

**NONLINEAR AXISYMMETRIC ELASTIC
ANALYSIS OF DEEP IMPERFECT SPHERICAL
SHELLS**

by

David William Smith

A Dissertation submitted to the University of London
for the Degree of Doctor of Philosophy (Ph.D.)

ACKNOWLEDGEMENTS

The work presented in this dissertation was conducted in the Department of Civil and Municipal Engineering of University College London, and the programs were executed on the Computers of the University of London Computer Centre. I would especially like to thank Professor James Croll of the Department of Civil and Municipal Engineering of University College London for his guidance and patience throughout the duration of this work.

I would also like to thank both of my parents for their generous support, assistance, and interest in this work. Special thanks is owed to my mother for the many hours she has spent entering the text and equations, and for proof reading this thesis. Thanks are also due to my wife for the unfailing encouragement she has always shown me.

ABSTRACT

The particular problem that is addressed in this thesis is the nonlinear elastic analysis of incomplete thin deep spherical shells, where the displacements on the boundary surface are fully restrained and the shell is loaded by a uniform pressure load. The shell may contain initial axisymmetric geometric or stress imperfections, and the initial response of the shell, the fundamental path, is axisymmetric. Solution techniques are developed and presented for the nonlinear fundamental path, and the nonlinear eigenvalue problem that yields the location of the points of the axisymmetric or periodic secondary paths that bifurcate from the axisymmetric fundamental path and the initial mode shapes of the secondary paths at the point of bifurcation of the secondary paths from the nonlinear axisymmetric fundamental path. Using the nonlinear elastic deep shell theory developed in this thesis, the behaviour of perfect and imperfect incomplete spherical shells with fully restrained boundary surface displacements under uniform pressure loading is examined.

This thesis also attempts to derive and present the equations and solution methods used in the nonlinear elastic analysis of thin spherical caps in as general a way as possible, in order that the solution methods developed in the thesis may be applied to shell structures composed of one or more incomplete thin elastic shells of arbitrary shape under arbitrary loading. By extending the derivation of the strain-displacement expressions for shells to include the terms that are quartic in displacements, the limitations present in linear thin shell theory may be lifted, and partial differential equations governing the nonlinear elastic behaviour of thin shells of arbitrary shape may be developed. The methods used to develop the total potential energy functional for pressure loaded spherical shells may be extended and used to express the total potential energy of shell structures composed of one or more incomplete shells of arbitrary shape under arbitrary loading.

NONLINEAR AXISYMMETRIC ELASTIC ANALYSIS OF DEEP SPHERICAL SHELLS

TABLE OF CONTENTS

| | Page |
|--|------|
| 1 INTRODUCTION | 4 |
| 2 THE KIRCHHOFF THIN SHELL EQUATIONS | 14 |
| 3 CLASSICAL AND AXISYMMETRIC POSTBUCKLING ANALYSIS OF COMPLETE SPHERICAL SHELLS | 44 |
| 4 GENERAL SOLUTION METHODS FOR THE NONLINEAR FUNDAMENTAL PATH AND THE LINEARISED SECONDARY PATH | 54 |
| 5 NUMERICAL SOLUTION ALGORITHMS, BASED ON FINITE DIFFERENCE SOLUTIONS OF THE KIRCHHOFF EQUATIONS | 94 |
| 6 VALIDATION OF THE COMPUTER PROGRAM | 117 |
| 7 PRESENTATION OF RESULTS | 139 |
| 8 CONCLUSIONS | 181 |
| REFERENCES | 187 |
| APPENDIX A AXISYMMETRIC POST BUCKLING ANALYSIS OF COMPLETE SPHERICAL SHELLS | 189 |
| APPENDIX B COMPUTER PROGRAM, SOURCE AND OUTPUT LISTINGS | 199 |

CHAPTER ONE

INTRODUCTION

CHAPTER ONE

CONTENTS

- 1.1 THE RESEARCH TOPIC**
- 1.2 THE PROBLEM**
- 1.3 THE MATHEMATICS**
- 1.4 THE PHYSICS - THERMODYNAMICS**
- 1.5 THIN SHELL THEORY**

INTRODUCTION

1.1 THE RESEARCH TOPIC

The theory of shells forms a part of the theory of elasticity concerned with the study of the deformation of elastic bodies under the influence of given loads. In this thesis it will be assumed that the material of the shell is isotropic and obeys Hooke's Law. There are two distinct classes of shells, thick shells and thin shells. A shell will be called thin if the maximum value of the ratio t/R , where t is the thickness of the shell and R is the radius of curvature of the middle surface, can be neglected in comparison with unity. Correspondingly, shells will be called thick whenever such terms cannot be neglected. If the displacements at a point are small in comparison with the thickness of the shell the governing differential equations are linear. If this limitation is not imposed the governing differential equations become nonlinear, and their solution becomes correspondingly more difficult. This thesis is concerned with the development and solution of the nonlinear differential equations that govern the nonlinear elastic behaviour of thin shells.

The method and notation used in deriving the nonlinear strain-displacement relations for thin shells of arbitrary shape, contained in Section 2.2 of Chapter Two, are based on the work of V.V. Novozhilov, Reference [1]. The two hypotheses of Kirchhoff, concerning the normals to the middle surface and the stresses normal to the middle surface, are used. This allows the study of the deformation of the shell to be expressed in terms of the deformation of the middle surface, in the same way as the hypothesis regarding plane sections in the bending of a beam reduces that problem to the study of the bending of the neutral axis. However, the derivation of the strain-displacement relations contained in this work has been extended, by comparison to that given by Novozhilov in Reference [1], to include the terms that are cubic and quartic in the displacements of the middle surface.

As a consequence of using the Kirchhoff assumptions we follow Novozhilov in expressing the opinion " ... that a simpler approach to the study of thin shells is impossible if one has in mind a theory which is to apply to all problems." On the basis of the Kirchhoff assumptions, with their inherent errors, one is thus justified in calling the theory developed in this work the Elastic Nonlinear Technical Theory of Thin Shells.

The nonlinear elastic analysis of thin shells will be illustrated using incomplete spherical shells as an example. In particular the equations and solution methods required for the nonlinear elastic analysis of deep spherical shells, with or without initial axisymmetric imperfections, under a uniform pressure load, and the solution of the linearised eigenvalue problem that yields the initial mode shapes and bifurcation loads of the secondary equilibrium paths which bifurcate from the axisymmetric fundamental equilibrium path are presented in this work. The

classical buckling and postbuckling analysis of complete spherical shells is presented in Chapter Three. Results for initially perfect incomplete spherical shells, with geometric slenderness values of between 3.5 and 60, and for initially imperfect spherical caps with slenderness values of 4, 6, 9, 12 and 30 are presented in Chapter Seven.

The introduction of those useful fictions of an incompressible weightless fluid and of an infinitely rigid material from which to construct a container allow the idealised 'system' under consideration to be represented in Figure 1.1.

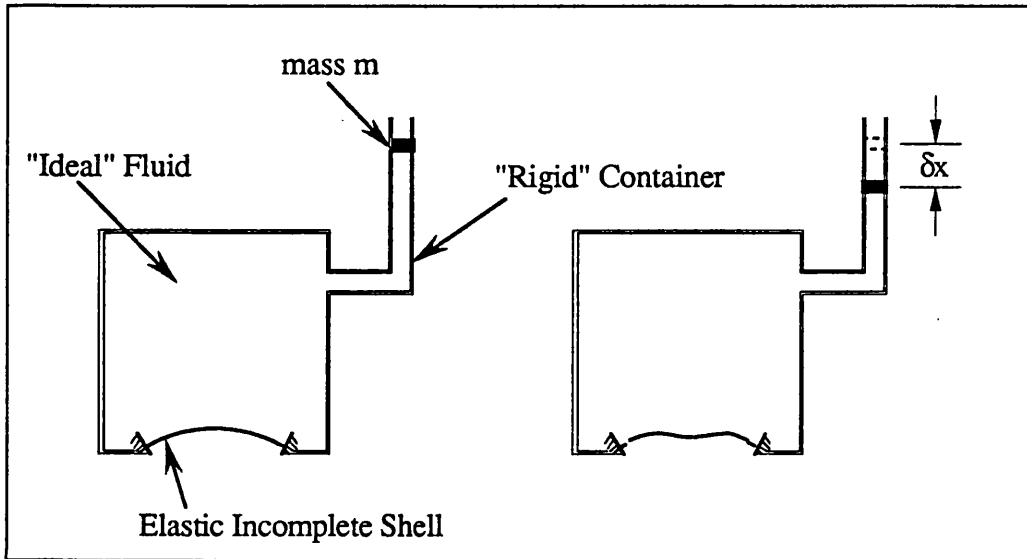


Figure 1.1 The Idealised System Under Consideration

1.2 THE PROBLEM

The particular problem that is addressed in this thesis is the nonlinear elastic analysis of incomplete thin deep spherical shells, where the displacements on the boundary surface are fully restrained and the shell is loaded by a uniform pressure load. The shell may contain initial axisymmetric geometric or stress imperfections, and the initial response of the shell, the fundamental path, is axisymmetric. Solution techniques are developed and presented for the nonlinear fundamental path, and the nonlinear eigenvalue problem that yields the location of the points of the axisymmetric or periodic secondary paths that bifurcate from the axisymmetric fundamental path and the initial mode shapes of the secondary paths at the point of bifurcation of the secondary paths from the nonlinear axisymmetric fundamental path. Using the nonlinear elastic deep shell theory developed in this thesis, the behaviour of perfect and imperfect incomplete spherical shells with fully restrained boundary surface displacements under uniform pressure loading is examined.

This thesis also attempts to derive and present the equations and solution methods used in the nonlinear elastic analysis of thin spherical caps in as general a way as possible, in order that the solution methods developed in the thesis may be applied to shell structures composed of one or more incomplete thin elastic shells of arbitrary shape under arbitrary loading. By extending the derivation of the strain-displacement expressions for shells to include the terms that are quartic in displacements, the limitations present in linear thin shell theory may be lifted, and partial differential equations governing the nonlinear elastic behaviour of thin shells of arbitrary shape may be developed. The methods used to develop the total potential energy functional for pressure loaded spherical shells may be extended and used to express the total potential energy of shell structures composed of one or more incomplete shells of arbitrary shape under arbitrary loading.

1.3 THE MATHEMATICS

To quote from Courant and Robbins, Reference [2]

"The number continuum, whether it is accepted as a matter of course or only after a critical examination, has been the basis of mathematics – and in particular of analytic geometry and the calculus – since the seventeenth century."

The brief summary of the mathematical concepts implicitly used in the development of the nonlinear differential equations that govern the elastic behaviour of thin shells that is given below is taken, almost entirely, from Reference [2].

The Number Continuum

In passing from the adjective "infinite", meaning simply "without end", to the noun "infinity" we must not make the assumption that "infinity", usually expressed by the special symbol ∞ , can be considered as though it were an ordinary number. The symbol ∞ cannot be included in the real number system and at the same time preserve the fundamental rules of arithmetic. Nevertheless the concept of the infinite pervades all of mathematics, since mathematical objects are usually studied not as individuals, but as members of classes or aggregates containing infinitely many objects of the same type, such as the totality of integers or of real numbers. For this reason it is necessary to analyze the mathematical infinite in a precise way. The modern theory of sets, created by Georg Cantor and his school at the end of the nineteenth century, has met this challenge with success. Cantor's theory of sets has influenced many fields of mathematics, and is of basic importance in the study of the logical and philosophical foundations of mathematics, Reference [2].

If the elements in two sets A and B may be paired with each other in such a way that there is a one to one correspondence between the elements of A and the elements of B, then the correspondence is said to be biunique, and A and B are said to be equivalent. Cantor's idea was to extend the concept of equivalence to infinite sets in order to define an "arithmetic" of infinities. Quoting from Courant and Robbins, Reference [2]

"Cantor made the very significant discovery that *the set of all real numbers*, rational and irrational, *is not denumerable*. In other words, the totality of real numbers presents a radically different and, so to speak, higher type of infinity than that of the integers or of the rational numbers alone."

It may be imagined that the reason for the non-denumerability of the number continuum lies in the fact that the straight line is infinite in extent, and that a finite segment of the line would contain only a denumerable infinity of points. This is not the case, for it is easy to show that the entire number continuum is equivalent to any finite segment, say the segment from 0 to 1 with the endpoints excluded, and it follows that even a finite segment of the number axis

contains a non-denumerable infinity of points. It is this non-denumerable number continuum, say the segment from 0 to 1 with the endpoints excluded, that forms the mathematical basis for both the analytic geometry and the calculus.

Uses of Analytic Geometry and the Calculus

The mathematical tools used in deriving the strain-displacement relations for thin shells of arbitrary geometry are analytic geometry and the differential calculus. The introduction of the assumption that the material is isotropic and obeys Hooke's Law allows the stresses within the shell to be expressed in terms of the strains. Then the First Law of thermodynamics, or the principle that energy is conserved, provides the physical reason for considering the total potential energy of the 'system' and the integral calculus allows the total potential energy of the 'system' to be expressed in the form of an integral. The Second Law of thermodynamics provides the physical justification for studying the equilibrium states of the 'system', and the calculus of variations, in particular the Euler equation, provides the necessary and sufficient condition for equilibrium of the 'system'.

The stability of equilibrium states is not considered in this thesis, however it is of interest to note that stability will be intimately associated with the definition of the 'system'. In particular the inclusion in the 'system' of the fictitious materials is tantamount to the inclusion of infinity in the continuum of the fluid and material elasticities, and therefore in the mathematics describing the 'system'. In the recent past the mathematical proof of the necessary and sufficient conditions, in the calculus of variations, for the stability of an equilibrium state of a system has not been rigorously established, see for example Thompson and Hunt Reference [3]. It may be the case that the recent contribution by S.J.G. Gift, Reference [4], to the calculus of variations of the fifth necessary condition will allow the necessary and sufficient conditions for stability to be proved with mathematical rigour.

1.4 THE PHYSICS - THERMODYNAMICS

The First Law of thermodynamics is a general statement of the principle of conservation of energy. The following statement of the First Law of thermodynamics is taken from D.E. Atkinson, Reference [5].

"A system may exchange energy with its surroundings in two ways: by gain or loss of heat or by doing work on the surroundings or having work done on it by the surroundings. In its thermodynamic sense, 'work' merely means any energy exchange except heat flow.

The First Law of thermodynamics is usually stated by the equation

$$\Delta E = q - w$$

where ΔE is the change in energy of the system, q is heat transferred to the system from the surroundings, and w is work done by the system on the surroundings. This Law is simple and self-evident." ?

An adequate statement of the principle of conservation of energy for the frictionless adiabatic system considered in this thesis, Figure 1.1, could also be derived from Newton's Laws.

The Second Law of Thermodynamics is concerned with the equilibrium of the system, and may be stated in a number of ways, the following is one of the statements of Second Law given by Atkinson in Reference [5].

"For any process that involves energy flow (or energy transduction) there is an equilibrium situation, and if the process proceeds spontaneously it must proceed in the direction of equilibrium."

Quoting from Reference [5] once more

"In discussions of the Second Law, it is often made to seem that systems go toward equilibrium because they must "obey" the Law. But of course equilibrium states exist in themselves quite independently of any Law or other product of human thought. Thus the Second Law is at base merely a descriptive and intuitively obvious statement concerning equilibrium states. Anyone who has a common-sense feeling that equilibrium states exist, and that systems that are not at equilibrium tend to go toward equilibrium and cannot spontaneously move away from it understand as much of the conceptual basis of the Second Law as there is to understand." X

When no heat is transferred to or from the 'system', an adiabatic process, the First Law of thermodynamics allows the energy of the 'system' to be expressed in terms of the potential energy (the elastic strain energy of the deformed shell and the potential energy of the load, i.e. of the mass m in a gravitational field) and the kinetic energy of the shell and the mass m . In this thesis we will consider only static adiabatic conditions, and as a result of imposing these limitations we need only consider the total potential energy of the 'system'. The Second Law of thermodynamics is a formal statement of Physics describing the obvious fact that the equilibrium states of the system are of particular interest.

1.5 THIN SHELL THEORY

In the theory of elasticity, the term shell is applied to bodies bounded by two curved surfaces when the distance between the surfaces is small in comparison with the other dimensions. The locus of points which lie at equal distances from these two surfaces defines the middle surface of the shell. The length intercepted between the two surfaces of the shell by a line perpendicular to the middle surface at any arbitrary point on the middle surface determines the thickness, t , of the shell at that point. The thickness may vary in magnitude, however, in the present work only shells of constant thickness are considered. If the shell has no boundary other than the two surfaces mentioned above it will be called complete, otherwise the shell will be referred to as incomplete. It will be assumed that each edge (also referred to as a boundary, e.g. boundary conditions) of an incomplete shell is a plane surface and that the edge surface and the middle surface of the shell intersect at right angles. The middle surface, thickness, and edges completely define the geometry of a shell. X

As mentioned in Section 1.1, it will be assumed that the material of the shell is isotropic and obey Hooke's Law, and that the shell is thin, i.e. that the ratio of the radius of curvature of the shell to the thickness of the shell, t/R , may be neglected in comparison with unity. For most technical applications an admissible maximum value of the ratio of the thickness of the shell to the radius of curvature of the shell of less than $1/50$, $t/R < 1/50$, will result in sufficiently accurate calculations, and shells for which this inequality is violated will be regarded as thick shells.

The similarity between plates and shells was recognised toward the end of the last century, when Aron first presented a theory of shells based on the assumptions used by Kirchhoff in the theory of plates, Reference [1]. As a result of the similarities between plates and shells the development of both thick and thin shell theories is closely related to the development of the theory of plates. There are two fundamentally different methods for the solution of problems in the classical theory of plates. The first method, which was proposed by Cauchy and Poisson, is based on the expansion of the displacements and stresses in the plate in power series of z , the distance of a given point from the middle plane of the plate, and results in universal approach to the theory of plates. However, the conditions under which the series converge, and the number of boundary conditions and their formulation, gave rise to arguments, Reference [1]. The second method, which was proposed by Kirchhoff, introduced physical meaning into the theory of plates and remains in use today. Kirchhoff based his reasoning on several assumptions, analogous to those used in the theory of beams. The Kirchhoff assumptions used in the theory of plates may be stated as follows

- The straight fibres of a plate which are perpendicular to the middle surface before deformation remain so after deformation and do not change their length. X

- The normal stresses acting on planes parallel to the middle surface may be neglected in comparison with the other stresses.

The method of Kirchhoff introduced into the basic theory of plates a simplification which had a definite physical interpretation and which was a completely obvious extension of the well proven theory of beams. The introduction of the concepts of internal forces and moments produced a further link between the theory of plates and the theory of beams. The development of a theory of plates or shells based on the Kirchhoff assumptions reduces the study of the three dimensional plate or shell to that of the two dimensional middle surface, and as a consequence the theory cannot be developed into a more accurate theory. In contrast the Cauchy-Poisson theory has the advantage that, in principle at least, an exact theory may be developed.

Inaccuracies in the thin shell theory developed by Aron were corrected by Love in his theory of thin shells, which is also based on the Kirchhoff theory of plates, References [1] and [6]. However, the development given by Love is inconsistent with regard to small terms, and as a consequence many different versions of the thin shell formulae have resulted.

The deficiencies and limitations that result from the use of the Kirchhoff assumptions as a basis for developing a thin shell theory have been studied by the Russian School in the theory of shells, and summarised by Novozhilov in Reference [1] from which the following quote is taken.

"Although the works of Galerkin [93, 94, 128] relate to thick shells, he was able by his original methods to obtain all the formulae of the theory of shells from the equations of the general theory of elasticity. He thus played an important part in the development of a mathematically rigorous theory for thin shells. The equations of the theory of thin shells were for the first time deduced in this way by A.I. Lur'e [15, 17] who, however, was not able to give the necessary criterion for simplifying his formulae. This criterion was given in the papers by Novozhilov [30, 28] where the errors introduced by Kirchhoff into the theory of thin shells were elucidated and where it was proved that these errors are of the order t/R in comparison with unity. In this way it was established that the above mentioned assumptions are sufficient for the construction of the theory of thin shells."

The derivation of the strain-displacement relations contained in Chapter Two include the terms that are cubic and quartic in the displacements of the middle surface, and the limitations present in Reference [1], that displacements at a point are small in comparison with the thickness of the shell, may be lifted resulting in the Elastic Nonlinear Technical Theory of Thin Shells.

CHAPTER TWO

THE KIRCHHOFF THIN SHELL EQUATIONS

CHAPTER TWO

CONTENTS

- 2.1 INTRODUCTION**
- 2.2 STRAIN DISPLACEMENT RELATIONS**
 - 2.2.1 Theory of Surfaces**
 - 2.2.2 Deformation of the Shell and the Nonlinear Variation of the Displacements Within the Thickness of the Shell**
 - 2.2.3 Incomplete Shells and Continuity of Displacements**
 - 2.2.4 Nonlinear Strain-Displacement Relations**
 - 2.2.5 Nonlinear Strain-Displacement Relations Specialised for Spherical Shells.**
- 2.3 THE STRAIN ENERGY FOR A DEFORMED SPHERICAL SHELL**
- 2.4 THE LOAD POTENTIAL ENERGY FOR A DEFORMED SPHERICAL SHELL**
- 2.5 THE EQUILIBRIUM EQUATIONS FOR THIN SPHERICAL SHELLS**
- 2.6 BOUNDARY CONDITIONS FOR INCOMPLETE CLAMPED SPHERES**
 - 2.6.1 Boundary Conditions at the Pole**
 - 2.6.2 Boundary Conditions for Clamped Incomplete Spheres (Caps)**

THE KIRCHHOFF THIN SHELL EQUATIONS

2.1 INTRODUCTION

In this chapter nonlinear strain-displacement relations are derived for thin shells of arbitrary shape based on the two assumptions of Kirchhoff. The method and notation used in deriving the strain displacement relations is based on the work of V.V.Novozhilov, Reference [1]. However, by extending the derivations to include the terms that are cubic and quartic in displacements the limitation present in the work of Novozhilov,

"that displacements at a point are small in comparison with the thickness of the shell"

may be lifted; and for all technical applications 'exact' partial differential equations governing the behaviour of elastic isotropic thin shells are available.

The nonlinear strain displacement relations for thin shells are developed in Section 2.2. These relations are then specialised for shells of spherical geometry. Then in Section 2.3 they are used to express the strain energy of the deformed shell, and integration across the thickness of the shell is performed. At this stage the middle surface strain expressions include cubic and quartic terms, while only linear and quadratic terms are maintained in the curvature expressions.

The load potential energy for uniform pressure loading is derived in Section 2.4, allowing the total potential energy functional to be expressed in terms of the middle surface displacements and their derivatives.

Equilibrium and stability of the system are considered in Section 2.5, and the Euler equation is introduced. Finally, in anticipation of the solution of the equilibrium equations, boundary conditions for spherical shells at the singular points (poles) and for clamped edges are given in Section 2.6.

2.2 STRAIN DISPLACEMENT RELATIONS

The nonlinear strain displacement relations for thin shells are developed in this Section. First some fundamental results from the theory of surfaces are presented in Section 2.2.1.

In Section 2.2.2 the first Kirchhoff assumption is introduced, allowing the displacements through the thickness of the shell (u_z, v_z, w_z) to be expressed in terms of the middle surface (reference surface) displacements and their derivatives.

Then, in Section 2.2.3, the conditions that are required at the boundary of incomplete shells in order that the displacements are continuous within the shell are briefly considered.

The nonlinear strain displacement relations are derived in Section 2.2.4. In Section 2.2.5 the notation that is to be used for spherical shells is introduced, and the nonlinear strain displacement relations for spherical shells are given.

2.2.1 Theory of Surfaces

Let α_1 and α_2 be the curvilinear coordinates of the surface describing lines of principal curvature and hence orthogonal. Then in general the surface of the shell may be described by,

$$\begin{aligned}x &= f_1(\alpha_1, \alpha_2) \\y &= f_2(\alpha_1, \alpha_2) \\z &= f_3(\alpha_1, \alpha_2)\end{aligned}\tag{2.1}$$

and in particular for spherical shells,

$$\begin{aligned}x &= r \cos\theta \sin\phi \\y &= r \sin\theta \sin\phi \\z &= r \cos\phi\end{aligned}\tag{2.2}$$

where $\phi = \alpha_1$, $\theta = \alpha_2$, see Figure 2.1.

The surface may also be defined by the vector equation,

$$\mathbf{r} = \mathbf{r}(\alpha_1, \alpha_2)\tag{2.3}$$

and introducing the following notation for derivatives:

$$\mathbf{r}_{\alpha_1} = \frac{\partial \mathbf{r}}{\partial \alpha_1}, \quad \mathbf{r}_{\alpha_2} = \frac{\partial \mathbf{r}}{\partial \alpha_2}\tag{2.4}$$

For spherical shells these expressions reduce to,

$$\mathbf{r}_\phi = r \mathbf{e}_1, \quad \mathbf{r}_\theta = r \sin\phi \mathbf{e}_2$$

where \mathbf{e}_1 and \mathbf{e}_2 are unit vectors parallel to the α_1 and α_2 (ϕ and θ) coordinate lines of the surface.

The surface vector associated with a small change in α_1 and α_2 is given by,

$$ds = r_{\alpha_1} d\alpha_1 + r_{\alpha_2} d\alpha_2 \quad (2.5)$$

and the square of its length is given by,

$$ds^2 = (r_{\alpha_1}, r_{\alpha_1}) d\alpha_1^2 + 2(r_{\alpha_1}, r_{\alpha_2}) d\alpha_1 d\alpha_2 + (r_{\alpha_2}, r_{\alpha_2}) d\alpha_2^2 \quad (2.6)$$

where (r_i, r_j) denotes the scalar product, and as r_{α_1} and r_{α_2} are orthogonal $(r_{\alpha_1}, r_{\alpha_2}) \equiv 0$

The Lamé parameters may now be defined as:

$$A_1^2 = (r_{\alpha_1}, r_{\alpha_1}) = \left(\frac{\partial x}{\partial \alpha_1}\right)^2 + \left(\frac{\partial y}{\partial \alpha_1}\right)^2 + \left(\frac{\partial z}{\partial \alpha_1}\right)^2 \quad (2.7)$$

$$A_2^2 = (r_{\alpha_2}, r_{\alpha_2}) = \left(\frac{\partial x}{\partial \alpha_2}\right)^2 + \left(\frac{\partial y}{\partial \alpha_2}\right)^2 + \left(\frac{\partial z}{\partial \alpha_2}\right)^2$$

Hence,

$$ds^2 = A_1^2 d\alpha_1^2 + A_2^2 d\alpha_2^2 \quad (2.8)$$

and when only α_1 or α_2 vary we have

$$ds_1 = A_1 d\alpha_1 ; \quad ds_2 = A_2 d\alpha_2 \quad (2.9)$$

Defining the surface unit vectors as the right handed set (e_1, e_2, e_n) we have

$$e_1 = \frac{1}{A_1} r_{\alpha_1} \quad e_2 = \frac{1}{A_2} r_{\alpha_2} \quad e_n = [e_1 \bullet e_2] \quad (2.10)$$

where $[e_1 \bullet e_2]$ is the vector product.

Differentiation of unit vectors, Figure 2.2, may be defined as follows:

$$\frac{|\Delta(e_n)|}{|e_n|} = \frac{M_1 M_2}{R_1} = \frac{(A_1 d\alpha_1)}{R_1} e_1$$

Hence,

$$\frac{\partial e_n}{\partial \alpha_1} = \frac{A_1}{R_1} e_1 \quad (2.11)$$

similarly

$$\frac{\partial \mathbf{e}_n}{\partial \alpha_2} = \frac{A_2}{R_2} \mathbf{e}_2 \quad (2.12)$$

The expressions (2.11) and (2.12) are valid only when α_1 and α_2 are lines of principal curvature and therefore orthogonal, the proof of this is known as the 'Theorem of Rodrigues' in the theory of surfaces.

To find $\frac{\partial \mathbf{e}_i}{\partial \alpha_j}$ where, $i = 1, 2$ and $j = 1, 2$ we note that,

$$\frac{\partial \mathbf{r}_{\alpha_1}}{\partial \alpha_2} = \frac{\partial \mathbf{r}_{\alpha_2}}{\partial \alpha_1} = \frac{\partial^2 \mathbf{r}}{\partial \alpha_1 \partial \alpha_2} \quad (2.13)$$

and using equation (2.10) we have

$$\frac{\partial A_1 \mathbf{e}_1}{\partial \alpha_2} = \frac{\partial A_2 \mathbf{e}_2}{\partial \alpha_1} \quad (2.14)$$

Consider next the projection of $\frac{\partial \mathbf{e}_1}{\partial \alpha_1}$ and $\frac{\partial \mathbf{e}_1}{\partial \alpha_2}$ on the $\mathbf{e}_1, \mathbf{e}_2, \mathbf{e}_n$ axes, noting that

$$\left(\mathbf{e}_1, \frac{\partial \mathbf{e}_1}{\partial \alpha_1} \right) \equiv \left(\mathbf{e}_1, \frac{\partial \mathbf{e}_1}{\partial \alpha_2} \right) \equiv 0$$

and

$$\left(\mathbf{e}_2, \frac{\partial \mathbf{e}_1}{\partial \alpha_1} \right) = \frac{\partial (\mathbf{e}_2, \mathbf{e}_1)}{\partial \alpha_1} - \left(\mathbf{e}_1, \frac{\partial \mathbf{e}_2}{\partial \alpha_1} \right) = - \left(\mathbf{e}_1, \frac{\partial \mathbf{e}_2}{\partial \alpha_1} \right) \quad (2.15)$$

From (2.14) we have,

$$\frac{\partial \mathbf{e}_2}{\partial \alpha_1} = \frac{1}{A_2} \frac{\partial A_1 \mathbf{e}_1}{\partial \alpha_2} - \frac{1}{A_2} \frac{\partial A_2}{\partial \alpha_1} \mathbf{e}_2 \quad (2.16)$$

Hence:

$$\begin{aligned} \left(\mathbf{e}_2, \frac{\partial \mathbf{e}_1}{\partial \alpha_1} \right) &= -\frac{1}{A_2} \left(\mathbf{e}_1, \frac{\partial A_1 \mathbf{e}_1}{\partial \alpha_2} \right) + \frac{1}{A_2} \frac{\partial A_2}{\partial \alpha_1} (\mathbf{e}_1, \mathbf{e}_2) \\ &= -\frac{A_1}{A_2} \left(\mathbf{e}_1, \frac{\partial \mathbf{e}_1}{\partial \alpha_2} \right) - \frac{1}{A_2} \frac{\partial A_1}{\partial \alpha_2} (\mathbf{e}_1, \mathbf{e}_1) \\ &= -\frac{1}{A_2} \frac{\partial A_1}{\partial \alpha_2} (\mathbf{e}_1, \mathbf{e}_1) \end{aligned}$$

therefore

$$\left(\mathbf{e}_2, \frac{\partial \mathbf{e}_1}{\partial \alpha_1} \right) = -\frac{1}{A_2} \frac{\partial A_1}{\partial \alpha_2} \quad (2.17)$$

also

$$\left(\mathbf{e}_n, \frac{\partial \mathbf{e}_1}{\partial \alpha_1} \right) = \frac{\partial (\mathbf{e}_n, \mathbf{e}_1)}{\partial \alpha_1} - \left(\mathbf{e}_1, \frac{\partial \mathbf{e}_n}{\partial \alpha_1} \right) = - \left(\mathbf{e}_1, \frac{\partial \mathbf{e}_n}{\partial \alpha_1} \right)$$

and using equation (2.11)

$$\left(\mathbf{e}_n, \frac{\partial \mathbf{e}_1}{\partial \alpha_1} \right) = -(\mathbf{e}_1, \mathbf{e}_1) \frac{A_1}{R_1} = -\frac{A_1}{R_1} \quad (2.18)$$

Similarly (2.14) and (2.12) may be used to derive the projections of $\frac{d\mathbf{e}_1}{d\alpha_2}$ on \mathbf{e}_2 and \mathbf{e}_n giving

$$\left(\mathbf{e}_2, \frac{\partial \mathbf{e}_1}{\partial \alpha_2} \right) = \frac{1}{A_1} \frac{\partial A_2}{\partial \alpha_1} \quad (2.19)$$

$$\left(\mathbf{e}_n, \frac{\partial \mathbf{e}_1}{\partial \alpha_2} \right) = 0 \quad (2.20)$$

The derivatives of \mathbf{e}_2 may be found in a similar fashion giving the results listed below.

$$\begin{aligned} \frac{\partial \mathbf{e}_1}{\partial \alpha_1} &= -\frac{1}{A_2} \frac{\partial A_1}{\partial \alpha_2} \mathbf{e}_2 - \frac{A_1}{R_1} \mathbf{e}_n \\ \frac{\partial \mathbf{e}_1}{\partial \alpha_2} &= \frac{1}{A_1} \frac{\partial A_2}{\partial \alpha_1} \mathbf{e}_2 \\ \frac{\partial \mathbf{e}_2}{\partial \alpha_2} &= -\frac{1}{A_1} \frac{\partial A_2}{\partial \alpha_1} \mathbf{e}_1 - \frac{A_2}{R_2} \mathbf{e}_n \\ \frac{\partial \mathbf{e}_2}{\partial \alpha_1} &= \frac{1}{A_2} \frac{\partial A_1}{\partial \alpha_2} \mathbf{e}_1 \\ \frac{\partial \mathbf{e}_n}{\partial \alpha_1} &= \frac{A_1}{R_1} \mathbf{e}_1 \\ \frac{\partial \mathbf{e}_n}{\partial \alpha_2} &= \frac{A_2}{R_2} \mathbf{e}_2 \end{aligned} \quad (2.21)$$

Also the conditions of Codazzi and Gauss may be derived by considering the following identities:

$$\frac{\partial^2 \mathbf{e}_n}{\partial \alpha_1 \partial \alpha_2} = \frac{\partial^2 \mathbf{e}_n}{\partial \alpha_2 \partial \alpha_1} \quad \text{and} \quad \frac{\partial^2 \mathbf{e}_1}{\partial \alpha_1 \partial \alpha_2} = \frac{\partial^2 \mathbf{e}_1}{\partial \alpha_2 \partial \alpha_1}$$

Substituting from equation (2.21) into the first of the identities above, yields the condition of Codazzi

$$\begin{aligned}\frac{\partial}{\partial \alpha_1} \left(\frac{A_2}{R_2} \right) &= \frac{1}{R_1} \frac{\partial A_2}{\partial \alpha_1} \\ \frac{\partial}{\partial \alpha_2} \left(\frac{A_1}{R_1} \right) &= \frac{1}{R_2} \frac{\partial A_1}{\partial \alpha_2}\end{aligned}\quad (2.22)$$

and using equation (2.21) in the second identity results in the condition of Gauss.

$$\frac{\partial}{\partial \alpha_1} \left(\frac{1}{A_1} \frac{\partial A_2}{\partial \alpha_1} \right) + \frac{\partial}{\partial \alpha_2} \left(\frac{1}{A_2} \frac{\partial A_1}{\partial \alpha_2} \right) = -\frac{A_1 A_2}{R_1 R_2}\quad (2.23)$$

We now have sufficient relations, in equations (2.21), (2.22), and (2.23), to derive the strain displacement expressions for the shell.

2.2.2. Deformation of the Shell and the Nonlinear Variation of the Displacements Within the Thickness of the Shell

Let the arbitrary point O on the middle surface of the shell undergo the displacement Δ as a result of the shell's deformation, Figure 2.3. The point O_1 located on the normal to the middle surface passing through O , and at a distance z from O undergoes the displacement Δ_z . That is, during the process of deformation the point O moves to the position O' and the point O_1 to the position O'_1 , Figure 2.3.

Making use of the first of the Kirchhoff assumptions:

- The straight fibres of the shell which are perpendicular to the middle surface before deformation remain so after deformation and do not change their length.

It follows that the segment $O'O'_1$ will be perpendicular to the deformed middle surface and that its length will be equal to that of OO_1 , namely z . Hence we have the vector equations

$$z\mathbf{e}_n + \Delta_z = \Delta + z\mathbf{e}'_n$$

$$\Delta_z = \Delta + (\mathbf{e}'_n - \mathbf{e}_n)z\quad (2.24)$$

and

$$\mathbf{e}'_n = [\mathbf{e}'_1 \cdot \mathbf{e}'_2]$$

where $\mathbf{e}'_1, \mathbf{e}'_2, \mathbf{e}'_n$ are the unit vectors of the deformed middle surface.

Defining the projections of Δ and Δ_z on \mathbf{e}_1 , \mathbf{e}_2 , and \mathbf{e}_n as u , v , w and u_z , v_z , w_z respectively, the vector equation of the deformed middle surface may be written as,

$$\mathbf{R} = \mathbf{r} + \Delta = \mathbf{r} + u\mathbf{e}_1 + v\mathbf{e}_2 + w\mathbf{e}_n \quad (2.25)$$

On differentiation of (2.25) and substitution from (2.21) we have

$$\frac{1}{A_1} \frac{\partial \mathbf{R}}{\partial \alpha_1} = (1 + \varepsilon_1)\mathbf{e}_1 + \omega_1\mathbf{e}_2 - \vartheta\mathbf{e}_n \quad (2.26a)$$

where

$$\varepsilon_1 = \frac{1}{A_1} \frac{\partial u}{\partial \alpha_1} + \frac{1}{A_1 A_2} \frac{\partial A_1}{\partial \alpha_2} v + \frac{w}{R_1} \quad (2.27a)$$

$$\omega_1 = \frac{1}{A_1} \frac{\partial v}{\partial \alpha_1} - \frac{1}{A_1 A_2} \frac{\partial A_1}{\partial \alpha_2} u$$

$$\vartheta = -\frac{1}{A_1} \frac{\partial w}{\partial \alpha_1} + \frac{u}{R_1}$$

Similarly

$$\frac{1}{A_2} \frac{\partial \mathbf{R}}{\partial \alpha_2} = \omega_2\mathbf{e}_1 + (1 + \varepsilon_2)\mathbf{e}_2 - \psi\mathbf{e}_n \quad (2.26b)$$

where

$$\varepsilon_2 = \frac{1}{A_2} \frac{\partial v}{\partial \alpha_2} + \frac{1}{A_1 A_2} \frac{\partial A_2}{\partial \alpha_1} u + \frac{w}{R_2} \quad (2.27b)$$

$$\omega_2 = \frac{1}{A_2} \frac{\partial u}{\partial \alpha_2} - \frac{1}{A_1 A_2} \frac{\partial A_2}{\partial \alpha_1} v$$

$$\psi = -\frac{1}{A_2} \frac{\partial w}{\partial \alpha_2} + \frac{v}{R_2}$$

The local coordinate frame of the deformed middle surface ($\mathbf{e}'_1, \mathbf{e}'_2, \mathbf{e}'_n$) is given by (2.10) as

$$\mathbf{e}'_1 = \frac{1}{A_1} \frac{\partial \mathbf{R}}{\partial \alpha_1}; \quad \mathbf{e}'_2 = \frac{1}{A_2} \frac{\partial \mathbf{R}}{\partial \alpha_2}; \quad \mathbf{e}'_n = \left[\mathbf{e}'_1 \bullet \mathbf{e}'_2 \right] \quad (2.28)$$

and A'_1 and A'_2 are the Lamé parameters of the deformed middle surface given by equation (2.7) as

$$A'_1 = \left\{ \left(\frac{\partial \mathbf{R}}{\partial \alpha_1}, \frac{\partial \mathbf{R}}{\partial \alpha_1} \right) \right\}^{\frac{1}{2}} \quad A'_2 = \left\{ \left(\frac{\partial \mathbf{R}}{\partial \alpha_2}, \frac{\partial \mathbf{R}}{\partial \alpha_2} \right) \right\}^{\frac{1}{2}}$$

Hence

$$\dot{A}_1 = A_1[(1 + \varepsilon_1)^2 + \omega_1^2 + \vartheta^2]^{\frac{1}{2}} \quad (2.29)$$

$$\dot{A}_1 = A_1\left[1 + \varepsilon_1 + \frac{1}{2}(\omega_1^2 + \vartheta^2) - \frac{1}{2}\varepsilon_1(\omega_1^2 + \vartheta^2) + \frac{1}{2}\varepsilon_1^2(\omega_1^2 + \vartheta^2) - \frac{1}{8}(\omega_1^2 + \vartheta^2)^2 + O 5th\right]$$

similarly

$$\dot{A}_2 = A_2\left[1 + \varepsilon_2 + \frac{1}{2}(\omega_2^2 + \psi^2) - \frac{1}{2}\varepsilon_2(\omega_2^2 + \psi^2) + \frac{1}{2}\varepsilon_2^2(\omega_2^2 + \psi^2) - \frac{1}{8}(\omega_2^2 + \psi^2)^2 + O 5th\right]$$

and

$$\dot{\mathbf{e}}_1 = \frac{1}{A_1} \frac{\partial \mathbf{R}}{\partial \alpha_1} = \frac{A_1}{A_1} [(1 + \varepsilon_1)\mathbf{e}_1 + \omega_1\mathbf{e}_2 - \vartheta\mathbf{e}_n]$$

$$\begin{aligned} \dot{\mathbf{e}}_1 = & \left[1 - \frac{1}{2}(\omega_1^2 + \vartheta^2) + \varepsilon_1(\omega_1^2 + \vartheta^2) - \frac{3}{2}\varepsilon_1^2(\omega_1^2 + \vartheta^2) + \frac{3}{8}(\omega_1^2 + \vartheta^2)^2 + O 5th\right]\mathbf{e}_1 \\ & + \omega_1\left[1 - \varepsilon_1 - \frac{1}{2}(\omega_1^2 + \vartheta^2) + \varepsilon_1^2 + \frac{3}{2}\varepsilon_1(\omega_1^2 + \vartheta^2) - \varepsilon_1^3 + O 4th\right]\mathbf{e}_2 \\ & - \vartheta\left[1 - \varepsilon_1 - \frac{1}{2}(\omega_1^2 + \vartheta^2) + \varepsilon_1^2 + \frac{3}{2}\varepsilon_1(\omega_1^2 + \vartheta^2) - \varepsilon_1^3 + O 4th\right]\mathbf{e}_n \end{aligned} \quad (2.30)$$

Similarly

$$\begin{aligned} \dot{\mathbf{e}}_2 = & \omega_2\left[1 - \varepsilon_2 - \frac{1}{2}(\omega_2^2 + \psi^2) + \varepsilon_2^2 + \frac{3}{2}\varepsilon_2(\omega_2^2 + \psi^2) - \varepsilon_2^3 + O 4th\right]\mathbf{e}_1 \\ & + \left[1 - \frac{1}{2}(\omega_2^2 + \psi^2) + \varepsilon_2(\omega_2^2 + \psi^2) - \frac{3}{2}\varepsilon_2^2(\omega_2^2 + \psi^2) + \frac{3}{8}(\omega_2^2 + \psi^2)^2 + O 5th\right]\mathbf{e}_2 \\ & - \psi\left[1 - \varepsilon_2 - \frac{1}{2}(\omega_2^2 + \psi^2) + \varepsilon_2^2 + \frac{3}{2}\varepsilon_2(\omega_2^2 + \psi^2) - \varepsilon_2^3 + O 4th\right]\mathbf{e}_n \end{aligned} \quad (2.31)$$

also

$$\dot{\mathbf{e}}_n = [\dot{\mathbf{e}}_1 \bullet \dot{\mathbf{e}}_2]$$

$$\begin{aligned} \dot{\mathbf{e}}_n = & \left[\vartheta - \varepsilon_1\vartheta - \omega_1\psi - \frac{1}{2}\vartheta(\omega_1^2 + \vartheta^2 + \omega_2^2 + \psi^2 - 2\varepsilon_1^2)\right. \\ & + \omega_1\psi(\varepsilon_1 + \varepsilon_2) + \frac{1}{2}\omega_1\psi(\omega_1^2 + \vartheta^2 + \omega_2^2 + \psi^2 - 2\varepsilon_1^2 - 2\varepsilon_2^2 - 2\varepsilon_1\varepsilon_2) \\ & + \vartheta(\omega_2^2 + \psi^2)(\varepsilon_2 + \frac{1}{2}\varepsilon_1) - \vartheta\varepsilon_1^3 + \frac{3}{2}\vartheta\varepsilon_1(\omega_1^2 + \vartheta^2) + O 5th \left. \right] \mathbf{e}_1 \\ & + \left[\psi - \varepsilon_2\psi - \vartheta\omega_2 - \frac{1}{2}\psi(\omega_1^2 + \vartheta^2 + \omega_2^2 + \psi^2 - 2\varepsilon_2^2)\right. \\ & + \vartheta\omega_2(\varepsilon_1 + \varepsilon_2) + \frac{1}{2}\omega_2\vartheta(\omega_1^2 + \vartheta^2 + \omega_2^2 + \psi^2 - 2\varepsilon_1^2 - 2\varepsilon_2^2 - 2\varepsilon_1\varepsilon_2) \\ & + \psi(\omega_1^2 + \vartheta^2)(\varepsilon_1 + \frac{1}{2}\varepsilon_2) - \psi\varepsilon_2^3 + \frac{3}{2}\psi\varepsilon_2(\omega_2^2 + \psi^2) + O 5th \left. \right] \mathbf{e}_2 \\ & + \left[1 - \omega_1\omega_2 - \frac{1}{2}(\omega_1^2 + \omega_2^2 + \vartheta^2 + \psi^2) + \omega_1\omega_2(\varepsilon_1 + \varepsilon_2) + \varepsilon_1(\omega_1^2 + \vartheta^2)\right. \\ & + \varepsilon_2(\omega_2^2 + \psi^2) + \frac{1}{2}\omega_1\omega_2(\omega_1^2 + \omega_2^2 + \vartheta^2 + \psi^2 - 2\varepsilon_1^2 - 2\varepsilon_2^2 - 2\varepsilon_1\varepsilon_2) \\ & - \frac{3}{2}\varepsilon_1^2(\omega_1^2 + \vartheta^2) - \frac{3}{2}\varepsilon_2^2(\omega_2^2 + \psi^2) + \frac{3}{8}(\omega_1^2 + \vartheta^2)^2 \\ & + \frac{3}{8}(\omega_2^2 + \psi^2)^2 + \frac{1}{4}(\omega_1^2 + \vartheta^2)(\omega_2^2 + \psi^2) + O 5th \left. \right] \mathbf{e}_n \end{aligned} \quad (2.32)$$

From equation (2.24), $\Delta_z = \Delta + (e'_n - e_n)z$ where $\Delta = ue_1 + ve_2 + we_n$ and substituting for e'_n from equation (2.32) the variation of the displacement as a function of z is given by:

$$\Delta_z = u_z e_1 + v_z e_2 + w_z e_n$$

where

$$\begin{aligned} u_z = u + z [& \vartheta - \vartheta \varepsilon_1 - \omega_1 \psi - \frac{1}{2} \vartheta (\omega_1^2 + \vartheta^2 + \omega_2^2 + \psi^2 - 2\varepsilon_1^2) \\ & + \omega_1 \psi (\varepsilon_1 + \varepsilon_2) + \frac{1}{2} \omega_1 \psi (\omega_1^2 + \vartheta^2 + \omega_2^2 + \psi^2 - 2\varepsilon_1^2 - 2\varepsilon_2^2 - 2\varepsilon_1 \varepsilon_2) \\ & + \vartheta (\omega_2^2 + \psi^2) (\varepsilon_2 + \frac{1}{2} \varepsilon_1) - \vartheta \varepsilon_1^3 + \frac{3}{2} \vartheta \varepsilon_1 (\omega_1^2 + \vartheta^2) + O 5th] \end{aligned} \quad (2.33)$$

$$\begin{aligned} v_z = v + z [& \psi - \psi \varepsilon_2 - \omega_2 \vartheta - \frac{1}{2} \psi (\omega_1^2 + \vartheta^2 + \omega_2^2 + \psi^2 - 2\varepsilon_2^2) \\ & + \vartheta \omega_2 (\varepsilon_1 + \varepsilon_2) + \frac{1}{2} \omega_2 \vartheta (\omega_1^2 + \vartheta^2 + \omega_2^2 + \psi^2 - 2\varepsilon_1^2 - 2\varepsilon_2^2 - 2\varepsilon_1 \varepsilon_2) \\ & + \psi (\omega_1^2 + \vartheta^2) (\varepsilon_1 + \frac{1}{2} \varepsilon_2) - \psi \varepsilon_2^3 + \frac{3}{2} \psi \varepsilon_2 (\omega_2^2 + \psi^2) + O 5th] \end{aligned}$$

$$\begin{aligned} w_z = w - z [& \frac{1}{2} (\omega_1 + \omega_2)^2 + \frac{1}{2} (\vartheta^2 + \psi^2) - \omega_1 \omega_2 (\varepsilon_1 + \varepsilon_2) \\ & - \varepsilon_1 (\omega_1^2 + \vartheta^2) - \varepsilon_2 (\omega_2^2 + \psi^2) + \frac{3}{2} \varepsilon_1^2 (\omega_1^2 + \vartheta^2) \\ & - \frac{1}{2} \omega_1 \omega_2 (\omega_1^2 + \vartheta^2 + \omega_2^2 + \psi^2 - 2\varepsilon_1^2 - 2\varepsilon_2^2 - 2\varepsilon_1 \varepsilon_2) \\ & + \frac{3}{2} \varepsilon_2^2 (\omega_2^2 + \psi^2) - \frac{3}{8} (\omega_1^2 + \vartheta^2)^2 - \frac{3}{8} (\omega_2^2 + \psi^2)^2 \\ & - \frac{1}{4} (\omega_1^2 + \vartheta^2) (\omega_2^2 + \psi^2) + O 5th] \end{aligned}$$

2.2.3 Incomplete Shells and Continuity of Displacements

The intersection of a boundary surface and the middle surface of the shell may be written as,

$$g(\alpha_1, \alpha_2) = 0 \quad \text{or} \quad \alpha_1 = f_1(\xi), \quad \alpha_2 = f_2(\xi) \quad (2.34)$$

where α_1 and α_2 are the curvilinear coordinates of the shell middle surface describing the lines of principal curvature and therefore orthogonal, and ξ is the curvilinear coordinate, of the boundary, on the middle surface defined by $g(\alpha_1, \alpha_2) = 0$.

Hence at the boundary,

$$\left(\frac{d\alpha_1}{d\xi} \right)^2 + \left(\frac{d\alpha_2}{d\xi} \right)^2 = 1 \quad (2.35)$$

The displacements of the shell u_z, v_z and w_z are given by equations (2.33) and (2.27) on the region $g(\alpha_1, \alpha_2) < 0$ (or $g(\alpha_1, \alpha_2) > 0$), where the use of the first Kirchhoff assumption has allowed u_z, v_z and w_z to be defined by the middle surface displacements (u, v, w) , their

derivatives with respect to α_1 and α_2 ($\delta u/\delta\alpha_1$, $\delta u/\delta\alpha_2$, $\delta v/\delta\alpha_1$, $\delta v/\delta\alpha_2$, $\delta w/\delta\alpha_1$, $\delta w/\delta\alpha_2$) and the distance normal to the middle surface (z). The limitations of thin shell theory will therefore require the boundary surface to intersect the middle surface of the shell at right angles. Also in order that the derivatives of u , v , and w with respect to α_1 and α_2 are defined on the region $g(\alpha_1, \alpha_2) < 0$ (or $g(\alpha_1, \alpha_2) > 0$) u , v , and w must be continuous functions of α_1 and α_2 on the region $g(\alpha_1, \alpha_2) \leq 0$ (or $g(\alpha_1, \alpha_2) \geq 0$). And as the choice of the middle surface as the reference surface is arbitrary u_z, v_z and w_z are also required to be continuous on the region $g(\alpha_1, \alpha_2) \leq 0$ (or $g(\alpha_1, \alpha_2) \geq 0$).

When u , v , and w are continuous on only one side of the boundary $g(\alpha_1, \alpha_2) = 0$ (a one-sided neighbourhood of $g(\alpha_1, \alpha_2) = 0$), then the derivatives of u , v , and w with respect to α_1 and α_2 at the boundary $g(\alpha_1, \alpha_2) = 0$ are not defined. Consequently the derivatives of u , v , and w with respect to α_1 and α_2 at the boundary $g(\alpha_1, \alpha_2) = 0$ will be determined so that the displacements u_z, v_z and w_z are continuous on the region $g(\alpha_1, \alpha_2) \leq 0$ (or $g(\alpha_1, \alpha_2) \geq 0$).

Let $\bar{u}_z(\xi)$, $\bar{v}_z(\xi)$ and $\bar{w}_z(\xi)$ be the orthogonal set of displacements of the boundary surface $g(\alpha_1, \alpha_2) = 0$ such that,

$$\begin{aligned}\bar{u}_z &= \bar{u}_0 + z\bar{u}_1 = u_z \frac{d\alpha_2}{d\xi} + v_z \frac{d\alpha_1}{d\xi} \\ \bar{v}_z &= \bar{v}_0 + z\bar{v}_1 = v_z \frac{d\alpha_2}{d\xi} - u_z \frac{d\alpha_1}{d\xi} \\ \bar{w}_z &= \bar{w}_0 + z\bar{w}_1 = w_z\end{aligned}\tag{2.36}$$

Hence

$$\begin{aligned}u &= \bar{u}_0 \frac{d\alpha_2}{d\xi} - \bar{v}_0 \frac{d\alpha_1}{d\xi} \\ v &= \bar{v}_0 \frac{d\alpha_2}{d\xi} + \bar{u}_0 \frac{d\alpha_1}{d\xi} \\ w &= \bar{w}_0\end{aligned}\tag{2.37}$$

and

$$\begin{aligned}K_u &= \bar{u}_1 \frac{d\alpha_2}{d\xi} - \bar{v}_1 \frac{d\alpha_1}{d\xi} \\ K_v &= \bar{v}_1 \frac{d\alpha_2}{d\xi} + \bar{u}_1 \frac{d\alpha_1}{d\xi} \\ K_w &= \bar{w}_1\end{aligned}\tag{2.38}$$

where

$$\begin{aligned}K_u &= \vartheta - \vartheta\varepsilon_1 - \omega_1 \psi - \frac{1}{2}\vartheta(\omega_1^2 + \vartheta^2 + \omega_2^2 + \psi^2 - 2\varepsilon_1^2) \\ &\quad + \omega_1 \psi(\varepsilon_1 + \varepsilon_2) + \frac{1}{2}\omega_1 \psi(\omega_1^2 + \vartheta^2 + \omega_2^2 + \psi^2 - 2\varepsilon_1^2 - 2\varepsilon_2^2 - 2\varepsilon_1\varepsilon_2) \\ &\quad + \vartheta(\omega_2^2 + \psi^2)(\varepsilon_2 + \frac{1}{2}\varepsilon_1) - \vartheta\varepsilon_1^3 + \frac{3}{2}\vartheta\varepsilon_1(\omega_1^2 + \vartheta^2) + O 5th\end{aligned}$$

$$\begin{aligned}
K_v = & \psi - \psi \varepsilon_2 - \omega_2 \vartheta - \frac{1}{2} \psi (\omega_1^2 + \vartheta^2 + \omega_2^2 + \psi^2 - 2\varepsilon_2^2) \\
& + \vartheta \omega_2 (\varepsilon_1 + \varepsilon_2) + \frac{1}{2} \omega_2 \vartheta (\omega_1^2 + \vartheta^2 + \omega_2^2 + \psi^2 - 2\varepsilon_1^2 - 2\varepsilon_2^2 - 2\varepsilon_1 \varepsilon_2) \\
& + \psi (\omega_1^2 + \vartheta^2) (\varepsilon_1 + \frac{1}{2} \varepsilon_2) - \psi \varepsilon_2^3 + \frac{3}{2} \psi \varepsilon_2 (\omega_2^2 + \psi^2) + O 5th
\end{aligned}$$

$$\begin{aligned}
K_w = & -\frac{1}{2} (\omega_1 + \omega_2)^2 - \frac{1}{2} (\vartheta^2 + \psi^2) + \omega_1 \omega_2 (\varepsilon_1 + \varepsilon_2) \\
& + \varepsilon_1 (\omega_1^2 + \vartheta^2) + \varepsilon_2 (\omega_2^2 + \psi^2) - \frac{3}{2} \varepsilon_1^2 (\omega_1^2 + \vartheta^2) \\
& + \frac{1}{2} \omega_1 \omega_2 (\omega_1^2 + \vartheta^2 + \omega_2^2 + \psi^2 - 2\varepsilon_1^2 - 2\varepsilon_2^2 - 2\varepsilon_1 \varepsilon_2) \\
& - \frac{3}{2} \varepsilon_2^2 (\omega_2^2 + \psi^2) + \frac{3}{8} (\omega_1^2 + \vartheta^2)^2 + \frac{3}{8} (\omega_2^2 + \psi^2)^2 \\
& + \frac{1}{4} (\omega_1^2 + \vartheta^2) (\omega_2^2 + \psi^2) + O 5th
\end{aligned}$$

and ε_1 , ω_1 , and ϑ and ε_2 , ω_2 , and ψ are given by equation (2.27).

Equations (2.37) and (2.38) are the boundary conditions that must be satisfied if the displacements u_z, v_z and w_z are to be defined by the thin shell equations (2.33) and (2.27) on the region $g(\alpha_1, \alpha_2) < 0$ (or $g(\alpha_1, \alpha_2) > 0$), and be continuous on the region $g(\alpha_1, \alpha_2) \leq 0$ (or $g(\alpha_1, \alpha_2) \geq 0$). The homogeneous boundary condition, all displacements on the boundary are zero, is of particular interest in its own right and in the idealized modelling of clamped shells and will be considered briefly below.

For a fully restrained boundary $\bar{u}_z(\xi) = \bar{v}_z(\xi) = \bar{w}_z(\xi) = 0$ for all ξ , hence

$$\bar{u}_0 = \bar{u}_1 = \frac{d\bar{u}_0}{d\xi} = 0 \quad (2.39)$$

$$\bar{v}_0 = \bar{v}_1 = \frac{d\bar{v}_0}{d\xi} = 0$$

$$\bar{w}_0 = \bar{w}_1 = \frac{d\bar{w}_0}{d\xi} = 0$$

When $d\alpha_1/d\xi = 0$ on the boundary ($\alpha_1 = f_1(\xi) = \text{constant}$, $\alpha_2 = \xi$) equations (2.37), (2.38) and (2.39) are satisfied when the displacements of the middle surface and their derivatives with respect to α_1 and α_2 at the boundary $g(\alpha_1, \alpha_2) = 0$ are given by,

$$u = 0 \quad \Rightarrow \quad \frac{\partial u}{\partial \alpha_2} = 0 \quad (2.40)$$

$$v = 0 \quad \Rightarrow \quad \frac{\partial v}{\partial \alpha_2} = 0$$

$$w = 0 \quad \Rightarrow \quad \frac{\partial w}{\partial \alpha_2} = 0$$

$$\frac{\partial w}{\partial \alpha_1} = 0$$

$$\frac{\partial u}{\partial \alpha_1} = a \quad \Rightarrow \quad \frac{\partial v}{\partial \alpha_1} = 0 \quad \text{or} \quad \frac{\partial v}{\partial \alpha_1} = \pm \sqrt{\frac{12a^2 - 8A_1 a + 4A_1^2}{3}}$$

Similarly when $d\alpha_2/d\xi = 0$ on the boundary ($\alpha_1 = \xi, \alpha_2 = f_2(\xi) = \text{constant}$) the middle surface displacements and their derivatives at the boundary are given by,

$$\begin{aligned}
 u = 0 & \Rightarrow \frac{\partial u}{\partial \alpha_1} = 0 & (2.41) \\
 v = 0 & \Rightarrow \frac{\partial v}{\partial \alpha_1} = 0 \\
 w = 0 & \Rightarrow \frac{\partial w}{\partial \alpha_1} = 0 \\
 \frac{\partial w}{\partial \alpha_2} & = 0 \\
 \frac{\partial v}{\partial \alpha_2} = a & \Rightarrow \frac{\partial u}{\partial \alpha_2} = 0 \text{ or } \frac{\partial u}{\partial \alpha_2} = \pm \sqrt{\frac{12a^2 - 8A_2a + 4A_2^2}{3}}
 \end{aligned}$$

When both $d\alpha_1/d\xi$ and $d\alpha_2/d\xi$ are non zero it may be shown that equations (2.37), (2.38) and (2.39) are satisfied when,

$$\begin{aligned}
 u & = 0 & (2.42a) \\
 v & = 0 \\
 w & = 0 \\
 \frac{\partial w}{\partial \alpha_1} = 0 & \Rightarrow \frac{\partial w}{\partial \alpha_2} = 0
 \end{aligned}$$

and the four first derivatives of u and v with respect to α_1 and α_2 at the boundary are chosen to satisfy the following three equations,

$$\begin{aligned}
 \frac{\partial u}{\partial \alpha_1} \frac{d\alpha_1}{d\xi} + \frac{\partial u}{\partial \alpha_2} \frac{d\alpha_2}{d\xi} & = 0 & (2.42b) \\
 \frac{\partial v}{\partial \alpha_1} \frac{d\alpha_1}{d\xi} + \frac{\partial v}{\partial \alpha_2} \frac{d\alpha_2}{d\xi} & = 0
 \end{aligned}$$

$$\begin{aligned}
 \frac{1}{2}(\omega_1 + \omega_2)^2 - (\omega_1 + \omega_2)(\omega_1 \varepsilon_1 + \omega_2 \varepsilon_2) - \frac{1}{8}(\omega_1 + \omega_2)^2(3\omega_1^2 - 2\omega_1\omega_2 + 3\omega_2^2) \\
 + \frac{1}{2}(\omega_1 + \omega_2)(3\omega_1 \varepsilon_1^2 + 3\omega_2 \varepsilon_2^2) - \frac{1}{2}\omega_1\omega_2(\varepsilon_1 - \varepsilon_2)^2 + O'5th = 0
 \end{aligned}$$

in which $\varepsilon_1, \omega_1, \varepsilon_2,$ and $\omega_2,$ are given in terms of the derivatives of u and v with respect to α_1 and α_2 by equation (2.27). Three of the four derivatives of u and v with respect to α_1 and α_2 may be expressed in terms of the fourth, which may be assigned arbitrarily. In particular when cubic expressions are used for the through thickness displacement relations of the shell, equations (2.42b) are satisfied by,

$$\begin{aligned}
 \frac{1}{A_1} \frac{\partial v}{\partial \alpha_1} \frac{d\alpha_1}{d\xi} + \frac{1}{A_1} \frac{\partial u}{\partial \alpha_2} \frac{d\alpha_2}{d\xi} & = 0 & (2.43) \\
 \frac{\partial u}{\partial \alpha_1} \frac{d\alpha_1}{d\xi} + \frac{\partial u}{\partial \alpha_2} \frac{d\alpha_2}{d\xi} & = 0 \\
 \frac{\partial v}{\partial \alpha_1} \frac{d\alpha_1}{d\xi} + \frac{\partial v}{\partial \alpha_2} \frac{d\alpha_2}{d\xi} & = 0
 \end{aligned}$$

which has the solution

$$\frac{\partial u}{\partial \alpha_1} = a \quad \Rightarrow \quad \frac{\partial v}{\partial \alpha_1} = \frac{A_1}{A_2} a, \quad \frac{\partial u}{\partial \alpha_2} = -a \frac{d\alpha_1}{d\alpha_2} \Big|_{\xi}, \quad \frac{\partial v}{\partial \alpha_2} = -\frac{A_1}{A_2} a \frac{d\alpha_1}{d\alpha_2} \Big|_{\xi} \quad (2.44)$$

where a is an arbitrary constant.

In general thin shell theory does not allow the middle surface displacements and their derivatives with respect to α_1 and α_2 to be uniquely determined at the boundary by the displacements of the boundary surface. A fifth condition involving either $\delta u / \delta \alpha_1$ or $\delta v / \delta \alpha_2$ at the boundary is required for the unique definition of the boundary values of the middle surface displacements and their derivatives with respect to α_1 and α_2 .

2.2.4 Nonlinear Strain Displacement Relations

The strains, ϵ , arising from the deformation of the shell's middle surface are given by,

$$\epsilon = \frac{ds - ds}{ds}$$

where

$$ds = A d\alpha, \quad ds = A' d\alpha$$

Making use of equation (2.29) to substitute for the Lamé parameters A, A' we have

$$\begin{aligned} \epsilon_{\alpha_1} = \frac{A_1 - A_1}{A_1} &= \epsilon_1 + \frac{1}{2}(\omega_1^2 + \vartheta^2) - \frac{1}{2}\epsilon_1(\omega_1^2 + \vartheta^2) \\ &+ \frac{1}{2}\epsilon_1^2(\omega_1^2 + \vartheta^2) - \frac{1}{8}(\omega_1^2 + \vartheta^2)^2 + O 5th \end{aligned} \quad (2.45)$$

$$\begin{aligned} \epsilon_{\alpha_2} = \frac{A_2 - A_2}{A_2} &= \epsilon_2 + \frac{1}{2}(\omega_2^2 + \psi^2) - \frac{1}{2}\epsilon_2(\omega_2^2 + \psi^2) \\ &+ \frac{1}{2}\epsilon_2^2(\omega_2^2 + \psi^2) - \frac{1}{8}(\omega_2^2 + \psi^2)^2 + O 5th \end{aligned} \quad (2.46)$$

The shear strain, ω , is given by

$$\sin(\omega) = \left(\mathbf{e}_1, \mathbf{e}_2 \right)$$

and substituting from equations (2.30) and (2.31) we have

$$\begin{aligned} \sin(\omega) &= \omega_1 + \omega_2 + (\vartheta\psi - \epsilon_2\omega_2 - \epsilon_1\omega_1) \\ &- \frac{1}{2}(\omega_1 + \omega_2)(\omega_1^2 + \vartheta^2 + \omega_2^2 + \psi^2) + \omega_2\epsilon_2^2 + \omega_1\epsilon_1^2 \\ &- \vartheta\psi(\epsilon_1 + \epsilon_2) + (\omega_1^2 + \vartheta^2)\left(\frac{1}{2}\epsilon_2\omega_2 + \frac{3}{2}\epsilon_1\omega_1 + \epsilon_1\omega_2\right) \\ &+ (\omega_2^2 + \psi^2)\left(\frac{1}{2}\epsilon_1\omega_1 + \frac{3}{2}\epsilon_2\omega_2 + \epsilon_2\omega_1\right) - \epsilon_2^3\omega_2 - \epsilon_1^3\omega_1 \\ &+ O 5th \end{aligned}$$

Making use of the expansion for x in terms of $\sin(x)$

$$x = \sin x + \frac{1}{6} \sin^3 x + \frac{9}{120} \sin^5 x + \dots$$

the shear strain may be expressed as follows:

$$\begin{aligned} \omega &= \omega_1 + \omega_2 + (\vartheta\psi - \varepsilon_2\omega_2 - \varepsilon_1\omega_1) & (2.47) \\ &- \frac{1}{2}(\omega_1 + \omega_2)(\omega_1^2 + \vartheta^2 + \omega_2^2 + \psi^2) + \frac{1}{6}(\omega_1 + \omega_2)^3 \\ &+ \omega_2\varepsilon_2^2 + \omega_1\varepsilon_1^2 - \vartheta\psi(\varepsilon_1 + \varepsilon_2) - \varepsilon_2^3\omega_2 - \varepsilon_1^3\omega_1 \\ &+ (\omega_1^2 + \vartheta^2)\left(\frac{1}{2}\varepsilon_2\omega_2 + \frac{3}{2}\varepsilon_1\omega_1 + \varepsilon_1\omega_2\right) \\ &+ (\omega_2^2 + \psi^2)\left(\frac{1}{2}\varepsilon_1\omega_1 + \frac{3}{2}\varepsilon_2\omega_2 + \varepsilon_2\omega_1\right) \\ &+ \frac{1}{2}(\omega_1 + \omega_2)^2(\vartheta\psi - \varepsilon_2\omega_2 - \varepsilon_1\omega_1) + O 5th \end{aligned}$$

To determine the curvature of the shell consider a surface parallel to the middle surface, at a distance z from the middle surface, see Figure 2.4, then we have

$$R_1^{(z)} = R_1 + z$$

$$R_2^{(z)} = R_2 + z$$

and

$$ds_1^{(z)} = A_1 \left(1 + \frac{z}{R_1}\right) d\alpha_1$$

$$ds_2^{(z)} = A_2 \left(1 + \frac{z}{R_2}\right) d\alpha_2$$

hence

$$A_1^{(z)} = A_1 \left(1 + \frac{z}{R_1}\right) \quad (2.48)$$

$$A_2^{(z)} = A_2 \left(1 + \frac{z}{R_2}\right)$$

We may now express the strain $\varepsilon_{\alpha_1}^{(z)}$ as a function of z by using equation (2.45) as follows :

$$\begin{aligned} \varepsilon_{\alpha_1}^{(z)} &= \varepsilon_1^{(z)} + \frac{1}{2}(\omega_1^{(z)2} + \vartheta^{(z)2}) - \frac{1}{2}\varepsilon_1^{(z)}(\omega_1^{(z)2} + \vartheta^{(z)2}) & (2.49) \\ &+ \frac{1}{2}\varepsilon_1^{(z)2}(\omega_1^{(z)2} + \vartheta^{(z)2}) - \frac{1}{8}(\omega_1^{(z)2} + \vartheta^{(z)2})^2 + O 5th \end{aligned}$$

With $\varepsilon_1^{(z)}$, $\omega_1^{(z)}$ and $\vartheta^{(z)}$ given by equations (2.27a) with A_1, A_2, R_1, R_2 and u, v, w replaced by $A_1^{(z)}, A_2^{(z)}, R_1^{(z)}, R_2^{(z)}$, and u_z, v_z, w_z . Performing these substitutions and using the conditions of Coddazi results in

$$\varepsilon_1^{(z)} = \frac{1}{1 + \frac{z}{R_1}} \left[\frac{1}{A_1} \frac{\partial u_z}{\partial \alpha_1} + \frac{1}{A_1 A_2} \frac{\partial A_1}{\partial \alpha_2} v_z + \frac{w_z}{R_1} \right] \quad (2.50)$$

$$\omega_1^{(z)} = \frac{1}{1 + \frac{z}{R_1}} \left[\frac{1}{A_1} \frac{\partial v_z}{\partial \alpha_1} - \frac{1}{A_1 A_2} \frac{\partial A_1}{\partial \alpha_2} u_z \right]$$

$$\vartheta^{(z)} = \frac{1}{1 + \frac{z}{R_1}} \left[-\frac{1}{A_1} \frac{\partial w_z}{\partial \alpha_1} + \frac{u_z}{R_1} \right]$$

Similarly, the strain $\varepsilon_{\alpha_2}^{(z)}$ may be written as,

$$\begin{aligned} \varepsilon_{\alpha_2}^{(z)} &= \varepsilon_2^{(z)} + \frac{1}{2} (\omega_2^{(z)^2} + \psi^{(z)^2}) - \frac{1}{2} \varepsilon_2^{(z)} (\omega_2^{(z)^2} + \psi^{(z)^2}) \\ &\quad + \frac{1}{2} \varepsilon_2^{(z)^2} (\omega_2^{(z)^2} + \psi^{(z)^2}) - \frac{1}{8} (\omega_2^{(z)^2} + \psi^{(z)^2})^2 + O_5 \text{th} \end{aligned} \quad (2.51)$$

with

$$\varepsilon_2^{(z)} = \frac{1}{1 + \frac{z}{R_2}} \left[\frac{1}{A_2} \frac{\partial v_z}{\partial \alpha_2} + \frac{1}{A_1 A_2} \frac{\partial A_2}{\partial \alpha_1} u_z + \frac{w_z}{R_2} \right] \quad (2.52)$$

$$\omega_2^{(z)} = \frac{1}{1 + \frac{z}{R_2}} \left[\frac{1}{A_2} \frac{\partial u_z}{\partial \alpha_2} - \frac{1}{A_1 A_2} \frac{\partial A_2}{\partial \alpha_1} v_z \right]$$

$$\psi^{(z)} = \frac{1}{1 + \frac{z}{R_2}} \left[-\frac{1}{A_2} \frac{\partial w_z}{\partial \alpha_2} + \frac{v_z}{R_2} \right]$$

Finally the shear strain, $\omega^{(z)}$, is given by

$$\begin{aligned} \omega^{(z)} &= \omega_1^{(z)} + \omega_2^{(z)} + (\vartheta^{(z)} \psi^{(z)} - \varepsilon_2^{(z)} \omega_2^{(z)} - \varepsilon_1^{(z)} \omega_1^{(z)}) \\ &\quad - \frac{1}{2} (\omega_1^{(z)} + \omega_2^{(z)}) (\omega_1^{(z)^2} + \vartheta^{(z)^2} + \omega_2^{(z)^2} + \psi^{(z)^2}) \\ &\quad + \frac{1}{6} (\omega_1^{(z)} + \omega_2^{(z)})^3 + \omega_2^{(z)} \varepsilon_2^{(z)^2} + \omega_1^{(z)} \varepsilon_1^{(z)^2} \\ &\quad - \vartheta^{(z)} \psi^{(z)} (\varepsilon_1^{(z)} + \varepsilon_2^{(z)}) - \varepsilon_2^{(z)^2} \omega_2^{(z)} - \varepsilon_1^{(z)^2} \omega_1^{(z)} \\ &\quad + (\omega_2^{(z)^2} + \vartheta^{(z)^2}) \left(\frac{1}{2} \varepsilon_2^{(z)} \omega_2^{(z)} + \frac{3}{2} \varepsilon_1^{(z)} \omega_1^{(z)} + \varepsilon_1^{(z)} \omega_2^{(z)} \right) \\ &\quad + (\omega_1^{(z)^2} + \psi^{(z)^2}) \left(\frac{1}{2} \varepsilon_1^{(z)} \omega_1^{(z)} + \frac{3}{2} \omega_2^{(z)} \varepsilon_2^{(z)} + \varepsilon_2^{(z)} \omega_1^{(z)} \right) \\ &\quad + \frac{1}{2} (\omega_1^{(z)} + \omega_2^{(z)})^2 (\vartheta^{(z)} \psi^{(z)} - \varepsilon_2^{(z)} \omega_2^{(z)} - \varepsilon_1^{(z)} \omega_1^{(z)}) + O_5 \text{th} \end{aligned} \quad (2.53)$$

The substitution of equations (2.33) into (2.50) and (2.52) will then allow the strains, equations (2.49), (2.51), (2.53), to be expressed in terms of the displacements of the middle surface u, v , and w and the distance, z , from the middle surface. The derivation of the nonlinear strains (as a function of z) presented above may be applied to any thin shell defined by equations (2.1) or (2.3).

2.2.5 Nonlinear Strain-Displacement Relations Specialised for Spherical Shells.

At this point in the derivation of the strain-displacement relations the formulae will be specialised for shells of spherical geometry. This will reduce the number of terms carried through successive substitutions.

The following notation will be used for shells of spherical geometry.

$$\phi \equiv \alpha_1 \quad , \quad \theta \equiv \alpha_2 \quad (2.54)$$

$$a \equiv R_1 \equiv R_2 \equiv r$$

$$A_1 \equiv a \quad , \quad A_2 \equiv a \sin \phi$$

and differentiation with respect to ϕ and θ will be denoted by,

$$\dot{u} \equiv \frac{\partial u}{\partial \phi} \quad , \quad \ddot{u} \equiv \frac{\partial^2 u}{\partial \phi^2} \quad , \quad \dots$$

$$\dot{u} \equiv \frac{\partial u}{\partial \theta} \quad , \quad \ddot{u} \equiv \frac{\partial^2 u}{\partial \theta^2} \quad , \quad \dots$$

The following notation will be used for the strain components of equation (2.27).

$$\epsilon_1 = \frac{1}{a} \left(\dot{u} + w \right) \quad (2.55)$$

$$\epsilon_2 = \frac{1}{a} \left(w + u \cot \phi + \dot{v} / \sin \phi \right)$$

$$\alpha = \omega_1 = \frac{1}{a} \dot{v}$$

$$\beta = \vartheta = \frac{1}{a} \left(u - \dot{w} \right)$$

$$\gamma = \omega_2 = \frac{1}{a} \left(\dot{u} / \sin \phi - v \cot \phi \right)$$

$$\delta = \psi = \frac{1}{a} \left(v - \dot{w} / \sin \phi \right)$$

On substitution of (2.33), (2.50) and (2.52) into (2.49), (2.51) and (2.53) we have,

$$\begin{aligned} \varepsilon_{\phi}^{(z)} = \varepsilon_{\alpha_1}^{(z)} = \frac{1}{1+\frac{z}{a}} [& \left\{ \varepsilon_1 + \frac{1}{2} (\alpha^2 + \beta^2) - \frac{1}{2} \varepsilon_1 (\alpha^2 + \beta^2) + \frac{1}{2} \varepsilon_1^2 (\alpha^2 + \beta^2) - \frac{1}{8} (\alpha^2 + \beta^2)^2 + O5th \right\} \\ & + \frac{z}{a} \left\{ \dot{\beta} - \dot{\beta} \varepsilon_1 - \dot{\beta} \varepsilon_1 - \dot{\alpha} \delta - \frac{1}{2} (\alpha + \gamma)^2 - \frac{1}{2} \alpha^2 - \frac{1}{2} \delta^2 + O3rd \right\}] \end{aligned} \quad (2.56)$$

$$\begin{aligned} \varepsilon_{\theta}^{(z)} = \varepsilon_{\alpha_2}^{(z)} = \frac{1}{1+\frac{z}{a}} [& \left\{ \varepsilon_2 + \frac{1}{2} (\gamma^2 + \delta^2) - \frac{1}{2} \varepsilon_2 (\gamma^2 + \delta^2) + \frac{1}{2} \varepsilon_2^2 (\gamma^2 + \delta^2) - \frac{1}{8} (\gamma^2 + \delta^2)^2 + O5th \right\} \\ & + \frac{z}{a} \left\{ \dot{\delta} / \sin \phi + \beta \cot \phi - (\dot{\delta} \varepsilon_2 + \delta \dot{\varepsilon}_2 + \dot{\gamma} \beta) / \sin \phi \right. \\ & \left. - (\beta \varepsilon_1 + \alpha \delta + \gamma \delta) \cot \phi - \frac{1}{2} (\alpha + \gamma)^2 - \frac{1}{2} \gamma^2 - \frac{1}{2} \beta^2 + O3rd \right\}] \end{aligned} \quad (2.57)$$

$$\begin{aligned} \varepsilon_{\theta\phi}^{(z)} = \frac{1}{2} \omega^{(z)} = \frac{1}{1+\frac{z}{a}} [& \frac{1}{2} \left\{ \alpha + \gamma + (\beta \delta - \varepsilon_2 \gamma - \varepsilon_1 \alpha) - \frac{1}{2} (\alpha + \gamma) (\alpha^2 + \beta^2 + \gamma^2 + \delta^2) \right. \\ & + \frac{1}{6} (\alpha + \gamma)^3 + \gamma \varepsilon_2^2 + \alpha \varepsilon_1^2 - \beta \delta (\varepsilon_1 + \varepsilon_2) - \varepsilon_2^3 \gamma - \varepsilon_1^3 \alpha \\ & + (\alpha^2 + \beta^2) \left(\frac{1}{2} \varepsilon_2 \gamma + \frac{3}{2} \varepsilon_1 \alpha + \varepsilon_1 \gamma \right) + (\gamma^2 + \delta^2) \left(\frac{1}{2} \varepsilon_1 \alpha + \frac{3}{2} \varepsilon_2 \gamma + \varepsilon_2 \alpha \right) \\ & \left. + \frac{1}{2} (\alpha + \gamma)^2 (\beta \delta - \varepsilon_2 \gamma - \varepsilon_1 \alpha) + O5th \right\} \\ & + \frac{z}{2a} \left\{ \dot{\delta} + \dot{\beta} / \sin \phi - \dot{\delta} \cot \phi - \dot{\delta} \varepsilon_2 - \delta \dot{\varepsilon}_2 - \dot{\gamma} \beta - \dot{\delta} \beta \right. \\ & \left. - \left(\dot{\beta} \varepsilon_1 + \dot{\beta} \varepsilon_1 + \dot{\alpha} \delta + \alpha \dot{\delta} \right) / \sin \phi + (\delta \varepsilon_2 + \gamma \beta) \cot \phi + \delta \beta \right. \\ & \left. - \alpha \dot{\beta} - \varepsilon_2 \left(\dot{\beta} / \sin \phi - \dot{\delta} \cot \phi - \dot{\gamma} \right) - \varepsilon_1 (\dot{\delta} - \dot{\alpha}) \right. \\ & \left. - \gamma \left(\dot{\delta} / \sin \phi + \beta \cot \phi \right) + O3rd \right\}] \end{aligned} \quad (2.58)$$

The nonlinear strain displacement relations for thin spherical shells are given by (2.56), (2.57) and (2.58), with the notation defined by (2.54) and linear strain components given by (2.55).

2.3 THE STRAIN ENERGY FOR A DEFORMED SPHERICAL SHELL

The second Kirchhoff assumption may be stated as follows:

- The normal stresses acting on planes parallel to the middle surface may be neglected in comparison with the other stresses.

This assumption allows the stress-strain relations for an isotropic linear elastic material (Hooke's Law) with modulus of elasticity E , and Poisson's ratio μ to be written as,

$$\sigma_{\phi}^{(z)} = \frac{E}{1-\mu^2} (\epsilon_{\phi}^{(z)} + \mu\epsilon_{\theta}^{(z)}) \quad (2.59)$$

$$\sigma_{\theta}^{(z)} = \frac{E}{1-\mu^2} (\epsilon_{\theta}^{(z)} + \mu\epsilon_{\phi}^{(z)})$$

$$\sigma_{\phi\theta}^{(z)} = \frac{E}{1+\mu} (\epsilon_{\theta\phi}^{(z)})$$

The elastic strain energy, U , of the spherical shell may then be written as

$$U = \frac{1}{2} \iiint [\sigma_{\phi}^{(z)}\epsilon_{\phi}^{(z)} + \sigma_{\theta}^{(z)}\epsilon_{\theta}^{(z)} + 2\sigma_{\phi\theta}^{(z)}\epsilon_{\phi\theta}^{(z)}] a^2 \left(1 + \frac{z}{a}\right)^2 \sin \phi \, d\theta d\phi dz \quad (2.60)$$

with the integration being performed over the entire volume of the shell.

Writing the nonlinear strain displacement relations (2.56), (2.57), (2.58) using the notation below,

$$\epsilon_{\phi}^{(z)} = \frac{1}{1 + \frac{z}{a}} (\epsilon_{\phi} + z\chi_{\phi}) \quad (2.61)$$

$$\epsilon_{\theta}^{(z)} = \frac{1}{1 + \frac{z}{a}} (\epsilon_{\theta} + z\chi_{\theta})$$

$$\epsilon_{\phi\theta}^{(z)} = \frac{1}{1 + \frac{z}{a}} (\epsilon_{\phi\theta} + z\chi_{\phi\theta})$$

allows the strain energy, U , to be expressed as

$$\begin{aligned} U = \frac{1}{2} \iiint & \left\{ \frac{E}{1-\mu^2} [\epsilon_{\phi} + z\chi_{\phi} + \mu(\epsilon_{\theta} + z\chi_{\theta})][\epsilon_{\phi} + z\chi_{\phi}] \right. \\ & + \frac{E}{1-\mu^2} [\epsilon_{\theta} + z\chi_{\theta} + \mu(\epsilon_{\phi} + z\chi_{\phi})][\epsilon_{\theta} + z\chi_{\theta}] \\ & \left. + \frac{2E}{1+\mu} [\epsilon_{\phi\theta} + z\chi_{\phi\theta}]^2 \right\} a^2 \sin \phi \, d\theta d\phi dz \quad (2.62) \end{aligned}$$

Performing the integration with respect to z from $-t/2$ to $+t/2$ results in

$$U = \frac{1}{2} \iint \frac{Et}{1-\mu^2} [\epsilon_\phi (\epsilon_\phi + \mu\epsilon_\theta) + \epsilon_\theta (\epsilon_\theta + \mu\epsilon_\phi) + 2(1-\mu)\epsilon_{\theta\phi}^2] a^2 \sin \phi \, d\theta \, d\phi$$

$$+ \frac{1}{2} \iint \frac{Et^3}{12(1-\mu^2)} [\chi_\phi (\chi_\phi + \mu\chi_\theta) + \chi_\theta (\chi_\theta + \mu\chi_\phi) + 2(1-\mu)\chi_{\theta\phi}^2] a^2 \sin \phi \, d\theta \, d\phi$$
(2.63)

Which may also be expressed as,

$$U = \frac{1}{2} \iint [N_\phi \epsilon_\phi + N_\theta \epsilon_\theta + 2N_{\theta\phi} \epsilon_{\theta\phi}] a^2 \sin \phi \, d\theta \, d\phi$$

$$+ \frac{1}{2} \iint [M_\phi \chi_\phi + M_\theta \chi_\theta + 2M_{\theta\phi} \chi_{\theta\phi}] a^2 \sin \phi \, d\theta \, d\phi$$
(2.64)

where

$$N_\phi = \frac{Et}{1-\mu^2} (\epsilon_\phi + \mu\epsilon_\theta) , \quad M_\phi = \frac{Et^3}{12(1-\mu^2)} (\chi_\phi + \mu\chi_\theta)$$

$$N_\theta = \frac{Et}{1-\mu^2} (\epsilon_\theta + \mu\epsilon_\phi) , \quad M_\theta = \frac{Et^3}{12(1-\mu^2)} (\chi_\theta + \mu\chi_\phi)$$

$$N_{\theta\phi} = \frac{Et}{1+\mu} \epsilon_{\theta\phi} , \quad M_{\theta\phi} = \frac{Et^3}{12(1+\mu)} \chi_{\theta\phi}$$
(2.65)

The nonlinear middle surface strains and curvatures first introduced in (2.61) are given by,

$$\epsilon_\phi = \epsilon_1 + \frac{1}{2}(\alpha^2 + \beta^2) - \frac{1}{2}\epsilon_1(\alpha^2 + \beta^2) + \frac{1}{2}\epsilon_1^2(\alpha^2 + \beta^2) - \frac{1}{8}(\alpha^2 + \beta^2)^2 + O5th$$
(2.66)

$$\epsilon_\theta = \epsilon_2 + \frac{1}{2}(\gamma^2 + \delta^2) - \frac{1}{2}\epsilon_2(\gamma^2 + \delta^2) + \frac{1}{2}\epsilon_2^2(\gamma^2 + \delta^2) - \frac{1}{8}(\gamma^2 + \delta^2)^2 + O5th$$

$$\epsilon_{\theta\phi} = \frac{1}{2}[(\alpha + \gamma) + (\beta\delta - \epsilon_2\gamma - \epsilon_1\alpha) - \frac{1}{2}(\alpha + \gamma)(\alpha^2 + \beta^2 + \gamma^2 + \delta^2)$$

$$+ \frac{1}{6}(\alpha + \gamma)^3 + \gamma\epsilon_2^2 + \alpha\epsilon_1^2 - \beta\delta(\epsilon_1 + \epsilon_2) - \epsilon_2^3\gamma - \epsilon_1^3\alpha$$

$$+ (\alpha^2 + \beta^2)(\frac{1}{2}\epsilon_2\gamma + \frac{3}{2}\epsilon_1\alpha + \epsilon_1\gamma) + (\gamma^2 + \delta^2)(\frac{1}{2}\epsilon_1\alpha + \frac{3}{2}\epsilon_2\gamma + \epsilon_2\alpha)$$

$$+ \frac{1}{2}(\alpha + \gamma)^2(\beta\delta - \epsilon_2\gamma - \epsilon_1\alpha) + O5th]$$

$$\chi_\phi = \frac{1}{a} \left[\beta - \beta\epsilon_1 - \beta\epsilon_1 - \alpha\delta - \frac{1}{2}(\alpha + \gamma)^2 - \frac{1}{2}\alpha^2 - \frac{1}{2}\delta^2 + O3rd \right]$$

$$\chi_\theta = \frac{1}{a} \left[\delta/\sin \phi + \beta \cot \phi - (\delta\epsilon_2 + \delta\epsilon_2 + \gamma\beta) / \sin \phi - \frac{1}{2}\beta^2 \right.$$

$$\left. - \frac{1}{2}\gamma^2 - \frac{1}{2}(\alpha + \gamma)^2 - (\beta\epsilon_1 + \alpha\delta + \gamma\delta) \cot \phi + O3rd \right]$$

(2.66 contd.)

$$\begin{aligned} \chi_{\theta\phi} = & \frac{1}{2a} [\dot{\delta} + \dot{\beta} / \sin \phi - \delta \cot \phi - \dot{\delta} \epsilon_2 - \dot{\delta} \epsilon_2 - \dot{\gamma} \beta - \dot{\gamma} \beta - \alpha \dot{\beta} + \delta \dot{\beta} \\ & - (\dot{\beta} \epsilon_1 + \dot{\beta} \epsilon_1 + \dot{\alpha} \delta + \alpha \dot{\delta}) / \sin \phi + (\delta \epsilon_2 + \gamma \beta) \cot \phi \\ & - \epsilon_2 (\dot{\beta} / \sin \phi - \delta \cot \phi - \gamma) - \gamma (\dot{\delta} / \sin \phi + \beta \cot \phi) \\ & - \epsilon_1 (\dot{\delta} - \alpha) + O3rd] \end{aligned}$$

and from equation (2.55)

$$\epsilon_1 = \frac{1}{a} (\dot{u} + \dot{w}) \quad , \quad \epsilon_2 = \frac{1}{a} (\dot{w} + u \cot \phi + \dot{v} / \sin \phi) \quad (2.67)$$

$$\alpha = \frac{1}{a} \dot{v} \quad , \quad \beta = \frac{1}{a} (u - \dot{w})$$

$$\gamma = \frac{1}{a} (\dot{u} / \sin \phi - v \cot \phi) \quad , \quad \delta = \frac{1}{a} (v - \dot{w} / \sin \phi)$$

The strain energy, U of the shell may now be expressed by equations (2.63) or (2.64) in terms of the displacements of the middle surface (u,v,w) with the aid of (2.66) and (2.67).

Within the limitations of the two Kirchhoff assumptions the expressions for the strain energy above contain all the terms in the displacements up to and including the fifth order terms in the membrane energy, and up to and including the cubic terms in the bending energy.

2.4 THE LOAD POTENTIAL ENERGY FOR SPHERICAL SHELLS

When the external loads are normal to the middle surface of the shell, the change in the load potential energy (J_L) due to the deformation of the shell is given by,

$$J_L = \iint P(\theta, \phi) \Delta V(\theta, \phi) d\theta d\phi \quad (2.68)$$

Where $P(\theta, \phi)$ is the load density and $\Delta V(\theta, \phi)$ is the elemental change in volume, and integration is over the entire middle surface of the shell. The volume enclosed by a deformed spherical surface is given by,

$$V = \iint \frac{1}{2} R_\theta XY d\theta d\phi$$

R_θ , X , and Y are defined in Figure 2.5, and given below, in which u, v, w are the middle surface displacements nondimensionalised by the radius (a).

$$R_\theta = a(1 + w + u \cot \phi) \sin \phi$$

$$X = R_\theta d\phi + au \sin \phi d\phi - aw \cos \phi d\phi$$

$$Y = R_\theta d\theta + av d\theta$$

For uniform external pressure loading, P is independent of θ and ϕ and the load potential energy may be written in the following form.

$$J_L = -P \iint \Delta V a^2 \sin \phi d\theta d\phi \quad (2.69)$$

with ΔV given by

$$\begin{aligned} \Delta V = \frac{1}{2} [& 3(w + u \cot \phi) + \dot{v}/\sin \phi + \dot{u} - \dot{w} \cot \phi \\ & + 3(w + u \cot \phi)^2 + (\dot{u} - \dot{w} \cot \phi) \dot{v}/\sin \phi \\ & + 2(w + u \cot \phi) (\dot{v}/\sin \phi + \dot{u} - \dot{w} \cot \phi) \\ & + (w + u \cot \phi)^3 + (w + u \cot \phi)^2 (\dot{v}/\sin \phi + \dot{u} - \dot{w} \cot \phi) \\ & + (w + u \cot \phi) (\dot{u} - \dot{w} \cot \phi) \dot{v}/\sin \phi] a \sin^2 \phi \end{aligned}$$

2.5 THE EQUILIBRIUM EQUATIONS FOR THIN SPHERICAL SHELLS

The total potential energy V of the system is given by the sum of strain energy U , equation (2.63), and the load potential energy J_L , equation (2.69).

$$V = U + J_L \quad (2.70)$$

By substitution from (2.55) and (2.56) we may write the total potential energy in the following form.

$$V = \iint F(P, \theta, \phi, u, v, w, \dot{u}, \dot{v}, \dot{w}, \ddot{u}, \ddot{v}, \ddot{w}, \dot{\dot{u}}, \dot{\dot{v}}, \dot{\dot{w}}) d\theta d\phi \quad (2.71)$$

Where θ and ϕ are independent variables and u , v , and w are continuously differentiable functions of θ , ϕ to be determined, and the integration is carried out over the two dimensional middle surface of the shell. X

For the system to be in a state of equilibrium it is necessary that the total potential energy be stationary with respect to any small kinematically admissible displacement function. For the equilibrium state to be stable the total potential energy must not only be stationary but must also be a complete relative minimum with respect to any small kinematically admissible displacements.

The calculus of variations, References [7] and [4], may be used to provide the necessary and sufficient conditions for equilibrium and stability. ✓

By expanding the total potential energy as a Taylor series

$$V = \bar{V} + \Delta V \quad (2.72)$$

$$\Delta V = \epsilon \delta V + \frac{1}{2!} \epsilon^2 \delta^2 V + \frac{1}{3!} \epsilon^3 \delta^3 V + \dots$$

where δV , $\delta^2 V$, $\delta^3 V$ are the first, second and third variations of V , the necessary condition for equilibrium is given by,

$$\delta V = 0 \quad (2.73)$$

Stability of the equilibrium state requires that,

$$\Delta V = \frac{1}{2!} \epsilon^2 \delta^2 V + \frac{1}{3!} \epsilon^3 \delta^3 V + \dots > 0 \quad (2.74)$$

and stability will depend upon the sign of the second variation, $\delta^2 V$. If the second variation is also zero then stability will depend on the third, fourth, etc. variations of the total potential energy.

For a uniform pressure loading P , independent of θ and ϕ , the necessary or stationary condition ($\delta V=0$) is given by the Euler equations as follows.

$$E_1 = 0; \quad \frac{d}{d\phi} \left(\frac{\partial F}{\partial \dot{u}} \right) + \frac{d}{d\theta} \left(\frac{\partial F}{\partial \dot{u}} \right) - \frac{\partial F}{\partial u} = 0 \quad (2.75)$$

$$E_2 = 0; \quad \frac{d}{d\phi} \left(\frac{\partial F}{\partial \dot{v}} \right) + \frac{d}{d\theta} \left(\frac{\partial F}{\partial \dot{v}} \right) - \frac{\partial F}{\partial v} = 0$$

$$E_3 = 0; \quad \frac{d^2}{d\phi^2} \left(\frac{\partial F}{\partial \dot{w}} \right) + \frac{d^2}{d\theta d\phi} \left(\frac{\partial F}{\partial \dot{w}} \right) + \frac{d^2}{d\theta^2} \left(\frac{\partial F}{\partial \dot{w}} \right) - \frac{d}{d\phi} \left(\frac{\partial F}{\partial \dot{w}} \right) - \frac{d}{d\theta} \left(\frac{\partial F}{\partial \dot{w}} \right) + \frac{\partial F}{\partial w} = 0$$

The Euler equations (2.75) are used in Chapter Four to derive the equilibrium equations for both the fundamental and secondary paths.

2.6 BOUNDARY CONDITIONS FOR INCOMPLETE CLAMPED SPHERES

The presentation of the boundary conditions in this Chapter anticipates the exact circumferential modelling of the shell equations introduced by equation (4.40) in Chapter Four.

In general five boundary conditions (four for the axisymmetric case as $v = 0$) are required at that pole ($\phi=0,\pi$) and at the edges of the spherical cap in order that the displacements are uniquely defined and continuous over the shell, see Section 2.2.3. At the pole the shell is continuous and the five boundary conditions required may be derived by considering symmetry and anti-symmetry. While at the edge of the shell the fifth supplementary boundary condition has been derived by requiring that the first of the Euler equations $E_1 = 0$, equation (2.75), is satisfied at the boundary.

2.6.1 Boundary Conditions at the Pole

The equilibrium equations become singular at the poles ($\phi=0,\pi$) and have been replaced by the following sets of boundary conditions,

$$i = 0 \quad u = \ddot{u} = 0 \quad (2.76)$$

$$(v \equiv 0)$$

$$\dot{w} = \dddot{w} = 0$$

$$i = 1, 3, 5, \dots \quad u = \dot{u} = 0$$

$$v = 0$$

$$w = \ddot{w} = 0$$

$$i = 2, 4, 6, \dots \quad u = \ddot{u} = 0$$

$$v = 0$$

$$w = \dot{w} = 0$$

2.6.2 Boundary Conditions for Clamped Incomplete Spheres (Caps)

The 'natural' boundary conditions of the variational calculus, Reference [7], correspond to boundaries at which no work is done. Either the edge deflections and/or rotations are prescribed, or the corresponding edge forces and/or moments are zero.

If work is done at the boundary supports, the supports yield, then the appropriate energy components expressed in terms of boundary integrals must be included in the total potential energy of the system.

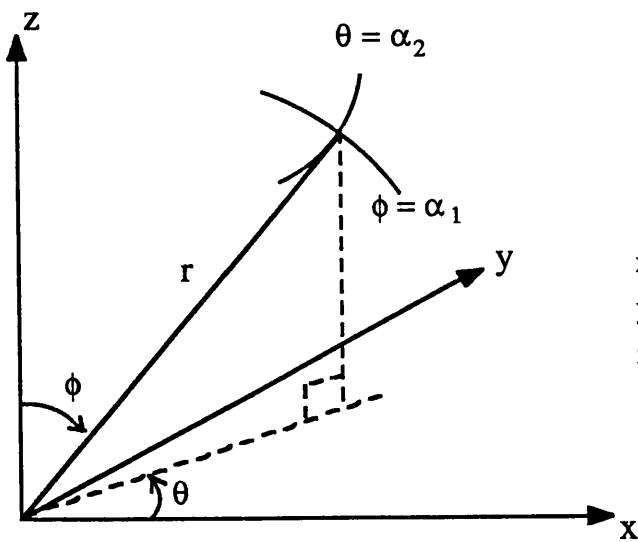
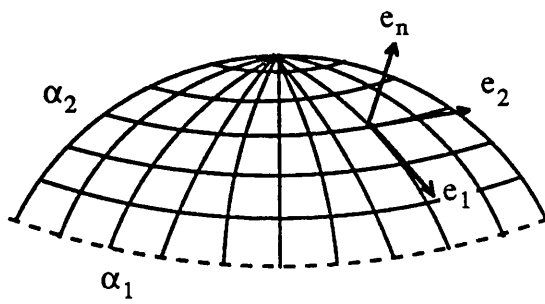
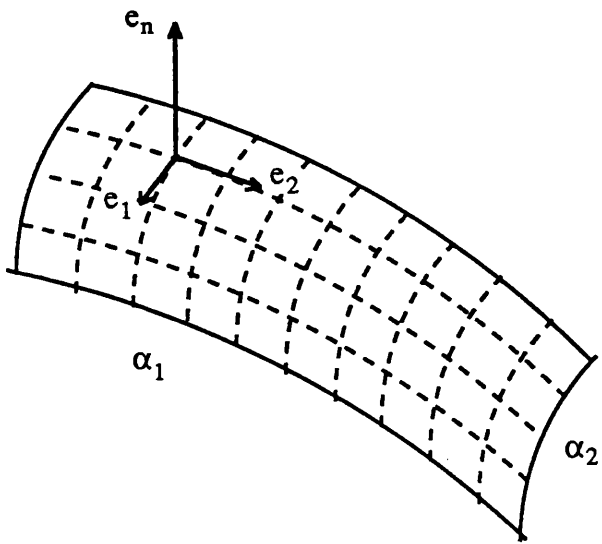
For a clamped edge at $\phi=\phi_b$ the following boundary conditions will be used for all circumferential modes ($i=0, 1, 2, \dots$)

$$u = 0, \quad (\dot{u} \cot \phi_b + \ddot{u})(1 + \alpha) + (\dot{w} \cot \phi_b + \ddot{w})\alpha = 0 \quad (2.77)$$

$$v = 0$$

$$w = \dot{w} = 0$$

The second supplementary condition for u has been derived by requiring that the first Euler equation $E_1 = 0$, equation (2.75) is satisfied at the boundary.



$$\begin{aligned} x &= r \cos \theta \sin \phi \\ y &= r \sin \theta \sin \phi \\ z &= r \cos \phi \end{aligned}$$

Figure 2.1 Shell Geometry

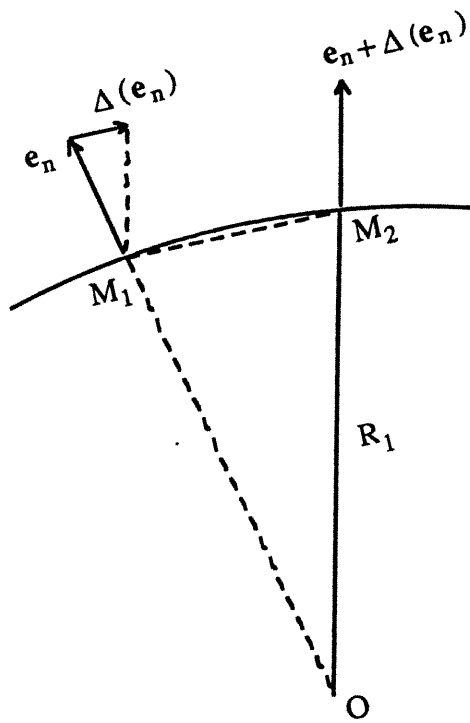


Figure 2.2 Differentiation of a unit vector.

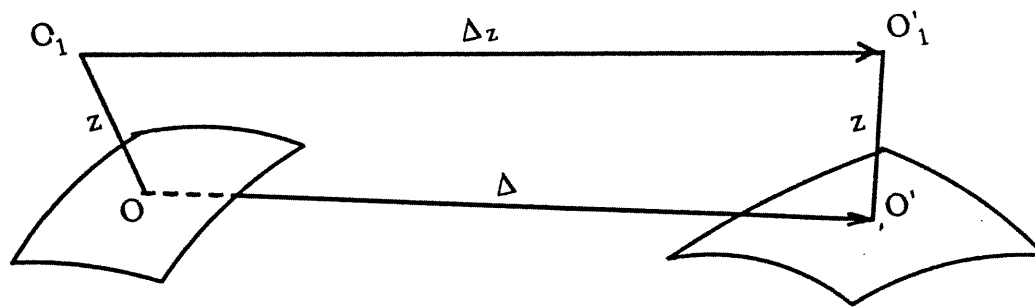


Figure 2.3 Deformations of the Shell.

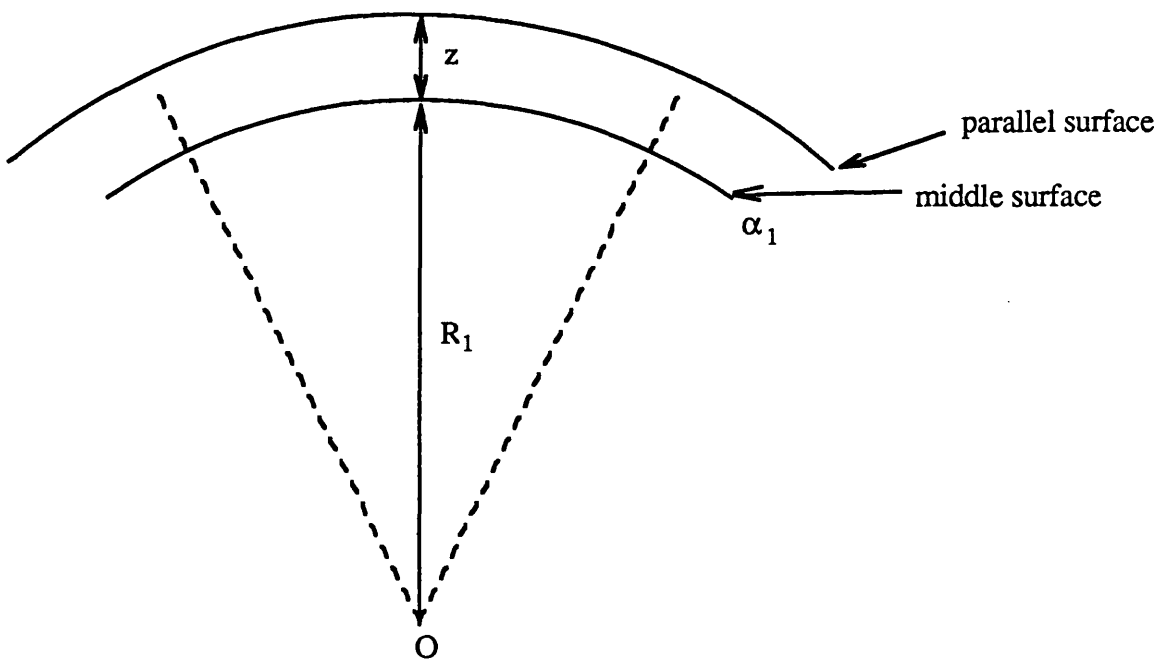


Figure 2.4 Parallel Surface.

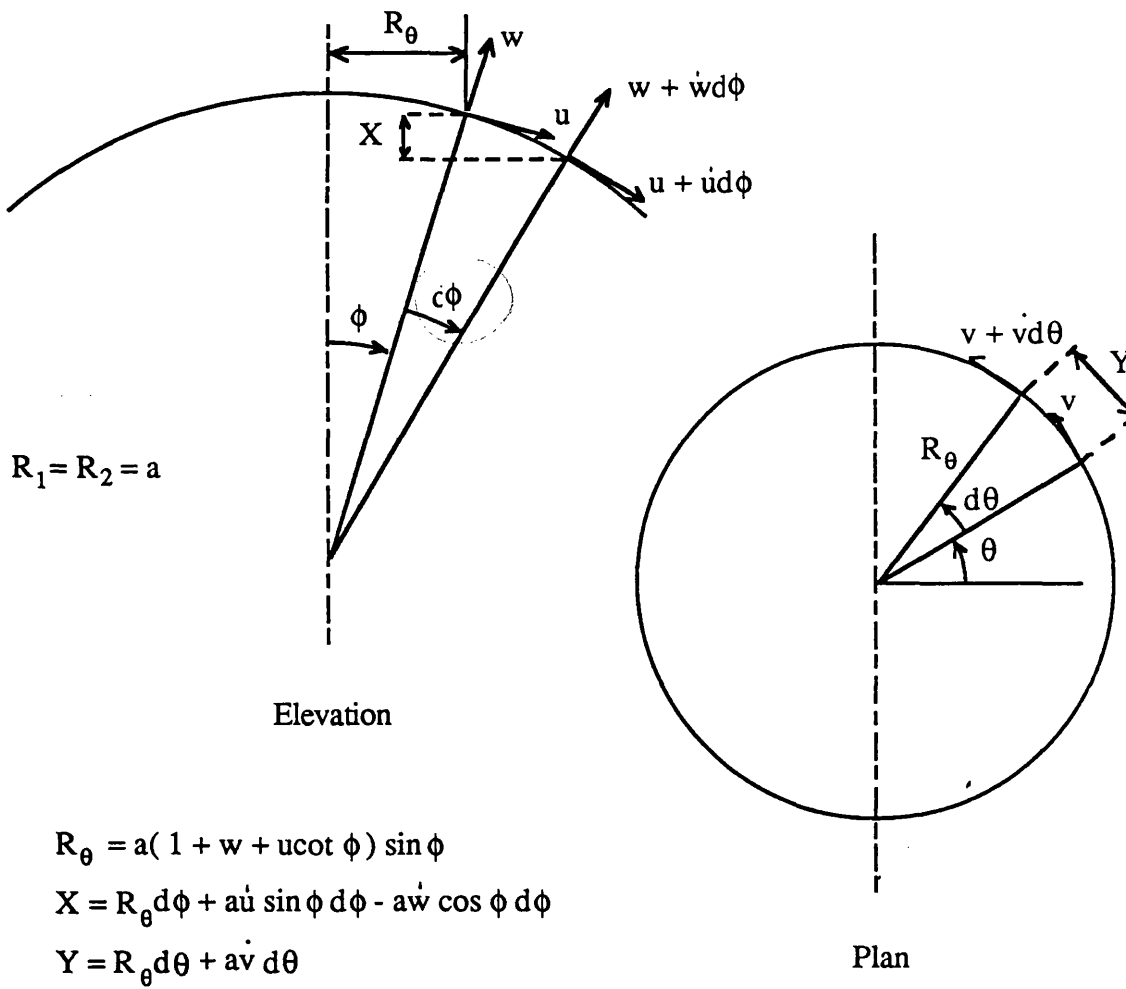


Figure 2.5 Volume of a Deformed Sphere

CHAPTER THREE

CLASSICAL AND AXISYMMETRIC POSTBUCKLING ANALYSIS OF COMPLETE SPHERICAL SHELLS

CHAPTER THREE

CONTENTS

3.1 INTRODUCTION

3.2 AXISYMMETRIC BUCKLING ANALYSIS OF COMPLETE SPHERICAL SHELLS

3.3 AXISYMMETRIC POSTBUCKLING ANALYSIS OF COMPLETE SPHERICAL SHELLS

CLASSICAL AND AXISYMMETRIC POSTBUCKLING ANALYSIS OF COMPLETE SPHERICAL SHELLS

3.1 INTRODUCTION

The first theoretical investigation of the elastic buckling of complete thin spherical shells under uniform pressure loading was undertaken by Zoelly in 1915. This method of analysis, and the lowest buckling or critical pressure that results, are frequently referred to as the classical analysis and the classical buckling or critical pressure of the perfect sphere. In the classical analysis of complete spherical shells buckling or bifurcation pressures are calculated from a linear eigenvalue problem, where the fundamental path consists of a pure radial contraction (membrane stresses) of the sphere, and the secondary or buckling mode is axisymmetric. This method of analysis has become a standard part of the analysis of complete spherical shells, see for example Timoshenko and Grere [8], Flugge [9] or Thompson and Hunt [3].

Although this method of analysis ignores buckling into nonaxisymmetric modes it has been claimed that, for the complete sphere, the eigenvalues associated with the nonaxisymmetric modes are coincident with the axisymmetric mode. This degeneracy being a consequence of the symmetry of the shell and loading. And that the nonaxisymmetric modes may be obtained by superposition of the axisymmetric modes with different orientations of the axes, while the number of possible modes increases with the radius to thickness ratio (r/t). A more detailed discussion of these coincident modes for the complete spherical shell is given by Hutchinson and Koiter [10], Thompson [11] and Silbiger [12].

Initial postbuckling analyses, for axisymmetric buckling of the complete spherical shell has been given by Koiter [13], Thompson [14], and Walker [15]. A multimode analysis which includes mode coupling between nonaxisymmetric and axisymmetric modes is also included in the work of Koiter [13]. In this work Koiter demonstrated that the range of validity of the axisymmetric postbuckling analysis tends to zero as the r/t ratio tends to infinity, as a result of mode coupling with the nonaxisymmetric periodic modes.

Although the classical analysis and the axisymmetric initial postbuckling analysis for complete spherical shells are limited by the considerations mentioned above, they are fundamental to the theoretical understanding of the elastic response of both complete and incomplete spherical shells, and are briefly reviewed below.

3.2 AXISYMMETRIC BUCKLING ANALYSIS OF COMPLETE SPHERICAL SHELLS

The notation used below for the axisymmetric buckling and the initial postbuckling analysis of complete spherical shells follows that used by Walker [15], the full derivation is contained in Appendix A, only the results of interest are presented below.

The axisymmetric strain displacement relations used in the classical analysis are given below, where the terms enclosed in the brackets, { }, are the terms derived in Chapter Two, that are required for consistency in the membrane and bending terms of the strain energy, these terms are neglected in the classical analysis.

$$\epsilon_{\phi} = \dot{u} + \dot{w} + \frac{1}{2}\dot{w}^2 + \{u^2 - 2uw - \frac{1}{2}(u+w)(u-w)^2\} \quad (3.1)$$

$$\epsilon_{\theta} = u \cot \phi + w$$

$$\chi_{\phi} = -\frac{1}{r}w'' + \left\{\frac{1}{r}\dot{u}\right\}$$

$$\chi_{\theta} = -\frac{1}{r}\dot{w} \cot \phi + \left\{\frac{1}{r}u \cot \phi\right\}$$

As a result of neglecting the terms in the brackets { } the expression for the strain energy, (A.2), is inconsistent in the quadratic terms of the bending energy, and the cubic and quartic terms of the membrane energy.

The load potential energy, (A.4) is given below, where similar linear, quadratic and cubic terms have been neglected from the complete expression given by equation (2.58).

$$J_L = -P2\pi r^3 \int_0^{\pi} w \sin \phi \, d\phi \quad (3.2)$$

As a result of using the above approximations, the fundamental path displacement is given by equation (A.6) as

$$w^f = \frac{Pr(1-\mu)}{2Et} \quad (3.3)$$

Where r is the radius of the shell, t is the thickness, E the modulus of elasticity, μ is Poisson's ratio, and P is the uniform pressure load, and w^f is the non-dimensional (with respect to r) radial displacement.

The classical critical pressure is then given by equation (A.15c) and (A.6) as

$$P_{ci} = \frac{2E}{\sqrt{3(1-\mu^2)}} \left(\frac{t^2}{r^2} \right) \quad (3.4)$$

The uniform radial contraction, W^f , at the classical critical pressure is given by,

$$\frac{W^f}{t} \Big|_{P = P_{ci}} = \frac{(1-\mu)}{\sqrt{3(1-\mu^2)}} \quad (3.5)$$

and for $\mu=0.3$ the radial membrane contraction at the classical buckling pressure is 42.4% of the shell thickness.

The critical, buckling mode is given by the Legendre polynomial of order N , where N is given by (A.15b) as

$$N(N+1) \approx \sqrt{12(1-\mu^2)} \frac{r}{t} \quad (3.6)$$

and for large values of N , $N \approx \sqrt[4]{12(1-\mu^2)} \sqrt{\frac{r}{t}}$, and for $\mu = 0.3$ then $N \approx 1.8 \sqrt{\frac{r}{t}}$.

The results of the classical buckling analysis for complete spherical shells described above are presented in the upper set of curves on Figure 3.1. The individual contributions to the quadratic term of the total potential energy, equation (A.9), that arise from the membrane and bending action of the shell, and the potential energy of the load are given by equation (A.36) of Appendix A. The axisymmetric nature of the buckling displacements in the classical analysis implies that these incremental displacements will develop circumferential bands of tension and compression. For the classical buckling of thin shells, equations (3.4) and (3.6), approximately 50% of the quadratic, buckling, strain energy of the shell is stored as circumferential membrane energy, with approximately the other 50% stored as meridional bending energy.

For buckling wavelengths that are longer than the classical critical wavelength, lower values of N , more than 50% of the incremental buckling strain energy of the shell is stored as circumferential membrane energy. The ability of the shell to develop circumferential bands of membrane compression will be sensitive to the presence of imperfections, therefore the effect of a reduction in the circumferential membrane stiffness on the buckling load will be of interest. The lower set of curves, on Figure 3.1, show the effect of performing the analysis described above with the circumferential membrane energy, $U_{2M\theta}$, set to zero. When the circumferential membrane energy is completely eliminated from the classical analysis the buckling wavelength increases and the buckling load reduces. For a shell with a r/t of 700 the buckling wavelength doubles by comparison to the classical wavelength, N reduces from 48 to 24, and the buckling load is reduced to approximately 20% of the classical value.

3.3 AXISYMMETRIC POSTBUCKLING ANALYSIS OF COMPLETE SPHERICAL SHELLS

The postbuckling path has been obtained by solving for the coefficients of a perturbation expansion about the critical, classical, bifurcation point, this is described in Appendix A. The perturbation series for the postbuckling path, equation (A.14), will contain cubic terms, as the expression for the total potential energy, equations (A.7) and (A.8), contained quartic terms

The postbuckling paths resulting from this analysis have been plotted in Figures 3.2 to 3.6 for values of the geometric slenderness parameter, λ , of between 12 and 70, where λ is defined as,

$$\lambda = \sqrt[4]{12(1 - \mu^2)} \sqrt{\frac{r}{t}} \alpha \quad (3.7)$$

in which α is the half angle of the spherical shell, for complete spheres $\alpha = \pi$.

For complete spheres the thin shell assumptions are not valid for values of λ less than about 26, corresponding to a r/t ratio of 20.7, however postbuckling paths have been calculated for λ values less than 26 as they may be representative of the behaviour exhibited by spherical caps, incomplete spherical shells, with equivalent λ values but larger radius to thickness ratios.

Figure 3.7 shows the effect of truncating the perturbation series after the linear, quadratic and cubic terms, for a spherical shell with a slenderness, λ , of 70.

Two points that arise from the classical buckling and postbuckling analysis of complete perfect spherical shells are of particular interest to the nonlinear elastic analysis of spherical caps. Firstly, the total prebuckling displacement, the fundamental path uniform radial contraction of the sphere, is approximately 42% of the shell thickness, equation (3.5), and the load carrying capacity of the shell on the postbuckling paths, Figure 3.2 to Figure 3.6, fall rapidly for small amplitudes of the incremental displacements. In most cases the load carrying capacity of the shell drops to zero for postbuckling displacements with an amplitude of about 20% of the thickness of the shell. Secondly, despite the relatively small amplitude of the displacements, it is at least necessary to model the postbuckling path using a cubic expression, that is the total potential energy must contain at least quartic terms.

The postbuckling behaviour of the complete perfect spherical shell will influence the response of imperfect complete spherical shells or incomplete spherical caps. Therefore, and as the results of the classical analyses described above indicate, it is expected that the nonlinear axisymmetric fundamental path analysis of incomplete spherical caps will require at least cubic terms to be included in the equilibrium equations, that is quartic terms in the expression for the total potential energy.

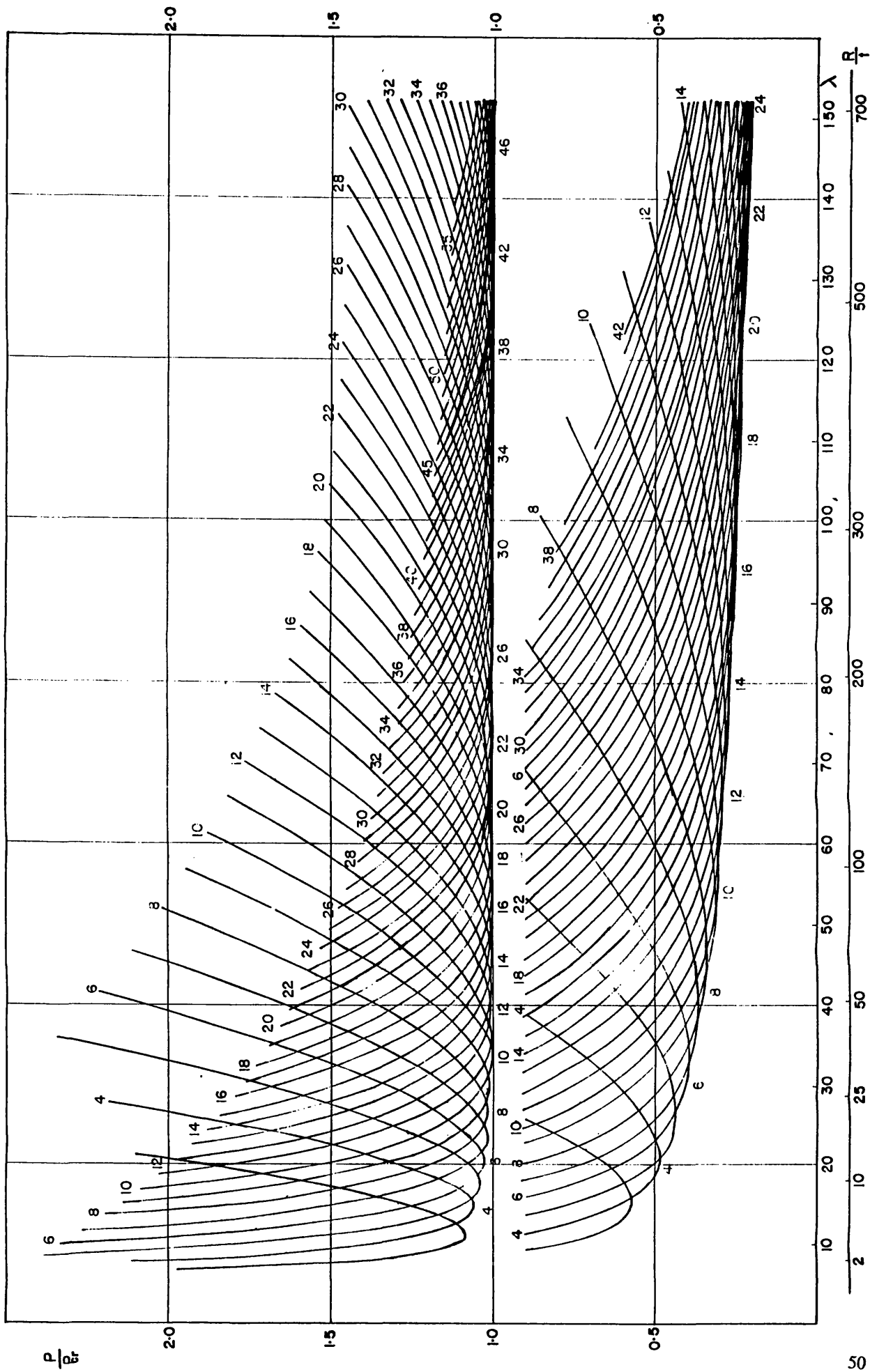


Figure 3.1 Classical Buckling Analysis of Perfect Complete Spherical Shells - upper set of curves, with $U_{2M_0}=0$ - lower set of curves. The order of the Legendre polynomial is indicated.

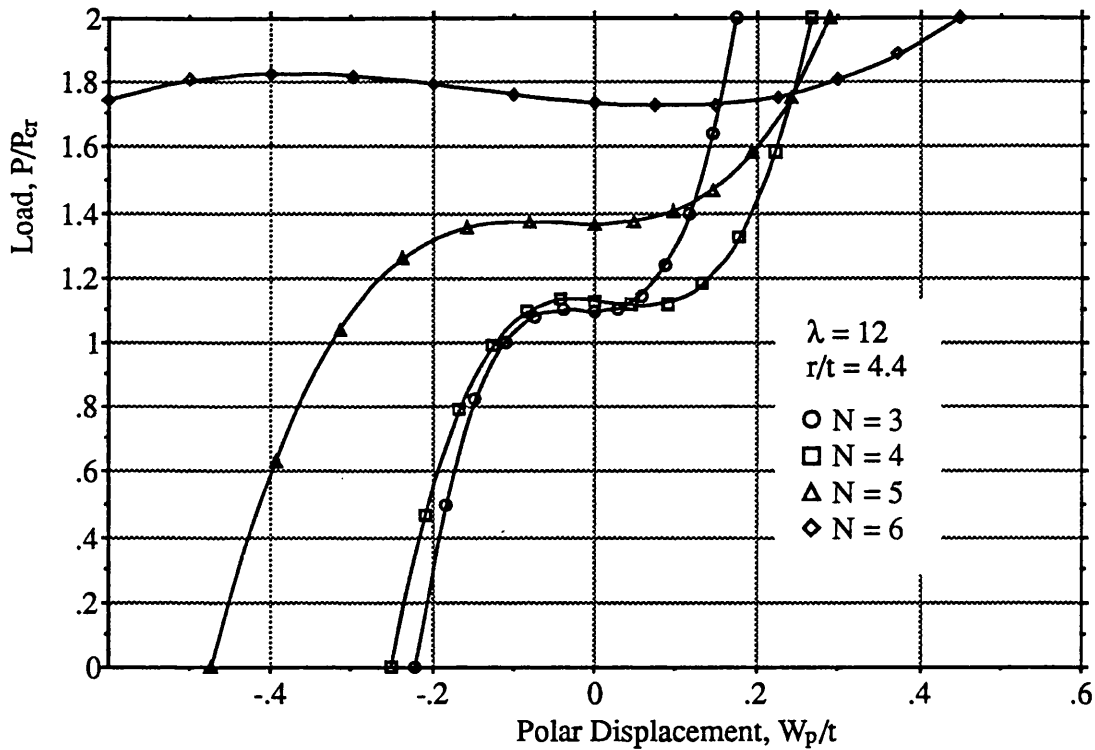


Figure 3.2 Post Buckling Paths for Complete Spherical Shells, $\lambda = 12$, N is the Order of the Legendre Polynomial of the Buckling mode.

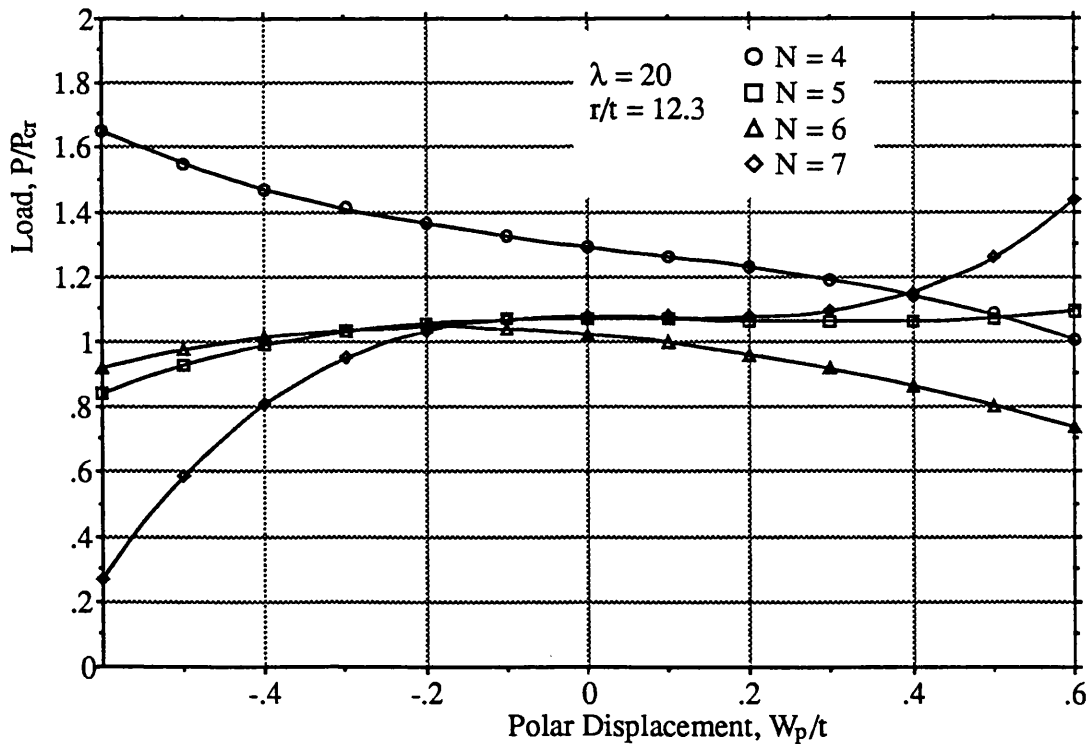


Figure 3.3 Post Buckling Paths for Complete Spherical Shells, $\lambda = 20$, N is the Order of the Legendre Polynomial of the Buckling mode.

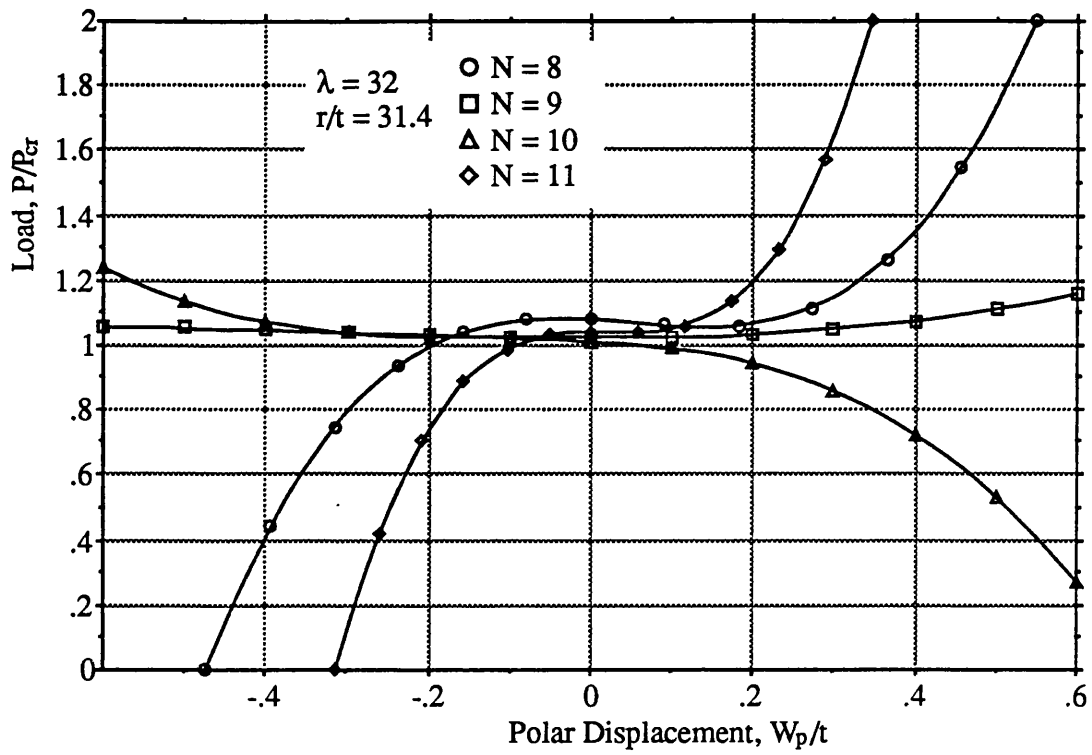


Figure 3.4 Post Buckling Paths for Complete Spherical Shells, $\lambda = 32$, N is the Order of the Legendre Polynomial of the Buckling mode.

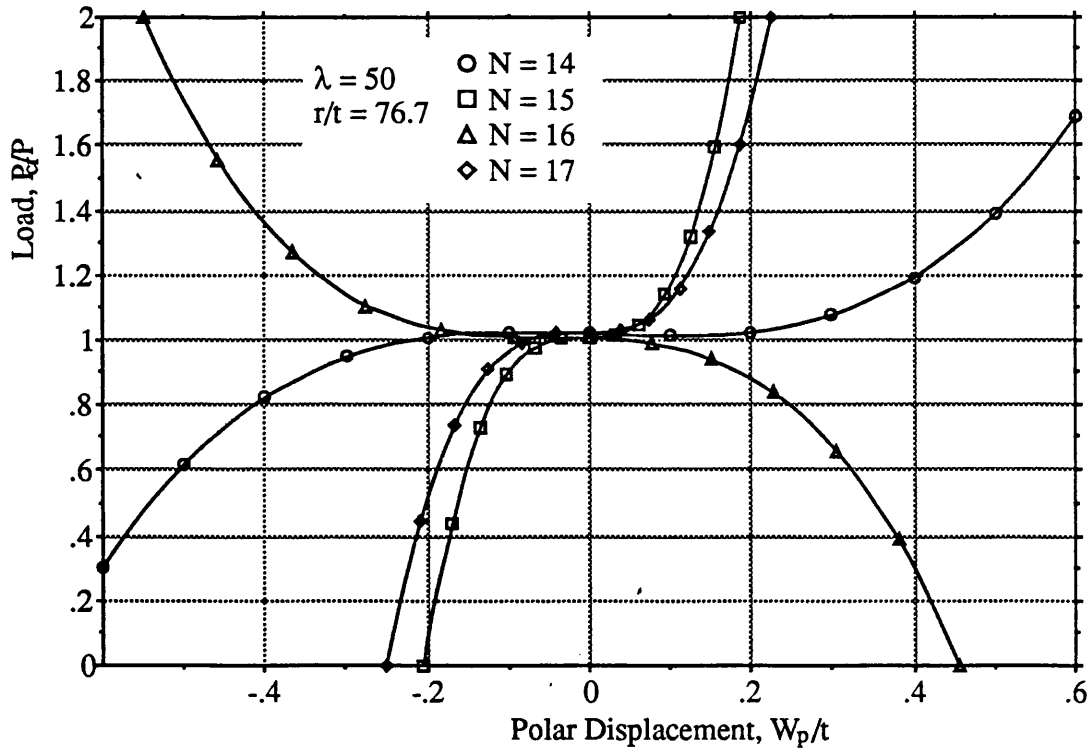


Figure 3.5 Post Buckling Paths for Complete Spherical Shells, $\lambda = 50$, N is the Order of the Legendre Polynomial of the Buckling mode.

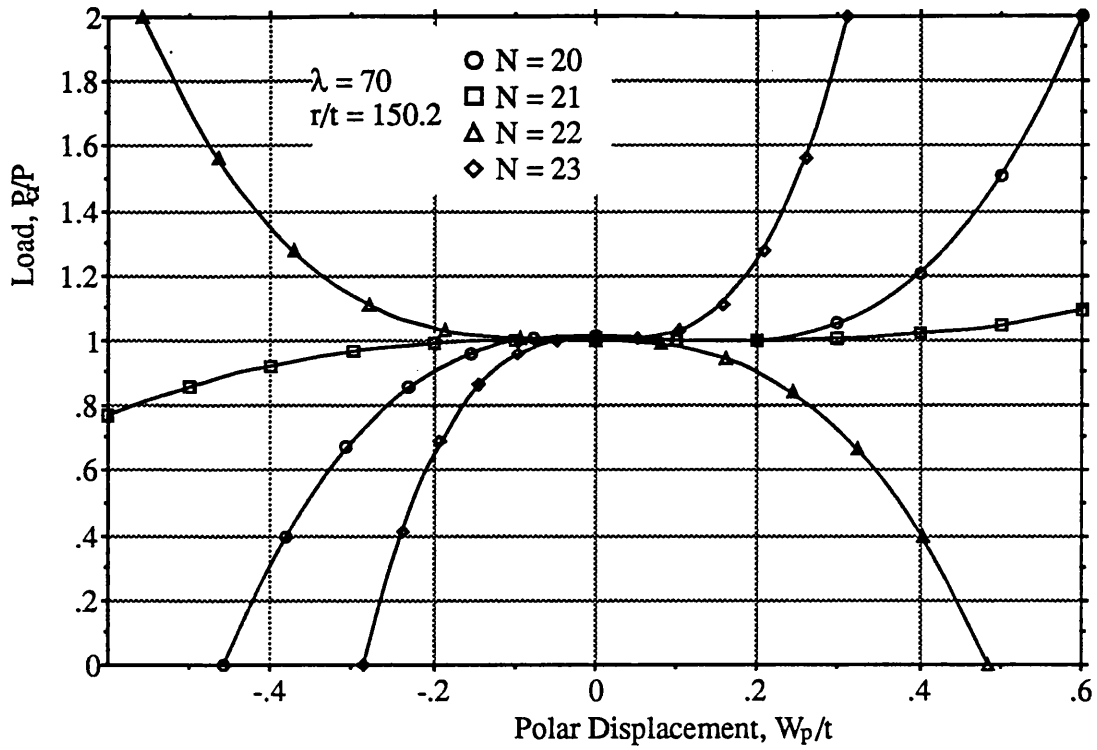


Figure 3.6 Post Buckling Paths for Complete Spherical Shells, $\lambda = 70$, N is the Order of the Legendre Polynomial of the Buckling mode.

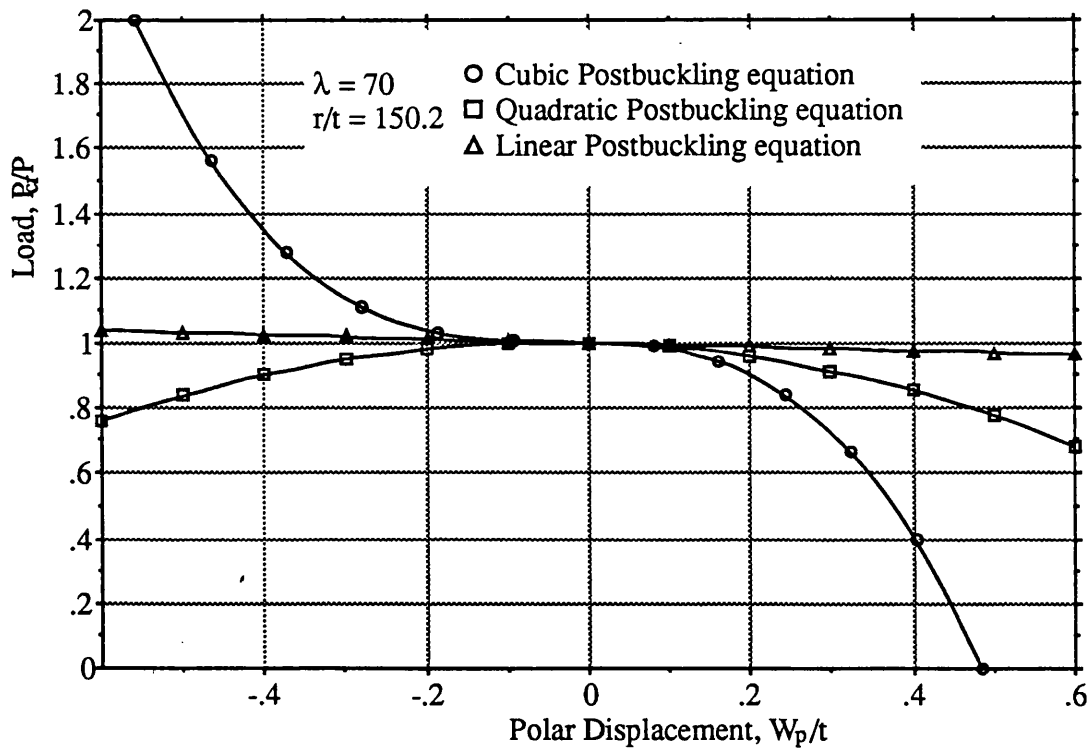


Figure 3.7 Comparisons of Cubic, Quadratic and Linear Post Buckling Paths for a Complete Spherical Shell, $\lambda = 70$.

CHAPTER FOUR

GENERAL SOLUTION METHODS FOR THE NONLINEAR FUNDAMENTAL PATH AND THE LINEARISED SECONDARY PATH

CHAPTER FOUR

CONTENTS

- 4.1 INTRODUCTION
- 4.2 THE NONLINEAR TOTAL POTENTIAL ENERGY FUNCTIONAL
 - 4.2.1 Displacement Notation
 - 4.2.2 Non-linear Strain Displacement Relations
 - 4.2.3 Stress Resultants and Strain Energy
 - 4.2.4 Load Potential Energy
 - 4.2.5 The Total Potential Energy Functional
- 4.3 THE FUNDAMENTAL PATH EQUILIBRIUM EQUATION
- 4.4 THE FUNDAMENTAL PATH PERTURBATION METHOD
- 4.5 THE SECONDARY PATH EQUATION
- 4.6 THE CIRCUMFERENTIAL MODELLING OF DISPLACEMENTS
- 4.7 THE ENERGY COMPONENTS OF THE FUNDAMENTAL AND SECONDARY PATHS
 - 4.7.1. Energy Components of the Fundamental Path (V_0)
 - 4.7.2. Incremental Linear Energy Components (V_1)
 - 4.7.3. Incremental Quadratic Energy Components (V_2)

GENERAL SOLUTION METHODS FOR THE NONLINEAR FUNDAMENTAL PATH AND THE LINEARISED SECONDARY PATH

4.1 INTRODUCTION

General solution methods are presented in this Chapter for the nonlinear axisymmetric fundamental path, and the nonlinear eigenvalue problem that yields the location of the points of secondary path bifurcation and the initial mode shapes of the secondary paths at the points of bifurcation of the secondary paths from the nonlinear fundamental path. The nonlinear equilibrium equations of the shell will be formulated in such a way that they lend themselves to a solution procedure based on a finite difference discretization. Numerical solution algorithms, based on finite difference approximations of the partial derivatives that occur in the differential equations of this Chapter, are contained in Chapter Five.

Solution methods developed in this Chapter assume an axisymmetric fundamental path that may contain axisymmetric initial imperfections of a general nature. At zero pressure the initial displacement field and/or stress field will be axisymmetric or zero, and at low pressures the displacements of the shell will remain axisymmetric. As the pressure increases and deformations grow, so periodic components of the deformations may grow.

The fundamental equilibrium path (ρ_1) may be represented by the curve O'ABCD in Figure 4.1. At the maximum pressure, P_{bk} , the path would become unstable and the shell would snap buckle to some distant equilibrium state. A general power, or perturbation, series solution method capable of evaluating any nonlinear fundamental path is developed in Section 4.4 of this Chapter.

Secondary equilibrium paths (ρ_2), with displacements that are periodic in the circumferential direction, may intersect the fundamental path at any point along its length, before or after the buckling point B. Secondary path solutions will consist of solving the nonlinear eigenvalue problem that yields the critical pressure, P_{cr} , and the initial mode shape associated with the secondary path at the point of bifurcation, point A in Figure 4.1.

Figure 4.2 provides a key to the methods and equations used in developing the fundamental and secondary path solutions. The total potential energy functional, Section 4.2, provides the common starting point for both the fundamental and secondary path analysis. Application of the stationary conditions, Sections 4.3 and 4.5, yield the nonlinear differential equations that govern equilibrium of the fundamental and secondary paths. A perturbation method is developed in Section 4.4 for solving the nonlinear fundamental path problem.

The linear terms of the secondary path equation, that is the terms of the secondary path that are linear in the incremental displacements x , give rise to a nonlinear eigenvalue/vector problem, equation (4.39) of Section 4.5. This eigenvalue problem is nonlinear in terms of the

fundamental path displacements and load. An 'efficient' strategy for solving the nonlinear eigenvalue problem is presented in Section 5.4 of Chapter Five.

A perturbation technique similar to that used for the solution of the nonlinear fundamental path could be used to obtain the nonlinear post bifurcation, or secondary, path solution if desired. This nonlinear secondary path perturbation problem is indicated in Figure 4.2 by the dotted box, and has not been attempted in the present work.

Exact circumferential modelling of the middle surface displacements is introduced in Section 4.6, making the derivatives contained in the equations presented in this Chapter functions of the meridional variable only. The energy components of the nonlinear fundamental path (the components of V_0 and V_1) and the quadratic components of the secondary path (the components of V_2) are given in Section 4.7.

Table 4.1 defines the terms of the nonlinear axisymmetric equilibrium equation for thin spherical shells under uniform pressure loading, i.e. the nonlinear axisymmetric fundamental path equation, equation (4.31). And Table 4.2 defines the terms of the linearised secondary path equilibrium equation, i.e. the nonlinear eigenvalue problem, equation (4.39).

4.2 THE NON-LINEAR TOTAL POTENTIAL ENERGY FUNCTIONAL

4.2.1 Displacement Notation

In the following notation the total displacements at the general point, (ϕ, θ) , on the middle surface of the spherical cap are written as,

$$u^T \equiv u^T(\phi, \theta)$$

$$v^T \equiv v^T(\phi, \theta)$$

$$w^T \equiv w^T(\phi, \theta)$$

and the uniform pressure, P , is independent of the coordinates ϕ and θ .

By introducing the standard sliding notation, extended to include the initial axisymmetric geometric imperfection, the total displacements (u^T, v^T, w^T) may be expressed as

$$u^T \equiv u^i + u^f + u \quad (4.1)$$

$$v^T \equiv v, \quad v^i \equiv v^f \equiv 0$$

$$w^T \equiv w^i + w^f + w$$

Where (u^i, w^i) are the axisymmetric initial geometric imperfections, and (u^f, w^f) are the axisymmetric fundamental path displacements, while (u, v, w) are the axisymmetric or periodic incremental displacements.

4.2.2 Non-linear strain displacement relations

Introducing the full nonlinear strain and the linear part of the curvature relations (2.66) and using x to denote the generalised displacements (u, v, w) with the superscript notation of (4.1) applying we have,

$$\begin{aligned} \epsilon_\phi^T = \epsilon_\phi(x^T) = & \epsilon_1^T + \frac{1}{2} \left\{ \left(\dot{v}^T \right)^2 + (\beta^T)^2 \right\} - \frac{1}{2} \epsilon_1^T \left\{ \left(\dot{v}^T \right)^2 + (\beta^T)^2 \right\} \\ & + \frac{1}{2} (\epsilon_1^T)^2 \left\{ \left(\dot{v}^T \right)^2 + (\beta^T)^2 \right\} - \frac{1}{8} \left\{ \left(\dot{v}^T \right)^2 + (\beta^T)^2 \right\}^2 + \dots \end{aligned} \quad (4.2)$$

$$\begin{aligned}\varepsilon_{\theta}^T &= \varepsilon_{\theta}(x^T) = \varepsilon_2^T + \frac{1}{2} \left\{ (\dot{\gamma}^T)^2 + (\dot{\delta}^T)^2 \right\} - \frac{1}{2} (\varepsilon_2^T) \left\{ (\dot{\gamma}^T)^2 + (\dot{\delta}^T)^2 \right\} \\ &\quad + \frac{1}{2} (\varepsilon_2^T)^2 \left\{ (\dot{\gamma}^T)^2 + (\dot{\delta}^T)^2 \right\} - \frac{1}{8} \left\{ (\dot{\gamma}^T)^2 + (\dot{\delta}^T)^2 \right\}^2 + \dots\end{aligned}$$

$$\begin{aligned}\varepsilon_{\theta\phi}^T &= \varepsilon_{\theta\phi}(x^T) = \frac{1}{2} \left[(\dot{v}^T + \dot{\gamma}^T) + (\beta^T \dot{\delta}^T - \varepsilon_1^T \dot{v}^T - \varepsilon_2^T \dot{\gamma}^T) \right. \\ &\quad \left. - \frac{1}{2} (\dot{v}^T + \dot{\gamma}^T) \left\{ (\dot{v}^T)^2 + (\dot{\gamma}^T)^2 + (\beta^T)^2 + (\dot{\delta}^T)^2 \right\} \right. \\ &\quad \left. + \frac{1}{6} (\dot{v}^T + \dot{\gamma}^T)^3 + \dot{\gamma}^T (\varepsilon_2^T)^2 + \dot{v}^T (\varepsilon_1^T)^2 \right. \\ &\quad \left. - \beta^T \dot{\gamma}^T (\varepsilon_1^T + \varepsilon_2^T) - (\varepsilon_2^T)^3 \dot{\gamma}^T - (\varepsilon_1^T)^3 \dot{v}^T \right. \\ &\quad \left. + \left\{ (\dot{v}^T)^2 + (\beta^T)^2 \right\} \left(\frac{1}{2} \varepsilon_2^T \dot{\gamma}^T + \frac{3}{2} \varepsilon_1^T \dot{v}^T + \varepsilon_1^T \dot{\gamma}^T \right) \right. \\ &\quad \left. + \left\{ (\dot{\gamma}^T)^2 + (\dot{\delta}^T)^2 \right\} \left(\frac{1}{2} \varepsilon_1^T \dot{v}^T + \frac{3}{2} \varepsilon_2^T \dot{\gamma}^T + \varepsilon_2^T \dot{\gamma}^T + \varepsilon_2^T \dot{v}^T \right) \right. \\ &\quad \left. + \frac{1}{2} (\dot{v}^T + \dot{\gamma}^T)^2 (\beta^T \dot{\delta}^T - \varepsilon_2^T \dot{\gamma}^T - \varepsilon_1^T \dot{v}^T) + \dots \right]\end{aligned}$$

$$\chi_{\phi}^T = \chi_{\phi}(x^T) = \frac{1}{a} \dot{\beta}^T + \dots$$

$$\chi_{\theta}^T = \chi_{\theta}(x^T) = \frac{1}{a} (\dot{\delta}^T / \sin \phi + \beta \cot \phi) + \dots$$

$$\chi_{\theta\phi}^T = \chi_{\theta\phi}(x^T) = \frac{1}{2a} (\dot{\delta}^T + \dot{\beta}^T / \sin \phi - \dot{\delta}^T \cot \phi) + \dots$$

with the linear components given by

$$\varepsilon_1^T = \varepsilon_1(x^T) = \dot{u}^T + \dot{w}^T \tag{4.3}$$

$$\varepsilon_2^T = \varepsilon_2(x^T) = \dot{w}^T + \dot{u}^T \cot \phi + \dot{v}^T / \sin \phi$$

$$\beta^T = \beta(x^T) = \dot{u}^T - \dot{w}^T$$

$$\gamma^T = \gamma(x^T) = \dot{u}^T / \sin \phi - \dot{v}^T \cot \phi$$

$$\delta^T = \delta(x^T) = \dot{v}^T - \dot{w}^T / \sin \phi$$

In equations (4.2) and (4.3) the sliding notation, introduced in (4.1), has been applied to the nonlinear strain and linear curvature expressions. As a consequence of the nonlinearity of the strain displacement relations, in general

$$\varepsilon_{\phi}^T \equiv \varepsilon_{\phi}(x^T = x^i + x^f + x) \neq \varepsilon_{\phi}(x^i) + \varepsilon_{\phi}(x^f) + \varepsilon_{\phi}(x) \equiv \varepsilon_{\phi}^i + \varepsilon_{\phi}^f + \varepsilon_{\phi} \tag{4.4}$$

where ε_{ϕ}^i , ε_{ϕ}^f , and ε_{ϕ} are given by the strain displacement relations, equation (4.2), operating upon x^i , x^f , and x respectively.

At the initial unloaded point O' in Figure 4.1 the displacements, x^i , are axisymmetric and the strains and curvatures are given by

$$\epsilon_{\phi}^i \equiv \epsilon_{\phi}(x^i) = \epsilon_1^i + \frac{1}{2}(\beta^i)^2 - \frac{1}{2}\epsilon_1^i (\beta^i)^2 + \frac{1}{2}(\epsilon_1^i)^2 (\beta^i)^2 - \frac{1}{8}(\beta^i)^4 + \dots \quad (4.5)$$

$$\epsilon_{\theta}^i \equiv \epsilon_{\theta}(x^i) = \epsilon_2^i$$

$$\epsilon_{\theta\phi}^i \equiv 0$$

$$\chi_{\phi}^i = \frac{1}{a}\beta^i$$

$$\chi_{\theta}^i = \frac{1}{a}\beta^i \cot \phi$$

$$\chi_{\theta\phi}^i \equiv 0$$

with the linear axisymmetric components given by

$$\epsilon_1^i \equiv \epsilon_1(x^i) = u^i + w^i \quad (4.6)$$

$$\epsilon_2^i \equiv \epsilon_2(x^i) = w^i + u^i \cot \phi$$

$$\beta^i \equiv \beta(x^i) = u^i - w^i$$

$$\gamma^i = \delta^i = v^i = 0$$

At any point along the axisymmetric fundamental path with displacements given by x^i+x^f , ($x \equiv 0$), the strains are given by the axisymmetric expressions (4.5) and (4.6) operating upon (x^i+x^f) . It should be noted that the change in meridional strain due to the fundamental path displacement x^f is given by $\epsilon_{\phi}(x^i+x^f) - \epsilon_{\phi}(x^i)$ and is not equal to $\epsilon_{\phi}(x^f)$.

However, as the circumferential strains and both meridional and circumferential curvatures are linear for axisymmetric displacements of the shell, the following relations hold

$$\epsilon_{\theta}(x^i+x^f) = \epsilon_{\theta}(x^i) + \epsilon_{\theta}(x^f) = \epsilon_2(x^i) + \epsilon_2(x^f) \quad (4.7)$$

$$\epsilon_{\theta\phi}(x^i+x^f) = 0$$

$$\chi_{\phi}(x^i+x^f) = \chi_{\phi}(x^i) + \chi_{\phi}(x^f) = \frac{1}{a}\beta(x^i) + \frac{1}{a}\beta(x^f)$$

$$\chi_{\theta}(x^i+x^f) = \chi_{\theta}(x^i) + \chi_{\theta}(x^f) = \frac{1}{a}\beta(x^i) \cot \phi + \frac{1}{a}\beta(x^f) \cot \phi$$

$$\chi_{\theta\phi}(x^i+x^f) = 0$$

and in this case ϵ_{θ}^f , χ_{ϕ}^f , χ_{θ}^f may be interpreted as the change in strains and curvatures due to the fundamental path displacements (x^f).

Similarly the secondary path periodic displacements (x) are responsible for changes in the strains and curvatures of the shell. If the displacements at the point A in Figure 4.1 are given by (x^i+x^f) , and the total displacements at a point on the secondary path ρ_2 are given by $x^T=x^i+x^f+x$, then the change in, say, the meridional strain from the initial unloaded state, O' in Figure 4.1, is given by $\epsilon_{\phi}(x^T=x^i+x^f+x) - \epsilon_{\phi}(x^i)$, which is not equal to $\epsilon_{\phi}(x^f+x)$. Similar inequalities are also true for the other non-linear strains ϵ_{θ} and $\epsilon_{\theta\phi}$.

Although the strain expressions (4.2) and (4.5) operating on the incremental periodic displacements (x) or the incremental fundamental displacement (x^f) respectively, are not in general equal to the corresponding incremental strains, they do provide a useful notation when expanding the total potential energy functional.

4.2.3 Stress Resultants and Strain Energy

The total membrane ($N_\phi^T, N_\theta^T, N_{\theta\phi}^T$) and bending ($M_\phi^T, M_\theta^T, M_{\theta\phi}^T$) stress resultants will be defined in terms of the corresponding strains by the use of equation (2.65), which is given below,

$$\begin{aligned}
 N_\phi^T &\equiv N_\phi(x^T) = \frac{Et}{1-\mu^2} (\epsilon_\phi^T + \mu\epsilon_\theta^T) & (4.8) \\
 N_\theta^T &\equiv N_\theta(x^T) = \frac{Et}{1-\mu^2} (\epsilon_\theta^T + \mu\epsilon_\phi^T) \\
 N_{\theta\phi}^T &\equiv N_{\theta\phi}(x^T) = \frac{Et}{1+\mu} \epsilon_{\theta\phi}^T \\
 M_\phi^T &\equiv M_\phi(x^T) = \frac{Et^3}{12(1-\mu^2)} (\chi_\phi^T + \mu\chi_\theta^T) \\
 M_\theta^T &\equiv M_\theta(x^T) = \frac{Et^3}{12(1-\mu^2)} (\chi_\theta^T + \mu\chi_\phi^T) \\
 M_{\theta\phi}^T &\equiv M_{\theta\phi}(x^T) = \frac{Et^3}{12(1+\mu)} \chi_{\theta\phi}^T
 \end{aligned}$$

in which the strains and curvatures are defined in equations (4.2) and (4.3), and the superscript notation of (4.1) applies.

If at the initial unloaded state O' in Figure 4.1 the displacements (x^i) are accompanied by strains and curvatures $\epsilon_\phi^i, \epsilon_\theta^i, \chi_\phi^i, \chi_\theta^i$, giving rise to stress resultants $N_\phi^i, N_\theta^i, M_\phi^i, M_\theta^i$, then the total membrane and bending stress resultants at the general point $x^T = x^i + x^f + x$ are given by (4.8), while the corresponding change in the strains (from the initial point O' to the general point x^T) are given by $(\epsilon_\phi^T - \epsilon_\phi^i), (\epsilon_\theta^T - \epsilon_\theta^i)$, etc.

However if the initial displacements (x^i) are unstressed (stress relieved), then due to the linearity between stresses and strains, (4.8), the stress resultants at the general point x^T are given by $N_\phi^T - N_\phi^i, N_\theta^T - N_\theta^i$ etc, where N_ϕ^i, N_θ^i , etc. are defined by (4.8) with the total strains $(\epsilon_\phi^T, \epsilon_\theta^T, \chi_\phi^T, \chi_\theta^T)$ replaced by the corresponding initial strains $(\epsilon_\phi^i, \epsilon_\theta^i, \chi_\phi^i, \chi_\theta^i)$.

It should be noted that the change in the strain, from the point O' to the general point x^T , remain the same, $(\epsilon_\phi^T - \epsilon_\phi^i)$, etc.) for stressed or stress free initial imperfection displacements (x^i).

If we wish to include axisymmetric residual stress fields ($N_\phi^R, N_\theta^R, M_\phi^R, M_\theta^R$) that may be independent of the initial displacements (x^i), then these residual stress resultants are simply added to the stress resultants N_ϕ^T , or $N_\phi^T - N_\phi^i$, etc. discussed above.

The membrane U_M and bending U_B strain energies, (2.64), are given by

$$U_M = \frac{1}{2} \int \int \left[\bar{N}_\phi (\epsilon_\phi^T - \epsilon_\phi^i) + \bar{N}_\theta (\epsilon_\theta^T - \epsilon_\theta^i) + 2\bar{N}_{\theta\phi} (\epsilon_{\theta\phi}^T - \epsilon_{\theta\phi}^i) \right] a^2 \sin \phi d\theta d\phi \quad (4.9)$$

$$U_B = \frac{1}{2} \int \int \left[\bar{M}_\phi (\chi_\phi^T - \chi_\phi^i) + \bar{M}_\theta (\chi_\theta^T - \chi_\theta^i) + 2\bar{M}_{\theta\phi} (\chi_{\theta\phi}^T - \chi_{\theta\phi}^i) \right] a^2 \sin \phi d\theta d\phi$$

where the integration is over the middle surface of the spherical cap.

In order that the strain energy is measured from a datum that corresponds to the unloaded initial state O' in Figure 4.1, the stress resultants are defined as

$$\begin{aligned} \bar{N}_\phi &= N_\phi^T - \langle N_\phi^i \rangle + N_\phi^R \\ \bar{N}_\theta &= N_\theta^T - \langle N_\theta^i \rangle + N_\theta^R \\ \bar{N}_{\theta\phi} &= N_{\theta\phi}^T \\ \bar{M}_\phi &= M_\phi^T - \langle M_\phi^i \rangle + M_\phi^R \\ \bar{M}_\theta &= M_\theta^T - \langle M_\theta^i \rangle + M_\theta^R \\ \bar{M}_{\theta\phi} &= M_{\theta\phi}^T \end{aligned} \quad (4.10)$$

where the following interpretations must be placed on the brackets $\langle \rangle$.

$$\begin{aligned} \langle N_\phi^i \rangle &= 0 \\ \langle N_\theta^i \rangle &= 0 && \text{for stressed initial imperfections} \\ \langle M_\phi^i \rangle &= 0 \\ \langle M_\theta^i \rangle &= 0 \\ \langle N_\phi^i \rangle &= N_\phi^i \\ \langle N_\theta^i \rangle &= N_\theta^i && \text{for stress - free initial imperfections} \\ \langle M_\phi^i \rangle &= M_\phi^i \\ \langle M_\theta^i \rangle &= M_\theta^i \end{aligned} \quad (4.11)$$

The introduction of the brackets, $\langle \rangle$, allows the derivation and solution of all axisymmetric imperfection types to be treated as a single case. It is only necessary to specify the initial imperfection displacements x^i , and whether they are stressed or stress free (the interpretation to be used for the brackets $\langle \rangle$), along with the initial residual stress resultants N_ϕ^R etc., when solving the resulting fundamental and secondary path equations.

4.2.4 Load Potential Energy

The load potential energy, J_L , for a uniform pressure load is given by

$$J_L = -\frac{P}{2} \iint 2[\Delta V(x^T) - \Delta V(x^i)] a^2 \sin \phi \, d\theta d\phi \quad (4.12)$$

Integration, over the middle surface of the shell, of the nonlinear change in volume $\Delta V(x^T)$ represents the difference in volume between the perfect spherical cap and the deformed shell with generalised displacements $x^T = x^i + x^f + x$, and $\Delta V(x^T)$ from equation (2.69), is given by

$$\begin{aligned} \Delta V^T \equiv \Delta V(x^T) = & \frac{1}{2} \{ 3(w^T + u^T \cot \phi) + \dot{v}^T / \sin \phi + \dot{u}^T - \dot{w}^T \cot \phi + 3(w^T + u^T \cot \phi)^2 \\ & + 2(w^T + u^T \cot \phi) \left(\dot{v}^T / \sin \phi + \dot{u}^T - \dot{w}^T \cot \phi \right) \\ & + \left(\dot{u}^T - \dot{w}^T \cot \phi \right) \dot{v}^T / \sin \phi + (w^T + u^T \cot \phi)^3 \\ & + (w^T + u^T \cot \phi)^2 \left(\dot{v}^T / \sin \phi + \dot{u}^T - \dot{w}^T \cot \phi \right) \\ & + (w^T + u^T \cot \phi) \left(\dot{u}^T - \dot{w}^T \cot \phi \right) \dot{v}^T / \sin \phi \} a \sin^2 \phi \end{aligned} \quad (4.13)$$

4.2.5 The Total Potential Energy Functional

The total potential energy, V , may be written as the sum of the strain energy and the load potential energy as

$$V = U_M + U_B + J_L \quad (4.14)$$

in which the membrane and bending strain energies (U_M , U_B) and the increase in the external load potential energy J_L for a uniformly loaded spherical shell are all measured from the initial unloaded state O' in Figure 4.1. Strain energies are given by equation (4.9) and may be written in terms of the generalised displacement by the use of equations (4.10), (4.8), (4.5), (4.6), (4.2), (4.3) and (4.1) with the notation of (4.11) defining the initial stress state, while the load potential energy is given by equation (4.12), and may be written in terms of the generalised displacements by using equation (4.13).

Expanding the total potential energy functional as a power series in the generalised incremental displacements (x), we have

$$V = V_0 + V_1 + V_2 + \dots \quad (4.15)$$

where V_0 is independent of the incremental displacement, (x), and V_1 and V_2 are linear and quadratic respectively in the incremental displacements (x).

Thus V_1 may be written as,

$$V_1 \equiv U_{1,M} + U_{1,B} + J_{1,L} \quad (4.16)$$

where the membrane ($U_{1,M}$), bending ($U_{1,B}$) and load potential ($J_{1,L}$) energies are given below

$$\begin{aligned} \frac{U_{1,M}}{Ka^2} = & \iint \left[\varepsilon_1 \left\{ (\varepsilon_\phi^s + \mu\varepsilon_\theta^s) \left(1 - \frac{1}{2}(\beta^s)^2 + \varepsilon_1^s (\beta^s)^2 + \dots \right) \right\} \right. \\ & + \beta \left\{ (\varepsilon_\phi^s + \mu\varepsilon_\theta^s) (\beta^s - \varepsilon_1^s \beta^s + (\varepsilon_1^s)^2 \beta^s - \frac{1}{2}(\beta^s)^3 + \dots) \right\} \\ & \left. + \varepsilon_2 \{ (\varepsilon_\theta^s + \mu\varepsilon_\phi^s) \} \right] \sin \phi \, d\theta d\phi \\ & - \frac{1}{2} \iint \left[\varepsilon_1 \left\{ Q_\phi^i \left(1 - \frac{1}{2}(\beta^s)^2 + \varepsilon_1^s (\beta^s)^2 + \dots \right) \right\} \right. \\ & + \beta \left\{ Q_\phi^i (\beta^s - \varepsilon_1^s \beta^s + (\varepsilon_1^s)^2 \beta^s - \frac{1}{2}(\beta^s)^3 + \dots) \right\} \\ & \left. + \varepsilon_2 \{ Q_\theta^i \} \right] \sin \phi \, d\theta d\phi \end{aligned} \quad (4.17)$$

$$\begin{aligned} \frac{U_{1,B}}{Ka^2} = & \alpha \iint \left[\left[\beta \left\{ \dot{\beta}^s + \mu\dot{\beta}^s \cot \phi \right\} + \beta \left\{ \dot{\beta}^s \cot \phi + \mu\dot{\beta}^s \right\} \cot \phi \right] \sin \phi \, d\theta d\phi \right. \\ & - \frac{\alpha}{2} \iint \left[\left[\beta \left\{ \dot{\beta}^i + \mu\dot{\beta}^i \cot \phi \right\} + \beta \left\{ \dot{\beta}^i \cot \phi + \mu\dot{\beta}^i \right\} \cot \phi \right. \right. \\ & \left. \left. + \left[\beta \left\{ \dot{\beta}^i + \mu\dot{\beta}^i \cot \phi \right\} + \beta \left\{ \dot{\beta}^i \cot \phi + \mu\dot{\beta}^i \right\} \cot \phi \right] \right] \sin \phi \, d\theta d\phi \right. \\ & \left. + \beta \left\{ \frac{M_\phi^R}{D} \right\} + \beta \left\{ \frac{M_\theta^R}{D} \right\} \right] \sin \phi \, d\theta d\phi \end{aligned} \quad (4.18)$$

$$\begin{aligned} \frac{J_{1,L}}{Ka^2} = & -\hat{p} \iint \left[(w + u \cot \phi) \left\{ 3 + 6\varepsilon_2^s + 3(\varepsilon_2^s)^2 + 2\varepsilon_3^s + 2\varepsilon_2^s \varepsilon_3^s \right\} \right. \\ & \left. + \varepsilon_3 \left\{ 1 + 2\varepsilon_2^s + (\varepsilon_2^s)^2 \right\} + \dot{v} / \sin \phi \left\{ 1 + 2\varepsilon_2^s + \varepsilon_3^s + (\varepsilon_2^s)^2 + \varepsilon_2^s \varepsilon_3^s \right\} \right] \sin^3 \phi \, d\theta d\phi \end{aligned} \quad (4.19)$$

In equations (4.17), (4.18), and (4.19) the following notations and definitions have been introduced

$$K = \frac{Et}{1-\mu^2}, \quad D = \frac{Et^3}{12(1-\mu^2)}, \quad \alpha = \frac{D}{Ka^2} = \frac{t^2}{12a^2} \quad (4.20)$$

$$\hat{p} = \frac{Pa}{2K} = \frac{Pa(1-\mu^2)}{2Et} \quad (4.21)$$

$$\varepsilon_3 = \dot{u} - w \cot \phi \quad (4.22)$$

$$Q_{\phi}^i = \varepsilon_{\phi}^i + \mu\varepsilon_{\theta}^i + \langle \varepsilon_{\phi}^i + \mu\varepsilon_{\theta}^i \rangle - \frac{N_{\phi}^R}{K} \quad (4.23)$$

$$Q_{\theta}^i = \varepsilon_{\theta}^i + \mu\varepsilon_{\phi}^i + \langle \varepsilon_{\theta}^i + \mu\varepsilon_{\phi}^i \rangle - \frac{N_{\theta}^R}{K}$$

and the superscript 's' has been introduced to denote displacements, strains and curvatures of the axisymmetric fundamental path, i.e. $x^s = x^i + x^f$, $e_{\phi}^s = \varepsilon_{\phi}(x^s)$ etc.

The terms of the total potential energy functional that are quadratic in the incremental displacements (x), may be treated in a similar manner to the linear terms as follows.

$$V_2 = U_{2,M} + U_{2,B} + J_{2,L} \quad (4.24)$$

Where the membrane ($U_{2,M}$), bending ($U_{2,B}$) and load potential ($J_{2,L}$) energies are given below.

X

$$\frac{U_{2,M}}{Ka^2} = \frac{1}{2} \int \int \left[\varepsilon_1^2 + \varepsilon_2^2 + 2\mu\varepsilon_1\varepsilon_2 + \frac{1}{2}(1-\mu)(v+\gamma)^2 \right] \sin \phi d\theta d\phi \quad (4.25)$$

$$\begin{aligned} & + \frac{1}{2} \int \int \left\{ 2 \left[\frac{1}{2}(v^2 + \beta^2) \left\{ (1 - \varepsilon_1^s + (\varepsilon_1^s)^2 - \frac{1}{2}(\beta^s)^2) (\varepsilon_1^s + \frac{1}{2}(\beta^s)^2 - \frac{1}{2}(\beta^s)^2 \varepsilon_1^s + \dots + \mu\varepsilon_2^s) \right\} \right. \right. \\ & \quad \left. \left. + \frac{1}{2}(\gamma^2 + \delta^2) \left\{ (1 - \varepsilon_2^s + (\varepsilon_2^s)^2) (\varepsilon_2^s + \mu(\varepsilon_1^s + \frac{1}{2}(\beta^s)^2 - \frac{1}{2}(\beta^s)^2 \varepsilon_1^s + \dots)) \right\} \right. \right. \\ & \quad \left. \left. + \left[\varepsilon_1 \beta \{-\beta^s + 2\beta^s \varepsilon_1^s\} + \varepsilon_1^2 \left\{ \frac{1}{2}(\beta^s)^2 \right\} + \beta^2 \left\{ -\frac{1}{2}(\beta^s)^2 \right\} \right] \left[\mu\varepsilon_2^s + \varepsilon_1^s + \frac{1}{2}(\beta^s)^2 \right] \right. \right. \\ & \quad \left. \left. + \varepsilon_1 \beta \{ \beta^s - \varepsilon_1^s \beta^s + (\varepsilon_1^s)^2 \beta^s - (\beta^s)^3 + \dots \} \right. \right. \\ & \quad \left. \left. + \varepsilon_1^2 \left\{ -\frac{1}{2}(\beta^s)^2 + \varepsilon_1^s (\beta^s)^2 + \dots \right\} + \beta^2 \left\{ \frac{1}{2}(\beta^s)^2 - \varepsilon_1^s (\beta^s)^2 \right\} \right. \right. \\ & \quad \left. \left. + \mu\varepsilon_2 \beta \left\{ (\beta^s)^2 - \varepsilon_1^s \beta^s + (\varepsilon_1^s)^2 \beta^s - \frac{1}{2}(\beta^s)^3 \right\} \right. \right. \\ & \quad \left. \left. + \mu\varepsilon_1 \varepsilon_2 \left\{ -\frac{1}{2}(\beta^s)^2 + \varepsilon_1^s (\beta^s)^2 \right\} \right. \right. \\ & \quad \left. \left. + (1-\mu) \left[v^2 \left\{ -\varepsilon_1^s - \frac{1}{2}(\beta^s)^2 + \frac{3}{2}(\varepsilon_1^s)^2 - 2(\varepsilon_1^s)^3 + 2\varepsilon_1^s (\beta^s)^2 \right\} \right. \right. \\ & \quad \left. \left. + \gamma^2 \left\{ -\varepsilon_2^s - \frac{1}{2}(\beta^s)^2 + \frac{3}{2}(\beta^s)^2 - 2(\varepsilon_2^s)^3 + 2\varepsilon_2^s (\beta^s)^2 + \varepsilon_1^s (\beta^s)^2 \right\} \right. \right. \\ & \quad \left. \left. + \delta^2 \left\{ \frac{1}{2}(\beta^s)^2 - (\beta^s)^2 (\varepsilon_1^s + \varepsilon_2^s) \right\} \right. \right. \\ & \quad \left. \left. + v\gamma \left\{ -(\varepsilon_1^s + \varepsilon_2^s) - (\beta^s)^2 + (\varepsilon_1^s)^2 + (\varepsilon_2^s)^2 + \varepsilon_1^s \varepsilon_2^s - (\varepsilon_2^s)^3 \right. \right. \right. \\ & \quad \left. \left. \left. - (\varepsilon_1^s)^3 + \varepsilon_2^s (\beta^s)^2 + 3\varepsilon_1^s (\beta^s)^2 - (\varepsilon_1^s)^2 \varepsilon_2^s - \varepsilon_1^s (\varepsilon_2^s)^2 \right\} \right. \right. \\ & \quad \left. \left. + v\delta \left\{ \beta^s - \beta^s (2\varepsilon_1^s + \varepsilon_2^s) - \frac{1}{2}(\beta^s)^3 + 2(\varepsilon_1^s)^2 \beta^s + \varepsilon_1^s \varepsilon_2^s \beta^s \right\} \right. \right. \\ & \quad \left. \left. + \gamma\delta \left\{ \beta^s - \beta^s (\varepsilon_1^s + 2\varepsilon_2^s) - \frac{1}{2}(\beta^s)^3 + 2(\varepsilon_2^s)^2 \beta^s + \varepsilon_1^s \varepsilon_2^s \beta^s \right\} \right] \right\} \sin \phi d\theta d\phi \end{aligned}$$

$$\begin{aligned} & - \frac{1}{2} \int \int \left[v^2 \left\{ \frac{1}{2} Q_\phi^i (1 - \varepsilon_1^s + (\varepsilon_1^s)^2 - \frac{1}{2}(\beta^s)^2 + \dots) \right\} \right. \\ & \quad \left. + \beta^2 \left\{ \frac{1}{2} Q_\phi^i (1 - \varepsilon_1^s + (\varepsilon_1^s)^2 - \frac{3}{2}(\beta^s)^2 + \dots) \right\} \right. \\ & \quad \left. + \gamma^2 \left\{ \frac{1}{2} Q_\theta^i (1 - \varepsilon_2^s + (\varepsilon_2^s)^2) \right\} + \delta^2 \left\{ \frac{1}{2} Q_\theta^i (1 - \varepsilon_2^s + (\varepsilon_2^s)^2) \right\} \right. \\ & \quad \left. + \varepsilon_1^2 \left\{ \frac{1}{2} Q_\phi^i (\beta^s)^2 \right\} + \varepsilon_1 \beta \left\{ Q_\phi^i (-\beta^s + 2\beta^s \varepsilon_1^s) \right\} \right] \sin \phi d\theta d\phi \end{aligned}$$

$$\frac{U_{2,B}}{Ka^2} = \frac{\alpha}{2} \iint [\beta^2 + (\dot{\delta}/\sin \phi + \beta \cot \phi)^2 + 2\mu\beta(\dot{\delta}/\sin \phi + \beta \cot \phi) + \frac{1}{2}(1-\mu)(\dot{\delta} + \beta/\sin \phi - \delta \cot \phi)^2] \sin \phi \, d\theta d\phi \quad (4.26)$$

$$\frac{J_{2,L}}{Ka^2} = -\hat{p} \iint [(w + u \cot \phi)^2 \{3 + 3\varepsilon_2^s + \varepsilon_3^s\} + \varepsilon_3 \dot{v}/\sin \phi \{1 + \varepsilon_2^s\} + 2(\dot{w} + u \cot \phi)(\dot{v}/\sin \phi + \varepsilon_3) \{1 + \varepsilon_2^s\}] \sin \phi \, d\theta d\phi \quad (4.27)$$

4.3 THE FUNDAMENTAL PATH EQUILIBRIUM EQUATION

A stationary value of the total potential energy with respect to the generalised coordinates (x) is necessary and sufficient for the equilibrium of the system. Hence for equilibrium of the system

$$\delta V = \delta V_1 + \delta V_2 + \dots = 0 \quad (4.28)$$

On the fundamental path the incremental displacements, x, are identically zero, therefore

$$\delta V_2 = \delta V_3 = \dots = 0 \quad (4.29)$$

and the fundamental path solution is given by the stationarity of V_1 with respect to any general incremental displacements (x). That is, $\delta V_1=0$ yields the fundamental path solution. The stationary condition (Chapter 2) is satisfied by the Euler equations, which for V_1 , given by (4.16), (4.17), (4.18) and (4.19), reduce to,

$$E_1 \text{ or } E_u : \frac{d}{d\phi} \left(\frac{\partial F}{\partial u} \right) - \frac{\partial F}{\partial u} = 0 \quad (4.30)$$

$$E_3 \text{ or } E_w : \frac{d^2}{d\phi^2} \left(\frac{\partial F}{\partial w} \right) - \frac{d}{d\phi} \left(\frac{\partial F}{\partial w} \right) + \frac{\partial F}{\partial w} = 0$$

where F is the complete integrand of V_1 .

When the Euler equations (4.30) are applied to the linear (in x) potential energy functional (V_1) a pair of fourth order nonlinear (in x^f) differential equations of the following form result:

$$\sum_{j=0}^4 A_{ij}(x^s)^j + \hat{p} \sum_{j=0}^3 B_{ij}(x^s)^j = 0 \quad \text{for } i = 1, 3 \quad (4.31)$$

in which $x^s = x^i + x^f$.

The terms of equation (4.31) have been calculated and are tabulated in Table 4.1, in which the $A_{i,0}$ and $A_{i,1}(x^s)$ terms are slightly different from those of expression (4.31). In anticipation of the solution method the constant and linear (in x^s) terms have been altered and are tabulated as follows:

$$A_{i,0}, \quad \text{of Table 4.1} = A_{i,0} + A_{i,1}(x^i), \quad \text{of equation (4.31)}$$

$$A_{i,1}(x^f), \quad \text{of Table 4.1} = A_{i,1}(x^s = x^i + x^f) - A_{i,1}(x^i), \quad \text{of equation (4.31)}$$

Fourth order expressions have been used for the strains and linear expressions for the curvatures in equation (4.2), allowing the fundamental path equilibrium equation, equation (4.31), to include consistent fourth order strain terms and linear curvature terms.

Originally the derivation of the equilibrium equations for the nonlinear fundamental path was based on the quartic strain displacement and the quadratic curvature displacement expressions given by equation (2.66). The eigenvalue problem that results from the linearised secondary path was based on strain displacement relations that contained all terms up to and including the cubic terms and only the 'largest' of the terms that arise from the quartic terms, while quadratic curvature displacement relations were used. Subsequently, these equations were solved, yielding the nonlinear axisymmetric fundamental path, and the initial mode shape and location (on the nonlinear axisymmetric fundamental path) of the secondary paths that bifurcate from the fundamental path. By neglecting higher order terms in the strain displacement and curvature displacement expressions and by comparing the order of magnitude of displacements, their derivatives, the linear strain components and the contributions to the total potential energy for both the fundamental and secondary paths, the order of accuracy required for the strain and curvature expressions was established, and this is presented in Section 6.2.3 of Chapter Six. It was found that cubic strain and linear curvature expressions are required for consistent and accurate modelling of the nonlinear elastic response of thin spherical caps, accurate but inconsistent modelling may be achieved with quadratic strain displacement and linear curvature displacement expression. As the terms that arise from the use of quadratic curvature expressions, equation (2.66), require the introduction of new, and unnecessary, notation they have been neglected in equation (4.2), and no quadratic curvature terms are given in Table 4.1.

4.4 THE FUNDAMENTAL PATH PERTURBATION METHOD

In order to solve the nonlinear differential equation (4.31) a perturbation technique will be adopted. If some general point on the fundamental path is given by $(\hat{p}_0, x_0^s \equiv x^i + x^f_0)$ which therefore satisfies the equilibrium equation (4.31), then we may construct the series

$$\begin{aligned} x^s &= x^i + x^f = x^i + x_0^f + x_1 e + x_2 e^2 + \dots = x_0^s + x_1 e + x_2 e^2 + \dots \\ \hat{p} &= \hat{p}_0 + \hat{p}_1 e + \hat{p}_2 e^2 + \dots \end{aligned} \quad (4.32)$$

where e is some suitably defined perturbation parameter, and the fundamental path superscript 'f' has been omitted from the individual linear, x_1 , quadratic, x_2 , etc. terms of the nonlinear fundamental path displacement x^f . We would like to solve for x_1, x_2, x_3, \dots and $\hat{p}_1, \hat{p}_2, \hat{p}_3, \dots$ such that x^s and \hat{p} also satisfy equation (4.31).

Using the form of equation (4.31) defined in Table 4.1 and substituting for x^s and \hat{p} from equation (4.32), and then collecting like powers of e together, we have an expression of the form

$$F_0 + F_1 e + F_2 e^2 + F_3 e^3 + \dots = 0 \quad (4.33)$$

in which the coefficients F_0, F_1, F_2, \dots are functions of x_0^i, \hat{p}_0, x_j , and \hat{p}_j only. As equation (4.33) must be satisfied for all values of e it follows that the individual coefficients F_0, F_1, \dots must be zero, and this condition yields the sequence of "perturbation equations" given below.

$$\begin{aligned} F_0 = 0 &\Rightarrow A_{i,1}(x_0^s) + A_{i,2} \{ (x_0^s)^2 \} + A_{i,3} \{ (x_0^s)^3 \} + A_{i,4} \{ (x_0^s)^4 \} + A_{i,0} = \\ &= -\hat{p}_0 [B_{i,1} \{ x_0^s \} + B_{i,2} \{ (x_0^s)^2 \} + B_{i,0}] \end{aligned} \quad (4.34)$$

$$F_1 = 0 \Rightarrow \bar{A}_i(x_1) = -\hat{p}_1 [\bar{B}_{i,0}]$$

$$\begin{aligned} F_2 = 0 \Rightarrow \bar{A}_i(x_2) &= -\hat{p}_2 [\bar{B}_{i,0}] - [A_{i,2} \{ (x_1)^2 \} + A_{i,3} \{ 3(x_0^s)(x_1)^2 \} \\ &+ A_{i,4} \{ 6(x_0^s)^2(x_1)^2 \} + \hat{p}_1 B_{i,1} \{ x_1 \} + \hat{p}_1 B_{i,2} \{ 2(x_0^s)x_1 \}] \end{aligned}$$

$$\begin{aligned} F_3 = 0 \Rightarrow \bar{A}_i(x_3) &= -\hat{p}_3 [\bar{B}_{i,0}] - [A_{i,2} \{ 2x_1 x_2 \} + A_{i,3} \{ (x_1)^3 + 6(x_0^s)x_1 x_2 \} \\ &+ A_{i,4} \{ 4(x_0^s)x_1^3 \} + A_{i,4} \{ 12(x_0^s)x_1 x_2 \} + \hat{p}_1 B_{i,1} \{ x_2 \} \\ &+ \hat{p}_2 B_{i,1} \{ x_1 \} + \hat{p}_1 B_{i,2} \{ (x_1)^2 \} + \hat{p}_1 B_{i,2} \{ (x_1)^2 \} \\ &+ \hat{p}_1 B_{i,2} \{ 2(x_0^s)x_2 \} + \hat{p}_2 B_{i,2} \{ 2(x_0^s)x_1 \} + \hat{p}_0 B_{i,2} \{ 2x_1 x_2 \}] \end{aligned}$$

where

$$\bar{A}_i(x_j) = A_{i,1}(x_j) + A_{i,2} \{2(x_0^s)x_j\} + A_{i,3} \{3(x_0^s)^2x_j\} + A_{i,4} \{4(x_0^s)^3x_j\} \\ + \hat{p}_0 [B_{i,1}x_j + B_2 \{2(x_0^s)x_j\}]$$

and

$$\bar{B}_{i,0} = B_{i,0} + B_{i,1}\{x_0^s\} + B_{i,2}\{(x_0^s)^2\}$$

In the above expressions $i=1$ and 3 and the terms $A_{i,j}(x)^j$ and $B_{i,j}(x)^j$ are defined in Table 4.1.

In order to solve sequentially equation (4.34) for $(\hat{p}_1, x_1), (\hat{p}_2, x_2), \dots$ only an expression relating \hat{p}_i and x_j is required, and by considering the choice of perturbation parameter we can find such a condition. For convenience it is desirable to choose the perturbation parameter so that it increases continuously along the fundamental equilibrium path. This will be achieved by identifying the perturbation parameter (e) with the arc length (s) of the fundamental path, where s is defined as

$$s = \int_0^e \left\{ \left(\frac{d\hat{p}}{de} \right)^2 + \left(\frac{dx^f}{de} \right)^2 \right\}^{\frac{1}{2}} de \quad (4.35)$$

Other, physically more obvious, definitions of perturbation parameter were tried, including the load parameter (\hat{p}), the change in volume of the shell, and the radial displacement at the pole. None of these definitions proved adequate as the nonlinear fundamental state was not always uniquely defined by the perturbation parameter. That is, these definitions of the perturbation parameter do not yield a continuously increasing (or decreasing) value of the perturbation parameter along the fundamental path.

In order to ensure the unique definition of the fundamental state for any value of the perturbation parameter the fundamental path arc length definition has been adopted. Substitution of (4.32) into (4.35) yields

$$s = \int_0^e \left\{ (\hat{p}_1 + 2\hat{p}_2e + 3\hat{p}_3e^2 + \dots)^2 + (x_1 + 2x_2e + 3x_3e^2 + \dots)^2 \right\}^{\frac{1}{2}} de$$

hence

$$\frac{ds}{de} = \left\{ [(\hat{p}_1)^2 + (x_1)^2] + 4[\hat{p}_1\hat{p}_2 + x_1x_2]e + [6\hat{p}_1\hat{p}_3 + 4(\hat{p}_2)^2 + 6x_1x_3 + 4(x_2)^2]e^2 + \dots \right\}^{\frac{1}{2}}$$

Now if we identify the perturbation parameter with the arc length, by putting $s = a e$, where a is some arbitrary non-zero constant, we may write

$$\frac{ds}{de} = a = \left\{ [(\hat{p}_1)^2 + (x_1)^2] + 4[\hat{p}_1\hat{p}_2 + x_1x_2] e + [6\hat{p}_1\hat{p}_3 + 4(\hat{p}_2)^2 + 6x_1x_3 + 4(x_2)^2] e^2 + \dots \right\}^{\frac{1}{2}}$$

which yields the following sequence of equations:

$$(\hat{p}_1)^2 + (x_1)^2 = a^2 \tag{4.36}$$

$$4\hat{p}_1\hat{p}_2 + 4x_1x_2 = 0$$

$$6\hat{p}_1\hat{p}_3 + 4(\hat{p}_2)^2 + 6x_1x_3 + 4(x_2)^2 = 0$$

$$8\hat{p}_1\hat{p}_4 + 12\hat{p}_2\hat{p}_3 + 8x_1x_4 + 12x_2x_3 = 0$$

etc.

Equations (4.34) and (4.36) may now be solved to yield the coefficients $x_1, x_2, x_3 \dots$ and $\hat{p}_1, \hat{p}_2, \hat{p}_3 \dots$ of the fundamental path series given by equation (4.32).

4.5 THE SECONDARY PATH EQUATION

The stationarity of V_1 with respect to the generalised displacement (x) has been used to determine the fundamental path solution. Hence the equilibrium of the system, equation (4.28), for general non-zero periodic or secondary path, displacements is given by:

$$\delta V_2 + \delta V_3 + \dots = 0 \quad (4.37)$$

The linearised secondary path solution consists of determining the critical pressure, P_{cr} and the initial mode shape of the secondary path at the point of bifurcation. This may be achieved by considering the solution of (4.37) which is linear in the generalised coordinate (x), that is $\delta V_2=0$.

If it were desired a perturbation method analogous to that used for the fundamental path solution could be set up for the secondary path. In which case the periodic displacement (x) and the uniform pressure load along the secondary path could be expressed in terms of a power series in the secondary path perturbation parameter. The solution of equation (4.37) would then be accomplished by setting the coefficients of like powers of the secondary path perturbation parameter to zero in a manner similar to that used in deriving equation (4.34). The present solution, given by putting $\delta V_2=0$, is identical to solving for the first term in the secondary path perturbation series.

The stationary condition, $\delta V_2=0$, is satisfied by the Euler equations

$$E_1 \text{ or } E_u; \quad \frac{d}{d\phi} \left(\frac{\partial F}{\partial \dot{u}} \right) + \frac{d}{d\theta} \left(\frac{\partial F}{\partial \dot{u}} \right) - \frac{\partial F}{\partial u} = 0 \quad (4.38)$$

$$E_2 \text{ or } E_v; \quad \frac{d}{d\phi} \left(\frac{\partial F}{\partial \dot{v}} \right) + \frac{d}{d\theta} \left(\frac{\partial F}{\partial \dot{v}} \right) - \frac{\partial F}{\partial v} = 0$$

$$E_3 \text{ or } E_w; \quad \frac{d^2}{d\phi^2} \left(\frac{\partial F}{\partial \dot{w}} \right) + \frac{d^2}{d\theta^2} \left(\frac{\partial F}{\partial \dot{w}} \right) + \frac{d^2}{d\phi d\theta} \left(\frac{\partial F}{\partial \dot{w}} \right) - \frac{d}{d\phi} \left(\frac{\partial F}{\partial \dot{w}} \right) - \frac{d}{d\theta} \left(\frac{\partial F}{\partial \dot{w}} \right) + \frac{\partial F}{\partial w} = 0$$

in which the quadratic (in the incremental displacements) components of the total potential energy V_2 are given by equations (4.24), (4.25), (4.26) and (4.27), and F is the complete integrand of V_2 .

When the Euler equations (4.38) are applied to V_2 a set of fourth order differential equations, linear in the incremental displacements (x) and their derivatives, but non-linear in the axisymmetric, fundamental path displacement (x^s) and their derivatives results, and is of the following form:

$$\sum_{j=0}^3 [A_{i,j}(x^s)^j](x) + \hat{p} \sum_{j=0}^1 [B_{i,j}(x^s)^j](x) = 0 \quad \text{for } i = 1, 2, 3 \quad (4.39)$$

The terms of equation (4.39) have been calculated and are presented in Table 4.2.

On substitution for x^s and \hat{p} from equation (4.32) into expression (4.39) a non-linear eigenvalue problem in terms of the fundamental path perturbation parameter (the eigenvalue) and the incremental displacement (x) (the eigenvector) results. It is the solution of this problem that yields the critical pressures and initial mode shapes of the secondary path displacement vector (x).

Fourth order expressions were used for the strain displacement and quadratic expressions for the curvatures displacement relations, equation (2.66), it is therefore possible to include consistent fourth order strain terms and quadratic curvature terms in equation (4.39). As for the fundamental path equilibrium equation, it is sufficient for consistent and accurate modelling of the elastic response of thin spherical caps to base the nonlinear eigenvalue problem, equation (4.39), on cubic strain and linear curvature expressions, and accurate but inconsistent modelling may be achieved with quadratic strain displacement and linear curvature displacement expression, see Chapter Six. For this reason the terms arising from the use of quadratic curvature expressions, equation (2.66), have been neglected in equation (4.2), and no quadratic curvature terms are given in Table 4.2. Also only the 'large' quartic terms (i.e. $[A_{i,3}(x^s)^3](x)$) arising from the use of quartic strain displacement relations, equation (4.2), are retained in Table 4.2.

4.6 THE CIRCUMFERENTIAL MODELLING OF DISPLACEMENTS.

Due to the axisymmetric properties of the spherical caps considered it is possible to express the displacements exactly as,

$$\begin{aligned} u &= u(\phi, \theta) = \sum_{i=0}^{\infty} u_i(\phi) \cos i\theta \\ v &= v(\phi, \theta) = \sum_{i=0}^{\infty} v_i(\phi) \sin i\theta \\ w &= w(\phi, \theta) = \sum_{i=0}^{\infty} w_i(\phi) \cos i\theta \end{aligned} \quad (4.40)$$

The functions $u_i(\phi)$, $v_i(\phi)$ and $w_i(\phi)$ are dependent on ϕ only, and no confusion will arise if we use the shorter notation of u_i , v_i and w_i for these functions of ϕ .

For the axisymmetric fundamental path, $i=0$, the fundamental path displacements are represented by

$$\begin{aligned} u^f &= u_0 \\ v^f &= v_0 = 0 \\ w^f &= w_0 \end{aligned} \quad (4.41)$$

Hence the fundamental path equations (4.32), (4.34) and (4.36) may be used exactly as they are, the displacements being functions of ϕ only.

For secondary path displacements i may take any zero or positive integer value. However the quadratic nature (quadratic in x) of the total potential energy functional (4.24) defining the secondary path, and the well known properties of the following integrals:

$$\begin{aligned} \int_0^{2\pi} \sin i\theta \sin j\theta \, d\theta &= \int_0^{2\pi} \cos i\theta \cos j\theta \, d\theta = 0 && \text{for } i \neq j \\ &= \pi && \text{for } i = j \end{aligned} \quad (4.42)$$

and

$$\int_0^{2\pi} \sin i\theta \cos j\theta \, d\theta = 0 \quad \text{for all } i \text{ and } j$$

allow equations (4.25), (4.26) and (4.27) to be used as they are, with the understanding that the circumferential mode number, i , is implied by u , v and w in the sense that

$$\begin{aligned} u &= u_i \cos i\theta \\ v &= v_i \sin i\theta \\ w &= w_i \cos i\theta \end{aligned} \tag{4.43}$$

Equations (4.39) are linear in the incremental displacements u , v and w and their derivatives, and it may be seen, from Table 4.2, that a constant factor of $\cos(i\theta)$ can be cancelled from the E_1 and E_3 equations, and a factor of $\sin(i\theta)$ from the E_2 equation.

Finally equation (4.39) and Table 4.2 may be used, provided the following interpretation is placed on the incremental displacements and their differentials:

$$\begin{array}{lll}
 u = u_i & v = v_i & w = w_i \\
 \dot{u} = -i\dot{u}_i & \dot{v} = +i\dot{v}_i & \dot{w} = -i\dot{w}_i \\
 \ddot{u} = -i^2\ddot{u}_i & \ddot{v} = -i^2\ddot{v}_i & \ddot{w} = -i^2\ddot{w}_i \\
 & \ddot{\dot{v}} = -i^3\ddot{\dot{v}}_i & \ddot{\dot{w}} = +i^3\ddot{\dot{w}}_i \\
 & & \ddot{\dot{\dot{w}}} = +i^4\ddot{\dot{\dot{w}}}_i
 \end{array} \tag{4.44}$$

By specifying the circumferential mode number, i , the incremental displacements of the secondary path, equation (4.39), are dependent upon ϕ only.

4.7 THE ENERGY COMPONENTS OF THE FUNDAMENTAL AND SECONDARY PATHS

The total potential energy functional defined as

$$V = U_M + U_B + J_L$$

and equations (4.9), (4.12) and (4.13) are the common starting point for the derivation of both the fundamental path equations ($\delta V_1=0$) and the secondary path eigenvalue problem ($\delta V_2=0$).

The solution (x^f, p^f) and (x, p) of the nonlinear fundamental path problem and the nonlinear eigenvalue problem may be substituted into the total potential energy functional

$$V = V_0 + V_1 + V_2 + \dots$$

This will give us an independent check on the derivation of the equilibrium equations, and the accuracy of the solution methods used. In effect we are able to check that the solution process has solved the original problem formulated by the total potential energy functional. The back substitution into the total potential energy functional also provides us with useful information as to the way in which the energy absorbed by the shell under loading is distributed through the shell. The subscript notation V_0, V_1, V_2 etc. will be used to denote the terms of the total potential energy that are independent, linear and quadratically dependent on the generalised incremental displacements.

4.7.1 Energy Components of the Fundamental Path (V_0)

The total potential energy at any point on the fundamental path ($x=0$), is given by,

$$V_0 = U_{0,M} + U_{0,B} + J_{0,L}$$

and for the axisymmetric fundamental path we have

$$\begin{aligned} U_{0,M} &= U_{0,M_\phi} + U_{0,M_\theta} \\ U_{0,B} &= U_{0,B_\phi} + U_{0,B_\theta} \\ U_{0,M_{\phi\theta}} &= U_{0,B_{\phi\theta}} = 0 \end{aligned} \tag{4.45}$$

The meridional and circumferential membrane ($U_{0,M\phi}$ $U_{0,M\theta}$) and bending ($U_{0,B\phi}$ $U_{0,B\theta}$) energies are

$$\begin{aligned} \frac{U_{0,M\phi}}{Ka^2} &= \frac{1}{2} \iint [\epsilon_\phi^s (\epsilon_\phi^s + \mu\epsilon_\theta^s)] \sin\phi d\theta d\phi \\ &+ \frac{1}{2} \iint \left[-\epsilon_\phi^s \left\{ \epsilon_\phi^i + \langle \epsilon_\phi^i + \mu\epsilon_\theta^i \rangle - \frac{N_\phi^R}{K} \right\} - \mu\epsilon_\theta^s \epsilon_\phi^i \right] \sin\phi d\theta d\phi \\ &+ \frac{1}{2} \iint \left[\epsilon_\phi^i \left\{ \langle \epsilon_\phi^i + \mu\epsilon_\theta^i \rangle - \frac{N_\phi^R}{K} \right\} \right] \sin\phi d\theta d\phi \end{aligned} \quad (4.46)$$

$$\begin{aligned} \frac{U_{0,M\theta}}{Ka^2} &= \frac{1}{2} \iint [\epsilon_\theta^s (\epsilon_\theta^s + \mu\epsilon_\phi^s)] \sin\phi d\theta d\phi \\ &+ \frac{1}{2} \iint \left[-\epsilon_\theta^s \left\{ \epsilon_\theta^i + \langle \epsilon_\theta^i + \mu\epsilon_\phi^i \rangle - \frac{N_\theta^R}{K} \right\} - \mu\epsilon_\phi^s \epsilon_\theta^i \right] \sin\phi d\theta d\phi \\ &+ \frac{1}{2} \iint \left[\epsilon_\theta^i \left\{ \langle \epsilon_\theta^i + \mu\epsilon_\phi^i \rangle - \frac{N_\theta^R}{K} \right\} \right] \sin\phi d\theta d\phi \end{aligned}$$

$$\begin{aligned} \frac{U_{0,B\phi}}{Ka^2} &= \frac{\alpha}{2} \iint [\chi_\phi^s (\chi_\phi^s + \mu\chi_\theta^s)] \sin\phi d\theta d\phi \\ &+ \frac{\alpha}{2} \iint \left[-\chi_\phi^s \left\{ \chi_\phi^i + \langle \chi_\phi^i + \mu\chi_\theta^i \rangle - \frac{M_\phi^R}{D} \right\} - \mu\chi_\theta^s \chi_\phi^i \right] \sin\phi d\theta d\phi \\ &+ \frac{\alpha}{2} \iint \left[\chi_\phi^i \left\{ \langle \chi_\phi^i + \mu\chi_\theta^i \rangle - \frac{M_\phi^R}{D} \right\} \right] \sin\phi d\theta d\phi \end{aligned}$$

$$\begin{aligned} \frac{U_{0,B\theta}}{Ka^2} &= \frac{\alpha}{2} \iint [\chi_\theta^s (\chi_\theta^s + \mu\chi_\phi^s)] \sin\phi d\theta d\phi \\ &+ \frac{\alpha}{2} \iint \left[-\chi_\theta^s \left\{ \chi_\theta^i + \langle \chi_\theta^i + \mu\chi_\phi^i \rangle - \frac{M_\theta^R}{D} \right\} - \mu\chi_\phi^s \chi_\theta^i \right] \sin\phi d\theta d\phi \\ &+ \frac{\alpha}{2} \iint \left[\chi_\theta^i \left\{ \langle \chi_\theta^i + \mu\chi_\phi^i \rangle - \frac{M_\theta^R}{D} \right\} \right] \sin\phi d\theta d\phi \end{aligned}$$

while the load potential energy, $J_{0,L}$ is

$$\begin{aligned} \frac{J_{0,L}}{Ka^2} &= -\hat{p} \iint [\{ 3\epsilon_2^s + (\epsilon_1^s - \epsilon_2^s + \beta^s \cot \phi) + 3(\epsilon_2^s)^2 + 2\epsilon_2^s (\epsilon_1^s - \epsilon_2^s + \beta^s \cot \phi) + (\epsilon_2^s)^3 \\ &+ (\epsilon_2^s)^2 (\epsilon_1^s - \epsilon_2^s + \beta^s \cot \phi) \} - \{ 3\epsilon_2^i + (\epsilon_1^i - \epsilon_2^i + \beta^i \cot \phi) + 3(\epsilon_2^i)^2 \\ &+ 2\epsilon_2^i (\epsilon_1^i - \epsilon_2^i + \beta^i \cot \phi) + (\epsilon_2^i)^3 + (\epsilon_2^i)^2 (\epsilon_1^i - \epsilon_2^i + \beta^i \cot \phi) \}] \sin\phi d\theta d\phi \end{aligned} \quad (4.47)$$

4.7.2 Incremental Linear Energy Components (V_1)

At any point on the fundamental path ($x=0$), the energy components associated with the linear terms of the total potential energy (V_1) represent the rates of change of the energy components associated with the incremental displacements along the fundamental path.

These components are

$$\begin{aligned}
 \frac{U_{1,M_\phi}}{Ka^2} &= \frac{1}{2} \int \int \left[\varepsilon_1 (2\varepsilon_\phi^s + \mu\varepsilon_\theta^s) \left(1 - \frac{1}{2}(\beta^s)^2\right) + \beta (2\varepsilon_\phi^s + \mu\varepsilon_\theta^s) (\beta^s - \varepsilon_1^s \beta^s) + \mu\varepsilon_2 \varepsilon_\phi^s \right] \sin\phi d\theta d\phi \\
 &\quad - \frac{1}{2} \int \int \left[\left\{ \varepsilon_1 \left(1 - \frac{1}{2}(\beta^s)^2\right) + \beta (\beta^s - \varepsilon_1^s \beta^s) \right\} \left\{ \varepsilon_\phi^i + \langle \varepsilon_\phi^i + \mu\varepsilon_\theta^i \rangle - \frac{N_\phi^R}{K} \right\} - \mu\varepsilon_2 \varepsilon_\phi^i \right] \sin\phi d\theta d\phi \\
 \frac{U_{1,M_\theta}}{Ka^2} &= \frac{1}{2} \int \int \left[\varepsilon_2 (2\varepsilon_\theta^s + \mu\varepsilon_\phi^s) + \varepsilon_1 \left\{ 1 - \frac{1}{2}(\beta^s)^2 \right\} \mu\varepsilon_2^s + \beta (\beta^s - \varepsilon_1^s \beta^s) \mu\varepsilon_2^s \right] \sin\phi d\theta d\phi \\
 &\quad - \frac{1}{2} \int \int \left[\varepsilon_2 \left(\varepsilon_\theta^i + \langle \varepsilon_\theta^i + \mu\varepsilon_\phi^i \rangle - \frac{N_\theta^R}{K} \right) + \varepsilon_1 \left\{ 1 - \frac{1}{2}(\beta^s)^2 \right\} \mu\varepsilon_\theta^i + \beta (\beta^s - \varepsilon_1^s \beta^s) \mu\varepsilon_\theta^i \right] \sin\phi d\theta d\phi \\
 \frac{U_{1,B_\phi}}{Ka^2} &= \frac{\alpha}{2} \int \int \left[\beta (2\dot{\beta}^s + \mu\dot{\beta}^s \cot \phi) + \beta (\mu\dot{\beta}^s \cot \phi) \right] \sin\phi d\theta d\phi \\
 &\quad - \frac{\alpha}{2} \int \int \left[\beta (\dot{\beta}^i + \langle \dot{\beta}^i + \mu\dot{\beta}^i \cot \phi \rangle - \frac{M_\phi^R}{D}) + \beta (\mu\dot{\beta}^i \cot \phi) \right] \sin\phi d\theta d\phi \\
 \frac{U_{1,B_\theta}}{Ka^2} &= \frac{\alpha}{2} \int \int \left[\beta \cot \phi (2\dot{\beta}^s \cot \phi + \mu\dot{\beta}^s) + \beta (\mu\dot{\beta}^s \cot \phi) \right] \sin\phi d\theta d\phi \\
 &\quad - \frac{\alpha}{2} \int \int \left[\beta \cot \phi (\dot{\beta}^i \cot \phi + \langle \dot{\beta}^i \cot \phi + \mu\dot{\beta}^i \rangle - \frac{M_\theta^R}{D}) + \beta (\mu\dot{\beta}^i \cot \phi) \right] \sin\phi d\theta d\phi
 \end{aligned}
 \tag{4.48}$$

while the rate of change of the load potential energy $J_{1,L}$ is

$$\begin{aligned}
 \frac{J_{1,L}}{Ka^2} &= -\hat{p} \int \int \left[(w + u \cot \phi) \{3 + 6\varepsilon_2^s + 3(\varepsilon_2^s)^2 + 2\varepsilon_3^s + 2\varepsilon_2^s \varepsilon_3^s\} \right. \\
 &\quad \left. + (u - w \cot \phi) \{1 + 2\varepsilon_2^s + (\varepsilon_2^s)^2\} \right] \sin^3 \phi d\theta d\phi
 \end{aligned}
 \tag{4.49}$$

4.7.3 Incremental Quadratic Energy Components (V_2)

Due to the non-linear strain displacement relations the incremental energy components associated with the initial mode shape of the secondary path, at the point of bifurcation from the nonlinear fundamental path, may be subdivided as follows

$$U_{2,M_\phi} = \frac{1}{2} \iint \left[\dot{N}_\phi \dot{\epsilon}_\phi + \overset{f'}{N}_\phi \overset{f'}{\epsilon}_\phi + \overset{f}{N}_\phi \overset{f''}{\epsilon}_\phi + \overset{f''}{N}_\phi \overset{f}{\epsilon}_\phi \right] \sin\phi \, d\theta d\phi \quad (4.50)$$

$$U_{2,M_\theta} = \frac{1}{2} \iint \left[\dot{N}_\theta \dot{\epsilon}_\theta + \overset{f'}{N}_\theta \overset{f'}{\epsilon}_\theta + \overset{f}{N}_\theta \overset{f''}{\epsilon}_\theta + \overset{f''}{N}_\theta \overset{f}{\epsilon}_\theta \right] \sin\phi \, d\theta d\phi$$

$$U_{2,M_{\theta\phi}} = \frac{1}{2} \iint 2 \left[\dot{N}_{\theta\phi} \dot{\epsilon}_{\theta\phi} + \overset{f'}{N}_{\theta\phi} \overset{f'}{\epsilon}_{\theta\phi} \right] \sin\phi \, d\theta d\phi$$

$$U_{2,B_\phi} = \frac{1}{2} \iint M_\phi \dot{\chi}_\phi a^2 \sin\phi \, d\theta d\phi$$

$$U_{2,B_\theta} = \frac{1}{2} \iint M_\theta \dot{\chi}_\theta a^2 \sin\phi \, d\theta d\phi$$

$$U_{2,B_{\theta\phi}} = \frac{1}{2} \iint 2 M_{\theta\phi} \dot{\chi}_{\theta\phi} a^2 \sin\phi \, d\theta d\phi$$

$$J_{2,L} = \frac{-P}{2} \iint 2 \left[\Delta \ddot{v} + \overset{f''}{\Delta v} \right] a^2 \sin\phi \, d\theta d\phi$$

In equation (4.50) the superscript notation has been introduced in order to indicate the dependence of the energy components upon the fundamental and secondary path displacements. In this notation a prime (') is used to indicate a strain or stress resultant that is linear in the periodic incremental displacements, a double prime (") indicates quadratic components, and the (f) indicates linear or nonlinear dependence on the fundamental path displacements. Using the same notation we may write the individual energy components as

$$\frac{\dot{N}_\phi \dot{\epsilon}_\phi}{Ka^2} = \frac{1}{2} \iint \epsilon_1 (\epsilon_1 + \mu \epsilon_2) \sin\phi \, d\theta d\phi \quad (4.51)$$

$$\frac{\dot{N}_\theta \dot{\epsilon}_\theta}{Ka^2} = \frac{1}{2} \iint \epsilon_2 (\epsilon_2 + \mu \epsilon_1) \sin\phi \, d\theta d\phi$$

$$\frac{\dot{N}_{\theta\phi} \dot{\epsilon}_{\theta\phi}}{Ka^2} = \frac{1}{2} \iint \frac{1}{2} (1 - \mu) (\nu + \gamma)^2 \sin\phi \, d\theta d\phi$$

$$\begin{aligned} \frac{\overset{f'}{N}_\phi \overset{f'}{\epsilon}_\phi}{Ka^2} = & \frac{1}{2} \iint \left[2\epsilon_1 \beta \left\{ \beta^s - \epsilon_1^s \beta^s + (\epsilon_1^s)^2 \beta^s - \frac{1}{2} (\beta^s)^3 \right\} + ((\epsilon_1)^2 - (\beta)^2) \left\{ -\frac{1}{2} (\beta^s)^2 + (\beta^s)^2 \epsilon_1^s \right\} \right. \\ & \left. + \mu \left\{ \epsilon_2 \beta \left\{ \beta^s - \epsilon_1^s \beta^s + (\epsilon_1^s)^2 \beta^s + \frac{1}{2} (\beta^s)^3 \right\} + \epsilon_1 \epsilon_2 \left\{ -\frac{1}{2} (\beta^s)^2 + (\beta^s)^2 \epsilon_1^s \right\} \right\} \right] \sin\phi \, d\theta d\phi \end{aligned}$$

$$\frac{\overset{f'}{N}_\theta \overset{f'}{\epsilon}_\theta}{Ka^2} = \frac{1}{2} \iint \left[\mu \left\{ \epsilon_2 \beta \left\{ \beta^s - \epsilon_1^s \beta^s + (\epsilon_1^s)^2 \beta^s + \frac{1}{2} (\beta^s)^3 \right\} + \epsilon_1 \epsilon_2 \left\{ -\frac{1}{2} (\beta^s)^2 + (\beta^s)^2 \epsilon_1^s \right\} \right\} \right] \sin\phi \, d\theta d\phi$$

$$\begin{aligned} \frac{\dot{N}_{\theta\phi}^f \dot{\epsilon}_{\theta\phi}^f}{Ka^2} &= \frac{1}{2} \iint \left[(1-\mu) \left[\dot{v}^2 \left\{ -\epsilon_1^s - \frac{1}{2}(\beta^s)^2 + \frac{3}{2}(\epsilon_1^s)^2 - 2(\epsilon_1^s)^3 + 2\epsilon_1^s(\beta^s)^2 \right\} \right. \right. \\ &\quad + \gamma^2 \left\{ -\epsilon_2^s - \frac{1}{2}(\beta^s)^2 + \frac{3}{2}(\epsilon_2^s)^2 - 2(\epsilon_2^s)^3 + \epsilon_2^s(\beta^s)^2 + \epsilon_1^s(\beta^s)^2 \right\} \\ &\quad + \delta^2 \left\{ \frac{1}{2}(\beta^s)^2 - \epsilon_1^s(\beta^s)^2 - \epsilon_2^s(\beta^s)^2 \right\} \\ &\quad + \nu\gamma \left\{ -\epsilon_1^s - \epsilon_2^s - (\beta^s)^2 + (\epsilon_1^s)^2 + (\epsilon_2^s)^2 + \epsilon_1^s\epsilon_2^s - (\epsilon_2^s)^3 \right. \\ &\quad \left. - (\epsilon_1^s)^3 + \epsilon_2^s(\beta^s)^2 + 3\epsilon_1^s(\beta^s)^2 - \epsilon_2^s(\epsilon_1^s)^2 - \epsilon_1^s(\epsilon_2^s)^2 \right\} \\ &\quad + \dot{v}\delta \left\{ \beta^s(1 - 2\epsilon_1^s + \epsilon_2^s) - \frac{1}{2}(\beta^s)^3 + 2(\epsilon_1^s)^2\beta^s + \epsilon_1^s\epsilon_2^s\beta^s \right\} \\ &\quad \left. + \gamma\delta \left\{ \beta^s(1 - 2\epsilon_2^s + \epsilon_1^s) - \frac{1}{2}(\beta^s)^3 + 2(\epsilon_2^s)^2\beta^s + \epsilon_1^s\epsilon_2^s\beta^s \right\} \right] \sin\phi \, d\theta d\phi \end{aligned}$$

$$\begin{aligned} \frac{\dot{N}_{\phi}^f \dot{\epsilon}_{\phi}^{\nu}}{Ka^2} &= \frac{1}{2} \iint \left[\frac{1}{2}(\dot{v}^2 + \beta^2) \left\{ \epsilon_1^s - (\epsilon_1^s)^2 + \frac{1}{2}(\beta^s)^2 - \frac{3}{2}\epsilon_1^s(\beta^s)^2 + (\epsilon_1^s)^3 \right\} \right. \\ &\quad + \epsilon_1\beta \left\{ -\epsilon_1^s\beta^s - 2(\epsilon_1^s)^2\beta^s - \frac{1}{2}(\beta^s)^3 \right\} + (\epsilon_1^2 - \beta^2) \left\{ \frac{1}{2}(\beta^s)^2\epsilon_1^s \right\} \\ &\quad + \mu \left\{ \frac{1}{2}(\dot{v}^2 + \beta^2) \left\{ \epsilon_2^s - \epsilon_2^s\epsilon_1^s + \epsilon_2^s(\epsilon_1^s)^2 - \frac{1}{2}(\beta^s)^2\epsilon_2^s \right\} \right. \\ &\quad \left. + \epsilon_1\beta(-\epsilon_2^s\beta^s - 2\epsilon_1^s\epsilon_2^s\beta^s) + (\epsilon_1^2 - \beta^2) \left\{ \frac{1}{2}(\beta^s)^2\epsilon_2^s \right\} \right] \sin\phi \, d\theta d\phi \end{aligned}$$

$$\begin{aligned} \frac{\dot{N}_{\phi}^{\nu} \dot{\epsilon}_{\phi}^f}{Ka^2} &= \frac{1}{2} \iint \left[\frac{1}{2}(\dot{v}^2 + \beta^2) \left\{ \epsilon_1^s - (\epsilon_1^s)^2 + \frac{1}{2}(\beta^s)^2 - \frac{3}{2}\epsilon_1^s(\beta^s)^2 + (\epsilon_1^s)^3 \right\} \right. \\ &\quad + \epsilon_1\beta \left\{ -\epsilon_2^s\beta^s - 2\epsilon_1^s\epsilon_2^s\beta^s \right\} + (\epsilon_1^2 - \beta^2) \left\{ \frac{1}{2}(\beta^s)^2\epsilon_1^s \right\} \\ &\quad \left. + \mu \left\{ \frac{1}{2}(\gamma^2 + \delta^2) \left\{ \epsilon_1^s + \frac{1}{2}(\beta^s)^2 - \epsilon_1^s\epsilon_2^s + \epsilon_1^s(\epsilon_2^s)^2 - \frac{1}{2}\epsilon_2^s(\beta^s)^2 - \frac{1}{2}\epsilon_1^s(\beta^s)^2 \right\} \right\} \right] \sin\phi \, d\theta d\phi \end{aligned}$$

$$\begin{aligned} \frac{\dot{N}_{\theta}^f \dot{\epsilon}_{\theta}^{\nu}}{Ka^2} &= \frac{1}{2} \iint \left[\frac{1}{2}(\gamma^2 + \delta^2) \left\{ \epsilon_2^s - (\epsilon_2^s)^2 + (\epsilon_2^s)^3 \right\} \right. \\ &\quad \left. + \frac{1}{2}\mu(\gamma^2 + \delta^2) \left\{ \epsilon_1^s - \epsilon_1^s\epsilon_2^s + \frac{1}{2}(\beta^s)^2 - \frac{1}{2}\epsilon_2^s(\beta^s)^2 - \frac{1}{2}\epsilon_1^s(\beta^s)^2 + \epsilon_1^s(\epsilon_2^s)^2 \right\} \right] \sin\phi \, d\theta d\phi \end{aligned}$$

$$\frac{f_{\theta}^{\prime\prime} \epsilon_{\theta}}{Ka^2} = \frac{1}{2} \iint \left[\frac{1}{2}(\gamma^2 + \delta^2) \{ \epsilon_2^s - (\epsilon_2^s)^2 + (\epsilon_2^s)^3 \} \right. \\ \left. + \mu \{ (\nu^2 + \beta^2) \left\{ \epsilon_2^s - \epsilon_1^s \epsilon_2^s + (\epsilon_1^s)^2 \epsilon_2^s - \frac{1}{2}(\beta^s)^2 \epsilon_2^s \right\} \right. \\ \left. + \epsilon_1 \beta (-\epsilon_2^s \beta^s + 2\epsilon_1^s \epsilon_2^s \beta^s) + (\epsilon_1^2 - \beta^2) \left\{ \frac{1}{2}(\beta^s)^2 \epsilon_2^s \right\} \right] \sin \phi \, d\theta \, d\phi$$

(4.51 contd.)

$$\frac{U_{2,B_{\theta}}}{Ka^2} = \frac{\alpha}{2} \iint \beta \left[\beta + \mu(\delta/\sin \phi + \beta \cot \phi) \right] \sin \phi \, d\theta \, d\phi$$

$$\frac{U_{2,B_{\theta}}}{Ka^2} = \frac{\alpha}{2} \iint (\delta/\sin \phi + \beta \cot \phi)(\delta/\sin \phi + \beta \cot \phi + \mu\beta) \sin \phi \, d\theta \, d\phi$$

$$\frac{U_{2,B_{\theta}}}{Ka^2} = \frac{\alpha}{2} \iint \frac{1}{2}(1 - \mu)(\delta + \beta/\sin \phi - \delta \cot \phi)^2 \sin \phi \, d\theta \, d\phi$$

$$\frac{P(\Delta \dot{V})}{Ka^2} = \hat{p} \iint \left[3(w + u \cot \phi)^2 + (u - w \cot \phi) \dot{v}/\sin \phi \right. \\ \left. + 2(w + u \cot \phi)(u - w \cot \phi + \dot{v}/\sin \phi) \right] \sin^3 \phi \, d\theta \, d\phi$$

$$\frac{P(\Delta \dot{V})}{Ka^2} = \hat{p} \iint \left[(w + u \cot \phi)^2 (3\epsilon_2^s + \epsilon_3^s) + (u - w \cot \phi) \dot{v}/\sin \phi (\epsilon_2^s) \right. \\ \left. + 2(w + u \cot \phi)(u - w \cot \phi + \dot{v}/\sin \phi)(\epsilon_2^s) \right. \\ \left. + (w + u \cot \phi) \dot{v}/\sin \phi (\epsilon_3^s) \right] \sin^3 \phi \, d\theta \, d\phi$$

TABLE 4.1; Definition of terms in equation (4.31), page 1 of 2.

| | |
|--------------------|--|
| $A_{1,1}(x^f) =$ | $u^f[-(1+\alpha)(\cot^2\phi+\mu)] + \dot{u}^f[(1+\alpha)\cot\phi] + \ddot{u}^f[1+\alpha]$ $+ \dot{w}^f[1+\mu+\alpha(\cot^2\phi+\mu)] + \ddot{w}^f[-\alpha\cot\phi] + \ddot{w}^f[-\alpha] + u^f[\frac{1}{2}Q_\phi^i] + \dot{w}^f[-\frac{1}{2}Q_\phi^i]$ |
| $A_{3,1}(x^f) =$ | $u^f[(1+\mu)\cot\phi - \alpha(1-\mu+1/\sin^2\phi)\cot\phi] + \dot{u}^f[(1+\mu)+\alpha(\mu+1/\sin^2\phi)]$ $+ \ddot{u}^f[-2\alpha\cot\phi] + \ddot{u}^f[-\alpha] + \dot{w}^f[2(1+\mu)] + \ddot{w}^f[\alpha(1-\mu+1/\sin^2\phi)\cot\phi]$ $+ \ddot{w}^f[-\alpha(\mu+1/\sin^2\phi)] + \ddot{w}^f[2\alpha\cot\phi] + \ddot{w}^f[\alpha]$ $+ u^f[-\frac{1}{2}Q_\phi^i - \frac{1}{2}Q_\phi^i\cot\phi] + \dot{u}^f[-\frac{1}{2}Q_\phi^i] + \dot{w}^f[\frac{1}{2}Q_\phi^i + \frac{1}{2}Q_\phi^i\cot\phi] + \ddot{w}^f[\frac{1}{2}Q_\phi^i]$ |
| $A_{1,2}(x^s)^2 =$ | $(\beta^s)^2[\frac{1}{2}(1-\mu)\cot\phi] + \beta^s\dot{\beta}^s - \beta^s\dot{\epsilon}_1^s[-1] + \beta^s\dot{\epsilon}_2^s[-\mu]$ $+ (\beta^s)^2[\frac{1}{4}Q_\phi^i + \frac{1}{4}Q_\phi^i\cot\phi] + \beta^s\dot{\beta}^s[\frac{1}{2}Q_\phi^i] + \beta^s\dot{\epsilon}_1^s[-\frac{1}{2}Q_\phi^i]$ |
| $A_{3,2}(x^s)^2 =$ | $(\beta^s)^2[\frac{1}{2}(1+\mu)] + \beta^s\dot{\epsilon}_1^s[\cot\phi] + \beta^s\dot{\epsilon}_2^s[\mu\cot\phi] + \dot{\beta}^s\dot{\epsilon}_1^s + \dot{\beta}^s\dot{\epsilon}_2^s[\mu] + \beta^s\dot{\epsilon}_1^s$ $+ \beta^s\dot{\epsilon}_2^s[\mu] + (\beta^s)^2[\frac{1}{4}Q_\phi^i] + \beta^s\dot{\epsilon}_1^s[\frac{1}{2}Q_\phi^i\cot\phi + \frac{1}{2}Q_\phi^i] + \beta^s\dot{\epsilon}_1^s[\frac{1}{2}Q_\phi^i] + \dot{\epsilon}_1^s\dot{\beta}^s[\frac{1}{2}Q_\phi^i]$ |
| $A_{1,3}(x^s)^3 =$ | $(\beta^s)^3[-\frac{1}{2}] + (\beta^s)^2\dot{\epsilon}_1^s[-(1-\frac{1}{2}\mu)\cot\phi] + (\beta^s)^2\dot{\epsilon}_2^s[-\frac{1}{2}\mu\cot\phi] + \beta^s\dot{\beta}^s\dot{\epsilon}_1^s[-2]$ $+ \beta^s(\dot{\epsilon}_1^s)^2 + \beta^s\dot{\epsilon}_1^s\dot{\epsilon}_2^s[\mu] + (\beta^s)^2\dot{\epsilon}_2^s[-\frac{1}{2}\mu] - (\beta^s)^2\dot{\epsilon}_1^s + \beta^s\dot{\beta}^s\dot{\epsilon}_2^s[-\mu]$ |
| $A_{3,3}(x^s)^3 =$ | $(\beta^s)^3[\frac{1}{2}\cot\phi] + (\beta^s)^2\dot{\beta}^s[\frac{3}{2}] + (\beta^s)^2\dot{\epsilon}_1^s[-1-\frac{1}{2}\mu] + (\beta^s)^2\dot{\epsilon}_2^s[-\frac{1}{2}\mu]$ $+ \beta^s(\dot{\epsilon}_1^s)^2[-\cot\phi] + \beta^s\dot{\epsilon}_1^s\dot{\epsilon}_2^s[-\mu\cot\phi] - \beta^s(\dot{\epsilon}_1^s)^2 + \beta^s\dot{\epsilon}_1^s\dot{\epsilon}_2^s[-\mu]$ $+ \beta^s\dot{\epsilon}_1^s\dot{\epsilon}_1^s[-2] + \dot{\beta}^s\dot{\epsilon}_1^s\dot{\epsilon}_2^s[-\mu] + \beta^s\dot{\epsilon}_1^s\dot{\epsilon}_2^s[-\mu]$ |
| $A_{1,4}(x^s)^4 =$ | $(\beta^s)^4[\frac{1}{8}\cot\phi(\mu-3)] + (\beta^s)^3\dot{\beta}^s[-\frac{3}{2}] + (\beta^s)^3\dot{\epsilon}_1^s[\frac{3}{2}] + (\beta^s)^3\dot{\epsilon}_2^s[\frac{1}{2}\mu]$ $+ (\beta^s)^2(\dot{\epsilon}_1^s)^2[\frac{1}{2}\cot\phi(3-\mu)] + (\beta^s)^2\dot{\epsilon}_1^s\dot{\epsilon}_2^s[\mu\cot\phi] + (\beta^s)^2\dot{\epsilon}_1^s\dot{\epsilon}_1^s[3] + (\beta^s)^2\dot{\epsilon}_1^s\dot{\epsilon}_2^s[\mu]$ $+ (\beta^s)^2\dot{\epsilon}_1^s\dot{\epsilon}_2^s[\mu] + \beta^s\dot{\beta}^s(\dot{\epsilon}_1^s)^2[3] + \beta^s\dot{\beta}^s\dot{\epsilon}_1^s\dot{\epsilon}_2^s[2\mu] - \beta^s(\dot{\epsilon}_1^s)^3 + \beta^s(\dot{\epsilon}_1^s)^2\dot{\epsilon}_2^s[-\mu]$ |
| $A_{3,4}(x^s)^4 =$ | $(\beta^s)^4[-\frac{1}{8}(3+\mu)] + (\beta^s)^3\dot{\epsilon}_1^s[-\frac{3}{2}\cot\phi] + (\beta^s)^3\dot{\epsilon}_2^s[-\frac{1}{2}\mu\cot\phi] + (\beta^s)^3\dot{\epsilon}_1^s[-\frac{3}{2}]$ $+ (\beta^s)^3\dot{\epsilon}_2^s[-\frac{1}{2}\mu] + (\beta^s)^2\dot{\beta}^s\dot{\epsilon}_1^s[-\frac{9}{2}] + (\beta^s)^2\dot{\beta}^s\dot{\epsilon}_2^s[-\frac{3}{2}\mu] + (\beta^s)^2(\dot{\epsilon}_1^s)^2[\frac{1}{2}(3+\mu)]$ $+ (\beta^s)^2\dot{\epsilon}_1^s\dot{\epsilon}_2^s[\mu] + \beta^s(\dot{\epsilon}_1^s)^3[\cot\phi] + \beta^s(\dot{\epsilon}_1^s)^2\dot{\epsilon}_2^s[\mu\cot\phi] + \beta^s(\dot{\epsilon}_1^s)^2\dot{\epsilon}_2^s[\mu]$ $+ \beta^s(\dot{\epsilon}_1^s)^2\dot{\epsilon}_2^s[\mu] + \beta^s\dot{\epsilon}_1^s\dot{\epsilon}_2^s\dot{\epsilon}_1^s[2\mu] + \beta^s(\dot{\epsilon}_1^s)^3 + \beta^s(\dot{\epsilon}_1^s)^2\dot{\epsilon}_1^s[3]$ |

TABLE 4.1; Definition of terms in equation (4.31), page 2 of 2.

| | | |
|------------------|---|---|
| $A_{1,0}$ | = | $\beta^i [\frac{1}{2} \beta^i (1 - \mu) \cot \phi + \beta^i - \epsilon_1^i - \mu \epsilon_2^i] + \beta^i \epsilon_1^i [-2\beta^i + \epsilon_1^i + \mu \epsilon_2^i]$ $+ (\beta^i)^2 [-\frac{1}{2} \beta^i - (1 - \frac{1}{2} \mu) \epsilon_1^i \cot \phi - \frac{1}{2} \mu \epsilon_2^i \cot \phi - \frac{1}{2} \mu \epsilon_2^i - \epsilon_1^i] + \beta^i \beta^i \epsilon_2^i [-\mu]$ $+ (\beta^i)^2 [\frac{1}{4} Q_\phi^i + \frac{1}{4} Q_\phi^i \cot \phi] + \epsilon_1^i \beta^i [-\frac{1}{2} Q_\phi^i] + \beta^i \beta^i [\frac{1}{2} Q_\phi^i]$ |
| $A_{3,0}$ | = | $\beta^i [\frac{1}{2} (1 + \mu) \beta^i + \epsilon_1^i \cot \phi + \mu \epsilon_2^i \cot \phi + \epsilon_1^i + \mu \epsilon_2^i] + \beta^i [\epsilon_1^i + \mu \epsilon_2^i]$ $+ (\beta^i)^2 [\frac{1}{2} \beta^i \cot \phi + \frac{3}{2} \beta^i - (1 + \frac{1}{2} \mu) \epsilon_1^i - \frac{1}{2} \mu \epsilon_2^i] + \beta^i \epsilon_1^i [-\epsilon_1^i - \mu \epsilon_2^i]$ $+ \beta^i \epsilon_1^i [-\epsilon_1^i \cot \phi - \mu \epsilon_2^i \cot \phi - 2\epsilon_1^i - \mu \epsilon_2^i] + \beta^i \epsilon_1^i \epsilon_2^i [-\mu] + (\beta^i)^2 [\frac{1}{4} Q_\phi^i]$ $+ \beta^i \epsilon_1^i [\frac{1}{2} Q_\phi^i \cot \phi + \frac{1}{2} Q_\phi^i] + \beta^i \epsilon_1^i [\frac{1}{2} Q_\phi^i] + \epsilon_1^i \beta^i [\frac{1}{2} Q_\phi^i]$ |
| $B_{1,1}(x^s)$ | = | $2\beta^s$ |
| $B_{3,1}(x^s)$ | = | $-2(\epsilon_1^s + \epsilon_2^s)$ |
| $B_{1,2}(x^s)^2$ | = | $2\beta^s \epsilon_2^s$ |
| $B_{3,2}(x^s)^2$ | = | $-2\epsilon_1^s \epsilon_2^s$ |
| $B_{1,0}$ | = | 0 |
| $B_{3,0}$ | = | -2 |

TABLE 4.2; Definition of terms in equation (4.39), page 1 of 6.

| | |
|---------------|---|
| $[A_{1,0}]_x$ | $=$ $ \begin{aligned} & u[-(1+\alpha)(\mu + \cot^2 \phi)] + \dot{u}[(1+\alpha) \cot \phi] + \ddot{u}[(1+\alpha)] \\ & + \ddot{u}\left[\frac{1}{2}(1+\alpha)(1-\mu)/\sin^2 \phi\right] + \dot{w}[(1+\mu) + \alpha(\mu + \cot^2 \phi)] + \ddot{w}[-\alpha \cot \phi] \\ & + \ddot{w}[-\alpha] + \ddot{w}[2\alpha \cot \phi/\sin^2 \phi] + \dot{w}[-\alpha/\sin^2 \phi] + \dot{v}\left[-\frac{1}{2}(1+\alpha)(3 - \mu \cot \phi/\sin \phi)\right] \\ & + \dot{v}\left[\frac{1}{2}(1+\alpha)(1+\mu)\right] + u\left[\frac{1}{2}Q_\phi^i\right] + \dot{w}\left[-\frac{1}{2}Q_\phi^i\right] + \ddot{u}\left[-\frac{1}{2}Q_\phi^i/\sin^2 \phi\right] + \dot{v}\left[\frac{1}{2}Q_\phi^i \cot \phi/\sin \phi\right] \end{aligned} $ |
| $[A_{2,0}]_x$ | $=$ $ \begin{aligned} & \dot{u}\left[\frac{1}{2}(1+\alpha)(3 - \mu) \cot \phi/\sin \phi\right] + \dot{u}\left[\frac{1}{2}(1+\alpha)(1+\mu)/\sin \phi\right] \\ & + \dot{v}\left[\frac{1}{2}(1+\alpha)(1-\mu)(1 - \cot^2 \phi)\right] + \dot{v}\left[\frac{1}{2}(1+\alpha)(1-\mu) \cot \phi\right] + \dot{v}\left[\frac{1}{2}(1+\alpha)(1-\mu)\right] \\ & + \ddot{v}[(1+\alpha)/\sin^2 \phi] + \dot{w}\left[-\alpha(1-\mu)/\sin \phi + (1+\mu)/\sin \phi\right] + \dot{w}[-\alpha \cot \phi/\sin \phi] \\ & + \ddot{w}[-\alpha/\sin \phi] + \ddot{w}[-\alpha/\sin^3 \phi] + \dot{u}\left[-\frac{1}{2}Q_\phi^i \cot \phi/\sin \phi\right] + \dot{v}\left[\frac{1}{2}Q_\phi^i/\sin^2 \phi\right] \\ & + \dot{w}\left[-\frac{1}{2}Q_\phi^i/\sin \phi\right] + \dot{v}\left[-\frac{1}{2}Q_\phi^i - \frac{1}{2}Q_\phi^i \cot \phi\right] + \dot{v}\left[-\frac{1}{2}Q_\phi^i\right] \end{aligned} $ |
| $[A_{3,0}]_x$ | $=$ $ \begin{aligned} & u[-\alpha(\cot \phi/\sin^2 \phi + (1-\mu) \cot \phi) + (1+\mu) \cot \phi] + \dot{u}[(1+\alpha)(1+\mu) + \alpha \cot^2 \phi] \\ & + \dot{u}[-2\alpha \cot \phi] + \ddot{u}[-\alpha] + \ddot{u}[-\alpha \cot \phi/\sin^2 \phi] + \ddot{u}[-\alpha/\sin^2 \phi] \\ & + \dot{v}[-\alpha(1/\sin^3 \phi + (1-\mu)/\sin \phi) + (1+\mu)/\sin \phi] + \dot{v}[\alpha \cot \phi/\sin \phi] + \dot{v}[-\alpha/\sin \phi] \\ & + \ddot{v}[-\alpha/\sin^3 \phi] + \dot{w}[2(1+\mu)] + \dot{w}[\alpha(\cot \phi/\sin^2 \phi + (1-\mu) \cot \phi)] \\ & + \ddot{w}[-\alpha(1+\mu + \cot^2 \phi)] + \ddot{w}[2\alpha \cot \phi] + \ddot{w}[\alpha] \\ & + \ddot{w}[4\cot^2 \phi/\sin^2 \phi + (3-\mu)/\sin^2 \phi] + \ddot{w}[-2\alpha \cot \phi/\sin^2 \phi] + \ddot{w}[2\alpha/\sin^2 \phi] \\ & + \ddot{w}[\alpha/\sin^4 \phi] + u\left[-\frac{1}{2}Q_\phi^i - \frac{1}{2}Q_\phi^i \cot \phi\right] + \dot{v}\left[-\frac{1}{2}Q_\phi^i/\sin \phi\right] + \dot{u}\left[-\frac{1}{2}Q_\phi^i\right] \\ & + \dot{w}\left[\frac{1}{2}Q_\phi^i + \frac{1}{2}Q_\phi^i \cot \phi\right] + \ddot{w}\left[\frac{1}{2}Q_\phi^i\right] + \ddot{w}\left[\frac{1}{2}Q_\phi^i \sin^2 \phi\right] \end{aligned} $ |

TABLE 4.2; Definition of terms in equation (4.39), page 2 of 6.

| | |
|----------------------|--|
| $[A_{1,1}(x^s)]_x =$ | $ \begin{aligned} & u[-\dot{\epsilon}_1^s - \mu\dot{\epsilon}_2^s + \dot{\beta}^s + (1 - 2\mu)\dot{\beta}^s \cot \phi] + w[-(1 + \mu)\dot{\beta}^s] \\ & + \dot{w}[\dot{\epsilon}_1^s + \mu\dot{\epsilon}_2^s - \dot{\beta}^s - (1 - \mu)\dot{\beta}^s \cot \phi] + \ddot{w}[-\dot{\beta}^s] + \ddot{u}[\mu(\dot{\epsilon}_1^s + \dot{\epsilon}_2^s)/\sin^2 \phi] \\ & + \ddot{w}[-\frac{1}{2}(1 - \mu)\dot{\beta}^s/\sin^2 \phi] + \dot{v}[-\mu(\dot{\epsilon}_1^s + \dot{\epsilon}_2^s)\cot \phi/\sin \phi + \frac{1}{2}(1 - 3\mu)\dot{\beta}^s/\sin \phi] \\ & + \dot{v}[-\frac{1}{2}(1 - \mu)(\dot{\epsilon}_1^s + \dot{\epsilon}_2^s)/\sin \phi] + u[\frac{1}{2}\dot{Q}_\phi^i \dot{\beta}^s - \frac{1}{2}\dot{Q}_\phi^i (\dot{\beta}^s + \dot{\beta}^s \cot \phi - \dot{\epsilon}_1^s)] + w[-\frac{1}{2}\dot{Q}_\phi^i \dot{\beta}^s] \\ & + \dot{w}[-\frac{1}{2}\dot{Q}_\phi^i \dot{\beta}^s + \frac{1}{2}\dot{Q}_\phi^i (\dot{\epsilon}_1^s - \dot{\beta}^s - \dot{\beta}^s \cot \phi)] + \ddot{u}[\frac{1}{2}\dot{Q}_\phi^i \dot{\epsilon}_2^s/\sin^2 \phi] + \dot{v}[-\frac{1}{2}\dot{Q}_\phi^i \dot{\epsilon}_2^s \cot \phi/\sin \phi] \\ & + \ddot{w}[-\frac{1}{2}\dot{Q}_\phi^i \dot{\beta}^s] \end{aligned} $ |
| $[A_{2,1}(x^s)]_x =$ | $ \begin{aligned} & \dot{u}[\mu(\dot{\epsilon}_1^s + \dot{\epsilon}_2^s)\cot \phi/\sin \phi - \frac{1}{2}(1 - \mu)(\dot{\epsilon}_1^s + \dot{\epsilon}_2^s)/\sin \phi - \frac{1}{2}(1 - 3\mu)\dot{\beta}^s/\sin \phi] \\ & + v[(1 - \frac{1}{2}(1 + \mu) - \mu\cot^2 \phi)\dot{\epsilon}_1^s + (-\frac{1}{2}(3 - \mu) - \mu\cot^2 \phi)\dot{\epsilon}_2^s + \frac{1}{2}(1 - \mu)(\dot{\epsilon}_1^s + \dot{\epsilon}_2^s)\cot \phi \\ & \quad + \frac{3}{2}(1 - \mu)\dot{\beta}^s \cot \phi + \frac{1}{2}(1 - \mu)\dot{\beta}^s] \\ & + \dot{w}[\mu\dot{\epsilon}_1^s/\sin \phi + \dot{\epsilon}_2^s/\sin \phi - \frac{1}{2}(1 - \mu)\dot{\beta}^s/\sin \phi - \frac{1}{2}(1 - \mu)\dot{\beta}^s \cot \phi/\sin \phi] \\ & + \dot{u}[-\frac{1}{2}(1 - \mu)(\dot{\epsilon}_1^s + \dot{\epsilon}_2^s)/\sin \phi] + \dot{v}[\mu(\dot{\epsilon}_1^s + \dot{\epsilon}_2^s) + \mu(\dot{\epsilon}_1^s + \dot{\epsilon}_2^s)\cot \phi] \\ & + \dot{w}[-\frac{1}{2}(1 + \mu)\dot{\beta}^s/\sin \phi] + \ddot{v}[\mu(\dot{\epsilon}_1^s + \dot{\epsilon}_2^s)] + \dot{u}[\frac{1}{2}\dot{Q}_\phi^i \dot{\epsilon}_2^s \cot \phi/\sin \phi] \\ & + v[-\frac{1}{2}\dot{Q}_\phi^i \dot{\epsilon}_2^s/\sin^2 \phi] + \dot{w}[\frac{1}{2}\dot{Q}_\phi^i \dot{\epsilon}_2^s/\sin \phi] + \dot{v}[\frac{1}{2}\dot{Q}_\phi^i \dot{\epsilon}_1^s + \frac{1}{2}\dot{Q}_\phi^i (\dot{\epsilon}_1^s + \dot{\epsilon}_1^s \cot \phi)] \\ & + \ddot{v}[\frac{1}{2}\dot{Q}_\phi^i \dot{\epsilon}_1^s] \end{aligned} $ |
| $[A_{3,1}(x^s)]_x =$ | $ \begin{aligned} & u[(\dot{\epsilon}_1^s + \mu\dot{\epsilon}_2^s)\cot \phi + \dot{\epsilon}_1^s + \mu\dot{\epsilon}_2^s + \dot{\beta}^s + \mu\dot{\beta}^s \cot \phi] \\ & + \dot{v}[(\mu\dot{\epsilon}_1^s + \dot{\epsilon}_2^s)/\sin \phi + \mu\dot{\beta}^s/\sin \phi - \frac{1}{2}(1 - \mu)\dot{\beta}^s \cot \phi/\sin \phi] \\ & + w[(1 + \mu)(\dot{\beta}^s + \dot{\beta}^s \cot \phi)] + u[\dot{\epsilon}_1^s + \mu\dot{\epsilon}_2^s + \dot{\beta}^s + (1 + \mu)\dot{\beta}^s \cot \phi] \\ & + \dot{v}[\frac{1}{2}(1 + \mu)\dot{\beta}^s/\sin \phi] + \dot{w}[-\dot{\epsilon}_1^s - \mu\dot{\epsilon}_2^s - (\dot{\epsilon}_1^s + \mu\dot{\epsilon}_2^s)\cot \phi] + \ddot{u}[\dot{\beta}^s] + \ddot{w}[-\dot{\epsilon}_1^s + \mu\dot{\epsilon}_2^s] \\ & + \ddot{w}[-(\dot{\epsilon}_2^s + \mu\dot{\epsilon}_1^s)/\sin^2 \phi] + \ddot{u}[\frac{1}{2}(1 - \mu)\dot{\beta}^s/\sin^2 \phi] \\ & + u[\frac{1}{2}\dot{Q}_\phi^i \dot{\epsilon}_1^s + \frac{1}{2}\dot{Q}_\phi^i (\dot{\epsilon}_1^s + \dot{\epsilon}_1^s \cot \phi + \dot{\beta}^s)] + \dot{v}[\frac{1}{2}\dot{Q}_\phi^i \dot{\epsilon}_2^s/\sin \phi] \\ & + w[\frac{1}{2}\dot{Q}_\phi^i \dot{\beta}^s + \frac{1}{2}\dot{Q}_\phi^i (\dot{\beta}^s + \dot{\beta}^s \cot \phi)] + u[\frac{1}{2}\dot{Q}_\phi^i \dot{\beta}^s + \frac{1}{2}\dot{Q}_\phi^i (\dot{\epsilon}_1^s + \dot{\beta}^s + \dot{\beta}^s \cot \phi)] \\ & + \dot{w}[-\frac{1}{2}\dot{Q}_\phi^i \dot{\epsilon}_1^s - \frac{1}{2}\dot{Q}_\phi^i (\dot{\epsilon}_1^s + \dot{\epsilon}_1^s \cot \phi)] + \ddot{u}[\frac{1}{2}\dot{Q}_\phi^i \dot{\beta}^s] + \ddot{w}[-\frac{1}{2}\dot{Q}_\phi^i \dot{\epsilon}_1^s] + \ddot{w}[-\frac{1}{2}\dot{Q}_\phi^i \dot{\epsilon}_2^s/\sin^2 \phi] \end{aligned} $ |

TABLE 4.2; Definition of terms in equation (4.39), page 3 of 6.

| | |
|------------------------|--|
| $[A_{1,2}(x^s)^2]_x =$ | $ \begin{aligned} & u \left[-\frac{1}{2}(3-\mu)(\beta^s)^2 + (\epsilon_1^s)^2 + \mu\epsilon_1^s \epsilon_2^s - \beta^s(2\epsilon_1^s + \mu\epsilon_2^s) - \beta^s(2\epsilon_1^s + \mu\epsilon_2^s) \right. \\ & \quad \left. - \beta^s(2\epsilon_1^s + \mu\epsilon_2^s) \cot \phi + 2\mu\epsilon_1^s \beta^s \cot \phi - \mu\beta^s \beta^s \cot \phi \right] \\ & + \dot{u}[-2\beta^s \beta^s - (\beta^s)^2 \cot \phi] + \ddot{u}[-(\beta^s)^2] \\ & + \ddot{u}[-\frac{1}{2}(1-2\mu)(\beta^s)^2 + \frac{1}{2}(1-3\mu)(\epsilon_2^s)^2 - \mu\epsilon_1^s \epsilon_2^s / \sin^2 \phi] \\ & + w[-(2+\mu)\beta^s \beta^s + (2+\mu)\beta^s \epsilon_1^s + \beta^s \epsilon_2^s - (\beta^s)^2 \cot \phi] \\ & + \dot{w} \left[\frac{1}{2}(1-\mu)(\beta^s)^2 - \epsilon_1^s (\epsilon_1^s + \mu\epsilon_2^s) + \beta^s(2\epsilon_1^s + \mu\epsilon_2^s) + \beta^s(2\epsilon_1^s + \mu\epsilon_2^s) \right. \\ & \quad \left. + \beta^s(2\epsilon_1^s + \mu\epsilon_2^s) \cot \phi - \mu\beta^s \epsilon_1^s \cot \phi \right] \\ & + \ddot{w}[\beta^s(2\epsilon_1^s + \mu\epsilon_2^s)] + \ddot{w}[\frac{1}{2}(1-\mu)\beta^s(\epsilon_1^s + 2\epsilon_2^s) / \sin^2 \phi] \\ & + \dot{v} \left[\left\{ \frac{1}{2}(1-2\mu)(\beta^s)^2 - \frac{1}{2}(1-3\mu)(\epsilon_2^s)^2 + \mu\epsilon_1^s \epsilon_2^s \right\} \cot \phi / \sin \phi \right. \\ & \quad \left. + \{ \mu\epsilon_1^s \beta^s - \mu\beta^s \beta^s - \frac{1}{2}(1-\mu)\beta^s(\epsilon_1^s + 2\epsilon_2^s) \} / \sin \phi \right] \\ & + \dot{v}[-\frac{1}{2}\mu(\beta^s)^2 / \sin \phi + \frac{1}{2}(1-\mu)((\epsilon_1^s)^2 + (\epsilon_2^s)^2 - (\beta^s)^2 + \epsilon_1^s \epsilon_2^s) / \sin \phi] \\ & + u[\frac{1}{2}Q_\phi^i((\epsilon_1^s)^2 - \frac{3}{2}(\beta^s)^2 - 2\beta^s \epsilon_1^s - 2\beta^s \epsilon_1^s - 2\beta^s \epsilon_1^s \cot \phi) - Q_\phi^i \epsilon_1^s \beta^s] \\ & + \dot{u}[-\frac{1}{2}Q_\phi^i(\beta^s)^2 - \frac{1}{2}Q_\phi^i((\beta^s)^2 \cot \phi + 2\beta^s \beta^s)] \\ & + w[-\frac{1}{2}Q_\phi^i(\beta^s)^2 - \frac{1}{2}Q_\phi^i((\beta^s)^2 \cot \phi + 2\beta^s \beta^s + 2\beta^s \epsilon_1^s)] \\ & + \dot{w}[-\frac{1}{2}Q_\phi^i((\epsilon_1^s)^2 - \frac{1}{2}(\beta^s)^2 - 2\beta^s \epsilon_1^s - 2\beta^s \epsilon_1^s - 2\beta^s \epsilon_1^s \cot \phi) - Q_\phi^i \beta^s \epsilon_1^s] \\ & + \ddot{u}[-\frac{1}{2}Q_\theta^i(\epsilon_2^s)^2 / \sin^2 \phi] + \dot{v}[\frac{1}{2}Q_\theta^i \epsilon_2^s \cot \phi / \sin \phi] + \ddot{u}[-\frac{1}{2}Q_\phi^i(\beta^s)^2] + \ddot{w}[Q_\phi^i \beta^s \epsilon_1^s] \end{aligned} $ |
|------------------------|--|

TABLE 4.2; Definition of terms in equation (4.39), page 4 of 6.

| | |
|------------------------|--|
| $[A_{2,2}(x^s)^2]_x =$ | $\begin{aligned} & \dot{u} \left[-\frac{1}{2}(1-2\mu)(\beta^s)^2 + \frac{1}{2}(1-3\mu)(\epsilon_2^s)^2 - \mu\epsilon_1^s \epsilon_2^s \right] \cot \phi / \sin \phi - \mu\epsilon_1^s \beta^s / \sin \phi \\ & + (1-\mu) \left\{ -\beta^s \dot{\beta}^s + \epsilon_1^s (\dot{\epsilon}_1^s + \frac{1}{2}\dot{\epsilon}_2^s) + \epsilon_2^s (\dot{\epsilon}_2^s + \frac{1}{2}\dot{\epsilon}_1^s) + \frac{1}{2}\beta^s (\dot{\epsilon}_1^s + 2\dot{\epsilon}_2^s) \right\} / \sin \phi \\ & + v \left[\left\{ \frac{1}{2}(1-2\mu)(\beta^s)^2 - \frac{1}{2}(1-3\mu)(\epsilon_2^s)^2 + \mu\epsilon_1^s \epsilon_2^s \right\} \cot^2 \phi - \frac{1}{2}(\beta^s)^2 + \epsilon_2^s (\epsilon_2^s + \mu\epsilon_1^s) \right. \\ & + (1-\mu) \left\{ \beta^s \dot{\beta}^s - \epsilon_1^s (\dot{\epsilon}_1^s + \frac{1}{2}\dot{\epsilon}_2^s) - \epsilon_2^s (\dot{\epsilon}_2^s + \frac{1}{2}\dot{\epsilon}_1^s) \right\} \cot \phi \\ & + (1-\mu) \left\{ -\frac{1}{2}(\beta^s)^2 + \frac{1}{2}(\epsilon_1^s)^2 + \frac{1}{2}(\epsilon_2^s)^2 + \frac{1}{2}\epsilon_1^s \epsilon_2^s \right\} \\ & - (1-\mu) \left\{ \frac{1}{2}\beta^s (2\dot{\epsilon}_1^s + \dot{\epsilon}_2^s) + \frac{1}{2}\beta^s (2\dot{\epsilon}_1^s + \dot{\epsilon}_2^s) \right\} \\ & \left. - (1-\mu) \left\{ \frac{1}{2}\beta^s (2\dot{\epsilon}_1^s + \dot{\epsilon}_2^s) + \beta^s (\dot{\epsilon}_1^s + 2\dot{\epsilon}_2^s) \right\} \cot \phi \right] \\ & + \dot{w} \left[\left\{ \frac{1}{2}(1-\mu)(\beta^s)^2 - \epsilon_2^s (\mu\epsilon_1^s + \epsilon_2^s) \right\} / \sin \phi \right. \\ & + (1-\mu) \left\{ \frac{1}{2}\beta^s (2\dot{\epsilon}_1^s + \dot{\epsilon}_2^s) + \frac{1}{2}\beta^s (2\dot{\epsilon}_1^s + \dot{\epsilon}_2^s) \right\} / \sin \phi \\ & \left. + \frac{1}{2}(1-\mu)\beta^s (\dot{\epsilon}_1^s + 2\dot{\epsilon}_2^s) \cot \phi / \sin \phi \right] \\ & + \dot{u} \left[-\frac{1}{2}(\beta^s)^2 / \sin \phi + \frac{1}{2}(1-\mu) \left\{ (\dot{\epsilon}_1^s)^2 + (\dot{\epsilon}_2^s)^2 + \dot{\epsilon}_1^s \dot{\epsilon}_2^s \right\} / \sin \phi \right] \\ & + \dot{w} \left[\beta^s \dot{\epsilon}_1^s / \sin \phi + \frac{1}{2}(1-\mu)\beta^s \dot{\epsilon}_2^s / \sin \phi \right] \\ & + v \left[\mu\beta^s \dot{\beta}^s + (1-3\mu)\dot{\epsilon}_1^s \dot{\epsilon}_1^s - \mu(\dot{\epsilon}_1^s \dot{\epsilon}_2^s + \dot{\epsilon}_1^s \dot{\epsilon}_2^s) \right. \\ & \left. + \left\{ \frac{1}{2}\mu(\beta^s)^2 + \frac{1}{2}(1-3\mu)(\epsilon_1^s)^2 - \mu\epsilon_1^s \epsilon_2^s \right\} \cot \phi \right] \\ & + v \left[\frac{1}{2}\mu(\beta^s)^2 + \frac{1}{2}(1-3\mu)(\epsilon_1^s)^2 - \mu\epsilon_1^s \epsilon_2^s \right] + \dot{u} \left[-\frac{1}{2}Q_8^i (\epsilon_2^s)^2 \cot \phi / \sin \phi \right] \\ & + v \left[\frac{1}{2}Q_8^i (\epsilon_2^s)^2 \cot^2 \phi + \frac{1}{2}Q_8^i (\epsilon_2^s)^2 \right] + \dot{w} \left[-\frac{1}{2}Q_8^i (\epsilon_2^s)^2 / \sin \phi \right] \\ & + v \left[-\frac{1}{2}Q_\phi^i \left\{ (\dot{\epsilon}_1^s)^2 - \frac{1}{2}(\beta^s)^2 \right\} - \frac{1}{2}Q_\phi^i \left\{ 2\dot{\epsilon}_1^s \dot{\epsilon}_1^s - \beta^s \dot{\beta}^s + (\dot{\epsilon}_1^s)^2 \cot \phi - \frac{1}{2}(\beta^s)^2 \cot \phi \right\} \right] \\ & + v \left[-\frac{1}{2}Q_\phi^i \left\{ (\dot{\epsilon}_1^s)^2 - \frac{1}{2}(\beta^s)^2 \right\} \right] \end{aligned}$ |
|------------------------|--|

TABLE 4.2; Definition of terms in equation (4.39), page 5 of 6.

| | |
|-----------------------|---|
| $[A_{3,2}(x^s)^2x] =$ | $ \begin{aligned} & u[3\beta^s\dot{\beta}^s - 2\dot{\epsilon}_1^s\dot{\epsilon}_1^s - \mu(\dot{\beta}^s\dot{\epsilon}_2^s + \dot{\epsilon}_1^s\dot{\epsilon}_2^s) + \beta^s(-2\dot{\epsilon}_1^s - \mu\dot{\epsilon}_2^s) \\ & \quad + \{\frac{3}{2}(\beta^s)^2 - (\dot{\epsilon}_1^s)^2 - \mu\dot{\epsilon}_1^s\dot{\epsilon}_2^s - \mu\dot{\beta}^s\dot{\epsilon}_1^s - \mu\dot{\beta}^s\dot{\epsilon}_1^s - \frac{1}{2}\mu(\beta^s)^2\} \cot \phi] \\ & + \dot{v}[\frac{1}{2}(1-\mu)(\beta^s)^2 - (\dot{\epsilon}_2^s)^2 - \mu\dot{\epsilon}_1^s\dot{\epsilon}_2^s - \mu\dot{\beta}^s\dot{\epsilon}_1^s - \mu\dot{\beta}^s\dot{\epsilon}_1^s] / \sin \phi \\ & \quad + \frac{1}{2}(1-\mu)\beta^s(2\dot{\epsilon}_2^s + \dot{\epsilon}_1^s) \cot \phi / \sin \phi] \\ & + w[-(1+\mu)(\beta^s)^2 - \beta^s(2\dot{\epsilon}_1^s + \mu\dot{\epsilon}_2^s) - \beta^s(2\dot{\epsilon}_1^s + \mu\dot{\epsilon}_2^s) - \mu(\dot{\epsilon}_1^s\dot{\beta}^s + \dot{\epsilon}_1^s\dot{\beta}^s) \\ & \quad - \beta^s(2\dot{\epsilon}_1^s + \mu\dot{\epsilon}_2^s) \cot \phi - \mu\dot{\epsilon}_1^s\dot{\beta}^s \cot \phi] \\ & + \dot{u}[-\frac{1}{2}(1+\mu)(\beta^s)^2 - \dot{\epsilon}_1^s(\dot{\epsilon}_1^s + \mu\dot{\epsilon}_2^s) - \beta^s(2\dot{\epsilon}_1^s + \mu\dot{\epsilon}_2^s) - \beta^s(2\dot{\epsilon}_1^s + \mu\dot{\epsilon}_2^s) \\ & \quad - \beta^s(2\dot{\epsilon}_1^s + \mu\dot{\epsilon}_2^s) \cot \phi - \mu\dot{\epsilon}_1^s\dot{\beta}^s \cot \phi] \\ & + \dot{w}[-3\beta^s\dot{\beta}^s + 2\dot{\epsilon}_1^s\dot{\epsilon}_1^s + \mu(\dot{\epsilon}_1^s\dot{\epsilon}_2^s + \dot{\epsilon}_1^s\dot{\epsilon}_2^s) + \{-\frac{3}{2}(\beta^s)^2 + (\dot{\epsilon}_1^s)^2 + \mu\dot{\epsilon}_1^s\dot{\epsilon}_2^s\} \cot \phi] \\ & + \dot{v}[-\mu\dot{\epsilon}_1^s\dot{\beta}^s / \sin \phi - \frac{1}{2}(1-\mu)\beta^s(2\dot{\epsilon}_1^s + \dot{\epsilon}_2^s) / \sin \phi] + \ddot{u}[-\beta^s(2\dot{\epsilon}_1^s + \mu\dot{\epsilon}_2^s)] \\ & + \ddot{w}[-\frac{3}{2}(\beta^s)^2 + (\dot{\epsilon}_1^s)^2 + \mu\dot{\epsilon}_1^s\dot{\epsilon}_2^s] + \ddot{w}[-\frac{1}{2}(\beta^s)^2 + (\dot{\epsilon}_2^s)^2 + \mu\dot{\epsilon}_1^s\dot{\epsilon}_2^s] / \sin^2 \phi] \\ & + \ddot{u}[-\frac{1}{2}(1-\mu)\beta^s(\dot{\epsilon}_1^s + 2\dot{\epsilon}_2^s) / \sin^2 \phi] \\ & + u[-\frac{1}{2}Q_\phi^i \{2\dot{\epsilon}_1^s\dot{\epsilon}_1^s - 3\beta^s\dot{\beta}^s + (\dot{\epsilon}_1^s)^2 \cot \phi - \frac{3}{2}(\beta^s)^2 \cot \phi + 2\beta^s\dot{\epsilon}_1^s\} \\ & \quad - \frac{1}{2}Q_\phi^i \{(\dot{\epsilon}_1^s)^2 - \frac{3}{2}(\beta^s)^2\}] \\ & + \dot{v}[-\frac{1}{2}Q_\phi^i (\dot{\epsilon}_2^s)^2 / \sin \phi] \\ & + w[-Q_\phi^i \beta^s\dot{\epsilon}_1^s - \frac{1}{2}Q_\phi^i \{2\beta^s\dot{\epsilon}_1^s + 2\beta^s\dot{\epsilon}_1^s + 2\beta^s\dot{\epsilon}_1^s \cot \phi + (\beta^s)^2\}] \\ & + \dot{u}[-Q_\phi^i \beta^s\dot{\epsilon}_1^s - \frac{1}{2}Q_\phi^i \{2\beta^s\dot{\epsilon}_1^s + 2\beta^s\dot{\epsilon}_1^s + 2\beta^s\dot{\epsilon}_1^s \cot \phi + (\dot{\epsilon}_1^s)^2 - \frac{1}{2}(\beta^s)^2\}] \\ & + \dot{w}[\frac{1}{2}Q_\phi^i \{(\dot{\epsilon}_1^s)^2 - \frac{3}{2}(\beta^s)^2\} + \frac{1}{2}Q_\phi^i \{2\dot{\epsilon}_1^s\dot{\epsilon}_1^s - 3\beta^s\dot{\beta}^s + (\dot{\epsilon}_1^s)^2 \cot \phi - \frac{3}{2}(\beta^s)^2 \cot \phi\}] \\ & + \ddot{u}[-Q_\phi^i \beta^s\dot{\epsilon}_1^s] + \ddot{w}[\frac{1}{2}Q_\phi^i \{(\dot{\epsilon}_1^s)^2 - \frac{3}{2}(\beta^s)^2\}] + \ddot{w}[\frac{1}{2}Q_\phi^i (\dot{\epsilon}_2^s)^2 / \sin^2 \phi] \end{aligned} $ |
| $[A_{1,3}(x^s)^3]x =$ | $ \begin{aligned} & u[-\frac{9}{2}\beta^s(\beta^s)^2] + \dot{u}[2\beta^s\dot{\beta}^s(3\dot{\epsilon}_1^s + \mu\dot{\epsilon}_2^s) + (\beta^s)^2(3\dot{\epsilon}_1^s + \mu\dot{\epsilon}_2^s) \cot \phi] \\ & + w[2\beta^s\dot{\beta}^s(3\dot{\epsilon}_1^s + \mu\dot{\epsilon}_2^s) + (\beta^s)^2(3\dot{\epsilon}_1^s + \mu\dot{\epsilon}_2^s) \cot \phi] + \dot{w}[\frac{9}{2}\beta^s(\beta^s)^2 \\ & \quad + \frac{1}{2}(3-\mu)(\beta^s)^3 \cot \phi] + \ddot{u}[\frac{1}{2}(2-3\mu)(\beta^s)^2(\dot{\epsilon}_1^s + \dot{\epsilon}_2^s) / \sin^2 \phi] \\ & + \ddot{w}[\frac{1}{4}(1-\mu)(\beta^s)^3 / \sin^2 \phi] + \dot{v}[2\mu\dot{\epsilon}_1^s\dot{\beta}^s\dot{\beta}^s / \sin \phi] + \ddot{u}[(\beta^s)^2(3\dot{\epsilon}_1^s + \mu\dot{\epsilon}_2^s)] \\ & + \ddot{w}[\frac{3}{2}(\beta^s)^3] + \dot{v}[\mu\dot{\epsilon}_1^s(\beta^s)^2 / \sin \phi + \frac{1}{2}(1-\mu)(\beta^s)^2(3\dot{\epsilon}_1^s + \dot{\epsilon}_2^s) / \sin \phi] \end{aligned} $ |

TABLE 4.2; Definition of terms in equation (4.39), page 6 of 6.

| | |
|-----------------------|---|
| $[A_{2,3}(x^s)^3]x =$ | $\begin{aligned} & \dot{u}[\frac{1}{2}(2-3\mu)(\beta^s)^2(\epsilon_1^s + \epsilon_2^s)\cot\phi/\sin\phi + (1-\mu)\beta^s\dot{\beta}^s(3\epsilon_1^s + \epsilon_2^s)/\sin\phi] \\ & + v[-\frac{1}{2}(2-3\mu)(\beta^s)^2(\epsilon_1^s + \epsilon_2^s)\cot^2\phi - \frac{3}{4}(1-\mu)(\beta^s)^2\dot{\beta}^s \\ & \quad - (1-\mu)\beta^s\dot{\beta}^s(3\epsilon_1^s + \epsilon_2^s)\cot\phi] \\ & + \dot{w}[\frac{3}{4}(1-\mu)(\beta^s)^2\dot{\beta}^s/\sin\phi] + \dot{u}[\mu\epsilon_1^s(\beta^s)^2/\sin\phi + \frac{1}{2}(1-\mu)(\beta^s)^2(3\epsilon_1^s + \epsilon_2^s)/\sin\phi] \\ & + \dot{v}[\beta^s\dot{\beta}^s(-\mu\epsilon_2^s + (1-4\mu)\epsilon_1^s)] \end{aligned}$ |
| $[A_{3,3}(x^s)^3]x =$ | $\begin{aligned} & u[\dot{\beta}^s\beta^s(-9\epsilon_1^s - 3\mu\epsilon_2^s) - \frac{3}{2}(\beta^s)^3 - \frac{3}{2}\mu(\beta^s)^2\dot{\beta}^s\cot\phi] + \dot{v}[-\frac{3}{2}\mu(\beta^s)^2\dot{\beta}^s/\sin\phi] \\ & + w[-\frac{9}{2}(\beta^s)^2\dot{\beta}^s - \frac{3}{2}(\beta^s)^3\cot\phi - \frac{3}{2}\mu(\beta^s)^2\dot{\beta}^s - \frac{1}{2}\mu(\beta^s)^3\cot\phi] \\ & + \dot{u}[-\frac{9}{2}(\beta^s)^2\dot{\beta}^s - \frac{1}{2}(3+\mu)(\beta^s)^3\cot\phi] \\ & + \dot{w}[\beta^s\dot{\beta}^s(9\epsilon_1^s + 3\mu\epsilon_2^s) + \frac{1}{2}(\beta^s)^2(9\epsilon_1^s + 3\mu\epsilon_2^s)\cot\phi] + \ddot{u}[-\frac{3}{2}(\beta^s)^3] \\ & + \ddot{w}[\frac{1}{2}(\beta^s)^2(9\epsilon_1^s + 3\mu\epsilon_2^s)] + \ddot{w}[\frac{1}{2}(2-\mu)(\beta^s)^2(\epsilon_1^s + \epsilon_2^s)/\sin^2\phi] \\ & + \ddot{u}[-\frac{1}{4}(1-\mu)(\beta^s)^3/\sin^2\phi] \end{aligned}$ |
| $[B_{1,0}]x =$ | $u[-2] + \dot{w}[2] + \dot{v}[\sin\phi]$ |
| $[B_{2,0}]x =$ | $\dot{u}[2\cos\phi] + \dot{u}[\sin\phi] + \dot{w}[2\sin\phi] + \dot{w}[-\cos\phi]$ |
| $[B_{3,0}]x =$ | $u[2\cot\phi] + w[4] + \dot{u}[2] + \dot{v}[1/\sin\phi] + \dot{v}[\cos\phi]$ |
| $[B_{1,1}(x^s)]x =$ | $u[-2\epsilon_2^s - 2\beta^s\cot\phi] + w[-2\beta^s] + \dot{v}[-\beta^s/\sin\phi] + \dot{w}[2\epsilon_2^s] + \dot{v}[\epsilon_2^s\sin\phi]$ |
| $[B_{2,1}(x^s)]x =$ | $\begin{aligned} & \dot{u}[(\epsilon_1^s + \epsilon_2^s + \beta^s\cot\phi)\cos\phi] + \dot{u}[\epsilon_2^s\sin\phi] + \dot{w}[(\epsilon_1^s + \epsilon_2^s + \beta^s\cot\phi)\sin\phi] \\ & + \dot{w}[-\epsilon_2^s\cos\phi] \end{aligned}$ |
| $[B_{3,1}(x^s)]x =$ | $u[2\epsilon_1^s\cot\phi] + w[2\epsilon_1^s + 2\epsilon_2^s] + \dot{u}[2\epsilon_2^s] + \dot{v}[\epsilon_1^s/\sin\phi] + \dot{v}[\epsilon_2^s\cos\phi]$ |

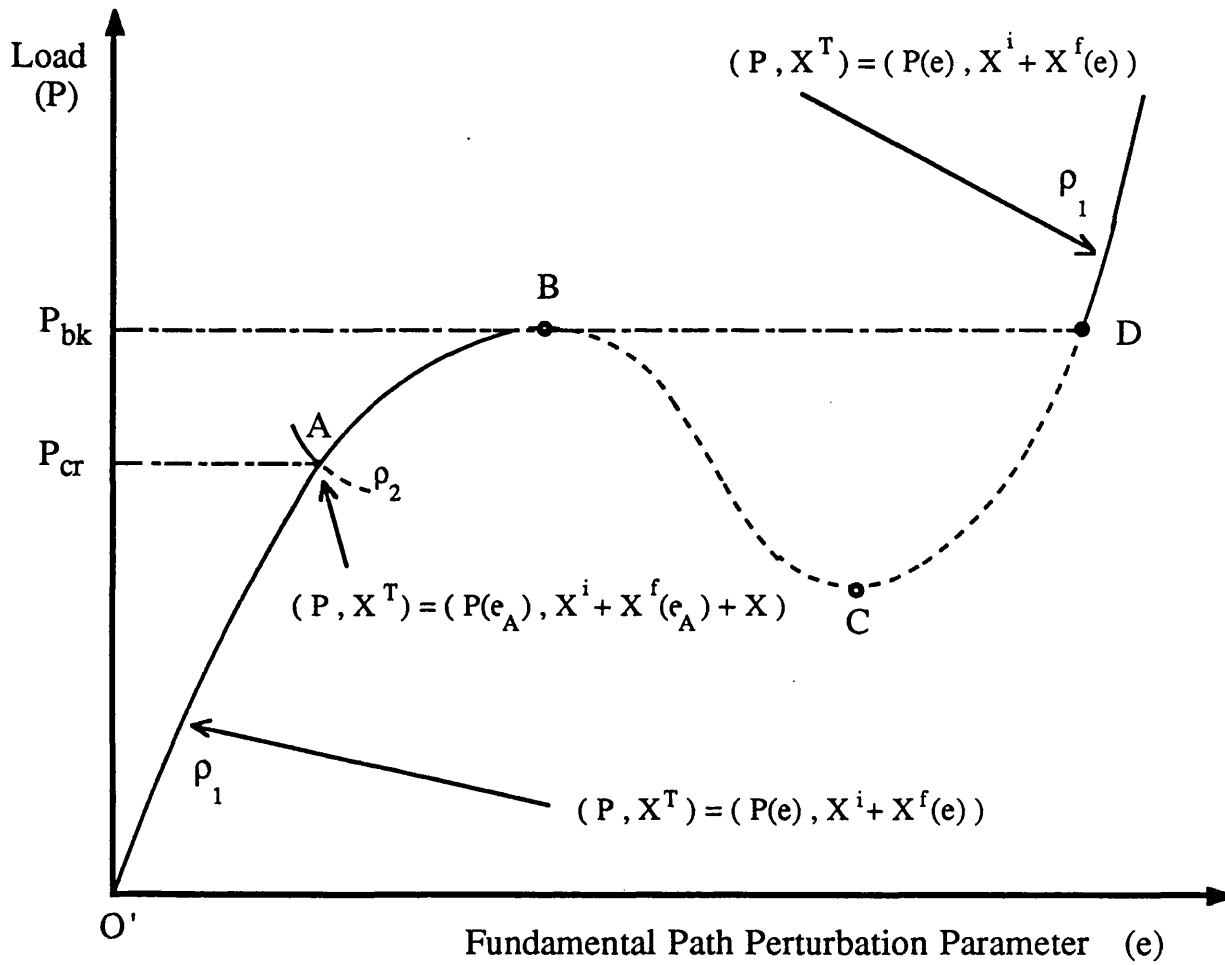
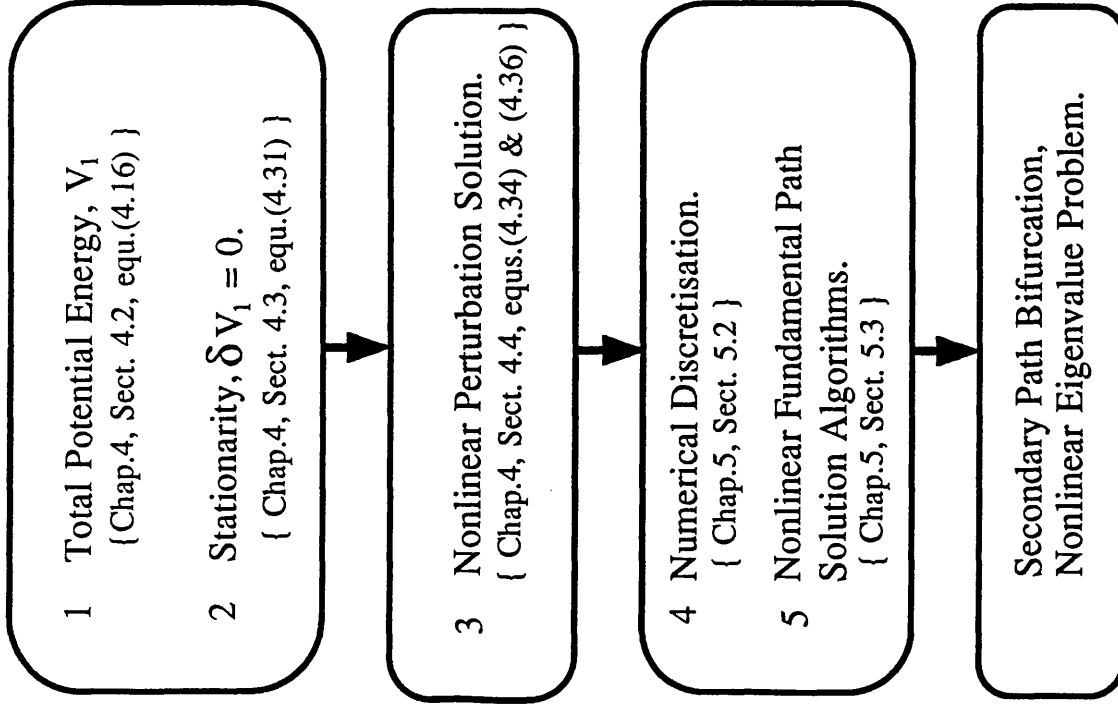


Figure 4.1 Fundamental and Secondary Equilibrium paths, Load -vs- Perturbation Parameter.

Nonlinear Fundamental Path



Secondary Path Bifurcation

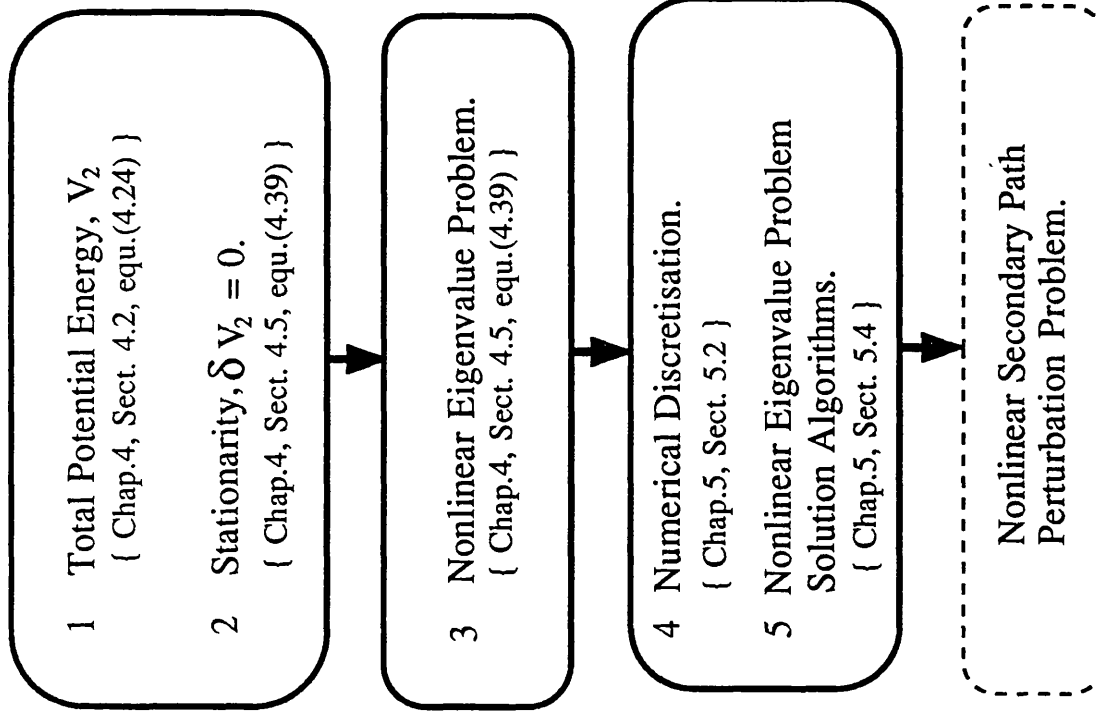


Figure 4.2 Key to Solution Methods for the Nonlinear Fundamental Path and Secondary Path Bifurcation

CHAPTER FIVE

NUMERICAL SOLUTION ALGORITHMS BASED ON FINITE DIFFERENCE SOLUTIONS OF THE KIRCHHOFF EQUATIONS

CHAPTER FIVE

CONTENTS

5.1 INTRODUCTION

5.2 THE FINITE DIFFERENCE DISCRETIZATION

5.3 THE FUNDAMENTAL PATH SOLUTION ALGORITHMS

5.4 THE SECONDARY PATH SOLUTION ALGORITHMS

5.4.1 The Linear Eigenvalue Problem

5.4.2 The Non-linear Eigenvalue Problem

NUMERICAL SOLUTION ALGORITHMS BASED ON FINITE DIFFERENCE SOLUTIONS OF THE KIRCHHOFF EQUATIONS

5.1 INTRODUCTION

The partial differential equations describing the fundamental path and the linearised secondary path equilibrium equations have been presented in Chapter Four. Exact circumferential modelling (the θ coordinate direction) was introduced in Chapter Four, leaving the generalised displacements $x=(u, v, w)$ as functions of only the meridional coordinate, ϕ . In this chapter numerical solution methods, based on finite difference approximations, are presented.

The accuracy with which finite difference expressions approximate the exact functions over the range of the function is (non-linearly) dependent upon the order of the finite difference expressions and the mesh or node spacing adopted. Storage requirements for banded matrices and vectors are linearly dependent on the nodal spacing, the order of the matrix or vector, while the order of the finite difference expressions have a weaker effect on the bandwidth of the matrices, and hence on storage requirements. For banded matrices the time required for computation varies for different parts of the solution algorithms, it is typically linearly dependent upon the order of the matrix, and either quadratically (Gaussian elimination) or linearly (back-substitution) dependent on the bandwidth. Due to these dependencies simple second order central finite difference expressions will not be the optimum expressions for use with the solution algorithms. //

The computer program was written in such a way that sets of finite difference expressions, and the portion of the shell surface over which they are to be applied, form part of the input data to the program. The expressions given in Section 5.2 are those that were adopted after conducting trials using various expressions. The effect of the order of finite difference expressions and nodal spacing on convergence is considered in more detail in Chapter Six.

The fundamental and secondary path equations that are the subject of the solution algorithms are both equilibrium equations, derived from the total potential energy functional. At various points during the solution method a check on the accuracy of the present solution is required, and these checks are performed within the context of the equilibrium equations.

The fundamental path solution algorithm is presented in Section 5.3 and the secondary path solution algorithm in Section 5.4. Once the fundamental and secondary path solutions have been determined, it is possible to calculate the various contributions to the strain and load terms of the total potential energy (Section 4.7). For a conservative system the sum of these various incremental energy contributions must be zero, therefore the error in the sum of these energy contributions may be used to provide a more independent check on the solution method and the internal accuracy required for the solution of the equilibrium equations.

5.2 THE FINITE DIFFERENCE DISCRETIZATION

Finite difference methods are based on approximating the dependent variable, $x(\phi)$, by a localised polynomial function \bar{x} , over a subregion of ϕ . If $x(\phi)$ is defined over the domain, $0 \leq \phi \leq l$ and the domain is divided into n equal intervals, $h=l/n$, then over the sub region r_j in the vicinity of ϕ_j the function x is approximated by \bar{x}_j

$$x \cong \bar{x}_j = \sum_{k=0}^l a_k z^k \quad (5.1)$$

where z is the local coordinate, $\phi = \phi_j + z$, as shown in Figure 5.1.

The derivatives in the sub region r_j are therefore approximated by

$$\frac{dx}{d\phi} \cong \frac{d\bar{x}_j}{dz} = \sum_{k=1}^l k a_k z^{k-1} \quad (5.2)$$

$$\frac{d^2x}{d\phi^2} \cong \frac{d^2\bar{x}_j}{dz^2} = \sum_{k=2}^l k(k-1) a_k z^{k-2}$$

$$\frac{d^3x}{d\phi^3} \cong \frac{d^3\bar{x}_j}{dz^3} = \sum_{k=3}^l k(k-1)(k-2) a_k z^{k-3}$$

$$\frac{d^4x}{d\phi^4} \cong \frac{d^4\bar{x}_j}{dz^4} = \sum_{k=4}^l k(k-1)(k-2)(k-3) a_k z^{k-4}$$

The coefficients a_k of the polynomial are defined by matching the values of \bar{x}_j with those of x at the $t+1$ nodes (..., $\phi_{j-3}, \phi_{j-2}, \phi_{j-1}, \phi_j, \phi_{j+1}, \phi_{j+2}, \dots$), which may be chosen symmetrically or not about ϕ_j . Choosing to match \bar{x}_j with x symmetrically about ϕ_j yields central finite differences, while varying degrees of forward or backward finite difference expressions result from appropriate non-symmetrical matching. //

$$\bar{x}_j \Big|_{z=ih} = x \Big|_{\phi_{j+i}} = x_{j+i} \quad ; \quad i = \dots -3, -2, -1, 0, 1, 2, \dots \quad (5.3)$$

Equation (5.1) subject to the conditions (5.3) results in a set of $t+1$ simultaneous equations which may be written as,

$$[H] \mathbf{a} = \mathbf{x} \quad (5.4)$$

and the solution is given by,

$$\mathbf{a} = [H]^{-1} \mathbf{x} \quad (5.5)$$

where \mathbf{a} is the coefficient vector $(a_0, a_1, a_2, \dots, a_t)^T$ and \mathbf{x} is the nodal value vector $(\dots, \bar{x}_{j-3}, \bar{x}_{j-2}, \bar{x}_{j-1}, \bar{x}_j, \bar{x}_{j+1}, \bar{x}_{j+2}, \dots)^T$, and the elements of $[H]$ are dependent on the node spacing h .

The derivatives of the local polynomial function \bar{x} , evaluated at ϕ_j , ($z=0$), are given by equation (5.2) as,

$$\left. \frac{d^s \bar{x}_j}{d\phi^s} \right|_{z=0} = s! a_s \quad (5.6)$$

and these are the finite difference approximations used in the discretization of the continuous differential equations presented in Chapter Four.

The accuracy of these expressions depends on the order of the polynomial, t , the order of the derivative, s , and the nodal spacing, h . By considering the largest of the neglected terms due to truncating the expression (5.2) at $k=t$, the error over the region r_j ; ($|z| \leq h/2$) may be evaluated and is of the order h^{t-s} .

The optimum choice of finite difference expressions for the discretization and subsequent computer solution for a particular problem is dependent on three main interrelated factors. The storage required by the program, the accuracy required, and the time taken to solve the problem; these all depend on the finite difference expressions selected. These factors influenced the choice of the finite difference expressions that were used, and will be discussed in Chapter Six with reference to the solution algorithms used by the computer program.

A computer program capable of generating finite difference expressions of any type and order of accuracy by the method outlined above was used. The finite difference expressions that were used are listed in Table 5.1, where they are written in the form,

$$\left. \frac{d^s x}{d\phi^s} \right|_{\phi_j} \cong \frac{d^s \bar{x}_j}{d\phi^s} = f_s \sum_{r=-5}^{+5} \alpha_{s,r} x_{j-r} \quad (5.7)$$

The coefficients, $\alpha_{s,r}$, and f_s , along with the order of accuracy of the expressions are all presented in Table 5.1.

The finite difference expressions are presented in seven groups for use with the shell equations, and two groups (one forward, one backward) for use with the boundary conditions. Figure 5.2 shows schematically at which of the equally spaced nodes on the spherical shell the various groups of finite difference expressions are used.

The fictitious nodes (0 and $n+1$) in Figure 5.2 are required for the application of the shell equations near the boundaries, and are defined by the boundary conditions at $\phi = 0$ and $\phi = \phi_b$.

Forward and backward finite difference expressions are used near the boundaries in order to avoid a need for more fictitious off shell nodes.

5.3 THE FUNDAMENTAL PATH SOLUTION ALGORITHMS

The solution algorithm for the nonlinear fundamental path is presented below in a general matrix/vector form.

The application of the finite difference expressions of Table 5.1 to equations (4.32), (4.34) and (4.36) allows them to be written in matrix form as follows.

From equation (4.32) we have,

$$\begin{aligned}\bar{x}^s &= \bar{x}^i + \bar{x}^f = \bar{x}^i + \bar{x}_0^f + \bar{x}_1 e + \bar{x}_2 e^2 + \dots = \bar{x}_0^s + \bar{x}_1 e + \bar{x}_2 e^2 + \dots \\ \hat{p} &= \hat{p}_0 + \hat{p}_1 e + \hat{p}_2 e^2 + \dots\end{aligned}\quad (5.8)$$

where $(\bar{x})^T = (u_1, w_1, u_2, w_2, \dots, u_n, w_n)$

Equation (4.34) yields a set of simultaneous equations which may be written in the form

$$[\bar{A}] (\bar{x}_r) = -\hat{p}_r (\bar{b}) - (\bar{d}_{r-1}) \quad (5.9)$$

Where the matrix $[\bar{A}]$ is given by

$$[\bar{A}] = \left[A_1 + A_2 \{2\bar{x}_0^s\} + A_3 \{3(\bar{x}_0^s)^2\} + A_4 \{4(\bar{x}_0^s)^3\} + \hat{p}_0 \{B_1 + B_2 2\bar{x}_0^s\} \right] \quad (5.10)$$

and the vectors \bar{b} and \bar{d}_{r-1} are defined by

$$\bar{b} = B_0 + B_1 \{\bar{x}_0^s\} + B_2 \{(\bar{x}_0^s)^2\} \quad (5.11)$$

$$\bar{d}_0 \equiv 0$$

$$\bar{d}_1 = -A_2 \{\bar{x}_1^2\} - A_3 \{3(\bar{x}_0^s) \bar{x}_1^2\} - A_4 \{6(\bar{x}_0^s)^2 \bar{x}_1^2\} - \hat{p}_1 B_1 \{\bar{x}_1\} - \hat{p}_1 B_2 \{2(\bar{x}_0^s) \bar{x}_1\}$$

$$\begin{aligned}\bar{d}_2 &= -A_2 \{2\bar{x}_1 \bar{x}_2\} - A_3 \{3(\bar{x}_1^3) + 6(\bar{x}_0^s) \bar{x}_1 \bar{x}_2\} - A_4 \{4(\bar{x}_0^s) \bar{x}_1^3\} \\ &\quad - A_4 \{12(\bar{x}_0^s) \bar{x}_1 \bar{x}_2\} - \hat{p}_1 B_1 \{\bar{x}_2\} - \hat{p}_2 B_1 \{\bar{x}_1\} - \hat{p}_1 B_2 \{\bar{x}_1^2\} \\ &\quad - \hat{p}_1 B_2 \{2(\bar{x}_0^s) \bar{x}_2\} - \hat{p}_2 B_2 \{2(\bar{x}_0^s) \bar{x}_1\} - \hat{p}_0 B_2 \{2\bar{x}_1 \bar{x}_2\}\end{aligned}$$

etc.

The matrix [A] is a 2n x 2n banded matrix, and the vectors (\bar{x}_r), (b) and (\bar{d}_{r-1}) are all of length 2n. In arriving at equations (5.9), (5.10) and (5.11) the equilibrium equations, E_i $i=1$ and 3 in equation (4.34), are taken in pairs at each of the on shell nodes of the finite difference grid, nodes 1 to n in Figure 5.2. And the boundary conditions, equations (2.76) and (2.77), are used to eliminate the non zero elements in the first and last four columns of the matrix, corresponding to the boundary and off shell fictitious nodes.

Finally equation (4.36) on application of the finite difference expression yields vector equations of the following form

$$(\hat{p}_1)^2 + (\bar{x}_1)^T \bar{x}_1 = a = \text{constant} \quad (5.12)$$

$$4\hat{p}_1 \hat{p}_2 + 4(\bar{x}_1)^T \bar{x}_2 = 0$$

$$6\hat{p}_1 \hat{p}_3 + 4(\hat{p}_2)^2 + 6(\bar{x}_1)^T \bar{x}_3 + 4(\bar{x}_2)^T \bar{x}_2 = 0$$

$$8\hat{p}_1 \hat{p}_4 + 12\hat{p}_2 \hat{p}_3 + 8(\bar{x}_1)^T \bar{x}_4 + 12(\bar{x}_2)^T \bar{x}_3 = 0$$

etc.

To solve the sequence of equations (5.9) for $r=1, 2, 3, \dots$ we may choose \hat{p}_1 arbitrarily and so solve for \bar{x}_1 ; in general we will need to make use of the condition (5.12) to solve for \hat{p}_r and \bar{x}_r , when $r \neq 1$.

Equation (5.9) may be manipulated to yield

$$[\bar{A}] (\bar{x}_r) = \frac{\hat{p}_r}{\hat{p}_1} [\bar{A}] (\bar{x}_1) + [\bar{A}] (\bar{x}_r^*) \quad (5.13)$$

in which

$$[\bar{A}] (\bar{x}_1) = -\hat{p}_1 (\bar{b})$$

$$[\bar{A}] (\bar{x}_r^*) = -(\bar{d}_{r-1})$$

and

$$\bar{x}_r = \bar{x}_r^* + \frac{\hat{p}_r}{\hat{p}_1} \bar{x}_1$$

Now (\bar{x}_r^*) is dependent on the previously known terms in (\bar{d}_{r-1}), and substituting for \bar{x}_r from (5.13) into (5.12) we arrive at,

$$(\hat{p}_1)^2 + (\bar{x}_1)^T \bar{x}_1 = a = \text{constant} \quad (5.14)$$

$$\hat{p}_2 = \frac{-4(\bar{x}_1)^T \bar{x}_2^*}{4(\hat{p}_1 + \frac{1}{\hat{p}_1} (\bar{x}_1)^T \bar{x}_1)}$$

$$\hat{p}_3 = \frac{-[4(\hat{p}_2)^2 + 4(\bar{x}_2)^T \bar{x}_2 + 6(\bar{x}_1)^T \bar{x}_3^*]}{6[\hat{p}_1 + \frac{1}{\hat{p}_1} (\bar{x}_1)^T \bar{x}_1]} \quad (5.14 \text{ contd.})$$

$$\hat{p}_4 = \frac{-[12\hat{p}_2\hat{p}_3 + 12(\bar{x}_2)^T \bar{x}_3 + 8(\bar{x}_1)^T \bar{x}_4^*]}{8[\hat{p}_1 + \frac{1}{\hat{p}_1} (\bar{x}_1)^T \bar{x}_1]}$$

etc.

And \hat{p}_r is now defined by the previously known terms $\hat{p}_{r-1}, \hat{p}_{r-2}, \dots$ and $\bar{x}_{r-1}, \bar{x}_{r-2}, \dots$, allowing both \hat{p}_r and \bar{x}_r to be evaluated. The solution algorithm is given schematically in Figure 5.3, where it is the portion of the total algorithm within the dotted line.

In setting up the $[\bar{A}]$ matrix and the (\bar{b}) vector, see Figure 5.3, equations (5.10) and (5.11) require \hat{p}_0, \bar{x}_0 and $\bar{x}^i, (\bar{x}_0 = \bar{x}^i + \bar{x}_0)$ to be specified. In general none of these are necessarily zero, but for the first entry ($t=1$) into the algorithm \hat{p}_0 and \bar{x}_0 will be zero, while \bar{x}^i will take the value specified by the initial imperfection profile. X

In using the perturbation method outlined here it was found that the fundamental path could not adequately be represented by a single polynomial series, equation (5.8). That is, the error in \bar{x}^f and \hat{p} increased, with 'e', reaching unacceptable levels within the range of 'e' that is of interest. It should be noted that this error is not entirely dependent on the number of terms in the series or on the choice of perturbation parameter, i.e. equation (5.14). That is equations (5.13) and $(\bar{d}_{r,1})$ defined by equation (5.11) are the result of specifying a perturbation series of the type (polynomial) given by equation (5.8). Choosing to identify the perturbation parameter with some physically or theoretically measurable path parameter, yields a condition, of the type given by equation (5.14), enabling \hat{p}_r to be specified in (5.13). Hence the magnitude of the vector \bar{x}_1 that is added to \bar{x}_r^i to give \bar{x}_r , equation (5.13), is determined. The convergence of the series, given by equation (5.8), at large values of 'e' will be limited by the inclusion of the \bar{x}_1 components in \bar{x}_r . And the \bar{x}_r vector may become divergent, increasing in magnitude and oscillating in sign as r increases.

The repeated use of the initial rate of change of the displacement profile, \bar{x}_1 , to force \bar{x}_r to satisfy the perturbation condition may be overcome by a repeated use of the perturbation method, so that it is the 'local initial' displacement vector $\bar{x}_{t,1}$ that is used to satisfy the perturbation condition.

We may write the general perturbation series as

$$\bar{x}_t^f = \bar{x}_{t,0} + \bar{x}_{t,1} e_l + \bar{x}_{t,2} e_l^2 + \dots \quad (5.15)$$

$$\hat{p}_t = \hat{p}_{t,0} + \hat{p}_{t,1} e_l + \hat{p}_{t,2} e_l^2 + \dots$$

where $e_l = e_g - a_{t-1}$ for $a_{t-1} \leq e_g \leq a_t$

and e_l is the local perturbation parameter, e_g the global perturbation parameter, and a_{t-1} and a_t are the lower and upper limits for e_g of the particular local perturbation series under consideration. The terms $\bar{x}_{t,0}$ and $\hat{p}_{t,0}$ are defined by

$$\bar{x}_{t,0} = \bar{x}_{t-1}^f \Big|_{e_g = a_{t-1}} \quad (5.16)$$

$$\hat{p}_{t,0} = \hat{p}_{t-1} \Big|_{e_g = a_{t-1}}$$

The solution algorithms described previously may be used to solve for the coefficients of the series given by equation (5.15). While the choice of $\hat{p}_{t,1}$ remains arbitrary, it will be helpful at a later stage to choose $\hat{p}_{t,1}$ such that the slope of the 'load-vs-e' graph is continuous, that is.

$$\hat{p}_{t,1} = \frac{d\hat{p}_{t-1}}{de_l} \Big|_{e_g = a_{t-1}} \quad (5.17)$$

After determining the coefficients of equation (5.15) an upper limit on e_g , say a_t , must be established, and this may be done by evaluating the shell equations (4.31) and checking the relative error between terms. The finite difference expressions, when applied to (4.31) yield the following vector equations

$$\bar{v}_1 = \bar{v}_2 - \bar{v}_3 \quad (5.18)$$

where

$$\bar{v}_1 = [A_{i,1}] (\bar{x}^f) \quad \text{for } i = 1, 3$$

$$\bar{v}_2 = - \left\{ \sum_{j=2}^4 [A_{i,j}] (\bar{x}^s)^j + \hat{p} \sum_{j=0}^2 [B_{i,j}] (\bar{x}^s)^j \right\}$$

$$\bar{v}_3 = A_{i,0}$$

The maximum relative error in equation (5.18) can be represented by

$$\text{ERROR} = \max \left(\frac{\bar{v}_1 - \bar{v}_2 + \bar{v}_3}{|\bar{v}_1| + |\bar{v}_2| + |\bar{v}_3|} \right) \quad (5.19)$$

where equation (5.19) is evaluated by comparing the individual elements of the vectors \bar{v}_1 , \bar{v}_2 , and \bar{v}_3 . The value of a_t is then set so that the error given by equation (5.19) is just less than or equal to some acceptable level when $e_g = a_t$.

Before reentering the solution routine for $t+1$ and $r=1$, it is necessary to improve the accuracy of $\bar{x}_{t+1,0}$ and $\hat{p}_{t+1,0}$ given by equation (5.16) to avoid a_{t+1} eventually being returned with the same value as a_t . This improvement of $(\bar{x}_{t+1,0}, \hat{p}_{t+1,0})$ may be accomplished by assuming that the total error is in the displacement vector. Then a Newton-Raphson iteration technique may be used to improve the vector, \bar{x} , until the error in the shell equation, given by equation (5.19), is reduced to an acceptable level.

The iteration scheme is given by

$$\bar{x}_{N+1} = \bar{x}_N - \bar{x}_{C,N} \quad (5.20)$$

where

$$f'(\bar{x}_N) \bar{x}_{C,N} = f(\bar{x}_N)$$

and $\bar{x}_{C,N}$ is the correction vector to \bar{x}_N . Using the shell equation as given in equation (5.18), the iteration scheme, equation (5.20), may be written as

$$[\bar{A}](\bar{x}_{C,N}) = -\bar{v}_1 + \bar{v}_2 - \bar{v}_3$$

where

$$[\bar{A}](\bar{x}_{C,N}) = \sum_{j=1}^4 [A_{i,j}] (j(\bar{x}_N)^{j-1}) (\bar{x}_{C,N}) + \hat{p}_{t+1,0} \sum_{j=1}^2 [B_{i,j}] (j(\bar{x}_N)^{j-1}) (\bar{x}_{C,N}) \quad (5.21)$$

$$\bar{v}_1 = [A_{i,1}] (\bar{x}_N) \quad \text{for } i = 1, 3$$

$$\bar{v}_2 = - \left\{ \sum_{j=2}^4 [A_{i,j}] (\bar{x}_N)^j + \hat{p}_{t+1,0} \sum_{j=0}^2 [B_{i,j}] (\bar{x}_N)^j \right\}$$

$$\bar{v}_3 = A_{i,0}$$

In setting up the matrix $[\bar{A}]$, equation (5.21), the same subroutines may be used that set up $[\bar{A}]$ for equation (5.10), similarly the vectors \bar{v}_1 and \bar{v}_2 may be evaluated by the subroutines used for equation (5.18).

The complete solution algorithm for the fundamental path is outlined in Figure 5.3. Using this algorithm the $[\bar{A}]$ matrix is only set up, and decomposed using a Gaussian elimination method with pivoting in the outer, t , loop which results in a routine that is fairly fast.

The resulting fundamental path may be represented by the dotted line in Figure 5.4. The error, or departure of the approximate path from the exact path, is controlled by specifying the allowable value of the error in (5.19) when determining a_t .

5.4 THE SECONDARY PATH SOLUTION ALGORITHM

The nonlinear eigenvalue problem that results from the introduction of finite difference expressions into equation (4.39) is solved by the use of iterative methods. First an inverse iteration method will be used to achieve an initial approximation to the eigenvalue and vector, then several shifts of origin followed by inverse iteration are used to achieve the desired accuracy on both the eigenvalue and vector. An orthogonalization of the eigenvector is also introduced into the iterative procedures, allowing the subdominant eigenvalues and vectors to be obtained.

Due to the somewhat cumbersome nature of the shorthand notation used for the equations of the nonlinear eigenvalue problem the method will first be described with reference to the linear eigenvalue problem.

5.4.1 The Linear Eigenvalue Problem

The inverse iteration schemes discussed here will lead to convergence on the eigenvalues of lowest absolute value, as we are interested in the lowest buckling pressures. It is usual, in the literature, Reference [16], to pose the eigenvalue problem so that convergence is on the largest eigenvalue first, and from this usage the inverse iterative process takes its name.

The linear eigenvalue problem

$$[A](\bar{x}) + \lambda[B](\bar{x}) = 0 \quad (5.22)$$

may be solved by using inverse iteration without a shift of origin, the solution algorithm is given by

$$[A]\bar{v}_{r+1} = -[B]\bar{u}_r$$

$$\bar{u}_{r+1} = \frac{\bar{v}_{r+1}}{\max(\bar{v}_{r+1})} \quad (5.23)$$

and

$$\lambda_{r+1} = \frac{1}{\max(\bar{v}_{r+1})}$$

where the notation $\max(\bar{v})$ is used to denote the element of maximum modulus of the vector \bar{v} . In the limit as $r \rightarrow \infty$, $\bar{u}_r \rightarrow \bar{x}_1$ and $\lambda_r \rightarrow \lambda_1$.

The rate of convergence may be established by considering the underlying reason for the method working. The property of eigenvectors, $\bar{x}_1, \bar{x}_2, \dots, \bar{x}_N$ of spanning the N-dimensional vector space, allows any general N-dimensional vector, \bar{z} , to be written as

$$\bar{z} = \sum_{i=1}^N \alpha_i \bar{x}_i \quad (5.24)$$

where the α_i 's are constants depending on the vector \bar{z} . Without loss of generality we may assume that the eigenvalue corresponding to the eigenvector \bar{x}_i is λ_i , for $i=1,2,3,\dots,N$ and that

$$|\lambda_1| \leq |\lambda_2| \leq |\lambda_3| \leq \dots \leq |\lambda_N| \quad (5.25)$$

Consider the effect on the general vector \bar{z} of a single step of the iterative process, we have

$$[A] (\bar{z}_{i+1}) = -[B] (\bar{z}_i) \quad (5.26)$$

or

$$[A] \left(\frac{\alpha_1 \bar{x}_1}{\lambda_1} + \frac{\alpha_2 \bar{x}_2}{\lambda_2} + \dots + \frac{\alpha_N \bar{x}_N}{\lambda_N} \right) = -[B] (\alpha_1 \bar{x}_1 + \alpha_2 \bar{x}_2 + \dots + \alpha_N \bar{x}_N)$$

It may be seen that the component of \bar{z}_{i+1} in the direction of \bar{x}_1 has increased by a factor of at least λ_2/λ_1 with respect to the other components. The rate of convergence is dependent on the ratio λ_2/λ_1 and the method will converge on the smallest (dominant) eigenvalue and vector (λ_1, \bar{x}_1) .

If the eigenvalue problem contains coincident roots, say $\lambda_1 = \lambda_2 = \dots = \lambda_r$ and $|\lambda_1| < |\lambda_{r+1}| \leq |\lambda_{r+2}| \dots \leq |\lambda_N|$, then the process will still converge on the dominant, coincident, eigenvalue. However the vector will not be uniquely defined, but will be dependent on the initial vector \bar{u}_0 , and will lie in the subspace spanned by $\bar{x}_1, \bar{x}_2, \dots, \bar{x}_r$.

If the ratio λ_2/λ_1 is close to unity then convergence is slow, and it may be desirable to use a shift of origin with the inverse iteration technique to improve the rate of convergence. If we have an approximation to λ_1 , say λ_e , then we may write the eigenvalues as

$$\lambda_i = \lambda_e + \delta_i \quad \text{and} \quad |\delta_1| \ll |\delta_2| \leq |\delta_3| \dots \leq |\delta_N| \quad (5.27)$$

Equation (5.22) may be written in the following form

$$[A + \lambda_e B](\bar{x}) = -\delta[B](\bar{x}) \quad (5.28)$$

or

$$[\tilde{A}](\bar{x}) = -\delta[B](\bar{x})$$

where

$$[\tilde{A}] = [A + \lambda_e B]$$

The solution algorithm is now given by

$$[\tilde{A}] \bar{v}_{r+1} = -[B] \bar{u}_r \quad (5.29)$$

$$\bar{u}_{r+1} = \frac{\bar{v}_{r+1}}{\max(\bar{v}_{r+1})}$$

and

$$\delta_{r+1} = \frac{1}{\max(\bar{v}_{r+1})}$$

The rate of convergence is now dependent on the ratio δ_2/δ_1 , and may be improved by further shifts of the origin to improved estimates of λ_e if this is required. An orthogonalization scheme may be introduced into the iterative cycle allowing subdominant eigenvalues and vectors to be determined. If we have found the first k eigenvalues and vectors then the $(k+1)$ 'th eigenvalue and vector may be found using the following algorithm

$$[A] \bar{v}_{r+1} = -[B] \bar{u}_r \quad (5.30)$$

$$\bar{w}_{r+1} = \bar{v}_{r+1} - \sum_{i=1}^k \frac{(\bar{v}_{r+1})^T \bar{x}_i}{\|\bar{x}_i\|} \bar{x}_i$$

$$\bar{u}_{r+1} = \frac{\bar{w}_{r+1}}{\max(\bar{w}_{r+1})}$$

$$\lambda_{r+1} = \frac{1}{\max(\bar{w}_{r+1})}$$

where

$$\|\bar{x}_i\| = (\bar{x}_i)^T \bar{x}_i$$

The vector \bar{w}_{r+1} is orthogonal to $\bar{x}_1, \bar{x}_2, \dots, \bar{x}_k$ hence $\alpha_1, \alpha_2, \dots, \alpha_k$ in the expression for \bar{z} in equation (5.24) are zero and hence convergence on $\lambda_1, \lambda_2, \dots, \lambda_k$ will be suppressed. It is not

necessary to orthogonalize at each step of the iteration. When a shift of the origin is used with a reasonable estimate to λ_{k+1} then the orthogonalization may be dropped completely from the inverse iteration as λ_{k+1} is dominant in any case.

The evaluation of subdominant eigenvalues enables the possibility of coincident eigenvalues to be investigated, and the verification that the lowest eigenvalue (buckling pressure) has been found. It is possible for the numerical procedures based on these algorithms to converge on subdominant ($\lambda_i, i \neq 1$) eigenvalues first, if the initial vector \bar{u}_0 has a large component in the direction of a subdominant eigenvector.

4.4.2 The Nonlinear Eigenvalue Problem

The application of finite difference expressions to the secondary path equation (4.39) results in a nonlinear eigenvalue problem which may be written in the following form

$$\sum_{j=0}^3 [A_j(\bar{x}^s)]^j (\bar{x}) + \hat{p} \sum_{j=0}^1 [B_j(\bar{x}^s)]^j (\bar{x}) = 0 \quad (5.31)$$

where

$$\bar{x}^s = \bar{x}^i + \bar{x}^f$$

and

$$\bar{x}_t^f = \bar{x}_{t,0} + \bar{x}_{t,1} e_t + \bar{x}_{t,2} e_t^2 + \dots \quad (5.32)$$

$$\hat{p} = \hat{p}_{t,0} + \hat{p}_{t,1} e_t + \hat{p}_{t,2} e_t^2 + \dots$$

for

$$a_{t-1} \leq e_g \leq a_t \quad \text{and} \quad e_t = e_g - a_{t-1}$$

The generalised displacement vectors are given by

$$(\bar{x}^s)^T = (u_1^s, w_1^s, u_2^s, w_2^s, \dots, u_n^s, w_n^s) \quad (5.33)$$

and

$$(\bar{x})^T = (u_1, v_1, w_1, u_2, v_2, w_2, \dots, u_n, v_n, w_n)$$

Equation (5.31) is a nonlinear eigenvalue problem in e_g and x ; by substituting for \bar{x}^s and \hat{p} from (5.32) it is possible to recast (5.31) in the standard form

$$[D_0](\bar{x}) + e_g [D_1](\bar{x}) + e_g^2 [D_2](\bar{x}) + \dots + e_g^m [D_m](\bar{x}) = 0 \quad (5.34)$$

Fortunately it is not necessary for the iterative solution method that the nonlinear eigenvalue problem be posed in the standard form given by equation (5.34). The iterative method based on the naturally occurring form of the eigenvalue problem given by equations (5.31) and (5.32) has the advantage that the nonlinearity is all contained in equation (5.32).

The iterative procedure for the solution of the nonlinear eigenvalue problem, without a shift of the origin, is given by analogy with equation (5.23) as follows

$$\begin{aligned}
 e_r &= \lambda_r - a_{r-1} \quad \text{where} \quad a_{r-1} \leq \lambda_r \leq a_r \\
 \bar{x}_r^s &= \bar{x}^i + \bar{x}_{r,0} + \bar{x}_{r,1} e_r + \bar{x}_{r,2} e_r^2 + \dots \\
 \hat{p}_r &= \hat{p}_{r,0} + \hat{p}_{r,1} e_r + \hat{p}_{r,2} e_r^2 + \dots \\
 [A_0] \bar{v}_{r+1} &= -\frac{1}{\lambda_r} \left\{ \sum_{j=1}^3 [A_j(\bar{x}_r^s)]^j (\bar{u}_r) + \hat{p}_r \sum_{j=0}^1 [B_j(\bar{x}_r^s)]^j (\bar{u}_r) \right\} \quad (5.35) \\
 \bar{w}_{r+1} &= \bar{v}_{r+1} - \sum_{i=1}^K \frac{(\bar{v}_{r+1})^T \bar{x}_i}{\|\bar{x}_i\|} \bar{x}_i \\
 \bar{u}_{r+1} &= \frac{\bar{w}_{r+1}}{\max(\bar{w}_{r+1})} \\
 \lambda_{r+1} &= \frac{1}{\max(\bar{w}_{r+1})}
 \end{aligned}$$

In equation (5.35) the eigenvalue λ is the global perturbation parameter, $\lambda \equiv e_g$ and e_r is the r 'th iterative estimate to the local perturbation parameter e_r .

Similarly by analogy with equations (5.28) and (5.30) the iterative procedure for use with a shift of origin is given by equations (5.36) and (5.37). The shift of origin to λ_e implies an estimate to the fundamental path displacements and load, given by $\bar{x}_{\lambda_e}^s$ and \hat{p}_{λ_e} and hence to the $[\bar{A}_0]$ matrix.

$$e_e = \lambda_e - a_{r-1} \quad \text{for} \quad a_{r-1} \leq \lambda_e \leq a_r \quad (5.36)$$

with

$$\bar{x}_{\lambda_e}^s = \bar{x}^i + \bar{x}_{t,0} + \bar{x}_{t,1} e_e + \bar{x}_{t,2} e_e^2 + \dots$$

$$\hat{p}_{\lambda_e} = \hat{p}_{t,0} + \hat{p}_{t,1} e_e + \hat{p}_{t,2} e_e^2 + \dots$$

and

$$[\bar{A}_0] = \sum_{j=0}^3 [A_j(\bar{x}_{\lambda_e}^s)]^j + \hat{p}_{\lambda_e} \sum_{j=0}^1 [B_j(\bar{x}_{\lambda_e}^s)]^j$$

The iterative scheme with a shift of origin is now given by:

$$\lambda_r = \lambda_e + \delta_r \quad \text{for} \quad a_{t-1} \leq \lambda_r \leq a_t \quad (5.37)$$

$$e_r = \lambda_r - a_{t-1}$$

$$\bar{x}_r^s = \bar{x}^i + \bar{x}_{t,0} + \bar{x}_{t,1} e_r + \bar{x}_{t,2} e_r^2 + \dots$$

$$\hat{p}_r = \hat{p}_{t,0} + \hat{p}_{t,1} e_r + \hat{p}_{t,2} e_r^2 + \dots$$

and

$$\begin{aligned} [\bar{A}_0] \bar{v}_{r+1} = \frac{-1}{\delta_r} \left\{ \sum_{j=1}^3 [A_j(\bar{x}_r^s)^j] \bar{u}_r + \hat{p}_r \sum_{j=0}^1 [B_j(\bar{x}_r^s)^j] \bar{u}_r \right. \\ \left. - \sum_{j=1}^3 [A_j(\bar{x}_{\lambda_e}^s)^j] \bar{u}_r - \hat{p}_{\lambda_e} \sum_{j=0}^1 [B_j(\bar{x}_{\lambda_e}^s)^j] \bar{u}_r \right\} \end{aligned}$$

$$\bar{w}_{r+1} = \bar{v}_{r+1} - \sum_{i=1}^K \frac{(\bar{v}_{r+1})^T \bar{x}_i}{\|\bar{x}_i\|} \bar{x}_i$$

$$\bar{u}_{r+1} = \frac{\bar{w}_{r+1}}{\max(\bar{w}_{r+1})}$$

$$\delta_{r+1} = \frac{1}{\max(\bar{w}_{r+1})}$$

The convergence of these iterative procedures, equations (5.35) and (5.37), apart from numerical stability, is again dependent on the n eigenvectors of equation (5.31) spanning the n -dimensional vector space. As equation (5.31) may be written in the standard form given by equation (5.34) it is sufficient to show that the eigenvectors of equation (5.34) span the n -dimensional vector space. The nonlinear eigenvalue problem, equation (5.34) may be written in the form of a standard linear eigenvalue problem, Reference [16], as follows.

$$\begin{bmatrix} 0 & I & 0 & 0 & \dots & 0 \\ 0 & 0 & I & 0 & \dots & 0 \\ 0 & 0 & 0 & I & \dots & 0 \\ \vdots & & & & & \\ \vdots & & & & & \\ \vdots & & & & & \\ 0 & 0 & 0 & 0 & \dots & I \\ D_m^{-1}D_0 & D_m^{-1}D_1 & D_m^{-1}D_2 & D_m^{-1}D_3 & \dots & D_m^{-1}D_{m-1} \end{bmatrix} \begin{bmatrix} X \\ Y_1 \\ Y_2 \\ \vdots \\ \vdots \\ Y_{m-2} \\ Y_{m-1} \end{bmatrix} = e_g \begin{bmatrix} X \\ Y_1 \\ Y_2 \\ \vdots \\ \vdots \\ Y_{m-2} \\ Y_{m-1} \end{bmatrix} \quad (5.38)$$

Where the partitioned matrix is mn by mn and the X, Y_i vectors are of length n , therefore the eigenvectors of equation (5.34) are independent.

The iterative routines given by equations (5.35), (5.36) and (5.37) are combined to form a solution algorithm, as shown in Figure 5.5. The convergence test used for iteration without a shift of origin is on the eigenvalue only, and is given by.

$$\text{ERROR} = \left| \frac{\lambda_{r+1} - \lambda_r}{\lambda_r} \right| \quad (5.39)$$

For iteration with a shift of origin convergence is checked on both the eigenvalue and vector, the error in the eigenvector is given by,

$$\text{ERROR} = \max \left(\frac{\bar{u}_{r+1} - \bar{u}_r}{\bar{u}_r} \right) \quad (5.40)$$

in which the error is the maximum value of the relative error as corresponding elements of the vectors \bar{u}_{r+1} and \bar{u}_r are compared. These convergence checks indicate that the iterative procedures are yielding stable eigenvalues and vectors, not that the eigenvalue and vector satisfy equation (5.31) or the original total potential energy functional equation (4.24).

| LOCATION (Figure 5.2) | REGION I EXPRESSIONS | | | | REGION II & VI EXPRESSIONS | | | |
|--------------------------|-------------------------|-----------------------------|-----------------------------|-----------------------------|----------------------------|-----------------------------|-----------------------------|-----------------------------|
| DERIVATIVE | $\frac{dx}{d\phi}, s=1$ | $\frac{d^2x}{d\phi^2}, s=2$ | $\frac{d^3x}{d\phi^3}, s=3$ | $\frac{d^4x}{d\phi^4}, s=4$ | $\frac{dx}{d\phi}, s=1$ | $\frac{d^2x}{d\phi^2}, s=2$ | $\frac{d^3x}{d\phi^3}, s=3$ | $\frac{d^4x}{d\phi^4}, s=4$ |
| ACCURACY | h^6 | h^6 | h^4 | h^4 | h^6 | h^6 | h^4 | h^4 |
| f_s r | $\frac{1}{60h}$ | $\frac{1}{180h^2}$ | $\frac{1}{8h^3}$ | $\frac{1}{6h^4}$ | $\frac{1}{60h}$ | $\frac{1}{180h^2}$ | $\frac{1}{8h^3}$ | $\frac{1}{6h^4}$ |
| -5 | 0 | 0 | 0 | 0 | 0 | 0 | 0 | 0 |
| -4 | 0 | 0 | 0 | 0 | 0 | 0 | 0 | 0 |
| -3 | 0 | 0 | 0 | 0 | -1 | 2 | 1 | -1 |
| -2 | 2 | -11 | -1 | 4 | 9 | -27 | -8 | 12 |
| -1 | -24 | 214 | -8 | -11 | -45 | 270 | 13 | -39 |
| 0 | -35 | -378 | 35 | 0 | 0 | -490 | 0 | 56 |
| 1 | 80 | 130 | -48 | 31 | 45 | 270 | -13 | -39 |
| 2 | -30 | 85 | 29 | -44 | -9 | -27 | 8 | 12 |
| 3 | 8 | -54 | -8 | 27 | 1 | 2 | -1 | -1 |
| 4 | -1 | 16 | 1 | -8 | 0 | 0 | 0 | 0 |
| 5 | 0 | -2 | 0 | 1 | 0 | 0 | 0 | 0 |

| LOCATION (Figure 5.2) | REGION III & V EXPRESSIONS | | | | REGION IV EXPRESSIONS | | | |
|--------------------------|----------------------------|-----------------------------|-----------------------------|-----------------------------|-------------------------|-----------------------------|-----------------------------|-----------------------------|
| DERIVATIVE | $\frac{dx}{d\phi}, s=1$ | $\frac{d^2x}{d\phi^2}, s=2$ | $\frac{d^3x}{d\phi^3}, s=3$ | $\frac{d^4x}{d\phi^4}, s=4$ | $\frac{dx}{d\phi}, s=1$ | $\frac{d^2x}{d\phi^2}, s=2$ | $\frac{d^3x}{d\phi^3}, s=3$ | $\frac{d^4x}{d\phi^4}, s=4$ |
| ACCURACY | h^8 | h^8 | h^6 | h^6 | h^{10} | h^{10} | h^8 | h^8 |
| f_s r | $\frac{1}{840h}$ | $\frac{1}{5040h^2}$ | $\frac{1}{240h^3}$ | $\frac{1}{240h^4}$ | $\frac{1}{2520h}$ | $\frac{1}{25200h^2}$ | $\frac{1}{30240h^3}$ | $\frac{1}{15120h^4}$ |
| -5 | 0 | 0 | 0 | 0 | -2 | 8 | 205 | -82 |
| -4 | 3 | -9 | -7 | 7 | 25 | -125 | -2522 | 1261 |
| -3 | -32 | 128 | 72 | -96 | -150 | 1000 | 14607 | -9738 |
| -2 | 168 | -1008 | -338 | 676 | 600 | -6000 | -52428 | 52428 |
| -1 | -672 | 8064 | 448 | -1952 | -2100 | 42000 | 70098 | -140196 |
| 0 | 0 | -14350 | 0 | 2730 | 0 | -73766 | 0 | 192654 |
| 1 | 672 | 8064 | -448 | -1952 | 2100 | 42000 | -70098 | -140196 |
| 2 | -168 | -1008 | 338 | 676 | -600 | -6000 | 52428 | 52428 |
| 3 | 32 | 128 | -72 | -96 | 150 | 1000 | -14607 | -9738 |
| 4 | -3 | -9 | 7 | 7 | -25 | -125 | 2522 | 1261 |
| 5 | 0 | 0 | 0 | 0 | 2 | 8 | -205 | -82 |

TABLE 5.1 Coefficients $\alpha_{s,r}$ and f_s of the Finite Difference Expressions;

$$\left. \frac{d^s x}{d\phi^s} \right|_{\phi_j} \cong \frac{d^s \bar{x}_j}{d\phi^s} = f_s \sum_{r=-5}^{+5} \alpha_{s,r} x_{j-r}, \text{ equation (5.7).}$$

| LOCATION (Figure 5.2) | REGION VII EXPRESSIONS | | | |
|--------------------------|-------------------------|-----------------------------|-----------------------------|-----------------------------|
| DERIVATIVE | $\frac{dx}{d\phi}, s=1$ | $\frac{d^2x}{d\phi^2}, s=2$ | $\frac{d^3x}{d\phi^3}, s=3$ | $\frac{d^4x}{d\phi^4}, s=4$ |
| ACCURACY | h^6 | h^6 | h^4 | h^4 |
| f_s r | $\frac{1}{60h}$ | $\frac{1}{180h^2}$ | $\frac{1}{8h^3}$ | $\frac{1}{6h^4}$ |
| -5 | 0 | -2 | 0 | 1 |
| -4 | 1 | 16 | -1 | -8 |
| -3 | -8 | -54 | 8 | 27 |
| -2 | 30 | 85 | -29 | -44 |
| -1 | -80 | 130 | 48 | 31 |
| 0 | 35 | -378 | -35 | 0 |
| 1 | 24 | 214 | 8 | -11 |
| 2 | -2 | -11 | 1 | 4 |
| 3 | 0 | 0 | 0 | 0 |
| 4 | 0 | 0 | 0 | 0 |
| 5 | 0 | 0 | 0 | 0 |

| LOCATION (Figure 5.2) | POLE BOUNDARY EXPRESSIONS | | |
|--------------------------|------------------------------|-----------------------------|-----------------------------|
| DERIVATIVE | $\frac{dx}{d\phi}, s=1$ | $\frac{d^2x}{d\phi^2}, s=2$ | $\frac{d^3x}{d\phi^3}, s=3$ |
| ACCURACY | h^6 | h^6 | h^6 |
| f_s r | $\frac{1}{60h}$ | $\frac{1}{180h^2}$ | $\frac{1}{240h^3}$ |
| -1 | -10 | 126 | -469 |
| 0 | -77 | -70 | 1818 |
| 1 | 150 | -486 | 2924 |
| 2 | -100 | 855 | 2690 |
| 3 | 50 | -670 | -1710 |
| 4 | -15 | 324 | 814 |
| 5 | 2 | -90 | -268 |
| 6 | 0 | 11 | 54 |
| 7 | 0 | 0 | -5 |

| LOCATION (Figure 5.2) | EDGE BOUNDARY EXPRESSIONS | | |
|--------------------------|------------------------------|-----------------------------|-----------------------------|
| DERIVATIVE | $\frac{dx}{d\phi}, s=1$ | $\frac{d^2x}{d\phi^2}, s=2$ | $\frac{d^3x}{d\phi^3}, s=3$ |
| ACCURACY | h^6 | h^6 | h^6 |
| f_s r | $\frac{1}{60h}$ | $\frac{1}{180h^2}$ | $\frac{1}{240h^3}$ |
| -6 | 0 | 11 | 0 |
| -5 | -2 | -90 | 1 |
| -4 | 15 | 324 | -8 |
| -3 | -50 | -670 | 29 |
| -2 | 100 | 855 | -64 |
| -1 | -150 | -486 | 83 |
| 0 | 77 | -70 | -56 |
| 1 | 10 | 126 | 15 |

TABLE 5.1 Coefficients $\alpha_{s,r}$ and f_s of the Finite Difference Expressions;

$$\left. \frac{d^s x}{d\phi^s} \right|_{\phi_j} \equiv \frac{d^s \bar{x}_j}{d\phi^s} = f_s \sum_{r=-6}^{+7} \alpha_{s,r} x_{j-r}, \text{ equation (5.7).}$$

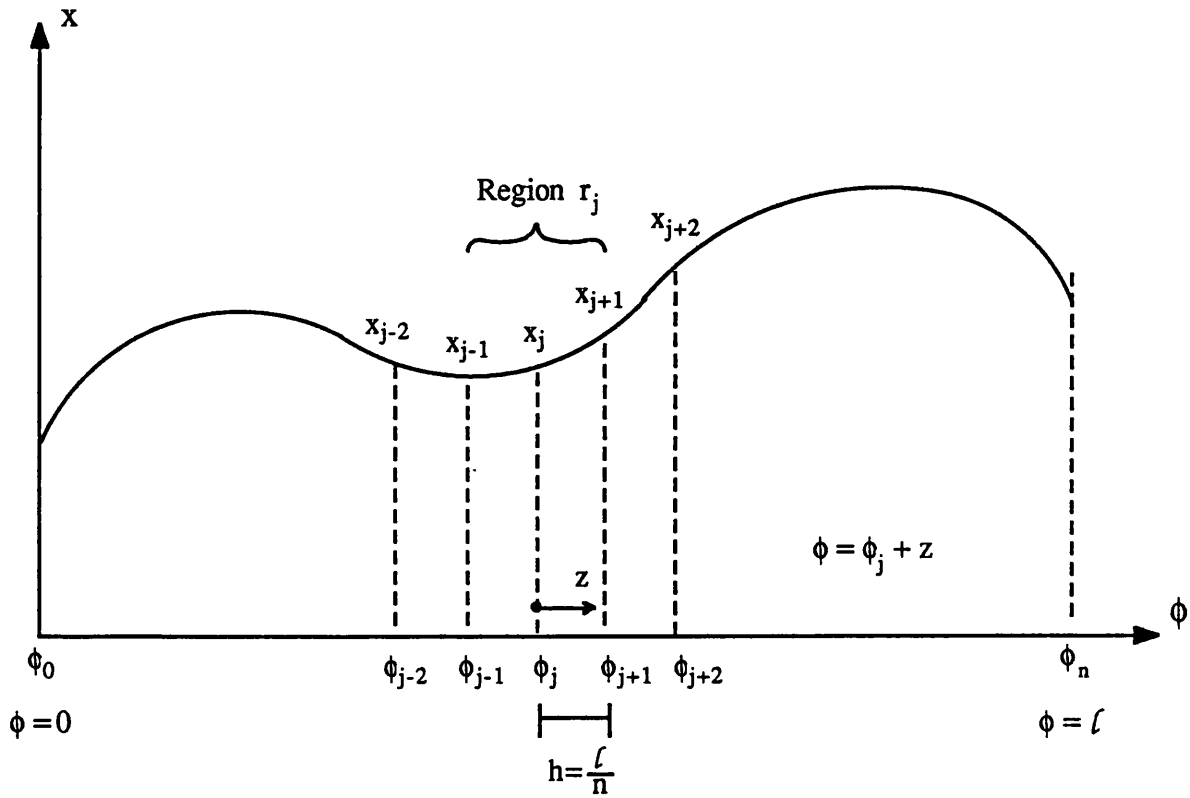


Figure 5.1 Finite Difference Collocation.

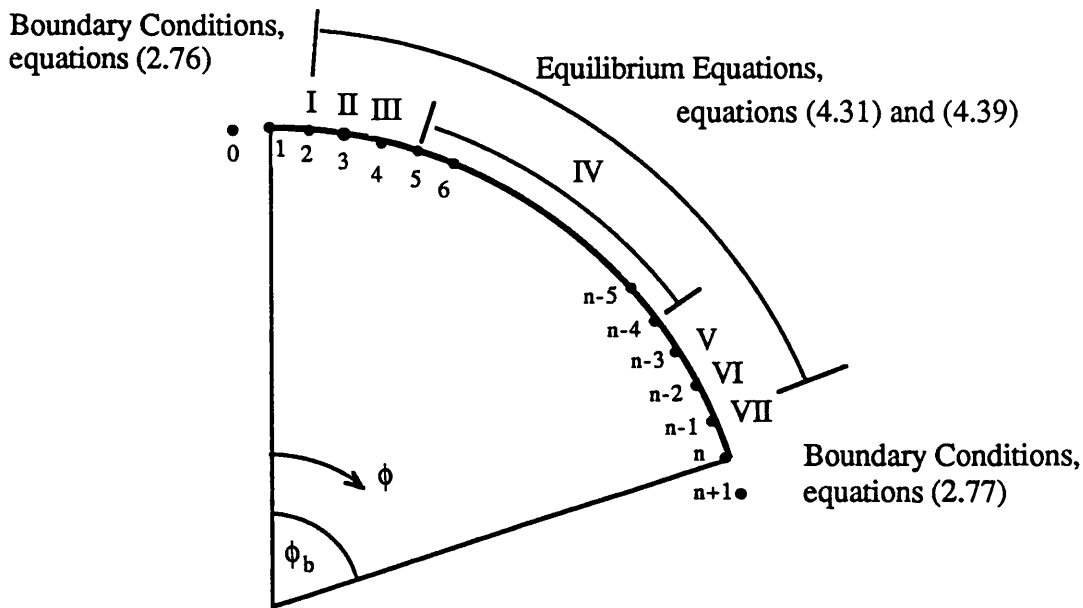


Figure 5.2 Finite Difference Mesh and Shell Regions (Table 5.1).

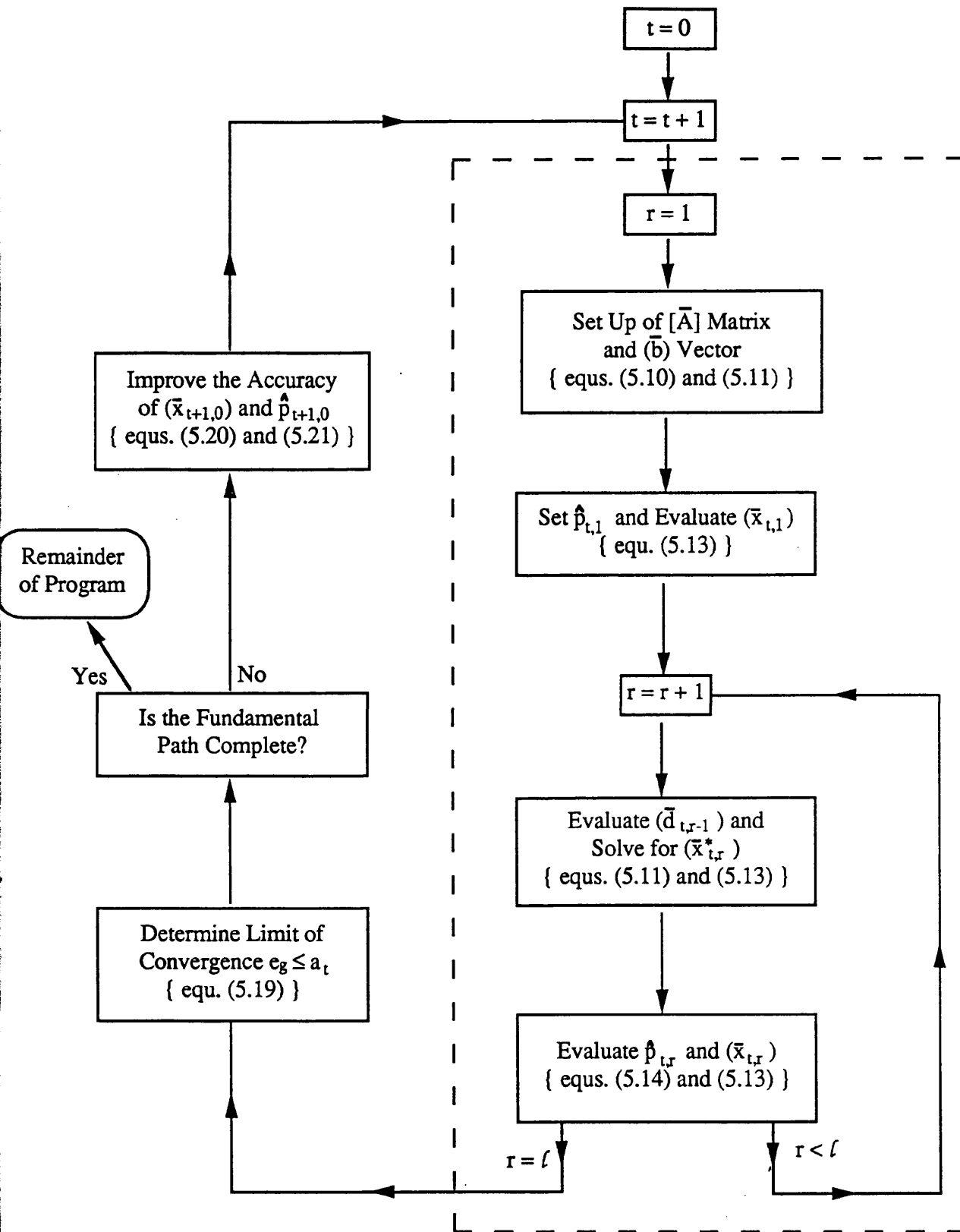


Figure 5.3 Solution Algorithm For The Nonlinear Fundamental Path

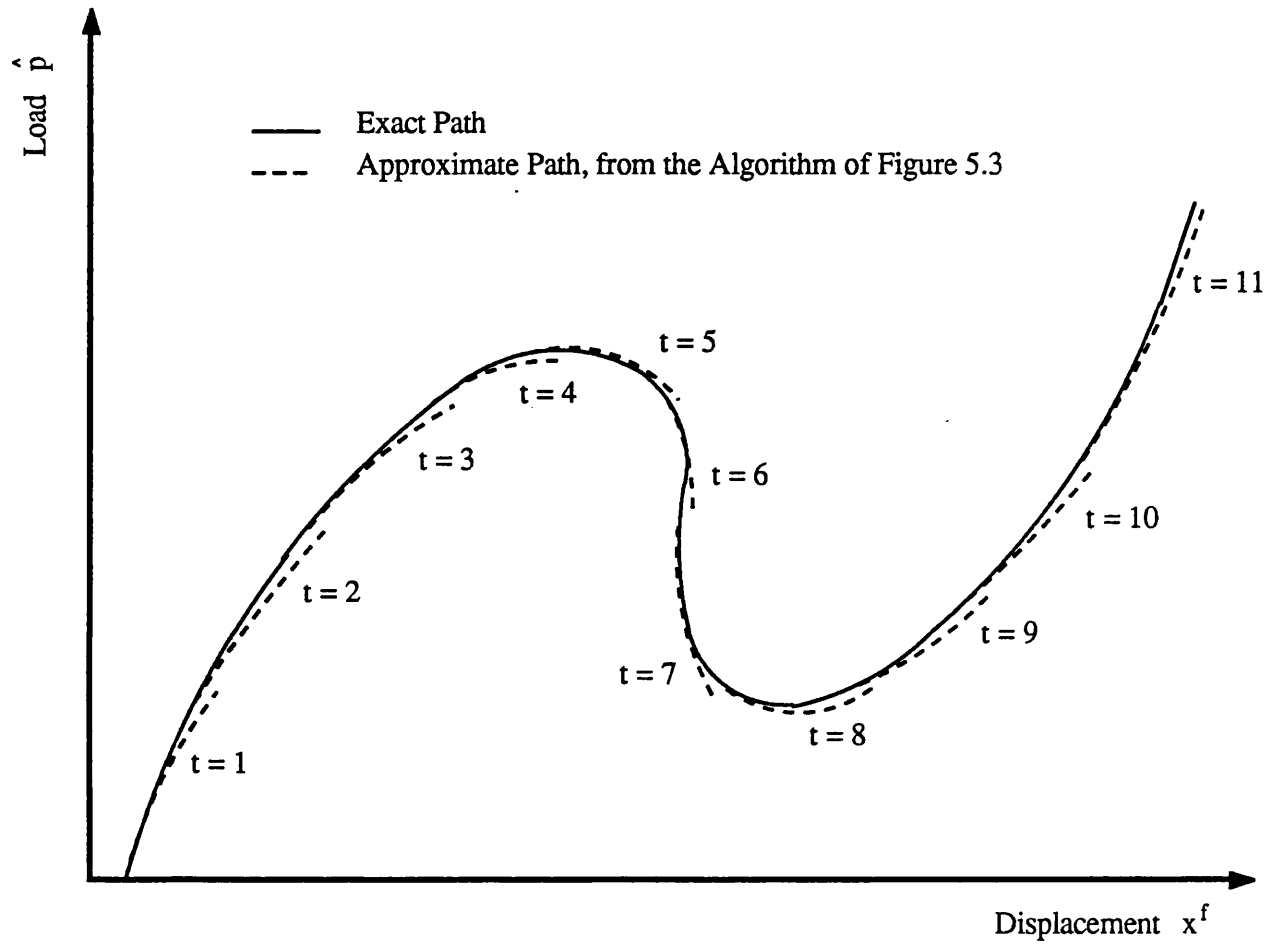


Figure 5.4 Piece-wise Continuous Modelling of the Nonlinear Fundamental Path

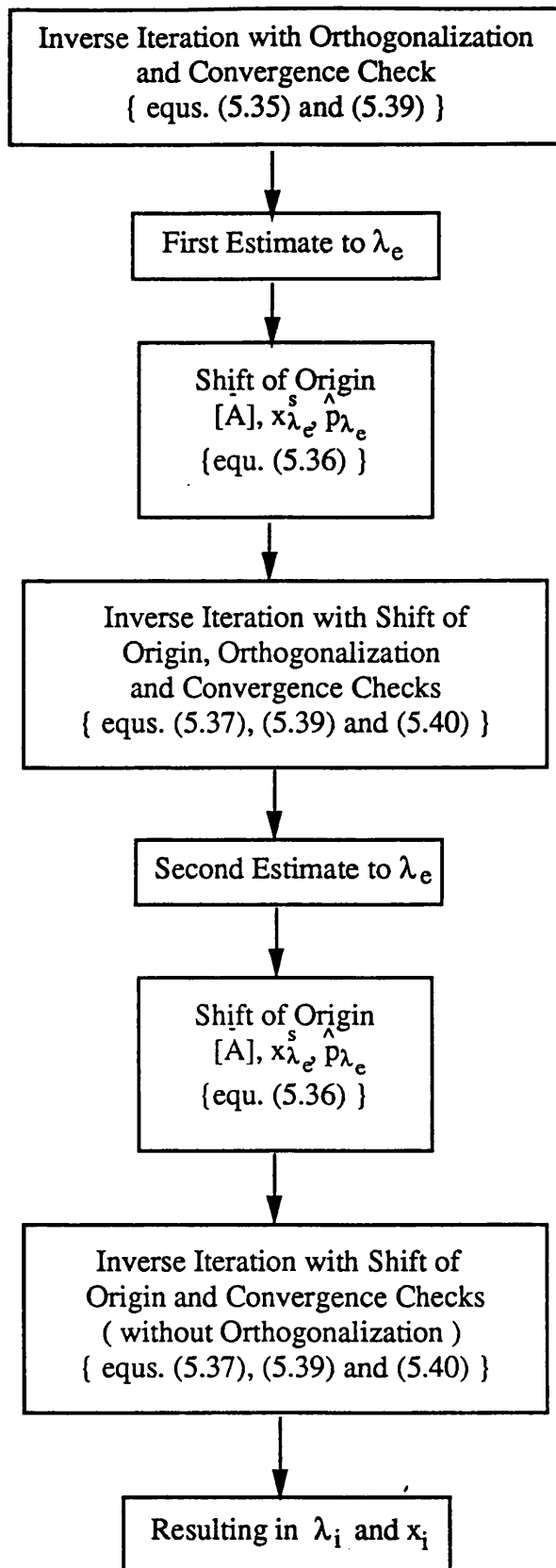


Figure 5.5 Solution Algorithms for the Nonlinear Eigenvalue Problem

CHAPTER SIX

VALIDATION OF THE COMPUTER PROGRAM

CHAPTER SIX

CONTENTS

6.1 INTRODUCTION

6.2 INTERNAL CONVERGENCE AND ERROR LIMITS

6.2.1 Finite Difference Expressions and Convergence

6.2.2 The Perturbation Series and Relative Error Limits used in the Solution of the Equilibrium Equations

6.2.3 Quadratic, Cubic and Quartic Terms of the Strain Displacement Relations and the Equilibrium Equation

6.2.4 Remarks on Accuracy and Efficiency

6.3 COMPARISONS WITH OTHER NUMERICAL RESULTS

6.3.1 Comparisons of Axisymmetric and Periodic Buckling Pressures for Perfect Spherical Caps with Clamped Edges

6.3.2 Comparisons of the Axisymmetric Nonlinear Fundamental Path Solutions with Initial Imperfections

VALIDATION OF THE COMPUTER PROGRAM

6.1 INTRODUCTION

Three computer programs were written in the course of the present work. Two of these programs were written to perform the classical axisymmetric bifurcation analysis, and the post bifurcation analysis for complete spherical shells. The mathematical basis of these programs has been described in Chapter Three and Appendix A. The validation of these two programs was performed by simple comparisons with results reported in the literature, and will not be reported here.

The third program, NLSPHERE, which implements the solution methods described in Chapters Four and Five, and in particular the validation of this program, are the concern of this Chapter. It is not intended to present a complete validation and description of the program NLSPHERE, but to draw attention to those features of the program and its operation which influence the accuracy and efficiency. The source listing (Fortran) and a typical output file are included in Appendix B.

The task of program validation has been separated into two parts. First, attention is focused on internal error limits and accuracy in Section 6.2. Then, comparisons between the present numerical results, and results obtained independently by other workers using nonlinear shallow shell theory are presented in Section 6.3.

6.2 INTERNAL CONVERGENCE AND ERROR LIMITS

6.2.1 Finite Difference Expression and Convergence

Replacing the continuous partial differentials of the 'exact' differential equations of Chapter Four with discrete finite difference approximations results in the set of simultaneous equations described in Chapter Five. The matrices that result will be 'banded', that is non-zero elements will be clustered about the principal diagonal of the matrix, all the solution techniques that have been used allow for the banded nature of the matrices to reduce both storage and the number of arithmetic operations required to perform a given computation. The accuracy with which the set of simultaneous equations models the 'exact' differential equations is nonlinearly dependent on both the accuracy of the finite difference expressions used in the transformation and the mesh spacing, h . The error may be reduced by using more accurate finite difference expressions, resulting in an increase in the number of non-zero elements in each row of the matrices, increasing the bandwidth K , or by reducing the mesh spacing h , resulting in a greater number of simultaneous equations to be solved, which increases both the order of the matrices and the length of the vectors, N . The use of central finite difference expressions with a high order of accuracy at or near the boundaries of the shell will increase the number of off shell 'fictitious nodes', while the use of highly accurate partial forward or backward expressions at or near the boundary may introduce errors due to the extra 'weight' attached to the near boundary nodes.

The computer program NLSPHERE requires the finite difference expression to be supplied as part of the input data file, and allows as many as seven sets of finite difference expressions to be used over the surface of the shell, the 'shell nodes'. The finite difference expressions used at the boundaries, the 'boundary nodes', are specified separately. This has been described in Chapter Five, in particular Figure 5.2 shows the node numbering and Table 5.1 presents the finite difference expressions that were eventually used.

The optimum (to minimise memory and CPU time required) choice of finite difference expressions and number of nodes will depend on the geometry of the shell under consideration. The degree of accuracy (the node spacing and the order of the finite difference expressions) required by the finite difference modelling of the elastic behaviour of the spherical shell will depend on the shortest wavelength present in the midsurface displacements. For spherical shells the wavelength of the buckling mode (both the axisymmetric buckling and periodic bifurcation modes) decreases as the geometric Bartdoff parameter, λ , increases. From the classical analysis of complete spherical shells $n \approx 1.81\sqrt{r/t}$, and for $\lambda \approx 56$ or $r/t=100$, then $n \approx 18$ where n is the order of the Legendre polynomial describing the buckling mode. In the numerical solution it is only necessary to model half of the spherical cap, therefore n is equal to the number of half waves modelled by the finite difference representation. The need for a

highly accurate finite difference discretization results from the presence of these short wavelength components of the midsurface displacements.

In the overall solution algorithm the boundary conditions are used to eliminate the boundary and off shell fictitious nodes from the matrices and vectors before the solution techniques described in Chapter Five are used. If the boundary and off shell fictitious nodes were not eliminated from the matrices of the nonlinear eigenvalue problem they would give rise to spurious eigen-values and vectors.

Storage requirements for banded matrices and vectors are linearly dependent on the nodal spacing, i.e. the order of the matrix or vector. The accuracy, or order, of the finite difference expressions will have a much weaker effect on the bandwidth of the matrices and will not affect the length of the vectors at all, hence the accuracy of the finite difference expressions used will have a weak effect on the overall storage requirements of the program. The product $N(K-1)$ where N is the order of the matrices, [$N=3 \times (\text{number of 'shell nodes'})$] and K is the bandwidth of the matrices [$K=3 \times (\text{number of nodes used by the finite difference expressions})$], is representative of the number of arithmetic operations, and therefore the CPU time, required to evaluate the derivative of a vector or perform back substitution of a decomposed matrix. Also the CPU time taken to perform Gaussian elimination with partial pivoting on banded matrices is proportional to $N(K-1)^2$. As a result of these nonlinear dependencies simple second order central finite difference expressions will not be the optimum expressions for use with the solution algorithms.

Convergence was studied in two parts, due to the large number of combinations of finite difference expressions and node spacings that were considered and tested. First a linear fundamental path problem ($w^f = Pr(1-\mu)/2Et$) with bifurcation into axisymmetric and periodic modes was used to select the optimum set of finite difference expressions. A typical comparison between finite difference expressions is shown in Figure 6.1, for a spherical cap with $\lambda \approx 32$. Figure 6.1 compares standard central finite difference expressions with a set of finite difference expressions in which all error terms are of order h^4 and with the set of finite difference expressions that were eventually used, i.e. the finite difference expressions in Table 5.1. After selecting the optimum set of finite difference expressions from the linear fundamental path convergence study, a second convergence study using the full nonlinear capabilities of the program was undertaken. Results from the second convergence study are shown in Figure 6.2, where the axisymmetric buckling pressure, \hat{p}_{bk} ($i=0$), and the minimum critical bifurcation pressure, \hat{p}_{cr} ($i=2$ and $i=26$), for two shells ($\lambda=6$ and $\lambda=38$) are compared, as the number of nodes is increased.

As a result of these convergence studies the finite difference expressions given in Table 5.1 with 51 shell and boundary nodes and two off shell fictitious nodes were used throughout. It is estimated that the relative errors introduced into the final numerical results due to the finite

difference discretization will for all the shells considered in this work, $3.5 \leq \lambda \leq 60$, be less than 1%, and usually less than 0.1%.

6.2.2 The Perturbation Series and Relative Error Limits used in the Solution of the Equilibrium Equations

The overall accuracy of the program depends on the accuracy with which the nonlinear fundamental path is modelled. The tendency, in the nonlinear modelling of the fundamental path, for errors to increase with increasing values of the perturbation parameter has been discussed in Chapter Five, (Section 5.3). As a consequence the local perturbation series was introduced, equation (5.15), and a measure of the relative error based on the equilibrium equations was defined, equation (5.19). Subsequently a Newton-Raphson iterative scheme for the improvement of the displacement vector prior to its use as the initial vector in the next local perturbation series was given by equation (5.20).

The computer program NLSPHERE requires the user to specify the number of terms used in a local perturbation series and the number of these local perturbation series that are used to model the complete fundamental path. Trials were undertaken in which the order of the local perturbation series was varied, resulting in the adoption of sixteen local perturbation series of ten terms each. As a result of tests, the upper bound relative error limit, equation (5.19), used in the evaluation of a_t was set at 0.005, with the Newton-Raphson iteration reducing this error to 10^{-6} , this 'improved' displacement vector is then used as the initial displacement vector for the next local perturbation series. Due to the adoption of the error limits discussed above, the relative errors introduced into the final numerical results by the nonlinear fundamental path solution method will in all cases be less than 0.5%.

The iterative solution method used for determining the eigen-values and vectors have been described in Chapter Five, (Section 5.2). The measure of the relative errors in the eigenvalues and eigenvectors have been defined by equations (5.39) and (5.40). Various error limits are used within the solution algorithms to determine when shifts of origin are to be performed. Each shift of origin requires the recalculation and decomposition (Gaussian elimination) of the banded $[A]$ matrix, equation (5.28), this improves the speed with which the iterative solution method converges, equation (5.29). Trials performed using various combinations of error limits and origin shifts resulted in the following rules being incorporated in the solution routines for the nonlinear eigenvalue problem.

- First - Inverse iteration and orthogonalization (if $j \geq 2$) are used until the relative change in the eigenvalue, equation (5.39), is less than 10^{-3}

Second - Inverse iteration with a shift of origin to λ_e and orthogonalization (if $j \geq 2$) are used until the relative change in the eigen-value and vector, equations (5.39) and (5.40), are both less than 10^{-5} .

Third - Inverse iteration with a shift of origin to λ_e without orthogonalization is used until the relative error in the eigen-value and vector, equations (5.39) and (5.40), are both less than 10^{-8} .

In practice the above rules were found to be a reasonable compromise between the increased rate of convergence that results from a shift of origin, and the CPU time used in setting up the $[\bar{A}]$ matrix and performing the Gaussian elimination with partial pivoting required by each shift of origin. It was found that the second and third error criteria, 10^{-5} and 10^{-8} above, were usually satisfied in less than ten iterations, when the estimate to the eigenvalue used for the shift of origin, λ_e , was given by the final value of the previous iterative step. The error limit of 10^{-8} on the final calculated value of the eigenvectors is important when subdominant eigenvalues are required, as the error introduced by the orthogonalization of the subdominant vectors during iteration depends on the errors present in the previously calculated 'dominant' eigenvectors. Also, as a result of using the final relative error limit of 10^{-8} on the eigenvalue and vector, the numerical solution algorithm used for the nonlinear eigenvalue problem, will be responsible for errors that are entirely negligible in comparison with those introduced by the finite difference discretization (0.1 to 1%) and the nonlinear fundamental path solution algorithm (<0.5%).

6.2.3 Quadratic, Cubic and Quartic Terms of the Strain Displacement Relations and the Equilibrium Equation

The fundamental path equilibrium equation, equation (4.31) and Table 4.1, contains the terms $A_1(x^s)$ and $\hat{p}B_0$, $A_2(x^s)^2$ and $\hat{p}B_1(x^s)$, $A_3(x^s)^3$ and $\hat{p}B_2(x^s)^2$, and $A_4(x^s)^4$; these are the linear, quadratic, cubic and quartic terms of the equilibrium equation. As mentioned in Chapter Four the derivation of the equilibrium equations for both the nonlinear fundamental path and the linearised secondary path were based on quartic strain and quadratic curvature expressions, equation (2.66). However for spherical shells with radius to thickness ratios greater than 100 ($\alpha = t^2/12r^2 < 8.3 \times 10^{-6}$) the quadratic curvature terms were found to have a negligible influence on the numerical results. As the inclusion of the quadratic curvature terms requires the notation used for the bending energy to be extended, and as for all cases considered these terms will for all practical purposes be zero, only the linear curvature terms are presented and discussed in the present work.

Figure 6.3 shows the effect on the nonlinear fundamental path for two, $\lambda=6$ and $\lambda=26$, perfect spherical caps. Pressure is plotted against perturbation parameter, when the equilibrium equations, equation (4.31), are used and all consistent terms up to and including the quadratic, the cubic, and the quartic are maintained. The necessity of maintaining terms in the equilibrium

equation up to and including the cubic terms is clearly demonstrated. The difference between the numerical results obtained from the consistent cubic and quartic expressions at most affected only the fifth significant figure.

Cubic terms in the equilibrium equation arise from quartic terms in the total potential energy functional. Which in turn arise from the product of cubic terms of the change in volume and the pressure load, equation (2.69), from the product of the quadratic terms of the strain displacement relations, and from the product of the cubic and linear terms of the strain displacement relations. Therefore consistent cubic terms in the equilibrium equation may only be achieved when the strain displacement relations and the change in volume are also consistent in their cubic terms. The 'largest' of the cubic terms in the equilibrium equation arise from the quadratic terms of the strain displacement relations, the classical axisymmetric analysis reported in Chapter Three is based on only the largest of the quadratic terms of the strain displacement relations, equation (3.1). The nonlinear, up to and including all cubic terms, strain displacement relations are given by

$$\varepsilon_{\phi} = \varepsilon_{\phi}(x) = \varepsilon_1 + \frac{1}{2} \left\{ \left(\dot{v} \right)^2 + (\beta)^2 \right\} - \frac{1}{2} \varepsilon_1 \left\{ \left(\dot{v} \right)^2 + (\beta)^2 \right\} + \dots \quad (6.1)$$

$$\varepsilon_{\theta} = \varepsilon_{\theta}(x) = \varepsilon_2 + \frac{1}{2} \left\{ (\gamma)^2 + (\delta)^2 \right\} - \frac{1}{2} (\varepsilon_2) \left\{ (\gamma)^2 + (\delta)^2 \right\} + \dots$$

$$\begin{aligned} \varepsilon_{\theta\phi} = \varepsilon_{\theta\phi}(x) = & \frac{1}{2} \left[\left(\dot{v} + \gamma \right) + \left(\beta\delta - \varepsilon_1 \dot{v} - \varepsilon_2 \gamma \right) - \frac{1}{2} \left(\dot{v} + \gamma \right) \left\{ \left(\dot{v} \right)^2 + (\gamma)^2 + (\beta)^2 + (\delta)^2 \right\} \right. \\ & \left. + \frac{1}{6} \left(\dot{v} + \gamma \right)^3 + \gamma (\varepsilon_2)^2 + \dot{v} (\varepsilon_1)^2 - \beta\gamma (\varepsilon_1 + \varepsilon_2) + \dots \right] \end{aligned}$$

where

$$\varepsilon_1 = u + w$$

$$\varepsilon_2 = w + u \cot \phi + \dot{v} / \sin \phi$$

$$\beta = u - w$$

$$\gamma = \dot{u} / \sin \phi - v \cot \phi$$

$$\delta = v - \dot{w} / \sin \phi$$

Profiles of the fundamental path displacements and their derivatives as well as the linear strain components, and the quartic contributions to the total membrane energy, are all presented in Figure 6.5 and Figure 6.6 at the axisymmetric buckling point, the fundamental paths for these shells, $\lambda=6$ and $\lambda=26$, are shown in Figure 6.3 and Figure 6.4. Profiles of the fundamental path displacements (normalised by the shell thickness) and their derivatives are shown in Figure 6.5 and Figure 6.6, (a) and (b), where the inplane displacement, u , and its derivative, u' , have been amplified by a factor of fifty ($\times 50$) to allow presentation on the same graph as the radial displacement, w , and its derivative, w' . The profiles of the axisymmetric linear

strain components, ϵ_1 , ϵ_2 , and β , are depicted in Figure 6.5 (c) and Figure 6.6 (c), where ϵ_1 and ϵ_2 have been amplified by a factor of ten ($\times 10$). Finally, in Figure 6.5 (d) and Figure 6.6 (d) the contributions to the total membrane energy, $U_{1,M}$, arising from the quadratic, $\beta^4/4$, and cubic, $(\epsilon_1^2 + \mu\epsilon_1\epsilon_2)\beta^2$, terms of the strain displacement relations are shown separately, the contribution from the cubic terms of strain displacement relations have been amplified by a factor of fifty ($\times 50$).

Figure 6.5 (d) and Figure 6.6 (d), show that the quartic contribution to the fundamental path membrane energy, $U_{1,M}$, from the quadratic terms, $\beta^4/4$, of the strain displacement relations decreases from approximately 10% for $\lambda=6$ to 5.5% for $\lambda=26$, at the maximum point on the profile. And the corresponding contribution from the cubic terms, $(\epsilon_1^2 + \mu\epsilon_1\epsilon_2)\beta^2$, of the strain displacement relations is approximately 0.1% for $\lambda=6$ and 0.05% for $\lambda=26$.

The linear terms of the secondary path equilibrium equation, the nonlinear eigenvalue problem given by equations (4.39) or (5.31) and Table 4.2, contain terms of orders $A_0(x)$, $[A_1(x^s)](x)$ and $\hat{p}B_0(x)$, $[A_2(x^s)^2](x)$ and $\hat{p}[B_1(x^s)](x)$, and $[A_3(x^s)^3](x)$, these are the terms that are linear, quadratic, cubic, and quartic in the generalised coordinates (\hat{p}, x^T) , $x^T = x^i + x^f + x$.

In the derivation of the quartic terms of the equilibrium equation, $[A_3(x^s)^3](x)$, only the 'largest' terms (those containing the radial displacement w and its derivatives) were maintained and included in the computer coding of the eigenvalue solution routines. Comparisons of eigenvalues and vectors resulting from the maintenance of all the cubic strain displacement terms, consistent cubic equilibrium equations, in both the fundamental path solution algorithm and the solution algorithm for the eigenvalue problem with the corresponding results when the equilibrium equations for the fundamental path contained consistent quartics, and the equilibrium equation for the secondary path contained consistent cubics and 'large' quartics, were performed, and resulted in differences in the fifth significant figure.

Bifurcation from the axisymmetric fundamental path into periodic modes occurs before the axisymmetric buckling pressure, P_{bk} , is reached for the two shells discussed above the critical periodic modes and buckling pressures are $i=2$ and $P_{cr}/P_{cl}=0.7618$ for $\lambda=6$ and $i=18$ and $P_{cr}/P_{cl}=0.7924$ for $\lambda=26$. Figure 6.7 and Figure 6.8 present profiles of the initial secondary path incremental displacements (the eigenvector), their derivatives, and the linear strain components; as these are all based on the eigenvector the vertical scale is arbitrary. Figure 6.7 and Figure 6.8, (a) and (b), use the same arbitrary vertical scale, and the inplane displacements, u and v , and their derivatives, \dot{u} , \dot{v} , \dot{u} , and \dot{v} , have all been amplified by a factor of fifty ($\times 50$) compared to the radial displacement, w , and its derivatives, \dot{w} and \dot{w} . In Figure 6.7 (c) and Figure 6.8 (c) the profiles of the initial secondary path linear strain components have been normalised by the largest value, and the components ϵ_1 , ϵ_2 , v , and γ have been amplified by a factor of fifty ($\times 50$) in comparison to the components β and δ .

By considering the contributions to the quartic terms of the strain energy that result from the inclusion of cubic terms of the strain displacement relations and by inspection of Figure 6.5 through Figure 6.8, it may be concluded that the inclusion of cubic terms in the strain displacement relations will in general make a difference to the strain energy of spherical shells of approximately 0.1%. The total potential energy and the equilibrium equations that result from the use of quadratic strain displacement relations will be inconsistent in their quartic and cubic terms respectively; however the errors introduced into the analysis by neglecting the cubic terms of the strain displacement relations should also be of the order of 0.1%.

For mathematical consistency and for practical reasons, as the extra terms that result from the use of cubic strain displacement expressions were already included in the coding of the computer program, and as the effect of including these extra terms on the CPU time and storage required for execution of the code are entirely negligible, the equilibrium equations for both the fundamental and the secondary paths used in this study are based on the cubic strain displacement expressions given by equation (6.1).

6.2.4 Remarks on Efficiency and Accuracy.

The solution algorithms presented in Chapter Five have been used with the finite difference discretization, fundamental path modelling, eigenvalue problem solution strategy, and error and accuracy limits discussed above, in the computer program NLSPHERE. It is of interest to note that the algorithm used for the solution of the nonlinear eigenvalue problem, equations (5.35) and (5.37), results in the CPU time required for the solution being very weakly dependent on the number of terms used in the local perturbation series, and completely independent of the total number of terms in the fundamental path. This program was compiled (Minnesota Fortran, MNF, compiler) and executed on the University of London Computer Centre CDC 7600 computer.

The program NLSPHERE evaluates a number of path parameters, mode shapes, and energy components associated with the fundamental and secondary paths, a sample output for a perfect spherical cap, $\lambda=12$ ($r/t=100$, $0 \leq i \leq 2$), is contained in Appendix B. The energy contributions to V_0 , V_1 , and V_2 of the total potential energy, equations (4.46) to (4.51), are calculated at four points along the fundamental path (contribution to V_0), at the point of axisymmetric buckling (contributions to V_0 and V_1) and at the point of 'bifurcation' into axisymmetric or periodic modes (contribution to V_0 , V_1 and V_2). The individual components of the membrane, bending and load potential energy are evaluated in the meridional direction by numerical integration using Simpson's rule.

The total potential energy functional, equations (4.14) and (4.15), is the starting point for the derivation of the equilibrium equations, therefore a final check on the accuracy of both the fundamental and secondary path solutions may be based on back substituting the displacement

vector and load into the total potential energy functional. This check is significant as it is independent of the solution methods used. The computer program evaluates the error in the terms of the total potential energy functional at the axisymmetric buckling point (V_1) and at all points of periodic bifurcation (V_1 and V_2). The relative error has been defined as twice the sum of all the individually integrated energy components divided by the sum of the absolute values of the same energy components, where the energy components are defined by equations (4.46) to (4.51). The relative error in the total potential energy based on this definition is typically of the order of 0.1%, this final and important check demonstrates that the fundamental path displacements, the bifurcation modes and the loads satisfy the total potential energy functional, which is the fundamental equation on which the analysis is based.

6.3 COMPARISONS WITH OTHER NUMERICAL RESULTS

The internal limits on errors and checks by back substitution, described in the first part of this chapter provide only a partial confirmation of the validity of the numerical results obtained from the program NLSPHERE. Independent confirmation of the present results by comparison with the published results of Huang, Reference [17], and Uchiyama and Yamada, Reference [18], are presented below.

Both Huang and Uchiyama and Yamada use shallow shell theory; the spherical geometry of the shell is replaced by a paraboloid and with the introduction of a stress function into the analysis they arrive at Marguerre's nonlinear differential equation, in polar coordinates for shallow spherical caps under uniform pressure loading. The derivation of Marguerre's nonlinear differential equation incorporates the Kirchhoff assumptions, discussed in Chapter Two, as well as the following assumptions.

- The ratio of rise height, $h = r(1 - \cos\alpha)$, to the base diameter or chord, $D = 2r \sin\alpha$, of the spherical cap is less than say $1/8$, or equivalently half the open angle of the cap, α , is less than 28 degrees. This is the shallow shell assumption, and the spherical geometry is represented by a paraboloid.
- The inplane meridional and circumferential displacements u and v are small in comparison with the radial displacement w . That is, the only nonlinear terms used in the expression for the middle surface strains are quadratic terms involving the radial displacement w .

The introduction of these assumptions in the work of Huang and Uchiyama and Yamada results in a different method of analysis and different solution techniques to those used in the present work. For this reason comparisons between the present results and those of Huang and Uchiyama and Yamada are comparisons between the results of different shell theories.

6.3.1 Comparison of Axisymmetric and Periodic Buckling Pressures for Perfect Spherical Caps with Clamped Edges.

The present results ($\mu=0.3$) are compared with those of Huang ($\mu=1/3$) and Uchiyama and Yamada ($\mu=0.3$) in Figure 6.9 where the axisymmetric ($i=0$) and periodic ($i=1,2,\dots$) buckling pressures have been plotted against the slenderness or Bartdoff parameter λ for perfect clamped shallow spherical caps.

The present results in Figure 6.9 are seen to be in good agreement with those of Huang, Reference [17], as well as Uchiyama and Yamada, Reference [18], especially when the different values of Poisson's ratio, μ , used by Huang and the differences between the shallow

shell derivations and the present analysis are considered. In general the difference between the present results and those based on shallow shell theory are of the same order as the differences between the two results obtained using shallow shell theory with slightly different values of Poisson's ratio. The greatest variation in results occurs for the antisymmetric ($i=1$) buckling mode, even so the differences in buckling pressures are less than 5%. The locus of the antisymmetric buckling pressures given by the present results have a similar shape to that of Uchiyama and Yamada and have an opposite curvature to the results of Huang. When displacement profiles of the fundamental path or periodic bifurcation modes were visually compared, as Uchiyama and Yamada give their results graphically, no differences between the profiles could be detected.

6.3.2 Comparisons of the Axisymmetric Nonlinear Fundamental Path Solution with Initial Imperfections.

Various comparisons between the results from the computer program NLSPHERE and those reported by Uchiyama and Yamada, Reference [18], for spherical caps with initial axisymmetric imperfections have been undertaken. Agreement between the results of the two methods are remarkably good, with relative errors of less than 5% in all cases. A single typical comparison will be presented.

Uchiyama and Yamada present graphs of pressure (Q) against displacement at the pole (δ) for a shallow spherical cap, $\lambda \approx 5.75$ or $H=5$ for different amplitudes of initial imperfection (A_2^0, W_2^0), in figure 10.2 of Reference [18].

The following notation is used by Uchiyama and Yamada,

$$Q = \frac{8H^2}{\sqrt{3(1-\mu^2)}} \left(\frac{P}{P_{cl}} \right) \quad (6.2)$$

$$H = \frac{h}{t}$$

$$\lambda = 2 \sqrt[4]{3(1-\mu^2)H^2}$$

$$W_2^0 = (1 - \xi^2)^2$$

$$\xi = \frac{\tan \phi}{\tan \alpha}$$

$$\mu = 0.3$$

$$A_2^0 = \text{imperfection amplitude}$$

in which h is the rise height and t the shell thickness. The parameter ξ , ($0 \leq \xi \leq 1$), used by Uchiyama and Yamada is the nondimensional distance measured along the chord of the cap from beneath the pole or apex, and is given above in terms of the meridional coordinate ϕ and the half open angle of the cap, α .

The same shape of initial imperfection (W_2^0), was used with the program NLSPHERE, resulting in the excellent agreement shown in Figure 6.10. The values of the imperfection amplitude shown in Figure 6.10 have been nondimensionalised with respect to the shell thickness and positive values indicate an initial imperfection with an outward displacement at the pole of the cap. Comparisons of other cases incorporating initial imperfections reported by Uchiyama and Yamada resulted in equally good agreement with the predictions from the program NLSPHERE.

As a result of the validation exercises reported in this Chapter, and other tests undertaken during the course of the work, it is believed that no significant 'bugs' or errors remain in the program source code.

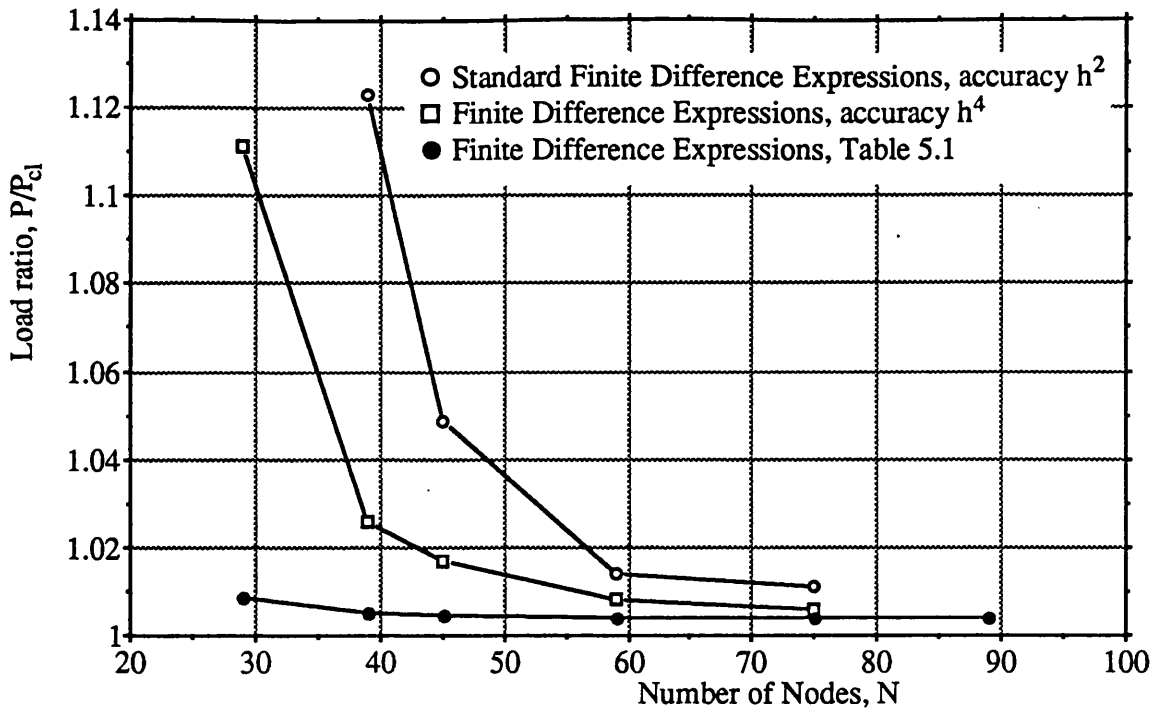


Figure 6.1 Comparison of Finite Difference Expressions, Lowest Buckling Load of Clamped Spherical Cap, Membrane Fundamental Path, $\lambda = 32$.

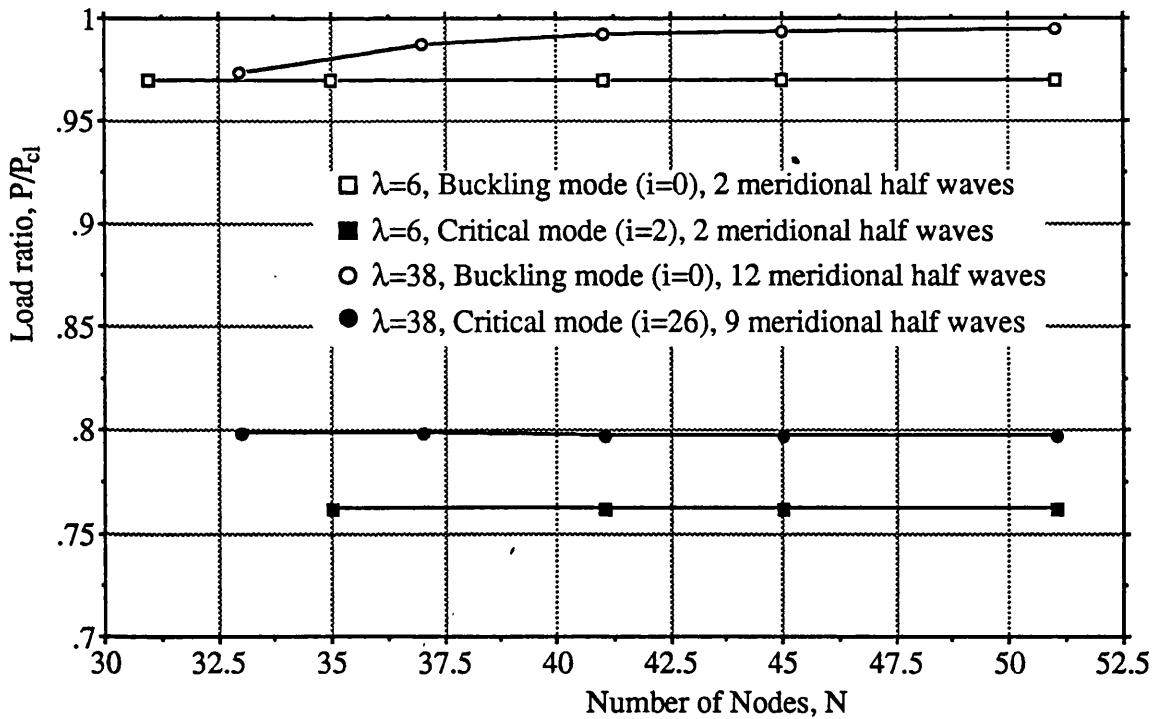


Figure 6.2 Convergence Study, Finite Difference Expressions in Table 5.1, Buckling and Critical Modes of Clamped Spherical Cap, Nonlinear Fundamental Path, $\lambda = 6$ and $\lambda = 38$

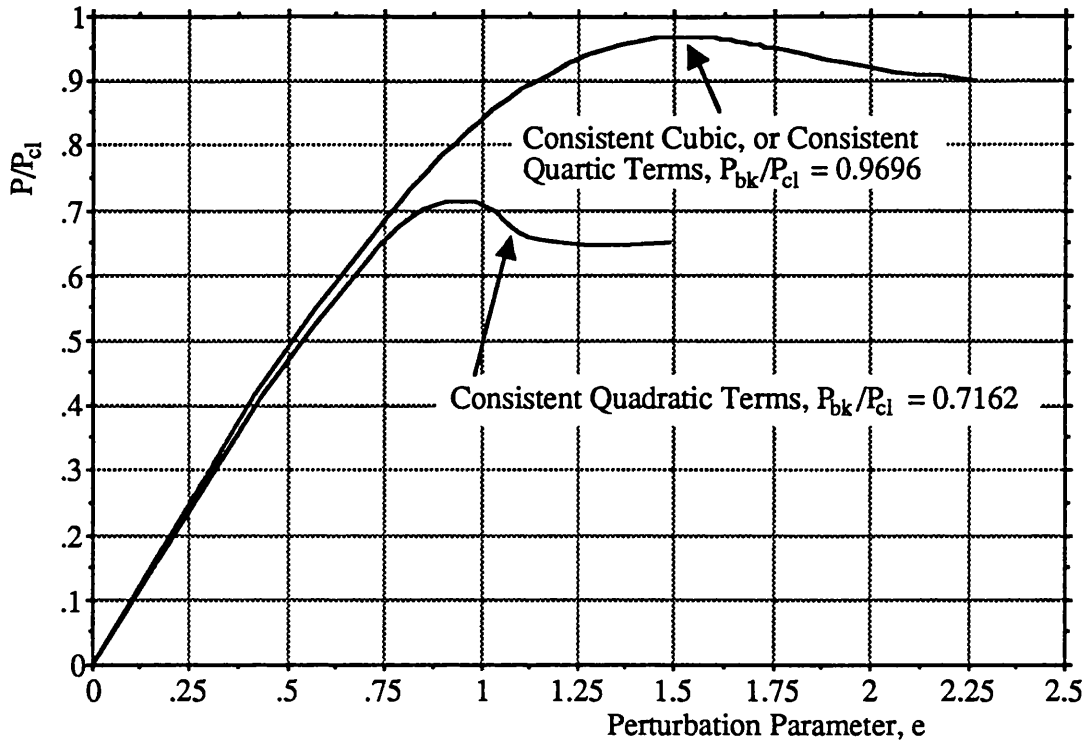


Figure 6.3 Nonlinear Fundamental Paths, based on Quadratic, Cubic, and "Quartic" Equilibrium Equations, for a Spherical Cap with $\lambda = 6$.

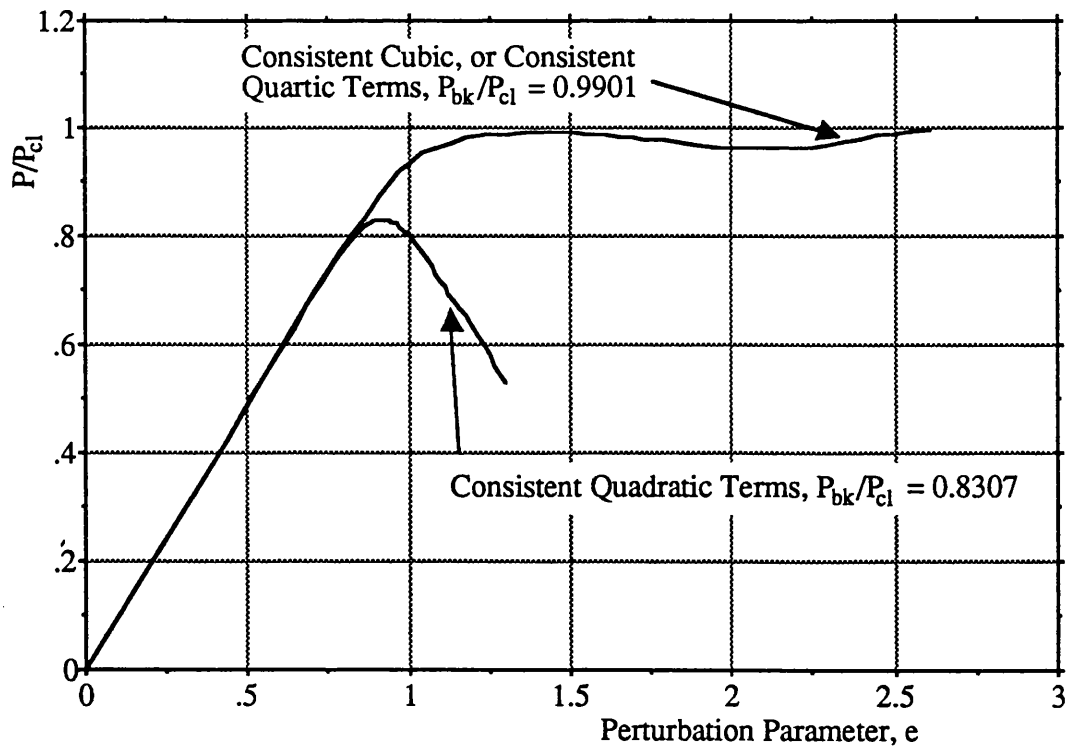


Figure 6.4 Nonlinear Fundamental Paths, based on Quadratic, Cubic, and "Quartic" Equilibrium Equations, for a Spherical Cap with $\lambda = 26$.

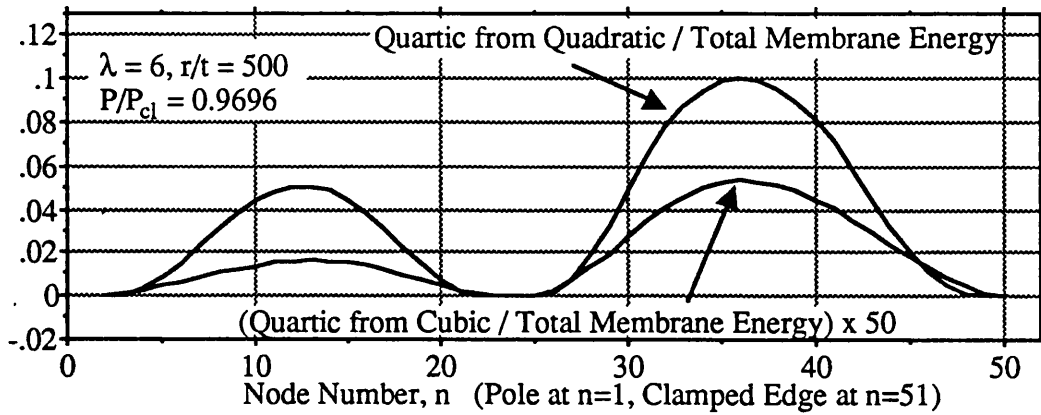
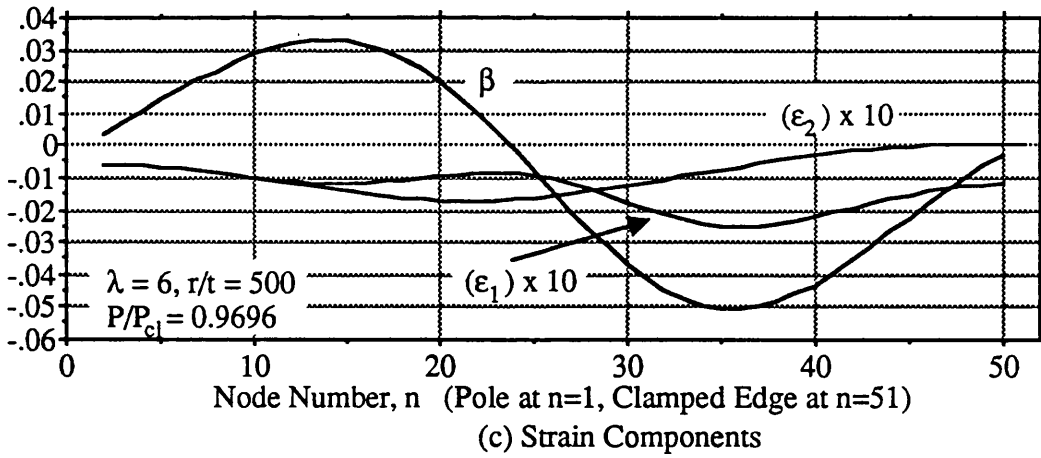
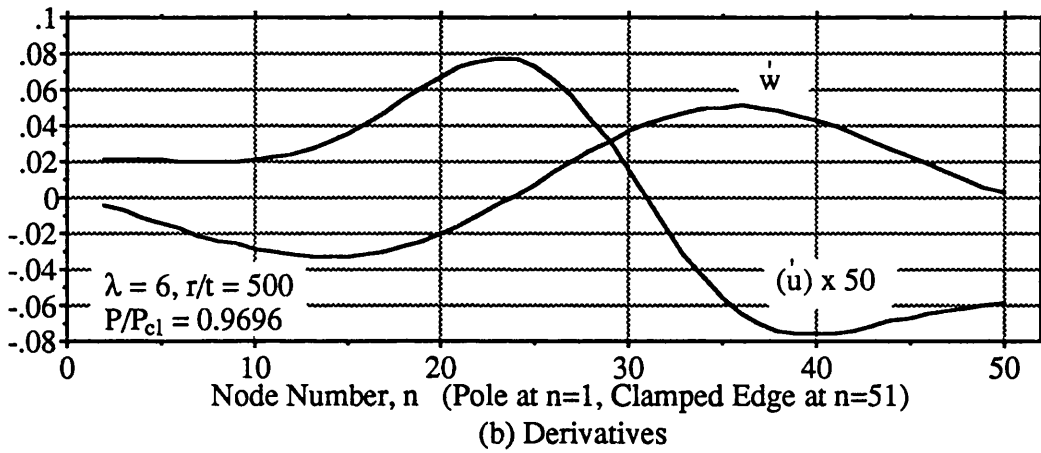
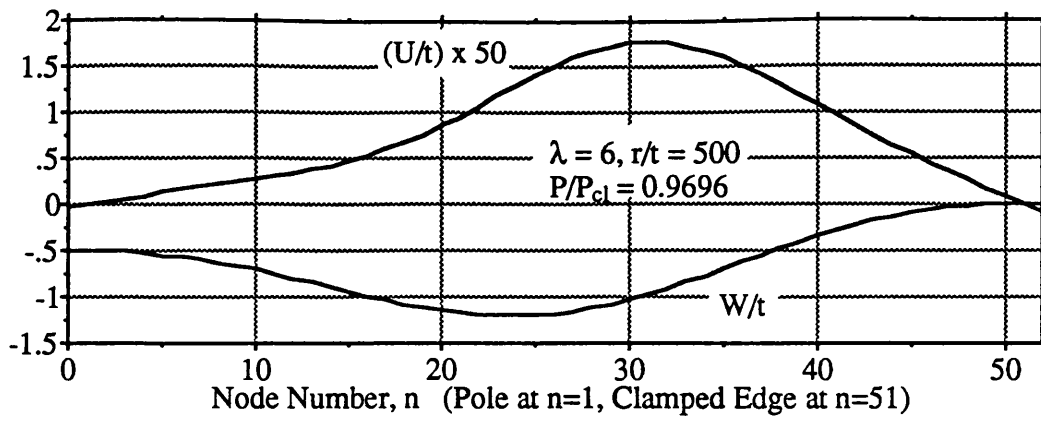


Figure 6.5 Fundamental Path Displacement, Strain, and Membrane Energy Profiles at the Axisymmetric Buckling Point, for $\lambda = 6$.

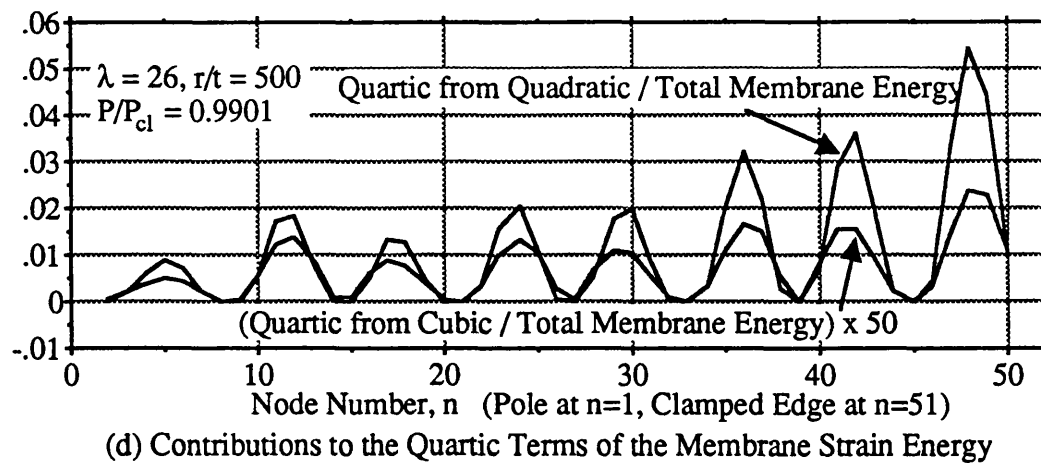
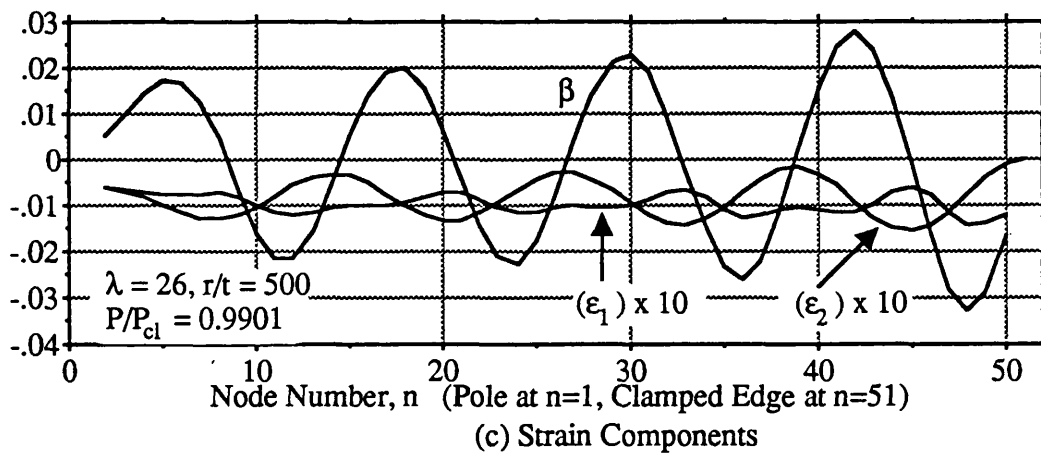
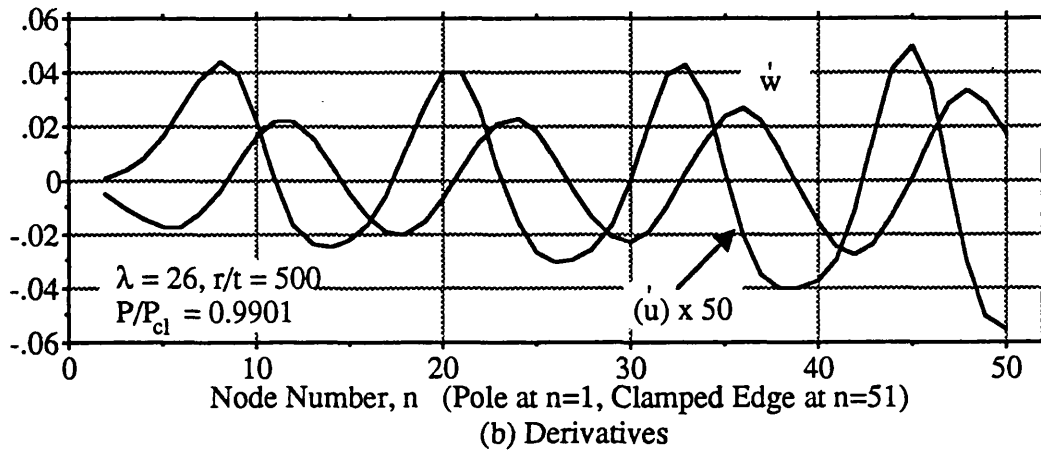
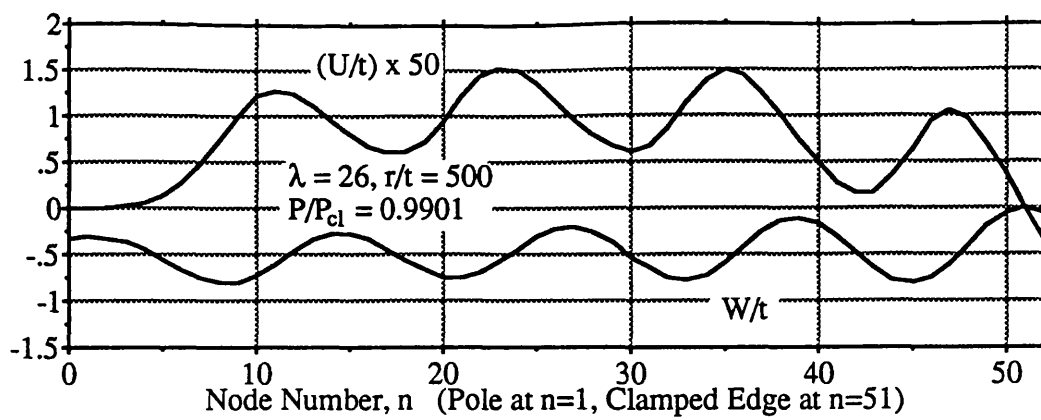
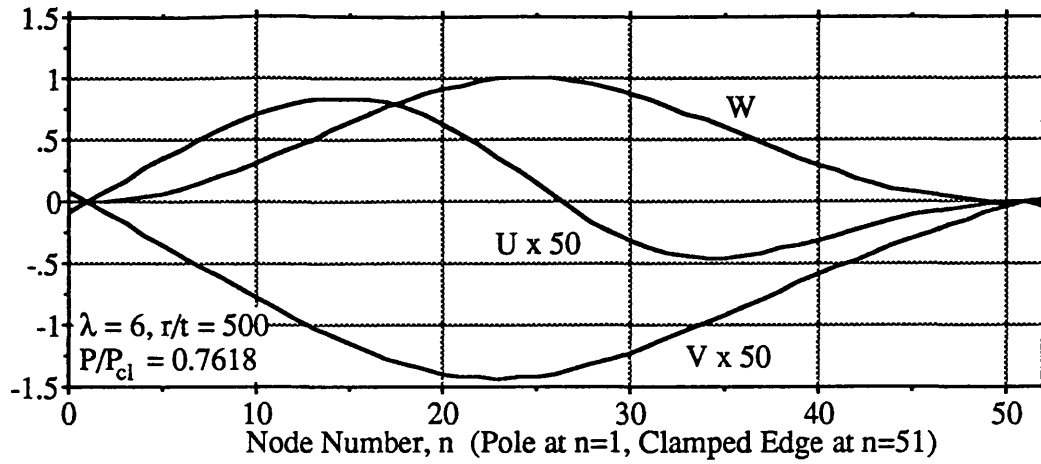
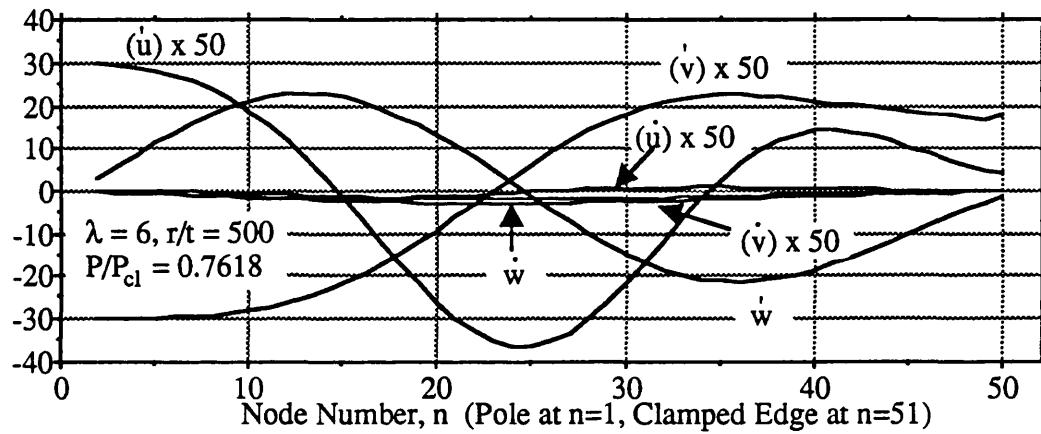


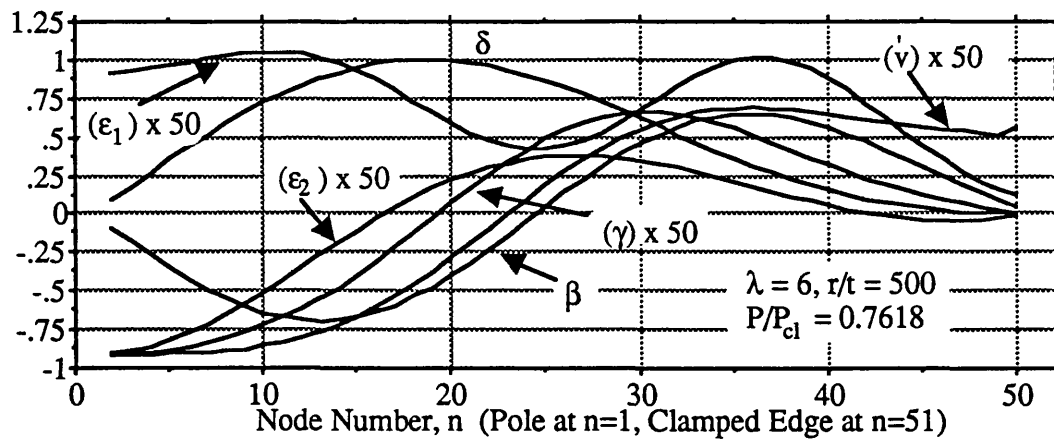
Figure 6.6 Fundamental Path Displacement, Strain, and Membrane Energy Profiles at the Axisymmetric Buckling Point, for $\lambda = 26$.



(a) Normalised Displacements

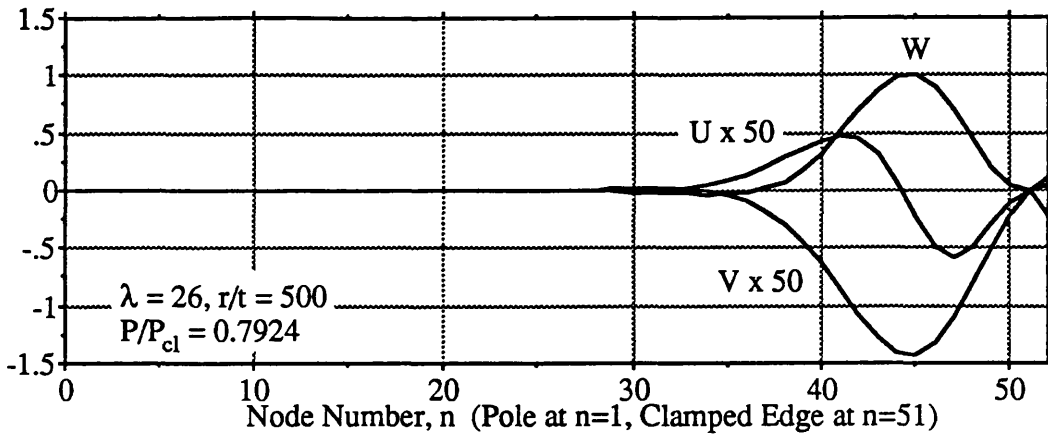


(b) Normalised Derivatives

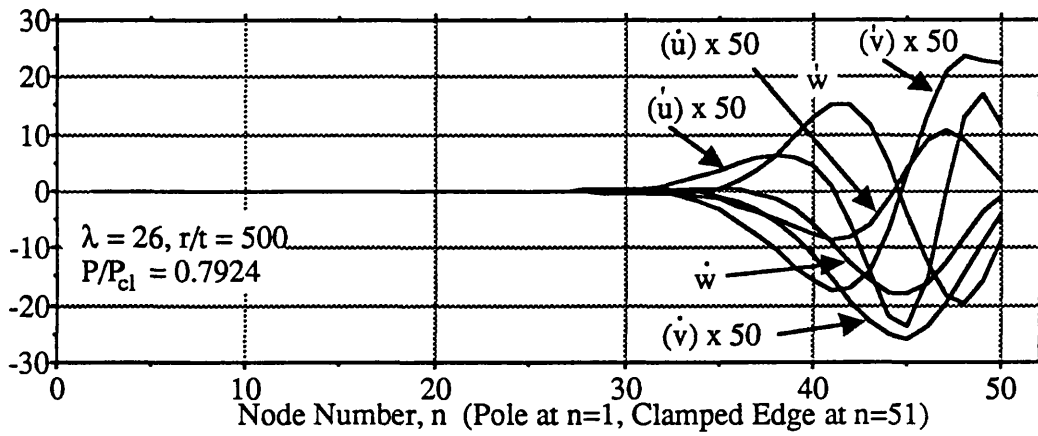


(c) Normalised Strain Components

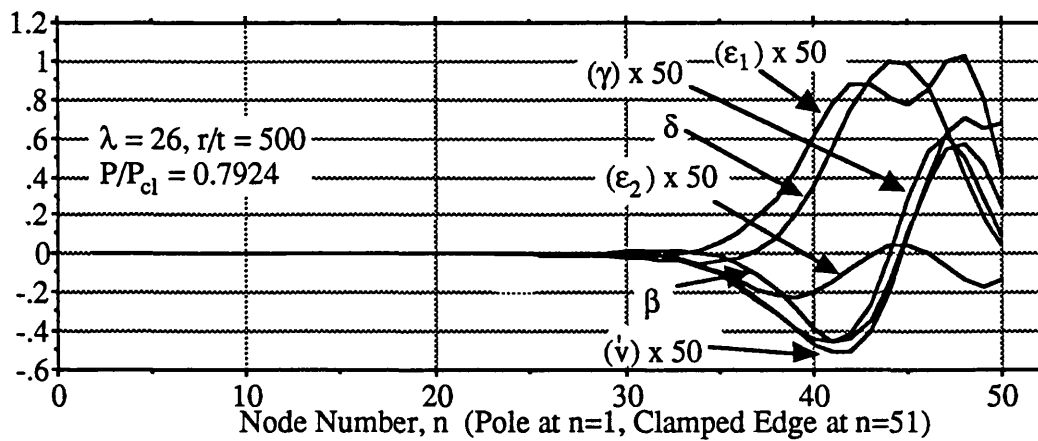
Figure 6.7 Secondary Path Initial Displacements, Derivatives, and Strain Components at the Point of Bifurcation into the Critical Periodic Mode, $i = 2$, for $\lambda = 6$.



(a) Normalised Displacements



(b) Normalised Derivatives



(c) Normalised Strain Components

Figure 6.8 Secondary Path Initial Displacements, Derivatives, and Strain Components at the Point of Bifurcation into the Critical Periodic Mode, $i = 18$, for $\lambda = 26$.

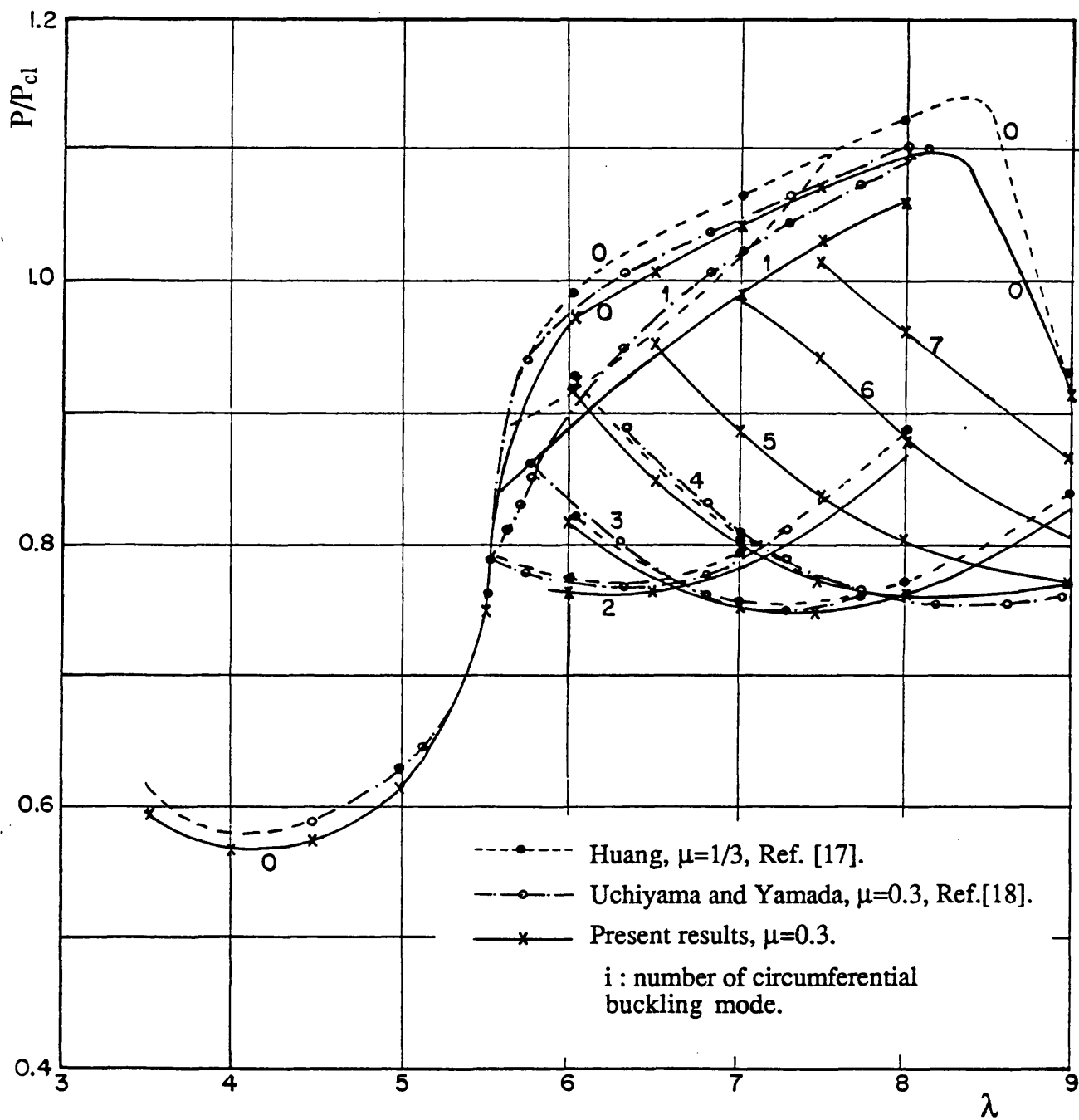


Figure 6.9 Comparisons of Axisymmetric and Periodic Buckling Pressures for Clamped Perfect Spherical Caps with Shallow Shell Theory Results, References [17] and [18]

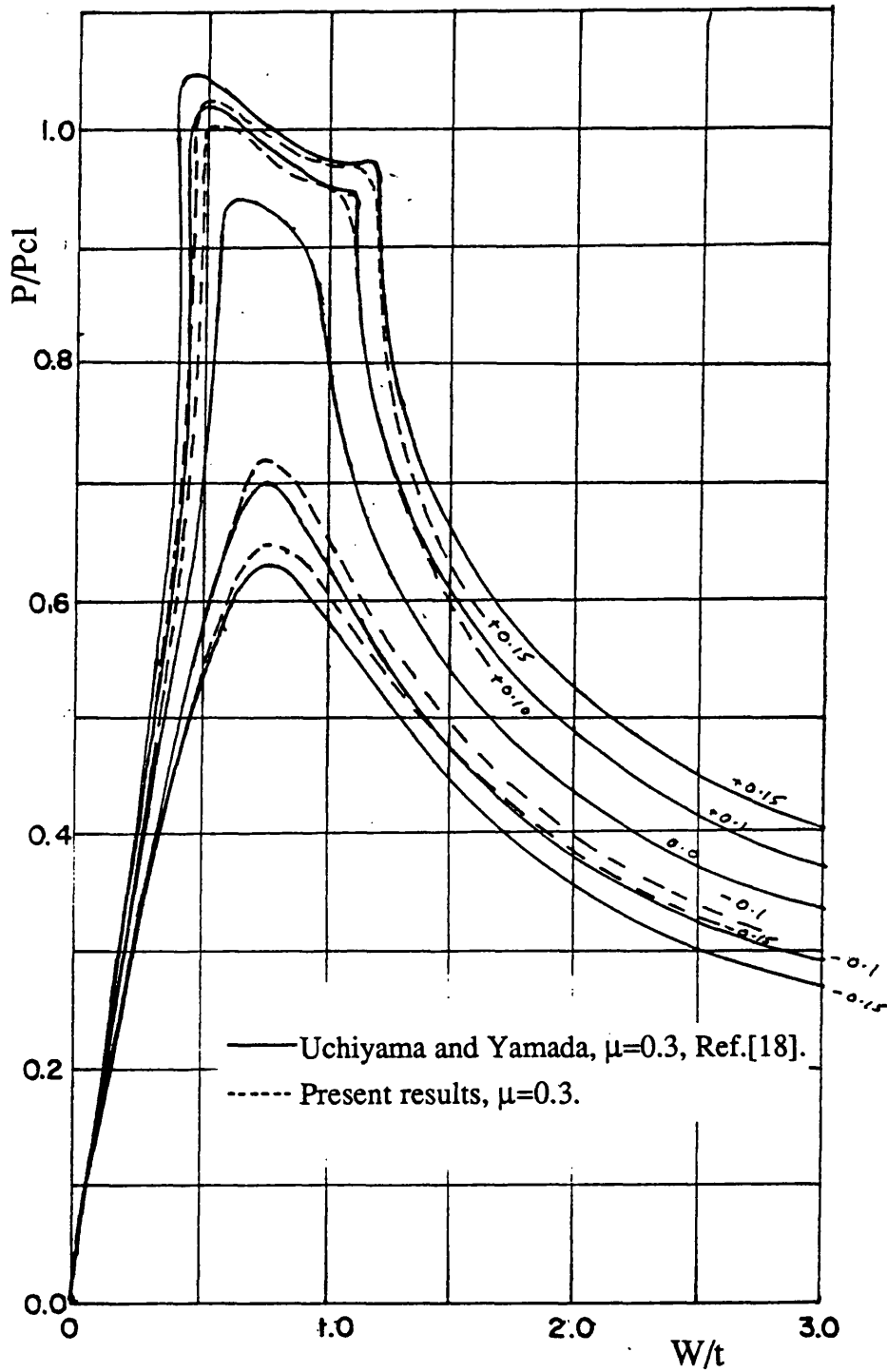


Figure 6.10 Comparisons of Nonlinear Fundamental Path for Clamped Imperfect Spherical Cap, $\lambda=5.75$, with Results from Shallow Shell Theory, Reference [18], Imperfection Amplitude is Indicated, see equation (6.2).

CHAPTER SEVEN

PRESENTATION OF RESULTS

CHAPTER SEVEN

CONTENTS

- 7.1 INTRODUCTION
- 7.2 THE GEOMETRIC SLENDERNESS OR BARTDOFF PARAMETER λ
- 7.3 PRESSURE LOADED PERFECT SPHERICAL CAPS CLAMPED AT THE BOUNDARY
- 7.4 PRESSURE LOADED SPHERICAL CAPS CLAMPED AT THE BOUNDARY WITH AXISYMMETRIC INITIAL IMPERFECTIONS

PRESENTATION OF RESULTS

7.1 INTRODUCTION

In this Chapter results from the computer program NLSPHERE, described in Chapters Five and validated in Chapter Six, are presented for perfect and imperfect spherical caps clamped at the boundary. Before the main results are presented in Section 7.3 and Section 7.4, results from different shells with the same value of the geometric slenderness or Bartdoff parameter, λ , are compared in Section 7.2. As a result of the comparisons presented in Section 7.2 the geometry of the spherical caps are described by the single slenderness or Bartdoff parameter λ in the remainder of the Chapter.

In Section 7.3 detailed results are presented for six perfect spherical caps with slenderness values of 3.5, 4, 6, 9, 12, and 30. And general results are given for perfect spherical caps with slenderness values between 3.5 and 60.

Section 7.4 presents detailed results for five spherical caps with initial axisymmetric imperfections and slenderness values of 4, 6, 9, 12, and 30. The initial axisymmetric imperfection mode that is used in the results presented in this Chapter is the buckling mode that results from a linear membrane fundamental path problem with boundary constraint imposed at the axisymmetric or periodic buckling point. This results in a linear eigenvalue problem, the eigenvector associated with the smallest eigenvalue is in all cases axisymmetric, and the radial component of the eigenvector associated with the smallest eigenvalue is used as the initial stress-free imperfection mode shape.

7.2 THE GEOMETRIC SLENDERNESS OR BARTDOFF PARAMETER λ

The geometric Bartdoff parameter λ for isotropic spherical shells is given by,

$$\lambda = \sqrt[4]{12(1-\mu^2)} \sqrt{\frac{r}{t}} \alpha \quad (7.1)$$

where

μ = Poisson's ratio

r = radius of the shell

t = the thickness of the shell

α = the open angle of half the shell, for a complete sphere $\alpha = \pi$

The geometric parameter λ is proportional to the ratio of the arc length, l ($l = \alpha r$) to the characteristic shell length (\sqrt{rt}), and by analogy with cylindrical shells is often referred to as the slenderness parameter. For complete spherical shells $\alpha = \pi$ and the slenderness parameter λ is proportional to $\sqrt{r/t}$. Also the order of the Legendre polynomial, N of the critical axisymmetric buckling mode is given by

$$N(N+1) \approx \left(\frac{\lambda}{\pi}\right)^2 = \sqrt{12(1-\mu^2)} \frac{r}{t} \quad (7.2)$$

The wavelength of the critical buckling mode, the critical wavelength, is inversely proportional to N for slender shells, large values of λ and N . The ratio of the characteristic shell length, $\sqrt{r/t}$, to the arc length, l , may be expressed as

$$\frac{C}{\lambda} = \frac{\sqrt[4]{12(1-\mu^2)}}{\lambda} = \frac{\sqrt{rt}}{l} \quad (7.3)$$

and this nondimensional parameter is indicated on many of the figures presented in this Chapter.

When shallow shell assumptions are used in the analysis of spherical caps the equilibrium equations governing the elastic behaviour of the shell may be written in a nondimensional form, which incorporates the shell geometry in terms of the single parameter λ . In the present work no attempt has been made in the derivation of the deep shell equations contained in Chapters Four and Five to express the shell geometry in terms of the single parameter λ . In the computer program NLSPHERE the geometry of the shell is specified by two parameters, the radius to thickness ratio r/t , and the open angle of the half shell α . For isotropic spherical caps, clamped at the boundary, the results of the nonlinear fundamental path and bifurcation analyses, when suitably nondimensionalised, were found to be dependent on λ alone.

For example Figure 7.1 (3 pages) compares results for two different shells with the same slenderness value of $\lambda=12$. These shells were specified by $r/t=100$ and $\alpha=0.660$ which does not satisfy the shallow shell conditions, and $r/t=500$ and $\alpha=0.295$ which does satisfy the shallow shell conditions.

In Figure 7.1 (a), (b) and (c) the nondimensional load, P/P_{cl} , is plotted against the perturbation parameter, e , the relative change in volume, $\Delta V/V$, and the displacement at the pole, δ , respectively. In the solution of the perturbation problem, Section 5.3 of Chapter Five, the value of $p_{1,1}$ is arbitrary. In the computer program NLSPHERE the first term of the perturbation series for the load, $p_{1,1}$, was set equal to the classical buckling pressure for the complete sphere, consequently the linear fundamental path solution, the solution for the complete sphere, would in all cases pass through the origin and the point with coordinates (1,1) in Figure 7.1 (a). Figure 7.1 (b) again shows the fundamental path, the load is plotted against the change in volume of the spherical cap, where the change in volume, ΔV , is normalised by the initial volume, V , of the spherical cap, and this is not the 'correct' nondimensionalisation. It may be shown that the 'correct' nondimensionalisation will result when the change in volume of the spherical cap is normalised by the change in volume of the complete sphere at the buckling load. The fundamental path is shown once again in Figure 7.1 (c), in this case the nondimensional load has been plotted against the displacement at the pole, δ , normalised by the shell thickness. For the complete spherical shell the radial contraction is proportional to the load and the contraction at the point of buckling is given by equation (3.5) of Chapter Three, for Poisson's ratio of 0.3 the radial contraction at buckling is equal to 42.4% of the shell thickness. The linear fundamental path solution, the solution for the complete sphere, would in all cases pass through the origin and the point with coordinates (0.424,1) in Figure 7.1 (c).

//?

The difference in the axisymmetric buckling pressures ($P_{bk}/P_{cl} \approx 0.960$) for the two shells is 0.11% which is within the limits of accuracy of the program NLSPHERE discussed in Chapter Six.

The radial, W , and inplane, U , displacements normalised by the shell thickness at the point of buckling are shown in Figure 7.1 (d) and (e) respectively for the two spherical caps. The radial displacements, Figure 7.1 (d), agree within the accuracy of the program, however there is a factor of $\sqrt{5}$ between the inplane displacements, Figure 7.1 (e). The 'correct' length to use in normalising the inplane, U , displacements is the arc length, $l=r\alpha$, of the spherical cap.

The difference in the critical periodic buckling pressures ($P_{cr}/P_{cl} \approx 0.772$, $i_{cr}=7$) for the two shells is approximately 0.13%, which is within the limits of accuracy of the program. Figure 7.1 (f) and (g) show the meridional, σ_ϕ , and circumferential, σ_θ , stress profiles at the critical load, $P_{cr}/P_{cl} \approx 0.772$, and at the axisymmetric buckling load, $P_{bk}/P_{cl} \approx 0.960$, and these stresses are normalised by the classical buckling stress, σ_{cl} , for the complete spherical shell. It is of

interest to note that the critical bifurcation load, $P_{cr}/P_{cl}=0.772$, occurs when the circumferential stress, σ_θ , first reaches the classical value, σ_{cl} . Comparisons of the critical meridional mode shape, $i_{cr}=7$, that result from the nonlinear eigenvalue problem have not been shown as the amplitude of the displacements is necessarily arbitrary.

When an axisymmetric initial imperfection with an amplitude of one tenth of the shell thickness is introduced into the analysis no periodic bifurcation from the nonlinear axisymmetric fundamental path occurs. This magnitude of initial imperfection reduces the axisymmetric buckling pressure for the two shells ($\lambda=12$, $r/t=100$ and $r/t=500$) to 0.596 of the classical pressure ($P_{bk}/P_{cl}\approx 0.596$), and the difference between the results obtained for the two shells is less than 0.3%.

The geometry of the spherical caps will be described by the single slenderness or Bartdoff parameter λ in this Chapter. As a point of interest a radius to thickness ratio of 500 has been used in all the cases presented below.

7.3 PRESSURE LOADED PERFECT SPHERICAL CAPS CLAMPED AT THE BOUNDARY

Periodic buckling occurs at a lower pressure than axisymmetric buckling for spherical caps with slenderness values, λ , of more than about 5.5, see Figure 6.9. In the detailed discussion and presentation of the results for perfect spherical caps below only the lowest bifurcation or critical load is mentioned. However as the slenderness increases, λ increases, the number of periodic bifurcation modes increase and the proximity of these periodic bifurcation modes also increases. The position of the points of bifurcation on the fundamental path of the dominant and subdominant periodic modes with circumferential mode numbers, i , between 16 and 33 are shown in Figure 7.2 for a perfect spherical cap with a slenderness value of 30.

In Figures 7.3 to 7.8, the nonlinear fundamental path, the fundamental path displacement profiles, the meridional and circumferential stress profiles, and the lowest, or critical, periodic buckling mode, eigenvector, are shown for caps with λ values of 3.5, 4, 6, 9, 12, and 30. In the graphs of the fundamental path radial displacement and stress profiles contained in Figures 7.3. to 7.8, the parameter 's' is the normalised arc length measured from the pole ($s=0$) to the clamped edge ($s=1$) of the spherical cap. To avoid confusion the value of the perturbation parameter, e , is used to indicate the location on the fundamental path to which the fundamental path displacement or stress profiles refer. The amplitude of the eigenvector resulting from the linearised eigenvalue problem is indeterminate, and the amplitude of the incremental mode shapes shown in Figures 7.5 to 7.8 have been normalised such that the maximum displacement is one.

Figure 7.3 $\lambda=3.5$

Figure 7.3 (a) shows the fundamental path, load is plotted against perturbation parameter, for a spherical cap with a λ value of 3.5. Axisymmetric buckling, a local maximum, occurs at $e=1.35$, when the load $P_{bk}/P_{cl}=0.597$, and a local minimum occurs at $e=2.54$, when the load $P/P_{cl}=0.559$. Figure 7.3 (b) and (c) show the radial, W , and inplane, U , displacement profiles at various positions along the fundamental path. For this spherical cap the rise height $h=1.85t$, and from inspection of Figure 7.3 (b) it may be seen that buckling, a local maximum, occurs at $e=1.35$ when the radial displacement at the pole $\delta=-1.1t$, and the local minimum occurs at $e=2.54$ when the radial displacement at the pole $\delta=-2.0t$, that is the shell turns 'inside out'. The meridional and circumferential stress profiles are shown in Figure 7.3 (d) and (e), the circumferential stress, σ_θ , at buckling, $e=1.35$, has a maximum value of approximately $1.1\sigma_{cl}$, Figure 7.3 (e). Both the meridional and circumferential stresses become tensile, negative in Figure 7.3 (d) and (e), near the pole for large values of the perturbation parameter, e.g. $e=4.89$. No periodic bifurcations from the fundamental path were found.

Figure 7.4, $\lambda=4$

The fundamental path for a spherical cap with a λ value of 4 is shown in Figure 7.4 (a) and (b), in (a) the load is plotted against perturbation parameter, and in (b) the load is plotted against the relative change in volume of the spherical cap. Axisymmetric buckling, a local maximum, occurs at $e=1.24$, when the load $P_{bk}/P_{cl}=0.563$, and a local minimum occurs at $e=3.84$, when the load $P/P_{cl}=0.381$. Figure 7.4 (c) and (d) show the radial, W , and inplane, U , displacement profiles at various positions along the fundamental path. For this spherical cap the rise height $h=2.42t$, and from inspection of Figure 7.4 (c) it may be seen that buckling occurs, a local maximum, at $e=1.24$ when the radial displacement at the pole $\delta \approx -1.0t$, and the local minimum occurs at $e=3.84$, when the radial displacement at the pole $\delta \approx -3.1t$. The behaviour of this spherical cap, $\lambda=4$, is similar to that described above for $\lambda=3.5$, the shell turns 'inside out' between the buckling load and the minimum load. The meridional and circumferential stress profiles are shown in Figure 7.4 (e) and (f), the circumferential stress, σ_θ , at buckling, $e=1.24$, has a maximum value of approximately $1.0\sigma_{cl}$, Figure 7.4 (f). Both the meridional and circumferential stresses become tensile near the pole for large values of the perturbation parameter. Once again no periodic bifurcations from the fundamental path occur.

Figure 7.5, $\lambda=6$

In Figure 7.5 (a), (b) and (c) the fundamental path for a spherical cap with a λ value of 6 is shown, in (a) the load is plotted against perturbation parameter, in (b) the load is plotted against the relative change in volume of the spherical cap, and in (c) the load is plotted against the radial displacement at the pole. Axisymmetric buckling occurs at $e=1.58$, when the load $P_{bk}/P_{cl}=0.970$. The radial, W , and inplane, U , displacement profiles at various positions along the fundamental path are shown in Figure 7.5 (d) and (e). From inspection of Figure 7.5 (c) and (d) it may be seen that axisymmetric buckling occurs, at $e=1.58$, when the radial displacement at the pole $\delta \approx -0.5t$, however at this load the maximum radial displacement is approximately $-1.2t$ and occurs at $s \approx 0.46$, Figure 7.5 (d).

For values of the perturbation parameter, e , of less than about 0.83 the behaviour of the spherical cap is fairly linear, while for values of the perturbation parameter greater than 0.83 the behaviour becomes highly nonlinear, Figure 7.5 (a), (b) and (c). Prior to buckling, $0.83 < e < 1.58$, the radial displacement at $s \approx 0.46$ grows rapidly with only small changes in the radial displacement at the pole. The radial displacement profile, Figure 7.5 (d), at buckling contains two points of inflection, $j=2$, and the radial displacement at the pole is a relative minimum. On the postbuckling part of the axisymmetric fundamental path, $1.58 < e < 3.33$, the displacement mode shape changes, the radial displacements at the pole increase rapidly, Figure 7.5 (c) and (d), the radial displacement at the pole becomes the maximum $j=1$, while the radial

displacement at $s=0.46$ decreases rapidly. This change in mode shape results in a decrease in the change in volume of the deformed shell, Figure 7.5 (b).

The meridional and circumferential stress profiles are shown in Figure 7.5 (f) and (g), the circumferential stress, σ_θ , at the axisymmetric buckling load, $e=1.58$, has a maximum value of approximately $1.82\sigma_{cl}$, Figure 7.5 (g).

Bifurcation from the axisymmetric fundamental path into periodic modes occurs before the axisymmetric buckling point is reached. The minimum or critical bifurcation is in the circumferential mode $i_{cr}=2$ at $e=0.90$ when the load $P_{cr}/P_{cl}=0.762$, and this occurs when the maximum value of the circumferential stress, σ_θ , is approximately equal to the classical value, σ_{cl} , Figure 7.5 (g). The shape of the critical mode is shown in Figure 7.5 (h).

Figure 7.6, $\lambda=9$

The fundamental path for a spherical cap with a λ value of 9 is shown in Figure 7.6 (a), (b) and (c). Axisymmetric buckling occurs at $e=1.14$, when the load $P_{bk}/P_{cl}=0.915$. The radial, W , and inplane, U , displacement profiles at various positions along the fundamental path are shown in Figure 7.6 (d) and (e). From Figure 7.6 (c) and (d) it may be seen that axisymmetric buckling occurs when the radial displacement at the pole $\delta \approx -0.6t$, however at this load the maximum radial displacement is approximately $-0.75t$ and occurs at $s=0.65$, Figure 7.6 (d).

The radial displacement profile, Figure 7.6 (d), at buckling contains three points of inflection, $j=3$, and the radial displacement at the pole is a relative maximum. The behaviour of the spherical cap is fairly linear for values of the perturbation parameter, e , of less than about 1.1, while for values of the perturbation parameter greater than 1.1 the behaviour becomes highly nonlinear, Figure 7.6 (a), (b) and (c). On the postbuckling part of the axisymmetric fundamental path, $1.14 < e < 9.26$, the displacement mode shape changes rapidly, the radial displacements at the pole increase, Figure 7.6 (c) and (d), and the radial displacement mode shape changes from $j=3$ to $j=1$. This change in mode shape results in a decrease in the change in volume of the deformed shell, Figure 7.6 (b), as the inward radial displacements at $s=0.65$ change to outward displacements.

The meridional and circumferential stress profiles are shown in Figure 7.6 (f) and (g), the circumferential stress, σ_θ , at the axisymmetric buckling load, $e=1.14$, has a maximum value of approximately $1.75\sigma_{cl}$, Figure 7.6 (g).

Before the axisymmetric buckling point is reached bifurcation from the axisymmetric fundamental path into periodic modes occurs. The minimum or critical bifurcation is in the circumferential mode $i_{cr}=4$ at $e=0.80$ when the load $P_{cr}/P_{cl}=0.767$, and this occurs when the

maximum value, at $s=0.61$, of the circumferential stress is approximately equal to the classical value, Figure 7.6 (g). The shape of the critical mode is shown in Figure 7.6 (h).

Figure 7.7, $\lambda=12$

Figure 7.7 (a), (b) and (c) show the fundamental path for a spherical cap with a λ value of 12. Axisymmetric buckling occurs at $e=1.28$, when the load $P_{bk}/P_{cl}=0.959$. Radial, W , and inplane, U , displacement profiles at various positions along the fundamental path are shown in Figure 7.7 (d) and (e). It may be seen from inspection of Figure 7.7 (c) and (d) that axisymmetric buckling occurs when the radial displacement at the pole $\delta \approx -0.55t$ is a local minimum, however at this load the radial displacement profile has two local maxima of approximately $-0.75t$ at $s=0.2$ and at $s=0.74$, Figure 7.7 (d).

For values of the perturbation parameter, e , of less than about 0.90 the behaviour of the spherical cap is fairly linear, while for values of the perturbation parameter greater than 0.90 the behaviour becomes highly nonlinear, Figure 7.7 (a), (b) and (c). Prior to buckling, $0.97 < e < 1.28$, the radial displacements at $s=0.2$ and $s=0.74$ grow rapidly with only small changes in the radial displacement at the pole. The radial displacement profile, Figure 7.7 (d), at buckling contains four points of inflection, $j=4$, and the radial displacement at the pole is a relative minimum. On the postbuckling part of the axisymmetric fundamental path the displacement mode shape changes, the radial displacements at the pole increase from approximately $-0.55t$ to approximately $-0.91t$ as e increases from 1.28 to 1.94, Figure 7.7 (c) and (d), and the radial displacement at the pole becomes a local maximum $j=3$, while the radial displacements at $s=0.2$ and $s=0.74$ decrease. This change in mode shape results in a decrease in the change in volume of the deformed shell, Figure 7.7 (b).

The meridional and circumferential stress profiles are shown in Figure 7.7 (f) and (g), the circumferential stress, σ_θ , at the axisymmetric buckling load, $e=1.28$, has a maximum value of approximately $1.5\sigma_{cl}$, Figure 7.5 (g).

Bifurcation from the axisymmetric fundamental path into periodic modes occurs before the axisymmetric buckling point is reached. The critical bifurcation is in the circumferential mode $i_{cr}=7$ at $e=0.82$ when the load $P_{cr}/P_{cl}=0.772$, and this occurs when the maximum value of the circumferential stress, σ_θ , is approximately equal to the classical value, σ_{cl} , Figure 7.7 (g). The shape of the critical mode is shown in Figure 7.7 (h).

Figure 7.8, $\lambda=30$

The fundamental path for a spherical cap with a λ value of 30 is shown in Figure 7.8 (a), (b) and (c). Axisymmetric buckling occurs at $e=1.05$, when the load $P_{bk}/P_{cl}=0.952$. From Figure 7.8 (c) and (d) it may be seen that axisymmetric buckling occurs when the radial displacement

at the pole $\delta \approx -0.52t$, is a local maximum. The radial displacement profile, at the buckling load, has four other local maxima the largest of which is approximately $-0.68t$ at $s \approx 0.90$, Figure 7.8 (d).

At buckling the radial displacement profile, Figure 7.8 (d), contains nine points of inflection, $j=9$, and the radial displacement at the pole is a relative maximum. The behaviour of the spherical cap is fairly linear for values of the perturbation parameter, e , of less than about 0.9, while for values of the perturbation parameter greater than 0.9 the behaviour becomes highly nonlinear, Figure 7.8 (a), (b) and (c). On the postbuckling part of the axisymmetric fundamental path the displacement mode shape changes, the radial displacements at the pole increase from approximately $-0.52t$ to approximately $-1.16t$ as e increases from 1.05 to 1.55, Figure 7.8 (c) and (d). The radial displacement mode shape also changes from $j=9$ at $e=1.05$ to $j=7$ at $e=1.55$, the radial displacement at the pole becoming the maximum displacement at $e=1.55$. This change in mode shape results in a decrease in the change in volume of the deformed shell, and the unloading path in Figure 7.8 (b) is virtually indistinguishable from the loading path.

The meridional and circumferential stress profiles are shown in Figure 7.8 (f) and (g), the circumferential stress at the axisymmetric buckling load, $e=1.05$, has a maximum value of approximately $1.38\sigma_{cl}$, Figure 7.8 (g).

Before the axisymmetric buckling point is reached bifurcation from the axisymmetric fundamental path into periodic modes occurs. The minimum or critical bifurcation is in the circumferential mode $i_{cr}=21$ at $e=0.80$ when the load $P_{cr}/P_{cl}=0.795$, and this occurs when the maximum value, at $s \approx 0.89$, of the circumferential stress is approximately equal to the classical value, Figure 7.8 (g). The shape of the critical mode is shown in Figure 7.8 (h).

Summary

The axisymmetric buckling and periodic bifurcation or critical pressures for clamped spherical caps where the slenderness parameter λ is in the range $3.5 \leq \lambda \leq 60$ are presented in Table 7.1(a) and (b) and graphically in Figure 7.9. When two values of the normalised axisymmetric buckling pressure are given in Table 7.1 this indicates that the fundamental path solution algorithm found a second (minimum) turning point, and this value is given as the second figure in Table 7.1. For example, when $\lambda=3.5$, see Figure 7.3, maxima and minima occur on the fundamental path at values of P/P_{cl} equal to 0.597 and 0.559 respectively. Also two values of the normalised periodic bifurcation pressure appearing in Table 7.1 for the same circumferential mode number, i , indicate that subdominant eigenvalues and vectors have been found by the computer program NLSPHERE. When subdominant eigenvalues have been found the load corresponding to the first bifurcation (lowest value of perturbation parameter) is given first. In

the case $\lambda=15$ and $i=5$, where the first value given in Table 7.1(a) is larger than the second, the second bifurcation occurs after the axisymmetric buckling point.

For spherical caps with values of the geometric parameter λ greater than about 5.5 bifurcation into periodic modes occurs at a lower pressure than axisymmetric buckling. The maximum radial displacement of the periodic critical mode and the maximum radial displacement of the axisymmetric fundamental path displacements at the critical load occur at approximately the same position on the shell. As λ increases the periodic buckling displacements affect a smaller area of the shell adjacent to the clamped boundary and the critical circumferential mode number i_{cr} increases, as may be seen from Figures 7.5 to 7.8. The number of periodic bifurcation modes, and their proximity to the critical mode also increases as λ increases. For a cap with a λ value of 30 some of these subcritical modes are shown in Figure 7.2.

For all spherical caps with λ values greater than 4 axisymmetric buckling, $4 \leq \lambda \leq 5.5$, or the lowest periodic bifurcation, $\lambda > 5.5$, occurs when the circumferential stress, σ_θ , first reaches the classical buckling stress, σ_{cl} , for the complete sphere with the same radius to thickness ratio.

For axisymmetric displacements j has been used to denote the meridional mode shape, and corresponds to the number of points of inflection ($j \geq 1$) occurring on the half shell ($0 \leq s \leq 1$), while N is reserved for the order of the Legendre polynomial of the buckling mode of the complete sphere. The values of j and N for clamped spherical caps and complete spheres respectively are also given in Figure 7.9, and are approximately equal for shells of equal slenderness, λ . Inspection of Figures 7.3 to 7.8 reveals that for axisymmetric displacements odd values of j occur when the displacement at the pole is a local maximum and even values of j are associated with a local minimum of the radial displacement at the pole. The undulating nature of the locus of axisymmetric buckling points in Figure 7.9 reflects the transition between odd and even values of j . Axisymmetric buckling pressures being locally less for odd values of j , and the odd j modes extend over a larger range of λ than the modes corresponding to even values of j .

Although the periodic post bifurcation paths have not been calculated in the present work, it may be of interest to speculate on the behaviour that they would reveal. For slender shells periodic bifurcation occurs before axisymmetric buckling and the critical mode shape affects the portion of the cap close to the boundary, the remainder of the cap being less affected by the initial critical bifurcation mode. However, if we consider the 'unaffected' part of the cap as a separate cap with a smaller slenderness value, λ , and 'softer' boundary conditions then it is reasonable to suppose that this part of the cap will have a lower buckling or critical load than the entire cap, see Figure 7.9. In this way it may be imagined that elastic buckling behaviour of slender spherical caps will start with periodic bifurcation near the boundary and then propagate towards the pole.

The terms of the total potential energy, V , that are independent, V_0 , linearly dependent, V_1 , and quadratically dependent, V_2 , on the incremental displacements are given in Chapter Four, by equations (4.46) to (4.51), and the program evaluates these terms at various points along the fundamental path. In evaluating the energy contributions to V_1 , the rate of change of the fundamental path displacement vector is used as the incremental vector, as all contributions to V_1 arising from periodic displacements are necessarily zero. The linearised eigenvalue problem that results from the application of the stationary condition to V_2 has axisymmetric solutions corresponding to the stationary points of the fundamental path, and periodic solutions when $\lambda > 5.5$ corresponding to the points of bifurcation to a periodic secondary path from the axisymmetric fundamental path. The contributions to the quadratic term of the total potential energy, V_2 , are evaluated for all eigenvalues and vectors, that is at both the points of axisymmetric 'snap' buckling and at the points of periodic bifurcation. In the sample output in Appendix B the evaluation of these energy contributions is shown.

For a spherical cap with a λ value of 12 the contributions to the quadratic terms of the total potential energy V_2 are plotted against the circumferential mode number, i , in Figure 7.10. As the sum of the quadratic energy contributions is zero and the amplitude of the eigenvector is indeterminate the quadratic energy contributions shown in Figure 7.10 have been normalised such that the total positive (stabilising) or negative (destabilising) energy is equal to one or minus one.

The destabilising energy contributions are due to the interaction between the axisymmetric fundamental path displacements and the periodic secondary path displacements. The stabilising contributions to the quadratic energy in all cases come from the terms that are functions of the secondary path displacements only, that is the positive energy is independent of the fundamental path displacements at the point of bifurcation. The quadratic components of the load potential energy J_{2L} given by equation (4.50) are not shown in Figure 7.10 as they are small by comparison to the other terms. Typically J_{2L} is responsible for less than 0.1% of the total destabilising energy.

The critical circumferential buckling mode, $i_{cr}=7$, occurs where the stabilising secondary path membrane and bending energies are equal in magnitude, as far as this is possible for integer values of i .

The stabilising and destabilising energy contributions to the circumferential membrane energy exhibit opposite trends, as the periodic buckling mode number, i , varies. At the critical buckling mode number, $i_{cr}=7$, the stabilising energy resulting from the secondary path circumferential membrane energy, $\dot{N}_\theta \dot{\epsilon}_\theta$, is small and decreases with increasing values of i . However the interaction between the secondary path and fundamental path circumferential stresses and strains, $\dot{N}_\theta \dot{\epsilon}_\theta$, $\dot{N}_\theta \ddot{\epsilon}_\theta$ and $\dot{N}_\theta \ddot{\epsilon}_\theta$, are responsible for approximately 50% of the destabilising energy at the critical buckling mode, and the relative magnitude of these energy

components increases with increasing i . This is a result of the interaction between the fundamental and secondary path displacement fields shown in Figures 7.5 to 7.8. Periodic bifurcation results in a release of this fundamental path circumferential membrane energy, which is present in the form of compressive strain energy.

The total bending energy ($U_{2B} = U_{2,B\phi} + U_{2,B\theta} + U_{2,B\theta\phi}$) is stabilising and increases when the periodic buckling mode number increases, this is almost entirely due to the increase in circumferential bending energy $U_{2,B\theta}$ which increases as i increases. All other energy contributions to both the stabilising and destabilising energy are either fairly insensitive to changes in the circumferential buckling mode number i , $\dot{N}_{\theta\phi}^{\phi}$ and $U_{2,B\theta\phi}$, or decrease as i increases, $\dot{N}_{\phi}^{\phi} + \dot{N}_{\phi}^{\theta} + \dot{N}_{\phi}^{\theta\phi}$, $\dot{N}_{\theta\phi}^{\theta}$, \dot{N}_{ϕ}^{θ} , $\dot{N}_{\theta}^{\theta}$, $U_{2,B\phi}$.

7.4 PRESSURE LOADED SPHERICAL CAPS CLAMPED AT THE BOUNDARY WITH AXISYMMETRIC INITIAL IMPERFECTIONS

The mode shape of the axisymmetric initial imperfection, the nonlinear fundamental path, the imperfection sensitivity, and the fundamental path radial displacement profiles and the meridional and circumferential stress profiles for the perfect spherical cap and for a cap with an axisymmetric imperfection with an amplitude of one tenth of the shell thickness, are compared for caps with λ values of 4, 6, 9, 12, and 30 in Figures 7.11 to 7.15 (two pages each). To avoid confusion the value of the perturbation parameter, e , is used to indicate the location on the fundamental path to which the fundamental path displacement or stress profiles refer.

A number of different initial axisymmetric imperfection mode shapes were tested, these included the buckling mode from the linear membrane fundamental path problem, the damped Legendre solution for a complete sphere of equivalent λ , the buckling mode resulting from the nonlinear solution of the perfect cap, the axisymmetric mode with the same meridional mode shape as the critical mode for the perfect cap, and the mode shape that results from a uniform radial edge displacement of the cap. Comparisons of the results for the different types of initial imperfections showed that the imperfection sensitivity was greatest, and almost identical, for the first two types of imperfection mentioned above, the buckling mode from the linear membrane fundamental path problem, and the damped Legendre mode for a complete sphere of equivalent λ . Results will be presented below for the initial axisymmetric imperfections that have the same radial shape as the buckling mode of the linear membrane fundamental path problem. That is a linear membrane fundamental path solution, radial displacements only, was used with boundary constraint, fully clamped, imposed at the axisymmetric or periodic buckling point, resulting in a linear eigenvalue problem; the eigenvector associated with the smallest eigenvalue is in all cases axisymmetric, and the radial component of the eigenvector associated with the smallest eigenvalue is the imperfection mode shape used below. In the computer program NLSPHERE these initial imperfections were treated as stress-free imperfections as described in Chapter Four by equations (4.9) to (4.11).

In all cases when the amplitude of the initial imperfection was greater than one tenth of the thickness of the spherical cap all periodic bifurcation was eliminated and the behaviour of the cap was entirely axisymmetric. In the results presented below no mention is made of periodic bifurcations from the imperfect axisymmetric fundamental path, as relatively small axisymmetric imperfections in the mode used are sufficient to eliminate any periodic behaviour.

Figure 7.11, $\lambda=4$

The stress-free initial imperfection mode shape, W^* , is shown in Figure 7.11 (a), for the spherical cap with a λ value of 4. The fundamental path is shown in Figure 7.11 (b), (c) and (d), in (b) the load is plotted against perturbation parameter, in (c) the load is plotted against the

relative change in volume of the spherical cap, and in (d) the load is plotted against the radial displacement at the pole, δ . The nondimensional amplitude of the initial imperfection with respect to the thickness of the shell, W^*/t , is indicated on Figure 7.11 (b), a negative amplitude indicates an inward initial displacement. Imperfection sensitivity, the locus of the maximum values or buckling loads on the fundamental path is shown in Figure 7.11 (e). Radial displacement profiles, and meridional and circumferential stress profiles at both the local maximum and minimum of the fundamental path, are shown in Figures 7.11 (f), (g), and (h) respectively.

For this spherical cap, $\lambda=4$, the rise height $h=2.42t$, and for all imperfections shown in Figure 7.11 the cap turns 'inside out' between the local maximum and minimum on the fundamental path, and the local minimum occurs for positive values of load. As the amplitude of the inward imperfection increases, the difference between the local maximum and minimum decreases, and for an imperfection amplitude of $W^*/t=-0.3$ no turning points were detected on the fundamental path, the maximum and minimum were completely eliminated and the load increased monotonically. The imperfection sensitivity shown in Figure 7.11 (e) represents the load at which buckling occurs, although in this case the spherical cap will support larger loads in the 'inside out' configuration.

Figure 7.12. $\lambda=6$

Figure 7.12 (a) shows the stress-free initial imperfection mode shape, W^* , for the spherical cap with a λ value of 6, and Figure 7.12 (b), (c) and (d) show the nonlinear fundamental path. The nondimensional amplitude of the initial imperfection with respect to the thickness of the shell, W^*/t , is indicated on Figure 7.12 (b), a negative amplitude indicates an inward initial displacement. Imperfection sensitivity, the locus of the maximum values or buckling loads on the fundamental path is shown in Figure 7.12 (e). The nonlinear fundamental path solution routine, in the program NLSPHERE, found no minimum value within the one hundred and sixty terms allowed for the fundamental path, and Figure 7.12 (b) suggests that the minimum value will occur for negative values of load. Radial displacement profiles, and meridional and circumferential stress profiles at the local maximum, $e=1.58$ for the perfect cap $W^*/t=0.0$, and $e=0.89$ for the imperfect cap $W^*/t=-0.1$, of the fundamental path and at the postbuckling points given by $e=2.50$, $P/P_{c1}=0.893$ for $W^*/t=0.0$ and $e=2.37$, $P/P_{c1}=0.329$ for $W^*/t=-0.1$ are shown in Figures 7.12 (f), (g), and (h).

For this spherical cap, $\lambda=6$, the rise height $h=5.44t$, and for all fundamental paths shown in Figure 7.12 no minimum load has been found, and the cap has not yet turned 'inside out', i.e. $\delta < 5.44t$ in Figure 7.12 (d). For the perfect cap periodic buckling occurs before axisymmetric buckling, when the circumferential stress first reaches the classical value for the complete spherical shell. For the imperfect spherical cap with an imperfection amplitude of $-0.1t$ the maximum meridional stress at buckling is approximately $1.1\sigma_{c1}$ at $s=0.28$, and the maximum

circumferential stress at buckling is approximately $0.9\sigma_{cl}$ at the pole, $s=0$, Figure 7.12 (g) and (h). The imperfection sensitivity is shown in Figure 7.12 (e), the axisymmetric buckling load is reduced by approximately 60% for an inwards imperfection with an amplitude of 30% of the shell thickness.

Figure 7.13, $\lambda=9$

For the spherical cap with a λ value of 9, Figure 7.13 (a) shows the stress-free initial imperfection mode shape, W^* , and Figure 7.13 (b), (c), and (d) show the nonlinear fundamental path. The nondimensional amplitude of the initial imperfection is indicated on Figure 7.13 (b). Figure 7.13 (e) shows the imperfection sensitivity for this value of the slenderness parameter, $\lambda=9$. The nonlinear fundamental path solution routine, in the program NLSPHERE, found no minimum values of load although negative loads were obtained for large values of the perturbation parameter, e , in a number of cases. Radial displacement profiles, and meridional and circumferential stress profiles at the local maximum, $e=1.14$ for the perfect cap $W^*/t=0.0$, and $e=0.86$ for the imperfect cap $W^*/t=-0.1$, on the fundamental path and at the postbuckling points given by $e=3.09$, $P/P_{cl}=0.549$ for $W^*/t=0.0$ and $e=1.56$, $P/P_{cl}=0.441$ for $W^*/t=-0.1$ are shown in Figures 7.13 (f), (g), and (h).

For the imperfect spherical cap with an imperfection amplitude of $-0.1t$ the maximum meridional stress at buckling is approximately $1.25\sigma_{cl}$ at $s=0.18$ and the maximum circumferential stress at buckling is approximately $0.85\sigma_{cl}$ at $s=0.12$, Figure 7.13 (g) and (h). The imperfection sensitivity is shown in Figure 7.13 (e), the axisymmetric buckling load is reduced by approximately 55% for an inwards imperfection with an amplitude of 30% of the shell thickness.

Figure 7.14, $\lambda=12$

Figure 7.14 (a) shows the stress-free initial imperfection mode shape, W^* , and Figure 7.14 (b), (c), and (d) show the nonlinear fundamental path for the spherical cap with a λ value of 12, and the amplitude of the initial imperfection is indicated on Figure 7.14 (b). Figure 7.14 (e) shows the imperfection sensitivity. The nonlinear fundamental path solution routine found no minimum values of load although in a number of cases negative loads were obtained for large values of the perturbation parameter. Radial displacement profiles, and meridional and circumferential stress profiles at the local maximum, $e=1.28$ for the perfect cap $W^*/t=0.0$, and $e=0.81$ for the imperfect cap $W^*/t=-0.1$, on the fundamental path and at the postbuckling points given by $e=1.94$, $P/P_{cl}=0.786$ for $W^*/t=0.0$ and $e=2.37$, $P/P_{cl}=0.316$ for $W^*/t=-0.1$ are shown in Figures 7.14 (f), (g), and (h).

The imperfect spherical cap with an imperfection amplitude of $-0.1t$ buckles axisymmetrically when the maximum meridional stress is approximately $1.20\sigma_{cl}$ at $s=0.13$ and the maximum

circumferential stress is approximately $0.80\sigma_{cI}$ at $s=0.08$, Figure 7.14 (g) and (h). The imperfection sensitivity is shown in Figure 7.14 (e). The axisymmetric buckling load is reduced by approximately 60% for an inwards imperfection with an amplitude of 30% of the shell thickness.

Figure 7.15, $\lambda=30$

The stress-free initial imperfection mode shape, W^* , is shown in Figure 7.15 (a). Figure 7.15 (b), (c), and (d) show the nonlinear fundamental path, and the amplitude of the initial imperfection is indicated on Figure 7.15 (b). The imperfection sensitivity is shown in Figure 7.14 (e). Once again the nonlinear fundamental path solution routine found no minimum values of load although in a number of cases negative loads were obtained for large values of the perturbation parameter. Figures 7.15 (f), (g), and (h) show the radial displacement profiles, and the meridional and circumferential stress profiles at the local maximum, $e=1.05$ for the perfect cap $W^*/t=0.0$, and $e=0.74$ for the imperfect cap $W^*/t=-0.1$, on the fundamental path and at the postbuckling points given by $e=1.55$, $P/P_{cI}=0.682$ for $W^*/t=0.0$ and $e=2.16$, $P/P_{cI}=0.321$ for $W^*/t=-0.1$.

The imperfect spherical cap with an imperfection amplitude of $-0.1t$ buckles axisymmetrically when the maximum meridional stress is approximately $1.20\sigma_{cI}$ at $s=0.06$ and the maximum circumferential stress is approximately $0.80\sigma_{cI}$ at $0<s<0.04$, Figure 7.15 (g) and (h). The imperfection sensitivity is shown in Figure 7.15 (e). The axisymmetric buckling load is reduced by approximately 60% for an inwards imperfection with an amplitude of 30% of the shell thickness.

Summary

As mentioned above when the initial axisymmetric imperfection is inwards and of the type used above, and when the amplitude of the imperfection is greater than one tenth of the thickness of the spherical cap all periodic behaviour of the cap is eliminated. The spherical cap buckles axisymmetrically with the radial displacement at the pole 'leading' the buckle. In some, but not all, cases a small outward initial imperfection of the type used resulted in a small increase in the axisymmetric buckling load. For spherical caps with slenderness values, λ , greater than 6 the results presented above indicate that the postbuckling path becomes negative before the cap turns 'inside out'.

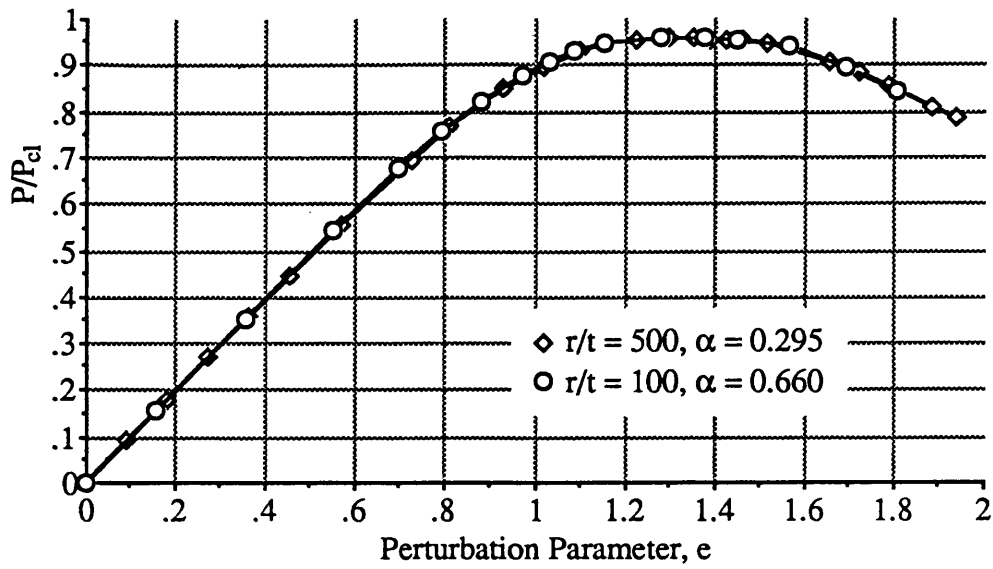
As a matter of interest the fundamental path solution algorithm implemented by the computer program NLSPHERE stops when the load reaches twice the classical buckling value, or when negative values of load are encountered, or when the one hundred and sixty terms allowed for fundamental path have all been utilised. In a large number of cases negative values of the load were encountered before the limit of one hundred and sixty terms was reached.

| I/λ | 3.5 | 4 | 4.5 | 5 | 5.5 | 6 | 6.5 | 7 | 7.5 | 8 | 9 | 10 | 11 | 12 | 13 | 14 | 15 | 16 | 17 | 18 | |
|-------------|----------------|----------------|-------|-------|-------|----------------|----------------|----------------|----------------|----------------|-------|-------|-------|-------|----------------|----------------|----------------|-------|-------|----------------|--|
| 0 | 0.597 0.559 | 0.563 0.381 | 0.573 | 0.616 | 0.746 | 0.970 | 1.009 | 1.042 | 1.073 | 1.102 | 0.915 | 0.811 | 0.807 | 0.959 | 0.964 0.904 | 0.977 0.896 | 0.988 | 0.902 | 0.888 | 0.922 | |
| 1 | | | | | | 0.886 0.943 | 0.944 0.980 | 0.990 0.980 | 1.029 1.073 | 1.065 1.095 | | | | | | | | | | | |
| 2 | | | | | | 0.762 | 0.760 | 0.780 | 0.819 | 0.873 | | | | | | | | | | | |
| 3 | | | | | | 0.818 | 0.772 | 0.750 | 0.748 | 0.763 | 0.831 | | | | | | | | | | |
| 4 | | | | | | 0.920 | 0.853 | 0.804 | 0.773 | 0.758 | 0.767 | 0.803 | | 0.884 | | | | | | | |
| 5 | | | | | | | 0.954 | 0.892 | 0.842 | 0.806 | 0.769 | 0.767 | 0.789 | 0.826 | 0.857 | 0.882 0.931 | 0.914 0.899 | | | | |
| 6 | | | | | | | | 0.988 | 0.954 | 0.880 | 0.809 | 0.772 | 0.767 | 0.786 | 0.812 | 0.838 0.968 | 0.862 0.934 | 0.881 | | | |
| 7 | | | | | | | | | 1.018 | 0.965 | 0.870 | 0.805 | 0.776 | 0.772 | 0.783 | 0.802 | 0.825 | 0.845 | 0.864 | 0.882 0.901 | |
| 8 | | | | | | | | | | 1.045 | | | 0.804 | 0.782 | 0.775 | 0.782 | 0.797 | 0.815 | 0.833 | 0.850 0.908 | |
| 9 | | | | | | | | | | | | | | 0.809 | 0.785 | 0.778 | 0.782 | 0.793 | 0.808 | 0.823 | |
| 10 | | | | | | | | | | | | | | 0.848 | 0.810 | 0.788 | 0.781 | 0.782 | 0.791 | 0.802 | |
| 11 | | | | | | | | | | | | | | 0.893 | 0.844 | 0.811 | 0.792 | 0.783 | 0.783 | 0.789 | |
| 12 | | | | | | | | | | | | | | 0.938 | 0.884 | 0.842 | 0.813 | 0.794 | 0.786 | 0.784 | |
| 13 | | | | | | | | | | | | | | | 0.925 | 0.878 | 0.841 | 0.814 | 0.797 | 0.788 | |
| 14 | | | | | | | | | | | | | | | 0.972 | 0.916 | 0.874 | 0.840 | 0.815 | 0.799 | |
| 15 | | | | | | | | | | | | | | | 1.021 | 0.952 | 0.909 | 0.870 | 0.839 | 0.817 | |
| 16 | | | | | | | | | | | | | | | 1.058 | 1.020 | 0.944 | | 0.867 | 0.839 | |
| 17 | | | | | | | | | | | | | | | | 1.061 | | | | 0.865 | |
| 18 | | | | | | | | | | | | | | | | 1.096 | | | | 0.893 | |

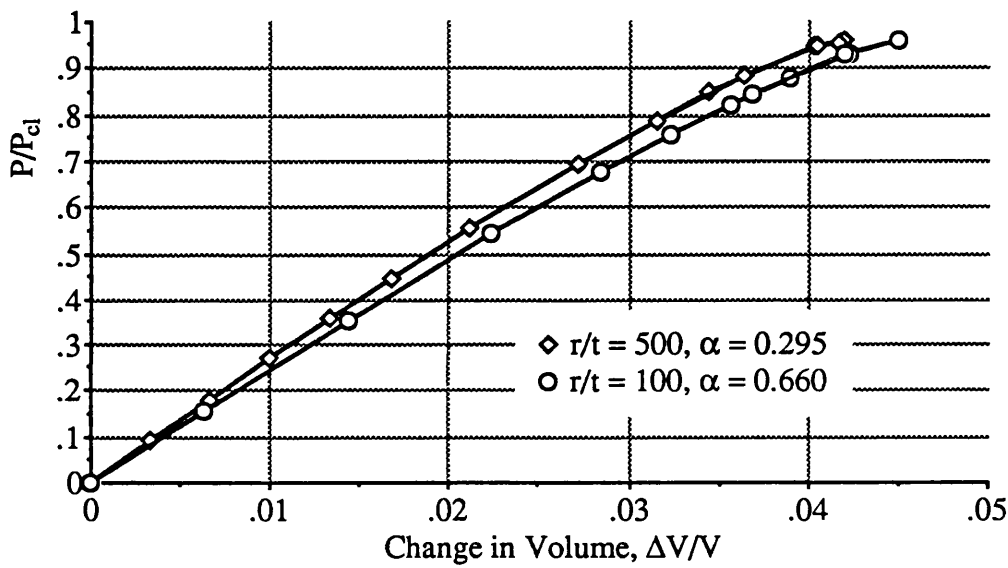
Table 7.1(a) Axisymmetric and Periodic Buckling Pressures for Clamped Perfect Spherical Caps, $3.5 \leq \lambda \leq 18$.

| λ | 20 | 22 | 24 | 26 | 28 | 30 | 32 | 34 | 36 | 38 | 40 | 42.5 | 45 | 47.5 | 50 | 52.5 | 55 | 57.5 | 60 | |
|-----------|----------------|----------------|----------------|----------------|----------------|----------------|----------------|----------------|----------------|----------------|----------------|----------------|----------------|----------------|----------------|----------------|----------------|----------------|----------------|----------------|
| 0 | 0.985 0.939 | 0.943 | 0.938 | 0.990 0.960 | 0.967 | 0.952 | 0.993 0.973 | 0.985 | 0.962 | 0.995 0.983 | 0.997 | 0.971 | 0.995 | 0.976 | 0.993 0.990 | 0.990 | 0.979 | 0.983 | 0.973 | |
| 9 | 0.854 0.905 | 0.883 0.912 | | | | | | | | | | | | | | | | | | |
| 10 | 0.829 0.911 | 0.857 0.906 | | | | | | | | | | | | | | | | | | |
| 11 | 0.810 0.925 | 0.834 0.907 | 0.858 0.910 | | | | | | | | | | | | | | | | | |
| 12 | 0.796 0.943 | 0.816 0.914 | 0.838 0.907 | 0.859 0.915 | | | | | | | | | | | | | | | | |
| 13 | 0.788 0.961 | 0.802 0.927 | 0.820 0.909 | 0.840 0.910 | | | | | | | | | | | | | | | | |
| 14 | 0.787 0.976 | 0.793 0.942 | 0.807 0.916 | 0.824 0.909 | 0.842 0.913 | | | | | | | | | | | | | | | |
| 15 | 0.793 0.985 | 0.789 | 0.797 0.927 | 0.811 0.912 | 0.827 0.913 | | | | | | | | | | | | | | | |
| 16 | 0.804 | 0.791 | 0.792 | 0.801 0.919 | 0.814 0.910 | 0.828 0.912 | 0.843 0.918 | 0.857 0.950 | 0.870 0.952 | | | | | | | | | | | |
| 17 | 0.820 | 0.797 | 0.791 | 0.795 0.929 | 0.804 0.914 | 0.816 0.911 | 0.829 0.915 | 0.842 0.920 | 0.855 0.951 | 0.867 0.932 | | | | | | | | | | |
| 18 | 0.840 | 0.808 | 0.794 | 0.792 0.941 | 0.798 0.921 | 0.807 0.912 | 0.818 0.912 | 0.830 0.916 | 0.842 0.951 | 0.853 0.952 | 0.863 | | | | | | | | | |
| 19 | 0.862 | 0.823 | 0.802 | 0.793 0.953 | 0.794 0.931 | 0.800 0.917 | 0.809 0.912 | 0.819 0.914 | 0.830 0.918 | 0.840 0.923 | 0.851 0.953 | | | | | | | | | |
| 20 | | 0.841 | 0.812 | 0.798 0.965 | 0.794 0.941 | 0.796 0.924 | 0.802 0.914 | 0.810 0.913 | 0.820 0.915 | 0.830 0.919 | 0.839 0.923 | 0.850 | 0.860 0.956 | | | | | | | |
| 21 | | 0.861 | 0.826 | 0.806 0.975 | 0.796 0.953 | 0.795 0.932 | 0.798 0.919 | 0.804 0.914 | 0.812 0.914 | 0.820 0.916 | 0.829 0.920 | 0.839 0.925 | 0.849 0.931 | | | | | | | |
| 22 | | 0.883 | 0.843 | 0.817 0.983 | 0.802 0.963 | 0.796 0.942 | 0.796 0.926 | 0.799 0.917 | 0.805 0.914 | 0.812 0.915 | 0.820 0.917 | 0.829 0.922 | 0.839 0.954 | | | | | | | |
| 23 | | 0.906 | 0.862 | 0.830 0.995 | 0.810 | 0.800 | 0.796 0.934 | 0.797 0.922 | 0.801 0.916 | 0.806 0.914 | 0.812 0.918 | 0.821 0.919 | 0.829 0.923 | 0.837 0.928 | | | | | | |
| 24 | | | 0.882 | 0.845 | 0.821 | 0.806 | 0.799 0.943 | 0.797 0.929 | 0.798 0.919 | 0.802 0.915 | 0.806 0.915 | 0.814 0.917 | 0.821 0.920 | 0.829 0.924 | 0.836 0.926 | | | | | |
| 25 | | | 0.902 | 0.863 | 0.834 | 0.815 | 0.804 0.953 | 0.798 0.936 | 0.797 0.925 | 0.799 0.918 | 0.802 0.915 | 0.808 0.916 | 0.814 0.918 | 0.821 0.921 | 0.827 0.925 | | 0.839 0.932 | | | |
| 26 | | | | 0.881 | 0.849 | 0.826 | 0.811 0.962 | 0.802 0.945 | 0.798 0.931 | 0.798 0.922 | 0.800 0.917 | 0.804 0.916 | 0.809 0.917 | 0.815 0.919 | 0.820 0.922 | 0.826 0.925 | 0.831 0.928 | | | |
| 27 | | | | | 0.865 | 0.838 | 0.820 0.970 | 0.808 0.954 | 0.802 0.939 | 0.799 0.928 | 0.799 0.920 | 0.801 0.916 | 0.805 0.916 | 0.809 0.918 | 0.814 0.920 | 0.819 0.923 | 0.824 0.925 | 0.828 0.928 | | |
| 28 | | | | | 0.882 | 0.852 | 0.831 0.978 | 0.816 0.962 | 0.806 0.947 | 0.801 0.934 | 0.799 0.925 | 0.799 0.919 | 0.802 0.916 | 0.805 0.917 | 0.809 0.918 | 0.814 0.921 | 0.818 0.921 | 0.821 0.921 | 0.824 0.924 | |
| 29 | | | | | | 0.867 | 0.843 0.984 | 0.825 0.970 | 0.813 0.955 | 0.806 0.942 | 0.801 0.931 | 0.800 0.922 | 0.800 0.918 | 0.803 0.917 | 0.806 0.917 | 0.809 0.919 | 0.812 0.921 | 0.816 0.921 | 0.818 0.924 | |
| 30 | | | | | | 0.883 | | 0.836 0.977 | 0.821 | 0.811 0.949 | 0.805 0.937 | 0.801 0.927 | 0.800 0.920 | 0.801 0.918 | 0.803 0.917 | 0.806 0.918 | 0.809 0.919 | 0.811 0.921 | 0.814 0.922 | |
| 31 | | | | | | | | 0.848 0.983 | | 0.819 0.957 | 0.810 0.944 | 0.805 | 0.802 0.924 | 0.801 0.920 | 0.802 0.918 | 0.803 0.918 | 0.806 0.918 | 0.808 0.919 | 0.810 0.920 | |
| 32 | | | | | | | | | | 0.827 0.964 | 0.817 0.952 | 0.809 0.938 | 0.804 0.929 | 0.802 0.923 | 0.802 0.920 | 0.802 0.918 | 0.804 0.918 | 0.805 0.918 | 0.807 0.919 | |
| 33 | | | | | | | | | | | 0.825 0.959 | 0.814 0.945 | 0.808 0.934 | 0.804 0.925 | 0.803 0.922 | 0.802 0.919 | 0.803 0.918 | 0.804 0.918 | 0.805 0.918 | |
| 34 | | | | | | | | | | | | 0.821 0.952 | 0.813 0.940 | 0.808 0.931 | 0.805 0.925 | 0.804 0.922 | 0.803 0.920 | 0.804 0.919 | 0.805 0.918 | |
| 35 | | | | | | | | | | | | | | 0.819 0.947 | 0.812 0.937 | 0.808 0.929 | 0.806 0.925 | 0.805 0.922 | 0.805 0.920 | |
| 36 | | | | | | | | | | | | | | | 0.826 0.953 | 0.813 0.934 | 0.809 0.928 | 0.807 0.924 | 0.806 0.922 | |
| 37 | | | | | | | | | | | | | | | | 0.835 0.959 | 0.818 0.940 | 0.814 0.933 | 0.811 0.928 | |
| 38 | | | | | | | | | | | | | | | | | 0.825 0.945 | 0.815 0.932 | 0.813 0.925 | |
| 39 | | | | | | | | | | | | | | | | | | 0.832 0.951 | 0.821 0.937 | |
| 40 | | | | | | | | | | | | | | | | | | | 0.827 0.942 | |
| 41 | | | | | | | | | | | | | | | | | | | | 0.834 0.947 |
| 42 | | | | | | | | | | | | | | | | | | | | 0.834 0.941 |
| 43 | | | | | | | | | | | | | | | | | | | | 0.841 0.946 |

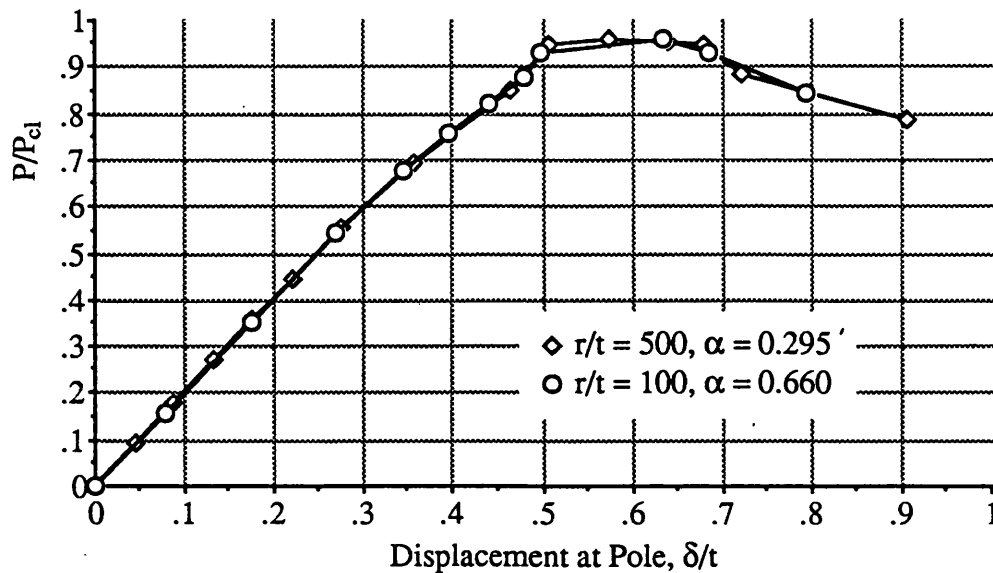
Table 7.1(b) Axisymmetric and Periodic Buckling Pressures for Clamped Perfect Spherical Caps, $20 \leq \lambda \leq 60$.



(a) Fundamental Path, P -vs- e



(b) Fundamental Path, P -vs- ΔV



(c) Fundamental Path, P -vs- δ

Figure 7.1 Fundamental Path and Shell Profiles for Perfect Shells, $\lambda=12$, $r/t=500$ and $r/t=100$.

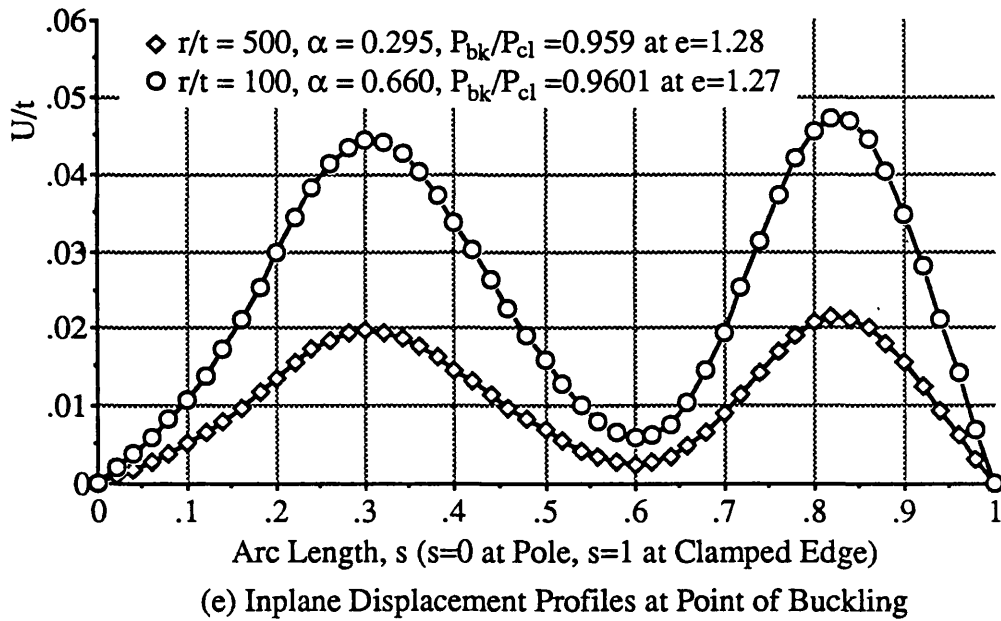
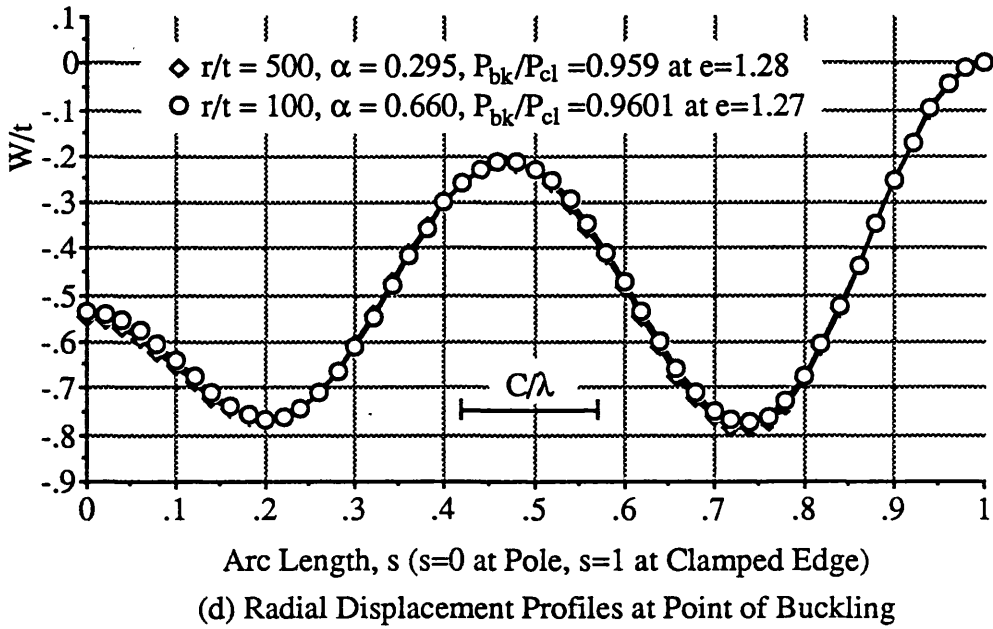
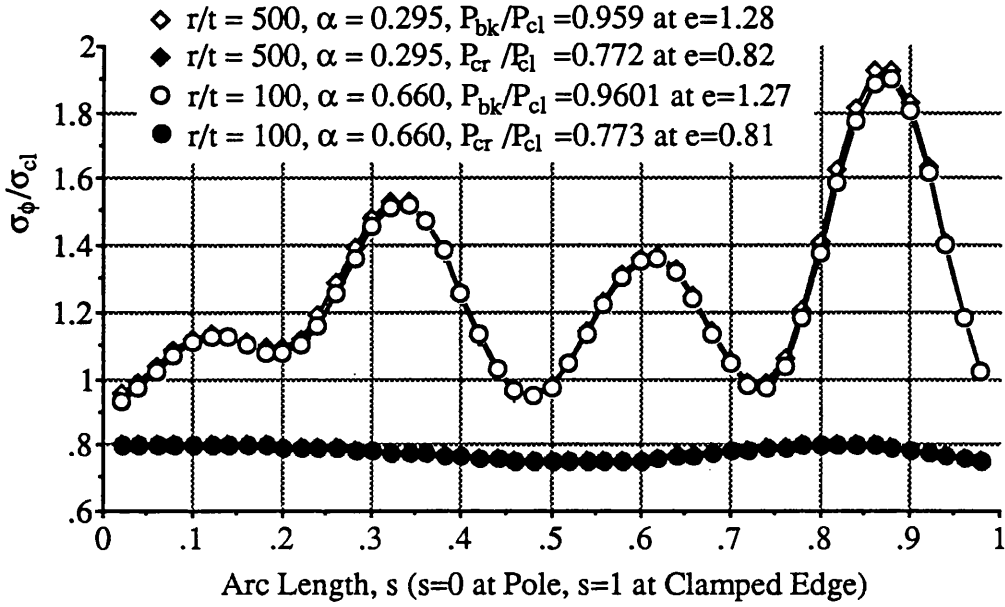
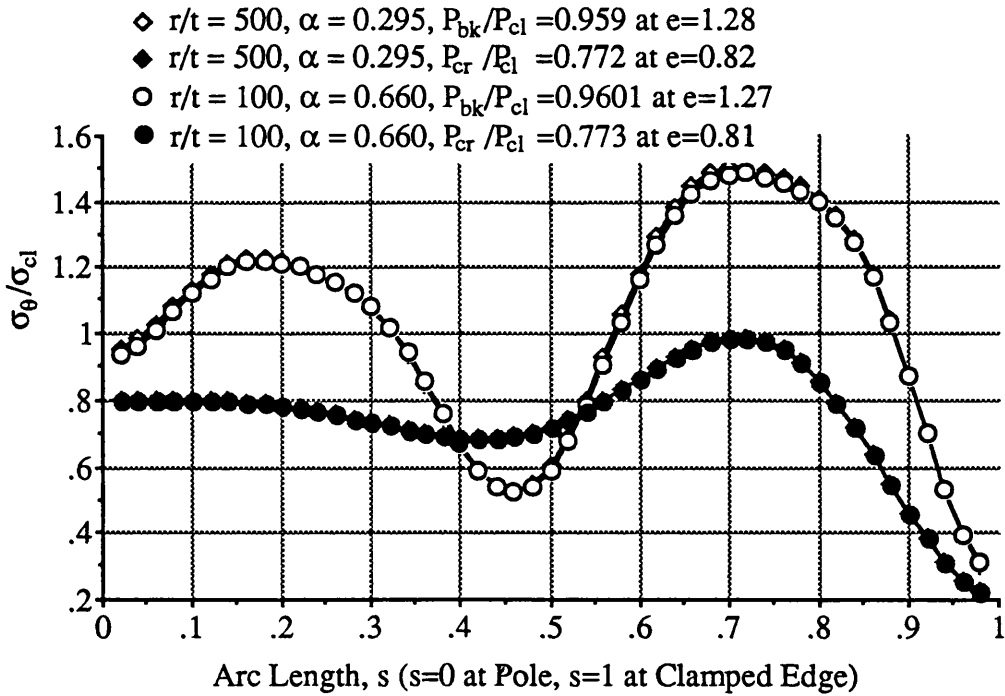


Figure 7.1 Fundamental Path and Shell Profiles for Perfect Shells, $\lambda=12$, $r/t=500$ and $r/t=100$.

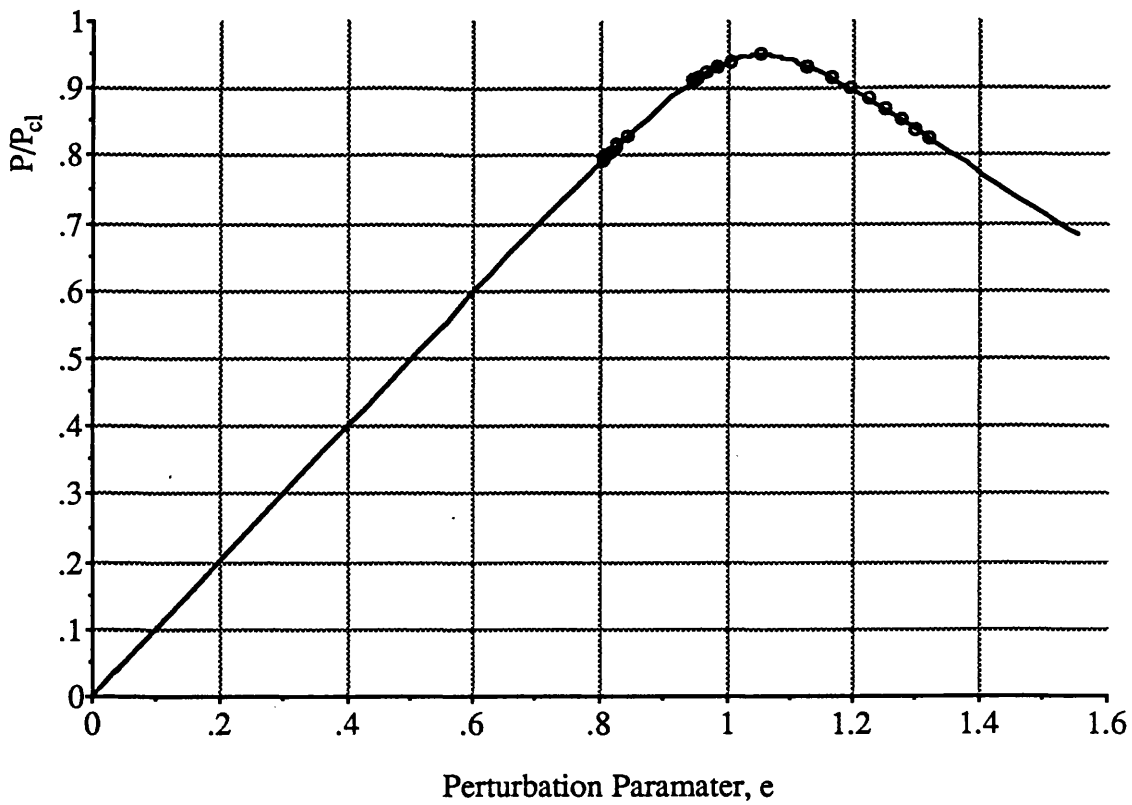


(f) Meridional Stress Profiles at Buckling Point and Critical Point

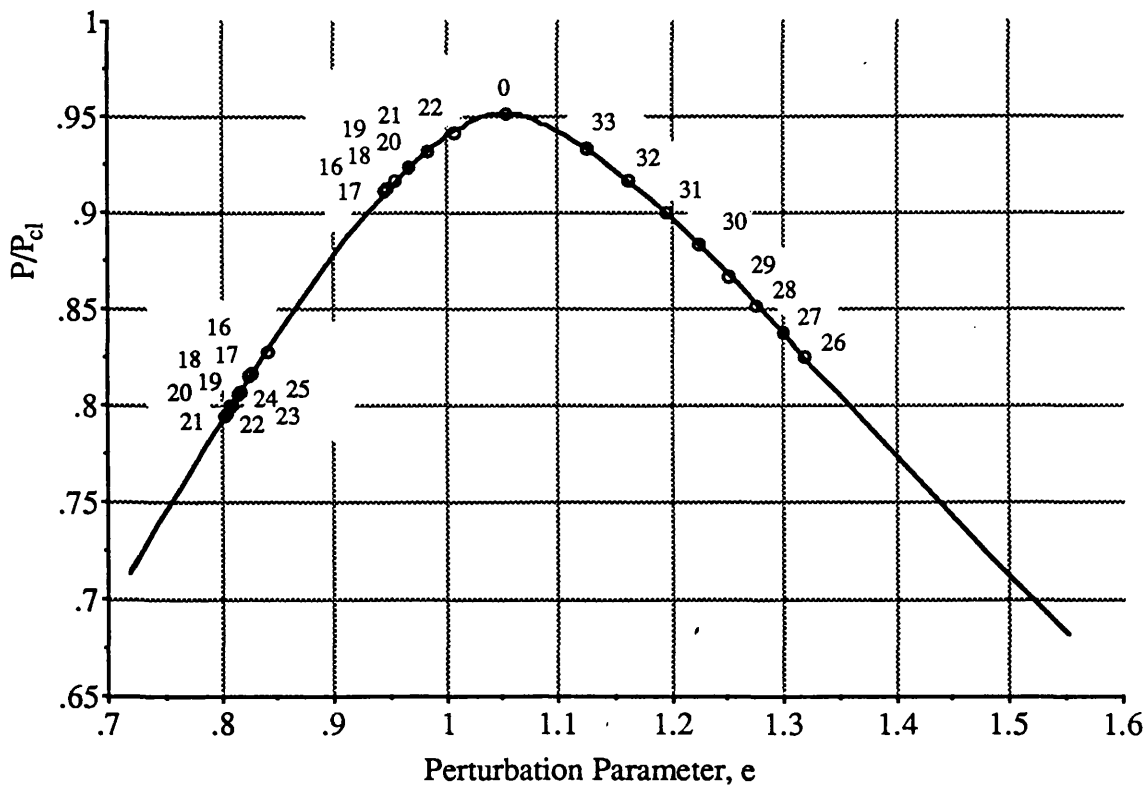


(g) Circumferential Stress Profiles at Buckling Point and Critical Point

Figure 7.1 Fundamental Path and Shell Profiles for Perfect Shells, $\lambda=12$, $r/t=500$ and $r/t=100$.

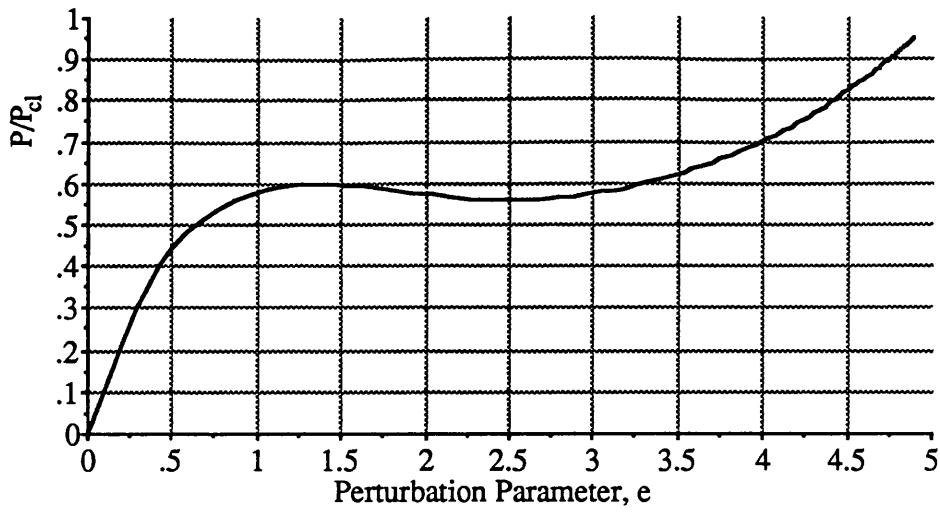


(a) Fundamental Path, P -vs- e , Showing Secondary Path Bifurcations

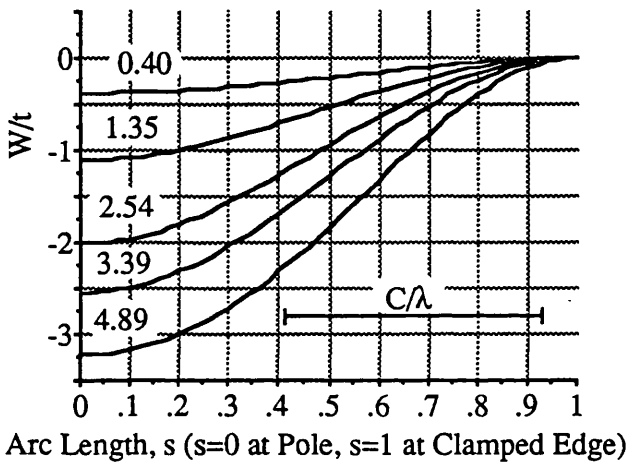


(b) Enlargement of Fundamental Path, P -vs- e , Showing Secondary Path Bifurcations

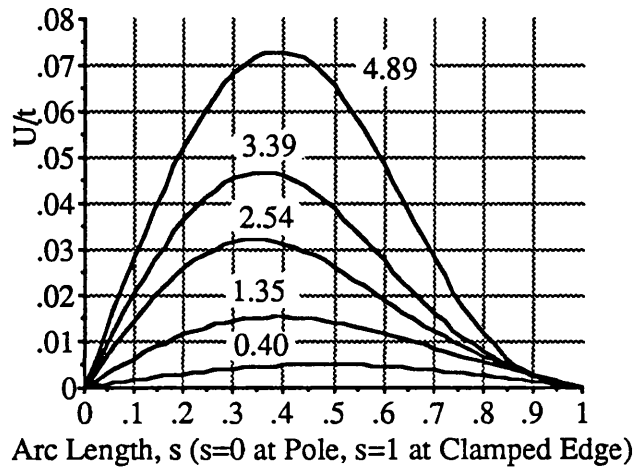
Figure 7.2 Fundamental Path and Secondary Path Bifurcations for Perfect Shell, $\lambda=30$, $r/t=500$. (on figure (b) the circumferential mode numbers, i , are indicated)



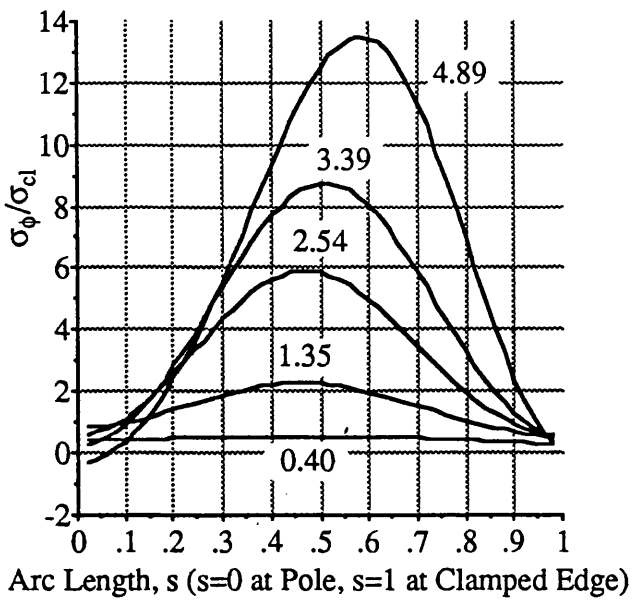
(a) Fundamental Path, P -vs- e



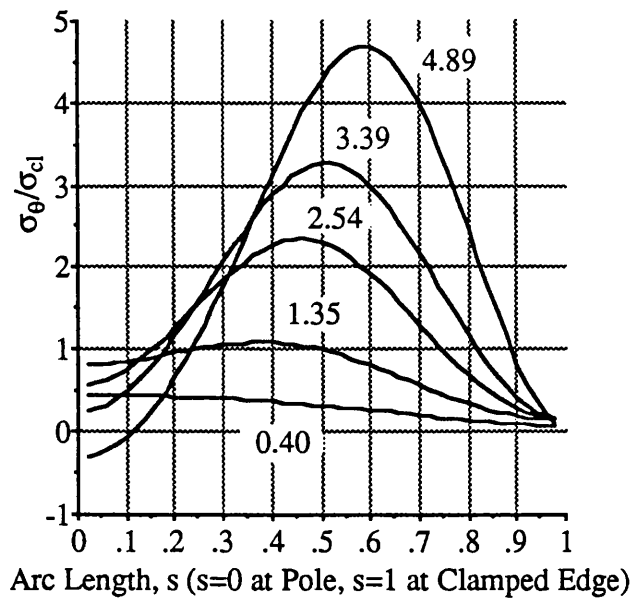
(b) Radial Displacement Profiles



(c) Inplane Displacement Profiles

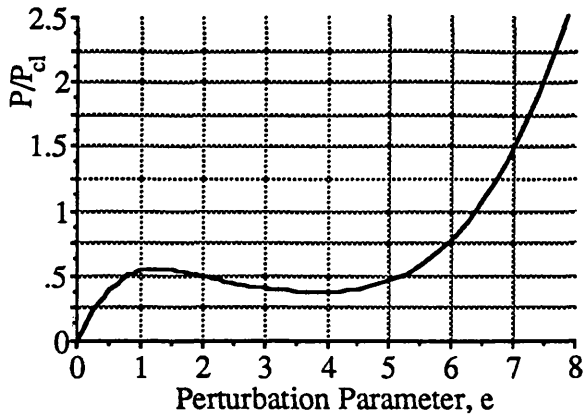


(d) Meridional Stress Profiles

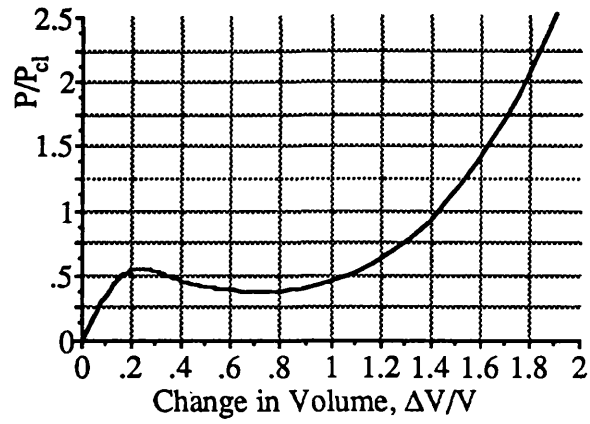


(e) Circumferential Stress Profiles

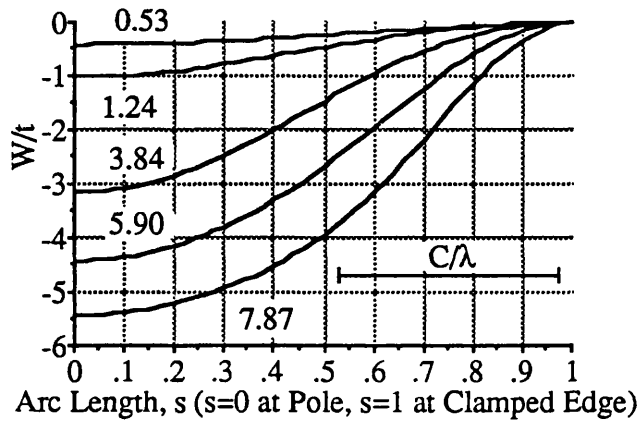
Figure 7.3 Fundamental Path and Shell Profiles for Perfect Shell, $\lambda=3.5$, $r/t=500$.
 $P_{bk}/P_{cl} = 0.597$, at $e=1.35$



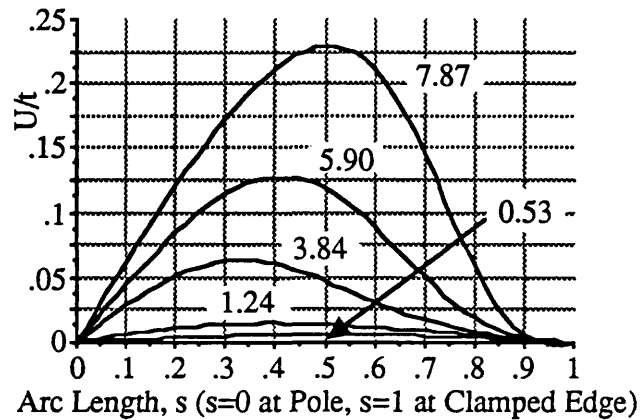
(a) Fundamental Path, P -vs- e



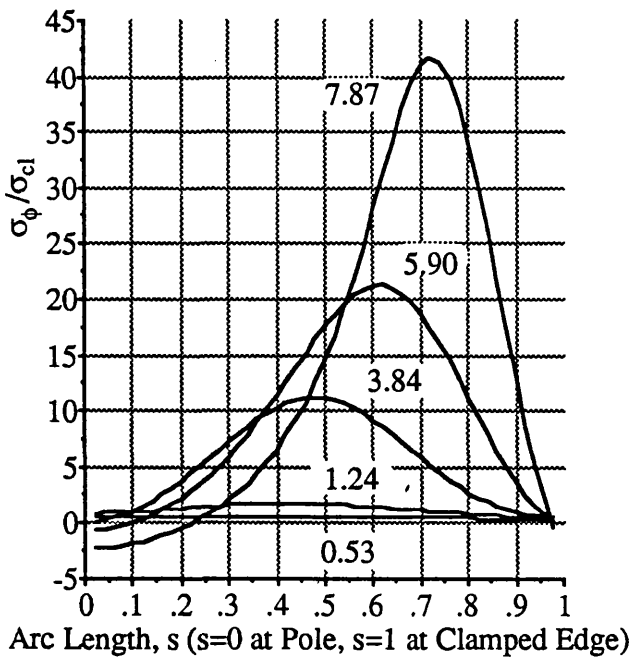
(b) Fundamental Path, P -vs- ΔV



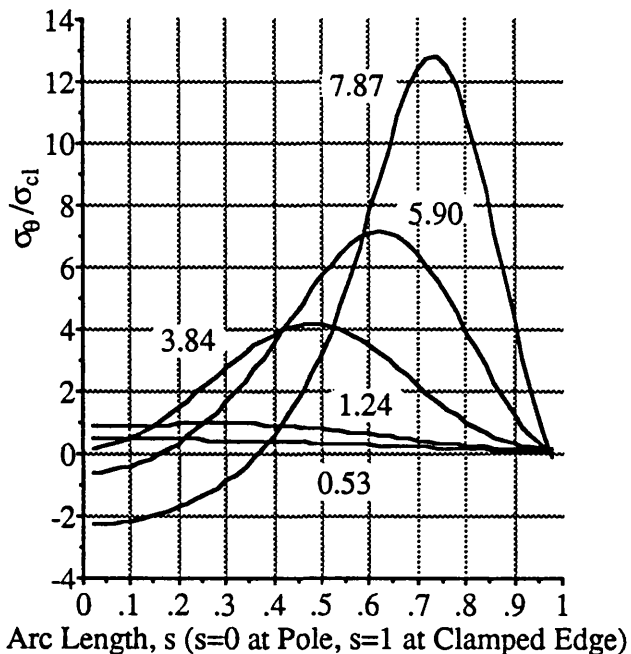
(c) Radial Displacement Profiles



(d) Inplane Displacement Profiles

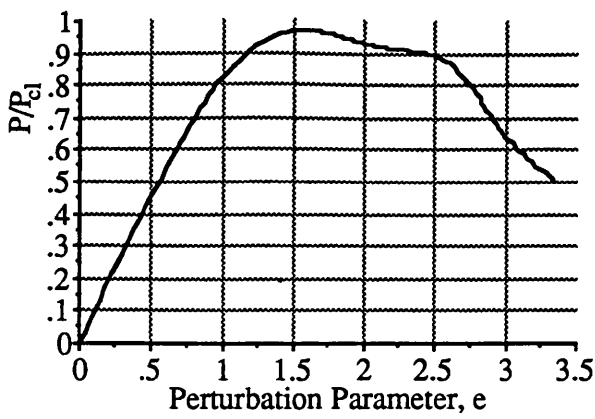


(e) Meridional Stress Profiles

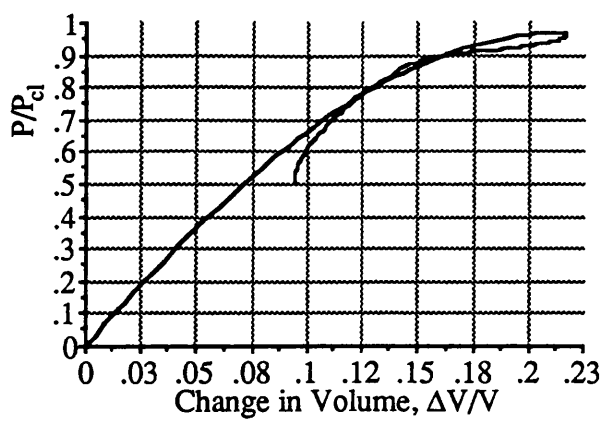


(f) Circumferential Stress Profiles

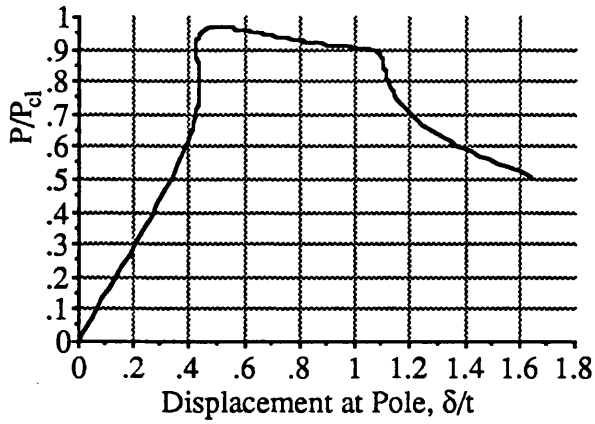
Figure 7.4 Fundamental Path and Shell Profiles for Perfect Shell, $\lambda=4$, $r/t=500$.
 $P_{bk}/P_{cl}=0.563$ at $e=1.24$.



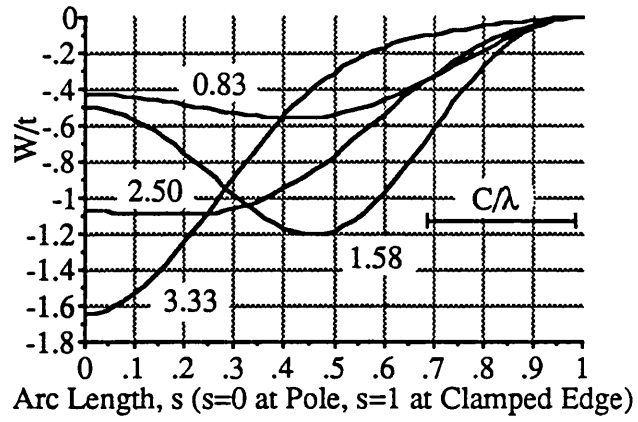
(a) Fundamental Path, P -vs- e



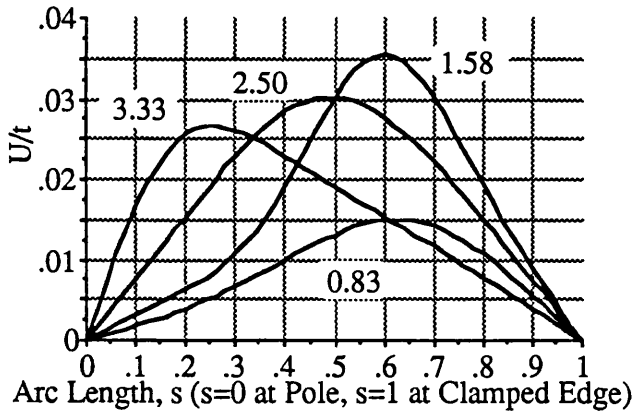
(b) Fundamental Path, P -vs- ΔV



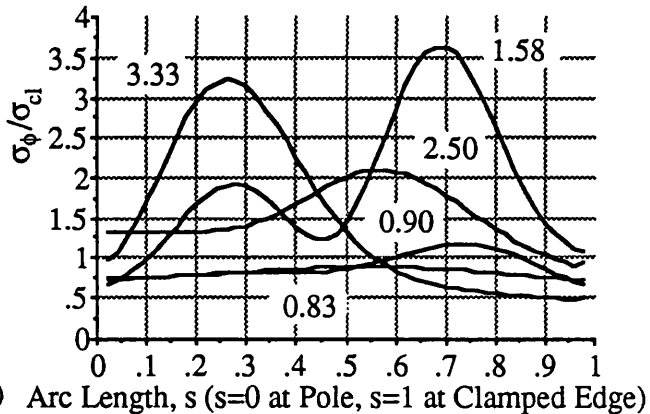
(c) Fundamental Path, P -vs- δ



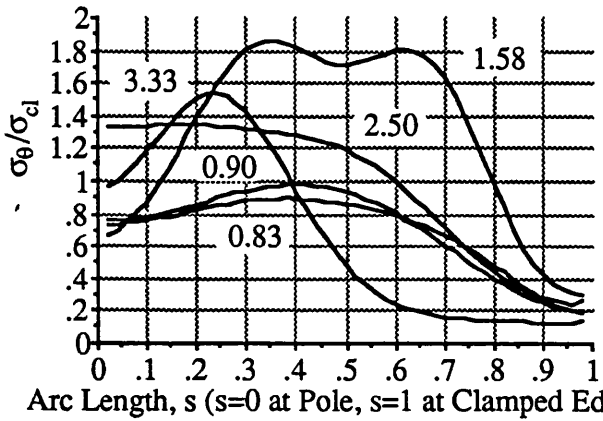
(d) Radial Displacement Profiles



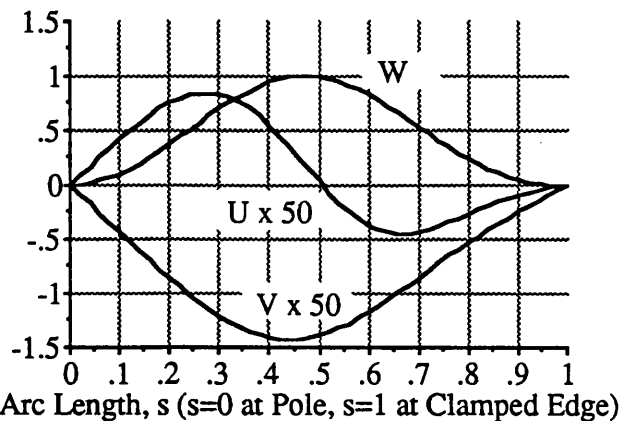
(e) Inplane Displacement Profiles



(f) Meridional Stress Profiles

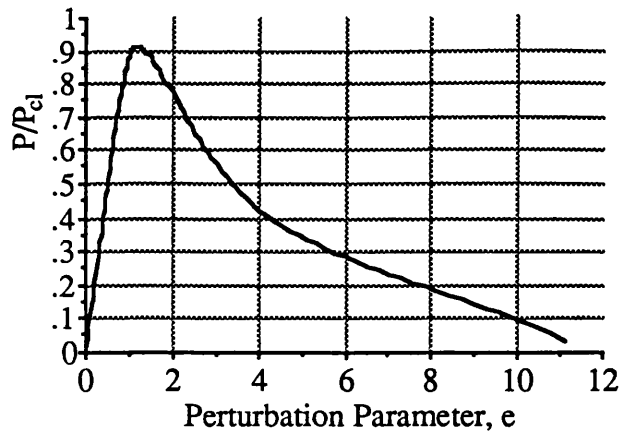


(g) Circumferential Stress Profiles

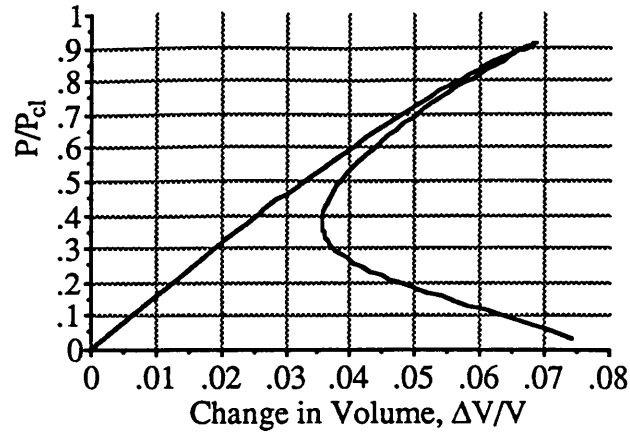


(h) Critical, $i=2$, Displacement Profiles

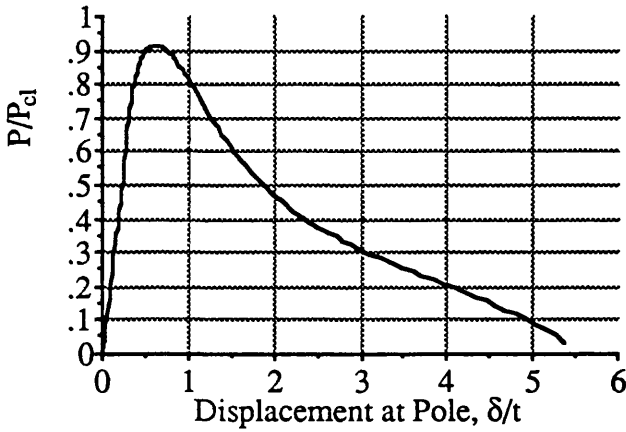
Figure 7.5 Fundamental Path and Shell Profiles for Perfect Shell, $\lambda=6$, $r/t=500$. $P_{bk}/P_{cl} = 0.970$, at $e=1.58$, $P_{cr}/P_{cl} = 0.775$, $i_{cr}=2$, at $e=0.90$.



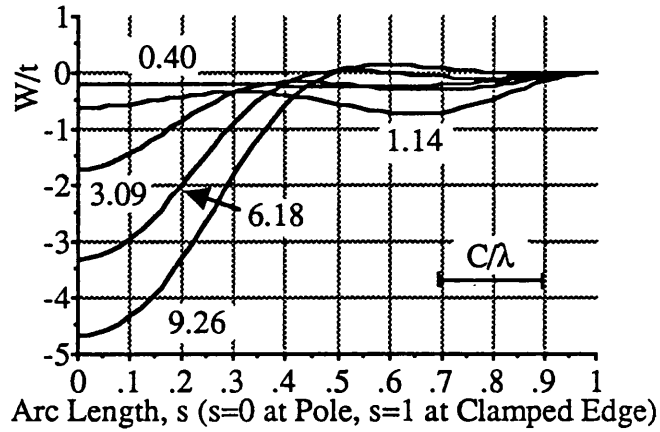
(a) Fundamental Path, P -vs- e



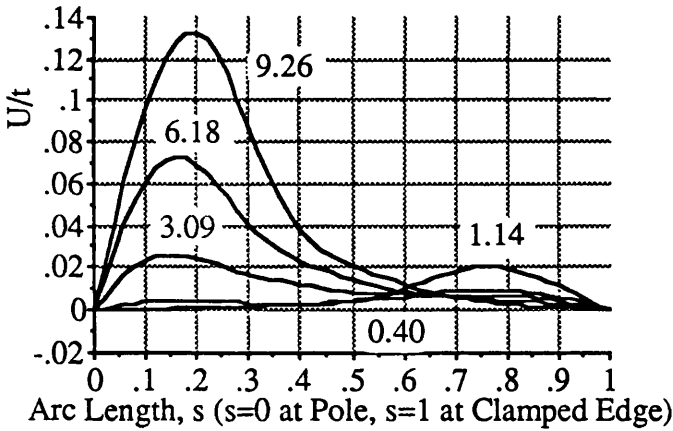
(b) Fundamental Path, P -vs- $\Delta V/V$



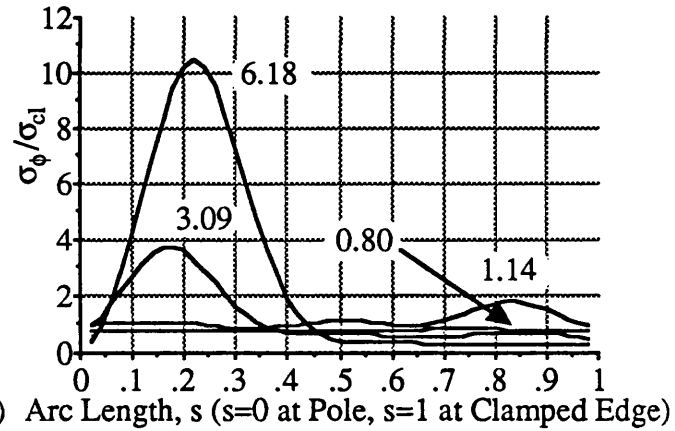
(c) Fundamental Path, P -vs- δ



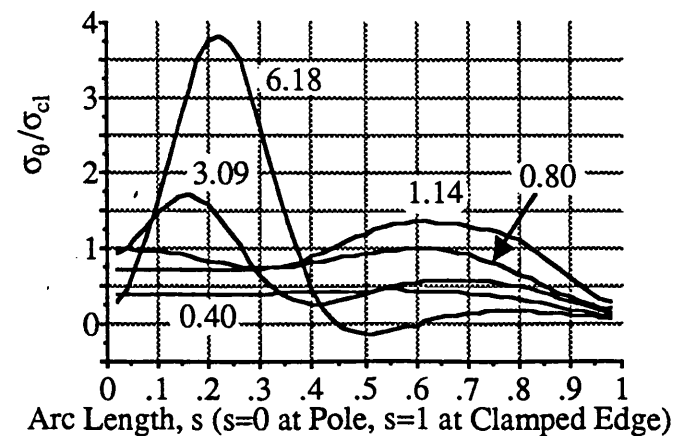
(d) Radial Displacement Profiles



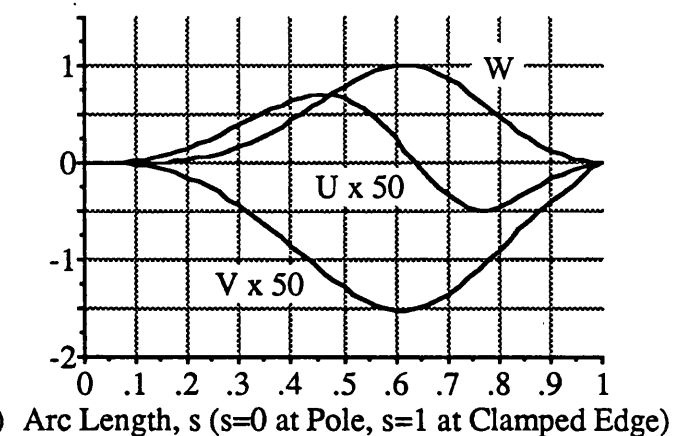
(e) Inplane Displacement Profiles



(f) Meridional Stress Profiles

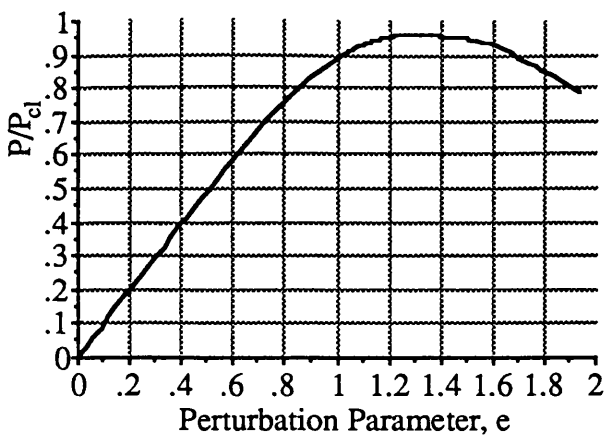


(g) Circumferential Stress Profiles

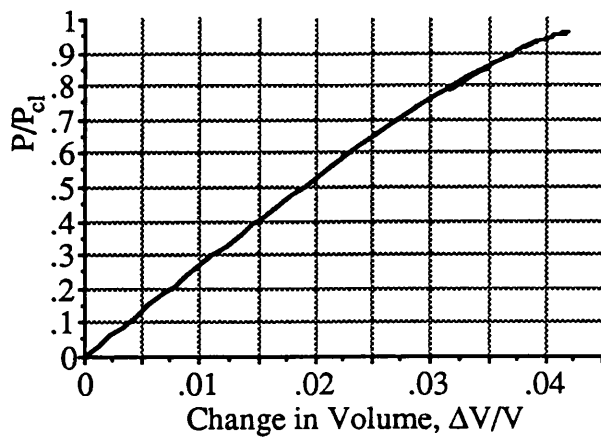


(h) Critical, $i=4$, Displacement Profiles

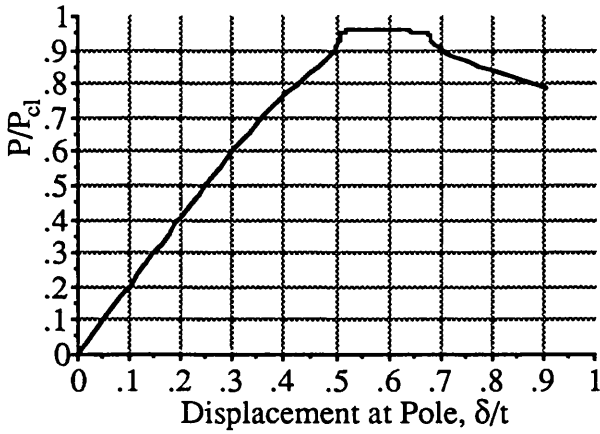
Figure 7.6 Fundamental Path and Shell Profiles for Perfect Shell, $\lambda=9$, $r/t=500$.
 $P_{bk}/P_{cl}=0.915$ at $e=1.14$, $P_{cr}/P_{cl}=0.767$, $i_{cr}=4$, at $e=0.80$.



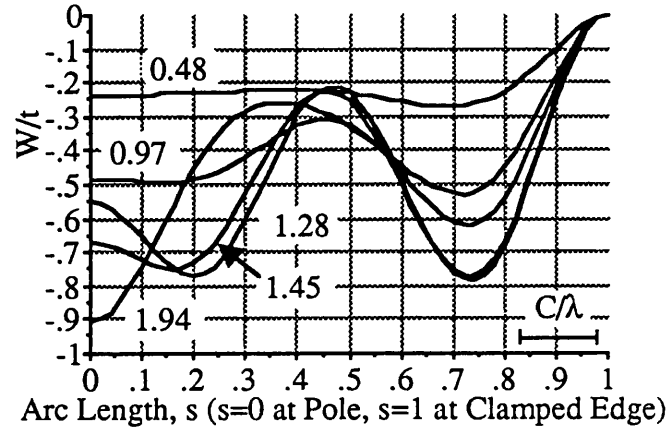
(a) Fundamental Path, P -vs- e



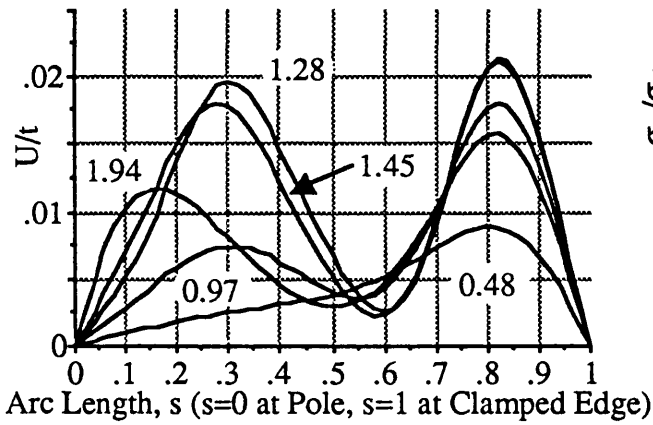
(b) Fundamental Path, P -vs- ΔV



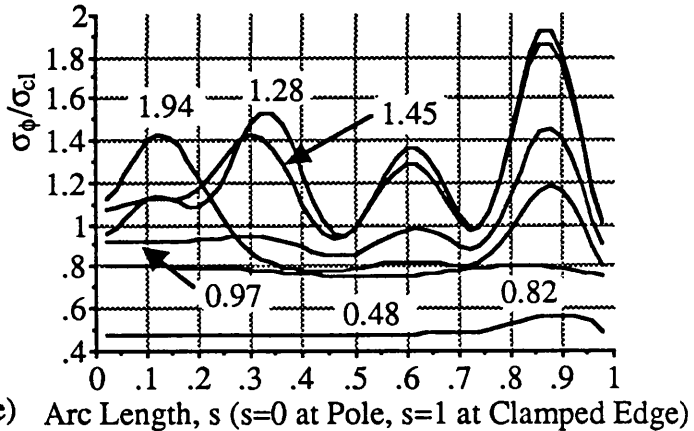
(c) Fundamental Path, P -vs- δ



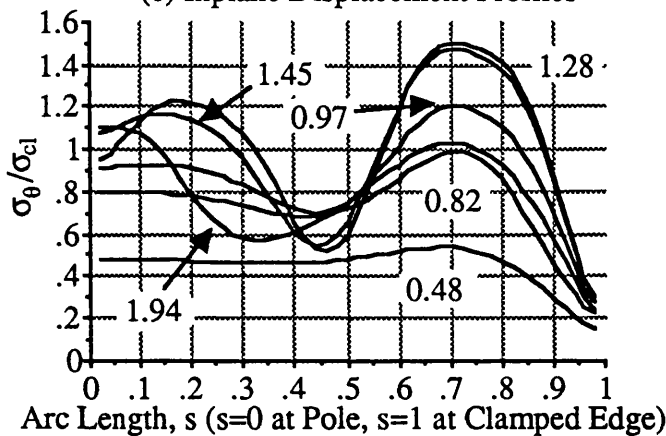
(d) Radial Displacement Profiles



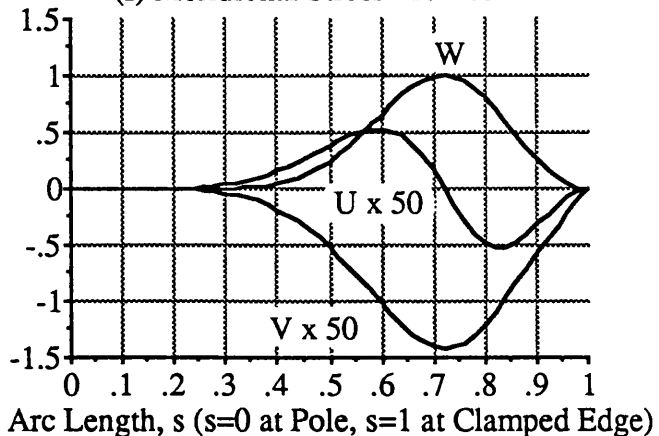
(e) Inplane Displacement Profiles



(f) Meridional Stress Profiles



(g) Circumferential Stress Profiles



(h) Critical, $i=7$, Displacement Profiles

Figure 7.7 Fundamental Path and Shell Profiles for Perfect Shell, $\lambda=12$, $r/t=500$.
 $P_{bk}/P_{cl}=0.959$ at $e=1.28$, $P_{cr}/P_{cl}=0.772$, $i_{cr}=7$ at $e=0.82$.

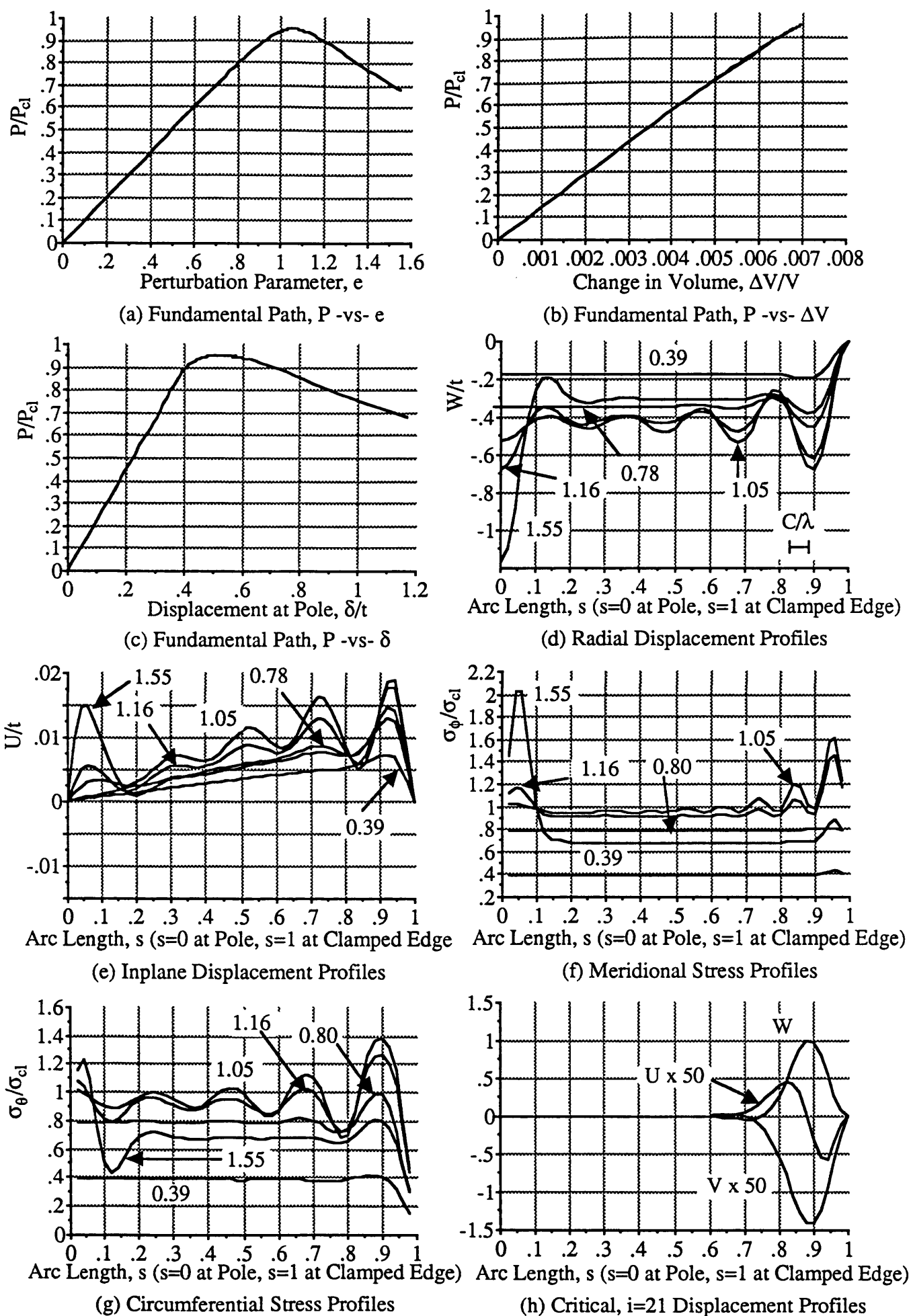


Figure 7.8 Fundamental Path and Shell Profiles for Perfect Shell, $\lambda=30$, $r/t=500$.
 $P_{bk}/P_{cl}=0.967$ at $e=1.05$, $P_{cr}/P_{cl}=0.794$, $i_{cr}=7$ at $e=0.80$.

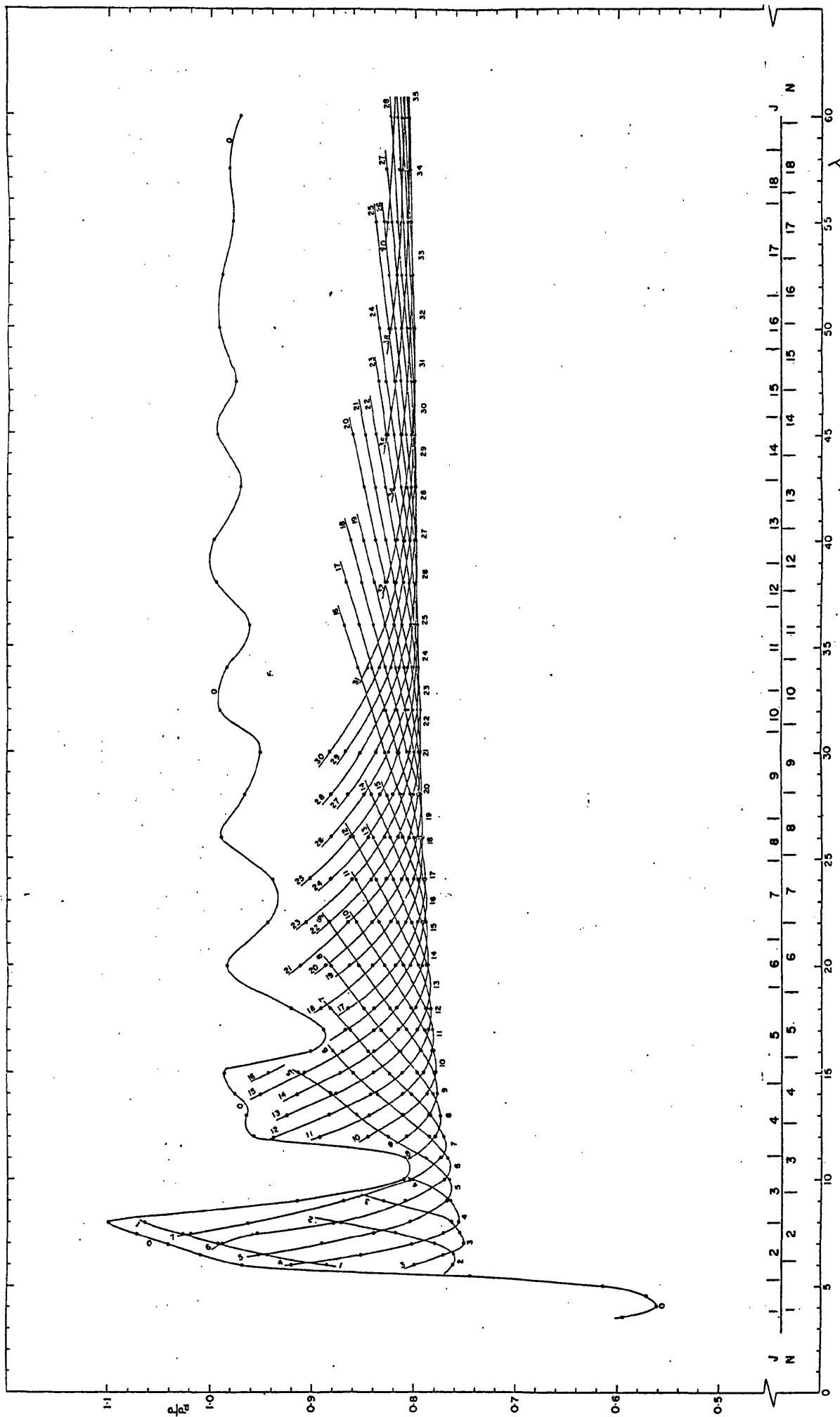
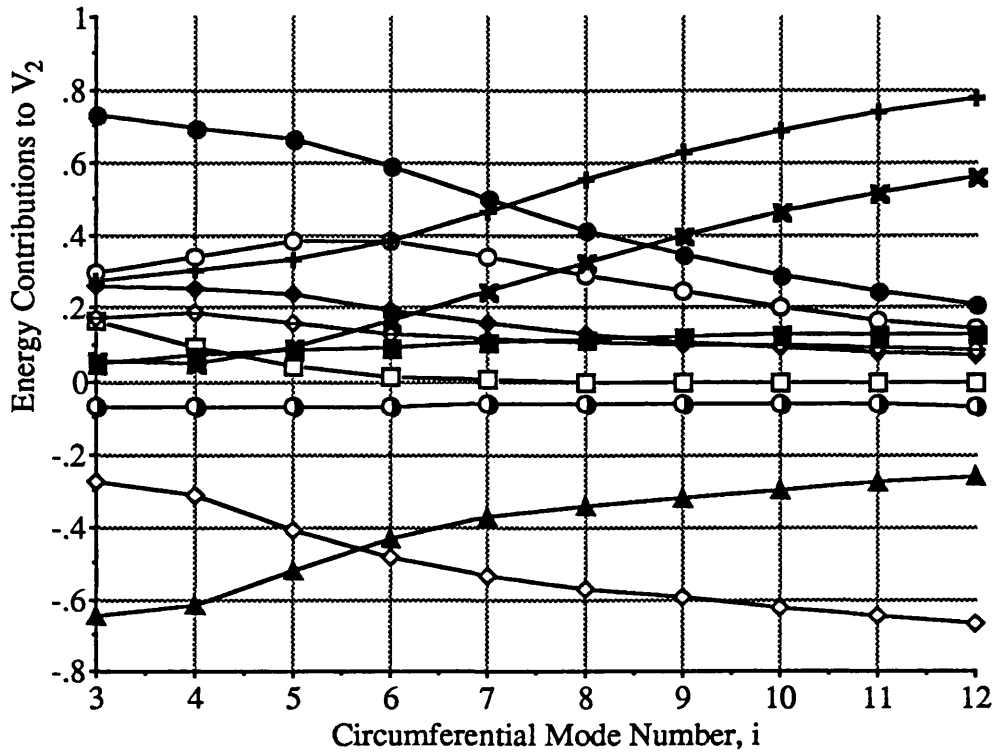


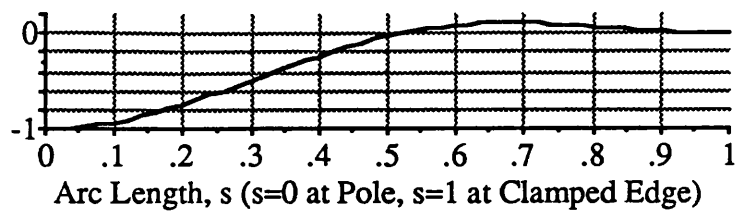
Figure 7.9 Axisymmetric and Periodic Buckling Pressures for Clamped Perfect Spherical Caps, $3.5 \leq \lambda \leq 60$, N - Legendre Polynomial for Complete Sphere, J - Mode Shape for Spherical Cap.



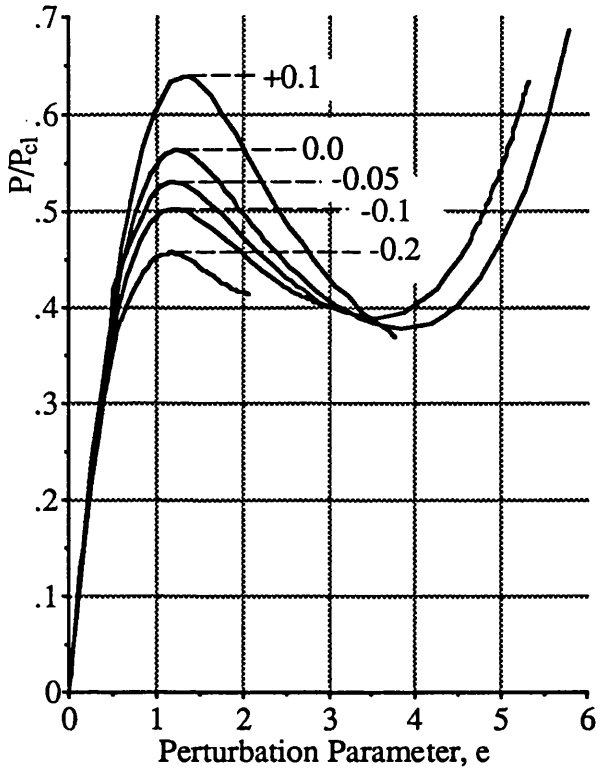
LEGEND

| Contributions to the Quadratic Terms of the Total Potential Energy, V_2 { notation defined by equation (4.51) } | | |
|--|--|---|
| "Stabilising Energy" Secondary Path Membrane Energy | "Stabilising Energy" Secondary Path Bending Energy | "Destabilising Energy" Interaction Between Fundamental and Secondary Path Displacements |
| <ul style="list-style-type: none"> ● $\dot{N}_\phi \dot{\epsilon}_\phi + \dot{N}_\theta \dot{\epsilon}_\theta + \dot{N}_{\theta\phi} \dot{\epsilon}_{\theta\phi}$ ○ $\dot{N}_\phi \dot{\epsilon}_\phi$ □ $\dot{N}_\theta \dot{\epsilon}_\theta$ ◆ $\dot{N}_{\theta\phi} \dot{\epsilon}_{\theta\phi}$ | <ul style="list-style-type: none"> + $U_{2,B_\phi} + U_{2,B_\theta} + U_{2,B_{\theta\phi}}$ ◇ U_{2,B_ϕ} × U_{2,B_θ} ■ $U_{2,B_{\theta\phi}}$ | <ul style="list-style-type: none"> ▲ $\dot{N}_\phi \dot{\epsilon}_\phi + \dot{N}_\phi \ddot{\epsilon}_\phi + \dot{N}_\phi \dot{\epsilon}_\phi$ ◇ $\dot{N}_\theta \dot{\epsilon}_\theta + \dot{N}_\theta \ddot{\epsilon}_\theta + \dot{N}_\theta \dot{\epsilon}_\theta$ ● $\dot{N}_{\theta\phi} \dot{\epsilon}_{\theta\phi}$ |

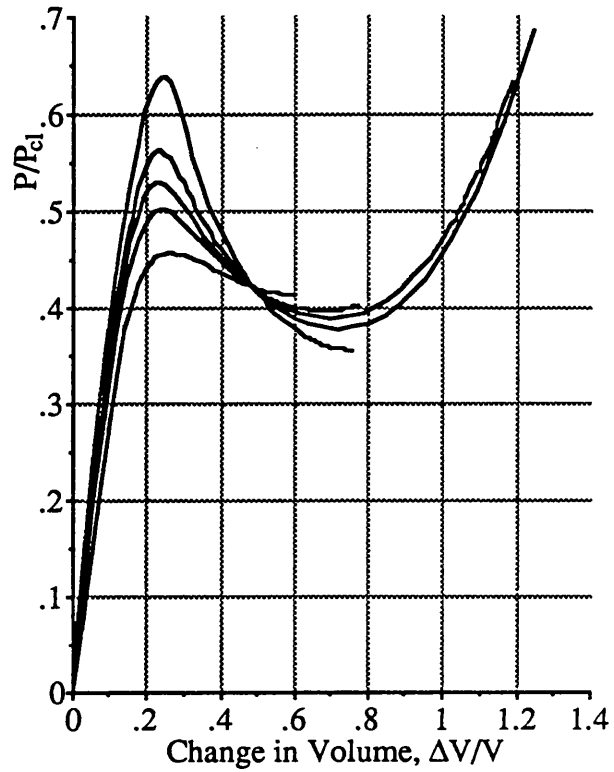
Figure 7.10 Relative Contributions to the Quadratic Terms of the Total Potential Energy as a Function of the Circumferential Mode number, for $\lambda=12$.



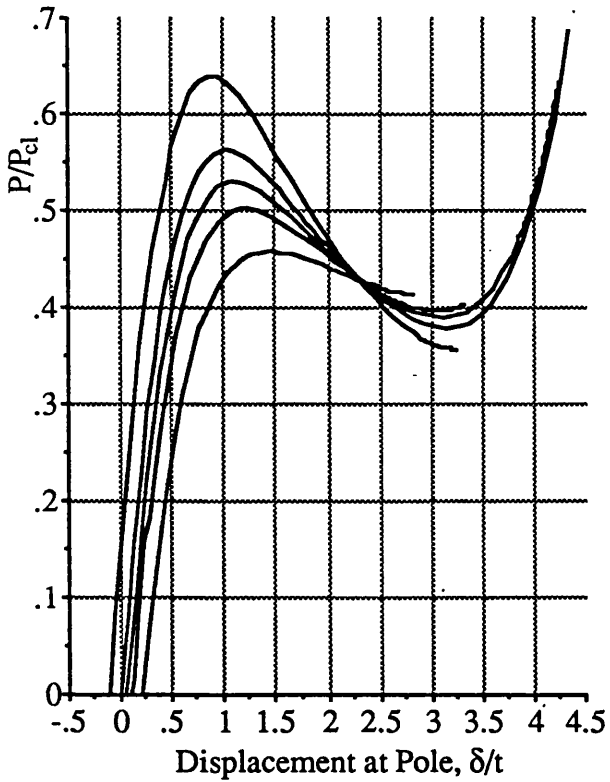
(a) Imperfection Shape, W^*



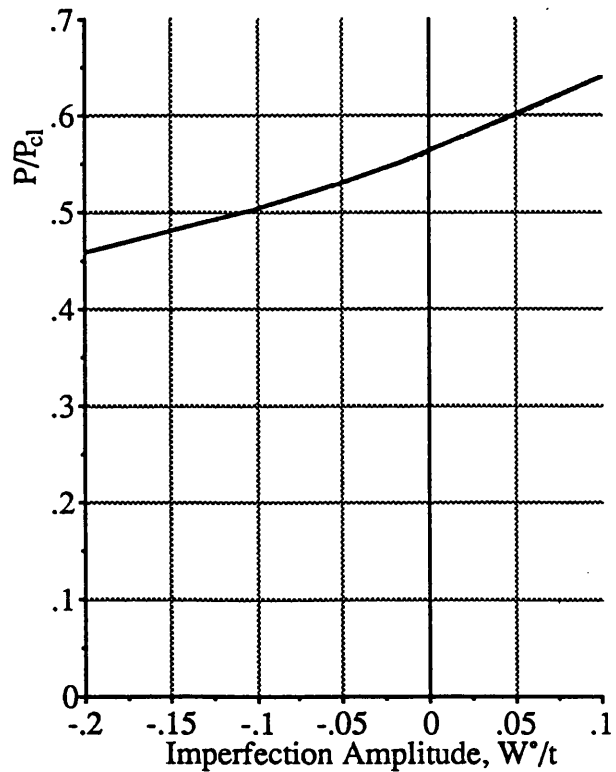
(b) Fundamental Path, P -vs- e



(c) Fundamental Path, P -vs- ΔV

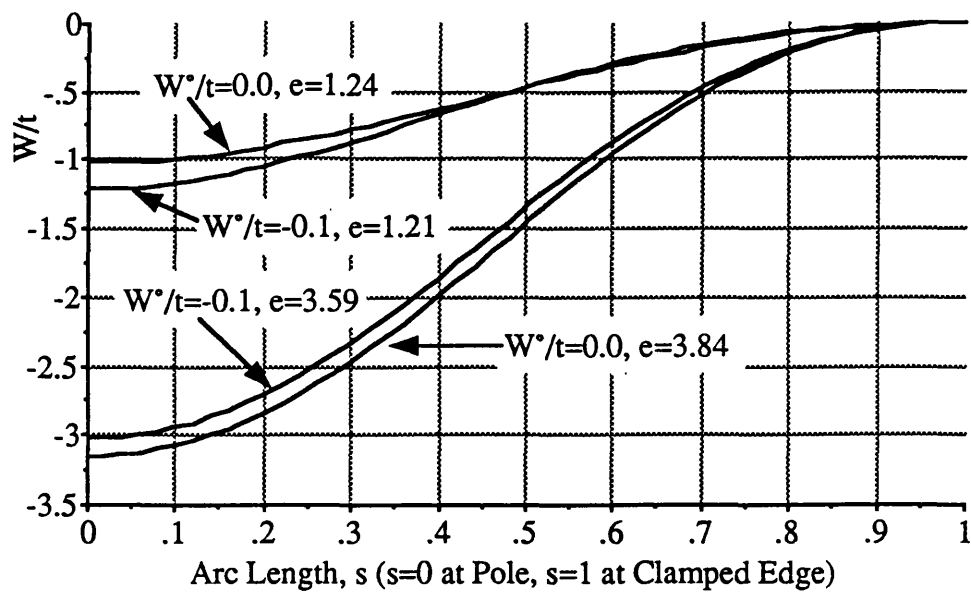


(d) Fundamental Path, P -vs- δ

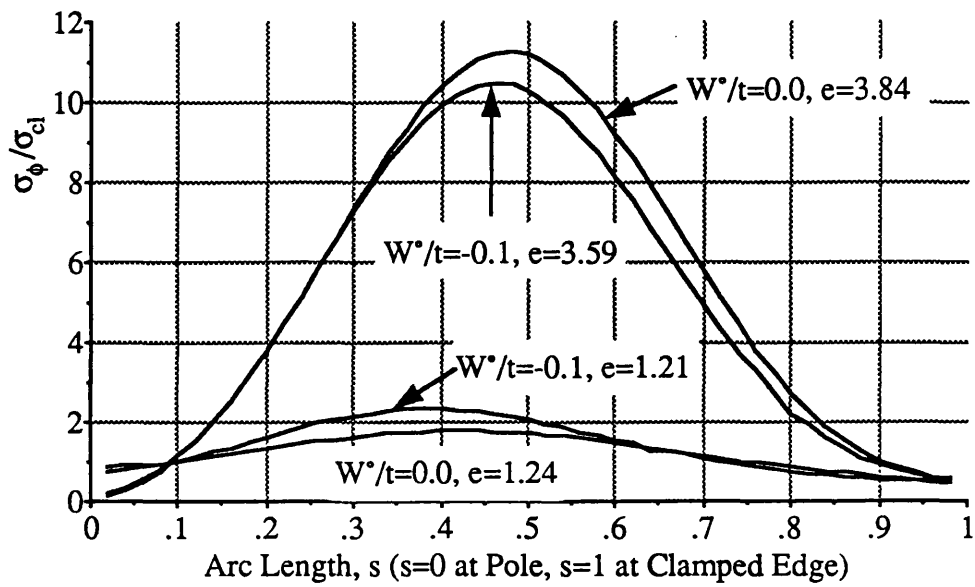


(e) Imperfection Sensitivity, W^*

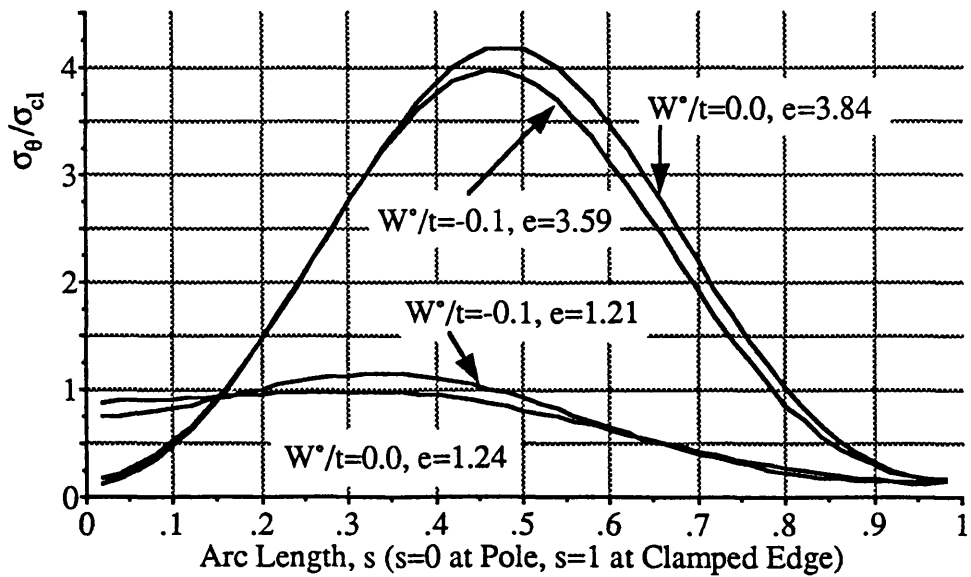
Figure 7.11 Fundamental Path and Shell Profiles for Imperfect Shells, $\lambda=4$, $r/t=500$.



(f) Radial Displacement Profiles

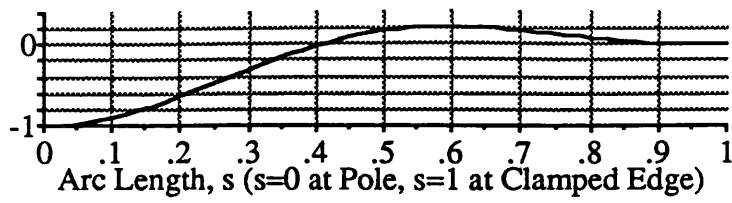


(g) Meridional Stress Profiles

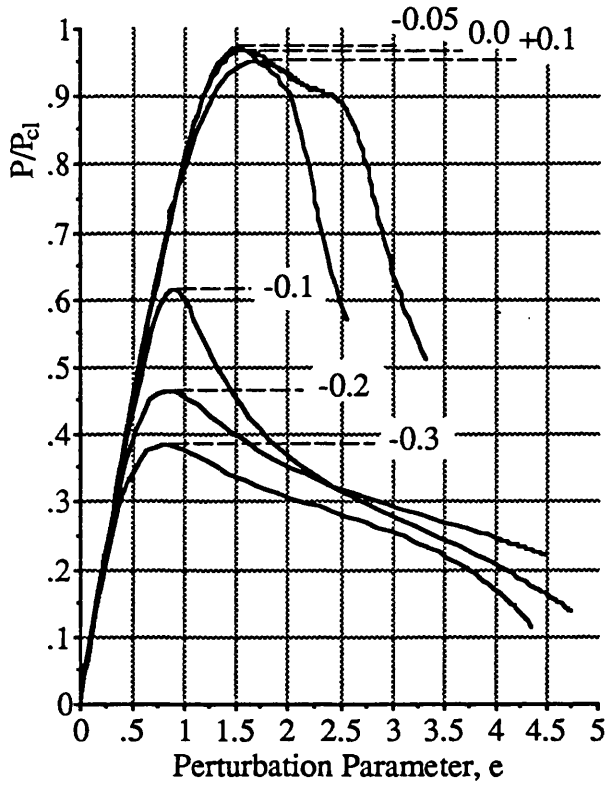


(h) Circumferential Stress Profiles

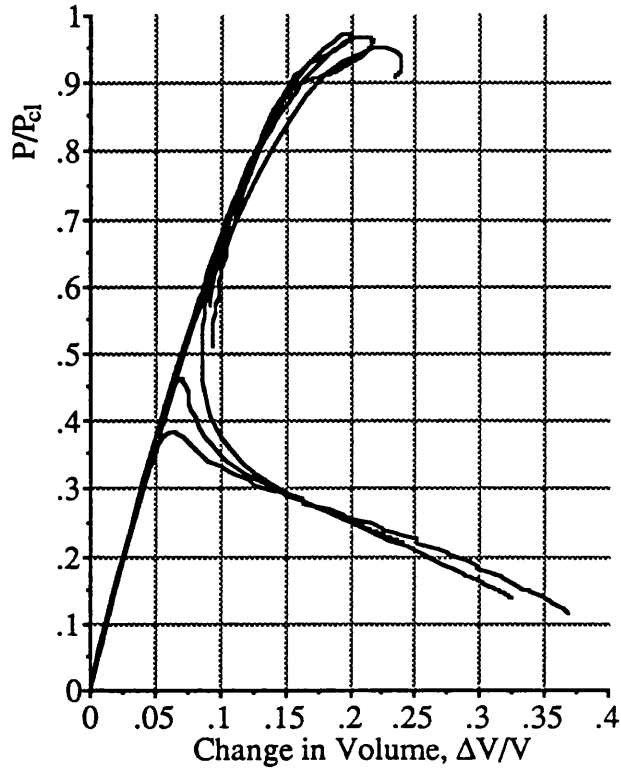
Figure 7.11 Fundamental Path and Shell Profiles for Imperfect Shells, $\lambda=4$, $r/t=500$.



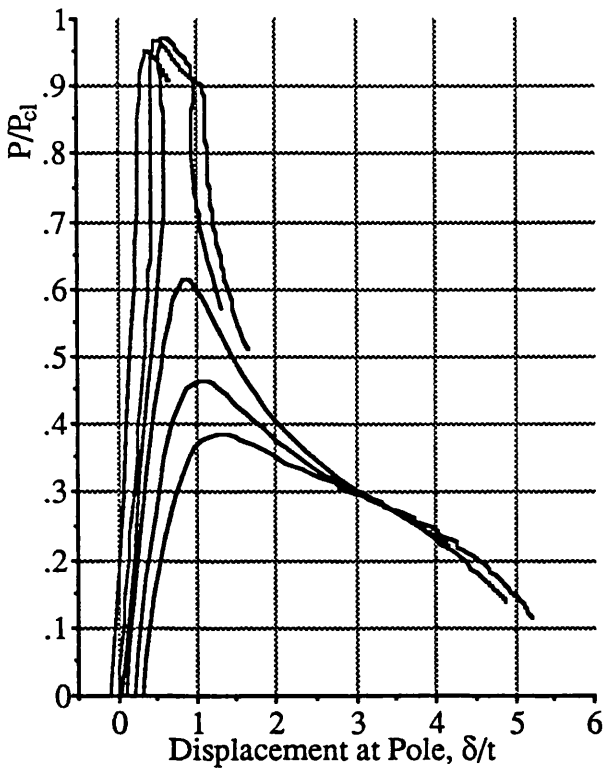
(a) Imperfection Shape, W^*



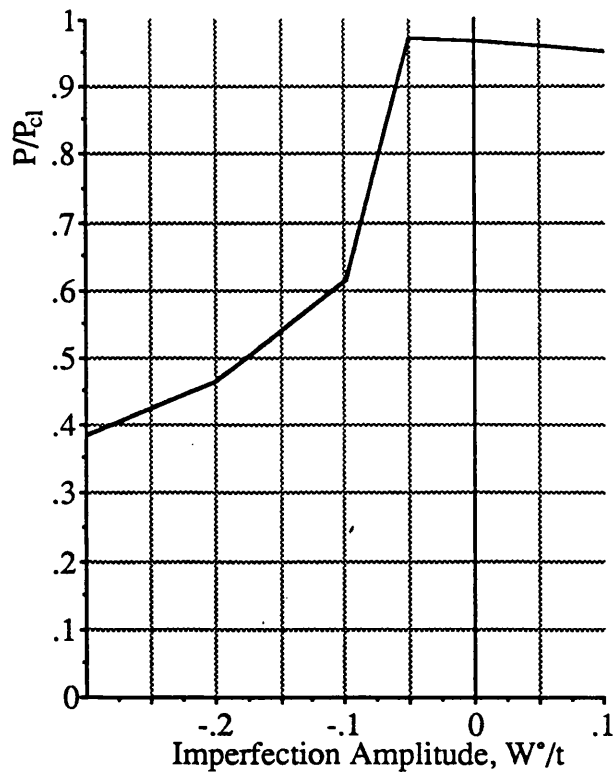
(b) Fundamental Path, P -vs- e



(c) Fundamental Path, P -vs- ΔV



(d) Fundamental Path, P -vs- δ



(e) Imperfection Sensitivity, W^*

Figure 7.12 Fundamental Path and Shell Profiles for Imperfect Shells, $\lambda=6$, $r/t=500$.

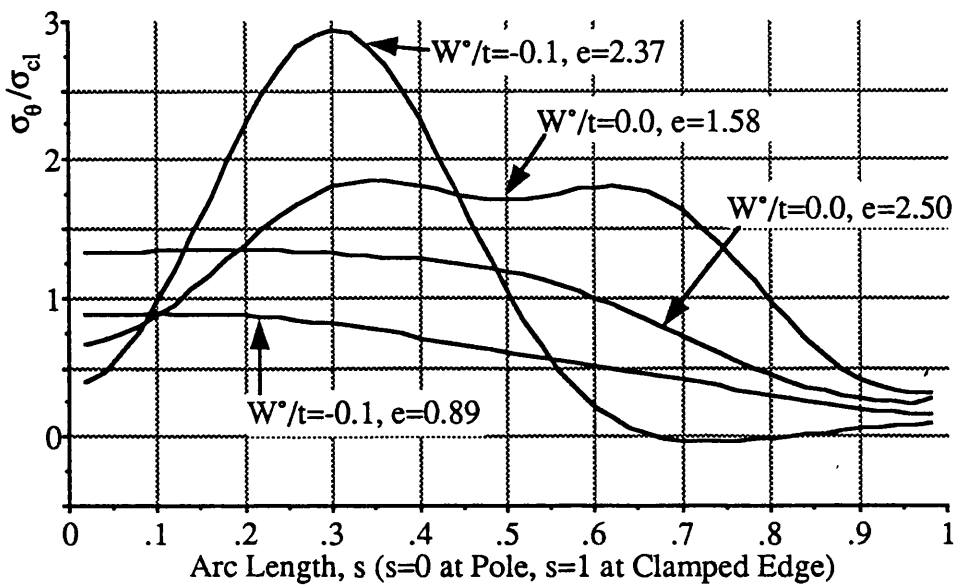
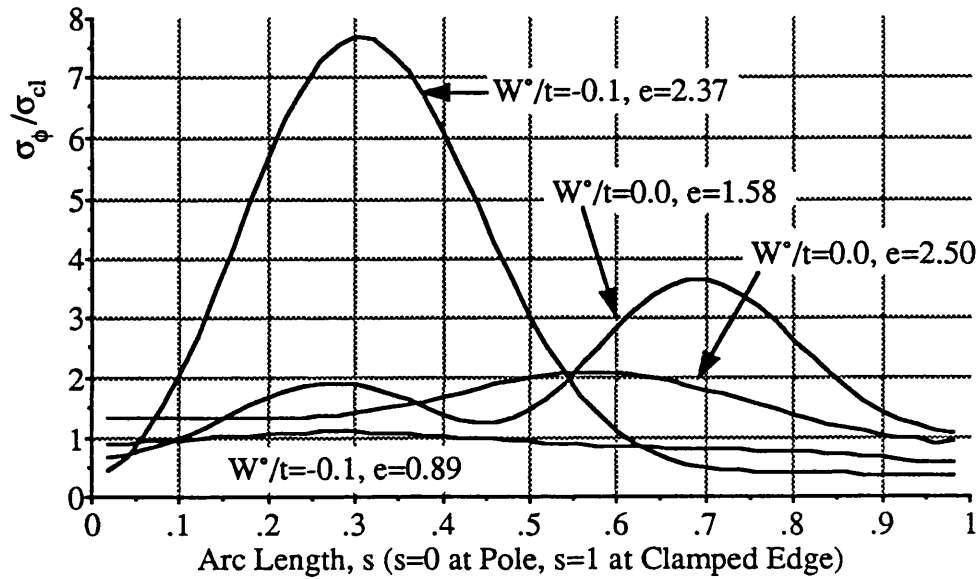
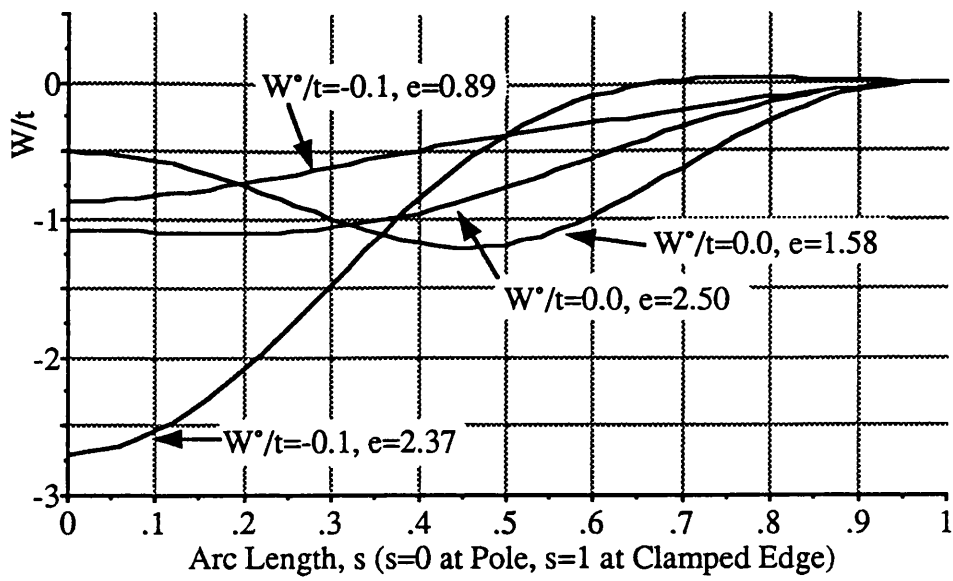
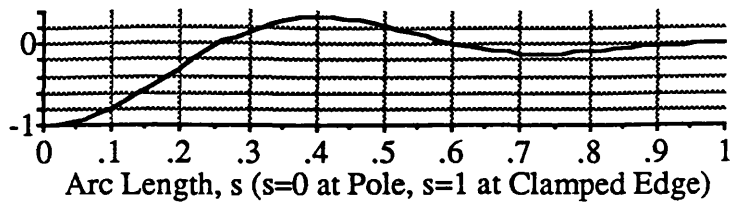
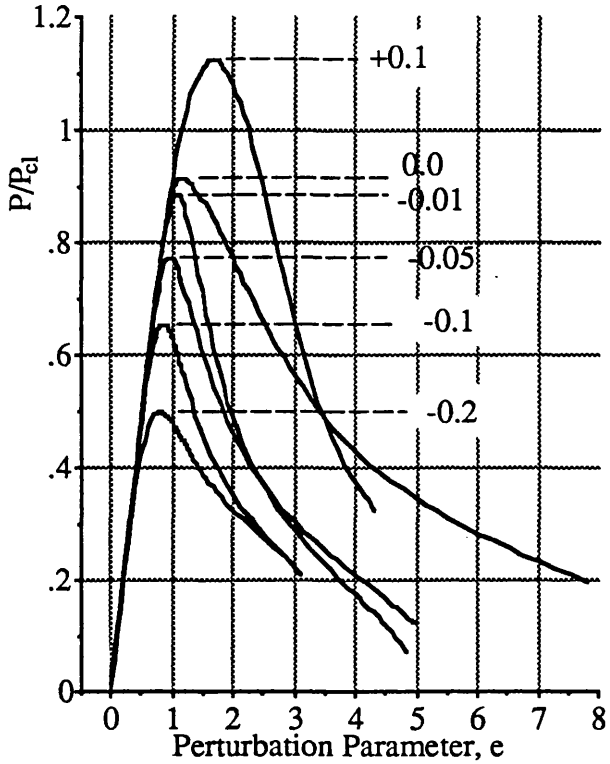


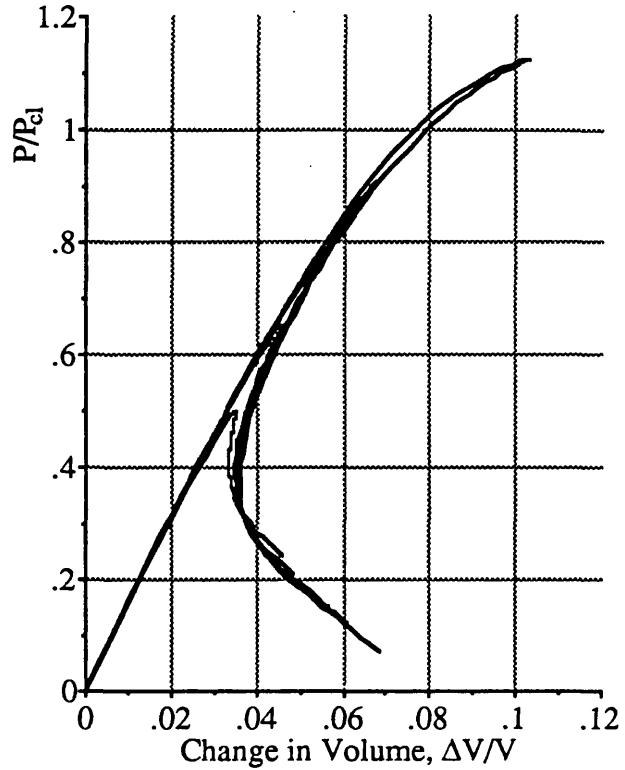
Figure 7.12 Fundamental Path and Shell Profiles for Imperfect Shells, $\lambda=6$, $r/t=500$.



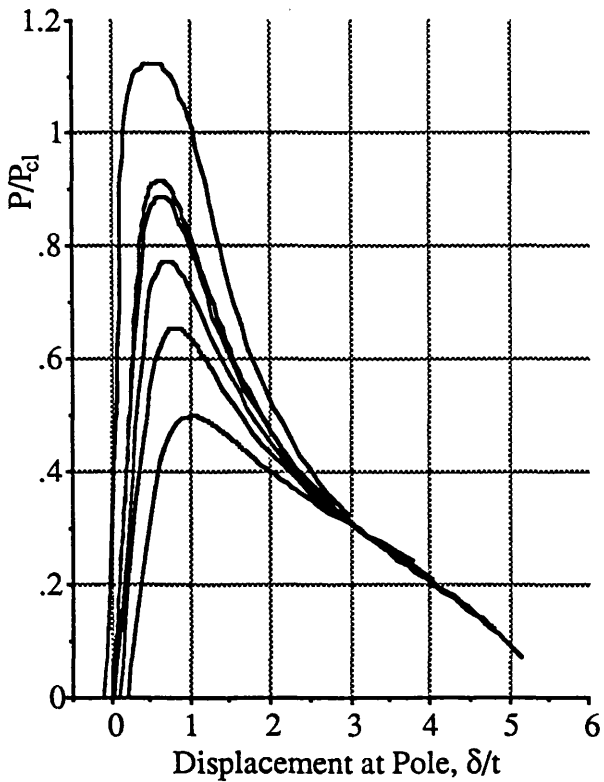
(a) Imperfection Shape, W^*



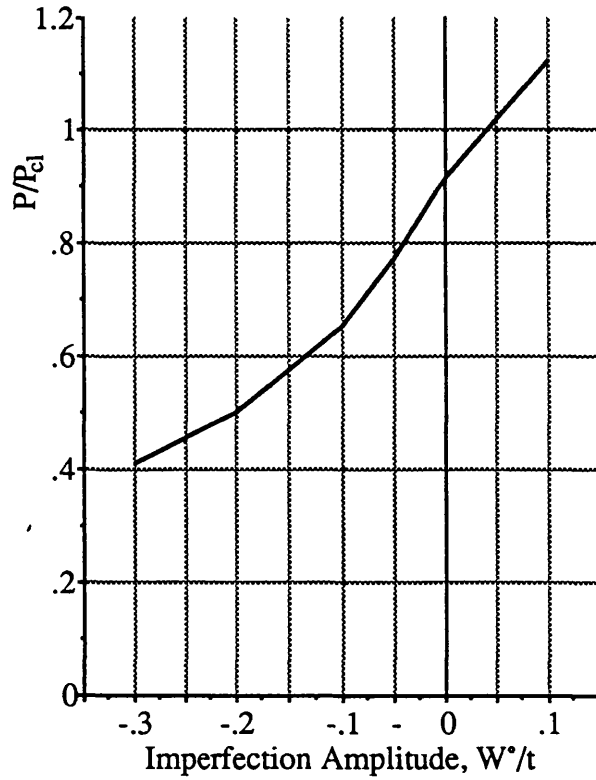
(b) Fundamental Path, P -vs- e



(c) Fundamental Path, P -vs- ΔV

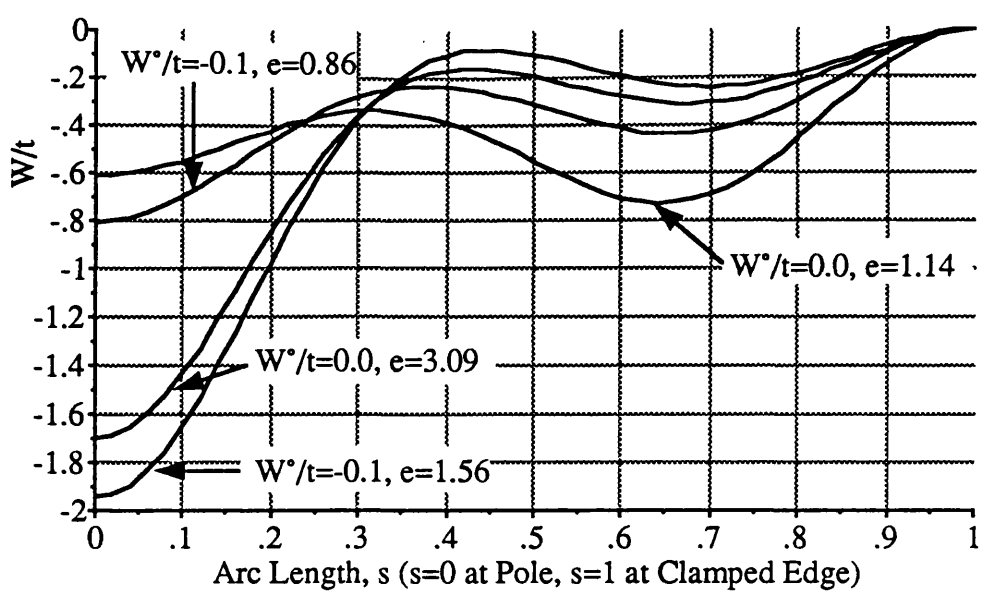


(d) Fundamental Path, P -vs- δ

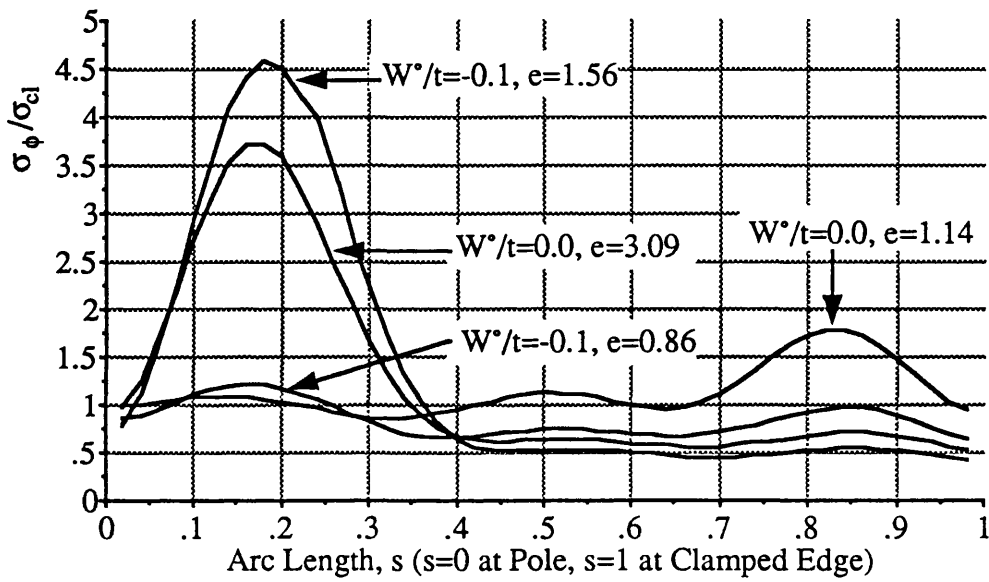


(e) Imperfection Sensitivity, W^*

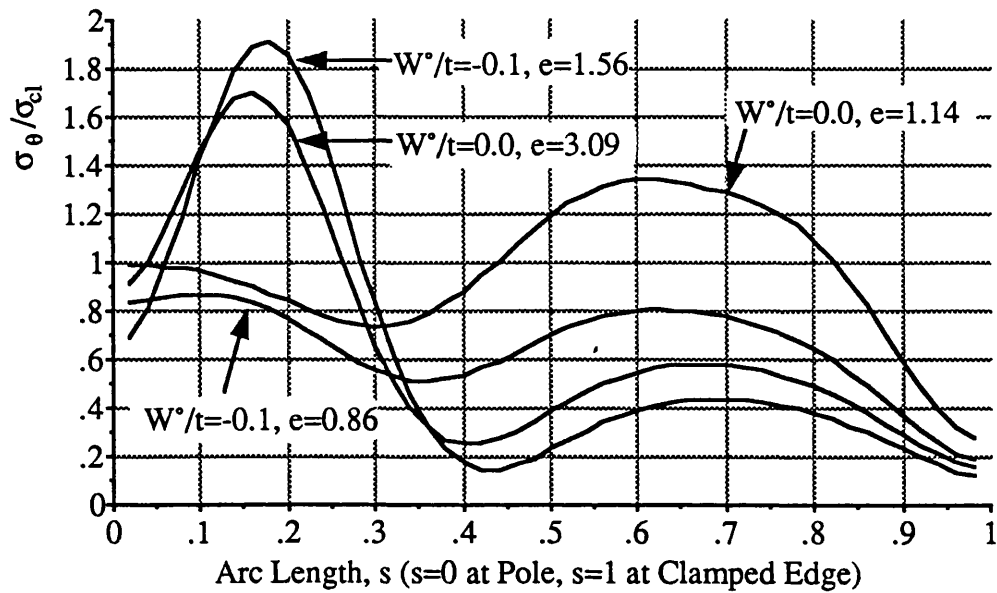
Figure 7.13 Fundamental Path and Shell Profiles for Imperfect Shells, $\lambda=9$, $r/t=500$.



(f) Radial Displacement Profiles

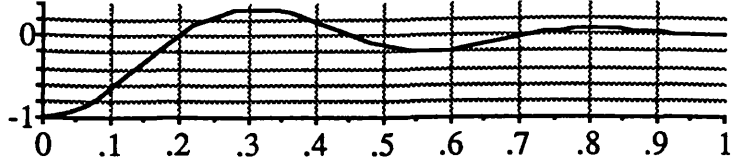


(g) Meridional Stress Profiles



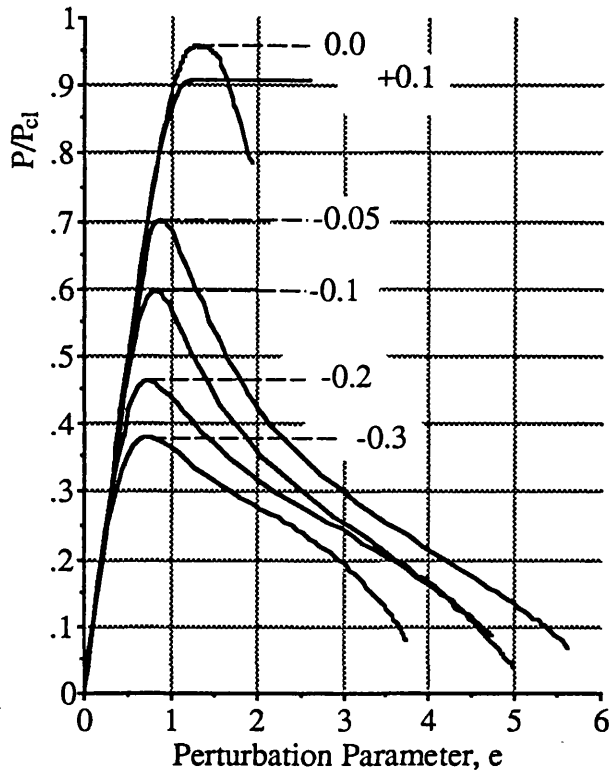
(h) Circumferential Stress Profiles

Figure 7.13 Fundamental Path and Shell Profiles for Imperfect Shells, $\lambda=9$, $r/t=500$.

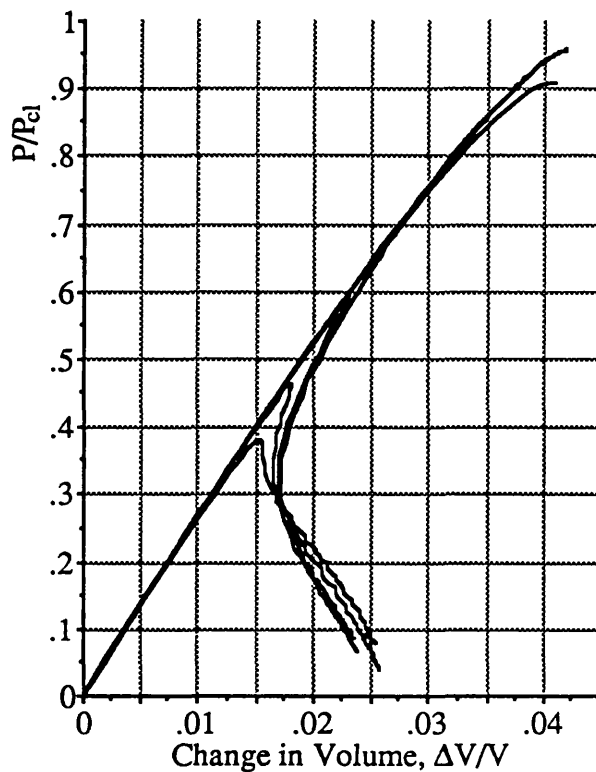


Arc Length, s ($s=0$ at Pole, $s=1$ at Clamped Edge)

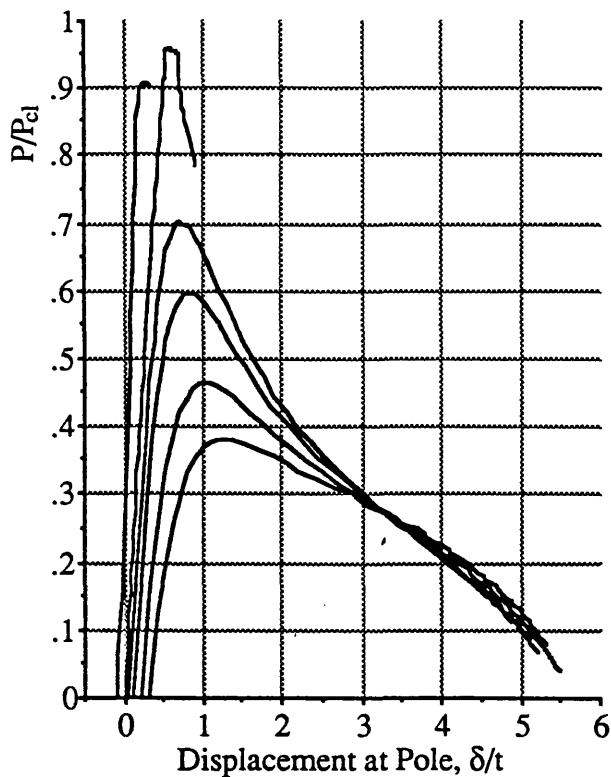
(a) Imperfection Shape, W^*



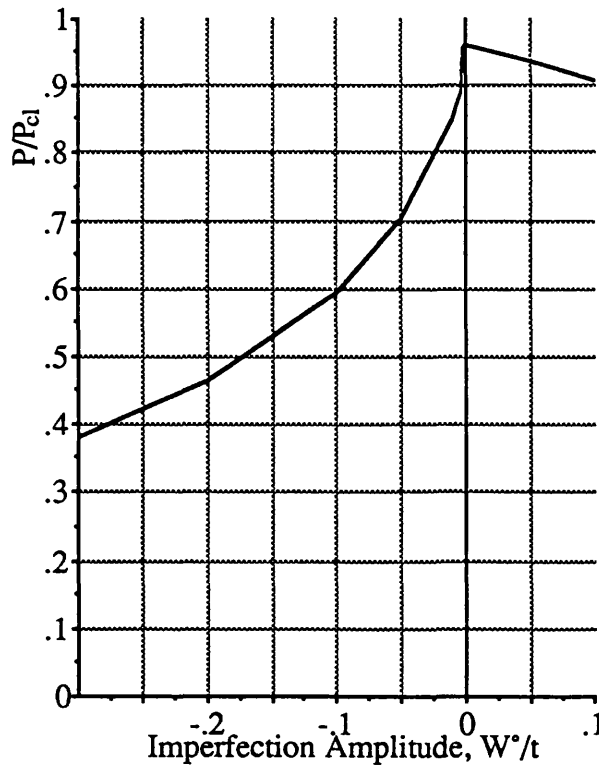
(b) Fundamental Path, P -vs- e



(c) Fundamental Path, P -vs- ΔV



(d) Fundamental Path, P -vs- δ



(e) Imperfection Sensitivity, W^*

Figure 7.14 Fundamental Path and Shell Profiles for Imperfect Shells, $\lambda=12$, $r/t=500$.

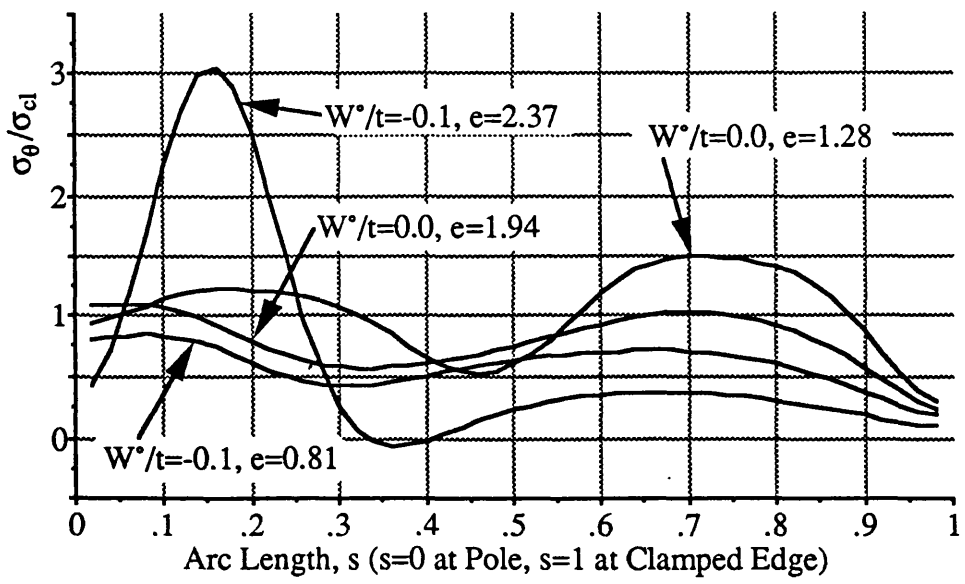
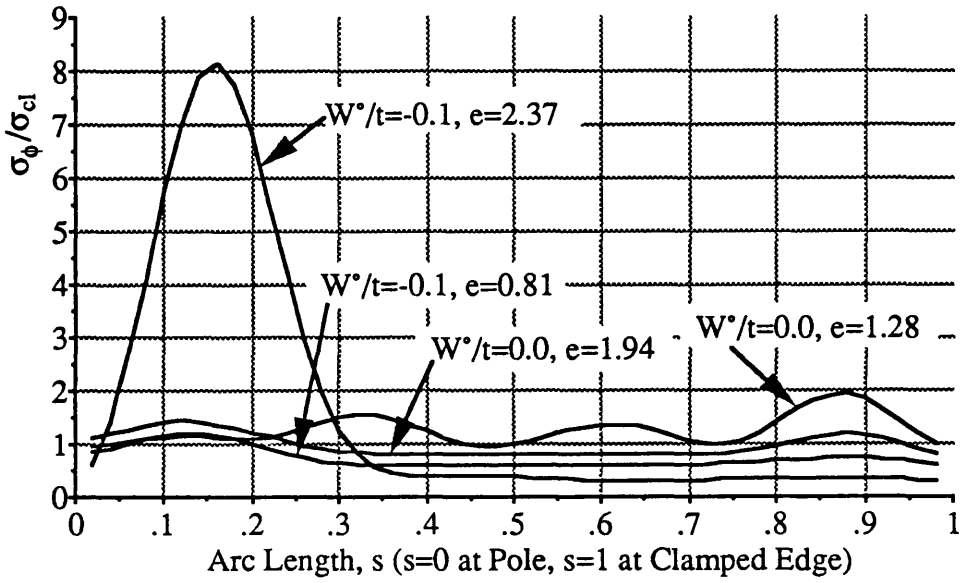
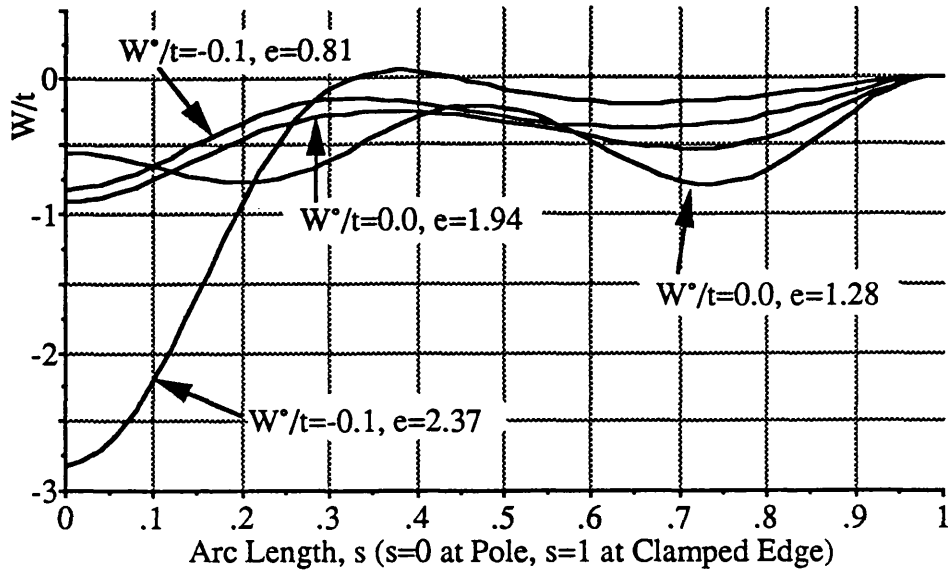
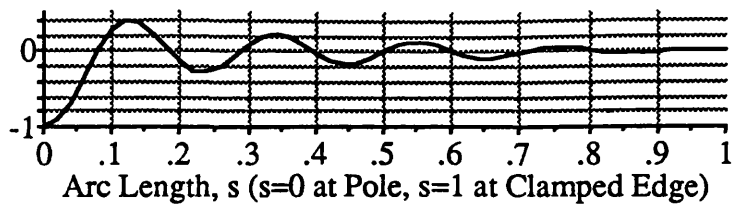
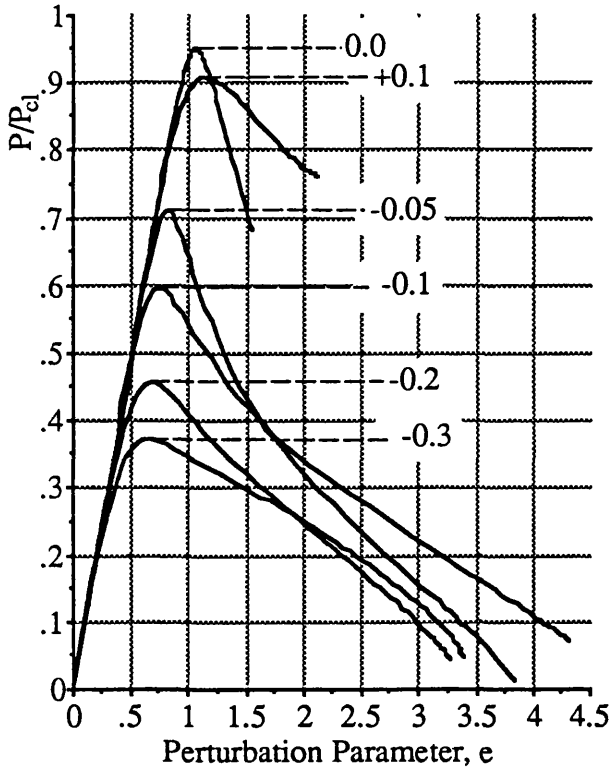


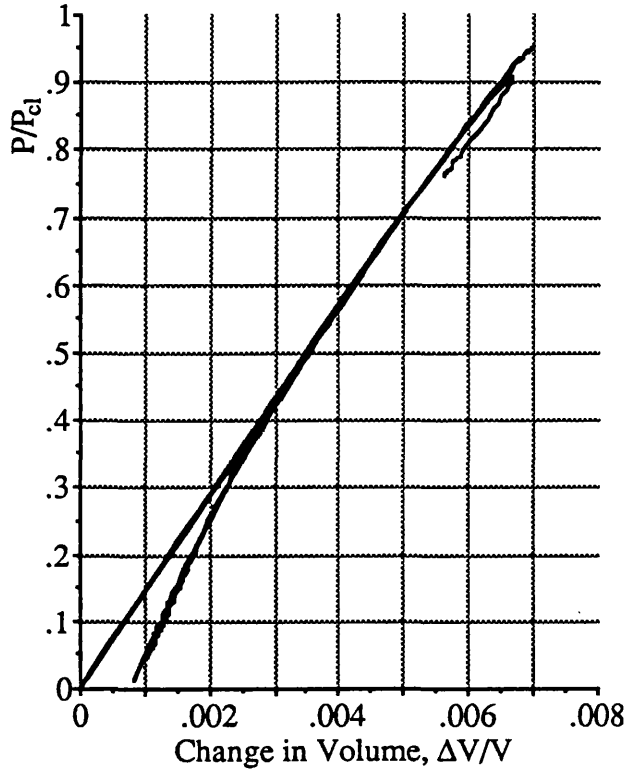
Figure 7.14 Fundamental Path and Shell Profiles for Imperfect Shells, $\lambda=12$, $r/t=500$.



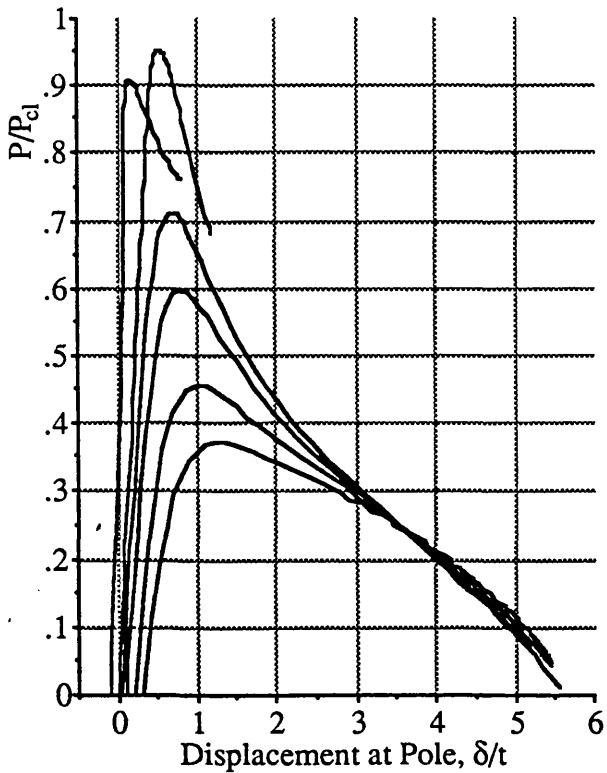
(a) Imperfection Shape, W^*



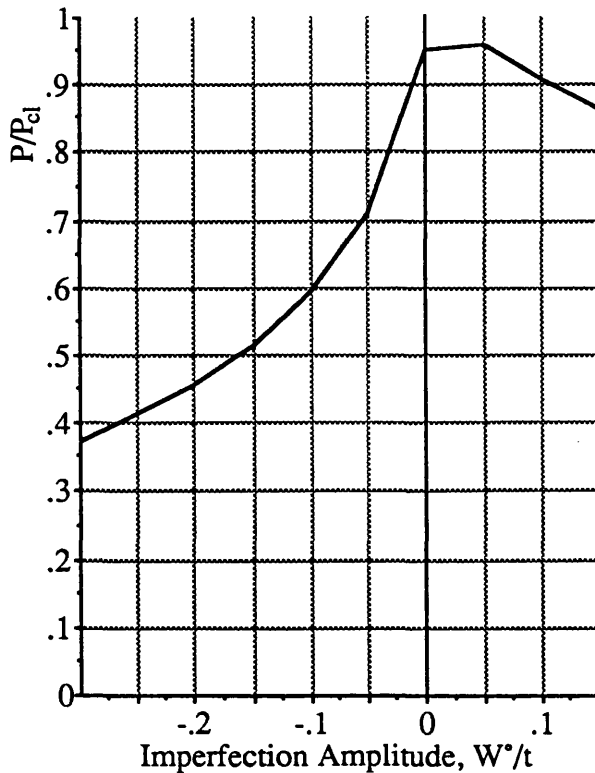
(b) Fundamental Path, P -vs- e



(c) Fundamental Path, P -vs- ΔV



(d) Fundamental Path, P -vs- δ



(e) Imperfection Sensitivity, W^*

Figure 7.15 Fundamental Path and Shell Profiles for Imperfect Shells, $\lambda=30$, $r/t=500$.

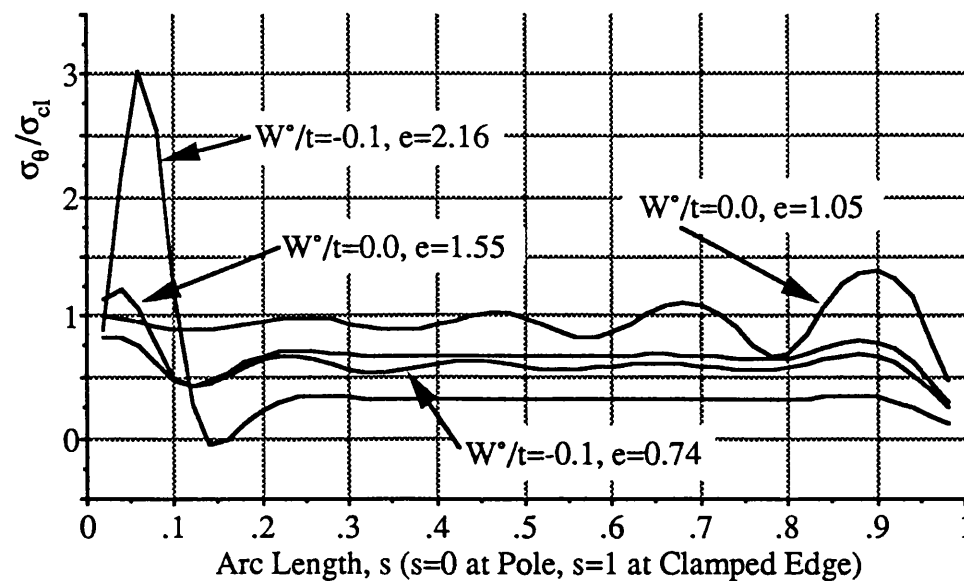
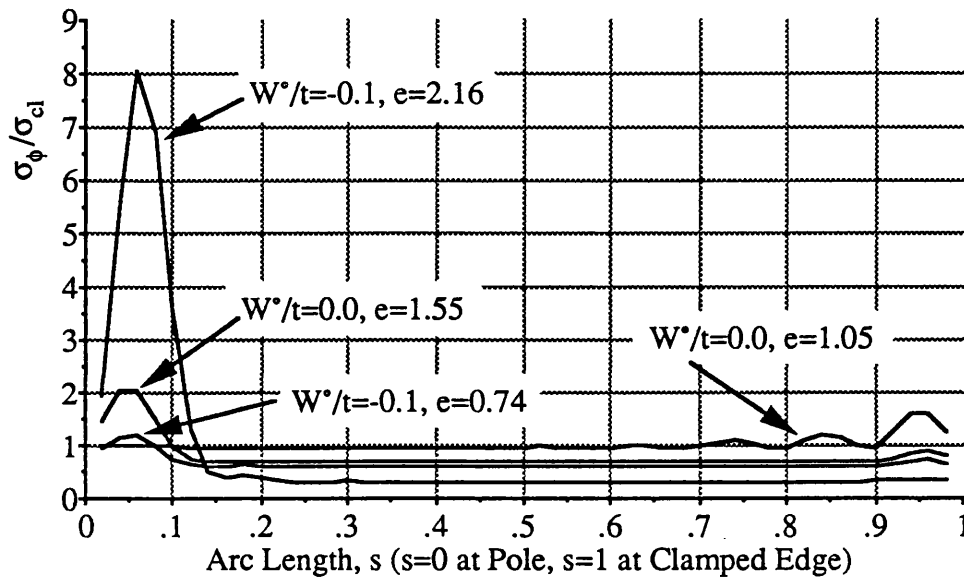
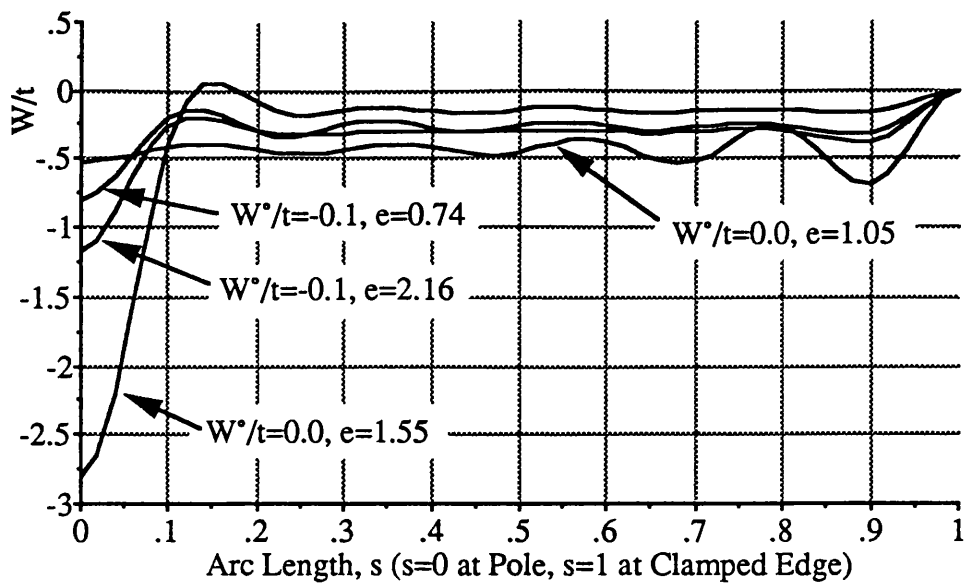


Figure 7.15 Fundamental Path and Shell Profiles for Imperfect Shells, $\lambda=30$, $r/t=500$.

CHAPTER EIGHT

CONCLUSIONS

CHAPTER EIGHT

CONTENTS

8.1 ELASTIC ANALYSIS OF SPHERICAL SHELLS

8.2 GENERAL CONCLUSIONS

CONCLUSIONS

8.1 ELASTIC ANALYSIS OF SPHERICAL SHELLS

In the classical analysis of complete spherical shells the bifurcation, or buckling, pressures are calculated from a linear eigenvalue problem in which the fundamental path consists of a pure radial contraction of the sphere, and the secondary path is axisymmetric. The total displacement of a complete perfect sphere under uniform external pressure loading at the lowest point of bifurcation on the fundamental path is approximately 42 per cent of the thickness of the shell, and the load carrying capacity of the shell on the secondary paths fall rapidly for small amplitudes of the secondary path displacements. In most cases the load carrying capacity of the shell drops to zero for secondary path displacements with an amplitude of about 20 per cent of the thickness of the shell. Despite the relatively small amplitude of the secondary path displacements, it is at least necessary to model the secondary path using a cubic expression, that is the total potential energy must contain at least quartic terms.

The axisymmetric nature of the secondary path displacements in the classical analysis implies that these displacements will cause circumferential bands of tension and compression to develop in the shell. The ability of the shell to develop circumferential bands of membrane compression will be sensitive to the presence of imperfections. When the circumferential membrane energy is completely eliminated from the classical analysis the bifurcation, or buckling, wavelength increases and the bifurcation, or buckling, loads decrease. For shells with radius to thickness ratios of more than 250 the critical buckling load is reduced to less than one quarter of the critical classical value, and the corresponding critical buckling wavelength doubles by comparison to the critical classical wavelength.

The comparisons for isotropic spherical caps clamped at the boundary under uniform pressure load, presented in Chapter Seven, show that the nonlinear fundamental path and bifurcation analysis are, when suitably nondimensionalised, dependent on the geometric slenderness parameter alone.

For initially perfect spherical caps with values of the geometric slenderness parameter greater than approximately 5.5, bifurcation into periodic modes occur at a lower pressures than axisymmetric buckling. The maximum radial displacement of the periodic critical mode and the maximum radial displacement of the axisymmetric fundamental path displacements at the critical load occur at approximately the same position on the shell. As the geometric slenderness parameter increases the periodic buckling displacements affect a smaller area of the shell adjacent to the clamped boundary, and the critical circumferential mode number increases. The number of periodic bifurcation modes and their proximity to the critical mode also increases as the geometric slenderness parameter increases.

For all initially perfect spherical caps with values of the geometric slenderness parameter of more than 4 the lowest buckling pressure, axisymmetric buckling or periodic bifurcation, occurs when the fundamental path circumferential stress first reaches the classical buckling stress for the complete sphere with the same radius to thickness ratio.

For perfect slender caps under uniform pressure loading periodic bifurcation occurs before axisymmetric buckling, and the initial displacements of the critical periodic buckling mode are large close to the boundary of the cap, and small in the central part of the cap. The periodic post bifurcation paths have not been calculated in the present work. However, if we consider the central part of the cap as a separate cap, with a smaller slenderness value and less restraint at the boundary, then it is reasonable to suppose that this part of the cap will have a lower bifurcation or axisymmetric buckling pressure than the entire cap. It may be imagined that the elastic buckling of perfect slender spherical caps under uniform external pressure, will be initiated by periodic bifurcation, in which the initial secondary path displacements near the boundary will be relatively large, the central portion of the spherical cap which has a lower critical pressure will then bifurcate or buckle axisymmetrically, and in this way the 'buckle' will propagate toward the pole.

The influence of one particular type of initial stress-free axisymmetric imperfection on the elastic behaviour of spherical caps has been examined in Chapter Seven. In all cases when the amplitude of the initial imperfection was greater than one tenth of the thickness of the spherical cap all periodic bifurcation was eliminated and the behaviour of the cap became entirely axisymmetric. Spherical caps with initial axisymmetric imperfections, of the type considered in Chapter Seven, buckle axisymmetrically with the radial displacement at the pole 'leading' the buckle.

For spherical caps with geometric slenderness values greater than 6 the results presented in Chapter Seven indicate that the postbuckling path becomes negative before the cap turns 'inside out'. In some cases, but not all, a small outward initial imperfection, of the type considered, resulted in a small increase in the axisymmetric buckling load.

8.2 GENERAL CONCLUSIONS

The derivation of the nonlinear strain-displacement expressions presented in Chapter Two makes use of the first Kirchhoff assumption and the resulting strain-displacement expressions may be applied to thin shells of arbitrary shape. By extending the derivation of the strain-displacement expressions to include the terms that are quartic in displacements, the limitations present in linear thin shell theory may be lifted and for all technical applications 'exact' partial differential equations governing the nonlinear elastic behaviour of thin shells are available.

The conditions that are required at the boundaries of incomplete shells in order that the displacements within the shell are continuous have been considered. In general, thin shell theory does not allow the reference surface displacements and their derivatives to be uniquely determined at the boundary by the displacements of the boundary surface alone. Five boundary conditions are required for the unique definition of the reference surface displacements and their derivatives. The 'natural' boundary conditions of the variational calculus correspond to boundaries at which no work is done. If work is done at the boundary supports, then the appropriate energy components expressed in terms of boundary integrals must be included in the total potential energy of the system. Particular boundary conditions for the spherical shells considered in this thesis are introduced in Chapter Two.

In the development of the total potential energy functional contained in Chapter Two, the use of the second Kirchhoff assumption and of Hooke's Law for an isotropic linear elastic material, allow the development of the expression for the strain energy of a spherical shell. The particular expression given in Chapter Two contains all the terms in the displacements up to and including the fifth order terms in the membrane energy, and up to and including the cubic terms in the bending energy. The expression for the load potential energy for a uniform external pressure load acting on a spherical shell is also derived in Chapter Two, allowing the total potential energy functional to be expressed in terms of the middle surface displacements and their derivatives. The methods used in the development of the total potential energy functional for pressure loaded spherical shells contained in Chapter Two are applicable to shell structures composed of one or more incomplete shells of arbitrary shape under arbitrary loading.

For a system to be in a state of equilibrium it is necessary that the total potential energy of the system be stationary with respect to any small kinematically admissible displacement function. The calculus of variations provides the necessary and sufficient conditions for equilibrium of the system. The total potential energy functional provides the common starting point for both the fundamental and secondary path analyses. Application of the stationary conditions yield the nonlinear differential equations that govern equilibrium of the fundamental and secondary paths.

A perturbation method is developed for solving the nonlinear fundamental path problem. The linear terms of the secondary path equation give rise to a nonlinear eigenvalue problem. The eigenvalue problem is nonlinear in terms of the fundamental path displacements and load. A method for solving the nonlinear eigenvalue problem is presented in Chapter Five. The solution of the nonlinear eigenvalue problem, in which the eigenvalue is the bifurcation load and the eigenvector is the initial displacement vector of the secondary path at the point of bifurcation, presented in Chapter Five is identical to solving for the first term in the secondary path perturbation series.

The fundamental and secondary path equations that are the subject of the solution algorithms are both equilibrium equations, and the fundamental and secondary path solutions, obtained by solving the equilibrium equations, have been used to calculate various contributions to the strain and load terms of the total potential energy. For a conservative system the sum of these various energy contributions must be zero, therefore the error in the sum of these energy contributions may be used to provide a check on the solution method. This check, back substituting the displacement vector and load into the total potential energy functional, is significant as it is independent of the solution methods used.

The methods used to solve the nonlinear partial differential equation, the equilibrium equation, for pressure loaded spherical shells presented in Chapters Four and Five take advantage of the axisymmetric nature of the problem to develop efficient solution routines. However, the solution methods and techniques developed in Chapters Four and Five may also be used for shell structures composed of one or more incomplete thin elastic shells of arbitrary shape under arbitrary loading.

REFERENCES

REFERENCES

- 1 Novozhilov V.V., 1964. "Thin Shell Theory", 2nd ed., Noordhoff Ltd., Gronongen The Netherlands.
- 2 Courant R., Robbins H., 1941. "What Is Mathematics", 4th ed., Oxford University Press, London New York Toronto.
- 3 Thompson J.M.T., Hunt G.W., 1973. "A General Theory Of Elastic Stability", John Wiley & Sons, London New York Sydney Toronto.
- 4 Gift S.J.G., 1987. "Contributions to the Calculus of Variations", Journal Of Optimization Theory And Applications, Vol. 52 No. 1.
- 5 Atkinson D.E., unpublished manuscript in preparation.
- 6 Calladine C.R., 1988. "The Theory of Thin Shell Structures 1888–1988", Proc. of The Institution of Mechanical Engineers, Vol. 202 No. 42.
- 7 Hildebrand F.B., 1965. "Methods Of Applied Mathematics", 2nd ed., Prentice-Hall Inc., Englewood Cliffs New Jersey.
- 8 Timoshenko S.P., Gere J.M., 1961. "Theory Of Elastic Stability", 2nd ed., McGraw-Hill, New York.
- 9 Flügge W., 1973. "Stresses In Shells", 2nd ed., Springer-Verlag, Berlin Heidelberg New York
- 10 Hutchinson J.W., Koiter W.T., 1970. "Postbuckling Theory", Applied Mechanics Reviews, Vol. 23.
- 11 Thompson J.M.T., 1962. "The Elastic Instability of a Complete Spherical Shell", Applied Mechanics Reviews, Vol. 15.
- 12 Silbiger A., 1962. "Nonaxisymmetric Modes of Vibration of Thin Spherical Shells".
- 13 Koiter W.T., 1969. "The Nonlinear Buckling Problem of a Complete Spherical Shell Under Uniform External Pressure", Proc. Kon. Ned. Ak. Wet, B72.
- 14 Thompson J.M.T., 1964. "The Rotationally Symmetric Branching Behaviour of a Complete Spherical Shell", Proc. Kon. Ned. Ak. Wet, B67.
- 15 Walker A.C., 1968. "An Analytical Study of the Rotationally Symmetric Non-Linear Buckling of a Complete Spherical Shell Under External Pressure", Int. Journal of Mechanical Science, Vol. 10.
- 16 Wilkinson J.H., 1965. "The Algebraic Eigenvalue Problem", Oxford University Press.
- 17 Huang N.C., 1964. "Unsymmetrical Buckling of Thin Shallow Spherical Shells", Transactions of the ASME Journal of Applied Mechanics.
- 18 Uchiyama K., Yamada M., 1974. "Buckling of Clamped Imperfect Thin Shallow Spherical Shells Under External Pressure I – The Effects of Geometrically Symmetrical Initial Imperfections –", Technology Reports Tohoku University, Vol. 39 No. 1.
- 19 Byerly E.W., 1893. "Fourier Series And Spherical Harmonics", Ginn & Co., Boston.
- 20 Adams J.C., 1878. "On the Expression of the Product of any two Legendre's Coefficients by means of a Series of Legendre's Coefficients", Proc. of The Royal Society, Vol.27.

APPENDIX A

AXISYMMETRIC ANALYSIS OF COMPLETE SPHERICAL SHELLS

AXISYMMETRIC ANALYSIS OF COMPLETE SPHERICAL SHELLS

A.1 POST BUCKLING ANALYSIS

Using the strain displacement relations

$$\epsilon_\phi = u - (w_f + w) + \frac{1}{2} \dot{w}^2 \quad (\text{A.1})$$

$$\epsilon_\theta = u \cot \phi - (w_f + w)$$

$$\chi_\phi = \frac{1}{r} \ddot{w}$$

$$\chi_\theta = \frac{1}{r} \dot{w} \cot \phi$$

The strain energy, U, is then given by

$$U = \int_0^\pi 2\pi r^2 K \sin \phi \, d\phi \quad (\text{A.2})$$

where

$$K = \frac{Et}{2(1-\mu^2)} (\epsilon_\phi^2 + \epsilon_\theta^2 + 2\mu\epsilon_\phi\epsilon_\theta) + \frac{Et^3}{24(1-\mu^2)} (\chi_\phi^2 + \chi_\theta^2 + 2\mu\chi_\phi\chi_\theta) \quad (\text{A.3})$$

The load potential energy, J_L, is given by

$$J_L = -P2\pi r^3 \int_0^\pi w \sin \phi \, d\phi \quad (\text{A.4})$$

The total potential energy functional may now be written as,

$$V(u, w) = V_0 + V_1(u, w) + V_2(u, w) + V_3(u, w) + \dots \quad (\text{A.5})$$

and the fundamental state is given by V₁(u, w) = 0, which yields

$$w_f = \frac{\lambda}{1+\mu} \quad \text{where} \quad \lambda = \frac{Pr(1-\mu^2)}{2Et} \quad (\text{A.6})$$

The total potential energy may now be written as

$$V(u, w, \lambda) = V_2(u, w, \lambda) + V_3(u, w) + V_4(w) \quad (\text{A.7})$$

where

$$V_2(u, w, \lambda) = \frac{\pi E t r^2}{1 - \mu^2} \int_0^\pi [(u + w)^2 + (u \cot \phi - w)^2 + 2\mu(u - w)(u \cot \phi - w) + \alpha(w^2 + w^2 \cot^2 \phi + 2\mu w w \cot \phi) - \lambda w^2] \sin \phi d\phi \quad (\text{A. 8})$$

$$V_3(u, w) = \frac{\pi E t r^2}{1 - \mu^2} \int_0^\pi [w^2(u - \mu u \cot \phi - (1 + \mu)w)] \sin \phi d\phi$$

$$V_4(w) = \frac{\pi E t r^2}{1 - \mu^2} \int_0^\pi \frac{1}{4} w^4 \sin \phi d\phi$$

$$\text{in which } \alpha = \frac{t^2}{12r^2}$$

The displacements of the middle surface, u and w , may be expressed in terms of the Legendre polynomials $P_i(x)$.

$$w(x) = a_i P_i(x)$$

$$u(x) = b_i z P_i(x)$$

Where repeated subscripts imply summation, and using the following notation,

$$x = \cos \phi, \quad z = (1 - x^2)^{\frac{1}{2}} = \sin \phi, \quad \beta_i = i(i + 1)$$

$$\dot{(\quad)} = \frac{d(\quad)}{dx}, \quad V^*(u, w) = \frac{1 - \mu^2}{\pi E t r^2} V(u, w)$$

equation (A. 8) may be written as

$$V_2^*(u, w, \lambda) = \int_{-1}^{+1} b_i^2 [\beta_i^2 P_i^2 + 2(1 - \mu) \{z^2 \ddot{P}_i - x \dot{P}_i\} \dot{P}_i x] + a_i b_i [-2(1 + \mu) \beta_i P_i^2] + a_i^2 [2(1 + \mu) P_i^2] + \alpha a_i^2 [\beta_i P_i^2 + 2(1 - \mu) (z^2 \ddot{P}_i - x \dot{P}_i) \dot{P}_i x] - \lambda a_i^2 [z^2 \dot{P}_i^2] dx \quad (\text{A. 9})$$

$$V_3^*(u, w) = \int_{-1}^{+1} [(1 + \mu) x z^2 \dot{P}_i \dot{P}_j \dot{P}_k b_i a_j a_k - z^4 \ddot{P}_i \dot{P}_j \dot{P}_k b_i a_j a_k - (1 + \mu) z^2 \dot{P}_i \dot{P}_j \dot{P}_k a_i a_j a_k] dx$$

$$V_4^*(w) = \int_{-1}^{+1} \frac{1}{4} z^4 \dot{P}_i \dot{P}_j \dot{P}_k \dot{P}_l a_i a_j a_k a_l dx$$

Using the Legendre integrals given in Section A.2 we may write the total potential energy as follows,

$$V^*(a, b, \lambda) = V_2^*(a, b, \lambda) + V_3^*(a, b) + V_4^*(a)$$

and

$$V^*(a_i, b_i, \lambda) = \sum_{m=0,1}^{\infty} ({}^m C_1 a_m^2 + {}^m C_2 a_m b_m + {}^m C_3 b_m^2 + \lambda {}^m C_4 a_m^2) \quad (\text{A.10})$$

$$+ {}^1 H_{ijk} b_i a_j a_k + {}^2 H_{ijk} a_i a_k a_k + H_{ijk\ell} a_i a_j a_k a_\ell$$

where

$${}^m C_1 = \frac{2}{2m+1} \{2(1+\mu) + \alpha(\beta_m - (1-\mu)\beta_m)\}$$

$${}^m C_2 = \frac{2}{2m+1} \{-2(1+\mu)\beta_m\}$$

$${}^m C_3 = \frac{2}{2m+1} \{\beta_m^2 - (1-\mu)\beta_m\}$$

$${}^m C_4 = \frac{2}{2m+1} \{-\beta_m\}$$

The use of the condition $\delta V^*/\delta b_r = 0$ allows the elimination of the passive coordinate,

$$\frac{\delta V^*}{\delta b_r} = 0 \Rightarrow b_r = \frac{1}{2 {}^r C_3} ({}^r C_2 a_r + {}^1 H_{rjk} a_j a_k) \quad (\text{A.11})$$

and

$$V^*(a_i, \lambda) = \sum_{m=0}^{\infty} ({}^m \dot{C}_1 + \lambda {}^m \dot{C}_2) a_m^2 + \frac{1}{2} {}^i \dot{C}_3 {}^1 H_{ijk} a_i a_j a_k \quad (\text{A.12})$$

$$+ \frac{1}{4} {}^i \dot{C}_4 {}^1 H_{ijk} {}^1 H_{i\ell p} a_j a_k a_\ell a_p + {}^2 H_{ijk} a_i a_j a_k + H_{ijk\ell} a_i a_j a_k a_\ell$$

where

$${}^m \dot{C}_1 = {}^m C_1 - \frac{({}^m C_2)^2}{4 {}^m C_3}, \quad {}^m \dot{C}_2 = {}^m C_4$$

$${}^i \dot{C}_3 = -\frac{{}^i C_2}{{}^i C_3}, \quad {}^i \dot{C}_4 = -\frac{1}{{}^i C_3}$$

The condition $\delta V^*/\delta a_r = 0$ yields

$$2({}^r \dot{C}_1 + {}^r \dot{C}_2 \lambda) a_r + \frac{1}{2} {}^r \dot{C}_3 {}^1 H_{rjk} a_j a_k + {}^i \dot{C}_3 {}^1 H_{irk} a_i a_k \quad (\text{A.13})$$

$$+ {}^2 H_{rjk} a_j a_k + 2 {}^2 H_{irk} a_i a_k + {}^i \dot{C}_4 {}^1 H_{irk} {}^1 H_{i\ell p} a_k a_\ell a_p + 4 H_{rjk\ell} a_j a_k a_\ell = 0$$

Introducing the perturbation series

$$a_i(s) = (\ddot{a}_N)s + \frac{1}{2}\ddot{a}_j s^2 + \frac{1}{6}\ddot{a}_j s^3 + \dots \quad \text{for } j \neq N \quad (\text{A.14})$$

$$\lambda(s) = \lambda_{cr} + \dot{\lambda}s + \frac{1}{2}\ddot{\lambda}s^2 + \frac{1}{6}\ddot{\lambda}s^3 + \dots$$

and identifying s with a_N :

$$s = a_N \Rightarrow \quad \dot{a}_N = 1, \quad \ddot{a}_N = \ddot{a}_{N+1} = \dots = 0; \quad \dot{a}_i = 0 \quad \text{for } i \neq N$$

By comparing coefficients of the powers of s , s^2 , s^3 , and s^4 we have

$$\text{From the } s \text{ term, or } \frac{\delta V^*}{\delta s} = 0.$$

$$\lambda_{cr} = -\frac{{}^N\bar{C}_1}{{}^N\bar{C}_2} = \frac{\alpha\beta_N^2 + (1 - \mu^2)}{\beta_N} \quad (\text{A.15a})$$

where

$$\beta_N = N(N+1) = \sqrt{\frac{1 - \mu^2}{\alpha}} \quad (\text{A.15b})$$

then

$$\frac{\delta \lambda_{cr}}{\delta \beta_N} = 0 \Rightarrow \quad (\lambda_{cr})_{\min} = 2\sqrt{\alpha(1 - \mu^2)} \quad (\text{A.15c})$$

$$\text{From the } s^2 \text{ term, or } \frac{\delta^2 V^*}{\delta s^2} = 0$$

$$\dot{\lambda} \Big|_{a_i=0}^{\lambda=\lambda_{cr}} = \frac{-1}{{}^N\bar{C}_2} (3 {}^N\bar{C}_3 {}^1H_{NNN} + 6 {}^2H_{NNN}) \quad (\text{A.16a})$$

$$\ddot{a}_r \Big|^{s=0} = -\frac{{}^r\bar{C}_3 {}^1H_{rNN} + 2 {}^N\bar{C}_3 {}^1H_{NrN} + 2 {}^2H_{rNN} + 4 {}^2H_{NrN}}{2({}^r\bar{C}_1 + {}^r\bar{C}_2\lambda_{cr})} \quad (\text{A.16b})$$

$$\text{From the } s^3 \text{ term, or } \frac{\delta^3 V^*}{\delta s^3} = 0$$

$$\ddot{\lambda} \Big|^{s=0} = \frac{1}{{}^N\bar{C}_2} (2 {}^N\bar{C}_3 {}^1H_{NjN}\ddot{a}_j + {}^i\bar{C}_3 {}^1H_{iNN}\ddot{a}_i + 2 {}^i\bar{C}_4 {}^1H_{iNN} {}^1H_{iNN} + 2 {}^2H_{iNN} \ddot{a}_i + 4 {}^2H_{NNk} \ddot{a}_k + 8H_{NNNN}) \quad (\text{A.17a})$$

and

$$\begin{aligned} \ddot{a}_r \Big|^{s=0} = & \frac{-3}{2(\bar{C}_1 + \bar{C}_2 \lambda_{cr})} (2 \bar{C}_2 \dot{\lambda} \ddot{a}_r + \bar{C}_3 {}^1H_{rjN} \ddot{a}_j + {}^i\bar{C}_3 {}^1H_{irN} \ddot{a}_i + {}^N\bar{C}_3 {}^1H_{Nr k} \ddot{a}_k \\ & + 2 {}^i\bar{C}_4 {}^1H_{irN} {}^1H_{iNN} + 2 {}^2H_{rjN} \ddot{a}_j + 2 {}^2H_{irN} \ddot{a}_i \\ & + 2 {}^2H_{Nr k} \ddot{a}_k + 8H_{rNNN}) \end{aligned} \quad (\text{A.17b})$$

From the s^4 term, or $\frac{\delta^4 V^*}{\delta s^4} = 0$

$$\begin{aligned} \ddot{\lambda} \Big|^{s=0} = & \frac{1}{8\bar{C}_2} (8 {}^N\bar{C}_3 {}^1H_{NjN} \ddot{a}_j + 3 {}^N\bar{C}_3 {}^1H_{Njk} \ddot{a}_j \ddot{a}_k + 4 {}^i\bar{C}_3 {}^1H_{iNN} \ddot{a}_i \\ & + 6 {}^i\bar{C}_3 {}^1H_{iNk} \ddot{a}_i \ddot{a}_k + 12 {}^i\bar{C}_4 {}^1H_{iNk} {}^1H_{iNN} \ddot{a}_k + 24 {}^i\bar{C}_4 {}^1H_{iNN} {}^1H_{iLN} \ddot{a}_L \\ & + 16 {}^2H_{NjN} \ddot{a}_j + 6 {}^2H_{Njk} \ddot{a}_j \ddot{a}_k + 8 {}^2H_{iNN} \ddot{a}_i + 12 {}^2H_{iNk} \ddot{a}_i \ddot{a}_k + 144 H_{jNNN} \ddot{a}_j) \end{aligned} \quad (\text{A.18})$$

A.2 THE LEGENDRE INTEGRAL FORMULAE

The Legendre equation and other related formulae are given by Byerly [19] The Legendre equation is,

$$z^2\ddot{P} - 2x\dot{P} + \beta P = 0, \quad \text{where } z^2 = (1 - x^2) \quad (\text{A.19})$$

and the Legendre polynomial of order N is given by,

$$P_N = \sum_{m=0}^M (-1)^m \frac{(2N-2m)! x^{(N-2m)}}{2^N m! (N-m)! (N-2m)!} \quad \begin{cases} M = \frac{N}{2}, & N \text{ even} \\ M = \frac{N-1}{2}, & N \text{ odd} \end{cases} \quad (\text{A.20})$$

Also,

$$\dot{P}_N = (2N-1)P_{N-1} + (2N-5)P_{N-3} + (2N-9)P_{N-5} + \dots + \begin{cases} +3P_1, & N \text{ even} \\ +1, & N \text{ odd} \end{cases} \quad (\text{A.21})$$

and,

$$(x^2 - 1)\dot{P}_N = NxP_N - NP_{N-1} \quad (\text{A.22})$$

hence $x\dot{P}_N$ may be written in terms of P_j where $j \leq N$, by using

$$x\dot{P}_N = NP_N + \dot{P}_{N-1} \quad (\text{A.23})$$

The integral of the product of Legendre polynomials is given by

$$\int_{-1}^{+1} P_m P_n = \begin{cases} \frac{2}{2m+1}, & m = n \\ 0, & m \neq n \end{cases} \quad (\text{A.24})$$

And the integrals of the quadratic terms of the total potential energy may be evaluated using the following formulae,

$$\int_{-1}^{+1} (z^2\ddot{P}_i - x\dot{P}_i)x\dot{P}_i dx = \int_{-1}^{+1} (x^2 - 1)\dot{P}_i^2 dx + \int_{-1}^{+1} \dot{P}_i^2 dx - \int_{-1}^{+1} \beta_i x\dot{P}_i P_i dx \quad (\text{A.25})$$

and

$$\int_{-1}^{+1} (x^2 - 1)\dot{P}_N^2 dx = \frac{-2}{2N+1}\beta_N, \quad \int_{-1}^{+1} \dot{P}_N^2 dx = \beta_N, \quad \int_{-1}^{+1} \beta_N x\dot{P}_N P_N dx = \left(\frac{2N}{2N+1}\right)\beta_N \quad (\text{A.26})$$

Hence

$$\int_{-1}^{+1} (z^2\ddot{P}_i - x\dot{P}_i)x\dot{P}_i dx = \int_{-1}^{+1} (x\dot{P}_i - \beta_i P_i)x\dot{P}_i dx = \int_{-1}^{+1} -\frac{1}{2}\beta_i P_i^2 dx = \int_{-1}^{+1} -\frac{1}{2}z^2\dot{P}_i^2 dx = \frac{-\beta_i}{2i+1} \quad (\text{A.27})$$

In order to evaluate the integrals that are cubic and quartic in the Legendre polynomials P we will need to make use of the following product formulae given by Adams[20].

$$P_\alpha P_\beta = \sum_{s=0,1}^{s=t} \frac{A(\alpha-s)A(s)A(\beta-s)}{A(\alpha+\beta-s)} \frac{(2\alpha+2\beta-4s+1)}{(2\alpha+2\beta-2s+1)} P_{\alpha+\beta-2s} \quad (\text{A.28})$$

where $t = \alpha$ if $\beta \geq \alpha$, or $t = \beta$ if $\alpha > \beta$, and

$$A(m) = \frac{1.3.5\dots(2m-1)}{1.2.3\dots m}; \quad \text{with } A(0) = 1, \text{ and } A(-m) = 0$$

Also

$$\dot{P}_\alpha \dot{P}_\beta = \sum_{r=0,1}^{r=u} \frac{B(\alpha-r-1)B(r)B(\beta-r-1)}{A(\alpha+\beta-r)} \frac{(2\alpha+2\beta-4r-1)}{(\alpha+\beta-2r-1)(\alpha+\beta-2r)} \dot{P}_{\alpha+\beta-2r-1} \quad (\text{A.29})$$

where $u = \alpha - 1$ if $\beta \geq \alpha$, or $u = \beta - 1$ if $\alpha > \beta$, and

$$B(m) = \frac{1.3.5\dots(2m+1)}{1.2.3\dots m}; \quad \text{with } B(0) = 1, \text{ and } B(-m) = 0$$

The cubic integrals ${}^1H_{ijk}$ and ${}^2H_{ijk}$ may be written as follows,

$$\begin{aligned} {}^1H_{ijk} &= {}^1H_{ikj} = \int_{-1}^{+1} [(1+\mu)xz^2\dot{P}_i\dot{P}_j\dot{P}_k - z^4\ddot{P}_i\dot{P}_j\dot{P}_k] dx \\ &= \frac{j(j+1)}{(2j+1)} \int_{-1}^{+1} \{i(i+\mu)[P_iP_{j-1}\dot{P}_k - P_iP_{j+1}\dot{P}_k] + (1-\mu)[\dot{P}_{i-1}P_kP_{j+1} - \dot{P}_{i-1}P_kP_{j-1}]\} dx \end{aligned} \quad (\text{A.30})$$

and

$${}^2H_{ijk} = {}^2H_{ikj} = \int_{-1}^{+1} -(1+\mu)z^2P_i\dot{P}_j\dot{P}_k dx = \frac{j(j+1)}{(2j+1)} \int_{-1}^{+1} (1+\mu)[P_iP_{j+1}\dot{P}_k - P_iP_{j-1}\dot{P}_k] dx \quad (\text{A.31})$$

The quartic integral, $H_{ijk\ell}$ may be written as,

$$\begin{aligned} H_{ijk\ell} &= \int_{-1}^{+1} z^4\dot{P}_i\dot{P}_j\dot{P}_k\dot{P}_\ell dx \\ &= \frac{k(k+1)(\ell+1)}{(2k+1)(2\ell+1)} \int_{-1}^{+1} [\dot{P}_i\dot{P}_j(P_{k-1}P_{\ell-1} - P_{k-1}P_{\ell+1} + P_{k+1}P_{\ell+1} - P_{k+1}P_{\ell-1})] dx \end{aligned} \quad (\text{A.32})$$

Finally the integrals of the cubic and quartic Legendre polynomials may be evaluated as follows.

$$\int_{-1}^{+1} \dot{P}_\alpha \dot{P}_\beta \dot{P}_\delta dx = \sum_{s=0,1}^t \Omega \frac{A(\alpha-s)A(s)A(\beta-s)}{A(\alpha+\beta-s)} \frac{(2\alpha+2\beta-4s+1)}{(2\alpha+2\beta-2s+1)} \quad (\text{A.33})$$

| | |
|--|---|
| $\Omega = 2$ if $\alpha \geq 0$ and $\beta \geq 0$ and $\delta \geq 0$ and $\alpha + \beta + \delta = 1, 3, 5, \dots$ (odd) and $\alpha + \beta - 2s < \delta$ | $\Omega = 0$ if $\alpha < 0$ or $\beta < 0$ or $\delta < 1$ or $\alpha + \beta + \delta = 2, 4, 6, \dots$ (even) or $\alpha + \beta - 2s \geq \delta$ |
|--|---|

$$\int_{-1}^{+1} \dot{P}_\alpha \dot{P}_\beta \dot{P}_\delta dx = \sum_{r=0,1}^{r=u} \Omega \frac{B(\alpha-r-1)B(r)B(\beta-r-1)}{A(\alpha+\beta-r)} \frac{(2\alpha+2\beta-4r-1)}{(\alpha+\beta-2r-1)(\alpha+\beta-2r)} \quad (\text{A.34})$$

| | |
|---|--|
| $\Omega = 2$ if $\alpha \geq 1$ and $\beta \geq 1$ and $\delta \geq 0$ and $\alpha + \beta + \delta = 2, 4, 6, \dots$ (even) and $\alpha + \beta - 2r - 1 > \delta$ | $\Omega = 0$ if $\alpha < 1$ or $\beta < 1$ or $\delta < 0$ or $\alpha + \beta + \delta = 1, 3, 5, \dots$ (odd) or $\alpha + \beta - 2r - 1 \leq \delta$ |
|---|--|

$$\int_{-1}^{+1} \dot{P}_\alpha \dot{P}_\beta \dot{P}_\delta \dot{P}_\gamma dx = \sum_{r=0,1}^{r=u} \sum_{s=0,1}^{s=t} \Omega \frac{B(\alpha-r-1)B(r)B(\beta-r-1)A(\delta-s)A(s)A(\gamma-s)}{A(\alpha+\beta-r)A(\delta+\gamma-s)} \otimes \quad (\text{A.35})$$

$$\otimes \frac{(2\alpha+2\beta-4r-1)(2\delta+2\gamma-4s+1)}{(\alpha+\beta-2r+1)(\alpha+\beta-2r)(2\delta+2\gamma-2s+1)}$$

| | |
|--|---|
| $\Omega = 2$ if $\alpha \geq 1$ and $\beta \geq 1$ and $\delta \geq 0$ and $\gamma \geq 0$ and $\alpha + \beta + \delta + \gamma = 0, 2, 4, \dots$ (even) and $\alpha + \beta - 2r - 1 > \delta + \gamma - 2s$ | $\Omega = 0$ if $\alpha < 1$ or $\beta < 1$ or $\delta < 0$ or $\gamma < 0$ or $\alpha + \beta + \gamma + \delta = 1, 3, 5, \dots$ (odd) or $\alpha + \beta - 2r - 1 \leq \delta + \gamma - 2s$ |
|--|---|

A.3 ENERGY CONTRIBUTIONS TO THE QUADRATIC TERMS OF THE TOTAL POTENTIAL ENERGY

The energy contributions to $V_2^*(u, w, \lambda)$ may be evaluated as follows.

$$U_{2M_\star} = \frac{2}{2m+1} \left\{ (1+\mu) + [2(m-\beta_m) - \mu\beta_m] \left(\frac{{}^m C_2}{2^m C_3} \right) + \left(\beta_m^2 - \frac{2m+1}{2} \beta_m + \frac{1}{2} \mu \beta_m \right) \left(\frac{{}^m C_2}{2^m C_3} \right) \right\} a_m^2$$

$$U_{2M_\circ} = \frac{2}{2m+1} \left\{ (1+\mu) + (2m + \mu\beta_m) \left(\frac{{}^m C_2}{2^m C_3} \right) + \left(\frac{2m-1}{2} \beta_m + \frac{1}{2} \mu \beta_m \right) \left(\frac{{}^m C_2}{2^m C_3} \right)^2 \right\} a_m^2$$

$$U_{2B_\star} = \frac{2\alpha}{2m+1} \left\{ \beta_m^2 - \frac{2m+1}{2} \beta_m + \frac{1}{2} \mu \beta_m \right\} a_m^2 \quad (\text{A.36})$$

$$U_{2B_\circ} = \frac{2\alpha}{2m+1} \left\{ \frac{2m-1}{2} \beta_m + \frac{1}{2} \mu \beta_m \right\} a_m^2$$

$$J_{2L} = \lambda \frac{2}{2m+1} \{-\beta_m\} a_m^2$$

APPENDIX B

COMPUTER PROGRAM, SOURCE AND OUTPUT LISTINGS


```

C
DAVID SMITH SPHERICAL SHELL FINITE DIFF. ANALYSIS VAR. F.D. EXPRESSIONS SPHERE 4
DAVID SMITH SPHERICAL SHELL FINITE DIFF. ANALYSIS VAR. F.D. EXPRESSIONS SPHERE 5
DIMENSION HA(147,62),A(147,41),UF(147,160),UFP(147,160),U(147,7) SPHERE 6
CX(159),V(147),V2(147),V3(147),V4(147),P(7),AF(7,4),AR(12,27),Z3(14 SPHERE 7
C7),Z4(149),PF(160),UFC(106,160),Z5(166),Z6(106) SPHERE 8
COMMON/COM1/ AN(7,4,12),ITYPE,ILN(7),JFN(7),JFH(7),KNOC(7) SPHERE 9
COMMON/COM2/ D0,D1,E2,D3,D4,AL,THETA,PCL,H,AI,IFR,ION SPHERE 10
COMMON /COM3/ JAC,JAW,JABW,IF,ID,IC,PT,12AP SPHERE 11
COMMON /COM4/ IN,N1,N2 SPHERE 12
COMMON /COM5/ VF(147,20),VFB(147,20),VFC(106,20),PFC(20),EFC(20) SPHERE 13
C, SF(147) SPHERE 14
COMMON UF,UFB,UFC SPHERE 15
LEVEL 2,UF,UFH,UFC SPHERE 16
CALL SECOND(AAA) SPHERE 17
WRITE (6,8000) AAA SPHERE 18
EG 1 J=1,20 SPHERE 19
PFC(I)=0.0 SPHERE 20
1 PFC(I)=0.0 SPHERE 21
I87=147 SPHERE 22
I99=159 SPHERE 23
KA=41 SPHERE 24
KHA=62 SPHERE 25
KUF=160 SPHERE 26
KU=7 SPHERE 27
KAP=27 SPHERE 28
NUFC=106 SPHERE 29
IFT=0 SPHERE 30
READ (5,1000) N,NMB,KU,ITYPE,IPP,AI,CO,ICN SPHERE 31
FORMAT (5I10,2F10,2,I10) SPHERE 32
READ (5,1005) R,DIV SPHERE 33
1005 FORMAT (2F10,2) SPHERE 34
DO 20 I=1,ITYPE SPHERE 35
DO 10 J=1,4 SPHERE 36
READ (5,1010) AF(I,J),(AN(I,J,K),K=1,7) SPHERE 37
READ (5,1020) (AK(I,J,K),K=8,12) SPHERE 38
10 CONTINUE SPHERE 39
READ(5,1030) IPN(I),ILN(I),JFN(I),JFH(I),KPCF(I) SPHERE 40
20 CONTINUE SPHERE 41
1010 FORMAT(RF10.1) SPHERE 42
1020 FORMAT(5F10.1) SPHERE 43
1030 FORMAT (5I10) SPHERE 44
READ (5,1040) IAC,IAPW,ISTEP SPHERE 45
1040 FORMAT (3I10) SPHERE 46
THETA=3.141592654/CIV SPHERE 47
ALAMP=SQRT(12.0*(1.0-DO*DO)) SPHERE 48
ALAMP=SQRT(ALAMP*R)*THETA SPHERE 49
AL=1.0/(12.0*(R**2)) SPHERE 50
D1=1.0+AL SPHERE 51
D2=1.0-DO SPHERE 52
D3=1.0+DO SPHERE 53
D4=3.0-DO SPHERE 54
BN=H SPHERE 55

[BN
H=THETA/(BN-1.0) SPHERE 56
FCI=-((1.0-DO*DO)/(SQRT(3.0*(1.0-DO*DO)))*R) SPHERE 57
NX=3*(R-7) SPHERE 58
NY=NX+12 SPHERE 59
N1=2*(A-2) SPHERE 60
N2=N1+8 SPHERE 61
JAC=(IAC*2)/3 SPHERE 62
JAW=2*JAC-1 SPHERE 63
JAPW=(IAPW*2)/3 SPHERE 64
IF=1 SPHERE 65
ID=4 SPHERE 66
IC=2 SPHERE 67
WRITE (6,2000) SPHERE 68
2000 FORMAT (1H1,10X,32H***** PARTIAL SPHERE ***** ) SPHERE 69
WRITE (6,2020) N,R,EG,THETA,ALAMP,IFR SPHERE 70
2020 FORMAT (1H0,2X,16HNUMBER OF NODES=,13,3X,4HR/T=,F8.3,3X,15HPUISSEN SPHERE 71
CS PATIC=,F5.3,3X,11HCPH ANGLE=,F7.3,3X,7HAMPRA=,F7.3,3X,11HPEFI SPHERE 72
CRRFER=,I3) SPHERE 73
DO 50 I=1,ITYPE SPHERE 74
ITCI=ILN(I) SPHERE 75
DO 50 J=1,4 SPHERE 76
AIT=H**J SPHERE 77
DO 50 K=1,ITCL SPHERE 78
AN(I,J,K)=AN(I,J,K)/(AF(I,J)*AIT) SPHERE 79
50 CONTINUE SPHERE 80
AIT=AI SPHERE 81
AI=0.0 SPHERE 82
ASTEP=ISTEP SPHERE 83
CALL IMPRFT(Z5,NUFC,P,HA,A,KHA,KA,I87,AP,KAP,UF,UFH,KUF,Z6,V2,V3, SPHERE 84
CV4,V) SPHERE 85
CALL FNDPTH (A,I87,KA,HA,KHA,X,I99,UF,KUF,AP,KAP,UFB,PF,Z4,F5N,ELM SPHERE 86
CT,E,V,UFC,NUFC,IFT,Z3,V2,V3,LNO,V4,Z5,Z6,U,KO) SPHERE 87
AI=AIT SPHERE 88
AI=AI-ASTEP SPHERE 89
KEFP=NC SPHERE 90
DO 370 I=1,NMB SPHERE 91
NO=KEFP SPHERE 92
AI=AI+ASTEP SPHERE 93
WRITE (6,2030) SPHERE 94
2030 FORMAT (1H0,25X,30H-----) SPHERE 95
WRITE (6,2040) AI SPHERE 96
2040 FORMAT(1H0,25X,10H---- AI=,F4.1,7H ---- ) SPHERE 97
WRITE (6,2030) SPHERE 98
AI2=AI**2 SPHERE 99
AI3=AI**3 SPHERE 100
AI4=AI**4 SPHERE 101
IF (AI.EQ.0.0) GO TO 60 SPHERE 102
IF (N1.EQ.4X) GO TO 60 SPHERE 103
N1=NX SPHERE 104
N2=NY SPHERE 105
JAD=IAD SPHERE 106
JAW=2*IAD-1 SPHERE 107
JABW=IABW SPHERE 108
IF=2 SPHERE 109

```

```

DO 120 J=1, JAW
  A(I, J)=0.0
DO 140 I=1, 12
  DO 140 J=1, JAW
    AP(I, J)=0.0
  PA=0.0
  AK=1.0
  AJ=1.0
  IF (ICN.FO.20.OR.ICN.EQ.30) AK=2.0
  IF (ICN.FO.20.OR.ICN.EQ.0) AJ=0.0
  DO 290 KK=1, JTYPF
    CALL FDDATA (KK, ITCL, MID, ISTART, IFIN)
    DC 280 IJ=ISTART, IFIN
    FA=PA+1.0
    PHI=PA*H
    S=SI*(PHI)
    C=COS(PHI)
    CT=C/S
    K1=IC*IJ-IE
    K2=K1+IE/2
    K3=K1+IF
    K4=3*IJ-7
    E0=VF(K4, 1)+(1.0-VF(K4, 1))*(VF(K4+2, 1)**2)/2.0+EC*VF(K4+1, 1)
    E1=VF(K4+1, 1)+D0*(VF(K4, 1)+(1.0-VF(K4, 1))*(VF(K4+2, 1)**2)/2.0)
    E01=VF(K4, 1)+(1.0-VF(K4, 1))*(VF(K4+2, 1)**2)/2.0+EC*VF(K4+1, 1)
    E11=VF(K4+1, 1)+D0*(VF(K4, 1)+(1.0-VF(K4, 1))*(VF(K4+2, 1)**2)/2.0)
    E0=EO*AK/2.0-AJ*SF(K4)/2.0
    E01=E01*AK/2.0-AJ*SF(K4+2)/2.0
    E1=E1*AK/2.0-AJ*SF(K4+1)/2.0
    DO 200 I=1, ITCL
      MA=JAD+IC*(I-VID)
      A(K1, MA)=A(K1, MA)+AN(KK, 1, I)*D1*CT+AN(KK, 2, I)*D1
      A(K1, MA+IE)=A(K1, MA+IE)+AN(KK, 1, I)*D3+AI*(D0+CT*CT)+AI2*AL/
      (S*S)-AI*(KK, 2, I)*AI*CT-AN(KK, 3, I)*AI
      A(K3, MA-IE)=A(K3, MA-IE)+AN(KK, 1, I)*D3+AI*(D0+CT*CT)+AI2
      *AL/(S*S)-2.0*AI*AN(KK, 2, I)*CT-AI*AN(KK, 3, I)
      A(K3, MA)=A(K3, MA)+AN(KK, 1, I)*AI*CT*(1.0/(S*S))+D2+2.0*AI2/(S
      *S)-AN(KK, 2, I)*AI*(D3+CT*CT+2.0*AI2/(S*S))+2.0*AI*CT*AN(KK, 3
      , I)+AI*AN(KK, 1, I)
    IF (ICN.FO.-10) GC TC 150
    A(K1, MA+IE)=A(K1, MA+IE)-AN(KK, 1, I)*EO
    A(K3, MA-IE)=A(K3, MA-IE)-AN(KK, 1, I)*FO
    A(K3, MA)=A(K3, MA)+AI*(KK, 1, I)*(E01+FO*CT)+AN(KK, 2, I)*EO
  150 CONTINUE
    IF (AI.EQ.0.0) GO TO 200
    A(K1, MA+1)=A(K1, MA+1)+AN(KK, 1, I)*AI*D1*D3/(2.0*S)
    A(K2, MA-1)=A(K2, MA-1)-AN(KK, 1, I)*AI*D1*D3/(2.0*S)
    A(K2, MA)=A(K2, MA)+AN(KK, 1, I)*E1*D2*CT/2.0+AN(KK, 2, I)*D1*D2/2
    A(K2, MA+1)=A(K2, MA+1)+AN(KK, 1, I)*AI*AI*CT/S+AN(KK, 2, I)*AI*AL
    /S
    A(K3, MA-1)=A(K3, MA-1)+AN(KK, 1, I)*AI*AL*CT/S-AN(KK, 2, I)*AI*AL
    /S
  200 CONTINUE
    A(K1, JAD)=A(K1, JAD)-D1*(D0+CT*CT)-AI2*D1*D2/(S*S*2.0)
    A(K1, JAD+IE)=A(K1, JAD+IE)-2.0*AI2*AL*CT/(S*S)
    A(K3, JAD-IE)=A(K3, JAD-IE)-AI*(CT/(S*S)+D2*CT)+D3*CT+AI2*AL*CT
    /S
    A(K3, JAD)=A(K3, JAD)+2.0*D3-AL*AI2*(4.0*((CT/S)**2)+D4/(S*S))+
    AI*AI4/(S**4)
  210 CONTINUE
    IF (ICN.EQ.-10) GC IC 210
    A(K1, JAD)=A(K1, JAD)+EO
    A(K3, JAD-IE)=A(K3, JAD-IE)-EO1-EO*CT
    IF (AI.EQ.0.0) GC TO 280
    A(K1, JAD+1)=A(K1, JAD+1)-AI*D1*CT*(1.0/S)
    A(K2, JAD-1)=A(K2, JAD-1)-AI*D1*CT*(1.0/S)
    A(K2, JAD)=A(K2, JAD)+D1*CT*(1.0-CT*CT)/2.0-AI2*D1/(S*S)
    A(K2, JAD+1)=A(K2, JAD+1)-AI*(C3-AL*CT2)/S-AI3*AL/(S**3)
    A(K3, JAD-1)=A(K3, JAD-1)-AI*AI*(1.0/(S**3)+CT/S)+AI*U3/S+AL*AI
    3/(S**3)
  280 CONTINUE
  290 CONTINUE
    THE BOUNDARY CONDITIONS
    THE BOUNDARY CONDITIONS
    IWILL=AI
    CALL BCOND (AB, KAB, IWILL, THETA, AL, H)
    END OF BOUNDARY CONDITIONS
    END OF BOUNDARY CONDITIONS
    CALL SECOND(AAA)
    AAB=AAA
    WRITE (6, 8001) AAA
    CONTROL OF SOLUTION AND ENERGY ROUTINES
    CONTROL OF SOLUTION AND ENERGY ROUTINES
    TZAF=0
    CALL REDUCE(A, AB, I87, KA, KAB, N1, AI, JAW, JAWP, I7AP, V, I87)
    CALL SECOND(AAA)
    AAC=AAA-AAB
    AAB=AAA
    WRITE (6, 8002) AAA, AAC
    IFAI=0
    CALL SLVTR(A, HA, I87, KA, KHA, UF, I87, KUF, UFP, I87, KUF, U, I87, KU, V2, V3,
    CIR7, X, I99, V, I87, P, KU, NC, IFAI, AH, KAB, NIK, Z3, 74, V4, PF, PSN, EI, MI, E,
    CUF, NUFC, IFT, LNC)

```

```

SPHERE 114
SPHERE 115
SPHERE 116
SPHERE 117
SPHERE 118
SPHERE 119
SPHERE 120
SPHERE 121
SPHERE 122
SPHERE 123
SPHERE 124
SPHERE 125
SPHERE 126
SPHERE 127
SPHERE 128
SPHERE 129
SPHERE 130
SPHERE 131
SPHERE 132
SPHERE 133
SPHERE 134
SPHERE 135
SPHERE 136
SPHERE 137
SPHERE 138
SPHERE 139
SPHERE 140
SPHERE 141
SPHERE 142
SPHERE 143
SPHERE 144
SPHERE 145
SPHERE 146
SPHERE 147
SPHERE 148
SPHERE 149
SPHERE 150
SPHERE 151
SPHERE 152
SPHERE 153
SPHERE 154
SPHERE 155
SPHERE 156
SPHERE 157
SPHERE 158
SPHERE 159
SPHERE 160
SPHERE 161
SPHERE 162
SPHERE 163
SPHERE 164
SPHERE 165
SPHERE 166
SPHERE 167
SPHERE 168
SPHERE 169
SPHERE 170
SPHERE 171
SPHERE 172
SPHERE 173
SPHERE 174
SPHERE 175
SPHERE 176
SPHERE 177
SPHERE 178
SPHERE 179
SPHERE 180
SPHERE 181
SPHERE 182
SPHERE 183
SPHERE 184
SPHERE 185
SPHERE 186
SPHERE 187
SPHERE 188
SPHERE 189
SPHERE 190
SPHERE 191
SPHERE 192
SPHERE 193
SPHERE 194
SPHERE 195
SPHERE 196
SPHERE 197
SPHERE 198
SPHERE 199
SPHERE 200
SPHERE 201
SPHERE 202
SPHERE 203
SPHERE 204
SPHERE 205
SPHERE 206
SPHERE 207
SPHERE 208
SPHERE 209
SPHERE 210
SPHERE 211
SPHERE 212
SPHERE 213
SPHERE 214
SPHERE 215
SPHERE 216
SPHERE 217
SPHERE 218
SPHERE 219
SPHERE 220

```

```

IF (IFAIL,EO,0) GC TO 360
WRITE (6,2050) L,IFAIL
IF(NIK,EO,0) GC TC 370
360 CONTINUE
CALL CNTP(L,A,IR7,KA,V,IR7,X,199,AR,KAR,UF,IR7,KUF,UFR,IR7,KUF,V2,
CV3,IR7,V1,IR7,P,KU,NIK,U,IR7,KU,CF,23,UFC,UFC,IFT,INU,FIM1,Z4)
CALL SECOND(AAA)
AAC=AAA-AAU
AAB=AAA
WRITE (6,8005) AAA,AAC
370 CONTINUE
2050 FCRMAT (1H ,5X,24HSLVTR HAS FAILED FOR L= ,I3,3X,6HIFAIL= ,I3)
8000 FCRMAT(1H ,2X,14HDELAYED TIME = ,F10.4)
8001 FCRMAT(1H ,75X,26HINT OF SET UP, TCTAL TIME= ,F9.3)
8002 FCRMAT(1H ,60X,5H1.1.=,F7.2,2X,10HT. RFLLCF=,F6.3)
8004 FCRMAT(1H ,60X,5H1.1.=,F7.2,2X,10HT. SLVTR=,F6.3)
8005 FCRMAT(1H ,60X,5H1.1.=,F7.7,2X,10HT. CCATPL=,F6.3)
STOP
FNC
** *DECK ENCPH
SUBROUTINE FNDPTH (A,NA,KA,HA,KHA,FV,NFV,U,KU,AP,KAB,UFP,PF,V,ESN,
CFIM1,F,VR,UFC,NDFC,IFT,23,02,V3,LNC,04,VIM0,Z6,XX,KX)
DIMENSION A(MA,KA),FA(MA,KHA),FV(NFV),U(KA,KU),AP(12,KAB),UFP(MA,
EU),PF(EU),V(NFV),VR(MA),UFC(NDFC,KU),73(PA),V2(MA),V3(MA),V4(MA)
C,VIMP(NDFC),Z6(NDFC),XX(MA,KX)
COMMON/COM1/ AN(7,4,12),ITYPE,ILN(7),IM(7),JSN(7),JFH(7),KHDE(7)
COMMON /COM2/ DO,D1,D2,D3,D4,AL,THETA,PCL,U,AT,IFR,ION
COMMON /COM3/ JAE,JAW,JARW,IC,IE,IF,PI,IZAP
COMMON /COM4/ IN,N1,K2
COMMON /COM5/ VF(147,20),VFR(147,20),VFC(106,20),PFC(20),EFC(20)
C,SF(147)
LFVEL,2,U,UFR,UFC
IFT=0
LNC=10
IPR1=30
NNH=3*(IN-2)
MM=IN+2
PA=0.0
DO 30 I=1,N1
DO 30 J=1,JAW
30 A(I,J)=0.0
DO 40 I=1,12
DO 40 J=1,JARW
40 A(I,J)=0.0
IF (ICN.EO.-10.CR.ICN.FO.-20) GO TC 65
I=1
CALL STFCP(VIMP,NDFC,U,NA,KU,UFR,NA,KU,I)
DO 50 I=1,N2
VFC(I,1)=VIMP(I)
50 VIMP(I)=0.0
DO 60 I=1,MM
VF(I,1)=U(I,1)
VFR(I,1)=UFR(I,1)
GC TO 85
65 DO 70 I=1,M2
VFC(I,1)=0.0
70 VIMP(I)=0.0
DO 80 I=1,MMH
VF(I,1)=0.0
80 VFR(I,1)=0.0
85 CONTINUE
AK=1.0
AJ=1.0
IF (ICN.EO.20.OR.ICN.EO.30) AK=2.0
IF (ICN.EO.20.OR.ICN.EO.0) AJ=0.0
DO 110 KK=1,ITYPE
CALL FDATA (KK,ITCL,MTR,ISTART,IFIN)
DO 100 IJ=ISTART,IFIN
PA=PA+L.0
PHI=PA*H
S=SIN(PHI)
C=COS(PHI)
CI=C/S
M1=3*IJ-2
M2=M1+1
M3=M1+2
K=2*IJ-1
K1=K+1
FO=AK*(VF(M1,1)+0.5*VF(M3,1))*2+DO*VF(M2,1)-AJ*SF(M1)
FO1=AK*(VFR(M1,1)+VFR(M3,1))*VF(M3,1)+DO*VFR(M2,1)-AJ*SF(M3)
DO 90 I=1,ITCL
MA=JAD+2*(I-MIC)
A(K,MA)=A(K,MA)+AN(KK,1,I)*D1*CI+AN(KK,2,I)*CI
A(K,MA+1)=A(K,MA+1)+AN(KK,1,I)*(D3+AL*(DO+CI*CT))-AL*AN(KK,2,I)
C )*CI-AJ*(KK,3,I)*AL
A(K1,MA-1)=A(K1,MA-1)+AN(KK,1,I)*(D3+AL*(DO+1.0/(S*S)))-2.0*AL
C*AN(KK,2,I)*CI-AL*AN(KK,3,I)
A(K1,MA)=A(K1,MA)+AN(KK,1,I)*(AL*(D2+CI*CT/(S*S)))-AL*AN(KK,2,
C I)*(DO+1.0/(S*S))+2.0*AL*AN(KK,3,I)*CI+AL*AN(KK,4,I)
IF (ICN.FO.-10) GO TC 90
A(K,MA+1)=A(K,MA+1)-AN(KK,1,I)*EO/2.0
A(K1,MA-1)=A(K1,MA-1)-AN(KK,1,I)*EO/2.0
A(K1,MA)=A(K1,MA)+AN(KK,1,I)*(EO+EO*CT)/2.0+AN(KK,2,I)*EO/2.0
90 CONTINUE
A(K,JAD)=A(K,JAD)-D1*(CI*CI+DO)
A(K1,JAD-1)=A(K1,JAD-1)+CI*(D3-AL*(D2+1.0/(S*S)))
A(K1,JAD)=A(K1,JAD)+2.0*D3
IF (ION.EO.-10) GC TC 100
A(K,JAC)=A(K,JAC)+EO/2.0
A(K1,JAC-1)=A(K1,JAC-1)-(EO*CT+EO1)/2.0
IF (ICN.EO.-20) GO TC 100
VIMP(K)=VF(M1,1)*(0.5*DO*VF(M3,1)*CI+VFR(M3,1)-VF(M1,1)-DO*VF(M2,1
1))+VF(M3,1)*(0.5*VF(M3,1)+1.0*VF(M3,1)+1.0*VF(M1,1)+DO*VF(M2,1
2)+VF(M2,1)*CT/2.0+EO*VF(M2,1)/2.0+VFR(M1,1)+VF(M1,1)*(-2.0*VFR(M3,1
3)+VF(M1,1)+DO*VF(M2,1))-DO*VF(M2,1)+VF(M3,1))
VIMP(K1)=VF(M3,1)*(0.5*DO*VF(M3,1)+VFR(M1,1)*CI+EO*VF(M2,1)*CT+VFR(

```

```

SPHERE 224
SPHERE 225
SPHERE 226
SPHERE 227
SPHERE 228
SPHERE 229
SPHERE 230
SPHERE 231
SPHERE 232
SPHERE 233
SPHERE 234
SPHERE 235
SPHERE 236
SPHERE 237
SPHERE 238
SPHERE 239
SPHERE 240
SPHERE 241
SPHERE 242
SPHERE 243
FNDPTH 1
FNDPTH 2
FNDPTH 3
FNDPTH 4
FNDPTH 5
FNDPTH 6
FNDPTH 7
FNDPTH 8
FNDPTH 9
FNDPTH 10
FNDPTH 11
FNDPTH 12
FNDPTH 13
FNDPTH 14
FNDPTH 15
FNDPTH 16
FNDPTH 17
FNDPTH 18
FNDPTH 19
FNDPTH 20
FNDPTH 21
FNDPTH 22
FNDPTH 23
FNDPTH 24
FNDPTH 25
FNDPTH 26
FNDPTH 27
FNDPTH 28
FNDPTH 29
FNDPTH 30
FNDPTH 31
FNDPTH 32

```

```

FNDPTH 33
FNDPTH 34
FNDPTH 35
FNDPTH 36
FNDPTH 37
FNDPTH 38
FNDPTH 39
FNDPTH 40
FNDPTH 41
FNDPTH 42
FNDPTH 43
FNDPTH 44
FNDPTH 45
FNDPTH 46
FNDPTH 47
FNDPTH 48
FNDPTH 49
FNDPTH 50
FNDPTH 51
FNDPTH 52
FNDPTH 53
FNDPTH 54
FNDPTH 55
FNDPTH 56
FNDPTH 57
FNDPTH 58
FNDPTH 59
FNDPTH 60
FNDPTH 61
FNDPTH 62
FNDPTH 63
FNDPTH 64
FNDPTH 65
FNDPTH 66
FNDPTH 67
FNDPTH 68
FNDPTH 69
FNDPTH 70
FNDPTH 71
FNDPTH 72
FNDPTH 73
FNDPTH 74
FNDPTH 75
FNDPTH 76
FNDPTH 77
FNDPTH 78
FNDPTH 79
FNDPTH 80
FNDPTH 81
FNDPTH 82
FNDPTH 83
FNDPTH 84
FNDPTH 85
FNDPTH 86
FNDPTH 87

```



```

340 WRITE (6,2050)
C **** EVALUATE F AND CHECK FOR TURNING POINTS ****
350 AK=1.0
    SAV=0.0
    K=0
    WRITE (6,2060)
    ITMP=0
    PMN=0.0
    DO 390 I=1,IFT
    IF(I.FG.1) GO TO 360
    EMN=EFC(I)-EFC(I-1)
    EMX=EFC(I-1)
360 EMN=EFC(I)
    EMX=0.0
370 DO 380 J=1,R
    AJ=J
    E=EMX+AJ*EMN/R.0
    CALL FUNVEC (U,UFB,KU,NA,UFC,NUFC,V,FV,FEV,VP,NA,PF,IO,IFT,LNO,E,
    CMN,IN,P,ITMP,IFAIL,ELMT)
    Z3(10+J)=P
    Z3(J)=F/PCL
    Z3(20+J)=E
    CALL VCLDIS(VB,NA,V,FEV,AJ,FMX)
    Z3(30+J)=AJ
    Z3(40+J)=PMX
    TEMP=AK*Z3(J)
    IF(TEMP.GT.SAV) SAV=TEMP
    IF(TEMP.FO.SAV) GO TO 380
    K=K+1
    Z3(100+K)=E-EMN/R.0
    Z3(50+K)=EMN/R.0
    AK=-AK
    SAV=-TEMP
380 CONTINUE
    WRITE (6,2070) I,(Z3(J),J=21,28)
    WRITE (6,2080) (Z3(J),J=11,18)
    WRITE (6,2090) (Z3(J),J=1,8)
    WRITE (6,2091) (Z3(J),J=11,38)
    WRITE (6,2092) (Z3(J),J=41,48)
390 CONTINUE
    ITMP=-1
    IG=LNC
    IF(K.FG.0) GO TO 490
C *** WE HAVE FOUND TURNING POINTS *****
    AK=1.0
    DO 460 I=1,K
    AK=-AK
    FE=Z3(50+I)
    E=Z3(100+I)
440 EMN=E-FE/2.0
    EMX=E+FE/2.0

```

```

FNDP1H 201
FNDP1H 202
FNDP1H 203
FNDP1H 204
FNDP1H 205
FNDP1H 206
FNDP1H 207
FNDP1H 208
FNDP1H 209
FNDP1H 210
FNDP1H 211
FNDP1H 212
FNDP1H 213
FNDP1H 214
FNDP1H 215
FNDP1H 216
FNCP1H 217
FNDP1H 218
FNDP1H 219
FNDP1H 220
FNDP1H 221
FNDP1H 222
FNDP1H 223
FNDP1H 224
FNDP1H 225
FNCP1H 226
FNDP1H 227
FNDP1H 228
FNDP1H 229
FNDP1H 230
FNDP1H 231
FNDP1H 232
FNDP1H 233
FNDP1H 234
FNCP1H 235
FNDP1H 236
FNDP1H 237
FNDP1H 238
FNDP1H 239
FNDP1H 240
FNDP1H 241
FNDP1H 242
FNDP1H 243
FNDP1H 244
FNDP1H 245
FNDP1H 246
FNDP1H 247
FNDP1H 248
FNDP1H 249
FNDP1H 250
FNDP1H 251
FNDP1H 252

```

```

    CALL FUNVEC (U,UFB,KU,NA,UFC,NUFC,V,FV,FEV,VP,NA,PF,IO,IFT,LNO,EMN
C,PMN,IN,P,ITMP,IFAIL,ELMT)
    V(1)=E*AK
    CALL FUNVEC (U,UFB,KU,NA,UFC,NUFC,V,FV,FEV,VP,NA,PF,IO,IFT,LNO,E,P
    CMN,IN,P,ITMP,IFAIL,ELMT)
    V(2)=E*AK
    CALL FUNVEC (U,UFB,KU,NA,UFC,NUFC,V,FV,FEV,VP,NA,PF,IO,IFT,LNO,EMX
C,PMN,IN,P,ITMP,IFAIL,ELMT)
    V(3)=E*AK
    IF(V(2).GT.V(1).AND.V(2).GT.V(3)) GO TO 450
    IF(V(2).LT.V(1)) E=EMN
    IF(V(2).LT.V(3)) E=EMX
    GO TO 440
450 TEMP=ABS((V(2)-V(3))/PCL)
    BEMP=ABS((V(2)-V(1))/PCL)
    PE=PE/2.0
    IF(BEMP.LT.TEMP) BEMP=TEMP
    IF(BEMP.GT.0.01) GO TO 440
    V(50+I)=F
460 CONTINUE
    WRITE (6,3000)
    ITMP=0
    DO 480 I=1,K
    E=V(50+I)
    CALL FUNVEC (U,UFB,KU,NA,UFC,NUFC,V2,Z3,NA,VP,NA,PF,IO,TFT,LNO,E,P
    CMN,IN,P,ITMP,IFAIL,ELMT)
    PE=P/PCI
    FSN=E
    DO 461 JK=1,20
    IK=21-JK
461 IF(E.LE.EFC(IK)) IKK=IK
    IF(IKK.GT.1) ESN=FSN-EFC(IKK-1)
    IK=LNC+(IKK-1)
    DO 462 JK=1,N2
462 XX(JK,I)=UFC(IK,IK+1)
    DO 463 JK=2,LNO
    AJ=JK
    A1=ESN*(JK-1)
    DO 463 J=1,N2
463 XX(J,I)=XX(J,I)+AJ*UFC(J,IK+JK)*A1
    TEMP=0.0
    DO 464 J=1,N2
    SAV=ABS(XX(J,I))
    IF(SAV.LE.TEMP) GO TO 464
    IK=J
    TEMP=SAV
464 CONTINUE
    DO 465 J=1,N2
465 XX(J,I)=XX(J,I)/TEMP
    WRITE (6,3010) I,E,F,PF
    WRITE (6,3020)
    DO 470 J=1,NMM
    JK=J-1
    IU=2*J-1
    IW=IU+1

```

```

FNDP1H 253
FNDP1H 254
FNDP1H 255
FNDP1H 256
FNDP1H 257
FNDP1H 258
FNDP1H 259
FNDP1H 260
FNDP1H 261
FNDP1H 262
FNDP1H 263
FNDP1H 264
FNDP1H 265
FNDP1H 266
FNDP1H 267
FNDP1H 268
FNDP1H 269
FNDP1H 270
FNDP1H 271
FNDP1H 272
FNDP1H 273
FNDP1H 274
FNDP1H 275
FNDP1H 276
FNDP1H 277
FNDP1H 278
FNDP1H 279
FNDP1H 280
FNDP1H 281
FNDP1H 282
FNDP1H 283
FNDP1H 284
FNDP1H 285
FNDP1H 286
FNDP1H 287
FNDP1H 288
FNDP1H 289
FNDP1H 290
FNDP1H 291
FNDP1H 292
FNDP1H 293
FNDP1H 294
FNDP1H 295
FNDP1H 296
FNDP1H 297
FNDP1H 298
FNDP1H 299
FNDP1H 300
FNDP1H 301
FNDP1H 302
FNDP1H 303
FNDP1H 304
FNDP1H 305
FNDP1H 306
FNDP1H 307

```

```

IF(E,IF,EFC(J)) IK=J
471 CONTINUE
KK=(IK-1)+LNO
A1=E
IF(IK,GT,1) A1=E-EFC(IK-1)
DO 472 J=1,NNM
V3(J)=U(J,KK+1)
472 V4(J)=HFR(J,KK+1)
DO 473 JK=2,LNO
AK=JK
KJ=JK-1
AJ=AK*(A1**KJ)
DO 473 J=1,NNN
V3(J)=V3(J)+U(J,KK+JK)*AJ
473 V4(J)=V4(J)+HFR(J,KK+JK)*AJ
MRK=0
CALL TFEV01(V3,V4,NA,V2,Z3,NA,FV,NFV,P,MRK)
WRITE(6,4000)
WRITE(6,4015) (FV(J),J=1,5)
WRITE(6,4020) (FV(J),J=6,10)
WRITE(6,4030)
WRITE(6,4010) (FV(J),J=51,55),FV(61)
WRITE(6,4020) (FV(J),J=56,60)
DO 474 J=1,10
474 FV(20+J)=FV(J)
MRK=-1
A1=E-0.05
CALL FUNVEC(U,UFB,KU,NA,UFC,NUFC,V2,Z3,NA,VR,NA,PF,IO,IFT,LNO,A1,
CMN,IN,F,ITMP,IFAIL,ELMT)
CALL TFEV01(V3,V4,NA,V2,Z3,NA,FV,NFV,P,MRK)
EMN=0.0
PF=0.0
DO 476 J=1,5
FV(40+J)=FV(20+J)-FV(J)
IF(FV(40+J).LT.0.0) GO TO 475
PE=PE+FV(40+J)
GO TO 476
475 FMN=EMN+FV(40+J)
476 CONTINUE
PF=(PE-FMN)/2.0
DO 477 J=1,5
477 FV(45+J)=FV(40+J)/PE
WRITE(6,4040)
WRITE(6,4015) (FV(J),J=41,45)
WRITE(6,4020) (FV(J),J=46,50)
480 CONTINUE
FSN=V(51)
GO TO 495
490 WRITE(6,3040)
FSN=2.0*ELMT
495 ITMP=0
MRK=-1

```

```

FNDPTH 311
FNDPTH 312
FNDPTH 313
FNDPTH 314
FNDPTH 315
FNDPTH 316
FNDPTH 317
FNDPTH 318
FNDPTH 319
FNDPTH 320
FNDPTH 321
FNDPTH 322
FNDPTH 323
FNDPTH 324
FNDPTH 325
FNDPTH 326
FNDPTH 327
FNDPTH 328
FNDPTH 329
FNDPTH 330
FNDPTH 331
FNDPTH 332
FNDPTH 333
FNDPTH 334
FNDPTH 335
FNDPTH 336
FNDPTH 337
FNDPTH 338
FNDPTH 339
FNDPTH 340
FNDPTH 341
FNDPTH 342
FNDPTH 343
FNDPTH 344
FNDPTH 345
FNDPTH 346
FNDPTH 347
FNDPTH 348
FNDPTH 349
FNDPTH 350
FNDPTH 351
FNDPTH 352
FNDPTH 353
FNDPTH 354
FNDPTH 355
FNDPTH 356
FNDPTH 357
FNDPTH 358
FNDPTH 359
FNDPTH 360
FNDPTH 361
FNDPTH 362

```

```

FMN=ELMT/4.0
E=0.0
E=F+FMN
CALL FUNVEC(U,UFB,KU,NA,UFC,NUFC,V4,FV,NA,VR,NA,FF,IO,IFT,LNO,E,P
CMN,IN,F,ITMP,IFAIL,ELMT)
V(1)=F
V(5)=P
V(9)=F/PCI
F=F+FMN
CALL TFEV01(Z3,VR,NA,V4,FV,NA,Z6,NUFC,P,MRK)
DO 496 J=1,10
496 Z6(40+J)=Z6(J)
CALL FUNVEC(U,UFB,KU,NA,UFC,NUFC,V4,FV,NA,Z3,NA,FF,IO,IFT,LNO,E,P
CMN,IN,F,ITMP,IFAIL,ELMT)
V(2)=E
V(6)=P
V(10)=F/PCI
F=F+FMN
CALL TFEV01(Z3,VR,NA,V4,FV,NA,Z6,NUFC,P,MRK)
DO 497 J=1,10
497 Z6(40+J)=Z6(J)
CALL FUNVEC(U,UFB,KU,NA,UFC,NUFC,V4,FV,NA,V2,NA,PF,IO,IFT,LNO,E,P
CMN,IN,F,ITMP,IFAIL,ELMT)
V(3)=E
V(7)=P
V(11)=F/PCI
F=F+FMN
CALL TFEV01(Z3,VR,NA,V4,FV,NA,Z6,NUFC,P,MRK)
DO 498 J=1,10
498 Z6(20+J)=Z6(J)
CALL FUNVEC(U,UFB,KU,NA,UFC,NUFC,V4,FV,NA,V3,NA,PF,IO,IFT,LNO,E,P
CMN,IN,P,ITMP,IFAIL,ELMT)
CALL TFEV01(Z3,VR,NA,V4,FV,NA,Z6,NUFC,P,MRK)
V(4)=E
V(8)=P
V(12)=F/PCI
WRITE(6,3050) (V(J),J=1,4)
WRITE(6,3051) (V(J),J=5,8)
WRITE(6,3052) (V(J),J=9,12)
WRITE(6,3060)
DO 500 I=1,MMM
JK=I-1
IU=2*I-1
IW=IU+1
500 WRITE(6,3070) JK,VR(IU),VR(IW),Z3(IU),Z3(IW),V2(IU),V2(IW),V3(IU)
C,V3(IW),JK
F=0.0
WRITE(6,5070)
WRITE(6,5000) Z6(61),Z6(41),Z6(21),Z6(1)
WRITE(6,5010) Z6(66),Z6(46),Z6(26),Z6(6)
WRITE(6,5020) Z6(62),Z6(42),Z6(22),Z6(2)
WRITE(6,5010) Z6(67),Z6(47),Z6(27),Z6(7)
WRITE(6,5030) Z6(63),Z6(43),Z6(23),Z6(3)
WRITE(6,5010) Z6(68),Z6(48),Z6(28),Z6(8)
WRITE(6,5040) Z6(64),Z6(44),Z6(24),Z6(4)

```

```

FNDPTH 363
FNDPTH 364
FNDPTH 365
FNDPTH 366
FNDPTH 367
FNDPTH 368
FNDPTH 369
FNDPTH 370
FNDPTH 371
FNDPTH 372
FNDPTH 373
FNDPTH 374
FNDPTH 375
FNDPTH 376
FNDPTH 377
FNDPTH 378
FNDPTH 379
FNDPTH 380
FNDPTH 381
FNDPTH 382
FNDPTH 383
FNDPTH 384
FNDPTH 385
FNDPTH 386
FNDPTH 387
FNDPTH 388
FNDPTH 389
FNDPTH 390
FNDPTH 391
FNDPTH 392
FNDPTH 393
FNDPTH 394
FNDPTH 395
FNDPTH 396
FNDPTH 397
FNDPTH 398
FNDPTH 399
FNDPTH 400
FNDPTH 401
FNDPTH 402
FNDPTH 403
FNDPTH 404
FNDPTH 405
FNDPTH 406
FNDPTH 407
FNDPTH 408
FNDPTH 409
FNDPTH 410
FNDPTH 411
FNDPTH 412
FNDPTH 413
FNDPTH 414
FNDPTH 415
FNDPTH 416
FNDPTH 417

```

```

RETURN
2000 FCRMAT (1H0,5X,14HPCF PERT PARM ,12,13H MAX LOCAL E=,E10.4,9H 1CT
CAL E=,F10.4,12H AT W/FICH B=,E10.4,6H P/CI=F10.4,7H P/CI2=,E10.4)
2020 FCRMAT (1H ,5X,14HPCF PERT PARM ,12,13H MAX LOCAL E=,E10.4,9H 1CT
** LACK OF STORAGE ** )
2040 FCRMAT (1H ,5X,36HPCF METHCD COMPLETF, ** P.C.T.0.0 ** )
2050 FCRMAT (1H ,5X,39HPCF METHCD COMPLETF, ** P.TC LARGE ** )
2060 FCRMAT (1H0,45X,6HF-VS-F )
2070 FCRMAT (1H0,2X,14HPCF PERT PARM= ,12,5X,2HF=,R(2X,E10.4))
2080 FCRMAT (1H ,22X,2HF=,R(2X,E10.4))
2090 FCRMAT (1H ,19X,6HF/FCL=,R(2X,E10.4))
2091 FCRMAT (1H ,20X,4HVC[=,R(2X,F10.4))
2092 FCRMAT (1H ,20X,4HVC[=,R(2X,F10.4))
3000 FCRMAT (1H0,5X,12HWF HAVE FOUND THE FOLLOWING TURNING POINTS )
3010 FCRMAT (1H0,5X,4HAC, ,12,6H AT E=,F10.4,3H P=,F10.4,7H P/CI=,F10.
C4,15X,13HBUCKLING VCEE )
3020 FCRMAT (1H ,4X,2(4HNCDF,10X,1HU,14X,1HW,10X,4HNOCF,10X))
3030 FCRMAT (1H ,5X,2(12,5X,E12.6,4X,F12.6,5X,12,10X))
3040 FCRMAT (1H0,5X,31HWF HAVE FOUND NO TURNING POINTS )
3050 FCRMAT (1H0,15X,4(2HF=,E12.6,11X))
3051 FCRMAT (1H ,15X,4(2HF=,E12.6,11X))
3052 FCRMAT (1H ,12X,4(6HF/PCL=,F12.6,6X))
3060 FCRMAT (1H ,5X,4HPCCF,6X,3(1HU,11X,1HW,11X),1HU,11X,1HW,5X,4HNOCF)
3070 FCRMAT (1H ,6X,12,2X,8(F10.4,2X),12)
4000 FCRMAT(1H0,3X,16HT.F.E. VO UMO,10X,3HUM0,10X,3HUB0,10X,3HUBC,10
CX,4HL.F. )
4010 FCRMAT (1H ,16X,5(E1C.4,3X),4X,13HENFRGY ERROR= ,F7.3,1X,8HPER CEN
CT)
4015 FCRMAT (1H ,16X,5(E1C.4,3X))
4020 FCRMAT (1H ,16X,5(E1C.4,3X))
4030 FCRMAT (1H ,3X,16HT.F.F. V1 UMO,10X,3HUM0,10X,3HUB0,10X,3HUBC,1
CX,4HL.F. )
4040 FCRMAT(1H0,1X,1RHTFF DELTA VO UMO,10X,3HUM0,10X,3HUB0,10X,3HUBC,
*10X,4HL.F. )
5000 FCRMAT(1H0,13X,4(5HUM0= ,E10.4,9X))
5010 FCRMAT(1H 18X,4(F10.4,14X))
5020 FCRMAT (1H0,13X,4(5HUM0= ,F10.4,9X))
5030 FCRMAT (1H0,13X,4(5HUM0= ,E10.4,9X))
5040 FCRMAT (1H0,13X,4(5HUM0= ,F10.4,9X))
5050 FCRMAT(1H0,12X,4(6HT.F.= ,E10.4,8X))
5070 FCRMAT (1H0,10X,36H---- TOTAL POTENTIAL ENERGY, VO ---- )
END
*DECK IMPRFT
SUBROUTINE IMPRFT(V,NUFC,R,HA,A,KHA,KA,NA,AP,KAPW,UF,UFR,KU,H,V2,
CV3,V4,V5)
DIMENSION V(NUFC),PA(NA,KHA),A(NA,KA),AE(12,KAPW),UF(NA,KU),UFR(NA
,KA),R(NUFC),V2(NA),V3(NA),V4(NA),V5(NA)
COMMON /COM1/ AN(7,4,12),ITYPE,ILN(7),IPA(7),JEN(7),JEN(7),KROE(7)
COMMON /COM2/ DO,C1,C2,D3,C1,AL,THETA,PCL,H,AT,IPR,ION
COMMON /COM3/ JAC,JAK,JABW,IF,IC,IC,ET,IZAP
COMMON /COM4/ IN,N1,N2
COMMON /COM5/ VF(147,20),VFR(147,20),VFC(106,20),PFC(20),EFC(20)
C,SF(147)

```

```

LEVEL 2,UF,UFR
ICID=0
NNN=3*(IN-2)
DO 5 I=1,NNN
5 SF(I)=0.0
DO 10 I=1,N2
10 V(I)=0.0
IF (ICN.LT.0) GC IC 1000
IF (ICN.EQ.20) GC IC 2000
IF (ICN.LT.40) GC IC 3000
C ION .GE. 40 --PERFECT SHELL --
IF (ICN.EQ.11) ICN=-10
IF (ICN.EQ.42) ICN=-20
WRITE (6,8000)
8000 FCRMAT(1H0,20X,23H*** PERFECT SHELL *** )
C -- ** IF ION.EQ.-20 SET SF(I) TO STRESS FIELD ** --
RETURN
1000 CONTINUE
C ION.LT.0 IMPERFECTICN PROFILE WILL BE READ IN IJU=0 ONLY W TERMS.
IF (ICN.EQ.-1) ICN=20
IF (ICN.EQ.-2) ICN=0
IF (ICN.EQ.-11) ICN=30
IF (ICN.EQ.-12) ION=10
READ (5,7000) WT,IJU
7000 FCRMAT(F10.6,110)
DO 1010 I=1,6
K=(I-1)*16+2
K2=K+14
J=K-1
J2=K2-1
IF (IJU.NE.0) HEAD(5,7010) (V(L),L=J,J2,2)
1010 READ(5,7010) (V(L),L=K,K2,2)
7010 FCRMAT(F10.6)
IF (IJU.NE.0) READ(5,7020) (V(J),J=97,105,2)
READ (5,7020) (V(J),J=98,106,2)
7020 FCRMAT(5F10,6)
WRITE (6,8010) WT,R
8010 FCRMAT(1H0,10X,45H*** IMPERFECT SHELL, PROFILE READ IN. W/T= ,
CF8.4,2X,4HR/T=,F9.3)
GC TO 5000
2000 CONTINUE
C ION.LT.20 IMPERFECTICN PROFILE OF LEGENDEE TYPE
IDID=1
IF (ICN.EQ.1) ICN=20
IF (ICN.EQ.2) ICN=0
IF (ICN.EQ.11) ICN=30
IF (ICN.EQ.12) ICN=10
RT=R*(THETA/3.141592654)**2
ALPHA=1.0/(12.0*RT*RT)
ALP=- (1.0+3.0*DO)+SQRT((1.0+3.0*DO)**2+(1.0-DO*DO)/ALPHA)
ANL=-0.5+0.5*SQRT(1.0+4.0*(ALB+2.0))
NN1=ANL
NN2=NN1+1
ALB=NN1*NN2-2
ALP2=NN2*(NN2+1)-2

```

```

1*(D0)
IF(PCR1,LT,PCR2) GO TO 2010
PCR1=PCR2
NN1=NN2
ALR=ALR2
2010 CONTINUE
BN=(ALPHA*ALR+1.0+CC+PCR1)/(ALR+1.0+D0+ECW1)
P=PCR1*SQR(3.0*(1.0-D0+D0)) *RT/(1.0-C0+D0)
CALL LEGEND (NN1,IN,PN,V,NUFC)
READ (5,7000) WT,IJU
IF(IJU,NE,0) GO TO 2030
DC 2020 I=1,N2,2
2020 V(I)=0.0
2030 WRITE (6,8020) NN1,E,WT,R
8020 FORMAT (1H0,10X,53H*** IMPERFECT SHELL, PROFILE OF LEGENDRE TYPE
COMPFR= ,12,14H *** P/PCL= ,E10.4,5H W/T=,FR.4,2X,4HR/1=,F9.3)
GO TO 5000
3000 CONTINUE
IN,LT,40 EDGE DISPLACEMENT TYPE IMPERFECTION PROFILE
IF (ICN,EQ,21) ICN=20
IF (ICN,EQ,22) ICN=0
IF (ICN,EQ,31) ICN=30
IF (ICN,EQ,32) ICN=10
READ (5,7000) WT,IJU
DC 3010 I=1,N2
3010 P(I)=0.0
DC 3020 I=1,N1
DC 3020 J=1,JAW
3020 A(I,J)=0.0
DC 3030 I=1,12
DC 3030 J=1,JABW
3030 AP(I,J)=0.0
PA=0.0
DC 3060 KK=1,ITYPE
CALL FCDATA (KK,ITCL,MID,ISTART,IFIN)
DC 3050 IJ=ISTART,IFIN
PA=PA+1.0
PHI=PA*H
S=SIN(PHI)
C=CCS(PHI)
CT=C/S
K=2*IJ-1
K1=K+1
DC 3040 I=1,ITCL
MA=JAD+2*(I-MID)
A(K,MA)=A(K,MA)+AN(KK,1,I)*D1*CT+AN(KK,2,I)*C1
A(K,MA+1)=A(K,MA+1)+AN(KK,1,I)*(D3+AL*(D2+1.0/(S*S)))-AL*AN(KK,2,I)
C *CT-AN(KK,3,I)*AL
A(K1,MA-1)=A(K1,MA-1)+AN(KK,1,I)*(D3+AL*(D2+1.0/(S*S)))-2.0*AL
C *AN(KK,2,I)*CT-AL*AN(KK,3,I)
A(K1,MA)=A(K1,MA)+AN(KK,1,I)*(AL*(D2*CT+CT/(S*S)))-AL*AN(KK,2,
C I)*(D0+1.0/(S*S))+2.0*AL*AN(KK,3,I)*CT+AL*AN(KK,4,I)
IMPRFT 70
IMPRFT 71
IMPRFT 72
IMPRFT 73
IMPRFT 74
IMPRFT 75
IMPRFT 76
IMPRFT 77
IMPRFT 78
IMPRFT 79
IMPRFT 80
IMPRFT 81
IMPRFT 82
IMPRFT 83
IMPRFT 84
IMPRFT 85
IMPRFT 86
IMPRFT 87
IMPRFT 88
IMPRFT 89
IMPRFT 90
IMPRFT 91
IMPRFT 92
IMPRFT 93
IMPRFT 94
IMPRFT 95
IMPRFT 96
IMPRFT 97
IMPRFT 98
IMPRFT 99
IMPRFT 100
IMPRFT 101
IMPRFT 102
IMPRFT 103
IMPRFT 104
IMPRFT 105
IMPRFT 106
IMPRFT 107
IMPRFT 108
IMPRFT 109
IMPRFT 110
IMPRFT 111
IMPRFT 112
IMPRFT 113
IMPRFT 114
IMPRFT 115
IMPRFT 116
IMPRFT 117
IMPRFT 118
IMPRFT 119
IMPRFT 120
IMPRFT 121

3040 CONTINUE
A(K,JAD)=A(K,JAD)-D1*(CT*CT+D0)
A(K1,JAD-1)=A(K1,JAD-1)+CT*(D3-AL*(D2+1.0/(S*S)))
A(K1,JAD)=A(K1,JAD)+2.0*E3
IMPRFT 122
IMPRFT 123
IMPRFT 124
IMPRFT 125
IMPRFT 126
IMPRFT 127
IMPRFT 128
IMPRFT 129
IMPRFT 130
IMPRFT 131
IMPRFT 132
IMPRFT 133
IMPRFT 134
IMPRFT 135
IMPRFT 136
IMPRFT 137
IMPRFT 138
IMPRFT 139
IMPRFT 140
IMPRFT 141
IMPRFT 142
IMPRFT 143
IMPRFT 144
IMPRFT 145
IMPRFT 146
IMPRFT 147
IMPRFT 148
IMPRFT 149
IMPRFT 150
IMPRFT 151
IMPRFT 152
IMPRFT 153
IMPRFT 154
IMPRFT 155
IMPRFT 156
IMPRFT 157
IMPRFT 158
IMPRFT 159
IMPRFT 160
IMPRFT 161
IMPRFT 162
IMPRFT 163
IMPRFT 164
IMPRFT 165
IMPRFT 166
IMPRFT 167
IMPRFT 168
IMPRFT 169
IMPRFT 170
IMPRFT 171
IMPRFT 172
IMPRFT 173
IMPRFT 174
IMPRFT 175
IMPRFT 176

3050 CONTINUE
3060 CONTINUE
E(N1+6)=1.0
IJ=0
CALL ECOND (AB,KAR,IJ,THETA,AL,H)
PT=1.0
IZAP=10
CALL REDUCE(A,AB,NA,KA,KAR,N1,AT,JAW,JABW,IZAP,P,NUFC)
DC 3070 I=1,N1
V(I)=E(I+1)
DC 3070 J=1,JAW
PA(I,J)=A(I,J)
3070 CALL MACR (HA,V,PA,N1,JAW,PT,KHA,NUFC)
AJ=-3.0
CALL PCKSUR(V,NUFC,AE,KAR,AJ,IN,JABW)
IF (IJU,NE,0) GO TO 3170
DC 3160 I=1,N2,2
3160 V(I)=0.0
3170 WRITE (6,9030) WT,R
9030 FORMAT (1H0,10X,58H*** IMPERFECT SHELL PROFILE DUE TO EDGE DISPLA
CEMENT ***,2X,4HW/T=FR.4,2X,4HR/1=,F9.3,3X,15H LINEAR SOLUTION )
5000 TEMP=0.0
IF (ICN,EQ,20,OR,ICN,EQ,30) WRITE (6,9020)
9020 FORMAT (1H ,60X,23H STRESS FREE DEFORMATION )
IF (ICN,EQ,0,OR,ICN,EQ,10) WRITE (6,9030)
9030 FORMAT (1H ,60X,21H STRESSSED DEFORMATION )
DC 5010 I=1,N2
HCLD=ABS(V(I))
IF(HCLC,LE,TEMP) GO TO 5010
BEPP=V(I)
TEMP=HCLD
5010 CONTINUE
DC 5020 I=1,N2
5020 V(I)=V(I)*WT/(BEPP*F)
WRITE (6,9000)
9000 FORMAT (1H ,10X,4H NCCF,8X,1HW,14X,1HW,8X,4H NCCF)
NNN=IN+2
DC 5030 I=1,NNN
J=1-1
K=2*I-1
K2=K+1
5030 WRITE (6,9010) J,V(K),V(K2),J
9010 FORMAT (1H ,11X,12,3X,F12.6,2X,E12.6,3X,12)
IF (ICID,EQ,0) RETURN
K=0
AJ=1.0
IF(V(2).GT,V(4)) AJ=-1.0
NN2=IN+1
DC 5040 I1=1,NN2
I=I1+2
TEMP=(V(I)-V(I-2))*AJ
IMPRFT 176

```



```

AJ=-AJ
V2(K)=I-2
5040 CONTINUE
I1=(V2(K-1)-2)/2
AJ=IN-I1
AJ=AJ/2
NN2=IN-2
DO 5050 I=I1,NN2
  J=I*2+3
  J1=J+1
  AK=I-I1+1
  TEMP=4.0*(AK-AJ)/(AJ-1.0)
  TEMP=0.5-0.5*TANH(TEMP)
  V(J)=V(J)+TEMP
5050 V(J1)=V(J1)+TEMP
V(N2-3)=0.0
V(N2-2)=0.0
V(N2-1)=-V(N2-5)
V(N2)=V(N2-4)
IDID=0
GC TO 5000
-- ** IF (IGN.FG.30,CR.IGN.FG.10) SET UP SF(I) FOR STRESS FIELD
** *DECK
END
LEGEND
SUPROUTINE LEGEND(N,IN,NN,V,NV)
DIMENSION V(NV)
DO 1 I=1,NV
  V(NV)=0.0
  ANN=IN-1
  NMM=IN*2
  NTERM=N/2+1
  IJ=2*N-1
  CCEFF=1.0
  DO 10 J=3,IJ,2
    AJ=J
  10 CCEFF=CCEFF/AJ
  DO 20 J=2,N
    AJ=J
  20 CCEFF=CCEFF/AJ
  CCEFF=2.0*CCEFF/(2.0+*N)
  ANN=N
  THEI=3.141592654/ANN
  SPCF=1.0
  K=-2
  DO 40 J=1,NTERM
    AJ=J
    K=K+2
    SUBN=N-K
    DO 30 I=1,NMM,2
      AI=(I+1)/2-1
      V(I+2)=V(I+2)-PN*CCEFF*SPCF*SUBN*SIN(SUBN*AI*THEI)
      V(I+3)=V(I+3)+CCEFF*SPCF*CCS(SUBN*AI*THEI)
  30 CONTINUE
    IF(J.NE.NTERM) GC TO 40
    SPCF=SPCF*(2.0*AJ-1.0)*(ANN+1.0-AJ)/(AJ*(2.0*ANN+1.0-2.0*AJ))
    IF(N.FG.2) SBCF=1.0/3.0
  40 CONTINUE
  V(1)=-V(5)
  V(2)=V(6)
  V(NMM+3)=-V(NMM-1)
  V(NMM+4)=V(NMM)
  RETURN
FNC
*DECK REDUCE
SUPROUTINE REDUCE(A,AR,NX,KAW,KARW,N,AT,IARW,IZAP,P,NP)
DIMENSION A(NX,KAW),AR(12,KARW),B(N6)
TO REDUCE BOTH AR AND A KAW MATRIX WHEN IZAP=0, WHEN IZAP.NE.0 AR MUST BE IN
REDUCED FORM ALLREADY
N=CRCR OF MATRIX A, AI=CIRCUM MODE NO. IARW=BANDWIDTH OF A IARW=BANDWIDTH
OF AR
TO REDUCE A(I,J) TO TRIANG. FORM, UPPER & LOWER
IAC=(IA+1)/2
IF(AT.FG.0.0) GO TO 10
IC=6
IE=14
GC TO 20
10 CONTINUE
IC=4
IF=10
20 CONTINUE
IAR=IARW-IC
ID=IAR+1
IF(IZAP.FG.10) GC TO 25
IF(IZAP.NE.0) GC TO 35
25 IF(IZAP.FG.10) IZAF=20
DO 30 I=2,IC
  IKI=I-1
  IKP=IE-I
  IKC=N+2*IC+2-I
  TEMP=1.0/AR(IKI,IC)
  REMP=1.0/AR(IKP,IC)
  J=0
  DO 30 JJ=1,IC
    J=J+1
    JB=IE-1-JJ
    JC=N+2*IC+1-JJ
    HCID=AR(JJ,IC-J)*TEMP
    BCID=AR(JB,IC+J)*REMP
    IF(IZAF.FG.20) B(JJ)=B(JJ)-B(IKI)*HCID
    IF(IZAF.FG.20) B(JC)=B(JC)-B(IKP)*BCID
    DO 30 K=1,IAR
      AR(JJ,IC-J+K)=AR(JJ,IC-J+K)-AR(IKI,IC+K)*HCID
      AR(JB,IC+J-K)=AR(JB,IC+J-K)-AR(IKP,IC+K)*BCID
  30 CONTINUE
  DO 50 I=1,IC
    IL=IAC-IC-1+I

```

```

IMPRFT 173
IMPRFT 180
IMPRFT 181
IMPRFT 182
IMPRFT 183
IMPRFT 184
IMPRFT 185
IMPRFT 186
IMPRFT 187
IMPRFT 188
IMPRFT 189
IMPRFT 190
IMPRFT 191
IMPRFT 192
IMPRFT 193
IMPRFT 194
IMPRFT 195
IMPRFT 196
IMPRFT 197
IMPRFT 198
IMPRFT 199
IMPRFT 200
IMPRFT 201
IMPRFT 202
LEGEND 1
LEGEND 2
LEGEND 3
LEGEND 4
LEGEND 5
LEGEND 6
LEGEND 7
LEGEND 8
LEGEND 9
LEGEND 10
LEGEND 11
LEGEND 12
LEGEND 13
LEGEND 14
LEGEND 15
LEGEND 16
LEGEND 17
LEGEND 18
LEGEND 19
LEGEND 20
LEGEND 21
LEGEND 22
LEGEND 23
LEGEND 24
LEGEND 25
LEGEND 26
LEGEND 27
LEGEND 28
LEGEND 29

```

```

LEGEND 30
LEGEND 31
LEGEND 32
LEGEND 33
LEGEND 34
LEGEND 35
LEGEND 36
LEGEND 37
LEGEND 38
LEGEND 39
LEGEND 40
REDUCE 1
REDUCE 2
REDUCE 3
REDUCE 4
REDUCE 5
REDUCE 6
REDUCE 7
REDUCE 8
REDUCE 9
REDUCE 10
REDUCE 11
REDUCE 12
REDUCE 13
REDUCE 14
REDUCE 15
REDUCE 16
REDUCE 17
REDUCE 18
REDUCE 19
REDUCE 20
REDUCE 21
REDUCE 22
REDUCE 23
REDUCE 24
REDUCE 25
REDUCE 26
REDUCE 27
REDUCE 28
REDUCE 29
REDUCE 30
REDUCE 31
REDUCE 32
REDUCE 33
REDUCE 34
REDUCE 35
REDUCE 36
REDUCE 37
REDUCE 38
REDUCE 39
REDUCE 40
REDUCE 41
REDUCE 42
REDUCE 43
REDUCE 44

```

```

TEMP=1.0/AR(I,IC)
PEMP=1.0/AR(I,IC)
DO 40 J=1,IL
  JB=N+1-J
  JC=JH+IC
  HCLD=A(J,IAD-IC+I-J)*TEMP
  BCLD=A(JB,IAD+I(-I+J)*BEMP
  IF (IZAF,EO,20) P(J+IC)=R(J+IC)-R(I)*HOIC
  IF (IZAF,EO,20) P(JC)=R(JC)-R(JD)*BCLD
  A(J,IAD-IC+I-J)=0.0
  A(JB,IAD+I(-I+J))=0.0
  DC 40 K=1,IAP
  KT=IAD-IC+I-J+K
  KP=IAD+I(-I+J)+K
  A(J,KT)=A(J,KT)-AR(I,IC+K)*HCLD
  A(JR,KP)=A(JR,KP)-AR(IE,ID-K)*POLC

```

```

40 CONTINUE
50 RETURN
END
*** *DFCK PERTBN
SUBROUTINE PERTBN (IFR,X,NFV,UFC,NUFC,PF,KU,PF,IFT,LNO)
DIMENSION X(NFV),UFC(NUFC,KU),PF(KU)
COMMON /COM2/ DO,D1,D2,D3,D4,AL,THETA,PCI,H,A1,IFR,IUN
COMMON /COM4/ IN,N1,N2
LEVEL 2,UFC
KK=0
IF (IFT,NF,0) KK=(IFT-1)*LNO
IF (IRR,EO,1) GO TO 100
AJ=2*IRR
HCLD=0.0
DO 20 I=1,N2
  HCLD=HCLD+UFC(I,KK+1)*X(I)*AJ
  IPR1=(IRR+1)/2
  IF (IPR1,LT,2) GO TO 50
  DC 30 I=2,IPR1
  J=IPR1-I
  K=(I+J)*2
  AK=K
  IF (I,FG,J) AK=AK/2.0
  HCLD=HCLD+AK*PF(I+KK)*PF(J+KK)
  DC 30 I=1,N2
  HCLD=HCLD+AK*UFC(I,I+KK)*UFC(L,I+KK)
30 CONTINUE
50 PF(IRR+KK)=-HCLD/(AJ*H1)
HCLD=PF(IRR+KK)/PF(I+KK)
DO 10 I=1,N2
  X(I)=X(I)+HCLD*UFC(I,I+KK)
10 UFC(I,IRR+KK)=X(I)
RETURN
100 PF(I+KK)=PE
DO 120 I=1,N2
  X(I)=X(I)*PE

```

REDUCE 47
REDUCE 48
REDUCE 49
REDUCE 50
REDUCE 51
REDUCE 52
REDUCE 53
REDUCE 54
REDUCF 55
REDUCE 56
REDUCE 57
REDUCE 58
REDUCE 59
REDUCE 60
REDUCE 61
REDUCE 62
REDUCE 63
REDUCE 64
REDUCE 65
REDUCE 66
PERTBN 1
PERTBN 2
PERTBN 3
PERTBN 4
PERTBN 5
PERTBN 6
PERTBN 7
PERTBN 8
PERTBN 9
PERTBN 10
PERTBN 11
PERTBN 12
PERTBN 13
PERTBN 14
PERTBN 15
PERTBN 16
PERTBN 17
PERTBN 18
PERTBN 19
PERTBN 20
PERTBN 21
PERTBN 22
PERTBN 23
PERTBN 24
PERTBN 25
PERTBN 26
PERTBN 27
PERTBN 28
PERTBN 29
PERTBN 30
PERTBN 31
PERTBN 32
PERTBN 33

```

120 UFC(I,KK+1)=X(I)
SAV=0.0
DO 125 I=1,N2
  SAV=SAV+X(I)*X(I)
125 BI=PE+SAV/PE
RETURN
END
*** *DFCK CNVRGE
SUBROUTINE CNVRGE(UFC,PF,NUFC,KU,UF,UFB,NUF,IFT,LNO,F,D,NP,U,NU,X,
CNX,Y,NY,V2,NV2,V,NV,A,NA,KA,VIMP)
DIMENSION UFC(NUFC,KU),PF(KU),UFB(NUF,KU),UF(NUF,KU),P(NP),U(NU),
CX(NX),Y(NY),V2(NV2),V(NV),A(NA,KA),VIMP(VIMP)
COMMON /COM4/ IN,N1,N2
COMMON /COM5/ VF(147,20),VFR(147,20),VFCC(106,20),PFCC(20),EFC(20)
C SF(147)
LEVEL 2,UF,UFB,UFC
CHK1=0.005
CHK2=1.0/(10.0**9)
KK=0
IF (IFT,NF,0) KK=(IFT-1)*LNO
NNN=3*(IN-2)
FMX=0.0
FMY=0.0
F=1.0
1 IF (IFT,EO,0) GO TO 220
DC 200 I=1,N1
  U(I)=VFC(I+4,IFT)-VFC(I+4,1)
200 DC 210 I=1,NNN
  X(I)=VF(I,IFT)
  Y(I)=VFR(I,IFT)
  PL=PFCC(IFT)
  GO TO 250
220 DC 230 I=1,N1
  U(I)=0.0
230 DC 240 I=1,NNN
  X(I)=0.0
  Y(I)=0.0
  PL=0.0
240 Y(I)=0.0
250 CONTINUE
TEMP=0.0
DO 20 J=1,LNO
  A1=E**J
  PL=PL+PF(KK+J)*A1
  DC 10 I=1,N1
  U(I)=U(I)+UFC(I+4,KK+J)*A1
10 DC 20 I=1,NNN
  X(I)=X(I)+UF(I,KK+J)*A1
  Y(I)=Y(I)+UFR(I,KK+J)*A1
20 CALL FVALFN(U,NU,X,NX,Y,NY,V2,NV2,V,NV,A,NA,KA,PL)
DC 30 I=1,N1
  BEMP=ARS(V(I))+ARS(V2(I))+ARS(VIMP(I))
  REMP=BEMP/3.0
  V(I)=V(I)-VIMP(I)
  IF (REMP,LE,CHK2) GO TO 30
HCLD=ARS((V2(I)+V(I))/PEMP)

```

PERTBN 34
PERTBN 35
PERTBN 36
PERTBN 37
PERTBN 38
PERTBN 39
PERTBN 40
CNVRGE 1
CNVRGE 2
CNVRGE 3
CNVRGE 4
CNVRGE 5
CNVRGE 6
CNVRGE 7
CNVRGE 8
CNVRGE 9
CNVRGE 10
CNVRGE 11
CNVRGE 12
CNVRGE 13
CNVRGE 14
CNVRGE 15
CNVRGE 16
CNVRGE 17
CNVRGE 18
CNVRGE 19
CNVRGE 20
CNVRGE 21
CNVRGE 22
CNVRGE 23
CNVRGE 24
CNVRGE 25
CNVRGE 26
CNVRGE 27
CNVRGE 28
CNVRGE 29
CNVRGE 30
CNVRGE 31
CNVRGE 32
CNVRGE 33
CNVRGE 34
CNVRGE 35
CNVRGE 36
CNVRGE 37
CNVRGE 38
CNVRGE 39
CNVRGE 40
CNVRGE 41
CNVRGE 42
CNVRGE 43
CNVRGE 44
CNVRGE 45
CNVRGE 46
CNVRGE 47
CNVRGE 48

```

IF(TEMP,LE,CHK1) GO TO 40
FMX=E
IF(EMN,NE,0.0) GC TC 50
E=FMX/2.0
GO TO 1
40 EMN=E
IF(EMX,NE,0.0) GC TC 50
E=EMN+EMX/2.0
GO TO 1
50 DO 100 K=1,6
E=(EMN+FMX)/2.0
IF(IFT,F0,0) GC TC 320
DO 300 I=1,N1
300 U(I)=VFC(I+4,IFT)-VFC(I+4,1)
DO 310 I=1,NNN
X(I)=VF(I,IFT)
310 Y(I)=VFH(I,IFT)
PL=PFC(IFT)
GC TC 350
320 DO 330 I=1,N1
330 U(I)=0.0
DO 340 I=1,NNN
X(I)=0.0
340 Y(I)=0.0
PL=0.0
350 CONTINUE
TEMP=0.0
DO 70 J=1,LNO
A1=E**J
FL=FL+PF(KK+J)*A1
DO 60 I=1,N1
60 U(I)=U(I)+UFC(I+4,KK+J)*A1
DO 70 I=1,NNN
X(I)=X(I)+UFC(I,KK+J)*A1
70 Y(I)=Y(I)+UFC(I,KK+J)*A1
CALL FVALFN(U,NU,X,NX,Y,NY,V2,NV2,V,NV,A,NA,KA,PI)
DO 80 I=1,N1
REMP=ABS(V(I))+ABS(V2(I))+ABS(VIMP(I))
REMP=REMP/3.0
V(I)=V(I)-VIMP(I)
IF(REMP,LE,CHK2) GC TO 80
HOLD=ABS((V2(I)+V(I))/REMP)
IF(HOLD,LE,TEMP) GC TO 80
TEMP=HOLD
80 CONTINUE
IF(TEMP,LE,CHK1) GC TO 90
FMX=E
GC TC 100
90 EMN=E
100 CONTINUE
RETURN
END

```

```

CNVRGE 52
CNVRGE 53
CNVRGE 54
CNVRGE 55
CNVRGE 56
CNVRGE 57
CNVRGE 58
CNVRGE 59
CNVRGE 60
CNVRGE 61
CNVRGE 62
CNVRGE 63
CNVRGE 64
CNVRGE 65
CNVRGE 66
CNVRGE 67
CNVRGE 68
CNVRGE 69
CNVRGE 70
CNVRGE 71
CNVRGE 72
CNVRGE 73
CNVRGE 74
CNVRGE 75
CNVRGE 76
CNVRGE 77
CNVRGE 78
CNVRGE 79
CNVRGE 80
CNVRGE 81
CNVRGE 82
CNVRGE 83
CNVRGE 84
CNVRGE 85
CNVRGE 86
CNVRGE 87
CNVRGE 88
CNVRGE 89
CNVRGE 90
CNVRGE 91
CNVRGE 92
CNVRGE 93
CNVRGE 94
CNVRGE 95
CNVRGE 96
CNVRGE 97
CNVRGE 98
CNVRGE 99
CNVRGE 100
CNVRGE 101
CNVRGE 102
CNVRGE 103

```

```

** *DFCK IMPRVE
SUBROUTINE IMPRVE (U,X,Y,NA,NFV,V1,V2,V3,V4,P,A,KA,HA,KHA,IFT,AB,K
CAP,UF,UFR,KU,UFC,NUFC,FE,II0,LNO,E,EMN,IFAT,FI*1,VIMP,Z6)
DIMENSION U(NA),X(NFV),Y(NFV),V1(NA),V2(NA),V3(NA),V4(NA),A(NA,KA)
C,HA(NA,KHA),AB(12,KAF),UF(NA,KU),UFC(NA,KU),NUFC(KU),PF(KU)
C,VIMP(NUFC),Z6(NUFC)
COMMON /COM2/ DO,D1,D2,D3,D4,AL,THEIA,FCI,H,AT,IFR,ION
COMMON /COM3/ JAF,JAW,JARW,IC,JE,IC,FT,TZAP
COMMON /COM4/ IN,N1,N2
COMMON /COM5/ VF(147,20),VFR(147,20),VFC(106,20),PFC(20),EFC(20)
C,SF(147)
LEVEL 2,UF,UFR,UFC
ICC=0
M1=0
PT=1.0
NNN=3*(IN-2)
IGT=IFT+1
LMT=15
IL=IPR
CHK1=1.0/(10.0**6)
CHK2=1.0/(10.0**9)
21 M1=M1+1
IF (M1.GT.LMT) GC TC 90
DO 5 I=1,N2
Z6(I)=U(I)
5 U(I)=U(I)-VFC(I,1)
DO 10 I=1,NNN
V1(I)=VF(I,IGT)
10 V2(I)=VFH(I,IGT)
DO 30 I=1,N1
U(I)=U(I+4)
DO 30 J=1,JAW
30 HA(I,J)=A(I,J)
CALL EVALFN(U,NA,V1,NA,V2,NA,V3,NA,V4,NA,A,NA,KA,P)
TEMP=0.0
DO 35 I=1,N1
REMP=ABS(V3(I))+ABS(V4(I))+ABS(VIMP(I))
REMP=REMP/3.0
V4(I)=V4(I)-VIMP(I)
IF(REMP,LE,CHK2) GO TO 35
HOLD=ABS((V3(I)+V4(I))/REMP)
IF (HOLD,LE,TEMP) GC TO 35
TEMP=HOLD
35 CONTINUE
IF (TEMP,LE,CHK1) GC TO 60
DO 40 I=1,N1
40 V3(I)=-V3(I)+V4(I)
CALL FKTHS(HA,NA,KHA,V4,NA,IGT)
CALL REDUCE (HA,AP,NA,KHA,KAP,N1,AT,JAW,JARW,TZAP,VIMP,NUFC)
CALL PAD7H (HA,V3,NA,N1,JAW,PI,KHA,NA)
CALL PKSUB(V3,NA,AP,KAB,AT,IN,JAB6)
DO 50 I=1,N2
50 U(I)=Z6(I)+V3(I)
CALL STRNCP(U,NA,UF,NA,KU,UFR,NA,KU,IL)
DO 55 I=1,NNN

```

```

IMPRVE 1
IMPRVE 2
IMPRVE 3
IMPRVE 4
IMPRVE 5
IMPRVE 6
IMPRVE 7
IMPRVE 8
IMPRVE 9
IMPRVE 10
IMPRVE 11
IMPRVE 12
IMPRVE 13
IMPRVE 14
IMPRVE 15
IMPRVE 16
IMPRVE 17
IMPRVE 18
IMPRVE 19
IMPRVE 20
IMPRVE 21
IMPRVE 22
IMPRVE 23
IMPRVE 24
IMPRVE 25
IMPRVE 26
IMPRVE 27
IMPRVE 28
IMPRVE 29
IMPRVE 30
IMPRVE 31
IMPRVE 32
IMPRVE 33
IMPRVE 34
IMPRVE 35
IMPRVE 36
IMPRVE 37
IMPRVE 38
IMPRVE 39
IMPRVE 40
IMPRVE 41
IMPRVE 42
IMPRVE 43
IMPRVE 44
IMPRVE 45
IMPRVE 46
IMPRVE 47
IMPRVE 48
IMPRVE 49
IMPRVE 50
IMPRVE 51
IMPRVE 52
IMPRVE 53
IMPRVE 54
IMPRVE 55

```

```

70 U(I)=26(I)
WRITE (6,2010) M1
DO 80 I=1,N2
80 VFC(I,IGT)=U(I)
RETURN
90 IF (ICC.GT.1) GO TC 140
WRITE (6,2010) M1
ICC=ICC+1
IF (IFT.LF.1) GO TC 100
EFC(IFT)=0.75*(EFC(IFT)-EFC(IFT-1))+EFC(IFT-1)
E=EFC(IFT)
GO TO 110
100 E=0.75*E
IF (IFT.FO.1) EFC(IFT)=E
110 CONTINUE
ITPF=0
CALL FUNVFC(UF,UFR,KU,NA,HFC,NUFC,X,Y,NFV,N,NA,FF,ILQ,IFT,INO,E,
CMN,IN,F,ITPF,IFAIL,FLHT)
PFC(IGT)=P
DO 120 J=1,NNN
VF(J,IGT)=X(J)
120 VFR(J,IGT)=Y(J)
DO 130 J=1,N2
130 VFC(J,IGT)=U(J)
M1=0
GO TC 21
140 WRITE (6,2000)
DO 150 I=1,NNN
VF(I,IGT)=X(I)
150 VFR(I,IGT)=Y(I)
RETURN
2000 FORMAT (1H,10X,17HIMPRVE HAS FAILED )
2010 FORMAT (1H,5X,3HM1=,I3)
END
*DFCK TFEV01
SUBROUTINE TFEV01 (XX,YY,NXX,X,Y,NX,V,NV,P,MPK)
DIMENSION XX(NXX),YY(NXX),X(NX),Y(NX),V(NV),V(NV)
COMMON /COM2/ D0,D1,C2,D3,C4,AL,THETA,PCI,H,AT,IFR,ICN
COMMON /COM4/ IH,N1,K2
COMMON /COM5/ VF(147,20),VFR(147,20),VFC(106,20),PFC(20),EFC(20)
C,SF(147)
AK=0.0
AJ=1.0
IF (ICN.EQ.20.OR.ICN.FO.30) AK=1.0
IF (ICN.EQ.20.OR.ICN.FO.0) AJ=0.0
IM=IN-2
IF (MRK.GT.0) GO TO 150
DO 10 I=1,5
10 V(I)=0.0
PA=0.0
DC 100 IJ=1,IM

```

```

IMPRVE 59
IMPRVE 60
IMPRVE 61
IMPRVE 62
IMPRVE 63
IMPRVE 64
IMPRVE 65
IMPRVF 66
IMPRVE 67
IMPRVF 68
IMPRVE 69
IMPRVE 70
IMPRVE 71
IMPRVE 72
IMPRVE 73
IMPRVE 74
IMPRVE 75
IMPRVE 76
IMPRVE 77
IMPRVE 78
IMPRVE 79
IMPRVE 80
IMPRVE 81
IMPRVE 82
IMPRVE 83
IMPRVE 84
IMPRVE 85
IMPRVE 86
IMPRVE 87
IMPRVE 88
IMPRVE 89
IMPRVE 90
IMPRVE 91
IMPRVE 92
IMPRVE 93
TFEVO1 1
TFEVO1 2
TFEVO1 3
TFEVO1 4
TFEVO1 5
TFEVO1 6
TFEVO1 7
TFEVO1 8
TFEVO1 9
TFEVO1 10
TFEVO1 11
TFEVO1 12
TFEVO1 13
TFEVO1 14
TFEVO1 15
TFEVO1 16
TFEVO1 17

```

```

K=IJ*3-2
K1=K+1
K2=K+2
IKT=IJ/2
IKT=IJ-2*IKT
AKT=IKT+1
PA=PA+1.0
PHI=PA*H
S=SIN(PHI)
C=COS(PHI)
CT=C/S
EOI=AK*(VF(K,1)*(1.0-0.5*VF(K2,1)**2)+0.5*VF(K2,1)**2+D0*VF(K1,1))
I-AJ*SF(K)
EOI=AK*(VF(K1,1)+D0*(VF(K,1)*(1.0-0.5*VF(K2,1)**2)+0.5*VF(K2,1)**2
I)-AJ*SF(K1)
XOI=AK*(VFB(K2,1)+D0*VF(K2,1)*CT)
XOI=AK*(VF(K2,1)*CT+D0*VFB(K2,1))
EOS=X(K)+0.5*(X(K2)**2)*(1.0-X(K))
EO=VF(K,1)+0.5*(VF(K2,1)**2)*(1.0-VF(K,1))
V(1)=V(1)+AKT*(EOS*(EOS+D0*X(K1)-FO-EOI)-D0*X(K1)*EO+EO*EOI)*S/2.0
V(2)=V(2)+AKT*(X(K1)*X(K2)+C0*EOS-VF(K1,1)-ECI)-D0*EOS*VF(K1,1)+
1VF(K1,1)*EOI)*S/2.0
V(3)=V(3)+AKT*AL*(Y(K2)+D0*X(K2)*CT-VFR(K2,1)-XOI)-D0*X(K2)
1*CT*VFR(K2,1)+VFR(K2,1)*XOI)*S/2.0
V(4)=V(4)+AKT*AL*(X(K2)*CT*(X(K2)*CT+D0*Y(K2)-VF(K2,1)*CT-XOI)-EC*
1Y(K2)*VF(K2,1)*CT+VF(K2,1)*CT*XOI)*S/2.0
100 CONTINUE
EOI=0.0
EOI=0.0
DO 120 I=1,5
IF (V(I).LE.0.0) GO TC 110
EOI=EOI+V(I)
GO TO 120
110 ECI=ECI+V(I)
120 CONTINUE
V(5)=-(EOI+EOI)
IF (V(5).LE.0.0) EOI=EOI+V(5)
IF (V(5).GE.0.0) EOI=EOI+V(5)
EOS=(EOI-EOI)/2.0
DO 130 I=1,5
V(I+5)=V(I)/EOS
130 V(I)=V(I)*H/3.0
IF (MRK.LT.0) RETURN
150 CONTINUE
DO 280 I=51,55
280 V(I)=0.0
PA=0.0
DC 300 IJ=1,IM
K=IJ*3-2
K1=K+1
K2=K+2
IKT=IJ/2
IKT=IJ-2*IKT
AKT=IKT+1
PA=PA+1.0

```

```

TFEVO1 18
TFEVO1 19
TFEVO1 20
TFEVO1 21
TFEVO1 22
TFEVO1 23
TFEVO1 24
TFEVO1 25
TFEVO1 26
TFEVO1 27
TFEVO1 28
TFEVO1 29
TFEVO1 30
TFEVO1 31
TFEVO1 32
TFEVO1 33
TFEVO1 34
TFEVO1 35
TFEVO1 36
TFEVO1 37
TFEVO1 38
TFEVO1 39
TFEVO1 40
TFEVO1 41
TFEVO1 42
TFEVO1 43
TFEVO1 44
TFEVO1 45
TFEVO1 46
TFEVO1 47
TFEVO1 48
TFEVO1 49
TFEVO1 50
TFEVO1 51
TFEVO1 52
TFEVO1 53
TFEVO1 54
TFEVO1 55
TFEVO1 56
TFEVO1 57
TFEVO1 58
TFEVO1 59
TFEVO1 60
TFEVO1 61
TFEVO1 62
TFEVO1 63
TFEVO1 64
TFEVO1 65
TFEVO1 66
TFEVO1 67
TFEVO1 68
TFEVO1 69
TFEVO1 70
TFEVO1 71
TFEVO1 72

```

```

F01=AK*(VF(K,1)+D0*(VF(K,1)*(1.0-0.5*VF(K2,1)**2)+0.5*VF(K2,1)**2)
1-AJ*SF(K)
FCI=AK*(VF(K,1)+D0*(VF(K,1)*(1.0-0.5*VF(K2,1)**2)+0.5*VF(K2,1)**2)
1))-AJ*SF(K1)
X0I=AK*(VF(K2,1)+D0*VF(K2,1)*CT)
XCI=AK*(VF(K2,1)+D0*VF(K2,1)*CT)
FOS=X(K)+0.5*(X(K2)**2)*(1.0-X(K))
FQ=VF(K,1)+0.5*(VF(K2,1)**2)*(1.0-VF(K,1))
V(51)=V(51)+AKT*(X(K)*(2.0*FOS+D0*X(K1))*(1.0-0.5*X(K2)**2)+X(K2)
1)*(2.0*EOS+D0*X(K1))*X(K2)*(1.0-X(K))*(E0+F0I)-D0*X(K1)*E0)*S/2.0
25*X(K2)**2)+X(K2)*X(K2)*(1.0-X(K))*(E0+F0I)-D0*X(K1)*E0)*S/2.0
V(52)=V(52)+AKT*(X(K1)*(2.0*X(K1)+D0*E0)+D0*X(K1)*X(K)*(1.0-0.
15*X(K2)**2)+X(K2)*X(K2)*(1.0-X(K)))-X(K1)*(VF(K1,1)+ECI)+D0*VF(
2K1,1)*X(K)*(1.0-0.5*X(K2)**2)+X(K2)*X(K2)*(1.0-X(K)))**S/2.0
V(53)=V(53)+AKT*AL*(Y(K2)*X(K2)*(2.0*Y(K2)+D0*X(K2)*CT)+X(K2)*D0*Y(K2)
1*CT-Y(K2)*VF(K2,1)+X0I)-D0*X(K2)*VF(K2,1)*CT)*S/2.0
1*CT-Y(K2)*Y(K2)+X0I)-D0*X(K2)*VF(K2,1)*CT)*S/2.0
V(54)=V(54)+AKT*AL*(X(K2)*CT*(2.0*X(K2)*CT+D0*Y(K2))+Y(K2)*D0*X(
1K2)*CT-X(K2)*X(K1)*CT*(2.0*X(K2)*CT+D0*Y(K2))*S/2.0
A1=X(K)-X(K1)+X(K2)*CT
A2=X(K)-X(K1)+X(K2)*CT
E0=VF(K,1)-VF(K1,1)+VF(K2,1)*CT
V(55)=V(55)+AKT*(X(K1)*(3.0+X(K1)+2.0*A2)+2.0*A2
1-VF(K1,1)*(6.0+6.0*X(K1)-3.0*VF(K1,1)+2.0*A2-2.0*E0)-E0*(2.0+2.0*X
2(K1)))+A1*(1.0+X(K1)*(2.0+X(K1))-VF(K1,1)*(2.0+2.0*X(K1)-VF(K1,1)
3))*S**3)
300 CCNTINUF
E0I=0.0
E0I=0.0
DC 320 I=51,55
IF(V(I).IE.0.0) GO TO 310
E0I=E0I+V(I)
GC TO 320
310 E0I=E0I+V(I)
320 CCNTINUF
V(61)=200.0*(E0I+E0I)/(E0I-E0I)
FOS=(E0I-E0I)/2.0
DC 330 I=51,55
V(1+5)=V(I)/E0S
330 V(I)=V(I)*H/3.0
RETURN
FNC
*** *DECK
VOLDIS
SUBROUTINE VOLDIS(U,II,X,IX,VOL,DELTA)
DIMENSION U(II),X(IX)
COMMON /COM2/ D0,D1,D2,D3,D4,AL,THETA,PCL,H,AT,IFR,ION
COMMON /COM4/ IN,N1,N2
VOL=0.0
FA=0.0
IM=IN-2
DC 100 IJ=1,IM

```

```

TPEV01 77
TPEV01 78
TPEV01 79
TPEV01 80
TPEV01 81
TPEV01 82
TPEV01 83
TPEV01 84
TPEV01 85
TPEV01 86
TPEV01 87
TPEV01 88
TPEV01 89
TPEV01 90
TPEV01 91
TPEV01 92
TPEV01 93
TPEV01 94
TPEV01 95
TPEV01 96
TPEV01 97
TPEV01 98
TPEV01 99
TPEV01 100
TPEV01 101
TPEV01 102
TPEV01 103
TPEV01 104
TPEV01 105
TPEV01 106
TPEV01 107
TPEV01 108
TPEV01 109
TPEV01 110
TPEV01 111
TPEV01 112
TPEV01 113
TPEV01 114
TPEV01 115
TPEV01 116
TPEV01 117
TPEV01 118
VOLDIS 1
VOLDIS 2
VOLDIS 3
VOLDIS 4
VOLDIS 5
VOLDIS 6
VOLDIS 7
VOLDIS 8
VOLDIS 9

```

```

K=IJ*3-2
K1=K+1
K2=K+2
IKT=IJ/2
IKT=IJ-2+IKT
AKT=IKT+1
PA=PA+1.0
PHI=PA*H
S=SIN(PHI)
C=COS(PHI)
CT=C/S
100 VOL=VOL+AKT*(3.0*X(K1)*(1.0+X(K1))+X(K1)**3+(X(K)-X(K1)+X(K2)*CT)
1*(1.0+X(K1)**2))*S**3)
PHI=PHI+H
C=COS(PHI)
S=SIN(PHI)
CT=C/S
E=U(N1+6)+U(N1+5)*CT
VCL=(H/3.0)*(2.0*VCL+(3.0*E*(1.0+E)+E**3))*S**3)
VCL=-VCL/((2.0-3.0*CT+C**3)/3.0)
DELTA=U(4)
RETURN
FNC
*** *DECK
EVALFN
SUBROUTINE EVALFN(U,NU,X,NX,Y,NY,V2,NV2,V,NV,A,NA,KA,P)
DIMENSION U(NU),X(NX),Y(NY),V2(NV2),V(NV),A(NA),KA)
COMMON /COM2/ D0,D1,D2,D3,D4,AL,THETA,PCL,H,AT,IFR,ION
COMMON /COM3/ JAR,JAR4,IE,IE,IC,IC,IZAP
COMMON /COM1/ IN,N1,N2
COMMON /COM5/ VF(147,20),VFB(147,20),VFC(106,20),FFC(20),EFC(20)
C,SE(147)
NNN=IN-2
CALL PROCUC (NA,KA,A,V2,U,N1,NV2,JAW)
PA=0.0
AK=1.0
AJ=1.0
IF (ICN.EQ.20.OR.ION.EQ.30) AK=2.0
IF (ICN.EQ.20.OR.ION.EQ.0) AJ=0.0
DC 50 I=1,NNN
PA=PA+1.0
PHI=PA*H
S=SIN(PHI)
C=COS(PHI)
CT=C/S
K1=I*2-1
K2=K1+1
L=I*3-2
L1=L+1
L2=L+2
V(K1)=X(L2)*(X(L2)*CT/2.0+Y(L2)-X(L))-D0*X(L1)
V(K2)=X(L2)*(D3*X(L2)/2.0+X(L)*CT+D0*X(L1)*CT+Y(L)+D0*Y(L
1))+Y(L2)*X(L1)+D0*X(L1)
V(K1)=V(K1)+2.0*P*X(L2)
V(K2)=V(K2)-2.0*P*(1.0+X(L)+X(L1))
V(K1)=V(K1)+X(L2)*X(L2)*(-X(L2)/2.0-(1.0-0.5*CT)*X(L)*CT-D0*CT

```

```

VOLDIS 10
VOLDIS 11
VOLDIS 12
VOLDIS 13
VOLDIS 14
VOLDIS 15
VOLDIS 16
VOLDIS 17
VOLDIS 18
VOLDIS 19
VOLDIS 20
VOLDIS 21
VOLDIS 22
VOLDIS 23
VOLDIS 24
VOLDIS 25
VOLDIS 26
VOLDIS 27
VOLDIS 28
VOLDIS 29
VOLDIS 30
VOLDIS 31
VOLDIS 32
EVALFN 1
EVALFN 2
EVALFN 3
EVALFN 4
EVALFN 5
EVALFN 6
EVALFN 7
EVALFN 8
EVALFN 9
EVALFN 10
EVALFN 11
EVALFN 12
EVALFN 13
EVALFN 14
EVALFN 15
EVALFN 16
EVALFN 17
EVALFN 18
EVALFN 19
EVALFN 20
EVALFN 21
EVALFN 22
EVALFN 23
EVALFN 24
EVALFN 25
EVALFN 26
EVALFN 27
EVALFN 28
EVALFN 29
EVALFN 30
EVALFN 31
EVALFN 32

```

```

1 (L1)=CO*(X(L1))/2.0+X(L2)*(-CT*(X(L1))-DO*(X(L1))-2.0*Y(L1))-X
2 0*Y(L1)*X(L1))+X(L2)*X(L1)*(-X(L1)-DO*(X(L1)))
V(K1)=V(K1)+2.0*P*(X(L1))*X(L1)
V(K2)=V(K2)-2.0*P*(X(L1))*X(L1)
E0=AK*(VF(L,1)+CO*VF(L1,1))-AJ*SF(L)
E01=AK*(VFR(L,1)+CO*VFR(L1,1))-AJ*SF(L2)
V(K1)=V(K1)+X(L2)*(X(L2)*(E01+FO*CT)/4.0-X(L1)*FO/2.0+Y(L2)*E0/2.0)
V(K2)=V(K2)+X(L2)*(X(L2)*(FO*CT+FO1)/2.0+Y(L1)*E0/2.0)
1+Y(L2)*X(L1)*E0/2.0
V(K1)=V(K1)-2.0*P*(1.0-VF(L1,1))*VF(L2,1)+X(L2)*VF(L1,1)+X(L1)*V
1 F(L2,1)
V(K2)=V(K2)+2.0*P*(VF(L,1)+VF(L1,1))-VF(L1,1)*VF(L,1)+X(L1)*(VF(L,
1 1)+VF(L1,1))+VF(L1,1)*(X(L1)-X(L1)))
50 CONTINUE
RETURN
END
FNDRHS
*** *DECK FNDRHS
SUBROUTINE FNDRHS (UF,NUF,KUF,UFR,IRF,V,KV,PF,IFT,LNO)
DIMENSION UF(NUF,KUF),UFR(NUF,KUF),V(NV),PF(KUF)
COMMON/CCM1/ AN(7,4,12),ITYPE,ILN(7),JMN(7),JSN(7),JEN(7),KBOE(7)
COMMON/CCM2/ DO,D1,D2,D3,D4,AL,THETA,PCL,H,A1,IFR,ION
COMMON/CCM4/ LN,L1,L2
COMMON/CCM5/ VF(147,20),VFR(147,20),VFC(106,20),FFC(20),FFC(20)
C, SF(147)
LEVEL 2,UF,UFR
IPR1=IPR-1
IPR2=IPR-2
JJ=0
IF(IFT.GT.1) JJ=(IFT-1)*LNO
FA=0.0
AK=1.0
AJ=1.0
IF (ICN.EQ.20.OR.ION.EQ.30) AK=2.0
IF (ICN.EQ.20.OR.ION.EQ.0) AJ=0.0
DO 10 I=1,L1
10 V(I)=0.0
DC 110 KK=1,ITYPE
CALL FDDATA (KK,ITCL,MID,ISTART,IFIN)
DO 100 IJ=ISTART,IFIN
PA=PA+1.0
PHI=PA*H
S=SIN(PHI)
C=COS(PHI)
CT=C/S
K=2*IJ-1
K1=K+1
N1=3*IJ-2
N2=N1+1
N3=N1+2
E0=AK*(VF(N1,1)+CO*VF(N2,1))-AJ*SF(N1)
E01=AK*(VFR(N1,1)+CO*VFR(N2,1))-AJ*SF(N3)
DC 20 I=1,IPR1
11=I+JJ
I2=IPR-I+JJ
V(K)=V(K)-UF(N3,I1)*(UF(N3,I2)*C2*CT/2.0+UFR(N3,I2)-UF(N1,I2)
1 -UF(N2,I2)*CO)
V(K1)=V(K1)-UF(N3,I1)*(UF(N3,I2)*D3/2.0+UF(N1,I2)*CT+UF(N2,I2)
1 *DO*CT+UFR(N1,I2)+UFR(N2,I2)*CO)-UFR(N3,I1)*(UF(N1,I2)+UF(N2
2 I2)*DO)
V(K)=V(K)-2.0*UF(N3,I1)*PF(I2)
V(K1)=V(K1)+2.0*(UF(N1,I1)+UF(N2,I1))*PF(I2)
IF (ICN.EQ.-10) GC TC 20
V(K)=V(K)-UF(N3,I1)*(UF(N3,I2)*(FO1+E0*CT)/4.0-UF(N1,I2)*E0/2.0+UF
1R(N3,I2)*FO/2.0)
V(K1)=V(K1)-UF(N3,I1)*(UF(N3,I2)*E0/4.0+UF(N1,I2)*(FO*CT+E01)/2.0+
1 UFR(N1,I2)*E0/2.0)-UF(N1,I1)*UFR(N3,I2)*FO/2.0
V(K)=V(K)+2.0*PF(I1)*(UF(N2,I2)*VF(N3,1)+UF(N3,I2)*VF(N2,1))
V(K1)=V(K1)-2.0*PF(I1)*(UF(N2,I2)*(VF(N1,1)+VF(N2,1))+VF(N2,1)*(U
1 F(N1,I2)-UF(N2,I2)))
20 CCNTINUE
IF (IPR.LT.3) GC TO 100
DC 40 I=1,IPR2
IHD=IPR-1-I
DC 30 J=1,IHD
I1=I+JJ
I2=J+JJ
I3=IPR-I-J+JJ
V(K)=V(K)-UF(N3,I1)*(UF(N3,I2)*(-UF(N3,I3))/2.0-UF(N1,I3)*CT*(
1 1.0-DO/2.0)-UFR(N2,I3)*CO/2.0-UFR(N1,I3)-UF(N2,I3)*DO*CT/2.0)
2 +UF(N1,I2)*(-UFR(N3,I3)*2.0+UF(N1,I3)+UF(N2,I3)*DO)-UF(N2,I2)
3 *UFR(N3,I3)*CO)
V(K1)=V(K1)-UF(N3,I1)*(UF(N3,I2)*(UF(N3,I3)*CT/2.0+UFR(N3,I3)
1 *3.0/2.0-UF(N1,I3)*(1.0+DO/2.0)-UF(N2,I3)*CO/2.0)+UF(N1,I2)*(
2 -UF(N1,I3)*CT-(UF(N2,I3)*DO*CT-UFR(N1,I3)*2.0-UFR(N2,I3)*DO)-U
3 F(N2,I2)+UFR(N1,I3)*DO)+UF(N1,I1)*(UF(N1,I2)*UFR(N3,I3)+DO*UF
4 (N2,I2)*UFR(N3,I3))
V(K)=V(K)-2.0*UF(N3,I1)*UF(N2,I2)*PF(I3)
V(K1)=V(K1)+2.0*UF(N1,I1)*UF(N2,I2)*PF(I3)
30 CCNTINUE
40 CCNTINUE
100 CONTINUE
110 CONTINUE
RETURN
END
FNDRHS
*** *DECK FNDRH2
SUBROUTINE FNDRH2 (UF,NUF,KUF,UFR,IRF,V,KV,PF,IFT,LNO)
DIMENSION UF(NUF,KUF),UFR(NUF,KUF),V(NV),PF(KUF)
COMMON/CCM1/ AN(7,4,12),ITYPE,ILN(7),JMN(7),JSN(7),JEN(7),KBOE(7)
COMMON/CCM2/ DO,D1,D2,D3,D4,AL,THETA,PCL,H,A1,IFR,ION
COMMON/CCM4/ LN,L1,L2
COMMON/CCM5/ VF(147,20),VFR(147,20),VFC(106,20),FFC(20),FFC(20)
C, SF(147)
LEVEL 2,UF,UFR
IPR1=IPR-1
JJ=(IFT-1)*LNO
PA=0.0
DO 110 KK=1,ITYPE
CALL FDDATA (KK,ITCL,MID,ISTART,IFIN)
FNDRH2 1
FNDRH2 2
FNDRH2 3
FNDRH2 4
FNDRH2 5
FNDRH2 6
FNDRH2 7
FNDRH2 8
FNDRH2 9
FNDRH2 10
FNDRH2 11
FNDRH2 12
FNDRH2 13

```

```

S=SIN(PHI)
C=CCS(PHI)
CT=C/S
K=2*IJ-1
K1=K+1
L=3*IJ-2
L1=L+1
L2=L+2
DO 70 I=1,IPR1
I1=I+JJ
I2=IRR-I+JJ
V(K)=V(K)-VF(L2,IFT)*UF(L2,I1)*(-1.5*UF(L2,I2)-(2.0-DO)*CT*UF(L2,I2)-DO*CT*UF(L1,I2)-DO*UF(L1,I2))*(-2.0+UF(L1,I2))*(-2.0+UF(L2,I2))+UF(L2,I2)+DO*UF(L1,I2)-DO*UF(L2,I1)+UF(L1,I2)-VF(L1,IFT)*UF(L2,I1)+(-1.0-0.5*DO)*UF(L2,I2)+2.0*UF(L1,I2)+DO*UF(L1,I2)-VF(L1,IFT)*UF(L2,I1)+(-1.0+DO)*CT*UF(L2,I2)/2.0+DO*(UF(L2,I2)-UF(L2,I1))+VFB(L2,IFT)+UF(L2,I1)*(2.0*UF(L1,I2)+DO*UF(L1,I2))+VFB(L1,IFT)*UF(L2,I1)+UF(L2,I2)*DO/2.0-2.0*(PFC(IFT)*UF(L2,I1)+UF(L1,I2)+VF(L2,IFT)*PF(11)*UF(L1,I2)+VF(L1,IFT)*PF(11)*UF(L2,I2))
V(K1)=V(K1)-VF(L2,IFT)*UF(L2,I1)*(1.5*UF(L2,I2)+CT+3.0*UF(L2,I2)-2.0-DO)*UF(L1,I2)+UF(L1,I1)*(-CT*UF(L1,I2)-DO*UF(L1,I2)+CT*2.0*UF(L1,I2)-DO*UF(L1,I2)-DO*UF(L1,I1)+UF(L1,I1)*UF(L1,I2))-VF(L1,IFT)*UF(L2,I1)+(-1.0+DO/2.0)*UF(L2,I2)-CT*(2.0*UF(L1,I2)+DO*UF(L1,I2))-2.0*UF(L1,I2)-DO*UF(L1,I2)-DO*UF(L1,I2)-DO*UF(L1,I2)-DO*UF(L1,I2)+DO*UF(L1,I2)+DO*UF(L1,I2)-VF(L1,IFT)*UF(L2,I1)+(-DO*(UF(L2,I2)/2.0+UF(L2,I2)+CT*UF(L1,I2)))-VFB(L2,I1)*UF(L1,I2)+DO*UF(L1,I2)+VFB(L1,IFT)*UF(L2,I1)+2.0*UF(L1,I2)+DO*UF(L1,I2)+VFB(L1,IFT)+DO*UF(L2,I1)*UF(L1,I2)+2.0*(PFC(IFT)*UF(L1,I1)+UF(L1,I2)+VF(L1,IFT)*PF(11)*UF(L1,I2)+VF(L1,IFT)*PF(11)*UF(L2,I2))
20 CONTINUE
100 CONTINUE
110 CONTINUE
RETURN
END

```

FNDLH2 17
FNDLH2 18
FNDLH2 19
FNDLH2 20
FNDLH2 21
FNDLH2 22
FNDLH2 23
FNDLH2 24
FNDLH2 25
FNDLH2 26
FNDLH2 27
FNDLH2 28
FNDLH2 29
FNDLH2 30
FNDLH2 31
FNDLH2 32
FNDLH2 33
FNDLH2 34
FNDLH2 35
FNDLH2 36
FNDLH2 37
FNDLH2 38
FNDLH2 39
FNDLH2 40
FNDLH2 41
FNDLH2 42
FNDLH2 43
FNDLH2 44
FNDLH2 45
FNDLH2 46
FNDLH2 47
FNDLH2 48
FNDLH2 49
FNDLH2 50
FNDLH2 51
FNDLH2 52
FNDLH2 1
FNDLH2 2
FNDLH2 3
FNDLH2 4
FNDLH2 5
FNDLH2 6
FNDLH2 7
FNDLH2 8
FNDLH2 9
FNDLH2 10
FNDLH2 11
FNDLH2 12
FNDLH2 13
FNDLH2 14
FNDLH2 15
FNDLH2 16

*DECK

```

SUBROUTINE FNDLHS (A,NA,KHA,V,NV,IK)
DIMENSION A(NA,KHA),V(NV)
COMMON/COM1/ AN(7,4,12),ITYPE,ILN(7),IMN(7),JSN(7),JEN(7),KHUE(7)
COMMON/COM2/ DO,D1,D2,D3,D4,AL,THE1A,PCI,H,AT,IFR,ION
COMMON/COM3/ JAC,JAK,JAW,JC,IE,IE,FT,IZAP
COMMON/COM4/ IN,N1,N2
COMMON/COM5/ VF(147,20),VFB(147,20),VFC(106,20),PFC(20),FPC(20)
C,SF(147)
P=PFC(1K)
PA=0.0
AK=1.0
AJ=1.0
IF (ICN.EQ.20.OR.ICN.EQ.30) AK=2.0
IF (ICN.EQ.20.OR.ION.EQ.0) AJ=0.0
DO 70 I=1,ITYPE

```

FNDLH2 17
FNDLH2 18
FNDLH2 19
FNDLH2 20
FNDLH2 21
FNDLH2 22
FNDLH2 23
FNDLH2 24
FNDLH2 25
FNDLH2 26
FNDLH2 27
FNDLH2 28
FNDLH2 29
FNDLH2 30
FNDLH2 31
FNDLH2 32
FNDLH2 33
FNDLH2 34
FNDLH2 35
FNDLH2 36
FNDLH2 37
FNDLH2 38
FNDLH2 39
FNDLH2 40
FNDLH2 41
FNDLH2 42
FNDLH2 43
FNDLH2 44
FNDLH2 45
FNDLH2 46
FNDLH2 47
FNDLH2 48
FNDLH2 49
FNDLH2 50
FNDLH2 51
FNDLH2 52
FNDLH2 53
FNDLH2 54
FNDLH2 55
FNDLH2 56
FNDLH2 57
FNDLH2 58
FNDLH2 59
FNDLH2 60
FNDLH2 61
FNDLH2 62
FNDLH2 63
FNDLH2 64
FNDLH2 65
FNDLH2 66
FNDLH2 67
FNDLH2 68
FNDLH2 69
FNDLH2 70
FNDLH2 71

```

CALL FDATA (KK,ITCL,MID,ISTART,IFIN)
DO 100 IJ=ISTART,IFIN
PA=PA+1.0
FHT=FA*H
S=SIN(PHI)
C=CCS(PHI)
CT=C/S
K=2*IJ-1
K1=K+1
L=3*IJ-2
L1=L+1
L2=L+2
FO=AK*(VF(L,1)+DO*VF(L1,1))-AJ*SF(L)
FO1=AK*(VFB(L,1)+DO*VFB(L1,1))-AJ*SF(L2)
DO 70 I=1,ITCL
MA=JAC+2*(I-1)C
A(K,MA+1)=A(K,MA+1)+AN(KK,1,I)*(-2.0*VF(L,IK)+DO*VF(L1,IK)-VFB(L2,IK)-DO*VF(L2,IK)*CT)+AN(KK,2,I)*(-VF(L2,IK))
A(K1,MA-1)=A(K1,MA-1)+AN(KK,1,I)*(-2.0*P*VF(L2,IK)*CT+VFB(L2,IK)+VF(L,IK)+DO*VF(L1,IK))+AN(KK,2,I)*VF(L2,IK)
A(K1,MA)=A(K1,MA)+AN(KK,1,I)*(-VF(L,IK)*CT-VFB(L,IK)-DO*(VF(L1,1K)*CT+VFB(L1,1K))+AN(KK,2,I)*(-VF(L,IK)-DO*VF(L1,IK)))
A(K,MA)=A(K,MA)+AN(KK,1,I)*VF(L2,IK)*VF(L2,IK)*CT+VFB(L2,IK)*2.0*AN(KK,2,I)*VF(L2,IK)*?
A(K,MA+1)=A(K,MA+1)+AN(KK,1,I)*(-2.0*VF(L1,IK)+VF(L2,IK)*(DO*VF(L2,IK)/2.0+(2.0-DO)*VF(L,IK)*CT+DO*CT*VF(L1,IK)+DO*VFB(L1,IK)+2.0*VFB(L,IK))+VF(L,IK)*2.0*VFB(L2,IK)-VF(L,IK)-DO*VF(L1,IK))+DO*VFB(L2,IK)*VF(L1,IK))+AN(KK,2,I)*VF(L2,IK)*2.0*VF(L,IK)+DO*VF(L1,IK))
A(K1,MA-1)=A(K1,MA-1)+AN(KK,1,I)*(-2.0*P*VF(L1,IK)+VF(L2,IK)*(C2*VF(L2,IK)/2.0-(2.0+DO)*VF(L,IK)*CT-DO*(VF(L1,IK)*CT+VFB(L1,IK))-2.0*VFB(L,IK))-VF(L,IK)*2.0*VFB(L2,IK)+VF(L,IK)+DO*VF(L1,IK))-DO*VFB(L2,IK)*VF(L1,IK))+AN(KK,2,I)*VF(L2,IK)*(-2.0*VF(L,IK)-DO*VF(L1,IK))
A(K1,MA)=A(K1,MA)+AN(KK,1,I)*(-VF(L2,IK)*VF(L2,IK)*1.5*CT+3.0*VFB(L2,IK))+VF(L,IK)*VF(L,IK)*CT+2.0*VFB(L,IK)+DO*(VF(L1,IK)*CT+VFB(L1,IK))+FO*VF(L1,IK))+AN(KK,2,I)*(-VF(L,IK)*VF(L,IK))+VF(L,IK)*VF(L,IK)+DO*VF(L1,IK))-1.5*VF(L2,IK)*?
IF (ICN.EQ.-10) GO TO 70
A(K,MA+1)=A(K,MA+1)+AN(KK,1,I)*(-EO*(VF(L2,IK)*CT-VFB(L,IK)+VFB(L2,IK))-VF(L2,IK)*EO1)/2.0-AN(KK,2,I)*VF(L2,IK)*FO/2.0
A(K1,MA-1)=A(K1,MA-1)+AN(KK,1,I)*EO*(VF(L2,IK)*CT+VFB(L2,IK)+VF(L1,IK))+VFB(L2,IK)*FO/2.0+AN(KK,2,I)*VF(L2,IK)*EO/2.0
A(K1,MA)=A(K1,MA)+AN(KK,1,I)*FO*(VF(L,IK)*CT+VFB(L,IK))+VF(L,IK)*FO/2.0-AN(KK,2,I)*VF(L,IK)*2.0*P*VF(L1,1)
A(K,MA+1)=A(K,MA+1)+AN(KK,1,I)*2.0*P*VF(L1,1)
A(K1,MA-1)=A(K1,MA-1)+AN(KK,1,I)*2.0*P*VF(L1,1)
70 CONTINUE
V(K)=-2.0*VF(L2,IK)
V(K1)=2.0*(1.0+VF(L,IK)+VF(L1,IK))
A(K,JAC)=A(K,JAC)+2.0*P*VFB(L2,IK)-VF(L,IK)-DO*VF(L1,IK)+(1.0-2.0*P)*VF(L2,IK)*CT
A(K,JAC+1)=A(K,JAC+1)-DO*VF(L2,IK)
A(K1,JAC-1)=A(K1,JAC-1)-2.0*P*CT+VF(L2,IK)+VF(L,IK)*CT+VFB(L,IK)
1+DO*(VFB(L2,IK)*CT+VFB(L1,IK)*CT+VFB(L1,IK))

```

```

1 A(K,JAD)=A(K,JAC)+2.0*P*(VF(L1,IK)+VF(L2,IK)*CT)-VF(L2,IK)*CT+0.5*
2 4*VF(L2,IK)+2.0*P*CT*VF(L,IK)+P*VF(L1,IK)*CT+VF(L1,IK)*VF(L2,IK)+VF(L
3 (L,IK)*CT)+2.0*VF(L,IK)+VF(L,IK)*VF(L,IK)-2.0*VF(L2,IK)+DO*VF(L
3 1,IK))-P*VF(L1,IK)*VF(L2,IK)
3 A(K,JAD+1)=A(K,JAC+1)+2.0*P*VF(L2,IK)+VF(L2,IK)*(-VF(L2,IK)*CT+2.
1 0*(VF(L,IK)-VF(L2,IK))+DO*(VF(L1,IK)+VF(L,IK)-VF(L2,IK)))
3 A(K1,JAC-1)=A(K1,JAC-1)-2.0*P*VF(L,IK)*CT+VF(L2,IK)*CT+VF(L2,IK)*
3 1K)/2.0-2.0*VF(L,IK)+3.0*VF(L2,IK)-DO*(VF(L1,IK)+VF(L,IK)*CT)-
2 VF(L,IK)*VF(L,IK)*CT+2.0*VF(L,IK)+DO*(VF(L1,IK)*CT+VF(L,IK)+V
3 F(L2,IK)*CT)-DO*VF(L,IK)*VF(L1,IK)
3 A(K1,JAC)=A(K1,JAC)-2.0*P*(VF(L,IK)+VF(L1,IK)+VF(L2,IK)*(-P3*VF(
1 I2,IK)-(2.0+DO)*(VF(L,IK)*CT+VF(L,IK))-DO*(VF(L1,IK)*CT+VF(L1,
2 K)))-VF(L,IK)*(2.0+P)*VF(L2,IK)-DO*VF(L2,IK)*VF(L1,IK)
3 IF(ICN.FO.-10) GO TO 100
A(K,JAC)=A(K,JAC)+EC*(VF(L2,IK)*CT-VF(L,IK)+VF(L2,IK))/2.0+VF(L2,
1 IK)*FO1/2.0
A(K,JAC+1)=A(K,JAC+1)-VF(L2,IK)*EO/2.0
A(K1,JAC-1)=A(K1,JAC-1)+EO*(VF(L2,IK)+VF(L,IK)*CT+VF(L,IK))/2.0+V
1 F(L,IK)*EO1/2.0
A(K1,JAC)=A(K1,JAC)+EO*(VF(L2,IK)*CT+VF(L2,IK))/2.0+VF(L2,IK)*EO1
1/2.0
A(K,JAD)=A(K,JAC)-2.0*P*(VF(L1,1)+VF(L2,1)*CT)
A(K,JAD+1)=A(K,JAC+1)-2.0*P*VF(L2,1)
A(K1,JAC-1)=A(K1,JAC-1)+2.0*P*VF(L,1)*CT
A(K1,JAC)=A(K1,JAC)-2.0*P*(VF(L,1)+VF(L1,1))
V(K)=V(K)+2.0*(C1-CV(L1,1))*VF(L2,1)+VF(L1,1)*VF(L2,1)+VF(L2,1
1 K)*VF(L1,1)
V(K1)=V(K1)-2.0*(VF(L,1)+VF(L1,1)-VF(L,1))*VF(L1,1)+VF(L1,1)*VF(
1 L,1)+VF(L1,1)*VF(L1,1)*VF(L,IK)-VF(L1,IK))
100 CONTINUE
110 CONTINUE
RETURN
END
** *DFCK STRNCF
SUBROUTINE STRNCF (X,NX,UF,NUF,KUF,UFK,KUUF,KUFP,IKK)
DIMENSION X(NX),UF(NCF,KUF),UFK(NUFB,KUFP)
COMMON /COM1/ AN(7,4,12),ITYPE,ILN(7),IPK(7),JSA(7),JEN(7),KROE(7)
COMMON /COM2/ DO,D1,E2,D3,D4,AL,THETA,PCL,H,AT,IFR,IUN
LEVEL 2,UF,UFH
PA=0.0
DO 100 KK=1,ITYPE
CALL FDATA (KK,ITCL,MID,ISTART,IFIN)
FO 90 IJ=ISTART,IFIN
PA=PA+1.0
PHI=PA*PI
S=SIN(PHI)
C=COS(PHI)
CT=C/S
K1=3*IJ-2
K2=K1+1
K3=K1+2
IJ=IJ*2+3
I4=IJ+1
ISU=IJ-2*MI
U1=0.0
U2=0.0
W1=0.0
W2=0.0
DO 90 K=1,ITCL
ICU=ISU+2*K
ICW=ICU+1
U1=U1+AN(KK,1,K)*X(ICW)
U2=U2+AN(KK,2,K)*X(ICU)
W1=W1+AN(KK,1,K)*X(ICW)
W2=W2+AN(KK,2,K)*X(ICW)
80 CONTINUE
UF(K1,IKK)=U1+X(I4)
UF(K2,IKK)=X(IU)*CT+X(IW)
UF(K3,IKK)=X(IU)-K1
UFK(K1,IKK)=U2+W1
UFK(K2,IKK)=W1+U1*CT-X(IU)/(S*S)
UFK(K3,IKK)=U1-W2
90 CONTINUE
100 CONTINUE
RETURN
END
** *DECK RCKSUP
SUBROUTINE RCKSUP (FV,NFV,AP,KAR,AI,IN,IABW)
DIMENSION FV(NFV),AP(12,KAR)
C TO FIND THE FIRST AND LAST 4/6 NODAL VALUES FROM THE BOUNDARY CONDITIONS
C ON ENTRY FV CONTAINS THE REDUCED VECTOR STARTING WITH FV(1)
C ON EXIT FV CONTAINS THE FULL VECTOR STARTING WITH FV(1)
IF(AI,IT,0.0) GO TO 10
IF(AI,EO,0.0) GO TO 10
ID=6
IC=3
GO TO 20
10 IC=4
IC=2
20 CONTINUE
IAB=IAPW-ID
IG=IAB+1
NNA=IC*(IN-2)
KJ=NNA+1
DO 30 JJ=1,NNA
J=KJ-JJ
FV(J+IC)=FV(J)
DO 50 IJ=1,ID
REMP=0.0
TEMP=0.0
DO 40 J=1,IAB
REMP=REMP+AB(IC+IJ,IC-J)*FV(NNA+ID+IJ-J)
TEMP=TEMP+AB(IC+1-IJ,IC+J)*FV(IC+1-IJ,J)
40 IHC=NNA+ID+IJ
IF(IHC.EQ.104,AND,AI,LT,0.0) REMP=REMP-1.0
FV(NNA+ID+IJ)=-REMP/AB(IC+IJ,IG)
50 FV(IC+1-IJ)=-TEMP/AB(IC+1-IJ,ID)

```



```

SUPRCUTIME FDDATA (KK,ITDL,MID,ISTART,IFIN)
COMMON/COM1/ AN(7,4,12),ITYPE,ILN(7),IMK(7),JSN(7),JEN(7),KROE(7)
COMMON/COM4/ IN,N1,A2
ITCL=IN(KK)
MID=IMN(KK)
10 IF(KRCE(KK)) 10,20,30
   ISTART=JSN(KK)
   IFIN=JEN(KK)
   RETURN
20 ISTART=JSN(KK)
   IFIN=IN-2-JEN(KK)
   RETURN
30 ISTART=IN-2-JSN(KK)
   IFIN=IN-2-JEN(KK)
   RETURN
END
*** *DECK FUNVEC
SUPRCUTIME FUNVEC (UF,UFB,KUF,MUF,UFC,MUFC,X,Y,NY,Z,NZ,FF,IPR,IFT,
CLHC,EF,FD,IN,PL,ICHS,IFAIL,ELMT)
DIMENSION UF(NUF,KUF),UFB(NUB,KUF),UFC(RUFC,KUF),PF(KUF),X(NY),Y(NZ)
COMMON/COM5/ VF(147,20),VFB(147,20),VFC(106,20),PFC(20),EFC(20)
C,GF(147)
LEVEL 2,UF,UFB,UFC
CK2=1.0/(10.0**6)
A1=E+FF
IF(A1.GT.ELMT.UR.A1.IT.CK2) GO TO 130
N1=3*(IN-2)
N2=2*(I+2)
IK=0
KK=0
IF(IFT.FO.0) GO TO 40
DO 1 IJ=1,20
  I=21-IJ
  IF (A1.LF.EFC(I)) IK=I
1 CONTINUE
  KK=(IK-1)*INC
  PL=PFC(IK)
  IF(IK.GT.1) A1=A1-EFC(IK-1)
  IF(ICHS.LT.0) GO TO 80
  IF (ICHS.EQ.2) GO TO 20
  DO 10 I=1,N
    X(I)=VF(I,IK)
10  Y(I)=VFB(I,IK)
    IF (ICHS.EQ.1) GO TO 80
20  DO 30 I=1,N2
    Z(I)=VFC(I,IK)
    GO TO 80
30  PL=0.0
    IF(ICHS.LT.0) GO TO 80
    IF (ICHS.EQ.2) GO TO 60
    DO 50 I=1,N

```

```

FDDATA 2
FDDATA 3
FDDATA 4
FDDATA 5
FDDATA 6
FDDATA 7
FDDATA 8
FDDATA 9
FDDATA 10
FDDATA 11
FDDATA 12
FDDATA 13
FDDATA 14
FDDATA 15
FDDATA 16
FDDATA 17
FUNVEC 1
FUNVEC 2
FUNVEC 3
FUNVEC 4
FUNVEC 5
FUNVEC 6
FUNVEC 7
FUNVEC 8
FUNVEC 9
FUNVEC 10
FUNVEC 11
FUNVEC 12
FUNVEC 13
FUNVEC 14
FUNVEC 15
FUNVEC 16
FUNVEC 17
FUNVEC 18
FUNVEC 19
FUNVEC 20
FUNVEC 21
FUNVEC 22
FUNVEC 23
FUNVEC 24
FUNVEC 25
FUNVEC 26
FUNVEC 27
FUNVEC 28
FUNVEC 29
FUNVEC 30
FUNVEC 31
FUNVEC 32
FUNVEC 33
FUNVEC 34
FUNVEC 35
FUNVEC 36

```

```

50  X(I)=0.0
    Y(I)=0.0
    IF (ICHS.EQ.1) GO TO 80
60  DO 70 I=1,N2
    Z(I)=0.0
70  DO 120 I=1,IPR
    AF=A1**I
    PI=PL+FF(I+KK)*AF
    IF (ICHS.LT.0) GO TO 120
    IF (ICHS.EQ.2) GO TO 100
    DO 90 J=1,N
      X(J)=X(J)+UF(J,I+KK)*AF
      Y(J)=Y(J)+UFB(J,I+KK)*AF
    IF (ICHS.EQ.1) GO TO 120
100  DO 110 J=1,N2
    Z(J)=Z(J)+UFC(J,I+KK)*AF
120 CONTINUE
    RETURN
130 IF(A1.GT.ELMT) IFAIL=1
    IF(A1.IT.CK2) IFAIL=2
    RETURN
END
*** *DECK SLVITR
SUPRCUTIME SLVITR (A,HA,NA,KA,KHA,UF,MUF,KUF,UFB,MUFB,KUFB,U,NU,KU
C,Z1,Z2,NZ,X,NX,V,NV,F,HP,NUM,IFAIL,AP,KAB,NIK,Z3,Z4,V4,FF,ESN,EPCL
C,E,UFC,MUFC,IFI,LNC)
DIMENSION A(NA,KA),FA(NA,KHA),UF(MUF,KUF),UFB(MUFB,KUFB),U(NU,KU)
CZ1(NZ),Z2(NZ),X(NX),V(NV),F(HP),AP(12,KAE),Z3(NZ),Z4(NZ),V4(NZ),FF
C(KUF),UFC(MUFC,KUF)
LEVEL 2,UF,UFB,UFC
C SLVITR CONTROLS THE ITERATIVE ROUTINES DIRITR AND INVITR WHICH SOLVE THE
C SECONDARY PATH EIGEN VALUE PROBLEM. THE A MATRIX IS UNCHANGED HA IS USFC
C TO STORE THE A MATRIX BEING WORKED ON
IFNV=0
DO 40 EKK=1,NUM
  PIF=MKK
  CALL DIRITR (A,HA,NA,KA,KHA,X,NX,UF,KUF,UFB,MUFB,KUFB,U,NU,KU
CZ1,Z2,NZ,V,NV,IFAIL,NIK,Y,AP,KAB,PF,FSN,EPCL,F,UFC,MUFC,IFT,LNO,IF
CIV)
  IF(IFAIL.NE.0) GO TO 20
10  CALL INVITR (A,HA,NA,KA,KHA,X,NX,Z1,Z2,NZ,V,NV,IFAIL,NIK,Y,U,NU,KU
C,UF,MUF,KUF,UFB,MUFB,KUFB,F,HP,AP,KAB,Z3,Z4,V4,FF,FSN,EPCL,F,UFC,
CNUFC,IFI,LNC,IFNV)
  IF(IFAIL.NE.0) GO TO 30
  GO TO 40
20  WRITE (6,8001)
  IFAIL=0
  GO TO 10
30  NIK=NIK-1
  WRITE (6,8002) NIK
  RETURN
40  CONTINUE
8001 FCPMAT (IH,10X,6HCIRFCT ITERATION HAS FAILED, INVERSE ITERATION
C WILL BE TRIED )
8002 FCPMAT (IH,10X,34HINVERSE ITERATION HAS FAILED WITH ,I3,IX,15H-E-V

```

```

FUNVEC 37
FUNVEC 38
FUNVEC 39
FUNVEC 40
FUNVEC 41
FUNVEC 42
FUNVEC 43
FUNVEC 44
FUNVEC 45
FUNVEC 46
FUNVEC 47
FUNVEC 48
FUNVEC 49
FUNVEC 50
FUNVEC 51
FUNVEC 52
FUNVEC 53
FUNVEC 54
FUNVEC 55
FUNVEC 56
FUNVEC 57
FUNVEC 58
SLVITR 1
SLVITR 2
SLVITR 3
SLVITR 4
SLVITR 5
SLVITR 6
SLVITR 7
SLVITR 8
SLVITR 9
SLVITR 10
SLVITR 11
SLVITR 12
SLVITR 13
SLVITR 14
SLVITR 15
SLVITR 16
SLVITR 17
SLVITR 18
SLVITR 19
SLVITR 20
SLVITR 21
SLVITR 22
SLVITR 23
SLVITR 24
SLVITR 25
SLVITR 26
SLVITR 27
SLVITR 28
SLVITR 29
SLVITR 30
SLVITR 31
SLVITR 32
SLVITR 33

```

```

*DECK DIRITR
SUBROUTINE DIRITR (A,HA,NA,KHA,X,NX,UF,XUF,NUF,KUF,UFB,NUFB,KUFB,U,
CNU,KU,Z1,Z2,NZ,V,NV,IFAIL,NTK,Y,AB,KAP,FF,FSN,ELMT,F,DFC,NDFC,IFT,
CLNC,IFNV)
DIMENSION A(HA,KA),HA(MA,KHA),X(NX),UF(MLF,KUF),UFB(NUFB,KUFB),
CU(MU,KU),Z1(MZ),Z2(NZ),V(NV),AB(12,KAB),FF(KUF),DFC(NDFC,KUF)
COMMON /COM2/ DO,C1,C2,D1,D4,AL,THE1A,PC,H,AT,IFR,ION
COMMON /COM3/ JAC,JAW,JABW,IE,ID,IC,ET,IZAB
COMMON /COM4/ IN,N1,N2
LEVEL=2,UF,UFB,DFC
TO PERFORM DIRECT ITERATION WHEN THE LEFT SIDE IS A BANDD MATRIX A (HA)
AND THE RHS IS CALCULATED AS A SINGL VECTOR V BY SDRHS SUB-DOMINANT E-VA
LUES/VECTORS ARE FOUND BY ORTHOGONALIZATION THE SMALLEST E-VAL IS FOUND
FIRST
ARGUMENTS *****
ARGUMENTS *****
A- LHS MATRIX(UNCHNGD), HA-WRKSPC(TRIANG DECOMT OF A ON EXIT), UF- FUND
PATH STRESS COMPONENTS (UNCHNGD) U- PREVIOUSLY FOUND VECTORS (USED BY
ORTHO. (UNCHNGD), V-WRKSPC,X- UNDEFINIC (APPRX E-VECT,NORM) Y- UNDEFINIC
(APPRX E-VAL) NTK- NO OF E-VALS BEING FOUND. OTHERS AS DEFINED BY MAIN
PROGRAM
THE FOLLOWING CCUID PF DEFINED ELSEWHERE
CK2=1.0/(10.0**6)
IQ=LRC
IF(IFT.EQ.0) IQ=IPR
ICHS=1
IFFV=0
YZ=0.0
LMT=30
CHK1=1.0/(10.0**3)
ISTEP=1
IWILL=3
LMT - NO. OF ITERATIONS THAT WILL BE ALLOWED ON FIRST TRY,CHK1 - A
CONVCRACY REQUIRED FOR E-VAL ISTEP - NO OF ITERATIONS PERFORMED PER
ICOUNT=ISTEP-1
FT=1.0
WITH CRTINGS. IWILL - NO OF ATTEMPTS I.E.40-10-10--FAIL.
ICID=0
Y=0.295*(E+0.05)
M1=0
DO 10 I=1,N1
DO 10 J=1,JAW
HA(I,J)=A(I,J)
10 CONTINUE
DO 30 I=1,N2
X(I)=1.0
30 CONTINUE
START OF DIRECT ITERATION
40 M1=M1+1
ICOUNT=ICOUNT+1
IF(M1.GT.LMT) GO TO 70
CALL FNVFC (UF,UFB,KUF,NUF,DFC,NDFC,Z1,Z2,NZ,V,NV,PF,IQ,IFT,LNC,Y
C YZ,IN,PL,ICHS,IFNV,ELMT)
IF(IFNV.NE.0) GO TO 70
CALL SDRHS(Z1,Z2,NZ,V,NV,X,NX,PL)
DO 45 I=1,N1
V(I)=V(I)/Y
45 CALL VACTR (HA,V,NA,A1,JAW,ET,KHA,NV)
FT=0.0
IF SUB-DOMINANT E-VECT ORTHOG
IF (M1.GT.1.AND.ICOUNT.GE.ISTEP) CALL CRTHO (NTK,ISTEP,ICOUNT,M1
C,V,U,KU,NV,KU)
FIND LARGEST ELEMENT OF V, V(IJJ)
SAV=0.0
DO 50 I=1,N1
TEMP=ABS(V(I))
IF(TEMP.GE.SAV) GO TO 50
SAV=TEMP
IJJ=I
50 CONTINUE
TEMP=V(IJJ)
DO 60 I=1,N1
X(I)=V(I)/TEMP
60 CONTINUE
TEST FOR CONVERGENCE ON E-VALUE
HOLD=1.0/TEMP
SAV=ABS((Y-HOLD)/HOLD)
Y=HOLD
CALL BCKSUB (X,NX,AB,KAB,A1,IN,JABW)
IF(SAV.GT.CHK1) GO TO 40
WRITE (6,8001) CHK1,M1,Y
RETURN
70 CONTINUE
IF(IFNV.EQ.0) GO TO 75
IFFV=IFFV+1
TH1=ELMT-ELMT/50.0
IF (Y.LE.CK2) TH1=0.6*ELMT
FSN=Y
Y=TH1
IFNV=0
IF(IFV.LE.4) GO TO 40
WRITE (6,8003) ELMT,FSN
IFAIL=IFAIL+1
RETURN
75 CONTINUE
WRITE (6,8002) CHK1,LMT,Y
ICID=ICID+1
IF(ICID.GE.IWILL) GO TO 80
LMT=10
IC0=2*(ICID/2)
IDO=ICID-IC0
LMT=LMT+IDO
M1=0
GO TO 40
80 IFAIL=IFAIL+1
RETURN
8001 FORMAT (1H ,28)CONVERGENCE ON E-VALUE (ERR= ,E10.3,8H) AFTER ,13,1
DIRITR 1
DIRITR 2
DIRITR 3
DIRITR 4
DIRITR 5
DIRITR 6
DIRITR 7
DIRITR 8
DIRITR 9
DIRITR 10
DIRITR 11
DIRITR 12
DIRITR 13
DIRITR 14
DIRITR 15
DIRITR 16
DIRITR 17
DIRITR 18
DIRITR 19
DIRITR 20
DIRITR 21
DIRITR 22
DIRITR 23
DIRITR 24
DIRITR 25
DIRITR 26
DIRITR 27
DIRITR 28
DIRITR 29
DIRITR 30
DIRITR 31
DIRITR 32
DIRITR 33
DIRITR 34
DIRITR 35
DIRITR 36
DIRITR 37
DIRITR 38
DIRITR 39
DIRITR 40
DIRITR 41
DIRITR 42
DIRITR 43
DIRITR 44
DIRITR 45
DIRITR 46
DIRITR 47
DIRITR 48
DIRITR 49
DIRITR 50
DIRITR 51
DIRITR 52
DIRITR 53
DIRITR 54
DIRITR 55
DIRITR 56
DIRITR 57
DIRITR 58
DIRITR 59
DIRITR 60
DIRITR 61
DIRITR 62
DIRITR 63
DIRITR 64
DIRITR 65
DIRITR 66
DIRITR 67
DIRITR 68
DIRITR 69
DIRITR 70
DIRITR 71
DIRITR 72
DIRITR 73
DIRITR 74
DIRITR 75
DIRITR 76
DIRITR 77
DIRITR 78
DIRITR 79
DIRITR 80
DIRITR 81
DIRITR 82
DIRITR 83
DIRITR 84
DIRITR 85
DIRITR 86
DIRITR 87
DIRITR 88
DIRITR 89
DIRITR 90
DIRITR 91
DIRITR 92
DIRITR 93
DIRITR 94
DIRITR 95
DIRITR 96
DIRITR 97
DIRITR 98
DIRITR 99
DIRITR 100
DIRITR 101
DIRITR 102
DIRITR 103
DIRITR 104
DIRITR 105
DIRITR 106
DIRITR 107

```

```

8003 FORMAT (1H,5X,29H) OUTSIDE OF FUNVEC RANGE, 0- ,E10.4,2X,2HY=,
1F10.4)
CIRITR 110
CIRITR 111
CIRITR 112
CIRITR 113
*** *DFCK INVITR 1
SUBROUTINE INVITR (A,HA,NA,KA,KHA,X,NX,Z1,Z2,NZ,V,NV,IFAIL,NIK,Y,
C U,NU,KU,UF,UUF,KUF,UFP,NUFP,KUFP,F,RF,AR,KAR,Z3,Z4,V4,PF,FSN,EPC1,
C UFC,UFC,NUFC,IFT,LNC,IFNV)
C DIMENSION A(NA,KA),HA(NA,KHA),X(NX),Z1(NZ),Z2(NZ),V(NV),U(NU,KU),
C UF(UF,KUF),UFP(NUFP,KUFP),P(NP),AP(12,PAP),Z3(NZ),Z4(NZ),V4(NZ)
C ,FF(KUF),UFC(NUFC,KUF)
C COMMON/COM2/ DO,D1,D2,D3,D4,AL,THETA,PCL,H,AT,TFR,ION
C COMMON/COM3/ JAC,JAW,JAW,IF,ID,IC,ET,IZAP
C COMMON/COM4/ IN,N1,N2
LEVEL 2,UF,UFP,UFC
TO PERFORM INVERSE ITERATION WITH MULTIPLE SHIFTS OF ORIGIN, WHEN THE LHS
IS A PARCELD MATRIX A AND THE APPROX E-VAL IS GIVEN BY Y AND INITIAL E-VECT
BY X. THE RHS IS CALCULATED BY SDRHS AS A SINGLE VECT V AND THE NEW LHS
PARCELD MATRIX BY SDRHS. ORTHOG IS USED TO FIND THE SUB-DOM E-VECT INITIAL
LY AND DROPPED (AS IT MAY INTRODUCE SIGNIFICANT ERRORS) FOR THE FINAL SET
OF ITERATIONS. F.G. SHIFT OF ORIGIN BY SDRHS TO Y ITERATION TO 10**-6
ACCURACY USING CRTHOG THEN NEW SHIFT OF ORIGIN BY SDRHS AND ITERATION TO
10**-9 WITHOUT CRTHOG.
C ARGUMENTS
C ARCHMENTS
A- LHS MATRIX (UNCHGD) HA-WRKSPACE, UF-FUND PATH STRESS COMPONENTS (UNCHG)
U- E-VECTORS (NEW VECT ADDED AS U( ,NIK), V-WRKSEC, X-APPROX E-VECTOR (FINA
L E-VECT), Y- APPROX E-VAL, P- E-VALS (NEW E-VAL ADDED AS P(NIK))
C THERE AS DEFINED IN THE CALLING PROGRAM
THE FOLLOWING COULD BE DEFINED ELSEWHERE.
CK2=1.0/(10.0**6)
IQ=LNC
IF(IFT.EQ.0) IQ=TPR
ICHS=1
IFFV=0
IZAP=1
LMT=40
CHK1=1.0/(10.0**5)
CHK2=1.0/(10.0**12)
ISTEP=1
IWILL = 5
KK12=1
NJK=NIK
PT=1.0
ITEST=0
ICOUNT=ISTEP-1
ICID=1
M1=0
Z=Y
PC=0.0
C CHK1-ALLOWED ERR IN E-VALUE AND E-VECTOR , CHK2 ELEMENT OF E-VECT
C LESS NOT CHECKED, ISTEPNO OF ITERATIVE STEPS BETWEEN ORTHOG, IWILL
C NO. OF ORIGIN SHIFTS TO BE TRIED. LMTNO OF ITERATIONS BEFORE SHIFT
INVITR 2
INVITR 3
INVITR 4
INVITR 5
INVITR 6
INVITR 7
INVITR 8
INVITR 9
INVITR 10
INVITR 11
INVITR 12
INVITR 13
INVITR 14
INVITR 15
INVITR 16
INVITR 17
INVITR 18
INVITR 19
INVITR 20
INVITR 21
INVITR 22
INVITR 23
INVITR 24
INVITR 25
INVITR 26
INVITR 27
INVITR 28
INVITR 29
INVITR 30
INVITR 31
INVITR 32
INVITR 33
INVITR 34
INVITR 35
INVITR 36
INVITR 37
INVITR 38
INVITR 39
INVITR 40
INVITR 41
INVITR 42
INVITR 43
INVITR 44
INVITR 45
INVITR 46
INVITR 47
INVITR 48
INVITR 49

```

```

C CF ORIGIN
C SHIFT OF ORIGIN I.F. SET UP HA=A+Y*B
1 FC 10 I=1,N1
GO 10 J=1,JAW
10 HA(I,J)=A(I,J)
CALL FUNVEC (UF,UFP,KUF,UUF,UFC,NUFC,Z3,Z4,NZ,V,NV,PF,IQ,IFT,LNC,Z
C ,FC,IN,PI,ICHS,IFNV,EPC1)
CALL SDRHS (HA,NA,KHA,Z3,Z4,NZ,PL)
CALL REDUCE (HA,AR,KA,KHA,KAP,N1,A1,JAW,JAW,IZAP,Z2,NZ)
FC=Z*CHK1*50.0
Z=Y+FC
C START OF INVERSE ITERATION
20 M1=M1+1
ICOUNT=ICOUNT+1
IF(M1.GT.LMT) GO TO 90
CALL FUNVEC (UF,UFP,KUF,UUF,UFC,NUFC,Z1,Z2,NZ,V,NV,PF,IQ,IFT,LNC,Y
C ,FC,IN,PI,ICHS,IFNV,EPC1)
IF(IFNV.NE.0) GO TO 60
CALL SDRHS(Z1,Z2,NZ,V,NV,X,NX,PL2)
CALL SDRHS(Z3,Z4,NZ,V4,NV,X,NX,PI)
FC 25 I=1,N1
25 V(I)=(V(I)-V4(I))/FC
CALL MAC7H (HA,V,NA,N1,JAW,PT,KHA,NV)
P1=0.0
IF SUB-DOMINANT E-VAL/VECT ORTOG
IF (NJK.GT.1.AND.ICOUNT.GE.ISTEP) CALL CRTHOG (NIK,ISTEP,ICOUNT,N1
C ,V,U,KU,NV,KU)
C FIND LARGEST ELEMENT OF V, V(IJJ)
SAV=0.0
DO 30 I=1,N1
TEMP=ABS(V(I))
IF (TEMP.LE.SAV) GO TO 30
SAV=TEMP
IJJ=I
30 CONTINUE
TEMP=V(IJJ)
PC=1.0/TEMP
TEST FOR CONVERGENCE ON E-VAL
K11=0
KLM=0
IKK=ITEST
HCLD=Y+1.0/TEMP
SAV=ABS((Z-HCLD)/HCLD)
Z=HCLD
IF (SAV.GT.CHK1) K11=1
TEST FOR CONVERGENCE ON E-VECTOR, AND COPY V ONTO X
DO 40 I=1,N1
V(I)=V(I)/TEMP
HOLD=ABS(V(I))
IF (HOLD.LE.CHK2) GO TO 40
HOLD=ABS((X(I+1D)-V(I))/V(I))
IF (HOLD.GT.CHK1) KLM=2
40 X(I)=V(I)
IKK=IKK+K11+KLM
CALL PCKSUB (X,NX,AP,KAP,AT,IN,JAW)
INVITR 50
INVITR 51
INVITR 52
INVITR 53
INVITR 54
INVITR 55
INVITR 56
INVITR 57
INVITR 58
INVITR 59
INVITR 60
INVITR 61
INVITR 62
INVITR 63
INVITR 64
INVITR 65
INVITR 66
INVITR 67
INVITR 68
INVITR 69
INVITR 70
INVITR 71
INVITR 72
INVITR 73
INVITR 74
INVITR 75
INVITR 76
INVITR 77
INVITR 78
INVITR 79
INVITR 80
INVITR 81
INVITR 82
INVITR 83
INVITR 84
INVITR 85
INVITR 86
INVITR 87
INVITR 88
INVITR 89
INVITR 90
INVITR 91
INVITR 92
INVITR 93
INVITR 94
INVITR 95
INVITR 96
INVITR 97
INVITR 98
INVITR 99
INVITR 100
INVITR 101
INVITR 102
INVITR 103
INVITR 104

```

```

IF (IKK.FO.1) WRITE (6,8001) CHK1,M1,Z
IF (IKK.FO.2) WRITE (6,8002) CHK1,M1
IFST=10
GO TO 20
CONTINUE
C 50 WILL COMPUTE ORIGIN KCH AND PERFORM FINAL ITERATIONS WITHOUT
IF (KK12.EQ.2) GO TO 60
WRITE (6,8003) CHK1,M1,Z
NJK=1
KK12=KK12+1
CHK1=CHK1/(10.0**3)
CHK2=CHK2/(10.0**3)
FC=0.0
FT=1.0
IFST=0
M1=0
Y=Z
LMT=40
ICID=1
GO TO 1
CONTINUE
C 60 REFORM NEW E-VAL/VECT
P(NIK)=Z
DO 70 I=1,N1
70 U(I,NIK)=V(I)
WRITE (6,8003) CHK1,M1,Z
C TO COMPUTE AND STORE EUCLIDIAN NORM OF NEW VECTOR
IF (NIK.EQ.KU) RETURN
U(N1-NIK,KU)=0.0
DO 80 I=1,N1
80 U(N1-NIK,KU)=U(N1-NIK,KU)+V(I)*V(I)
RETURN
90 CONTINUE
IF (IFNV.FO.0) GO TO 95
FSF=Y+FC
FC=EPCL-FPCL/25.0-Y
IF (Z,IF,CK2) PC=0.5*EPCL-Y
IFNV=0
IFFV=IFFV+1
IF (IFFV.LE.4) GO TO 20
WRITE (6,8006) EPCL,ESH
IFAIL=IFAIL+2
RETURN
95 WRITE (6,8004) LMT,Z
IF (ICID.EQ.1WILL) GO TO 100
FT=1.0
IFST=0
M1=0
Y=Z
LMT=20
ICD=2*(ICID/2)
ICD=ICD-ID0

```

```

INVTR 108
INVTR 109
INVTR 110
INVTR 111
INVTR 112
INVTR 113
INVTR 114
INVTR 115
INVTR 116
INVTR 117
INVTR 118
INVTR 119
INVTR 120
INVTR 121
INVTR 122
INVTR 123
INVTR 124
INVTR 125
INVTR 126
INVTR 127
INVTR 128
INVTR 129
INVTR 130
INVTR 131
INVTR 132
INVTR 133
INVTR 134
INVTR 135
INVTR 136
INVTR 137
INVTR 138
INVTR 139
INVTR 140
INVTR 141
INVTR 142
INVTR 143
INVTR 144
INVTR 145
INVTR 146
INVTR 147
INVTR 148
INVTR 149
INVTR 150
INVTR 151
INVTR 152
INVTR 153
INVTR 154
INVTR 155
INVTR 156
INVTR 157
INVTR 158
INVTR 159

```

```

LMT=LMT+ID0
ICID=ICID+1
WRITE (6,8005) Z
GO TO 1
100 IFAIL=IFAIL+2
RETURN
8001 FORMAT(1H,10X,29HCONVERGENCE ON E-VALUE (ERR<,F10.3,8H) AFTER ,I
C3,1X,12HITERATIONS ,E12.5)
8002 FORMAT(1H,10X,30HCONVERGENCE ON F-VECTOR (ERR<,E10.3,8H) AFTER ,
C13,1X,12HITERATIONS )
8003 FORMAT(1H,10X,39HCOMPLETE CONVERGENCE, E-VAL/VECT (ERR<,E10.3,8
CH) AFTER ,I3,1X,12HITERATIONS ,E12.5)
8004 FORMAT(1H,10X,50HFAILED TO CONVERGE USING INVERSE ITERATION WITHI
CN ,I3,1X,17HITERATIONS F-VAL= ,E12.5)
8005 FORMAT(1H,10X,36HWILL TRY ANOTHER SPLIT OF CRICIN TO ,E12.5)
8006 FORMAT(1H,5X,29HY OUTSIDE OF FUNVEC RANGE, 0- ,F10.4,2X,2HY=,E10
1.4)
END
*DFCK SMDRHS
SUBROUTINE SMDRHS (Z1,Z2,NZ,V,NV,X,NX,P)
DIMENSION Z1(NZ),Z2(NZ),V(NV),X(NX)
COMMON/CCM1/ AN(7,4,12),ITYPE,ILN(7),IMN(7),JSM(7),JFN(7),KBCF(7)
COMMON/CCM2/ DO,D1,D2,D3,D4,AL,THETA,PCL,H,AI,TPR,TOM
COMMON /COM3/ JAF,JAW,JAW*,IE,ID,IC,ET,IZAP
COMMON /COM4/ IN,N1,N2
COMMON/COM5/ VF(147,20),VFP(147,20),VFC(106,20),FFC(20),EFC(20)
C SF(147)
AI2=AI*AI
PA=0.0
DO 30 I=1,N1
30 V(I)=0.0
AK=1.0
AJ=1.0
IF (ICN.EQ.20.OR.ICN.EQ.30) AK=2.0
IF (ICN.FO.20.OR.TCN.EQ.0) AJ=0.0
DO 120 KK=1,ITYPE
CALL FDATA(KK,ITCL,MID,ISTART,IFIN)
DO 110 IJ=ISTART,IFIN
PA=PA+1.0
PHI=PA*H
S=SIN(PHI)
C=COS(PHI)
CT=C/S
K=IC*IJ-IE
K1=K+IE/2
K2=K+IE
L=3*TJ-2
L1=L+1
L2=L+2
FO=VF(L,1)+(1.0-VF(L,1))*(VF(L2,1)**2)/2.0+DO*VF(L1,1)
FG=VF(L1,1)+C0*(VF(L,1)+(1.0-VF(L,1))*(VF(L2,1)**2)/2.0)
LO1=VFB(L,1)+(1.0-VF(L,1))*VFB(L2,1)+VFE(L,1)*(VF(L2,1)**
12)/2.0+DO*VFB(L1,1)
FO=(AK*EO-AJ*SF(L))/2.0
FG=(AK*EO-AJ*SF(L1))/2.0

```

```

INVTR 160
INVTR 161
INVTR 162
INVTR 163
INVTR 164
INVTR 165
INVTR 166
INVTR 167
INVTR 168
INVTR 169
INVTR 170
INVTR 171
INVTR 172
INVTR 173
INVTR 174
INVTR 175
INVTR 176
INVTR 177
SMDRHS 1
SMDRHS 2
SMDRHS 3
SMDRHS 4
SMDRHS 5
SMDRHS 6
SMDRHS 7
SMDRHS 8
SMDRHS 9
SMDRHS 10
SMDRHS 11
SMDRHS 12
SMDRHS 13
SMDRHS 14
SMDRHS 15
SMDRHS 16
SMDRHS 17
SMDRHS 18
SMDRHS 19
SMDRHS 20
SMDRHS 21
SMDRHS 22
SMDRHS 23
SMDRHS 24
SMDRHS 25
SMDRHS 26
SMDRHS 27
SMDRHS 28
SMDRHS 29
SMDRHS 30
SMDRHS 31
SMDRHS 32
SMDRHS 33
SMDRHS 34
SMDRHS 35
SMDRHS 36
SMDRHS 37

```

```

M2=M1+IF/2
M3=M1+IF
V(K)=V(K)-AN(KK,1,I)*X(M3)*(Z1(L)+D0*Z1(L1)-C2*Z1(L2))*CT-Z2(L2)
-2.0*P)*AN(KK,2,I)*X(M3)*Z1(L2)
1 V(K2)=V(K2)-AN(KK,1,I)*X(M1)*(Z1(L)+D0*Z1(L1)+D3*Z1(L2))*CT+Z2(
1 12)-2.0*P)*X(M3)*(Z1(L)+D0*Z1(L1))+C2*Z2(L1))-AN(KK,2
1 I)*X(M1)*Z1(L2)-X(M3)*Z1(L1))
2 V(K)=V(K)-AN(KK,1,I)*X(M1)*(Z1(L2)+D0*Z1(L1)+D3*Z1(L2))*CT)+X(
M3)*(Z2(L2)+D0*Z1(L1)+D3*Z1(L2))*Z1(L1)+D0*Z1(L1)+D0*Z1(L1)
2 L1)*CT+Z1(L2)*Z1(L2)+D0*Z1(L1)+D0*Z1(L1)+D0*Z1(L1)+D0*Z1(L1)
3 +D0*Z1(L1)-2.0*P)*Z1(L1))-AN(KK,2,I)*X(M1)*(-Z1(L2)**2)+X(M3)*
4 Z1(L2)*(2.0*Z1(L1)+D0*Z1(L1))
1 V(K2)=V(K2)-AN(KK,1,I)*X(M1)*(-Z2(L2))*Z1(L1)+D0*Z1(L1)+Z1
1 (L2)*D2*Z1(L2)+D0*Z1(L1)-D0*Z1(L1)-Z1(L1)+D0*Z1(L1)
2 -Z1(L2)*(2.0*P)*Z1(L1)+C0*Z1(L1))*CT-2.0*P*Z1(L1)+X(M3)*(-3.
3 0*Z2(L2)*Z1(L1)+D0*Z1(L1)+D0*Z1(L1)+D0*Z1(L1)+D0*Z1(L1)+D0*Z1(L1)
4 (-1.5*Z1(L2)**2+Z1(L1))*Z1(L1)+D0*Z1(L1)*Z1(L1))*CT))-AN(KK,2,I)*X(M1)
5 *(-Z1(L2))*Z1(L1)+D0*Z1(L1))+X(M3)*(-1.5*Z1(L2)**2+Z1(L1))*
6 Z1(L2)*Z1(L1))
IF(ICN.EQ.-10) GC TC 50
V(K)=V(K)-AN(KK,1,I)*X(M3)*(E0*Z1(L)-Z1(L2))*(E0*CT+E01)-Z2(L2)+F0
1)+AN(KK,2,I)*Z1(L2)+F0*X(M3)
V(K2)=V(K2)-AN(KK,1,I)*X(M1)*(Z1(L2)+F0*CT+F01)+E0*(Z1(L)+Z2(L2
1 I))-X(M3)*(Z1(L)+F0*CT+F01)+Z2(L)*F0))-AN(KK,2,I)*X(M1)*Z1(L2)*
2 F0-X(M3)*Z1(L)*F0
V(K)=V(K)-AN(KK,1,I)*2.0*X(M3)*P*VF(L1,1)
V(K2)=V(K2)-AN(KK,1,I)*2.0*X(M1)*P*VF(L1,1)
50 CONTINUE
IF(AI.EQ.0.0) GC TC 80
V(K)=V(K)-AI*AN(KK,1,I)*X(M2)*(-C2*(Z1(L)+Z1(L1)))/(S*2.0)-P*S)
V(K2)=V(K2)-AI*AN(KK,1,I)*X(M2)*(C3*Z1(L2)/(2.0*S)-P*C)
V(K1)=V(K1)-AN(KK,1,I)*X(M1)*AI*(C2*(Z1(L)+Z1(L1)))/(2.0*S)+F*S
1 +X(M2)*(D0*(Z1(L)+Z2(L1))+D0*(Z1(L)+Z1(L1))*CT)+X(M3)*AI*(D3*Z
2 1(L2)/(2.0*S)-P*C))-AN(KK,2,I)*X(M2)*E0*(Z1(L)+Z1(L1))
V(K)=V(K)-AI*AN(KK,1,I)*X(M2)*(-Z1(L2)*Z1(L1))/(2.0*S)+D2*(Z1(L)
1 **2+Z1(L1))*Z1(L1)+Z1(L1))*Z1(L1))/(2.0*S)-F*Z1(L1)*S)
2 V(K2)=V(K2)+AI*AN(KK,1,I)*X(M2)*(Z1(L2)+Z1(L1)+D2*Z1(L1))/2.0)/S
1 +P*Z1(L1)*C)
2 V(K1)=V(K1)-AN(KK,1,I)*(-AI*X(M1)*(-Z1(L2)*Z1(L2))/(2.0*S)+D2*(Z
1 (L1)+Z1(L1))*Z1(L1)+Z1(L1))/(2.0*S)-F*Z1(L1)*S)+X(M2)*(D0*Z
2 1(L2)+Z2(L2)+(1.0-3.0*P0)*Z1(L1)+Z1(L1)-D0*(Z1(L1)+Z1(L1))*Z2
3 (L1))+D0*Z1(L1)+Z1(L1)+Z1(L1)+Z1(L1)+Z1(L1)+Z1(L1)+Z1(L1)+Z1(L1)
4 CT/2.0)-AI*X(M3)*(Z1(L2)+Z1(L1)+C2*Z1(L1))/2.0)/S)*Z1(L1)*C))-AN
5 (KK,2,I)*D0*(D0*Z1(L2)+Z1(L1))*Z1(L1)+D0*(1.0-3.0*P0)*Z1(L1)**2-D0*Z1(L1)*Z
6 1(L1))*X(M2)
IF(ICN.EQ.-10) GC TC 80
V(K1)=V(K1)-AN(KK,1,I)*X(M2)*(E0*CT+E01)*Z1(L)+E0*Z2(L))-AN(K
1 K,2,I)*X(M2)*E0*Z1(L)
V(K)=V(K)-AN(KK,1,I)*X(M2)*AI*P*VF(L1,1)*S
V(K1)=V(K1)+AN(KK,1,I)*X(M1)*AI*P*VF(L1,1)*S-X(M3)*AI*P*VF(L1,1)
1 *C)
V(K2)=V(K2)-AN(KK,1,I)*X(M2)*AI*P*VF(L1,1)*C
80 CONTINUE
V(K)=V(K)-X(K+ID)*Z2(L2)+Z1(L2)*(1.0-2.0*P0)*CT-Z1(L)-D0*Z1(L1)
1 +2.0*P)*X(K2+ID)*E3*Z1(L2)
V(K2)=V(K2)-X(K+ID)*(Z1(L2)+Z2(L1)+D0*Z2(L1)+(E0*Z2(L2)+Z1(L1)+E0
1 *Z1(L1))*CT-2.0*P*CT)-X(K2+ID)*(C3*Z2(L2)+E3*Z1(L2))*CT-4.0*P)
V(K)=V(K)-X(K+ID)*(-0.5*E1*Z1(L2)+Z1(L2)+D0*Z2(L1)+Z1(L1)+CT-Z1(L2)
1 *(2.0*P0*Z1(L1)+D0*Z1(L1))*CT-Z2(L1)+D0*Z1(L1))-Z1(L2
2 )*(2.0*Z2(L1)+D0*Z2(L1))+Z1(L1)+Z1(L1)+Z1(L1)+Z1(L1)+Z1(L1)+Z1(L1)
3 Z2(L1)*C*S+(Z1(L1)-Z1(L1)+Z1(L2))*CT)*C)X(K2+ID)*(-Z1(L2))*Z1(L1)
4 +D0*(Z1(L1)+Z1(L1)+D0*Z1(L1)-Z1(L2))*CT)-2.0*P*(Z2(L1))*S*S-(Z1(L
5 )-Z1(L1)+Z1(L1))*CT)*C*S)
V(K2)=V(K2)-X(K+ID)*(Z1(L2)*(3.0*Z2(L2)-2.0*Z1(L1)-D0*Z1(L1)+C4*
1 Z1(L2)*CT/2.0)-D0*Z2(L1)*CT)+Z1(L1)+Z1(L1)+Z1(L1)+Z1(L1)+Z1(L1)*CT
2 -D0*Z2(L2)*CT-D0*Z1(L1)*CT)-D0*Z2(L1)+Z1(L1)-2.0*P*(Z1(L1))*CT+Z2
3 (L1)*C*S+(Z1(L1)-Z1(L1)+Z1(L2))*CT)*C)X(K2+ID)*(-Z1(L2))*Z1(L1)
4 +D0*(Z1(L1)+Z1(L1)+D0*Z1(L1)-Z1(L2))*CT)-D0*Z2(L1)+Z1(L1)+Z1(L1)
5 *(2.0*P0)*Z1(L1)+C4*Z1(L1))-2.0*P*(2.0*Z1(L1)+Z2(L1))*S*C+(Z1(L1)-
6 Z1(L1)+Z1(L2))*CT)*S*S)
IF(ICN.EQ.-10) GC TC 100
V(K)=V(K)+X(K+ID)*E0*Z1(L)-Z1(L2)*(E01+F0*CT)-Z2(L2)*E0)+X(K2+ID
1 )*Z1(L2)*E0
V(K2)=V(K2)-X(K+ID)*(Z1(L1)*(E0*CT+E01)+E0*(Z2(L1)+Z1(L2)))-X(K2+ID
1 )*(Z1(L2)*(F0*CT+E01)+Z2(L2)*F0)
V(K)=V(K)+2.0*X(K+ID)*(VF(L1,1)+VF(L2,1))*CT)*F+2.0*X(K2+ID)*P*VF(L
1 1)
V(K2)=V(K2)-2.0*X(K+ID)*P*VF(L1,1)*CT-2.0*X(K2+ID)*P*(VF(L1,1)+VF(L
1 1))
100 CONTINUE
IF(AI.EQ.0.0) GC TC 110
V(K)=V(K)+AI2*X(K+ID)*D0*(Z1(L)+Z1(L1))/(S*S)-AI*X(K1+ID)*(1.0-
1 3.0*P0)*Z1(L2)/(2.0*S)-D0*(Z1(L)+Z1(L1))*CT/S)-AI2*X(K2+ID)*D2*Z
2 1(L2)/(S*S*2.0)
V(K2)=V(K2)+AI2*X(K+ID)*C2*Z1(L2)/(2.0*S*S)-AI*X(K1+ID)*(D0*Z2(L
1 2)/S+(Z1(L1)+D0*Z1(L1))/S-C2*Z1(L2)*CT/(2.0*S)-P/S)-AI2*X(K2+ID)
2 *(Z1(L1)+D0*Z1(L1))/S*S)
V(K1)=V(K1)+AI*X(K+ID)*((3.0*P0-1.0)*Z1(L2)/(2.0*S)-D2*(Z2(L)+Z2
1 (L1))/(2.0*S)+D0*(Z1(L1)+Z1(L1))*CT/S)-X(K1+ID)*(D2*Z2(L2
2 )/2.0-(3.0*P0)*Z1(L1)/2.0-C3*Z1(L1)/2.0+D2*(3.0*Z1(L2)+Z2(L1)+Z2(L
3 1))*CT/2.0-D0*(Z1(L1)+Z1(L1))*CT*CT)+AI*X(K2+ID)*(-D2*(Z1(L2)+Z1(L
4 2))*CT)/(2.0*S)+(Z1(L1)+D0*Z1(L1))/S-2.0*P*S)
V(K)=V(K)+AI*X(K+ID)*(-1.0-2.0*P0)*Z1(L2)+Z1(L1))*Z1(L1)*(1.0-3.0*
1 P0)*Z1(L1)-2.0*P0*Z1(L1))/(2.0*S*S)-AI*X(K1+ID)*(-Z1(L2)+D0*Z2(L
2 )/2.0-(3.0*P0)*Z1(L1)/2.0+D2*Z1(L1))/S+(1.0-2.0*P0)*Z1(L2)
3 **2-(0.5-1.5*P0)*Z1(L1)+2.0*Z1(L1)+Z1(L1))*CT/S-P*(Z2(L1))*S*(Z1
4 (L1)-Z1(L1)+Z1(L2))*CT)*C)+AI2*X(K2+ID)*D2*Z1(L2)*(Z1(L1)+2.0*Z1(L
5 1))/(2.0*S*S)
V(K1)=V(K1)+AI*X(K+ID)*(Z1(L2)*(-C2*Z2(L2)+(1.0-3.0*P0)*Z1(L1)+2
1 .0*P2*Z1(L1))/(2.0)*S+D2*(Z1(L1)+Z1(L1))*Z1(L1)+Z1(L1)+Z1(L1)+Z1(L1)
2 +(0.5*Z2(L1))/S+(C0-3.0*P0)*Z1(L2)**2+(0.5-1.5*P0)*Z1(L1)**2-D0*Z1
3 (L1)+Z1(L1))*CT/S-F*(Z1(L1))*CT+Z1(L1)-Z1(L1)+Z1(L1)+Z1(L1)+Z1(L1)
4 *I+IE)*(Z1(L2)*(-2.0*P0)*Z1(L2)-C2*(2.0*Z2(L1)+Z2(L1))+2.0*P2*Z2
5 (L2))*CT-D2*CT*(5.0*Z1(L1)+4.0*Z1(L1))+1.0-2.0*P0)*Z1(L2)*CT*Z1(L
6 2.0*(C2*Z2(L2)+2.0*Z1(L1)+Z1(L1))+C2*Z1(L1)+Z1(L1)+Z1(L1)+Z1(L1)+Z1(L1)
7 L1)*Z1(L1)-2.0*P2*CT*(Z1(L1)+Z1(L1))+0.5*Z2(L1)+Z1(L1))*Z1(L1)+0.
8 5*Z2(L1))-Z1(L1)*(1.0-3.0*P0)*Z1(L1)-E0*Z1(L1))*CT*CT)/2.0)+AI*X

```

```

SNDRRHS 40
SNDRRHS 41
SNDRRHS 42
SNDRRHS 43
SNDRRHS 44
SNDRRHS 45
SNDRRHS 46
SNDRRHS 47
SNDRRHS 48
SNDRRHS 49
SNDRRHS 50
SNDRRHS 51
SNDRRHS 52
SNDRRHS 53
SNDRRHS 54
SNDRRHS 55
SNDRRHS 56
SNDRRHS 57
SNDRRHS 58
SNDRRHS 59
SNDRRHS 60
SNDRRHS 61
SNDRRHS 62
SNDRRHS 63
SNDRRHS 64
SNDRRHS 65
SNDRRHS 66
SNDRRHS 67
SNDRRHS 68
SNDRRHS 69
SNDRRHS 70
SNDRRHS 71
SNDRRHS 72
SNDRRHS 73
SNDRRHS 74
SNDRRHS 75
SNDRRHS 76
SNDRRHS 77
SNDRRHS 78
SNDRRHS 79
SNDRRHS 80
SNDRRHS 81
SNDRRHS 82
SNDRRHS 83
SNDRRHS 84
SNDRRHS 85
SNDRRHS 86
SNDRRHS 87
SNDRRHS 88
SNDRRHS 89
SNDRRHS 90
SNDRRHS 91
SNDRRHS 92
SNDRRHS 93
SNDRRHS 94
SNDRRHS 95
SNDRRHS 96
SNDRRHS 97
SNDRRHS 98
SNDRRHS 99
SNDRRHS 100
SNDRRHS 101
SNDRRHS 102
SNDRRHS 103
SNDRRHS 104
SNDRRHS 105
SNDRRHS 106
SNDRRHS 107
SNDRRHS 108
SNDRRHS 109
SNDRRHS 110
SNDRRHS 111
SNDRRHS 112
SNDRRHS 113
SNDRRHS 114
SNDRRHS 115
SNDRRHS 116
SNDRRHS 117
SNDRRHS 118
SNDRRHS 119
SNDRRHS 120
SNDRRHS 121
SNDRRHS 122
SNDRRHS 123
SNDRRHS 124
SNDRRHS 125
SNDRRHS 126
SNDRRHS 127
SNDRRHS 128
SNDRRHS 129
SNDRRHS 130
SNDRRHS 131
SNDRRHS 132
SNDRRHS 133
SNDRRHS 134
SNDRRHS 135
SNDRRHS 136
SNDRRHS 137
SNDRRHS 138
SNDRRHS 139
SNDRRHS 140
SNDRRHS 141
SNDRRHS 142
SNDRRHS 143
SNDRRHS 144
SNDRRHS 145
SNDRRHS 146
SNDRRHS 147

```

```

1 V(K2)=V(K2)-AI*(K1+ID)*(Z1(L1)+Z2(L1))/2.0-D0*Z2(L1)+D2*(Z1(L1)+0.5*Z1(L1))*CT/S-71(L1)*(Z1(L1)+Z2(L1))*FO/S-Z1(L1)*2/S-P*(
2 Z1(L1)/S+Z2(L1)*C*(Z1(L1)-Z1(L1)+Z1(L1)*CT)*S)+AI2*(K2+ID)*(-0.5*Z1(L1)+Z1(L1)+Z1(L1)+Z1(L1))/S)*AI2*(K2+ID)*D2*Z1(L1)
3 2)*(Z1(L1)+2.0*Z1(L1))/(2.0*S*S)
4 IF (TCN.EQ.-10) GO TO 110
V(K)=V(K)+X(K+IC)*AI2*EO*Z1(L1)/(S*S)+X(K1+ID)*AI*EO*Z1(L1)*CT/S
V(K1)=V(K1)+X(K+IC)*AI*EO*Z1(L1)*CT/S+X(K1+ID)*FO*Z1(L1)/(S*S)+X(K2+IC)*AI*FO*Z1(L1)/S
1 V(K2)=V(K2)-X(K1+IC)*AI*EO*Z1(L1)/S-X(K2+ID)*AI2*FO*Z1(L1)/(S*S)
V(K)=V(K)+X(K+IC)*AI*P*VF(L2,1)/S
V(K1)=V(K1)+X(K+IC)*C*X(K2+ID)*S)*AI*F*(VF(L1,1)+VF(L,1)+VF(L2,1))*CT)
110 V(K2)=V(K2)-X(K1+ID)*AI*P*VF(L,1)/S
120 CONTINUE
CONTINUE
RETURN
END
**** *DECK
SNELHS
SUPROUTINE SNELHS (A,NA,KA,Z1,Z2,NZ,F)
DIMENSION A(NA,KA),Z1(NZ),Z2(NZ)
COMMON/COM1/ AN(7,4,12),ITYPE,ITLN(7),IMP(7),JSN(7),JLN(7),KHOF(7)
COMMON/COM2/ DO,D1,E2,D3,E4,AL,THETA,ECL,H,A1,IFR,IOM
COMMON /COM3/ JAR,JAW,JARW,IF,ID,IC,ET,I2AP
COMMON /COM4/ I1,N1,A2
COMMON/COM5/ VFC(147,20),VFC(106,20),FFC(20),FFC(20)
C,SF(147)
FA=0.0
AI2=AI*AI
AK=1.0
AJ=1.0
IF (TCN.EQ.20.OR.ICN.EQ.30) AK=2.0
IF (TCN.EQ.20.OR.ICN.EQ.0) AJ=0.0
DC 110 KK=1,ITYPE
CALL FCDATA (KK,ITCL,MID,ISTART,IFIN)
DO 100 IJ=ISTART,IFIN
PA=PA+1.0
PHI=PA*H
S=SIN(PHI)
C=COS(PHI)
CT=C/S
K=IC*IJ-IF
K1=K+IF/2
K2=K+IF
L=3*IJ-2
L1=L+1
L2=L+2
EO=VF(L1,1)+(1.0-VF(L1,1))*(VF(L2,1)+2)/2.0+D0*VF(L1,1)
FO=VF(L1,1)+D0*(VF(L1,1)+(1.0-VF(L1,1))*(VF(L2,1)+2)/2.0)
FO1=VF(L1,1)+(1.0-VF(L1,1))*VF(L2,1)*VF(L2,1)-VFC(L,1)*(VF(L2,1)+2)/2.0+D0*VF(L1,1)
FO=(AK*EO-AJ*SF(I))/2.0

```

```

2 SNDRHS 151
2 SNDRHS 152
2 SNDRHS 153
2 SNDRHS 154
2 SNDRHS 155
2 SNDRHS 156
2 SNDRHS 157
2 SNDRHS 158
2 SNDRHS 159
2 SNDRHS 160
2 SNDRHS 161
2 SNDRHS 162
2 SNDRHS 163
2 SNDRHS 164
2 SNDRHS 165
2 SNDRHS 166
2 SNDRHS 167
2 SNDRHS 168
2 SNDRHS 169
2 SNDRHS 170
2 SNDRHS 171
2 SNDRHS 172
2 SNDRHS 173
2 SNDRHS 174
2 SNDRHS 175
2 SNDRHS 176
2 SNDRHS 177
2 SNDRHS 178
2 SNDRHS 179
2 SNDRHS 180
2 SNDRHS 181
2 SNDRHS 182
2 SNDRHS 183
2 SNDRHS 184
2 SNDRHS 185
2 SNDRHS 186
2 SNDRHS 187
2 SNDRHS 188
2 SNDRHS 189
2 SNDRHS 190
2 SNDRHS 191
2 SNDRHS 192
2 SNDRHS 193
2 SNDRHS 194
2 SNDRHS 195
2 SNDRHS 196
2 SNDRHS 197
2 SNDRHS 198
2 SNDRHS 199
2 SNDRHS 200
2 SNDRHS 201
2 SNDRHS 202
2 SNDRHS 203
2 SNDRHS 204
2 SNDRHS 205
2 SNDRHS 206
2 SNDRHS 207
2 SNDRHS 208
2 SNDRHS 209
2 SNDRHS 210
2 SNDRHS 211
2 SNDRHS 212
2 SNDRHS 213
2 SNDRHS 214
2 SNDRHS 215
2 SNDRHS 216
2 SNDRHS 217
2 SNDRHS 218
2 SNDRHS 219
2 SNDRHS 220
2 SNDRHS 221
2 SNDRHS 222
2 SNDRHS 223
2 SNDRHS 224
2 SNDRHS 225
2 SNDRHS 226
2 SNDRHS 227
2 SNDRHS 228
2 SNDRHS 229
2 SNDRHS 230
2 SNDRHS 231
2 SNDRHS 232
2 SNDRHS 233
2 SNDRHS 234

```

```

FC=(AK*EO-AJ*SF(I))/2.0
FO1=(AK*EO1-AJ*SF(L2))/2.0
DC 70 I=1,ITCL
MA=JAD+IC*(I-NIC)
1 A(K,MA+IE)=A(K,MA+IE)+AN(KK,1,I)*(Z1(L1)+D0*Z1(L1)-D2*Z1(L2)*CT-Z2(L2)-2.0*F)-AN(KK,2,1)*Z1(L2)
1 A(K2,MA-IF)=A(K2,MA-IF)+AN(KK,1,I)*(Z1(L1)+D0*Z1(L1)+D3*Z1(L2)*CT+Z2(L2)-2.0*P)+AN(KK,2,1)*Z1(L2)
1 A(K2,MA)=A(K2,MA)-AN(KK,1,I)*(Z2(L1)+D0*Z2(L1)+(Z1(L1)+D0*Z1(L1))*CT)-AN(KK,2,1)*(Z1(L1)+D0*Z1(L1))
1 A(K,MA)=A(K,MA)-AN(KK,1,I)*(Z1(L2)+2.0*Z2(L2)+Z1(L2)*CT)-AN(KK,2,1)*Z1(L2)**2
1 A(K,MA+IF)=A(K,MA+IE)+AN(KK,1,I)*(Z1(L2)*(D2*Z1(L2))/2.0+(2.0*Z2(L1)+D0*Z2(L1))*(2.0-C-D0)*Z1(L1)+D0*Z1(L1)-Z1(L2)*(Z1(L1)+D0*Z1(L1))+Z2(L2)*(2.0*Z1(L1)+D0*Z1(L1))-2.0*F*Z1(L1))+AN(KK,2,1)*Z1(L2)**2+(2.0*Z1(L1)+D0*Z1(L1))
1 A(K2,MA-IF)=A(K2,MA-IE)+AN(KK,1,I)*(Z1(L2)*(D2*Z1(L2))/2.0-2.0*Z2(L1)-D0*Z2(L1)-(2.0+C+D0)*Z1(L1)+D0*Z1(L1))*CT-Z1(L2)*(Z1(L1)+D0*Z1(L1))-Z2(L2)*(2.0*Z1(L1)+D0*Z1(L1))-2.0*F*Z1(L1)-AN(KK,2,1)*Z2(L2)**2+(2.0*Z1(L1)+D0*Z1(L1))
1 A(K2,MA)=A(K2,MA)+AN(KK,1,I)*(-3.0*Z1(L2)*Z2(L2)+2.0*Z1(L1)*Z2(L1)+D0*(Z1(L1)*Z2(L1)+Z1(L1)*Z2(L1)))+(-1.5*Z1(L2)**2+Z1(L1)*Z1(L1)+D0*(Z1(L1)*CT)+AN(KK,2,1)*(-1.5*Z1(L2)**2+Z1(L1)*Z1(L1)+D0*Z1(L1))
IF (TCN.EQ.-10) GO TO 70
A(K,MA+IE)=A(K,MA+IE)+AN(KK,1,I)*(FO*Z1(L1)-Z1(L2)*(FO*CT+FO1))-Z2(L2)*FO-AN(KK,2,1)*Z1(L2)*EO
A(K2,MA-IE)=A(K2,MA-IE)+AN(KK,1,I)*(Z1(L2)*(FO*CT+FO1)+(Z1(L1)+Z2(L2))*EO)+AN(KK,2,1)*Z1(L2)*EO
1 A(K2,MA)=A(K2,MA)-AN(KK,1,I)*(Z1(L1)*(EO*CT+FO1)+Z2(L1)*EO)-AN(KK,2,1)*Z1(L1)*EO
A(K,MA+IE)=A(K,MA+IE)+AN(KK,1,I)*2.0*P*VF(L1,1)
A(K2,MA-IF)=A(K2,MA-IF)+AN(KK,1,I)*2.0*P*VF(L1,1)
20 CONTINUE
IF (AI.EQ.0.0) GO TO 70
A(K,MA+1)=A(K,MA+1)-AI*AN(KK,1,I)*(D2*(Z1(L1)+Z1(L1))/(2.0*S)+F*S)
1 A(K1,MA-1)=A(K1,MA-1)+AI*AN(KK,1,I)*(C2*(Z1(L1)+Z1(L1))/(2.0*S)+P*S)
1 A(K1,MA)=A(K1,MA)+AN(KK,1,I)*(D0*(Z1(L1)+Z1(L1))*CT+D0*(Z2(L1)+Z2(L1))+AN(KK,2,1)*D0*(Z1(L1)+Z1(L1))
A(F1,MA+1)=A(K1,MA+1)+AI*AN(KK,1,I)*(C3*Z1(L2)/(2.0*S)-P*C)
A(K2,MA-1)=A(K2,MA-1)+AI*AN(KK,1,I)*(C3*Z1(L2)/(2.0*S)-P*C)
1 A(K,MA+1)=A(K,MA+1)+AI*AN(KK,1,I)*(-Z1(L2)*Z1(L1)/(2.0*S)+F2*(Z1(L1)+Z1(L1))*2-Z1(L1)*Z1(L1))/(2.0*S)-F*Z1(L1)*S)
1 A(K1,MA-1)=A(K1,MA-1)-AI*AN(KK,1,I)*(C2*(Z1(L1)+Z1(L1))*2-Z1(L1)*Z1(L1))-Z1(L2)*Z1(L1)/(2.0*S)-P*Z1(L1)*S)
1 A(K1,MA)=A(K1,MA)+AN(KK,1,I)*(Z1(L2)+Z1(L2)*CT/2.0)*D0+Z1(L1)*(1.0-3.0*D0)*(Z2(L1)+Z1(L1)*CT/2.0)-D0*(Z2(L1)+Z1(L1)*CT)-D0*Z2(L1)*Z1(L1)+AN(KK,2,1)*(0.5*D0*Z1(L2)**2+(1.0-D0*3.0)*0.5*Z1(L1)**2-D0*Z1(L1)*Z1(L1))
1 A(K1,MA+1)=A(K1,MA+1)-AI*AN(KK,1,I)*((2.0*Z1(L1)+D2*Z1(L1))*Z1(L2)/(2.0*S)+P*Z1(L1)*C)
A(K2,MA-1)=A(K2,MA-1)+AI*AN(KK,1,I)*((2.0*Z1(L1)+D2*Z1(L1))*Z1(L2)/(2.0*S)-P*Z1(L1)*C)
1 IF (TCN.EQ.-10) GO TO 70

```

```

2 SNDRHS 35
2 SNDRHS 36
2 SNDRHS 37
2 SNDRHS 38
2 SNDRHS 39
2 SNDRHS 40
2 SNDRHS 41
2 SNDRHS 42
2 SNDRHS 43
2 SNDRHS 44
2 SNDRHS 45
2 SNDRHS 46
2 SNDRHS 47
2 SNDRHS 48
2 SNDRHS 49
2 SNDRHS 50
2 SNDRHS 51
2 SNDRHS 52
2 SNDRHS 53
2 SNDRHS 54
2 SNDRHS 55
2 SNDRHS 56
2 SNDRHS 57
2 SNDRHS 58
2 SNDRHS 59
2 SNDRHS 60
2 SNDRHS 61
2 SNDRHS 62
2 SNDRHS 63
2 SNDRHS 64
2 SNDRHS 65
2 SNDRHS 66
2 SNDRHS 67
2 SNDRHS 68
2 SNDRHS 69
2 SNDRHS 70
2 SNDRHS 71
2 SNDRHS 72
2 SNDRHS 73
2 SNDRHS 74
2 SNDRHS 75
2 SNDRHS 76
2 SNDRHS 77
2 SNDRHS 78
2 SNDRHS 79
2 SNDRHS 80
2 SNDRHS 81
2 SNDRHS 82
2 SNDRHS 83
2 SNDRHS 84
2 SNDRHS 85
2 SNDRHS 86
2 SNDRHS 87
2 SNDRHS 88
2 SNDRHS 89

```

```

A(K1,PA-1)=A(K1,PA-1)-AN(KK,1,I)*A1*P*VF(L1,1)*S
A(K1,PA+1)=A(K1,PA+1)+AN(KK,1,I)*A1*P*VF(L1,1)*C
A(K2,PA-1)=A(K2,PA-1)+AN(KK,1,I)*A1*P*VF(L1,1)*C
70 CONTINUE
A(K,JAD)=A(K,JAD)+Z2(L2)-Z1(L1)-D0*Z1(L1)+(1.0-2.0*D0)*Z1(L2)*CT+
1 2.0*P
A(K,JAD+IE)=A(K,JAD+IE)-D3*Z1(L2)
A(K2,JAD-IE)=A(K2,JAD-IE)+Z1(L2)+Z2(L1)+E0*Z2(L1)+(D0*Z2(L2)+Z1(L1)
1 +D0*Z1(L1))*CT-2.0*F*CT
A(K2,JAD)=A(K2,JAD)+D3*Z2(L2)+D3*Z1(L2)*CT-4.0*F
A(K,JAD)=A(K,JAD)-Z1(L2)*C4*Z1(L2)/2.0+(D0*Z2(L2)+2.0*F*Z1(L1)+D
1 0*Z1(L1))*CT+2.0*Z2(L1)+E0*Z2(L1)-Z2(L1)*(2.0*Z1(L1)+E0*Z1(L1))+Z1(L
2 1)*Z1(L1)+D0*Z1(L1)-2.0*F*(Z1(L1)+Z2(L1))*C*S-(Z1(L1)-Z1(L1))+Z1(L
3 2)*CT)*C*S
A(K,JAD+IE)=A(K,JAD+IE)+Z1(L2)*(-2.0+E0)*(Z2(L2)-Z1(L1))+E0*Z1(L1)
1 -Z1(L1)*CT-P*2.0*(Z2(L1))*S*S-(Z1(L1)-Z1(L1)+Z1(L2))*CT)*C*S
A(K2,JAD-IE)=A(K2,JAD-IE)+Z1(L2)*3.0*Z2(L2)-2.0*Z1(L1)+E0*Z1(L1)+
1 (E4*Z1(L2)+2.0*F*Z2(L1))*CT+Z1(L1)*(-2.0*Z2(L1)-E0*Z2(L1)+(D0*Z2(L1)
2 1)-Z1(L1)-D0*Z1(L1))*CT)-E0*Z2(L1)+Z1(L1)-2.0*F*(Z1(L1)+Z2(L1))*
3 C*S+(Z1(L1)-Z1(L1)+Z1(L2))*CT)*C*S
A(K2,JAD)=A(K2,JAD)-Z1(L2)*E3*Z1(L2)+(2.0+D0)*(Z2(L1)+Z1(L1))*CT+D
1 0*(Z2(L1)+Z1(L1))*CT)-Z2(L2)*(2.0+D0)*Z1(L1)+E0*Z1(L1)-2.0*P*(2.
2 0*Z1(L1)+Z2(L1))*S*(Z1(L1)-Z1(L1)+Z1(L2))*CT)*S*S
IF (ICH.EQ.-10) GO TO 90
A(K,JAD)=A(K,JAD)-FC*(Z1(L1)-Z2(L2)-Z1(L2))*CT+FC1*Z1(L2)
A(K,JAD+IE)=A(K,JAD+IE)-E0*Z1(L2)
A(K2,JAD-IE)=A(K2,JAD-IE)+E0*(Z1(L1)*CT+Z2(L1)+Z1(L2))+E01*Z1(L1)
A(K2,JAD)=A(K2,JAD)+E0*(Z1(L2)*CT+Z2(L2))+E01*Z1(L2)
A(K,JAD)=A(K,JAD)-2.0*P*(VF(L1,1)+VF(L2,1))*CT
A(K,JAD+IE)=A(K,JAD+IE)-2.0*P*VF(L2,1)
A(K2,JAD-IE)=A(K2,JAD-IE)+2.0*P*VF(L1,1)*CT
A(K2,JAD)=A(K2,JAD)+2.0*P*(VF(L1,1)+VF(L2,1))
90 CONTINUE
IF (AI.EQ.0.0) GO TO 100
A(K,JAD)=A(K,JAD)-A12*D0*(Z1(L1)+Z1(L1))/(S*S)
A(K,JAD+1)=A(K,JAD+1)+A1*(C1.0-3.0*D0)*Z1(L2)/(2.0*S)-D0*(Z1(L1)+Z
1 (L1))*CT/S
A(K,JAD+2)=A(K,JAD+2)+A12*D2*Z1(L2)/(2.0*S*S)
A(K1,JAD-1)=A(K1,JAD-1)-A1*(D0*(Z1(L1)+Z1(L1))*CT/S-(D2*(Z2(L1)+Z2(L
1 1))-1.0-3.0*D0)*Z1(L2))/(2.0*S)-2.0*F*CT
A(K1,JAD)=A(K1,JAD)+D2*Z2(L2)/2.0-Z1(L1)*C*(D4/2.0+CT*CT*E0)-Z1(L1)*
1 (L3/2.0+CT*CT*E0)+E2*CT*(3.0*Z1(L2)+Z2(L1)+Z2(L1))/2.0
A(K1,JAD+1)=A(K1,JAD+1)+A1*(D2*(Z2(L2)+Z1(L1))*CT)/(2.0*S)-(Z1(L1)
1 +D0*Z1(L1))/S+2.0*F*S
A(K2,JAD-2)=A(K2,JAD-2)-A12*D2*Z1(L2)/(2.0*S*S)
A(K2,JAD-1)=A(K2,JAD-1)+A1*(D0*(Z2(L2)+Z1(L1))+Z1(L1)-D2*Z1(L2))*C
1 T/2.0)/S-P/S
A(K2,JAD)=A(K2,JAD)+A12*(Z1(L1)+D0*Z1(L1))/(S*S)
A(K,JAD)=A(K,JAD)-A12*(Z1(L1))*C*(C1.0-3.0*D0)*Z1(L1)-2.0*D0*Z1(L1)-
1 (1.0-2.0*D0)*Z1(L2)*2)/(2.0*S*S)
A(K,JAD+1)=A(K,JAD+1)-A1*(Z1(L2))*C*(D0*Z2(L2)+(1.0-3.0*D0)*Z1(L2)/2.
1 0+D2*Z1(L1)-(1.0-2.0*D0)*Z1(L2))*CT/2.0)/S+Z1(L1))*C*(0.5-1.5*D0)*Z1(L
2 11)-D0*Z1(L1))*CT/S+FC*(Z2(L1))*S-(Z1(L1)-Z1(L1)+Z1(L2))*CT)*C))
A(K1,JAD-1)=A(K1,JAD-1)-A1*(Z1(L2))*C*(D2*Z2(L2)+(1.0-5-1.5*D0)*Z1(L1)
1 +D2*Z1(L1)-(1.0-5-1.5*D0)*Z1(L2))*CT)/S+Z1(L1)*C*(D2*(Z2(L1)+0.5*Z2(L1))-D0*
2 Z1(L1))*CT)/S+Z1(L1)*C*(Z2(L1)+0.5*Z2(L1))+C*(0.5-1.5*D0)*Z1(L1))*CT
3 /S-P*(2.0*Z1(L1))*C+(Z1(L1)-Z1(L1)+Z1(L2))*CT)*C))
A(K,JAD+2)=A(K,JAD+2)-A12*D2*Z1(L2)*(Z1(L1)+2.0*Z1(L1))/(2.0*S*S)
A(K1,JAD)=A(K1,JAD)+Z1(L2)*(-2.0-D0)*Z1(L2)-C2*(2.0*Z2(L1)+Z2(L1)
1 -(2.0*Z2(L2)-5.0*Z1(L1)-4.0*Z1(L1))*CT)+1.0-2.0*D0)*Z1(L2))*CT*CT)
2 /2.0-C2*Z2(L2)*(2.0*Z1(L1)+Z1(L1))/2.0+Z1(L1)*C*(Z2*Z1(L1)+D3*Z1(L1)-2
3 0*D2*(Z2(L1)+0.5*Z2(L1))*CT+2.0*E0*Z1(L1))*CT*CT)/2.0+Z1(L1)*C*(D4*Z
4 1(L1)-2.0*F*(Z2(L1)+0.5*Z2(L2))*CT-(1.0-3.0*D0)*Z1(L1))*CT*CT)/2.0
A(K1,JAD+1)=A(K1,JAD+1)-A1*(Z1(L2))*C*(Z1(L2)+D2*Z2(L2)+2.0*Z2(L1)
1 L)+Z2(L1)+Z1(L1)+2.0*Z1(L1))*CT)/(2.0*S)+C2*Z2(L2)*(2.0*Z1(L1)+Z1
2 (L1))/(2.0*S)-Z1(L1))*C*(D0*Z1(L1)+Z1(L1))/S-P*(Z1(L1)+Z1(L1)+Z1(L2))*C
3 T)*S)
A(K2,JAD-2)=A(K2,JAD-2)+A12*D2*Z1(L2)*(Z1(L1)+2.0*Z1(L1))/(2.0*S*S)
1 )
A(K2,JAD-1)=A(K2,JAD-1)+A1*(Z1(L2))*C*(D2*Z2(L2)-D0*Z2(L2)+2.0+D2*(2.
1 0*Z1(L1)+Z1(L1))*CT)/(2.0*S)-Z1(L1)*C*(D0*Z2(L2)+Z1(L1))/S-Z1(L1)*2
2 Z1(L1)/S-P*(Z1(L1))/S+Z2(L1)*C+(Z1(L1)-Z1(L1)+Z1(L2))*CT)*S))
A(K2,JAD)=A(K2,JAD)+A12*(Z1(L2)*Z1(L2)/2.0-Z1(L1)*(Z1(L1)+D0*Z1(L1)
1 ))/(S*S)
IF (ICH.EQ.-10) GO TO 100
A(K,JAD)=A(K,JAD)-A12*F0*Z1(L1)/(S*S)
A(K,JAD+1)=A(K,JAD+1)-A1*FC*Z1(L1)*CT/S
A(K1,JAD-1)=A(K1,JAD-1)-A1*E0*Z1(L1)*CT/S
A(K1,JAD)=A(K1,JAD)-FC*Z1(L1)/(S*S)
A(K1,JAD+1)=A(K1,JAD+1)-A1*F0*Z1(L1)/S
A(K2,JAD-1)=A(K2,JAD-1)+A1*FC*Z1(L1)/S
A(K2,JAD)=A(K2,JAD)+A12*EC*Z1(L1)/(S*S)
A(K,JAD+1)=A(K,JAD+1)-A1*P*VF(L2,1)/S
A(K1,JAD-1)=A(K1,JAD-1)-A1*F*(VF(L1,1)+VF(L2,1))*CT)*C
A(K1,JAD+1)=A(K1,JAD+1)-A1*F*(VF(L1,1)+VF(L2,1))*CT)*S
A(K2,JAD-1)=A(K2,JAD-1)+A1*F*VF(L1,1)/S
100 CONTINUE
110 CONTINUE
RETURN
END
** *DECK ORTHOG ORTHOG 1
SUBROUTINE ORTHOG (AIK,ISTEP,ICOUNT,N,V,U,NUM,IR7,KUW) ORTHOG 2
DIMENSION U(IR7,KUW) V(IR7) ORTHOG 3
FOR ORTHOG V W.R.T. ALL E-VECTORS ALIRFAC FOUND ORTHOG 4
FORMS V=V-SUM OF ((V(TRAN)*X)*X)/(X(TRAN)*X) ORTHOG 5
EXPECTS EUCLIDEAN NORM OF F-VECT TO BE STORED IN U(N-J,NUM) FOR I'RH VECT ORTHOG 6
ICOUNT=0 ORTHOG 7
IKN=NIK-1 ORTHOG 8
DO 20 I=1,IKN ORTHOG 9
SAV=0.0 ORTHOG 10
DO 10 J=1,N ORTHOG 11
SAV=SAV+V(J)*U(J,I) ORTHOG 12
10 CONTINUE ORTHOG 13
DO 20 J=1,N ORTHOG 14
V(J)=V(J)-SAV*U(J,I)/U(N-I,NUM) ORTHOG 15
20 CONTINUE ORTHOG 16
RETURN ORTHOG 17

```

```

CCKFB, Z1, Z2, NZ, V, NV, F, NP, NO, D, NU, KU, EF, Z3, OFC, NUF, T, T, L, L, EI, AT, Z4
DIMENSION A(NA, KA), V1(NV1), X(NX), AR(12, KAR), OF(NUF, KUF), UFB(NUFB, K
CUBF), Z1(NZ), Z2(NZ), V(NV), F(NF), D(DU, KU), EF(EF), Z3(NZ), OFC(NUFC, KU
CF), Z4(NX)
COMMON/COM2/ DO, E1, E2, E3, D4, AL, THETA, PCL, H, AT, TFR, ION
COMMON /COM3/ JAF, JAK, JARW, IF, ID, IC, FT, IZAP
COMMON /COM4/ IN, NI, N2
LEVEL 2, UF, UFR, UFC
CONTRACTS CHECK AND ENERGY ROUTINES AND IN THE CASE OF AI=0.0 RE-ENTERS FND
PTH IN ORDER TO FIND EBF & ECF (STORED IN PLACE OF U, W) AS THESE STRESS
COMPONENTS ARE AFFECTED BY ENERGY
ARGUMENTS *****
ARGUMENTS *****
NI=NUMBER OF NODES (=NN IN MAIN PROGRAM) KM1=TAW OR IAWO KM3=IARW OR IARWO
OTHERS AS DEFINED IN MAIN PROGRAM
CALL SECOND(AAA)
AAP=AAA

IMODE=AI
DO 90 I=1, NO
  YP(I)
  DO 30 J=1, NI
    X(J)=U(J, I)
30  CALL PCKSUB (X, NUF, AP, KAR, AI, IN, JAPW)
    SAV=0.0
    IFF=1C+I
    IZZ=N2-IC
    DO 70 J=IFF, IZZ
      TEMP=ARS(X(J))
      IF(TEMP.LE.SAV) GO TO 70
      SAV=TEMP
      JJJ=J
70  CONTINUE
    TEMP=X(J, J)
    DO 80 J=1, N2
      X(J)=X(J)/TEMP
80  CALL NPWAVE (X, NX, IN, AI, ICCUNT)
    WRITE (6, 2000)
    WRITE (6, 2010) IMODE, I, ICCUNT
    WRITE (6, 2000)
    CALL ENERGY (X, NX, Y, V, Z1, Z2, NV, NZ, UF, NUF, KUF, UFR, NUFR, KUF, PF, Z3,
    CUF, NUFC, T, T, L, L, EI, AT, Z4)
    CALL SECOND(AAA)
    AAC=AAA-AAP
    AAB=AAA
    WRITE (6, 8010) AAA, AAC
90  CONTINUE
RETURN
2000  FORMAT (1H0, 5X, 110H-----)
2010  CFORMAT (1H0, 8X, 25HCIRCUMFERENTIAL MODE NO. = , I3, 3X, 22HEIGEN-VALUE
C POSITION = , 13, 4X, 37HNO. OF TURNING POINTS ON HALF SHELL = , I4)
8010  FORMAT(1P , 60X, 5HT. T. = , F7.2, 2X, 10HT. ENERGY = , F6.3)

```

```

*** *DECK END
      PRODC
      SUBROUTINE PRODC (NA, KA, A, V2, X, NI, NUF, KM1)
      DIMENSION A(NA, KA), V2(NA), X(NUF)
      C PERFORMS PRODUCT V2=A(X) WHERE A IS HANDLED WITH WIDTH KM1, AND ORDER NI
      NI=(KM1-1)/2
      DO 1 I=1, NI
        V2(I)=0.0
        NJ=NI+2-I
        K=0
        DO 1 J=NJ, KM1
          K=K+1
          V2(I)=V2(I)+A(I, J)*X(K)
1      NM=NI+1
        NL=NI-NI
        DO 2 I=NM, NL
          V2(I)=0.0
          K=I-NI-1
          DO 2 J=1, KM1
            K=K+1
            V2(I)=V2(I)+A(I, J)*X(K)
2      NM=NL+1
        M2=KM1
        DO 3 I=NM, M1
          V2(I)=0.0
          M2=M2-1
          K=I-NI-1
          DO 3 J=1, M2
            K=K+1
            V2(I)=V2(I)+A(I, J)*X(K)
3      RETURN
      END
*** *DECK MA07B
      SUBROUTINE MA07B (A, P, IA, N, NW, PT, JCKE, NIZ)
      DIMENSION A(IA, JCKE), P(NIZ)
      EQUIVALENCE (IP, I, N, NW, KIP, NCG), (NR12, NS, J, I, PU), (AMAXT, TREST, TEMP)
      C ALTERED VERSION OF HARWELL ROUTINE MA07E AND MA07C
      C PERFORMS GAUSSIAN ELIMINATION WITH PARTIAL PIVOTING ON Banded MATRIX A
      C SEE HARWELL LIBRARY FOR FULL DETAILS
      JCK1=IA*JCKE
      NR=(NW-1)/2
      NR1=NR+1
      NR2=NR1+NR
      NR32=NR2+NR1
      IF(PT.EQ.0.) GO TO 99
      DO 4 ISET=1, N
        NR12=MINO(NR2+1, N-ISET+NR1+1)
        DO 4 JSET=NR12, NR32
9     A(ISET, JSET)=0.0
        DO 22 K=1, N
          IP=K
          NS=NR1
          RESI=ABS(A(IP, NS))
          DO 7 NFI=1, NR
            IPT=K+NFI

```



```

IF (REST.GE.TPFST) GO TO 7
REST=TPFST
NS=NT
IP=IPT
7 CONTINUE
IF (K.FO.1) PT=REST
PT=AMINI(REST,PT)
IF (PFST.NE.0.) GO TO 5
WRITE (6,6)
6 FORMAT (1H ,80HZERO PIVOT FOUND IN MA07B. ATTEMPT TO SOLVE THE SY
STEM OF EQUATIONS ABANCONF. )
RETURN
5 A(K,NR32)=IP
IF (IP.FO.K) GO TO 3
DO 8 NV=1,NR2
TFMP=A(K,NR+NV)
A(K,NR+NV)=A(IP,NS+NV-1)
8 A(IP,NS+NV-1)=TFMP
C FLIMINATION AND COEFF. STORAGE
3 IF (K+NR.IE.N) GO TO 15
NL=N-K
IF (NL) 22,22,16
15 NL=NR
16 CONTINUE
CALL MA07C (A,NL,K,NR,IA,JOKI)
22 CONTINUE
C NCW B IS PROCESSED
99 DO 17 KB=1,N
NEX=A(KB,NR32)
IF (NEX.EQ.KB) GO TO 20
TFMP=B(KB)
B(KB)=B(NEX)
B(NEX)=TFMP
20 DO 17 IB=1,NR
KIP=KB+IB
IF (KIP.GT.N) GO TO 17
B(KIB)=B(KIB)-B(KP)*A(KB,IB)
17 CONTINUE
C PACK SUBSTITUTE
DO 25 NBACK=1,N
NCC=N+1-NBACK
PNCO=B(NCO)
L2=MINO(NR2,NBACK)
IF (L2.FO.1) GO TO 25
DO 31 LCO=2,L2
31 PNCO=PNCO-A(LCO+NCC-1)*A(NCC,LCO+NR)
25 B(NCC)=PNCO/A(NCC,NR1)
RETURN
END
*DECK MA07C
SUBROUTINE MA07C (A,NL,K,NR,IA,JOKI)
DIMENSION A(JOKI)

```

```

MA07B 27
MA07B 28
MA07B 29
MA07B 30
MA07B 31
MA07B 32
MA07B 33
MA07B 34
MA07B 35
MA07B 36
MA07B 37
MA07B 38
MA07B 39
MA07B 40
MA07B 41
MA07B 42
MA07B 43
MA07B 44
MA07B 45
MA07B 46
MA07B 47
MA07B 48
MA07B 49
MA07B 50
MA07B 51
MA07B 52
MA07B 53
MA07B 54
MA07B 55
MA07B 56
MA07B 57
MA07B 58
MA07B 59
MA07B 60
MA07B 61
MA07B 62
MA07B 63
MA07B 64
MA07B 65
MA07B 66
MA07B 67
MA07B 68
MA07B 69
MA07B 70
MA07B 71
MA07B 72
MA07B 73
MA07B 74
MA07B 75
MA07C 1
MA07C 2
MA07C 3

```

```

NR1=NR+1
NR3=3*NR
J4=K+NR*IA
PIVT=A(J4)
DO 9 IK=1,NL
I=IK+K
J1=I+(NR-1K)*IA
TEMP=-A(J1)/PIVT
A(K+(IK-1)*IA)=-TEMP
J2=I+(NR3-1K)*IA
J3=J4
DO 9 J=J1,J2,IA
A(J)=A(J)+A(J3)*TEMP
9 CONTINUE
RETURN
END
*DECK BCCND
SUBROUTINE BCCND (AP,KAPW,IWILL,THETA,AL,N)
DIMENSION AP(12,KAPW)
C SETS UP THE BOUNDARY CONDITIONS IN AP FOR A10.0, A1=1,3,5... A1=2,4,6....
C 1ST & 2ND DERIVATIVES H**6, 3RD DERIVATIVES H**4
C=COS(THETA)
S=SIN(THETA)
CT=C/S
AL1=AL+1.0
IF (IWILL.EQ.0) GO TO 300
IWCN= 2*(IWILL/2)
IF (IWILL-IWCN) 310,320,310
C
C
C 300
AP(1,4)=126.0
AP(1,6)=-70.0
AP(1,8)=-486.0
AP(1,10)=855.0
AP(1,12)=-670.0
AP(1,14)=324.0
AP(1,16)=-90.0
AP(1,18)=11.0
AP(3,4)=1.0
AP(2,4)=-10.0
AP(2,6)=-77.0
AP(2,8)=150.0
AP(2,10)=-100.0
AP(2,12)=50.0
AP(2,14)=-15.0
AP(2,16)=2.0
AP(4,2)=-489.0
AP(4,4)=1818.0
AP(4,6)=-2924.0
AP(4,8)=2690.0
AP(4,10)=-1710.0
AP(4,12)=814.0
AP(4,14)=-268.0

```

```

MA07C 4
MA07C 5
MA07C 6
MA07C 7
MA07C 8
MA07C 9
MA07C 10
MA07C 11
MA07C 12
MA07C 13
MA07C 14
MA07C 15
MA07C 16
MA07C 17
MA07C 18
MA07C 19
MA07C 20
BCOND 1
BCOND 2
BCOND 3
BCOND 4
BCOND 5
BCOND 6
BCOND 7
BCOND 8
BCOND 9
BCOND 10
BCOND 11
BCOND 12
BCOND 13
BCOND 14
BCOND 15
BCOND 16
BCOND 17
BCOND 18
BCOND 19
BCOND 20
BCOND 21
BCOND 22
BCOND 23
BCOND 24
BCOND 25
BCOND 26
BCOND 27
BCOND 28
BCOND 29
BCOND 30
BCOND 31
BCOND 32
BCOND 33
BCOND 34
BCOND 35
BCOND 36
BCOND 37
BCOND 38

```

```

C FCR I=1,3,5...
310 CONTINUE
  AP(1,6)=-10.0
  AB(1,9)=-77.0
  AP(1,12)=150.0
  AB(1,15)=-100.0
  AP(1,18)=50.0
  AB(1,21)=-15.0
  AP(1,24)=2.0
  GO TO 387
22 FCR I=2,4,6...
  CONTINUE
  AP(1,6)=126.0
  AB(1,9)=-70.0
  AP(1,12)=-486.0
  AB(1,15)=855.0
  AP(1,18)=-670.0
  AB(1,21)=324.0
  AP(1,24)=-90.0
  AB(1,27)=11.0
  GO TO 387
24 FCR I=2,4,6...
  CONTINUE
  AP(1,6)=126.0
  AB(1,9)=-70.0
  AP(1,12)=-486.0
  AB(1,15)=855.0
  AP(1,18)=-670.0
  AB(1,21)=324.0
  AP(1,24)=-90.0
  AB(1,27)=11.0
  GO TO 387
C FCR CIAMPED EDGE
C FCR CIAMPED EDGF
406 CONTINUE
  AP(5,15)=1.0

```

```

PCOND 42
PCOND 43
PCOND 44
PCOND 45
PCOND 46
PCOND 47
PCOND 48
PCOND 49
PCOND 50
PCOND 51
PCOND 52
PCOND 53
PCOND 54
PCOND 55
PCOND 56
PCOND 57
PCOND 58
PCOND 59
PCOND 60
PCOND 61
PCOND 62
PCOND 63
PCOND 64
PCOND 65
PCOND 66
PCOND 67
PCOND 68
PCOND 69
PCOND 70
PCOND 71
PCOND 72
PCOND 73
PCOND 74
PCOND 75
PCOND 76
PCOND 77
PCOND 78
PCOND 79
PCOND 80
PCOND 81
PCOND 82
PCOND 83
PCOND 84
PCOND 85
PCOND 86
PCOND 87
PCOND 88
PCOND 89
PCOND 90
PCOND 91
PCOND 92
PCOND 93

```

```

AP(6,15)=1.0
AP(7,15)=(30.0*CT+126.0/H)*AL1
AP(7,13)=(231.0*CT-70.0/H)*AL1
AB(7,11)=(-450.0*CT-486.0/H)*AL1
AP(7,9)=(300.0*CT+855.0/H)*AL1
AP(7,7)=(-150.0*CT-670.0/H)*AL1
AB(7,5)=(45.0*CT+324.0/H)*AL1
AP(7,3)=(-6.0*CT-90.0/H)*AL1
AB(7,1)=11.0*AL1/H
AB(7,16)=(-126.0*CT-22.5*15.0/H)*AL/H
AB(7,14)=(70.0*CT+56.0*22.5/H)*AL/H
AP(7,12)=(486.0*CT-22.5*83.0/H)*AL/H
AB(7,10)=(-855.0*CT+22.5*64.0/H)*AL/H
AB(7,8)=(670.0*CT-22.5*29.0/H)*AL/H
AB(7,6)=(-324.0*CT+22.5*8.0/H)*AL/H
AP(7,4)=(90.0*CT-22.5/H)*AL/H
AB(7,2)=-11.0*CT*AL/H
AB(8,15)=10.0
AB(8,13)=77.0
AB(8,11)=-150.0
AB(8,9)=100.0
AB(8,7)=-50.0
AB(8,5)=15.0
AB(8,3)=-2.0
GO TO 340
387 CONTINUE
  AP(7,22)=1.0
  AB(8,22)=1.0
  AP(9,22)=1.0
  AB(10,22)=(30.0*CT+126.0/H)*AL1
  AP(10,19)=(231.0*CT-70.0/H)*AL1
  AB(10,16)=(-450.0*CT-486.0/H)*AL1
  AP(10,13)=(300.0*CT+855.0/H)*AL1
  AP(10,10)=(-150.0*CT-670.0/H)*AL1
  AB(10,7)=(45.0*CT+324.0/H)*AL1
  AP(10,4)=(-6.0*CT-90.0/H)*AL1
  AB(10,1)=11.0*AL1/H
  AB(10,24)=(-126.0*CT-22.5*15.0/H)*AL/H
  AB(10,21)=(70.0*CT+56.0*22.5/H)*AL/H
  AP(10,18)=(486.0*CT-22.5*83.0/H)*AL/H
  AB(10,15)=(-855.0*CT+22.5*64.0/H)*AL/H
  AB(10,12)=(670.0*CT-22.5*29.0/H)*AL/H
  AB(10,9)=(-324.0*CT+22.5*8.0/H)*AL/H
  AP(10,6)=(90.0*CT-22.5/H)*AL/H
  AB(10,3)=-11.0*CT*AL/H
  AP(11,22)=10.0
  AB(11,19)=77.0
  AB(11,16)=-150.0
  AB(11,13)=100.0
  AB(11,10)=-50.0
  AB(11,7)=15.0
  AB(11,4)=-2.0
  GO TO 340
7 AB(12,1)=AB(11,1)
GO TO 340

```

```

PCOND 94
PCOND 95
PCOND 96
PCOND 97
PCOND 98
PCOND 99
PCOND 100
PCOND 101
PCOND 102
PCOND 103
PCOND 104
PCOND 105
PCOND 106
PCOND 107
PCOND 108
PCOND 109
PCOND 110
PCOND 111
PCOND 112
PCOND 113
PCOND 114
PCOND 115
PCOND 116
PCOND 117
PCOND 118
PCOND 119
PCOND 120
PCOND 121
PCOND 122
PCOND 123
PCOND 124
PCOND 125
PCOND 126
PCOND 127
PCOND 128
PCOND 129
PCOND 130
PCOND 131
PCOND 132
PCOND 133
PCOND 134
PCOND 135
PCOND 136
PCOND 137
PCOND 138
PCOND 139
PCOND 140
PCOND 141
PCOND 142
PCOND 143
PCOND 144
PCOND 145
PCOND 146
PCOND 147
PCOND 148

```

```

*DECK NFWAVE
SUBROUTINE NFWAVE (W, I90, IN, AI, ICCUNT)
DIMENSION W(199)
C CALCULATES THE NUMBER OF TURNING POINTS IN THE W PROFILE, RETURNS THEM AS
C ICCUNT
IF(AI.FO.0.0) GO TO 5
ISTEP=3
GO TO 6
5 ISTEP=2
5 ICCUNT=0
KOLD=12
I=ISTEP
J=I*2
DO 100 IJ=2, IN
(I=I+ISTEP
J=J+ISTEP
IF(W(I)-W(J)) 20,30,40
20 KK=-1
GO TO 50
30 KOLD=0
GO TO 100
40 KK=1
50 CONTINUE
IF(KK.FO.KOLD) GO TO 100
ICCNT=ICCNT+1
KOLD=KK
100 CONTINUE
J=ISTEP*3
TEMP=W(ISTEP)*W(J)
IF(TEMP.LT.0.0) ICCUNT=ICCNT-1
RETURN
END
** *DFCK ENERGY
SUBROUTINE ENERGY (U, IX, P, V, V2, V3, NV, NZ, UF, NUF, KUF, UFB, NUFB, KUFB,
CPF, Z3, UFC, NUFC, IFT, LNO, ELMT, Z9, NV1, Z4)
DIMENSION U(IX), UF(NUF, KUF), V(NV), V2(NV), V3(NZ), UFB(NUFB, KUFB), PF(
C KUF), Z3(NV), UFC(NUFC, KUF), Z9(NV1), Z4(IX)
COMMON/CCM1/ AN(7,4,12), ITYPE, ILN(7), IAK(7), JSN(7), JKN(7), KBOE(7)
COMMON/CCM2/ DO, C1, C2, C3, C4, AL, THETA, PCL, H, AI, IFR, ION
COMMON /COM3/ JAC, JAW, JAW, JF, ID, IC, FT, IZAP
COMMON /COM4/ IN, N1, N2
COMMON/CCM5/ VF(147,20), VFB(147,20), VFC(106,20), PFC(20), FFC(20)
C, SF(147)
LEVEL 2, UF, UFB, UFC
IQ=LNC
IF(IFT.FO.0) IQ=IPR
ICHS=1
IFAII=0
C CALCULATES THE ENERGY COMPONENTS OF THE TOTAL POTENTIAL ENERGY GIVING RISE
C TO THE SECONDARY PATH EQUATIONS. PRINTS OUT THE SOLUTION VECTOR AND THE EN
C ERGY COMPONENTS
C ARGUMENTS *****

```

```

ENERGY 1
ENERGY 2
ENERGY 3
ENERGY 4
ENERGY 5
ENERGY 6
ENERGY 7
ENERGY 8
ENERGY 9
ENERGY 10
ENERGY 11
ENERGY 12
ENERGY 13
ENERGY 14
ENERGY 15
ENERGY 16
ENERGY 17
ENERGY 18
ENERGY 19
ENERGY 20
ENERGY 21
ENERGY 22
ENERGY 23
ENERGY 24
ENERGY 25
ENERGY 26
ENERGY 27
ENERGY 28
ENERGY 29
ENERGY 30
ENERGY 31
ENERGY 32
ENERGY 33
ENERGY 34
ENERGY 35
ENERGY 36
ENERGY 37
ENERGY 38
ENERGY 39
ENERGY 40
ENERGY 41
ENERGY 42
ENERGY 43
ENERGY 44
ENERGY 45
ENERGY 46
ENERGY 47
ENERGY 48
ENERGY 49
ENERGY 50
ENERGY 51
ENERGY 52
ENERGY 53
ENERGY 54
ENERGY 55
ENERGY 56
ENERGY 57
ENERGY 58
ENERGY 59
ENERGY 60
ENERGY 61
ENERGY 62
ENERGY 63
ENERGY 64
ENERGY 65
ENERGY 66
ENERGY 67
ENERGY 68
ENERGY 69
ENERGY 70
ENERGY 71
ENERGY 72
ENERGY 73
ENERGY 74
ENERGY 75

```

```

WRITE (6,4000)
AI2=AI*AI
PA=0.0
AK=1.0
AJ=1.0
IF (ICN.EQ.20.OR.ICN.EQ.30) AK=2.0
IF (ICN.EQ.20.OR.ICN.EQ.0) AJ=0.0
DC 110 KK=1,1TYPE
CALL FRDATA (KK,ITCL,MTD,ISTART,IFIN)
DO 100 IJ=ISTART,IFIN
  PA=PA+1.0
  PHI=PA*H
  S=SIN(PHI)
  C=COS(PHI)
  CT=C/S
  U1=0.0
  V1=0.0
  W1=0.0
  W2=0.0
  IU=IC*(IJ+1)+1
  IV=IU+IE/2
  IW=IU+IE
  K1=3*IJ-2
  K2=K1+1
  K3=K1+2
  ISU=IU-IC*MI
  DO 80 K=1,ITCL
    ICU=ISU+IC*K
    ICV=ICU+IE/2
    ICW=ICU+IE
    U1=U1+AN(KK,1,K)*U(ICU)
    W1=W1+AN(KK,1,K)*U(ICW)
    W2=W2+AN(KK,2,K)*U(ICW)
    IF(AJ.EQ.0.0) GC TO 80
    V1=V1+AN(KK,1,K)*U(ICV)
  CCNTINUE
  EQ=U1+U(IW)
  EC=U(IW)+U(IU)*CT
  EOC=0.0
  E20=(U(IU)-W1)**2/2.0
  E2C=0.0
  XO=U1-W2
  XC=U(IU)*CT-W1*CT
  XOC=0.0
  E1=U(IU)+CT+U(IW)
  E2=U1-W1*CT
  E3=0.0
  F4=0.0
  E5=0.0
  BU=U(IU)-W1
  IF(AI.FO.0.0) GC TO 90
  FC=EQ+AI*U(IV)/S

```

```

ENERGY 78
ENERGY 79
ENERGY 80
ENERGY 81
ENERGY 82
ENERGY 83
ENERGY 84
ENERGY 85
ENERGY 86
ENERGY 87
ENERGY 88
ENERGY 89
ENERGY 90
ENERGY 91
ENERGY 92
ENERGY 93
ENERGY 94
ENERGY 95
ENERGY 96
ENERGY 97
ENERGY 98
ENERGY 99
ENERGY 100
ENERGY 101
ENERGY 102
ENERGY 103
ENERGY 104
ENERGY 105
ENERGY 106
ENERGY 107
ENERGY 108
ENERGY 109
ENERGY 110
ENERGY 111
ENERGY 112
ENERGY 113
ENERGY 114
ENERGY 115
ENERGY 116
ENERGY 117
ENERGY 118
ENERGY 119
ENERGY 120
ENERGY 121
ENERGY 122
ENERGY 123
ENERGY 124
ENERGY 125
ENERGY 126
ENERGY 127
ENERGY 128
ENERGY 129
ENERGY 130

```

```

FOC=FOC+(V1-U(IV)*CT-AI*U(IU)/S)/2.0
E20=E20+V1*V1/2.0
E2C=E20+((-AI*U(IU)/S-U(IV)*CT)**2+(U(IV)+AI*U(IW)/S)**2)/2.0
XC=XO+AI*U(IV)/S+AI2*U(IW)/(S*S)
XOC=XOC+(-U(IV)*CT+V1+2.0*AI*W1/S-2.0*AI*U(IW)*CT/S-AI*U(IU)/S)/2.0
C
E3=E3+AI*U(IV)/S
E4=E4-AI*U(IU)/S-U(IV)*CT
F5=F5+AI*U(IW)/S+U(IV)
90
CCNTINUE
Z3(K1)=FO
Z3(K2)=FC
Z3(K3)=FOO
IKT=IJ/2
IKT=IJ-2*IKT
AKT=IKT+1
EA=1.0-V2(K1)*(1.0-V2(K1))-V2(K3)*V2(K3)/2.0
FF=V2(K3)*(-1.0+3.0*V2(K1))
EX=(V1*V1+BU*BU)*FA/2.0+EO*PU*EF+(EO*EO-BU*BU)*V2(K3)*V2(K3)/2.0
E2=(E4*F4+E5*F5)*(1.0-V2(K2)+V2(K2)*V2(K2))/2.0
FA=EA+V2(K3)
FE=V2(K3)*FE
V(1)=V(1)+AKT*EO*EO*S
V(2)=V(2)+AKT*EC*EC*S
V(3)=V(3)+AKT*DO*2.0*EO*FO*S
V(4)=V(4)+AKT*2.0*(1.0-DO)*EO*EO*EC*S
V(5)=V(5)+AKT*(2.0*FO*PU*FA+FO*EO*EF-PU*BU*FE)*S
V(6)=V(6)+AKT*DO*2.0*(FO*PU*EA+FO*EO*FE/2.0)*S
V(7)=V(7)+AKT*(1.0-FC)*(V1*V1*(V2(K1)-V2(K3))*V2(K3)/2.0+1.5*V2(K1)*V2(K1)+F4*F4*(V2(K2)-V2(K3))*V2(K3)/2.0+1.5*V2(K2)**2)+E5*E5
V(8)=V(8)+AKT*(V1*V1*(V2(K1)-V2(K2))-V2(K3)*V2(K3)+V2(K1)+V2(K2)+F4*F4*V2(K3)*(1.0-V2(K1))-2.0*V2(K2))*S
V(9)=V(9)+AKT*(1.0-EC)*(V1*V1*2.0*V2(K1)+V2(K3)**2-V2(K1)**2)+E4*E4
V(10)=V(10)+AKT*(V1*V1*(V2(K1)-V2(K3))*V2(K3)+V2(K2)))*S
V(11)=V(11)+AKT*(V1*V1*(V2(K1)-V2(K3))*V2(K3)+V2(K1)+0.5*V2(K3)**2-2.0*V2(K1)**2)*(FO*EO-BU*BU)*V2(K1)*V2(K3)+V2(K3)/2.0)*S
V(12)=V(12)+AKT*2.0*E2*V2(K2)*S
V(13)=V(13)+AKT*2.0*(FO*FO*V2(K2)*S
V(14)=V(14)+AKT*2.0*(FO*FO*V2(K2)*S
V(15)=V(15)+AKT*2.0*(FO*FO*V2(K2)*S
V(16)=V(16)+AKT*2.0*(FO*FO*V2(K2)*S
V(17)=V(17)+AKT*2.0*(1.0-DO)*XO*XOC*S*AL
V(61)=-FO*EO*V2(K3)**2

```

```

ENERGY 131
ENERGY 132
ENERGY 133
ENERGY 134
ENERGY 135
ENERGY 136
ENERGY 137
ENERGY 138
ENERGY 139
ENERGY 140
ENERGY 141
ENERGY 142
ENERGY 143
ENERGY 144
ENERGY 145
ENERGY 146
ENERGY 147
ENERGY 148
ENERGY 149
ENERGY 150
ENERGY 151
ENERGY 152
ENERGY 153
ENERGY 154
ENERGY 155
ENERGY 156
ENERGY 157
ENERGY 158
ENERGY 159
ENERGY 160
ENERGY 161
ENERGY 162
ENERGY 163
ENERGY 164
ENERGY 165
ENERGY 166
ENERGY 167
ENERGY 168
ENERGY 169
ENERGY 170
ENERGY 171
ENERGY 172
ENERGY 173
ENERGY 174
ENERGY 175
ENERGY 176
ENERGY 177
ENERGY 178
ENERGY 179
ENERGY 180
ENERGY 181
ENERGY 182
ENERGY 183
ENERGY 184
ENERGY 185

```

```

1(K2))
V(65)=FO*RU*(2.0*DO*V2(K3)*(1.0-V2(K1)))
V(66)=V1*V1*((1.0-V2(K1))*(V2(K1)+CO*V2(K2))+0.5*V2(K3)**2-D2*(V2(K1)+0.5*V2(K3)**2-1.5*V2(K1)**2))
V(67)=F4*F4*((1.0-V2(K2))*(V2(K2)+DO*V2(K1))+0.5*DO*V2(K3)**2-D2*(V2(K2)+0.5*V2(K3)**2-1.5*V2(K2)**2))
V(68)=F5*F5*((1.0-V2(K2))*(V2(K2)+CO*V2(K1))+0.5*DO*V2(K3)**2+D2*V2(K3)+V2(K3)/2.0)
V(69)=-V1*F4*DO*(V2(K1)*(1.0-V2(K1)-V2(K2))+V2(K2)*(1.0-V2(K2))+V2(K3)**2)
V(70)=V1*E5*DO*V2(K3)*(1.0-2.0*V2(K1)-V2(K2))
V(71)=E1*F5*DO*V2(K3)*(1.0-V2(K1)-2.0*V2(K2))
IF (ICM.FO.-10) GO TC 94
O1=AK*(VF(K1,1)+0.5*VF(K3,1)**2-0.5*VF(K1,1)*VF(K3,1)**2)-AJ*(SF(K1)-DO*SF(K2))/(1.0+CO*DO)
O2=AK*(VF(K2,1))-AJ*(SF(K2)-CO*SF(K1))/(1.0+FO*DO)
V(8)=V(8)-AKT*EX*Q1*S
V(9)=V(9)-AKT*EZ*Q2*S
V(10)=V(10)-AKT*EO*EX*Q2*S
V(11)=V(11)-AKT*EO*EZ*Q1*S
V(63)=V(63)+EO*RU*V2(K3)*(G1+DO*Q2)
V(64)=V(64)-RU*RU*(1.0-V2(K1))*(O1+CO*Q2)/2.0
V(66)=V(66)-V1*V1*(1.0-V2(K1))*(O1+FO*Q2)/2.0
V(67)=V(67)-F4*F4*(1.0-V2(K2))*(O2+CO*Q1)/2.0
V(68)=V(68)-F5*F5*(1.0-V2(K2))*(O2+CO*Q1)/2.0
V(13)=V(13)+2.0*AKT*E1*(E1*E1*(VF(K1,1)+2.0*VF(K2,1)+VF(K3,1)*CT)+F1*F2*2.0*VF(K2,1)+F1*E3*(VF(K1,1)+VF(K2,1)+VF(K3,1)*CT)+F2*F3*VF(K2,1))*(S**3)
94 CONTINUE
ILL1=ILL1+1
IF (ILL1.FO.4.NR.III1.LT.0) GO TO 95
GO TO 98
95 WRITE (6,4010) IKK1,(V(J),J=61,71),IKK1
IKK1=IKK1+4
IF (ILL1.LT.0) IKK1=IKK1-1
ILL1=0
98 GO 99 J=61,71
99 V(J+20)=V(J+20)+AKT*V(J)*S
100 CONTINUE
110 CONTINUE
EPCS=0.0
ENFG=0.0
DO 130 I=1,17
IF (V(I).GT.0.0) GO TO 120
ENEG=ENEG+V(I)
GO TC 130
120 EPOS=EPOS+V(I)
130 CONTINUE
ERP=(2.0*(EPCS+ENFG)/(EPOS-ENEG))*100.0
TEMP=(EPOS-ENEG)/2.0
DO 140 I=1,17
V(I+17)=V(I)/TEMP

```

ENERGY 188
ENERGY 190
ENERGY 191
ENERGY 192
ENERGY 193
ENERGY 194
ENERGY 195
ENERGY 196
ENERGY 197
ENERGY 198
ENERGY 199
ENERGY 200
ENERGY 201
ENERGY 202
ENERGY 203
ENERGY 204
ENERGY 205
ENERGY 206
ENERGY 207
ENERGY 208
ENERGY 209
ENERGY 210
ENERGY 211
ENERGY 212
ENERGY 213
ENERGY 214
ENERGY 215
ENERGY 216
ENERGY 217
ENERGY 218
ENERGY 219
ENERGY 220
ENERGY 221
ENERGY 222
ENERGY 223
ENERGY 224
ENERGY 225
ENERGY 226
ENERGY 227
ENERGY 228
ENERGY 229
ENERGY 230
ENERGY 231
ENERGY 232
ENERGY 233
ENERGY 234
ENERGY 235
ENERGY 236
ENERGY 237
ENERGY 238
ENERGY 239
ENERGY 240

```

140 V(I)=V(I)*H/3.0
WRITE (6,2030)
DO 145 I=R1,91
145 V(I+20)=V(I)/TEMP
WRITE (6,2000)
IF (AL.FO.0.0) GO TC 160
IJ=0
WRITE (6,2010) IJ,U(1),U(2),U(3),IJ
IJ=1
WRITE (6,2010) IJ,U(4),U(5),U(6),IJ
NNN=N2-6
DO 150 I=7,NNN,3
IJ=IJ+1
J=I+1
K=I+2
K1=I-6
K2=J-6
K3=K-6
TEMP=V2(K1)+0.5*V2(K3)+V2(K3)*(1.0-V2(K1)+V2(K1)+V2(K1)-0.25*V2(K3)**2)
150 WRITE (6,2011) IJ,U(I),U(J),U(K),Z3(K1),Z3(K2),Z3(K3),TEMP,V2(K2),
CIJ
IJ=IJ+1
J=I+1
K=I+2
WRITE (6,2010) IJ,U(I),U(J),U(K),IJ
IJ=IJ+1
I=I+3
J=I+1
K=I+2
WRITE (6,2010) IJ,U(I),U(J),U(K),IJ
GO TO 180
160 BEMP=0.0
IJ=0
WRITE (6,2010) IJ,U(1),BEMP,U(2),IJ
IJ=1
WRITE (6,2010) IJ,U(3),BEMP,U(4),IJ
NNN=N2-4
DO 170 I=5,NNN,2
IJ=IJ+1
J=I+1
K1=(IJ-1)*3-2
K2=K1+1
K3=K1+2
TEMP=V2(K1)+0.5*V2(K3)+V2(K3)*(1.0-V2(K1)+V2(K1)+V2(K1)-0.25*V2(K3)**2)
170 WRITE (6,2011) IJ,U(I),BEMP,U(J),Z3(K1),Z3(K2),Z3(K3),TEMP,V2(K2),
CIJ
IJ=IJ+1
J=I+1
WRITE (6,2010) IJ,U(I),BEMP,U(J),IJ
IJ=IJ+1
I=I+2
J=I+1
WRITE (6,2010) IJ,U(I),BEMP,U(J),IJ

```

ENERGY 241
ENERGY 242
ENERGY 243
ENERGY 244
ENERGY 245
ENERGY 246
ENERGY 247
ENERGY 248
ENERGY 249
ENERGY 250
ENERGY 251
ENERGY 252
ENERGY 253
ENERGY 254
ENERGY 255
ENERGY 256
ENERGY 257
ENERGY 258
ENERGY 259
ENERGY 260
ENERGY 261
ENERGY 262
ENERGY 263
ENERGY 264
ENERGY 265
ENERGY 266
ENERGY 267
ENERGY 268
ENERGY 269
ENERGY 270
ENERGY 271
ENERGY 272
ENERGY 273
ENERGY 274
ENERGY 275
ENERGY 276
ENERGY 277
ENERGY 278
ENERGY 279
ENERGY 280
ENERGY 281
ENERGY 282
ENERGY 283
ENERGY 284
ENERGY 285
ENERGY 286
ENERGY 287
ENERGY 288
ENERGY 289
ENERGY 290
ENERGY 291
ENERGY 292
ENERGY 293
ENERGY 294
ENERGY 295

```

FNPCL=PI*PI*SQRT(1.0-DO*DO)/(1.0-DO*DO)
PEMP=0.0
WRITE (6,2030)
WRITE (6,2030)
WRITE (6,2111)
WRITE (6,2110)
V(40)=V(12)+V(13)
V(41)=V(29)+V(30)
WRITE (6,2120)
WRITE (6,2130) V(12),V(13),V(40)
WRITE (6,2130) V(29),V(30),V(41)
WRITE (6,2030)
WRITE (6,2111)
WRITE (6,2140)
V(12)=V(1)+V(3)/2.0
V(13)=V(2)+V(3)/2.0
V(29)=V(18)+V(20)/2.0
V(30)=V(19)+V(20)/2.0
V(40)=V(12)+V(13)+V(4)
V(41)=V(29)+V(30)+V(21)
WRITE (6,2030)
WRITE (6,2150)
WRITE (6,2160) V(12),V(13),V(4),V(40)
WRITE (6,2160) V(29),V(30),V(21),V(41)
V(1)=V(5)+V(6)/2.0
V(2)=V(6)/2.0
V(3)=V(7)
V(18)=V(22)+V(23)/2.0
V(19)=V(23)/2.0
V(20)=V(24)
V(40)=V(1)+V(2)+V(3)
V(41)=V(18)+V(19)+V(20)
WRITE (6,2170)
WRITE (6,2180) (V(I),I=1,3),V(40)
WRITE (6,2180) (V(I),I=18,20),V(41)
V(4)=(V(8)+V(10))/2.0
V(5)=(V(8)+V(11))/2.0
V(6)=(V(9)+V(11))/2.0
V(7)=(V(9)+V(10))/2.0
V(21)=(V(25)+V(27))/2.0
V(22)=(V(25)+V(28))/2.0
V(23)=(V(26)+V(28))/2.0
V(24)=(V(26)+V(27))/2.0
V(42)=V(4)+V(5)+V(6)+V(7)
V(43)=V(21)+V(22)+V(23)+V(24)
WRITE (6,2190)
WRITE (6,2200) (V(I),I=4,7),V(42)
WRITE (6,2200) (V(I),I=21,24),V(43)
V(1)=V(1)+V(4)+V(5)
V(2)=V(2)+V(6)+V(7)
V(18)=V(18)+V(21)+V(22)
V(19)=V(19)+V(23)+V(24)
V(40)=V(40)+V(42)

```

```

ENERGY 298
ENERGY 299
ENERGY 300
ENERGY 301
ENERGY 302
ENERGY 303
ENERGY 304
ENERGY 305
ENERGY 306
ENERGY 307
ENERGY 308
ENERGY 309
ENERGY 310
ENERGY 311
ENERGY 312
ENERGY 313
ENERGY 314
ENERGY 315
ENERGY 316
ENERGY 317
ENERGY 318
ENERGY 319
ENERGY 320
ENERGY 321
ENERGY 322
ENERGY 323
ENERGY 324
ENERGY 325
ENERGY 326
ENERGY 327
ENERGY 328
ENERGY 329
ENERGY 330
ENERGY 331
ENERGY 332
ENERGY 333
ENERGY 334
ENERGY 335
ENERGY 336
ENERGY 337
ENERGY 338
ENERGY 339
ENERGY 340
ENERGY 341
ENERGY 342
ENERGY 343
ENERGY 344
ENERGY 345
ENERGY 346
ENERGY 347
ENERGY 348
ENERGY 349
ENERGY 350

```

```

V(41)=V(41)+V(43)
WRITE (6,2210)
WRITE (6,2220)
WRITE (6,2230) (V(I),I=1,3),V(40)
WRITE (6,2230) (V(I),I=18,20),V(41)
WRITE (6,2210)
V(14)=V(14)+V(16)/2.0
V(15)=V(15)+V(16)/2.0
V(16)=V(17)
V(31)=V(31)+V(33)/2.0
V(32)=V(32)+V(33)/2.0
V(33)=V(34)
V(40)=V(14)+V(15)+V(16)
V(41)=V(31)+V(32)+V(33)
WRITE (6,2240)
WRITE (6,2250) (V(I),I=14,16),V(40)
WRITE (6,2250) (V(I),I=31,33),V(41)
WRITE (6,2030)
WRITE (6,4020)
WRITE (6,4030) (V(I),I=81,86)
WRITE (6,4030) (V(I),I=101,106)
WRITE (6,4040)
WRITE (6,4050) (V(I),I=87,91)
WRITE (6,4050) (V(I),I=107,111)
WRITE (6,2030)
WRITE (6,2030)
WRITE (6,2260) ERR
WRITE (6,2270) FI,PN,FNPCL
WRITE (6,2030)
RETURN
2000 FCRMAT (1H0,4HNCCF,9X,1H0,13X,1HV,14X,1HW,12X,5HFO(S),10X,5HFO(S),
C9X,6HFO(S),10X,5HFO(F),10X,5HFO(F),8X,4HNDDF)
2010 FCRMAT (1H,1X,13,3(E13.6,2X),75X,13)
2011 FCRMAT (1H,1X,13,8(E13.6,2X),13)
2111 FCRMAT (1H0)
2030 FCRMAT (1H0,5X,100H- - - - - )
C 4 - - - - - )
2040 FCRMAT (1H0,10X,11HFC(S)*EO(S),7X,11HFC(S)*FC(S),4X,16H2*DO*EO(S)*
FC(S),2X,22H2*(1-DO)*EO(S)*EO(S),2X,5HTOTAL)
2050 FCRMAT (1H,9X,3(E12.4,6X),3X,E12.4,6X,E12.4)
2060 FCRMAT (1H0,6X,15HFO(F,S)*EO(F,S),4X,15HFO(F,S)*EO(F,S),4X,20H2*DO
C*EO(F,S)*EO(F,S),2X,26H2*(1-DO)*FOC(F,S)*EO(F,S),2X,5HTOTAL)
2070 FCRMAT (1H,7X,1(E12.4,7X),3X,E12.4,16X,E12.4)
2080 FCRMAT (1H0,8X,15H2*FO(F,S)*EO(F,S),4X,15H2*FO(F,S)*EO(F,S),4X,18H2*DO
C*EO(F,S)*EO(F,S),4X,16H2*DO*FO(F,S)*EO(F,S),4X,5HTOTAL)
2090 FCRMAT (1H,9X,3(E12.4,7X),4X,E12.4,7X,E12.4)
2100 FCRMAT (1H0,10X,11HXC(S)*XO(S),7X,11HXC(S)*XO(S),4X,16H2*DO*XO(S)*
CX(S),2X,22H2*(1-DO)*XO(S)*XO(S),2X,5HTOTAL)
2110 FCRMAT (1H0,30X,14HLCAP POTENTIAL)
2120 FCRMAT (1H0,20X,7HP*CV(S),8X,9HP*CV(S),10X,5HTOTAL)
2130 FCRMAT (1H,18X,E12.4,4X,E12.4,7X,E12.4)
2140 FCRMAT (1H0,40X,28HSTRESS*STRAIN,FCMFM*CURV.)
2150 FCRMAT (1H0,10X,11HNC(S)*EO(S),7X,11HNC(S)*FC(S),6X,13HNO(S)*EOC(
CS),5X,5HTOTAL)
2160 FCRMAT (1H,9X,4(E12.4,6X))

```

```

ENERGY 351
ENERGY 352
ENERGY 353
ENERGY 354
ENERGY 355
ENERGY 356
ENERGY 357
ENERGY 358
ENERGY 359
ENERGY 360
ENERGY 361
ENERGY 362
ENERGY 363
ENERGY 364
ENERGY 365
ENERGY 366
ENERGY 367
ENERGY 368
ENERGY 369
ENERGY 370
ENERGY 371
ENERGY 372
ENERGY 373
ENERGY 374
ENERGY 375
ENERGY 376
ENERGY 377
ENERGY 378
ENERGY 379
ENERGY 380
ENERGY 381
ENERGY 382
ENERGY 383
ENERGY 384
ENERGY 385
ENERGY 386
ENERGY 387
ENERGY 388
ENERGY 389
ENERGY 390
ENERGY 391
ENERGY 392
ENERGY 393
ENERGY 394
ENERGY 395
ENERGY 396
ENERGY 397
ENERGY 398
ENERGY 399
ENERGY 400
ENERGY 401
ENERGY 402
ENERGY 403
ENERGY 404
ENERGY 405

```

```

2190 FORMAT (1H,10X,13HNO(F)*F0(F,S),5X,13HNO(F),5X,13HNO(F)*E
CO(F,S),5X,13HNO(F,S)*F0(F),5X,5HTOTAL)
2200 FORMAT (1H,10X,5(E12.4,6X))
2210 FORMAT (1H,10X,80H-----)
C-----)
2220 FORMAT (1H,3X,9HNSUP TOTAL,3X,11HNO*F0,(F,S),6X,11HNO*EC,(F,S),6X,
C13HNO*F00,(F,S),6X,5HTOTAL)
2230 FORMAT (1H,14X,4(E12.4,6X))
2240 FORMAT (1H,10X,11HNO(S)*X0(S),5X,11HNO(S)*X0(S),6X,13HNO(S)*X0(S)
C),7X,5HTOTAL)
2250 FORMAT (1H,7X,4(E12.4,6X))
2260 FORMAT (1H,90X,16HENERGY FRPCR IS ,F7.3,9H PEP CFMT)
2270 FORMAT (1H,20X,14HCRITICAL LCAD=,F16.8,3X,6HPPN/P =,F16.8,3X,8HPPN/P
CCL =,F16.8)
4000 FORMAT (1H,1X,4HPCCE,3X,5HE1*E1,5X,5HE1*F2,6X,4HE1*B,7X,3HB*B,6X,4
CHE2*B,5X,5HV1*V1,5X,5HE4*E4,5X,5HE5*F5,5X,5HV1*F4,5X,5HV1*E5,5X,5H
CE4*F5,3X,4HNCDF)
4010 FORMAT (1H,2X,12,2X,11(E9.3,1X),1X,12)
4020 FORMAT (1H,10X,5HE1*E1,10X,5HE1*F2,11X,4HE1*B,12X,3HB*B,11X,4HE2*
C),10X,5HV1*V1)
4030 FORMAT (1H,6X,6(E12.6,3X))
4040 FORMAT (1H,10X,5HE4*E4,10X,5HE5*F5,10X,5HV1*E4,10X,5HV1*F5,10X,5HE
C4*F5)
4050 FORMAT (1H,6X,5(E12.6,3X))
5000 FORMAT (1H,3X,16HT.F.F. V0 UMO,10X,3FUMO,10X,3HUR0,10X,3HUPO,10
CX,4HL.F.)
5010 FORMAT (1H,16X,5(F10.4,3X),4X,13HENERGY FRPCR =,F7.3,1X,8HPER CEN
CT)
5015 FORMAT (1H,16X,5(E10.4,3X))
5020 FORMAT (1H,16X,5(E10.4,3X))
5030 FORMAT (1H,3X,16HT.F.F. V1 UMO,10X,3FUMO,10X,3HUR0,10X,3HURC,1
CX,4HL.F.)
5040 FORMAT (1H,1X,18PTE DELTA V0 UMO,10X,3FUMO,10X,3HUR0,10X,3HURC,
"10X,4HL.F.)
END
ENERGY 409
ENERGY 410
ENERGY 411
ENERGY 412
ENERGY 413
ENERGY 414
ENERGY 415
ENERGY 416
ENERGY 417
ENERGY 418
ENERGY 419
ENERGY 420
ENERGY 421
ENERGY 422
ENERGY 423
ENERGY 424
ENERGY 425
ENERGY 426
ENERGY 427
ENERGY 428
ENERGY 429
ENERGY 430
ENERGY 431
ENERGY 432
ENERGY 433
ENERGY 434
ENERGY 435
ENERGY 436
ENERGY 437
ENERGY 438
ENERGY 439
ENERGY 440
ENERGY 441
ENERGY 442
ENERGY 443

```

CORRECTION ITEMS ARE LISTED IN CHRONOLOGICAL ORDER OF INSERTION

| SPHERE | FNCPTH | IMPRFT | LEGEND | REDUCE | PERTPN | CNVRGE | IMPRVE |
|--------|--------|--------|--------|--------|--------|--------|--------|
| TPEV01 | VCLDIS | EVALFN | FNDRHS | FNCRR2 | FNDLHS | STRNCP | BCKSUH |
| EDDATA | FUNVFC | SLVTR | DIRLTR | INVTR | SNDLHS | ENFRGY | CRTHOG |
| CONTRL | PRCDUC | MAC7P | MAC7C | RCCND | NOWAVE | | |

CKS ARE LISTED IN THE ORDER OF THEIR OCCURRENCE ON A NEW PROGRAM LIBRARY IF ONE IS CREATED BY THIS UPDATE

| YANKSSS | SPHERE | FNCPTH | IMPRFT | LEGEND | REDUCE | PERTPN | CNVRGE |
|---------|--------|--------|--------|--------|--------|--------|--------|
| IMPRVE | TPEV01 | VCLDIS | EVALFN | FNDRHS | FNCRR2 | FNDLHS | STRNCP |
| BCKSUP | EDDATA | FUNVFC | SLVTR | DIRLTR | INVTR | SNDLHS | SNDLHS |
| CRTHOG | CONTRL | PRCDUC | MAC7P | MAC7C | RCCND | NOWAVE | ENERGY |

DECKS WRITTEN TO COMPILE FILE

| SPHERE | FNCPTH | IMPRFT | LEGEND | REDUCE | PERTPN | CNVRGE | IMPRVE |
|--------|--------|--------|--------|--------|--------|--------|--------|
| TPEV01 | VCLDIS | EVALFN | FNDRHS | FNCRR2 | FNDLHS | STRNCP | BCKSUH |
| EDDATA | FUNVFC | SLVTR | DIRLTR | INVTR | SNDLHS | ENFRGY | CRTHOG |
| CONTRL | PRCDUC | MAC7P | MAC7C | RCCND | NOWAVE | | |

THIS UPDATE REQUIRED 25100B WORDS OF SCM
AND 07000B WORDS OF LCM.

***** PARTIAL SPHERE *****
 NUMBER OF NODES= 51 R/T= 100.000 PCISECSNS RATIO= .300 CPEN ANGLE= .660 LAMBDA= 12.000 PERT CMDCR=160

*** PERFECT SHELL ***
 M1= 2
 FCR PERT PARM 1 MAX LCCAL E= .2539E+00 TOTAL E= .2539E+00 AT WHICH P=-.1395E-02 PCIF=-.5472E-02 PDIF2= .2908E-03
 M1= 2
 FCR PERT PARM 2 MAX LCCAL E= .2695E+00 TOTAL E= .5234E+00 AT WHICH P=-.2850E-02 PDIF=-.5267E-02 PDIF2= .1543E-02
 M1= 2
 FCR PERT PARM 3 MAX LCCAL E= .1973E+00 TOTAL E= .7207E+00 AT WHICH P=-.3844E-02 PDIF=-.4717E-02 PDIF2= .4393E-02
 M1= 2
 FCR PERT PARM 4 MAX LCCAL E= .1123E+00 TOTAL E= .8330E+00 AT WHICH P=-.4341E-02 PDIF=-.4103E-02 PDIF2= .6467E-02
 M1= 2
 FCR PERT PARM 5 MAX LCCAL E= .1309E+00 TOTAL E= .9639E+00 AT WHICH P=-.4818E-02 PDIF=-.3150E-02 PDIF2= .8194E-02
 M1= 2
 FCR PERT PARM 6 MAX LCCAL E= .7715E-01 TOTAL E= .1041E+01 AT WHICH P=-.5034E-02 PDIF=-.2409E-02 PDIF2= .1127E-01
 M1= 2
 FCR PERT PARM 7 MAX LCCAL E= .7715E-01 TOTAL E= .1118E+01 AT WHICH P=-.5185E-02 PDIF=-.1493E-02 PDIF2= .1180E-01
 M1= 3
 FCR PERT PARM 8 MAX LCCAL E= .9668E-01 TOTAL E= .1215E+01 AT WHICH P=-.5277E-02 PDIF=-.4466E-03 PDIF2= .9837E-02
 M1= 3
 FCR PERT PARM 9 MAX LCCAL E= .1084E+00 TOTAL E= .1323E+01 AT WHICH P=-.5279E-02 PDIF= .2377E-03 PDIF2=-.1229E-02
 M1= 3
 FCR PERT PARM 10 MAX LCCAL E= .4736E-01 TOTAL E= .1371E+01 AT WHICH P=-.5270E-02 PDIF= .7653E-04 PDIF2=-.4624E-02
 M1= 2
 FCR PERT PARM 11 MAX LCCAL E= .4443E-01 TOTAL E= .1415E+01 AT WHICH P=-.5268E-02 PDIF= .9510E-04 PDIF2= .3439E-02
 M1= 2
 FCR PERT PARM 12 MAX LCCAL E= .5811E-01 TOTAL E= .1473E+01 AT WHICH P=-.5254E-02 PDIF= .4298E-03 PDIF2= .7401E-02
 M1= 2
 FCR PERT PARM 13 MAX LCCAL E= .7715E-01 TOTAL E= .1550E+01 AT WHICH P=-.5196E-02 PDIF= .1103E-02 PDIF2= .9782E-02
 M1= 2
 FCR PERT PARM 14 MAX LCCAL E= .9277E-01 TOTAL E= .1643E+01 AT WHICH P=-.5048E-02 PDIF= .2075E-02 PDIF2= .9626E-02
 M1= 2
 FCR PERT PARM 15 MAX LCCAL E= .7715E-01 TOTAL E= .1720E+01 AT WHICH P=-.4866E-02 PDIF= .2550E-02 PDIF2= .3048E-02
 FCR PERT PARM 16 MAX LOCAL E= .8691E-01 TOTAL E= .1807E+01 AT WHICH P=-.4639E-02 PDIF= .2645E-02 PDIF2= .7753E-03
 FEET METHOD COMPLETE, ** LACK OF STORAGE **

P-VS-E
 FOR PERT PARM= 1 E= .3174E-01 .6348E-01 .9521E-01 .1270E+00 .1587E+00 .1904E+00 .2222E+00 .2539E+00
 P/FCL= .1748E-03 .3495E-03 .5241E-03 .6986E-03 .8730E-03 .1047E-02 .1221E-02 .1395E-02
 VCL= .1256E-02 .2517E-02 .3782E-02 .5053E-02 .6328E-02 .7609E-02 .8895E-02 .1019E-01
 CIS= .1581E-03 .3156E-03 .4726E-03 .6291E-03 .7850E-03 .9406E-03 .1096E-02 .1251E-02
 FOR PERT PARM= 2 E= .2876E+00 .3213E+00 .3550E+00 .3887E+00 .4224E+00 .4561E+00 .4897E+00 .5234E+00
 P/FCL= .1579E-02 .1763E-02 .1946E-02 .2129E-02 .2311E-02 .2492E-02 .2671E-02 .2850E-02
 VCL= .2867E+00 .3201E+00 .3534E+00 .3865E+00 .4196E+00 .4524E+00 .4850E+00 .5174E+00
 CIS= .1156E-01 .1294E-01 .1433E-01 .1572E-01 .1712E-01 .1851E-01 .1992E-01 .2132E-01
 .1415E-02 .1579E-02 .1743E-02 .1907E-02 .2071E-02 .2236E-02 .2401E-02 .2568E-02

| | | | | | | | | | |
|------------------|-------|----------|----------|----------|----------|----------|----------|----------|----------|
| FOR FERT PARM= 3 | F= | 5481F+C0 | 5728E+00 | 5974E+00 | 6221F+00 | 6467E+00 | 6714E+00 | 6960E+00 | 7207E+00 |
| | P | 2979F+C2 | 3107E-02 | 3234F-02 | 3360E-02 | 3484F-02 | 3606F-02 | 3720E-02 | 3844E-02 |
| | P/VCL | 5409F+C0 | 5642E+00 | 5873F+00 | 6101F+00 | 6326F+00 | 6547E+00 | 6765E+00 | 6979E+00 |
| | VCL | 2235E-01 | 2338E-01 | 2446E-01 | 2543E-01 | 2645E-01 | 2746E-01 | 2847E-01 | 2948E-01 |
| | DTS | 2690E-02 | 2814E-02 | 2938E-02 | 3063E-02 | 3189E-02 | 3316E-02 | 3447E-02 | 3573E-02 |
| FOR FERT PARM= 4 | E= | 7347E+C0 | 7488F+00 | 7628F+00 | 7769E+00 | 7909F+00 | 8049F+00 | 8190E+00 | 8330F+00 |
| | P | 3909F+C2 | 3974F-02 | 4038F-02 | 4101E-02 | 4163E-02 | 4225E-02 | 4287E-02 | 4349E-02 |
| | P/VCL | 7098F+C0 | 7216E+00 | 7332F+00 | 7446E+00 | 7555E+00 | 7668F+00 | 7776F+00 | 7881E+00 |
| | VCL | 3004E-C1 | 3061E-01 | 3116F-01 | 3172E-01 | 3227E-01 | 3282E-01 | 3336E-01 | 3389E-01 |
| | DTS | 3046F-02 | 3120E-02 | 3194F-02 | 3268E-02 | 3343E-02 | 3417F-02 | 3490E-02 | 3564E-02 |
| FOR FERT PARM= 5 | E= | 8491F+C0 | 8657F+00 | 8821F+00 | 8984F+00 | 9148E+00 | 9312E+00 | 9475E+00 | 9639F+00 |
| | P | 4107F-02 | 4172E-02 | 4234E-02 | 4295E-02 | 4355E-02 | 4415E-02 | 4475E-02 | 4535E-02 |
| | P/VCL | 8002F+C0 | 8119E+00 | 8233F+00 | 8343E+00 | 8450E+00 | 8552E+00 | 8652E+00 | 8748E+00 |
| | VCL | 3451E-C1 | 3512E-01 | 3572E-01 | 3632E-01 | 3690E-01 | 3747E-01 | 3804E-01 | 3859E-01 |
| | DTS | 4249F-02 | 4332F-02 | 4414F-02 | 4494F-02 | 4571E-02 | 4645E-02 | 4713E-02 | 4776E-02 |
| FOR FERT PARM= 6 | E= | 9735E+C0 | 9892E+00 | 1002E+01 | 1002E+01 | 1022E+01 | 1022E+01 | 1031E+01 | 1041E+01 |
| | P | 4818F-02 | 4875E-02 | 4933F-02 | 4990E-02 | 5046E-02 | 5102E-02 | 5158E-02 | 5214E-02 |
| | P/VCL | 8802F+C0 | 8855E+00 | 8907F+00 | 8958E+00 | 9005E+00 | 9052E+00 | 9097E+00 | 9140E+00 |
| | VCL | 3892E-C1 | 3923E-01 | 3955E-01 | 3986E-01 | 4016E-01 | 4046E-01 | 4075E-01 | 4104E-01 |
| | DTS | 4810E-02 | 4842E-02 | 4874F-02 | 4905E-02 | 4936F-02 | 4967E-02 | 4997E-02 | 5028E-02 |
| FOR FERT PARM= 7 | E= | 1051E+C1 | 1060E+01 | 1070E+01 | 1080F+01 | 1089E+01 | 1099E+01 | 1109E+01 | 1118E+01 |
| | P | 5057E-02 | 5078E-02 | 5099E-02 | 5118E-02 | 5136E-02 | 5154E-02 | 5170E-02 | 5185E-02 |
| | P/VCL | 9181F+C0 | 9220E+00 | 9258F+00 | 9293E+00 | 9324E+00 | 9357E+00 | 9386E+00 | 9414E+00 |
| | VCL | 4132E-C1 | 4159E-01 | 4186F-01 | 4211E-01 | 4236E-01 | 4260E-01 | 4283E-01 | 4305E-01 |
| | DTS | 4969F-02 | 4974F-02 | 4977F-02 | 4978E-02 | 4978E-02 | 4977E-02 | 4976E-02 | 4975E-02 |
| FOR FERT PARM= 8 | E= | 1120F+C1 | 1142E+01 | 1154E+01 | 1167F+01 | 1179F+01 | 1191E+01 | 1203E+01 | 1215E+01 |
| | P | 5202E-02 | 5217E-02 | 5231E-02 | 5243E-02 | 5255E-02 | 5266E-02 | 5277E-02 | 5287E-02 |
| | P/VCL | 9445E+C0 | 9473E+00 | 9498E+00 | 9520E+00 | 9540E+00 | 9556E+00 | 9570E+00 | 9581E+00 |
| | VCL | 4331E-C1 | 4356E-01 | 4379F-01 | 4401E-01 | 4421E-01 | 4439E-01 | 4456E-01 | 4471E-01 |
| | DTS | 4976F-02 | 4980E-02 | 4987F-02 | 4998E-02 | 5014E-02 | 5036E-02 | 5054E-02 | 5099E-02 |
| FOR FERT PARM= 9 | E= | 1228E+C1 | 1242E+01 | 1255E+01 | 1269E+01 | 1283E+01 | 1296E+01 | 1310E+01 | 1323E+01 |
| | P | 5282E-02 | 5285E-02 | 5287E-02 | 5288E-02 | 5289E-02 | 5289E-02 | 5289E-02 | 5279E-02 |
| | P/VCL | 9591E+C0 | 9595E+00 | 9598E+00 | 9601F+00 | 9599E+00 | 9595E+00 | 9590E+00 | 9584E+00 |
| | VCL | 4486E-01 | 4499E-01 | 4509E-01 | 4517E-01 | 4523E-01 | 4527E-01 | 4527E-01 | 4525E-01 |
| | DTS | 5148E-02 | 5206E-02 | 5276F-02 | 5358E-02 | 5452F-02 | 5561E-02 | 5683E-02 | 5820E-02 |
| FOR FERT PARM=10 | E= | 1329F+C1 | 1335E+01 | 1341E+01 | 1347E+01 | 1353E+01 | 1359E+01 | 1365E+01 | 1371E+01 |
| | P | 5279E-02 | 5276E-02 | 5275E-02 | 5274E-02 | 5273E-02 | 5272E-02 | 5271E-02 | 5270E-02 |
| | P/VCL | 9592E+C0 | 9570E+00 | 9577E+00 | 9575E+00 | 9571E+00 | 9572E+00 | 9571E+00 | 9570E+00 |
| | VCL | 4521F-01 | 4522E-01 | 4520E-01 | 4517E-01 | 4514E-01 | 4511E-01 | 4508E-01 | 4505E-01 |
| | DTS | 5877E-02 | 5939E-02 | 6003E-02 | 6066E-02 | 6129E-02 | 6191E-02 | 6251E-02 | 6308E-02 |
| FOR FERT PARM=11 | E= | 1376E+C1 | 1382E+01 | 1387F+01 | 1393E+01 | 1398E+01 | 1404E+01 | 1409E+01 | 1415E+01 |
| | P | 5270E-02 | 5270E-02 | 5269F-02 | 5269E-02 | 5269E-02 | 5269E-02 | 5268E-02 | 5268E-02 |
| | P/VCL | 9569E+C0 | 9568E+00 | 9568F+00 | 9567E+00 | 9567E+00 | 9566E+00 | 9565E+00 | 9564E+00 |
| | VCL | 4502E-01 | 4498E-01 | 4495E-01 | 4492E-01 | 4488E-01 | 4485E-01 | 4481E-01 | 4477E-01 |
| | DTS | 6351E-02 | 6396E-02 | 6437F-02 | 6477E-02 | 6514E-02 | 6549E-02 | 6581E-02 | 6610E-02 |
| FOR FERT PARM=12 | E= | 1422E+C1 | 1430E+01 | 1437F+01 | 1444E+01 | 1451E+01 | 1459E+01 | 1466E+01 | 1473E+01 |
| | P | 5266E-02 | 5266E-02 | 5265F-02 | 5263E-02 | 5261E-02 | 5259E-02 | 5257E-02 | 5255E-02 |
| | P/VCL | 9563F+C0 | 9551E+00 | 9559E+00 | 9553E+00 | 9549E+00 | 9549E+00 | 9549E+00 | 9549E+00 |
| | VCL | 4472E-01 | 4466E-01 | 4463E-01 | 4454E-01 | 4441E-01 | 4433E-01 | 4426E-01 | 4420E-01 |
| | DTS | 6646E-02 | 6678E-02 | 6707E-02 | 6732E-02 | 6754E-02 | 6773E-02 | 6789E-02 | 6803E-02 |
| FOR FERT PARM=13 | E= | 1483E+C1 | 1492E+01 | 1502E+01 | 1512E+01 | 1521E+01 | 1531E+01 | 1541E+01 | 1550E+01 |
| | P | 5249E-02 | 5244E-02 | 5238F-02 | 5231E-02 | 5223E-02 | 5215E-02 | 5206E-02 | 5196E-02 |
| | P/VCL | 9531E+C0 | 9521E+00 | 9510E+00 | 9498E+00 | 9485E+00 | 9469E+00 | 9452E+00 | 9433E+00 |
| | VCL | 4415E-C1 | 4404E-01 | 4392E-01 | 4379E-01 | 4355E-01 | 4336E-01 | 4316E-01 | 4290E-01 |
| | DTS | 6818E-02 | 6833E-02 | 6844E-02 | 6844E-02 | 6848E-02 | 6850E-02 | 6851E-02 | 6851E-02 |

CIRCUMFERENTIAL MODE NO.= C EIGEN-VALUE POSITION = I NO. OF TURNING POINTS ON HALF SHELL = 4

T.P.E. V0 UMC 1.196E-05 UMC 1.230E-05 UMC 2.395E-06 UMC 5.871E-08 UMC 2.671E-05
 .4477E+00 .4604E+00 .8969E-01 .2198E-02 .1000E+01
 T.P.E. V1 UMC 2.283E-06 UMC 1.407E-06 UMC 2.528E-06 UMC 1.1785E-07 UMC 6.372E-06
 .3576E+00 .2204E+00 .3960E+00 .2796E-01 .9981E+00
 ENERGY ERRCR= .381 PER CENT

TPE DELTA V0 UMC 1.508E-07 UMC 1.592E-07 UMC 1.690E-07 UMC 1.007E-08 UMC 1.891E-07
 .3083E+00 .3255E+00 .3456E+00 .2059E-01 .1000E+01

| NCDE | U | V | E0(S) | EC(S) | F0(S) | EC(F) |
|------|---|---|-------------|--------------|--------------|--------------|
| 0 | 0 | 0 | 9.63916E-01 | 2.35630E+00 | 2.37278E+00 | 3.942179E-02 |
| 1 | 0 | 0 | 1.12364E-01 | 1.099946E+00 | 1.875899E+00 | 4.254492E-02 |
| 2 | 0 | 0 | 1.96024E-02 | 3.07535E-01 | 1.092712E+00 | 4.490902E-02 |
| 3 | 0 | 0 | 5.45520E-02 | 2.310680E-01 | 3.88431E-02 | 4.254492E-02 |
| 4 | 0 | 0 | 7.39835E-02 | 2.55735E+00 | 1.092712E+00 | 4.490902E-02 |
| 5 | 0 | 0 | 9.88332E-02 | 2.55735E+00 | 1.092712E+00 | 4.490902E-02 |
| 6 | 0 | 0 | 1.37546E-01 | 3.95130E+00 | 2.25605E+00 | 4.99644E-02 |
| 7 | 0 | 0 | 1.67328E-01 | 5.10787E+00 | 3.38431E+00 | 5.20754E-02 |
| 8 | 0 | 0 | 2.66439E-01 | 8.09903E+00 | 4.34346E+00 | 5.54197E-02 |
| 9 | 0 | 0 | 3.88377E-01 | 1.1396E+00 | 5.04679E+00 | 5.54197E-02 |
| 10 | 0 | 0 | 5.27676E-01 | 1.77271E+00 | 5.43487E+00 | 5.54197E-02 |
| 11 | 0 | 0 | 6.82996E-01 | 2.77071E+00 | 5.48110E+00 | 5.54197E-02 |
| 12 | 0 | 0 | 8.62296E-01 | 4.00000E+00 | 5.48110E+00 | 5.54197E-02 |
| 13 | 0 | 0 | 1.06420E-01 | 5.975616E+00 | 5.19119E+00 | 4.49839E-02 |
| 14 | 0 | 0 | 1.28990E-01 | 8.04522E+00 | 4.59742E+00 | 4.71368E-02 |
| 15 | 0 | 0 | 1.54520E-01 | 1.01702E+00 | 3.70840E+00 | 4.32233E-02 |
| 16 | 0 | 0 | 1.82733E-01 | 1.4181E+00 | 2.70840E+00 | 3.89380E-02 |
| 17 | 0 | 0 | 2.14552E-01 | 1.77071E+00 | 1.53620E+00 | 3.43204E-02 |
| 18 | 0 | 0 | 2.50897E-01 | 2.2277E+00 | 2.98085E-01 | 2.96221E-02 |
| 19 | 0 | 0 | 2.91847E-01 | 2.77071E+00 | 5.40322E-01 | 2.51549E-02 |
| 20 | 0 | 0 | 3.37532E-01 | 3.35432E+00 | 2.11327E+00 | 2.1582E-02 |
| 21 | 0 | 0 | 3.87891E-01 | 4.00000E+00 | 3.15740E+00 | 1.78778E-02 |
| 22 | 0 | 0 | 4.42895E-01 | 4.7332E+00 | 4.01843E+00 | 1.55351E-02 |
| 23 | 0 | 0 | 5.02866E-01 | 5.5533E+00 | 4.64676E+00 | 1.43102E-02 |
| 24 | 0 | 0 | 5.67366E-01 | 6.4551E+00 | 5.02238E+00 | 1.31046E-02 |
| 25 | 0 | 0 | 6.36337E-01 | 7.4255E+00 | 5.22235E+00 | 1.19844E-02 |
| 26 | 0 | 0 | 7.09900E-01 | 8.4646E+00 | 5.33735E+00 | 1.09354E-02 |
| 27 | 0 | 0 | 7.87660E-01 | 9.5676E+00 | 5.00664E+00 | 1.00000E-02 |
| 28 | 0 | 0 | 8.69990E-01 | 1.07376E+00 | 4.66121E+00 | 9.22090E-02 |

| | | | | | | | |
|----|------------|----|------------|-------------|------------|------------|------------|
| 29 | 169501E-01 | 0. | 307097E+00 | 260141E+00 | 350841E+00 | 377058E-02 | 327200E-02 |
| 30 | 168728E-02 | 0. | 256183E+00 | 272865E+00 | 280236E+00 | 377141E-02 | 390460E-02 |
| 31 | 308619E-02 | 0. | 200034E+00 | 266968E+00 | 207414E+00 | 358211E-02 | 456478E-02 |
| 32 | 44713E-02 | 0. | 142273E+00 | 240819E+00 | 136401E+00 | 341125E-02 | 521844E-02 |
| 33 | 695657E-02 | 0. | 858485E-01 | 196878E+00 | 703739E-01 | 326715E-02 | 582288E-02 |
| 34 | 997390E-02 | 0. | 330714E-01 | 196557E+00 | 116459E-01 | 315912E-02 | 678692E-02 |
| 35 | 115422E-01 | 0. | 142804E-01 | 790433E-01 | 382428E-01 | 309322E-02 | 878692E-02 |
| 36 | 117260E-01 | 0. | 548538E-01 | 202810E-01 | 783978E-01 | 307542E-02 | 707105E-02 |
| 37 | 107701E-01 | 0. | 376385E-01 | 279676E-01 | 108449E+00 | 310887E-02 | 714333E-02 |
| 38 | 878628E-02 | 0. | 111933E+00 | 1138914E+00 | 128468E+00 | 332877E-02 | 714333E-02 |
| 39 | 673361E-02 | 0. | 127381E+00 | 591004E+00 | 138914E+00 | 332877E-02 | 691433E-02 |
| 40 | 373361E-02 | 0. | 134007E+00 | 272687E-01 | 140609E+00 | 350841E-02 | 855788E-02 |
| 41 | 139138E-02 | 0. | 123322E+00 | 271653E-01 | 122643E+00 | 337279E-02 | 855788E-02 |
| 42 | 408834E-03 | 0. | 108527E+00 | 515923E-01 | 106118E+00 | 396774E-02 | 327449E-02 |
| 43 | 151647E-02 | 0. | 108533E-01 | 803094E-01 | 869360E-01 | 422538E-02 | 449624E-02 |
| 44 | 194338E-02 | 0. | 899833E-01 | 921993E-01 | 869360E-01 | 448225E-02 | 449624E-02 |
| 45 | 183940E-02 | 0. | 697091E-01 | 866569E-01 | 669072E-01 | 472375E-02 | 282008E-02 |
| 46 | 142876E-02 | 0. | 498146E-01 | 683115E-01 | 476995E-01 | 493646E-02 | 282008E-02 |
| 47 | 932859E-03 | 0. | 320609E-01 | 683115E-01 | 307185E-01 | 510934E-02 | 129050E-02 |
| 48 | 506933E-03 | 0. | 177388E-01 | 446938E-01 | 170223E-01 | 523036E-02 | 693397E-02 |
| 49 | 229120E-03 | 0. | 757990E-02 | 233567E-01 | 726810E-02 | 530221E-02 | 260764E-02 |
| 50 | 790459E-04 | 0. | 177958E-02 | 954306E-02 | 167494E-02 | 530221E-02 | 226652E-02 |
| 51 | 0. | 0. | 0. | 0. | 0. | 0. | 0. |
| 52 | 746135E-04 | 0. | 144534E-02 | 0. | 0. | 0. | 0. |

LCAD POTENTIAL

F*DV(S) F*DV(F,S) TCTAL.
 -.5781E-04 .2023E-07 -.5779E-04
 -.2662E-02 .9316E-06 -.2661E-02

STRESS*STRAIN MOMENT*CURV.

| | | | |
|-----------------|-----------------|-----------------|------------|
| NO(S)*EO(S) | NO(S)*EC(S) | NO(S)*FC(S) | TOTAL |
| .6519E-02 | .5504E-02 | 0. | .1202E-01 |
| .3002E+00 | .2535E+00 | 0. | .5537E+00 |
| NO(F,S)*FO(F,S) | NO(F,S)*FC(F,S) | NO(F,S)*EC(F,S) | TOTAL |
| -.5843E-02 | .1716E-03 | 0. | -.5971E-02 |
| -.2691E+00 | .7903E-02 | 0. | -.2612E+00 |
| NO(F)*FO(F,S) | NO(F)*EC(F,S) | NO(F,S)*EC(F) | TOTAL |
| -.3170E+00 | -.5639E-02 | -.1245E-02 | -.1377E-01 |
| | -.2597E+00 | -.5735E-01 | -.6341E+00 |

SUB TOTAL NO*EO (F,S) NO*FC (F,S) NO*EC (F,S) TOTAL

-.1837E-01 -.1944E-01
 -.8458E+00 -.8952E+00

```

-----
M0(S)*X0(S)      MC(S)*XC(S)      M0C(S)*X0C(S)      TOTAL
.7117E-02        .6265E-03          0.                .7943E-02
.3277E+00        .3804E-01          0.                .3658E+00
-----
E1+E1           E1*F2           E1*H           B*H           E2*H           V1*V1
-.301741E-02    .142397E-03      -.225230E+01    -.226384E+01    .778927E-01    0.
-.611501E-03    .288577E-04      -.456446E+00    -.458784E+00    .157856E-01    0.
-----
E4+E4           0.              0.              V1*F5           E4*E5
0.              0.              0.              0.              0.
0.              0.              0.              0.              0.
-----
CRITICAL LCAD= -.52877566E-02  PN/E = .11621443E-03  PN/PCL = .9600877E+00
ENERGY ERROR IS 2.155 PER CENT
-----
T.T.= 29.37  T. REDUCE= .005
T.T.= 29.35  T. ENERGY= .081
T.T.= 29.35  T. CONTRA= .082
-----
AI= 1.0
-----

```

```

-----
CONVERGENCE ON F-VALUE (ERR<.100E-02) AFTER 18 ITERATIONS
CONVERGENCE ON F-VECT (ERR<.100E-04) AFTER 4 ITERATIONS
COMPLETE CONVERGENCE ON F-VAL/VECT (ERR<.100E-04) AFTER 6 ITERATIONS
COMPLETE CONVERGENCE ON E-VECT (ERR<.100E-07) AFTER 3 ITERATIONS
COMPLETE CONVERGENCE ON VAL/VECT (ERR<.100E-07) AFTER 5 ITERATIONS
CODE OF CONVERGENCE, 0=1807E+01 Y=2337E+01
Y CUTSIDE OF FUNVEC RANGE, 0=1A07E+01 INVERSE ITERATION WILL BE TRIED
Y CUTSIDE OF FUNVEC RANGE, 0=1A07E+01 INVERSE ITERATION WILL BE TRIED
INVERSE ITERATION HAS FAILED WITH 1 E-VALUES FOUND
T.T.= 32.01  T. SLVTR= 2.637
SLVTR HAS FAILED FOR L= 2  IFAIL= 2
-----
END OF SET UP, TOTAL TIME= 29.364

```

```

-----
CIRCUMFERENTIAL MODE NO.= 1  EIGEN-VALUE POSITION = 1  NO. OF TURNING POINTS ON HALF SHELL = 3
-----
T.F.E. V0      UMO      UMC      URO      L.P.
.1103E-05      .1099E-05      .1612E-06      .2453E-08      L.P.264E-05
.4665E+00      .4643E+00      .6820E-01      .1037E-02      -.2364E-05
T.F.E. V1      UMO      UMC      URO      L.P.
.8669E-06      .1287E-05      .5027E-06      .1441E-07      L.P.1000E+01
.3238E+00      .4808E+00      .1877E+00      .5380E-02      .2684E-05
-----
TPE DELTA V0  UMO      UMC      URO      L.P.
.4870E-07      .897E-07      .2434E-07      .6114E-09      L.P.1436E-06
.3391E+00      .4872E+00      .1694E+00      .4257E-02      -.1000E+01
-----
FNFKGY ERROR= -.471 PER CENT

```


45 --.192186E-02
 46 --.143217E-02
 47 --.189204E-03
 48 --.640445E-03
 49 --.382305E-03
 50 --.180855E-03
 51 C .174174E-03
 52

--.184021E-03
 --.175302E-03
 --.153837E-03
 --.123161E-03
 --.85057E-04
 --.396298E-04
 0. --.164001E-03
 C. --.329165E-03

.264622E-01
 .164198E-01
 .862949E-02
 .357443E-02
 .937196E-03
 .553922E-04
 C. --.329165E-03

.934425E-01
 .527047E-01
 .388552E-01
 .262841E-01
 .178344E-01
 .141616E-01
 C. --.329165E-03

.235993E-01
 .139866E-01
 .693645E-02
 .246650E-02
 .273290E-03
 .249788E-03
 --.249788E-03

.191268E-02
 .200999E-02
 .197907E-02
 .195729E-02
 .188652E-02
 .213677E-02
 --.249788E-03

.458528E-02
 .477557E-02
 .493228E-02
 .504631E-02
 .510996E-02
 .511689E-02
 --.249788E-03

.260451E-02
 .187316E-02
 .120998E-03
 .656122E-03
 .249146E-04
 .223384E-04
 --.249788E-03

LCAC POTENTIAL

F*DV(S) F*CV(F,S) TCTAL
 --.1599E-04 --.2642E-07 --.1601E-04
 --.1079E-02 --.1782E-05 --.1080E-02

STRESS*STRAIN MOMENT*CURV.

NO(S)*EO(S) NO(S)*EC(S) NOC(S)*EOC(S) TOTAL
 .3025E-02 .3553F-02 .1871E-02 .8452E-02
 .2041F+00 .2397F+00 .1264E+00 .5702F+00
 NO(F,S)*EO(F,S) NO(F,S)*EO(F,S) NOC(F,S)*EOC(F,S) TCTAL
 --.2119E-02 --.9741F-04 --.6572E-02 --.2058E-02
 --.1427E+00 --.1721E-02 --.3993E-04 --.1386E+00
 NO(F)*EO(F,S) NO(F,S)*FO(F,S) NO(F,S)*EO(F,S) TOTAL
 .4207E-02 .3721E-02 .1723E-02 .1186E-01
 .2838E+00 .2510E+00 .1162E+00 .8001E+00

SUE TOTAL NO*EO,(F,S) NC*EC,(F,S) NOC*FCC,(F,S) TOTAL
 --.1004E-01 --.3835E-02 --.3993E-04 --.1392E-01
 --.6776E+00 --.2587E+00 --.2694E-02 --.9389E+00

MC(S)*XC(S) MC(S)*XC(S) NOC(S)*XOC(S) TOTAL
 .4075E-02 .7572E-03 .5553E-01 .5655E-02
 .2749E+00 .5108E-01 .5553E-01 .3815E+00

E1*E1 .348126E-04 E1*E2 .701280E+00 E2*E2 .442458E-01
 .128262E-03 .103355E-04 .206204E+00 .509360F+00 .131362E-01
 E4*E4 .775296E+00 V1*F4 .112462E-02 F4*F4 .577029E-02
 .459103E-03 .230178E+00 .300660E-03 .333888F-02 .171315E-02

.191268E-02
 .200999E-02
 .197907E-02
 .195729E-02
 .188652E-02
 .213677E-02
 --.249788E-03

.235993E-01
 .139866E-01
 .693645E-02
 .246650E-02
 .273290E-03
 .249788E-03
 --.249788E-03

.934425E-01
 .527047E-01
 .388552E-01
 .262841E-01
 .178344E-01
 .141616E-01
 C. --.329165E-03

.264622E-01
 .164198E-01
 .862949E-02
 .357443E-02
 .937196E-03
 .553922E-04
 C. --.329165E-03

.934425E-01
 .527047E-01
 .388552E-01
 .262841E-01
 .178344E-01
 .141616E-01
 C. --.329165E-03

.235993E-01
 .139866E-01
 .693645E-02
 .246650E-02
 .273290E-03
 .249788E-03
 --.249788E-03

.191268E-02
 .200999E-02
 .197907E-02
 .195729E-02
 .188652E-02
 .213677E-02
 --.249788E-03

.458528E-02
 .477557E-02
 .493228E-02
 .504631E-02
 .510996E-02
 .511689E-02
 --.249788E-03

ENERGY ERROR IS 1.169 PER CENT

CRITICAL LCAD= -.51298651E-02 PA/F = .11274429E-03 FM/PCL = .93142067E+00

T.T.= 32.09 T. FENERGY= .084
T.T.= 32.09 T. CCNTRL= .085

AI= 2.0

END CF SET UP, ICIAL TIME= 32.104
T. REDUCE= .006

CONVERGENCE ON E-VALUE (ERR< 100E-02) AFTER 5 ITERATIONS
CONVERGENCE ON E-VECTCP (ERR< 100E-04) AFTER 3 ITERATIONS
COMPLETE CONVERGENCE, E-VAL/VECT (FRR< 100E-04) AFTER 6 ITERATIONS
CONVERGENCE ON E-VECTCP (FRR< 100E-07) AFTER 2 ITERATIONS
COMPLETE CONVERGENCE, E-VAL/VECT (ERR< 100E-07) AFTER 3 ITERATIONS
Y CUTSIDE OF FUNVEC RANGE, 0-180VE+01
DIPECT ITERATION HAS FAILED, INVERSE ITERATION WILL BE TRIED
Y CUTSIDE OF FUNVEC RANGE, 0-180VF+01
INVERSE ITERATION HAS FAILED WITH 1 E-VALUES FOUND

SLVTR HAS FAILED FOR L= 3 IFAIL= 2
T.T.= 34.65 T. SLVTR= 2.543

CIRCUMFERENTIAL MODE NO.= 2 EAGEN-VALUE POSITION = 1 NO. CF TURNING POINTS CN HALF SHELL = 4

| NCDE | E1#E1 | E1#E2 | E1#E | U#B | E2#H | V1#V1 | E4#E4 | E5#E5 | V1#E4 | V1#E5 | E4#E5 | NCDE |
|------|----------|----------|----------|----------|----------|----------|----------|----------|----------|----------|-----------|------|
| 1 | .223E-05 | .649E-06 | .794E-02 | .369E-01 | .231E-02 | .932E-03 | .925E-03 | .369E-01 | .217E-02 | .278E-02 | .277E-02 | 1 |
| 4 | .703E-04 | .293E-05 | .889E-01 | .498E+00 | .127E-01 | .559E-03 | .411E-03 | .719E+00 | .111E-02 | .294E-01 | .251E-01 | 4 |
| 8 | .778E-04 | .997E-09 | .121E-02 | .250E+00 | .155E-03 | .299E-04 | .374E-05 | .119E+01 | .248E-04 | .271E-01 | .960E-04 | 8 |
| 12 | .181E-04 | .652E-05 | .264E-01 | .443E-01 | .933E-02 | .194E-03 | .422E-03 | .66E+00 | .652E-03 | .340E-01 | .193E-01 | 12 |
| 16 | .812E-04 | .110E-04 | .175E+00 | .146E+00 | .238E-01 | .348E-03 | .486E-03 | .125E+00 | .899E-03 | .340E-01 | .183E-02 | 16 |
| 20 | .864E-06 | .109E-05 | .482E-01 | .326E+00 | .608E-02 | .159E-03 | .186E-03 | .205E-02 | .395E-03 | .171E-02 | .183E-02 | 20 |
| 24 | .873E-06 | .891E-06 | .518E-02 | .358E-02 | .527E-02 | .244E-05 | .470E-04 | .536E-02 | .958E-02 | .135E-02 | .149E-02 | 24 |
| 28 | .349E-05 | .607E-05 | .739E-01 | .616E-02 | .346E-02 | .210E-05 | .304E-05 | .158E-02 | .587E-05 | .855E-03 | .1942E-03 | 28 |
| 32 | .376E-07 | .970E-08 | .60CE-01 | .100E-01 | .178E-03 | .419E-05 | .394E-05 | .322E-01 | .952E-05 | .828E-05 | .330E-05 | 32 |
| 36 | .337E-05 | .183E-06 | .337E-03 | .246E-02 | .180E-03 | .449E-05 | .345E-05 | .382E-01 | .731E-06 | .144E-04 | .875E-05 | 36 |
| 40 | .386E-05 | .123E-05 | .348E-02 | .146E-02 | .160E-02 | .177E-05 | .159E-04 | .382E-01 | .620E-06 | .119E-03 | .874E-05 | 40 |
| 44 | .946E-10 | .905E-10 | .571E-05 | .405E-03 | .544E-05 | .204E-07 | .270E-10 | .591E-07 | .165E-08 | .272E-06 | .9556E-08 | 44 |
| 48 | | | | | | | | | | | | 48 |

T.P.E. V0 UMO .1068E-05 UMC .1047E-05 UPO .1430E-06 URO .1980E-08 L.P. .2260E-05
 .4726E+00 UMC .4633E+00 UBO .6330E-01 URO .8761E-03 L.P. .1000E+01

T.P.E. V1 UMO .1026E-05 UMC .1451E-05 UBO .4781E-06 URO .1119E-07 L.P. .2982E-05
 .344PE+00 UMC .4880E+00 UBO .1609E+00 URO .3763E-02 L.P. .1003E+01

TPE DELTA V0 UMO .5600E-07 UMC .7628E-07 UBO .2259E-07 L.BG .1669E-09 L.P. .1553E-06
 .3605E+00 UMC .4911E+00 UBO .1454E+00 L.BG .3006E-02 L.P. .1000E+01

ENERGY ERRCR= -.531 PER CENT

| NCDF | II | V | F0(S) | EC(S) | F0F(S) | EU(F) | FC(F) | NCDF |
|------|------------|-------------|------------|------------|------------|-----------|-------------|------|
| 1 | 823637E-02 | 827693E-02 | 176120E-01 | 630659E+00 | 629975E+00 | 17440E+00 | 3999337E-02 | 1 |
| 2 | 230324E-01 | 827998E-02 | 176122E-01 | 633397E+00 | 599777E+00 | 17440E+00 | 4083260E-02 | 2 |
| 3 | 433322E-01 | 1633099E-01 | 151179E+00 | 632647E+00 | 605284E+00 | 17440E+00 | 4083450E-02 | 3 |
| 4 | 298062E-01 | 3153703E-01 | 157757E+00 | 622747E+00 | 590724E+00 | 17440E+00 | 4114350E-02 | 4 |
| 5 | 324727E-01 | 3821140E-01 | 381449E+00 | 555280E+00 | 485944E+00 | 17440E+00 | 421707E-02 | 5 |
| 6 | 334197E-01 | 4103328E-01 | 135332E+00 | 55280E+00 | 485944E+00 | 17440E+00 | 431564E-02 | 6 |
| 7 | 335197E-01 | 487958E-01 | 197687E+00 | 197687E+00 | 590091E+01 | 17440E+00 | 4333740E-02 | 7 |
| 8 | 303210E-01 | 5342747E-01 | 643674E+00 | 131198E+00 | 590091E+01 | 17440E+00 | 432907E-02 | 8 |
| 9 | 247650E-01 | 551157E-01 | 867669E+00 | 156136E+00 | 351330E-01 | 17440E+00 | 420495E-02 | 9 |
| 10 | 222233E-01 | 511572E-01 | 984013E+00 | 311581E+00 | 172608E+00 | 17440E+00 | 408349E-02 | 10 |
| 11 | 127357E-02 | 523362E-01 | 100000E+01 | 270865E+00 | 337801E+00 | 17440E+00 | 408369E-02 | 11 |
| 12 | 166986E-01 | 450777E-01 | 976032E+00 | 287041E+00 | 358717E+00 | 17440E+00 | 395460E-02 | 12 |
| 13 | 192579E-01 | 45049E-01 | 920035E+00 | 326446E+00 | 395498E+00 | 17440E+00 | 375321E-02 | 13 |
| 14 | 264014E-01 | 402597E-01 | 835328E+00 | 241766E+00 | 424182E+00 | 17440E+00 | 355046E-02 | 14 |
| 15 | 318053E-01 | 351163E-01 | 728119E+00 | 388275E+00 | 431806E+00 | 17440E+00 | 333591E-02 | 15 |
| 16 | 372383E-01 | 294751E-01 | 605431E+00 | 181996E+00 | 421433E+00 | 17440E+00 | 312064E-02 | 16 |
| 17 | 427524E-01 | 247512E-01 | 471741E+00 | 110688E+00 | 398643E+00 | 17440E+00 | 291674E-02 | 17 |
| 18 | 476912E-01 | 192233E-01 | 34280E+00 | 35958E+00 | 366224E+00 | 17440E+00 | 273309E-02 | 18 |
| 19 | 529157E-01 | 155069E-01 | 217521E+00 | 37500E+00 | 328934E+00 | 17440E+00 | 259309E-02 | 19 |
| 20 | 583090E-01 | 115697E-01 | 102767E+00 | 108445E+00 | 288936E+00 | 17440E+00 | 249749E-02 | 20 |
| 21 | 637383E-01 | 813913E-01 | 292991E-02 | 161571E+00 | 249405E+00 | 17440E+00 | 245996E-02 | 21 |
| 22 | 693033E-01 | 521234E-02 | 795256E-01 | 211353E+00 | 175744E+00 | 17440E+00 | 248937E-02 | 22 |
| 23 | 753947E-01 | 270708E-02 | 143070E+00 | 244837E+00 | 142606E+00 | 17440E+00 | 258301E-02 | 23 |
| 24 | 815096E-01 | 770352E-02 | 217276E+00 | 68890E-01 | 11894E+00 | 17440E+00 | 300875E-02 | 24 |
| 25 | 880478E-01 | 815096E-01 | 228936E+00 | 712663E-01 | 11894E+00 | 17440E+00 | 332033E-02 | 25 |
| 26 | 950061E-01 | 200061E-02 | 228936E+00 | 795907E-01 | 222249E+00 | 17440E+00 | 368767E-02 | 26 |
| 27 | 102655E-02 | 347065E-02 | 169441E+00 | 898822E-01 | 248814E+00 | 17440E+00 | 406924E-02 | 27 |
| 28 | 110734E-02 | 377005E-02 | 196336E+00 | 962531E-01 | 15140E+00 | 17440E+00 | 452682E-02 | 28 |
| 29 | 120259E-02 | 383233E-02 | 169442E+00 | 956485E-01 | 15140E+00 | 17440E+00 | 495857E-02 | 29 |
| 30 | 125229E-02 | 360333E-02 | 138164E+00 | 878266E-01 | 134631E+00 | 17440E+00 | 532272E-02 | 30 |
| 31 | 135259E-02 | 339154E-02 | 105392E+00 | 678666E-01 | 78035E-01 | 17440E+00 | 572310E-02 | 31 |
| 32 | 145266E-02 | 246866E-02 | 720019E-01 | 424301E-01 | 334628E-01 | 17440E+00 | 600554E-02 | 32 |
| 33 | 155277E-02 | 193593E-02 | 398622E-01 | 124356E-01 | 33303E-01 | 17440E+00 | 618964E-02 | 33 |
| 34 | 165299E-02 | 141212E-02 | 103522E-01 | 173813E-01 | 408187E-01 | 17440E+00 | 625827E-02 | 34 |
| 35 | 175316E-02 | 932306E-02 | 363212E-01 | 490329E-01 | 377965E-01 | 17440E+00 | 619205E-02 | 35 |
| 36 | 185333E-02 | 523740E-02 | 518535E-01 | 53000E-01 | 325707E-01 | 17440E+00 | 565275E-02 | 36 |
| 37 | 195350E-02 | 206448E-02 | 616016E-01 | 638084E-01 | 186708E-01 | 17440E+00 | 518840E-02 | 37 |
| 38 | 205367E-02 | 212257E-02 | 955907E-01 | 835072E-01 | 119870E-01 | 17440E+00 | 466154E-02 | 38 |
| 39 | 215384E-02 | 162256E-02 | 642590E-01 | 659077E-01 | 64072E-01 | 17440E+00 | 395794E-02 | 39 |
| 40 | 225401E-02 | 131519E-02 | 581224E-01 | 583451E-01 | 41072E-02 | 17440E+00 | 324804E-02 | 40 |
| 41 | 235418E-02 | 246182E-02 | 382218E-01 | 485302E-01 | 299073E-02 | 17440E+00 | 252177E-02 | 41 |
| 42 | 245435E-02 | 224882E-02 | 267389E-01 | 373820E-01 | 163707E-02 | 17440E+00 | 181773E-02 | 42 |
| 43 | 255452E-02 | 133458E-02 | 267389E-01 | 331950E-01 | 205333E-02 | 17440E+00 | 117730E-02 | 43 |
| 44 | 265469E-02 | 827915E-02 | 160920E-01 | 224506E-01 | 205333E-02 | 17440E+00 | 640358E-02 | 44 |
| 45 | 275486E-02 | 344440E-02 | 151428E-02 | 595330E-01 | 176884E-02 | 17440E+00 | 221601E-02 | 45 |
| 46 | 285503E-02 | 126687E-02 | 194310E-02 | 180843E-02 | 176884E-02 | 17440E+00 | 221601E-02 | 46 |
| 47 | 295520E-02 | | | | | | | 47 |
| 48 | 305537E-02 | | | | | | | 48 |
| 49 | 315554E-02 | | | | | | | 49 |
| 50 | 325571E-02 | | | | | | | 50 |
| 51 | 335588E-02 | | | | | | | 51 |
| 52 | 345605E-02 | | | | | | | 52 |

LOAD POTENTIAL

P*UV(S) F*CV(F,S) TOTAL
 .5120E-04 .2020E-06 .5100F-04
 .2622E-02 .1035E-04 .2612E-02

STRESS*STRAIN MOMENT*CURV.

| | | | |
|-----------------|-----------------|------------------|-----------|
| NO(S)*EO(S) | NO(S)*FC(S) | NO(S)*FOC(S) | TOTAL |
| .3176E-02 | .2365E-02 | .4024E-02 | .4566E-02 |
| .1627E+00 | .1211E+00 | .2061E+00 | .4899E+00 |
| NO(F,S)*EO(F,S) | NO(F,S)*FC(F,S) | NO(F,S)*FOC(F,S) | TOTAL |
| .1407E-02 | .1039E-04 | .8381E-03 | .2286E-02 |
| .7208F-01 | .2069E-02 | .4292E-01 | .1171E+00 |
| NO(F)*EO(F,S) | NO(F)*FC(F,S) | NO(F,S)*EO(F) | TOTAL |
| .4128E-02 | .4378E-02 | .4233E-02 | .1722E-01 |
| .2114E+00 | .2242E+00 | .2168E+00 | .8820E+00 |

SUB TOTAL NO*FO (F,S) NC*EO (F,S) NOC*EOC (F,S) TOTAL
 .9913E-02 .8756E-02 .8381E-03 .1951E-01
 .5077E+00 .4485E+00 .4292E-01 .9991E+00

MO(S)*XC(S) MO(S)*XC(S) MO(C(S))*XC(S) TOTAL
 .4166E-02 .3462E-02 .2238E-02 .9881E-02
 .2149E+00 .1773E+00 .1139E+00 .5061E+00

| | | | | |
|-------------|-------------|-------------|-------------|-------------|
| E1*E1 | F1*E2 | F1*E4 | H*E4 | V1*V1 |
| .198429E-03 | .146332E-05 | .423158E+00 | .176205E+01 | .133635E-02 |
| .447240E-04 | .329818E-06 | .953758E-01 | .397150F+00 | .301201E-03 |
| E4*E4 | F5*E5 | V1*E4 | V1*F5 | E4*E5 |
| .174330E-02 | .201381E+01 | .334759E-02 | .985403E-01 | .118996E+00 |
| .392923E-03 | .453894E+00 | .754514E-03 | .222100E-01 | .268205E-01 |

CRITICAL LGAD= .50520654E-02 PN/E = .11103440E-03 FN/PCL = .91729472E+00
 ENERGY ERRCR IS -.052 PER CENT

T.T.= 34.74 I. ENFHCY= .085
 T.T.= 34.74 I. CCNTHL= .085

*** 7000 SCOPE 2.1.5 I.VL 533P MAY 1982 13/10/83 832H6
 SYS DEVICES 819/ 4/PP FLS=200K FIL=764K MXS=164K MXI=415K MXP=415R

